B cell signalling in mechanisms of central and peripheral tolerance

Theresa Thalhamer

A thesis submitted to the Faculty of Medicine, University of Glasgow for the degree of Doctor of Philosophy

Division of Immunology, Infection and Inflammation
Glasgow Biomedical Research Centre
120 University Place
University of Glasgow
Glasgow
G12 8TA

September 2009

Summary

Tolerance against self is a necessary feature of the immune system to prevent autoimmunity. Hence during B cell development, a number of central and peripheral developmental checkpoints ensure the deletion of self-reactive B cells and selection of tolerant B cells. For example, antigen-driven ligation of the B cell receptor (BCR) on immature B cells results, by default, in receptor editing, anergy and/or apoptosis, whereas it provides survival, proliferative and effector differentiation signals to mature B cells. Moreover, various factors can influence the functional outcome downstream of BCR ligation. Thus, T helper cell-derived signals, such as those following ligation of the CD40 receptor, can rescue pathogen-specific immature B cells from growth arrest and apoptosis, thereby providing a mechanism in which cells programmed to die because of their immature status can survive after receiving appropriate T cell help. On the other hand, mitogenic BCR-mediated signalling of mature B cells can be suppressed by co-ligation of the inhibitory receptor FcγRIIb. This allows the maintenance of B cell homeostasis in the periphery, as cross-linking of the BCR and FcγRIIb by immune complexes enables the system to terminate ongoing immune responses following clearance of pathogens. The precise signalling mechanisms involved in dictating these differential functional outcomes remain to be elucidated but it is becoming increasingly clear that the developmental stage as well as the integration of various extracellular signals decide the cell's fate. The core aim of this study has therefore been to characterise the signalling pathways coupling BCR ligation to survival, proliferation and apoptosis during development. In particular, it was planned to focus on the differential signalling mechanisms involved in the negative selection of immature B cells and FcγRIIb-mediated homeostatic regulation of mature B cells.

Negative selection of self-reactive immature B cells constitutes a major mechanism of sustaining central tolerance. The WEHI-231 cell line provides a well-established model system for dissecting the signalling mechanism underlying such clonal deletion of immature B cells as these cells, which have the phenotype of immature B cells, undergo growth arrest and apoptosis following stimulation of their BCR. Previously, this laboratory has identified ERK signalling as a key regulator of immature B cell fate. Thus, spontaneously proliferating WEHI-231 B cells exhibit a sustained yet cyclic pattern of ERK activation that is necessary for their survival and proliferation. By contrast, BCR-ligation induces a strong transient activation of ERK followed by sustained downregulation of the cyclic activation pattern observed in spontaneously proliferating cells. However, the pathways linking BCR ligation with suppression of ERK signalling and consequent growth arrest have not been delineated in full. For example, in B cells, the Ras/Raf-1/MEK cascade is considered to be a major

pathway regulating ERK activation and consistent with this, this laboratory has previously shown that overexpression of Ras can rescue WEHI-231 B cells from BCR-mediated growth arrest. However, although MEK activation was found to be compromised under conditions of BCR-driven growth arrest, such BCR-signalling did not suppress Ras activation indicating that other pathways normally contributed to the MEK-dependent activation of ERK in spontaneously proliferating WEHI-231 cells.

The data presented in this thesis now provide evidence for the existence of a second pathway controlling ERK activation in immature B cells, the Rap/B-Raf/MEK cascade, which has now been implicated in the maintenance of cycling ERK activation observed in spontaneously proliferating WEHI-231 B cells. BCR signalling was found to reduce the levels of active Rap, hence providing a mechanism for the BCR-mediated uncoupling of the Ras-independent, MEK-dependent ERK activation contributing to the cycling ERK signalling responsible for survival and proliferation of WEHI-231 cells. Consistent with the role of Rap in promoting such ERK signalling, additionally, it has now been demonstrated that levels of SPA-1, a negative regulator of Rap, increase upon BCR-stimulation indicating that this may be the mechanism by which the BCR signals to uncouple the Rap/B-Raf/MEK pathway.

Although ERK had previously been identified as the major regulatory element governing survival and proliferation of immature B cells, the pathways linking ERK to the regulation of survival/apoptosis and cell cycle progression have been only poorly characterised. This study has now highlighted the connection between sustained ERK signalling and the stabilisation of c-Myc protein levels. For example, abrogation of ERK activity by BCR-ligation, or pharmacological inhibition, reduced c-Myc levels in a transcription-independent fashion indicating regulation at the post-translational level. This proposal was corroborated by analysis of the phosphorylation status of c-Myc that indicated that ERK signalling promoted the expression of stabilised forms (S62) of c-Myc and reduced the expression of those (T58) targeting c-Myc for proteosomal degradation. The importance of such c-Myc stabilisation was illustrated by Laser Scanning Cytometric analysis that revealed that the increasing levels of c-Myc expressed by individual WEHI-231 B cells correlated with their cell cycle progression, presumably reflecting widely established findings that c-Myc promotes cell cycle progression by increasing the expression and activation of cyclin/Cdk complexes and reducing the levels of Cdk inhibitors such as p27. Consistent with this, negative signalling via the BCR, or suppression of ERK activation by pharmacological inhibition, also increased p27 levels and resulted in the reduction of the hyperphosphorylation of retinoblastoma (Rb) proteins required for transition through the G1-S-phase checkpoint. As Rb is a target of cyclin/Cdks, collectively these data further confirm the

links not only between BCR-signalling and c-Myc stability but also the differential cell fate decisions of apoptosis, survival and/or cell cycle progression.

By contrast, in mature B cells, BCR-signalling is linked to survival and proliferation. However, to prevent autoimmunity resulting from an expanded pool of potentially weakly autoreactive B cells, such survival and proliferation of mature B cells needs to be homeostatically regulated. Hence, the immune system has evolved inhibitory signalling cascades such as that triggered by cognate immune-complexes co-ligating the BCR and FcγRIIb to terminate ongoing antigen-driven responses. This study has emphasised the crucial role of caspase 8 in the apoptosis of mature B cells resulting from such co-ligation of the BCR and FcγRIIb and has indicated that such caspase 8 activation is likely to be downstream of Fas signalling. Consistent with this, blocking the Fas/FasL death receptor cascade was found to reduce the levels of apoptosis detected and B cells from MRL/MpJ-*Fas*^{lpr} mice, a strain harbouring a mutation causing the abrogation of Fas expression, exhibited defective apototic responses upon such BCR/FcγRIIb co-ligation. Thus, Fas/FasL death receptor signalling might be a major mechanism underpinning the FcγRIIb-mediated apoptosis pathway.

Finally, to determine whether dysfunctional regulation of FcγRIIb-mediated signalling plays a role in human autoimmune conditions, B cells from patients with Rheumatoid arthritis and Systemic lupus erythematosus were examined. Overall, the homeostatic regulatory responses between B cells from healthy controls and RA and SLE patients were not found to be significantly different. However, the B cells derived from a small proportion of RA and SLE patients were found to exhibit defective FcγRIIb-mediated inhibitory responses. Moreover, significant differences were found in the ratio of FcγRIIb1/FcγRIIb2 expression between the cohorts of healthy controls and RA and SLE patients. The RA and SLE patients expressed relatively higher levels of the FcγRIIb2 isoform which promotes antigen-processing suggesting that these B cells may play some role in priming autoreactive responses in such individuals. Thus, as these inflammatory disorders constitute spectrum diseases, such defects in the regulation of B cell responses could be one of the contributing factors aggravating autoimmune disease development in some subgroups of patients.

Declaration

The work presented in this thesis represents original work carried out by the author. This thesis has not been submitted in any form to any other University.

Theresa Thalhamer
University of Glasgow
September 2009

Acknowledgements

I want to thank my supervisor Maggie Harnett for all the support and patience during the last few years. Thank you very much for the encouragement and advice, especially during the writing of this thesis.

I would like to thank The Nuffield Foundation/Oliver Bird Rheumatism Programme for funding my PhD. Moreover, thanks to Iain McInnes, the head of the Oliver Bird Rheumatism Programme in Glasgow, who first pointed out this great programme to me.

A big “Thank you” goes to everybody, past and present, in the Division of Immunology. I am not going to try and list you all as I don’t want to risk missing out anyone. It has been a pleasure to work with so many great people. A special thanks to all the past and present members of the Harnett Lab, specifically Mairi and Angela for the last few years filled with lots of fun, cups of tea and great support. Also, I would like to thank Verica, Vuk and Andy for kindly reading my thesis.

I want to thank Erica Lacey, Eleanor Forbes as well as Kirsty Brown for their contributions. Furthermore, a big thanks to Ashley Gilmour for carrying out the FACS sorting. I also want to thank Mairi for running the SLE model, Angela for all the help with immunofluorescent staining and kindly giving me permission to reproduce some of her figures and Rinako for providing cell samples.

I want to thank the patients for donating blood samples and the nurses and doctors at the Glasgow Royal Infirmary for collecting the samples.

A very special mention has to go to my friend Chrisu who has put up with my incessant moaning during our undergraduate studies as well as during my PhD and writing up period. You have always managed to brighten my day with a few encouraging words. Thanks so much for everything.

Finally, I’d like to thank my parents and my sister and brother for all their patience and support through the last few years.

Table of contents

List of figures and tables

1 Introduction

2 Materials and Methods

3 Signalling involved in negative selection of immature B cells

5 General Discussion

List of abbreviations

AA	Arachidonic acid
Ab	Antibody
ACPA	Anti-citrunillated protein antigens
Ag	Antigen
ANA	Anti-nuclear antigen
APAF-1	Apoptotic peptidase activating factor 1
APC	Antigen presenting cell
ASK1	Activator of S-phase kinase
ATF	Activating transcription factor
BAFF	B-cell-activating factor
BCAP	B-cell PI3K adaptor
BCR	B cell receptor
BH	Breakpoint cluster region homology
BH	Bcl-2 homology
bHLHZip	Basic-region/helix-loop-helix/leucin-zipper
BIC	B-cell integration cluster
Blimp-1	B lymphocyte induced maturation protein-***1***
BLNK	***B cell*** linker
Btk	Bruton Tyrosine Kinase
CAD	Caspase-actived DNAse
CAK	Cdk activating kinase
CD	Cluster of differentiation
Cdk	Cyclin-dependent kinases
CDR	Complementary determining regions
C3G	Crk SH3-domain-binding guanine-nucleotide releasing factor
CKI	Cdk inhibitor
cPLA2	Cytosolic phospholipase A2
CLP	Common lymphoid progenitor
Cox2	Cycloxygenase 2
CTL	Cytotoxic T cell
DAG	Diacylglycerol
DD	Death domain
DED	Death effector domain
DISC	Death-inducing signalling complex
DLK	Dual leucine zipper-bearing kinase
DNA-PK	DNA-dependent protein kinase
DUB	Deubiquitinating enzyme
DUSP	Dual-specificity phosphatase
EAE	Experimental autoimmune encephalomyelitis
Elk	Ets-like transcription factor

ERK	Extra-cellular signal-regulated kinase
Ets	E26-AMV virus oncogene cellular homolog
FACS	Fluorescent-activated cell sorting
FADD	Fas-associated death domain
FCS	Foetal calf serum
FLIP	FLICE-like inhibitory protein
GC	Germinal centre
GEF	Guanine nucleotide exchange factor
GPRC	G-protein coupled receptors
Grap	Grb2-like accessory protein
GRD	GAP-related domain
GSK3	Glycogen synthase kinase 3
GTPase	Guanine triphosphatase
HePTP	Hematopoeitic protein tyrosine phosphatase
HRP	Horse radish peroxidase
HSC	Haematopoietic stem cell
hsp1	Heat shock factor transcription factor 1
IFN	Interferon
Ig	Immunoglobulin
IL	Interleukin
ILK	Integrin-linked kinase
IP_3	Inositol-(1,4,5)-P_3
IRES	Internal ribosome entry site
ITAM	Immunoreceptor tyrosine-based activation motif
ITIM	Immunoreceptor Tyrosine-Based Inhibitory Motif
J chain	Joining chain
JNK	c-Jun NH_2-terminal kinase
KAP	CDK associated phosphatase
KSR	Kinase suppressor of Ras
Lox	Lipoxygenase
LPS	Lipopolysaccharide
MAPK	Mitogen activated protein kinase
Mdm2	Murine double minute 2
MEK	MAP/ERK kinase
MEKK	MAP/ERK kinase kinase
MEKKK	MAP/ERK kinase kinase kinase
MHC	Major histocompatibility complex
MLK	Mixed lineage kinase
MKP	MAPK phosphatase
MMP	Mitochondrial membrane potential
MNK	MAPK interacting serine/threonine kinase
MOMP	Mitochondrial outer membrane permeabilization

MSK	Mitogen-and stress-activated protein kinase
mTOR	Mammalian target of rapamycin
MZ	Marginal zone
NF-κB	Nuclear factor – κB
NFAT	Nuclear factor of activated T cells
NK cells	Natural Killer cells
NO	Nitric oxide
PAC-1	Phosphatase of activated cells-1
PAK	p21-activated kinase
PAMP	Pathogen associated molecular patterns
PARP	Poly(ADP-ribose) polymerase
PBMC	Peripheral blood mononuclear cell
PDK	3′-phosphoinositide-dependent protein ***kinase***
PH	Pleckstrin homology
PI	Propidium iodide
PI3 kinase	Pphosphoinositide-3-kinase
PIP_3	PI-(3,4,5)-P_3
PLD	Phospholipase D
PKB	Protein kinase B
PKC	Protein kinase C
PLC	Phospholipase C
PP2A	Protein phosphatase 2A
PRR	Pattern recognition receptors
PTK	Protein tyrosine kinase
RA	Rheumatoid arthritis
RAG	Recombination-activating gene
Rap	Ras proximity
Rb	Retinoblastoma
RalGDS-RBD	Ras binding domain of the Ral guanine nucleotide dissociation stimulator
RF	Rheumatoid factor
RIP	Receptor-interacting protein
RSK	90 kDa ribosomal S6 kinase
SCID	Severe combined immunodeficiency
SLC	Surrogate light chain
SLE	Systemic Lupus Erythematosus
SH2	Src homology 2
SHIP	SH2 domain containing inositol 5’ phosphatase
snRNPs	Small nuclear ribonucleoproteins
Sos	Son of sevenless
SPA-L	SPA-1-like
STAT	Signal transducer and activator of ***transcription***
STEP	Striatal enriched phosphatase

TAK1	TGFβ-activated kinase
TCR	T cell receptor
TdT	Terminal deoxynucleotidyl transferase
TGF	Transforming growth factor
T_H cell	T helper cell
TKB	Tyrosine kinase-binding
Tpl2	Tumor progression locus 2
TLR	Toll-like receptor
TRAF	TNF-receptor associated factor
TRAIL	TNF-related apoptosis inducing ligand
TSC	Tuberous sclerosis complex
UBD	Ubiquitin binding domain
XIAP	X-linked inhibitor of apoptosis proteins

g	gram
mg	milligram
µg	microgram
M	molar
mM	millimolar
µM	micromolar
ml	millilitres
µl	microlitres
min	minutes
s	seconds
h	hours
wks	weeks
rpm	revolutions per minute
g	times gravity
V	volts

1 Introduction

1.1 The immune system

The immune system is the body's defence against infections caused by pathogens like bacteria, viruses and parasites. It consists of cells and molecules that ensure that the pathogen is removed from the body before it can cause too much damage. The first barriers a pathogen has to overcome to enter the host are of a physical nature. Thus, the skin and the mucosal surfaces can prevent the entry of the majority of pathogens and inactivate others by the production of antimicrobial substances. If a microbe passes these first barriers, then innate immunity provided by cells such as phagocytes (macrophages and granulocytes) and natural killer (NK) cells provides the first line of defense. The major mechanism for recognition of foreign antigens by these cells are PRRs (pattern recognition receptors) which bind PAMPs (pathogen associated molecular patterns) leading to the initiation of an innate immune response. The specificities of these innate immune system receptors are germ-line encoded meaning that their repertoire for pathogen recognition is limited and predetermined. PAMPs are structures shared by many classes of pathogens ensuring that the innate immune response recognises and combats a broad spectrum of pathogens in the first few days of infection whilst the adaptive immune system becomes activated. Moreover, innate cells, via their role in antigen presentation are crucial for priming of the specific adaptive response.

The adaptive immune response is highly specific and extremely diverse and comprises two branches: humoral (B cells) and cellular (T cells) immunity. T cells are not able to recognise protein antigen in its native form. Their antigen recognition receptor, the TCR (T cell receptor) binds to peptides derived from antigen in the context of MHC (major histocompatibility complex) molecules expressed at the surface of cells. Depending on the class of MHC (I or II) the T cell is able to interact with, one can differentiate between cytotoxic T cells (CTLs) which recognise peptide presented in combination with MHC class I (present on all nucleated cells) and T helper cells (T_H cells) which recognise peptide bound to MHC II (mainly expressed on antigen presenting cells; APCs). The major function of CTLs is the killing of infected or tumour cells whereas T_H cells provide help to other cell classes in the form of either cytokines or engagement of surface costimulatory molecules. There is a third class of T cells, the so called T regulatory cells which play a homeostatic

role in keeping an ongoing immune response in check after the removal of the pathogen and by this way preventing a harmful overreaction of the immune system.

The other arm of the adaptive immune response is humoral immunity which is dependent on B cells, the producers of antibodies. The Immunoglobulin (Ig) molecule is made up of four chains, two identical heavy (55-70kD) and light chains (~24kD) linked by disulphide bonds. Both heavy and light chains consist of Ig domains – two in each light chain and varying numbers, depending on the antibody subclass, on the heavy chain. The heavy and light chains both feature an amino terminal V (variable) region and a constant (C) region at the carboxy terminus of the protein. The amino acid sequence of the variable regions varies between molecules from different B cell clones thereby creating the specificity of antibodies as the opposing V regions of the heavy and light chains comprise the antigen binding site (Fig.1.1). The high number of antibodies with different V regions and hence different binding specificities is achieved by random genetic recombination of the genes encoding the variable regions of the heavy and light chain. Thus, the variable region of the heavy chain is generated by the recombination of D_H segments to J_H segments followed by the joining of the V_H region to the pre-assembled D_HJ_H segment (Fig.1.2). The mammalian genome encodes about 300 variable (V_H) genes, 30 diversity (D_H) genes and 6 joining (J_H) genes allowing the potential creation of 50,000 different heavy chains via somatic recombination. To further increase diversity the enzyme TdT (terminal deoxynucleotide transferase) randomly adds nucleotides into the heavy chain genes without following a template. Similarly to the heavy chain, the light chain protein is also generated by somatic recombination but it is encoded by two genes, kappa and lambda, which further doubles the number of potential light chains, as both genes encode multiple V and J segments. In contrary to the heavy chain gene, the gene encoding the light chain lacks a D segment and is therefore created via a single recombination event. The V region furthermore contains three so called CDRs (complementarity-determining region). These regions are areas of high variability where most mutations occur during somatic hypermutation. They are located in the part of the V region which takes part in the antibody-antigen interaction and thus influences the binding capacity of the antibody (Fig.1.3).

The B cell receptor (BCR) consists of an antigen-binding component – the membrane bound Ig molecule – and the signal-transducing units Igα and Igβ (CD79a and b, reviewed in [1]). In the majority of cases, binding of antigen to the BCR on a naïve mature B cell will lead to its activation when T cell help is provided. Ultimately the B cell will develop into an antibody-secreting cell producing large amounts of antibody specific for the antigen which activated the B cell in the first place. Every B cell clone produces an

antibody with a unique specificity that can carry out various functions depending on their isotype. There are five different antibody isotypes: IgA, IgD, IgE, IgG and IgM (Fig.1.1). Before their activation naïve mature B cells express IgM and IgD on their surface and upon activation some clones can secrete IgM. The IgD isotype has so far not been found in a secreted form and its major function therefore seems to be signal transduction. Secreted IgM can form a pentamer thereby increasing antigen binding-avidity and a major function of soluble IgM is the activation of the classical pathway of complement. The complement system comprises a family of proteins which can bind to antibody-coated pathogens, or directly to pathogens and initiate a cascade which ultimately leads to the creation of a pore-forming complex and hence the destruction of the pathogen.

Upon receiving T cell help in the form of cytokines and CD40-ligation, B cells can undergo isotype-switching. This process leads to the expression of heavy chains other than the μ chain (IgM). The precise inflammatory environment and the specific types of cytokines generated dictate the isotype that the B cell produces subsequently. The infection with, for example, large parasites such as helminths, induces an inflammatory environment favourable to the production of IgE antibodies which then coat the parasite and drive the activation of granulocytes, a cell class which can release their cytotoxic granular contents, helping to combat pathogens that are too big to be engulfed by phagocytes. On the other hand, a bacterial or viral infection induces cytokines that drive B cells to switch to the expression of IgG isotypes. These antibodies can coat pathogens by binding to their specific antigen expressed on the microbe's surface and thus carry out various functions such as the opsonisation of pathogens, thereby targeting them for enhanced recognition by phagocytes. Moreover, binding of IgG can cause neutralisation which inactivates the pathogen or its toxins and prevents their entry into host cells. Finally, IgA antibodies comprise a very specialised isoytpe. IgA dimers or trimers, joined via the so called J chain (joining chain) can be transported across the epithelial barrier into the mucosal surfaces of the gastro-intestinal and respiratory tract creating an additional barrier to pathogens entering through these surfaces. Through the production of different isotypes B cells can therefore adjust to various pathogens creating a specific inflammatory environment ensuring the production of antibody isotypes best suited to protect against the different types of pathogens.

1.2 B cell development

There are three major subsets of B cells – B-2 follicular B cells, marginal zone (MZ) B cells and B-1 B cells. The follicular B cell subset is the major B cell class involved in the

adaptive humoral immune response, whilst B-1 B cells and marginal zone B cells appear to function as more innate-like subsets of B cells. For example, B-1 B cells are the major producers of “natural antibodies”, a class of IgM antibodies which are polyreactive and function to provide a first line of defense against microbial infection [2]. These antibodies are able to bind to multiple different self and foreign antigens although usually with relatively low affinity. Natural antibodies are present in healthy individuals in the absence of antigenic stimulation and as they recognise conserved pathogen antigens such as phosphorylcholine or lipopolysaccharide (LPS), can hence contribute to the initial innate immune response [2]. Furthermore, B-1 B cells express a reduced number of BCR specificities, compared to B-2 follicular B cells [2] again consistent with their status of innate-like immune cells, similar to γδ T cells. B-1 B cells are mainly found in the peritoneal and pleural cavities but also in the spleen and the intestine and they make up about 5% of the general B cell population (reviewed in [3]).

B-1 B cells are therefore a first line of defence which leads to the rapid production of antibodies especially against T-independent antigens like phosphorylcholine or LPS [2]. There are two subtypes of B-1 cells, B-1a and B-1b. Both cell types express low levels of CD11b, but only B-1a cells express CD5, a marker which was originally used to distinguish B-1 from B-2 B cells [2]. It has recently been shown that B-1a and B-1b B cells have distinct functions. Thus, B-1a B cells were found to provide protection from acute *Streptococcus pneumoniae* infection through the production of natural antibodies whereas B-1b cells contributed to the adaptive antibody response to this infection [4]. Moreover, B-1b but not B-1a B cells were found to be crucial for the induction of long-lasting T-cell independent immunity to *Borrelia hermsii* due to the production of pathogen-specific IgM [5]. MZ B cells, similarly to B-1 B cells, are important in the rapid response against pathogens, particularly blood-borne bacteria. MZ B cells reside in the marginal zone of the spleen, locating them at the blood-lymphoid interface between white and red pulp. The blood circulating through the spleen slows down in this area allowing the efficient encounter of MZ B cells with their antigens. Similarly to B-1 B cells, MZ B cells rapidly develop into antibody-producing cells thereby providing protection from blood-borne pathogens during the time it takes for the adaptive immune response to become established [6]. The B cell subclass crucial for the humoral adaptive immune response are conventional, follicular B-2 B cells. Unlike B-1 and MZ B cells these cells undergo somatic hypermutation and isotype switching and therefore contribute to the production of high affinity antibodies.

In mice, follicular B cells start their development in the bone marrow but also in the foetal liver before birth. Their progenitors are haematopoietic stem cells (HSC) which are

pluripotent and potentially able to develop into other immune cell lineages, like T cells, or myeloid lineage cells. The first step in their developmental process is the commitment of HSC to the lymphoid lineage as indicated by their expression of c-kit and the Interleukin-7 (IL-7) receptor α-chain (CD127) [7]. At this stage, called common lymphoid progenitor (CLP), the progeny can give rise to B, T and NK cells. The major transcription factors determining whether pluripotent cells commit to the B cell lineage are the paired box transcription factors PAX-5/BSAP, E2A and EBF1 (reviewed in [8]). The first stage at which cells are recognised as committed B cells is called the pre-pro-B cell stage and this can be distinguished by the expression of the B220 isoform of CD45, the lack of CD19, low levels of CD24 and little or no immunoglobulin (Ig) rearrangement [9] (Fig.1.4). The regulation of this step of lineage commitment depends on expression of different transcription factors. For example, the lack of E2A [10] was shown to impair the development of B cells at the pro-B cell stage whilst EBF-deficient cells do not progress to the pre-B cell stage [11].

Pro-B cells are the next stage in the development at which the cells upregulate CD19 and express CD10 but not surface immunoglobulin. These cells also upregulate recombination-activating gene-1 (RAG-1) and RAG-2, enzymes that are necessary to generate double stranded DNA breaks during the heavy and light chain rearrangement process. If those molecules are missing no μ heavy chain can be produced and the cells do not undergo any further development [12]. The DNA-PK repair complex has also been shown to be needed for successful rearrangement as B cells from Scid/Scid (severe combined immunodeficiency) mice display a developmental block at the pro-B cell stage [13]. This is because the scid mutation affects the activity of the DNA-PK repair complex which is involved in the joining of the segments during V(D)J recombination [14]. Consistent with upregulation of RAG-1 and RAG-2, the early pro-B cell stage is identified by the initiation of heavy chain rearrangement starting with the joining of one D_H and one J_H gene. The transition to the late pro-B cell stage is marked by the joining of a V_H segment to the pre-arranged D_HJ_H complex (Fig.1.2). Pro-B cells are also the first developmental stage expressing Igα and Igβ (CD79a and CD79b). These signalling molecules are expressed in a complex with the chaperone molecule calnexin and were found to be crucial for further developmental progress, as mice lacking Igα and/or Igβ are arrested at the pro-B cell stage [15]. Presumably, Igα/Igβ are needed for the transduction of signals permitting the survival and development of pro-B cells into pre-B cells. Consistent with this, cross-linking of CD79b was shown to induce the phosphorylation of various signalling transducers such as Syk, Btk and Vav leading to the activation of ERK (extracellular signal-regulated kinase) [15,16]. Moreover, such CD79b-mediated signalling

allowed arrested pro-B cells to mature into pre-B cells further confirming the importance of Igβ [16]. Interestingly, heavy chain rearrangement did not depend on this Igα/Igβ-mediated signalling indicating that different pathways regulate V(D)J recombination and developmental progress [17]. The succesful expression and signalling of Igα/Igβ initiates the maturation to pre-B cell. At this stage the B cell expresses the rearranged μ heavy chain in combination with λ5 and VpreB (SLC, surrogate light chain) to yield the pre-BCR which associates with Igα and Igβ on the surface of the cell [18] (Fig.1.5). A functional pre-BCR is necessary to permit the B cell to reach the next developmental stage. For example, it has been postulated that the association of the rearranged heavy chain with the invariant SLC allows signalling that ensures that only B cells expressing correctly folded heavy chains can develop further [19]. It is not clear what exact role the pre-BCR plays in the downregulation of RAG and TdT enzymes and progression to the next developmental stage, as pre-B cells from mice unable to express SLC were still capable of downregulating RAG and TdT [20]. Recently, it has been shown that the pre-BCR might also provide one of the earliest checkpoints in negative selection of autoreactive B cell clones. For example, autoreactive B cells from mice lacking expression of SLC were found to be able to escape negative selection leading to higher production of anti-nuclear DNA antibodies in these mice [21]. Thus, in the presence of SLC, pre-B cells expressing heavy chains likely to produce DNA-reactive antibodies undergo negative selection [21]. This process seems to be antigen-independent as pro-B cells expressing these specific heavy chains intracellularly were also depleted from the repertoire [21]. Besides taking part in positive and negative selection of pre-B cells, the successful expression of a functional heavy chain also leads to the block of rearrangement on the other heavy chain allele, a process called allelic exclusion [22,23]. If the rearrangement of both heavy chain alleles fails the cell undergoes programmed cell death by apoptosis.

Following allelic exclusion, the expression of the functional pre-BCR also initiates light chain rearrangement. Thus, V to J recombination leads to the expression of functional κ or λ light chain which then associates with the μ heavy chain (Fig.1.4). Surface expression of functional μ heavy and light chain complexes (IgM) is a characteristic feature of immature B cells. From the immature B cell stage onwards, the clonal selection process is Ag-dependent. Thus, immature B cells binding with high affinity to self-antigen are subjected to a process called negative selection which leads to either receptor editing or apoptosis [24] depending on the localisation of the cells. Thus, autoreactive immature B cells in the bone marrow default to receptor editing whereas apoptosis and therefore deletion seems to be the default response for immature B cells in the periphery [25]. Upon binding to self-antigen, induction of receptor editing allows immature B cells to express the

RAG genes again and undergo further light chain recombination in this way producing a new light chain molecule which might change the specificity of the BCR, therefore allowing the cell to escape deletion or anergy [26]. The response of immature B cells with low affinity for self-antigens is less well characterised. For example, it has been shown that membrane-bound low-affinity auto-antigens are as effective at inducing negative selection as high-affinity antigens [27]. Soluble low-affinity self-antigens on the other hand were found to preferentially induce positive selection of B cells into the B-2 B cell pool [28]. Thus, depending on the nature and affinity/avidity of the self-antigen, B cells will undergo either positive or negative selection.

Immature B cells that survive negative selection are released from the bone marrow into the circulation to migrate to the secondary lymphoid organs such as the spleen. These transitional-immature (T1) B cells are sensitive to BCR-induced apoptosis for a few days following their emigration from the bone marrow [29], a feature that ensures that self-reactive B cells that do not encounter their specific antigen in the bone marrow are deleted in the periphery. The initiation of IgD expression on T1 B cells indicates their development into (T2) transitional B cells. Recently, the existence of another transitional B cell subset (T3) has been proposed. These cells can be identified as $B220^{+}AA4.1^{+}CD23^{+}sIgM^{low}$ thereby only differing from T2 cells in their lower expression of IgM [30]. It has therefore been hypothesised that these cells simply represent T2 cells on the brink of developing into mature B cells or alternatively, B cells targeted for deletion or anergy. In support of the latter, Merrell *et al* defined this T3 population as an antigen-induced unresponsive population in a transgenic BCR model and consistent with this, also found a high percentage of self-reactive cells to be present in the T3 population of non-transgenic mice [31].

The survival of T2 cells and mature B cells depends on multiple factors, the major being BCR and B cell activating factor (BAFF) signalling. Many molecules involved in BCR signalling, such as Syk, BLNK (B cell linker protein, also known as SLP-65), Btk and NF-κB (Nuclear factor- κB) signalling have been found to be necessary for the survival of T2 and mature peripheral B cells indicating that BCR signalling initiates signals needed for the developmental progression or survival of these cells [32]. In recent years, the importance of BAFF in the survival and development of B cells has become clear as loss of BAFF signalling was shown to lead to loss of mature and T2 B cells [33]. There appears to be crosstalk between BCR AND BAFF receptor signalling as BCR signalling was shown to upregulate BAFF receptor expression [34] and BCR and BAFF receptor signalling appears to be integrated at the level of NF-κB regulation. For example, BCR signalling provides optimal levels of p100 NF-κB which are then processed downstream of BAFF receptor

signalling stimulating survival [35]. Thus, transitional B cells which are not or only weakly self-reactive and able to induce BCR and BAFF receptor signalling progress to the next developmental stage, mature naïve B cells [36].

Antigen ligation of the BCR on mature B cells leads to activation, proliferation and differentiation rather than cell cycle arrest or apoptosis as seen with immature cells. Nevertheless, antigen has to be recognised in the right environment as the full development into an activated effector B cell generally depends on the presence of T_H cells, their cytokines or other activation signals like TLR (Toll-like receptor) ligands [37]. Indeed, a mature B cell has three main developmental possibilities after activation – becoming an antibody secreting plasma cell, a memory B cell or participating in the germinal centre (GC) reaction. In a T cell-dependent response, the initial antibody production is due to the rapid extrafollicular proliferative focus response [38]. The first step in this response is the acquisition of antigen by B cells in the blood or in lymph nodes while they are re-circulating [39]. B cells encountering antigen in the blood will migrate to the T cell zone of the spleen [39] where antigen-stimulated B cells will interact with primed T cells resulting in entry into the cell cycle as well as commitment to the plasma cell programme induced by the upregulation of B lymphocyte induced maturation protein-1 (Blimp-1; reviewed in [40]). Moreover, such antigen-activated B cells form extrafollicular foci where they can further differentiate into, often short-lived, plasma cells and secret antibodies. Notably, during this type of response, B cells do not undergo somatic hypermutation [41].

Alternatively, B cells that do not develop into such plasma cells can enter primary follicles where they initiate the GC reaction and undergo somatic hypermutation with the help of follicular T_H and dendritic cells [42]. The major objective of somatic hypermutation is the selection of B cells with higher affinity for their antigen. Why some B cells enter the plasma cell development pathway directly rather than take part in the GC reaction remains to be elucidated. However, a recent publication by Paus and colleagues [43] indicates that the affinity of the B cell determines whether it takes part in the GC reaction or not. For example, by testing various antigen concentrations and densities in a transgenic mouse model they found that high affinity clones are preferentially recruited into the extrafollicular reaction whilst intermediate and low affinity B cells are more likely to enter the GC reaction where they have the chance to increase their binding affinity, and hence, positive selection.

The GC reaction starts around day 4-5 after antigen encounter: activated B cells first migrate into the dark zone of the germinal centre where they keep proliferating, lose surface Ig expression and start somatic hypermutation (centroblasts) (Fig.1.6). After

having mutated their Ig CDRs, the cells stop dividing (centrocytes) and express their new receptor. The migration between light and dark zone is regulated by a chemokine gradient and differential expression of chemokine receptors on centroblasts and centrocytes. For example, centroblasts express CXCR4 and follow the CXCL12 gradient towards the light zone, whereas centrocytes express CXCR5 which makes them responsive to CXCL13 expressed in the dark zone thereby allowing shuttling of cells between the dark and light zone [44]. Only centrocytes with high affinity receptors are selected and allowed to survive. The major criteria influencing the decision between survival and death of B cells in the germinal centre include the affinity of the mutated BCR as well as costimulatory signals received. Thus, expression of CD40 has been shown to be crucial during GC reactions, as lack of this molecule or its ligand abrogates GC formation [45]. CD40 ligand (CD154) is expressed not only on activated T cells taking part in the GC reaction, but also by B cells themselves [46] with interaction of CD40 and its ligand resulting in survival and cell cycle progression of GC B cells [47]. As GC B cells are by default prone to apoptosis due to a changed balance of anti- and pro-apoptotic Bcl-2-family members and other regulators of apoptosis such as Fas and p53 [48,49], the lack of positive signals such as CD40 ligation will otherwise lead to cell death. Changes in transcription factor expression are also very important for determining B cell selection and plasma cell development. Indeed, Bcl-6 expression has been found to be essential for the formation of germinal centres and GC B cells [50] due to its' repression of Blimp-1, the major regulator of plasma cell induction. Cells positively selected during the GC reaction then either develop into plasma cells or memory cells. The mechanisms underlying the decision between these two options have not been fully elucidated yet, but there is evidence that expression of a high affinity BCR skews towards selection into the plasma cell pool [51], whereas memory B cell selection might be a more random process as indicated by the constant recruitment of B cells into the memory B cell pool during the GC reaction [52].

Development of plasma cells is highly regulated, especially at the transcriptional level. In order for B cells to develop into plasma cells, Pax5 needs to be downregulated [53] and Blimp-1 expression induced [54] leading to cell cycle arrest due to c-Myc downregulation [55] and induction of the immunoglobulin secretory programme [56]. Blimp-1 itself can be upregulated by multiple signals including cytokines, such as IL-21 [57], and TLR ligation and more effectively if these signals are combined with BCR ligation [58]. Moreover, cells that have been selected into the plasma cell pool are then allowed to leave the GC reaction by way of Blimp-1 induced downregulation of CXCR5 expression [56] and upregulation of CXCR4 and CXCR3 resulting in the migration of these cells to the bone marrow or sites of inflammation [59]. Plasma cells migrating to the bone marrow can

become part of the long-lived (> 1 year) plasma cell compartment creating a source of long-lasting antibody production [60]. By contrast, the other fate of post-GC cells is to become memory cells which are important for the secondary response to repeated encounter with the same pathogen. These cells express high affinity antigen receptors and can rapidly develop into plasma cells ensuring a fast response if the same pathogen infects the organism again [61].

Besides follicular B cells, B-1 cells and MZ B cells can also develop into antibody producing plasma cells upon antigen-stimulation, usually providing a quicker response than follicular B cells due to the lack of time-consuming selection and mutation processes seen in GC reactions [40]. The exact mechanisms leading to development of marginal zone and B-1 B cells are not fully elucidated yet, but there has recently been a plethora of studies using multiple systems to further dissect these developmental pathways. A major contribution to the field has come from Montecino-Rodriguez and co-workers who showed the existence of a B-1 B cell specific progenitor which can be found in foetal and adult bone marrow [62] (Fig.1.7). These cells are lineage (lin)-negative (negative for markers expressed on macrophages, granulocytes, natural killer cells and T cells, as well as IgM^+ B cells) and further defined by the expression of CD19, AA4.1 and the lack or low levels of CD45R. Reconstitution experiments showed that they preferentially develop into B-1 B cells. This strengthens the hypothesis of two different lineages developing seperately into B-1 and B-2 B cells, a theory that has its origin in studies showing that foetal-derived progenitors preferably reconstitute the B-1 B cell compartment whereas adult bone marrow progenitors are more efficient at reconstitution of the B-2 B cell pool [63,64] which could be explained by the higher percentage of $CD19^+CD45R^{-/low}$ B-1 B cell progenitors in the foetal compartment. Further confirmation of the above-mentioned studies has come from Tung *et al* [65] using CD138 and MHC II as additional markers to distinguish between the different developmental progenitors. Thus, according to their classification $CD138^-$, $CD138^{int}$, and $CD138^{hi}$, respectively, CD138 provided a further marker to differentiate the progenitors for B-1a, B-1b, and B-2 cells. By contrast, follicular and MZ B cells are thought to derive from the same bone marrow derived precursor [66], diverging into two different populations after the T2 stage of development, thus splenocytes defined by $B220^+AA4.1^{low}CD21/35^{high}$ $CD23^+$ expression are thought to be MZ B cell precursors [67].

An alternative hypothesis which was favoured before distinct B-1 B cell progenitors had been discovered, proposed one common progenitor for both B-1 and B-2 B cells and explained the development of separate lineages by differences in antigen-dependent BCR-signalling. Thus, after encountering certain B-1 B cell-specific antigens, B-2 B cells were found to develop a B-1 B cell phenotype [68]. Due to the discovery of specific progenitors,

this hypothesis has now been questioned but the general idea that varying strength of BCR-antigen interaction influences the development of different B cell subsets still holds true suggesting that despite the existence of distinct lineage progenitors, there may be plasticity in development. For example, it has been shown that development of B-2 follicular B cells, MZ or B-1 B cells can depend on the BCR-antigen binding specificity and affinity [69]. Thus, in general, in the preferred model, weak BCR-antigen interactions are thought to lead to MZ B cell development whereas intermediate and strong interactions would lead to follicular and B-1 B cell development, respectively (reviewed in [70]). Besides BCR-antigen affinity, BCR specificity seems to be important in the B cell selection process as shown by preferential selection of weakly autoreactive specificities into the B-1 and MZ B cell pool [70].

1.3 B cell tolerance

The development and maturation of lymphocytes is tightly regulated to ensure tolerance against self with B and T cells having to pass through a process called negative selection during their early development. In the case of B cells this happens in the bone marrow at the immature B cell stage as a high percentage, up to 75% [71], of early immature B cells express BCRs that are polyreactive or self-reactive with high affinity. Immature B cells and newly emigrated transitional B cells (see also section 1.2) therefore need to react to antigenic stimulation in a different way from mature B cells. Thus cross-linking of the BCR on immature, but not mature, B cells leads to induction of either anergy or apoptosis. Anergy is a state of unresponsiveness in which B cells receiving constant signalling through the BCR lose the ability to be activated by antigenic stimulation. Some of the features defining anergic B cells include a reduced lifespan and an impaired ability to interact with T cells [72]. Anergy therefore silences potentially harmful autoreactive B cells preventing their activation.

However, some self-reactive cells manage to evade negative selection in the bone marrow (central tolerance) which has made it necessary for the immune system to evolve further checkpoints in the periphery to deal with lower affinity autoreactive B cells (Fig.1.8). The mechanisms of peripheral tolerance include induction of anergy [72], downregulation of B cell responses by inhibitory receptors such as FcγRIIb [73] and exclusion of autoreactive clones from GC reactions [74]. Moreover, the dependence of the majority of B cells on a second (T cell-dependent) signal to get activated upon antigen encounter ensures that autoreactive B cells generally do not get activated in the periphery. Thus, if a

naïve mature B cell binds its antigen without further cognate T cell help (CD40 engagement or cytokine help) it will be rendered unresponsive or undergo apoptosis.

In people with autoimmune disease one or more of the tolerance checkpoints mentioned above may be disturbed. For example, it has been shown that exclusion of autoreactive clones from the GC reaction is faulty in Systemic lupus erythematosus (SLE) patients [75]. Furthermore, analysis of the self- and poly-reactive antibody repertoire in SLE and Rheumatoid arthritis (RA) patients indicated the disturbance of various checkpoints in peripheral B cell development, allowing a higher percentage of self-reactive clones to escape from selection compared to healthy controls [76]. The implications of defects in B cell selection in autoimmune disease will be further discussed in Chapter 4.

1.4 Effector functions of B cells

Recently, evidence has accumulated that B cells do not only act as antibody-secreting cells. For example, they are effective secondary antigen presenting cells (APC) [77] due to their efficient antigen uptake following BCR internalisation. In addition, they can also act as effector B cells producing cytokines or indeed, as regulatory cells dampening ongoing immune responses. B effector cells were originally thought only to originate from follicular B cells rather than B-1 or MZ B cells [78] as the first reports indicating the importance of B cell-produced cytokines came from studies showing that development of follicles depends on lymphotoxin-α produced by B cells [79]. Similar to T_H cells, effector B cells can be divided into two subsets, Be-1 and Be-2 B cells: thus, Be-1 cells are induced by T_H1 cells resulting in IL-12 and IFNγ production by those B cells [80] whereas Be-2 B cells develop in a T_H2 specific milieu further inducing IL-13 and IL-4 production [80,81]. Cytokines produced by these activated Be-1 and Be-2 cells can then in turn influence the immune response by further skewing T_H cell differentiation towards expansion of T_H1 or T_H2 cells.

The third functional subset of B effector cells are regulatory B cells (reviewed in [82]). Thus, B cells have been shown to be able to regulate auto-inflammatory diseases such as inflammatory bowel disease, EAE (Experimental autoimmune encephalomyelitis), and disease models of SLE and RA [82,83]. The regulatory function of these cells in the above-mentioned studies appears to be IL-10 dependent, but further studies have shown that TFGβ-producing B cells might be able to carry out regulatory functions as well [84]. Regulatory B cells cannot be detected in normal healthy individuals as they are only induced upon inflammation and need an inflammatory environment for their development [82]. In addition to IL-10 production, such regulatory B cells might have other properties

such as the ability to downregulate ongoing T cell responses or recruit T regulatory cells via their Ag-presenting capacity. Moreover, antibodies produced by such B cells might help clear apoptotic bodies containing potentially dangerous auto-antigens or regulate dendritic cells through engagement of various Fc receptors such as the inhibitory receptor FcγRIIb [85]. The origin of regulatory B cells is still controversial as all three B cell subsets are capable of producing IL-10, with B-1 and MZ B cells being the major producers of this cytokine. This led to the hypothesis that most regulatory B cells originate from B-1 or MZ B cells and transfer studies have confirmed the existence of regulatory B cells in these subsets [86,87]. Furthermore, multiple studies have recently defined B regulatory cells which share features with MZ or MZ-precursor cells [86]. Nevertheless, there is evidence that B regulatory cells might also originate from B-2 follicular B cells, as indicated by their production of IgG and IgA by these cells rather than the B-1/MZ B cell-associated IgM [82].

1.5 B cell signalling

The Ig component of the BCR is not able to signal *per se* but rather signals through its' accessory transducing molecules, Igα and Igβ. These proteins both contain ITAMs (immunoreceptor tyrosine-based activation motif) which confer their signalling ability [88]. ITAMs comprise an 15-20 amino acid long motif that is defined by two YxxL sequences flanking seven to twelve variable residues ($YxxLx_{(7-12)}YxxL$). Upon receptor stimulation, members of the Src-family of non-receptor PTKs (protein tyrosine kinases) become activated enabling them to phosphorylate the tyrosines in the ITAMs [89]. Thus, PTKs like Lyn are normally associated with the BCR in an inactive form and unfold upon BCR stimulation to adopt their active conformation. Once activated they phosphorylate the ITAM [90] which enables it to bind SH2 (Src homology 2) domain-containing proteins like Lyn itself, Syk, Btk, PLCγ (Phospholipase Cγ), BLNK, Grb2 and Vav all of which play important roles in various downstream signalling cascades. Moreover, the number of docking sites for SH2 containing transducers is further increased by phosphorylation of adaptor proteins like BLNK by Syk.

B cells can react in various ways to BCR ligation including proliferation, growth arrest, apoptosis and differentiation depending on their maturation status, costimulatory or regulatory signals, signal strength and duration. It is therefore no surprise that the signal cascades activated by BCR ligation are complex involving crosstalk between pathways and differential recruitment of component isoforms. Nevertheless, the three major pathways associated with BCR signalling in mature B cells are the PI3 kinase

(phosphoinositide-3-kinase), PLCγ and MAP (mitogen-activated protein) kinase pathways [91] (Fig.1.9).

1.5.1 PI3 kinase pathway

PI3 kinases catalyse the phosphorylation of the inositol lipids like PI, PI-(4)-P and PI-(4,5)-P_2 to produce PI-(3)-P, PI-(3,4)-P_2 and PI-(3,4,5)-P_3 (PIP_3), respectively [92], molecules which are normally present in the cell at very low levels and are able to recruit SH2 and PH (pleckstrin homology) domain-containing proteins to the membrane where they can be activated. PLCγ, Btk, Vav, PDK1/2 (3′-phosphoinositide-dependent protein kinase) and Akt are a few such signalling proteins that can bind to PI-(3,4)-P_2 and PI-(3,4,5)-P_3 via their SH2 or PH domains [93-96]. PI3 kinases can be divided into four subclasses: IA, IB, II and III [97]. Of those four, only class IA and IB enzymes were found to be able to produce PI-(3,4,5)-P_3. Class IA PI3 kinases are made up of a catalytic (p110α, p110β or p110δ) and a regulatory subunit (p85α, p55α, p50α, p85β, p55γ) and the various isoforms of the regulatory and catalytic subunits can bind to each other interchangeably creating multiple different combinations. The binding to tyrosine-phosphorylated motifs on receptors such as the BCR is mediated by two SH2 domains located in the regulatory subunit [98]. Some of the isoforms of the regulatory subunits contain further domains such as SH3 and breakpoint cluster region homology (BH) domains, the latter of which is responsible for the interaction of PI3 kinase with members of the Rac and Cdc42 subfamilies [97]. The second class of PI3 kinases able to produce PI-(3,4,5)-P_3, IB, so far only consists of one family member PI3 Kγ, composed of the catalytic p110γ and the regulatory p101 subunits. PI3 Kγ appears to be mainly activated downstream of G-protein coupled receptors (GPRC) such as chemokine receptors [97]. Expression of the p110γ and p110δ subunits is mainly restricted to lymphocytes whereas the other class I subunits are ubiquitously expressed. The function of class II and III PI3 kinases is not as well studied as the class I molecules, but it has been shown that they are involved in vesicular trafficking [97]. PI3 kinase inhibitors wortmannin and LY294004 have been useful tools in defining the role of PI3 kinase in specific cellular processes [97], however, these inhibitors are not isoform-specific and therefore other tools, such as using gene targeting in mice, have had to be used to dissect the importance of specific PI3 kinase isoforms.

For example, with respect to the regulatory subunits, deletion of p85β indicated a negative regulatory role for this isoform in T cell expansion, as $p85\beta^{-/-}$ cells showed increased levels of proliferation and were less susceptible to cell death due to CD3 and IL-2 stimulation [99]. Furthermore, p85β appears to be involved in CD28 signalling in T cells

as shown by reduced c-Cbl and Cbl-b downregulation and defective T cell differentiation and induction of secondary immune responses in p85β-deficient mice [100]. By contrast, in insulin signalling depletion of p85α was found to increase PI3 kinase dependent responses [97]. Moreover, p85α was found to be involved in regulating separation of the cytosol during fibroblast cytokinesis by way of influencing Cdc42 and septin-2 activation and localisation, respectively [101]. Interestingly, this latter function of p85α seems to be independent of PI3 kinase activity further increasing the complexity of PI3 kinase signalling by showing that regulatory subunits can influence signalling in the absence of dimerisation with a catalytic subunit [101]. The above mentioned studies have to be interpreted carefully though, as the effects of p85 deletion are complicated by the role the p85 subunits appear to play in the stabilisation of the p110 catalytic subunits [97].

Similarly, there are many studies analysing the effect of genetic deletion or mutation of the catalytic subunits. Thus, by introducing an inactivating mutation, the p110δ isoform has been shown to be involved in many different cellular processes. For example, p110δ was shown to be needed for T_H1 and T_H2 cell cytokine secretion [102], differentiation of T_H1 and T_H2 cells *in vitro* as well as clonal expansion and differentiation of T cells *in vivo* [103]. Furthermore, $CD4^+CD25^+Foxp3^+$ Treg activity was found to be reduced due to lack of p110δ [104]. Another catalytic subunit, p110γ, also seems to play an important role in the regulation of T cell responses but in this case, p110γ-deficient CD4 and CD8 T cells displayed reduced ability to migrate to sites of inflammation in the periphery *in vivo* [105,106]. Moreover, during T cell development, deficiency of p110γ leads to a partial defect in pre-TCR-dependent differentiation inducing a change in the CD4/CD8 T cell ratio [107]. T cells are not the only subset of immune cells in which PI3 kinase signalling plays an important role. For example, the third catalytic subunit, p110β, seems to play a role in macrophage signalling. Indeed, deletion of p110β in RAW 264.7 cells increased LPS-stimulated inducible nitric oxide (NO) synthase as well as IL-12 expression indicating its negative regulatory role in TLR-induced activation of these processes [108]. In addition, it was shown to be required for Fcγ receptor-mediated phagocytosis by primary macrophages [109]. Further studies in macrophages showed that p110β, contrary to what was thought to that point, can be coupled to GPCR (stromal cell-derived factor, sphingosine-1-phosphate and lysophosphatidic acid ligand/receptor interactions) as well as tyrosine kinase signalling. Hence, p110β might allow GPCR-linked PI3 kinase signalling in cell populations with little or no p110γ expression, the subunit normally activated by GPCR signalling [110].

1.5.1.1 PI3 kinases & B cell responses

A number of studies dissecting the role of specific subunits of the PI3 kinase family have underscored the importance of this signalling cascade in B cell responses. To analyse the effects of the lack of all three p85α isoforms (p85α, p55α and p50α) triple-knockout mice deficient for all three isoforms of p85α were created. However, due to the premature death of these animals, chimeric RAG-2-deficient mice had to be created to study the full impact of deletion of all these regulatory subunits. The lack of all three p85α isoforms led to a reduction in peripheral mature B cells and serum antibody levels. Furthermore, the surviving B cells showed reduced responsiveness to BCR or CD40 stimulation as well as modulated survival responses upon IL-4 treatment [111]. Similarly, mice deficient for p85α, but still expressing the short p85α isoforms p55α and p50α, were found to suffer from a severe reduction of transitional and mature follicular, MZ as well as $CD5^+$ peritoneal B cells indicating that p85α is involved in the differentiation of all these subsets. Indeed, in p85α-deficient mice, B cell development was found to be arrested at the pro-B cell stage. Moreover, the proliferative and T-independent antibody production responses of the residual B cells were inhibited [112] suggesting that lack of p85α expression can not be compensated for by its shorter isoforms p55α and p50α.

Consistent with these findings, the catalytic p110δ subunit seems to be especially important in B cell biology as p110δ-deficient animals were also found to display a reduction of follicular B cell numbers, due to a block in pro-B cell differentiation, as well as a lack of B-1 B cells. As with the regulatory mutants, the remainder of peripheral B cells in these p110δ deficient mice are characterised by reduced BCR-mediated Ca^{2+} signalling and proliferative capacity and *in vivo* the germinal centre reaction and responses to both T-dependent and T-independent antigens are severely compromised [113]. Moreover, expression of a dominant negative catalytically inactive form of p110δ leads to impaired B and T cell responses due to reduced antigen receptor signalling [114]. It was proposed that besides the primary effects of lack of p110δ on T cell signalling, such T cell responses might be downregulated due to a defect of B cell-mediated antigen presentation. Indeed, although B cells expressing the inactive form of p110δ were as effective at BCR-mediated antigen uptake as the wild-type (WT) cells, the mutant cells did show a marked defect in their ability to stimulate T cells. Thus, p110δ B cells presented lower levels of antigenic peptide-MHCII complexes on their surface leading to impaired F-actin polarisation at the T cell-interaction site and thereby hampering the effective interaction of B and T cells [115]. Further studies also showed that lack of p110δ diminishes chemotactic responses of B cells, particularly those to CXCL13, thereby reducing the migration to Peyer's patches and splenic white pulp cords [116]. Altered migration of B cells could therefore also influence

immune responses by inhibiting correct homing of cells to inflammatory sites or sites of B and T cell interaction important for initiation of an effective response.

1.5.1.2 PI3 kinases & B cell signalling

BCR ligation rapidly triggers PI3 kinase activation [97]. Multiple studies have indicated that Syk is important in such BCR-mediated activation of PI3 kinase in that this tyrosine kinase phosphorylates CD19 and the adaptor protein B-cell PI3 kinase adaptor (BCAP) on tyrosine in the right context for PI3 kinase binding [98]. In addition, another Syk-dependent mechanism of PI3 kinase activation involves the phosphorylation of Cbl and the downstream recruitment and activation of PI3 kinase due to a Cbl-induced conformational change of the p85 subunit [117]. However, PI3 kinases IA and IB can also be activated by Ras, potentially via allosteric modulation or reorientation of the PI3 kinase [118] and another Syk-independent mechanism for the activation of PI3 kinase might involve Vav3-dependent activation of Rac1 which in turn increases the activity of PI3 kinase [119].

One of the major downstream effectors of PI3 kinase signalling in B cells is Btk which can be recruited to the plasma membrane via its' PH domain by PI-(3,4,5)-P_3 produced by PI3 kinase (Fig.1.9). Activation of Btk is achieved by autophosphorylation of two regulatory tyrosines as well as phosphorylation by Lyn [120,121] and this is dependent on p110δ activity as p110δ-deficient B cells display reduced phosphorylation of Btk [122]. Recruitment of Btk is important for the induction of the PLCγ2 signalling pathway which in turn leads to production of Inositol-(1,4,5)-triphosphate (IP_3) and diacylglycerol (DAG) and consequent Ca^{2+} and protein kinase C (PKC) signalling. PI-(3,4,5)-P_3 produced by PI3 kinase plays additional roles in the activation of PLCγ2 by mediating its translocation to the membrane and thereby into close proximity to Btk, as well as ehancing PLCγ2 activity in an SH2 domain-dependent fashion [123,124]. Consistent with these findings, p110δ-deficient B cells displayed impaired IP_3 production, emphasising the importance of PI3 kinase in maximal PLCγ2 activation [122].

The other major downstream outcome of PI3 kinase signalling in B cells is activation of PKB (protein kinase B)/Akt which predominantly acts to promote cell survival. The initial step in this cascade is the recruitment of PDK1 to the membrane via its PH domain [95]. The exact mechanism for activation of PDK1 is not known, but autophosphorylation is the most likely event. PDK1 is needed for the phosphorylation of PKB/Akt on threonine 308 [125]. However, phosphorylation at this single residue is not sufficient for full activation as further phosphorylation on serine 473 was shown to be crucial for optimal PKB/Akt activity. The enzyme carrying out this modification has not been identified yet, but there are some

candidates such as mTOR (mammalian target of rapamycin), ILK (integrin-linked kinase) or even PKB/Akt itself by autophosphorylation [126].

Although fully activated PKB/Akt transduces several cellular responses, the major functional outcome is enhancement of survival. For example, PKB/Akt inhibits activation of the executioner apoptotic protease caspase 9 and regulates forkhead-related transcription factors [127]. These transcription factors are involved in the regulation of many genes associated with cell survival such that by regulating forkhead-related transcription factors, PKB/Akt is therefore able to suppress expression of Bim and Puma, two pro-apoptotic BH3-only proteins [126]. Moreover, PKB/Akt can phosphorylate the pro-apoptotic Bad at serine 136 initiating Bad's association with 14-3-3 proteins and thereby its' sequestration from the mitochondria and inactivation. Another pro-apoptotic Bcl-2-family member regulated by PKB/Akt is Bax which gets phosphorylated at an inhibitory site by PKB/Akt [128]. PKB/Akt does not only inhibit pro-apoptotic mechanisms as it also upregulates pathways inducing expression of survival factors such as the NF-κB pathway. For example, PKB/Akt activates IKKα, one of the kinases that phosphorylate IκB thereby leading to the targeting of IκB for degradation [129] and releasing the suppression of NF-κB which in turn is then able to upregulate the expression of Bcl-x_L, a pro-survival member of the Bcl-2-family. Moreover, recruitment of PKCζ to the plasma membrane via its PH domain is potentially another mechanism linking PI3 kinase, via creation of PH domain docking sites, to B cell survival via activation of NF-κB. Once recruited to the membrane PKCζ gets activated by Ras [130] allowing it to phosphorylate NF-κB thereby enhancing its transcriptional activity [131].

1.5.2 PLCγ pathway

PLCγ is recruited to the BCR by phosphorylated BLNK bringing it into close proximity with Btk and Syk leading to its phosphorylation and activation and subsequent downstream signalling [132]. Translocation of PLCγ to the plasma membrane is also required to bring it into close proximity to its substrate PI-(4,5)-P_2 which it converts to the important second messengers diacylglycerol (DAG) and Inositol-(1,4,5)-triphosphate (IP_3). IP_3 binds to IP_3-receptors on the endoplasmic reticulum leading to release of intracellular calcium followed by entry of extracellular calcium [132] thereby activating calcium sensitive molecules such as calcineurin, protein kinase C isoforms (the conventional isoforms α, β, γ) as well as JNK (c-Jun NH_2-terminal kinase) [133]. IP_3 binding to its receptors on the endoplasmic reticulum can further affect the localisation of molecules like Bcl-2 [134] and the activation of enzymes like PLA_2 [135], calpain [136] and protein kinase II. Likewise,

DAG is needed for the activation of all phorbol ester-sensitive isoforms of PKCs (α, β, γ, δ, ε, η, θ) [137] (Fig.1.9).

Thus, the family of PKC enzymes represent the major downstream effectors activated by PLCγ signalling. PKCs have been shown to play diverse roles in B cells ranging from the induction of proliferation to initiation of apoptosis, depending on the specific isoform and the developmental stage of the B cell involved. As indicated above, PKCs are dividided into three subtypes – the classical PKCs (α, β1, β2, γ), the novel PKCs (δ, ε, η, θ) and the atypical PKCs (ξ, λ, τ). The classical PKCs depend on Ca^{2+} as well as DAG for their activation whereas novel PKCs are regulated by DAG and the atypical PKCs need neither Ca^{2+} nor DAG for their activation [137]. B cells express many of these PKC isoforms (α, β, δ, ε, η, ξ, λ) and all of these have been shown to be recruited and activated downstream of BCR-ligation [138]. Due to the availability of isoform-specific PKC-deficient animals the importance of the different isoforms has been addressed, but PKCβ and PKCδ are the best-studied PKC isoforms in B cells. Thus, analysis of PKCβ knock-out animals indicated that this isoform is important in B cell responses as such mice displayed reduced numbers of B cells in the periphery, a complete lack of B-1 B cells and reduced antibody responses [139]. The defect in PKCβ knock-out B cells has been identified as an inability to activate NF-κB signalling downstream of the BCR, consistent with findings that NF-κB is a crucial transcription factor involved in the activation of genes involved in survival and activation of B cells by e.g. increasing the expression of anti-apoptotic molecules like Bcl-x_L and Bcl-2 [131,140]. The reduction of NF-κB activation in PKCβ-deficient B cells is due to the requirement of PKCβ for the efficient recruitment of IKK to the plasma membrane. As mentioned before, IKKβ activation is needed for the phosphorylation-mediated degradation of IκB and consequential release of NF-κB. The exact mechanism of how PKCβ-mediated localisation of IKKβ to the plasma membrane initiates its phophorylation is not known yet, but recent findings have implicated BCL10, MALT1 and Carma1 in the connection of PKC and NF-κB signalling, making them interesting candidates [138]. Unlike PKCβ, the novel PKC isoform PKCδ does not appear to transduce activatory signals downstream of the BCR, but rather, it appears to be an important mediator of negative regulation of B cells, as indicated by hyper B cell expansion and progressive development of an autoimmune phenotype in PKCδ deficient mice [141]. This autoimmune phenotype seems to be caused by a severe impairment of peripheral tolerance in these mice [141]. Although, the functional effectors of PKCδ in B cell signalling responsible for this phenotype have not yet been elucidated, modulation of NF-κB does not appear to be involved. By contrast, it has been proposed that negative regulation of IL-6 by PKCδ-mediated mechanisms may be responsible for this phenotype [138] as IL-6 is an important

B cell differentiation factor supporting the germinal center reaction and development of isotype-switched B cell clones [142]. Changes of IL-6 expression due to lack of inhibition by PKCδ could therefore induce de-regulated B cell differentiation and expansion.

1.5.3 The MAP kinase (MAPK) pathway

MAP kinase (mitogen activated protein kinase) is the generic term for a family of serine-threonine protein kinases which can be subdivided into three distinct groups. The ErkMAP kinases (extracellular signal-regulated kinase), the c-Jun N-terminal kinases (JNK) and the p38 MAP kinases all play roles in B cell signalling (reviewed in [143]). Generally, ERK MAPKs have been classified as being activated by growth factor stimulation, whereas JNK and p38 are considered to be responsive to stress stimuli such as osmotic shock and radiation as well as cytokines [144]. Nevertheless, all of the MAPKs get activated by phosphorylation of their tyrosine/threonine activation motif, which differs between the subfamilies. For example, ERK1/2 share a TEY motif in their activation loop whereas the JNK and p38 family of MAP kinases are activated upon phosphorylation of their TPY or TGY motif, respectively. This phosphorylation is carried out by specific tyrosine-threonine kinases called MAPKK (MAPK kinase) or MEK which themselves are activated by a family of serine-threonine kinases generically termed MAPKKK (MAPK kinase kinase) or MEKK. Upstream activation of GTPases (guanine triphosphatases) like Ras or Rap-1, which are able to activate MAPKKK, in this way initiates the appropriate MAPK pathways (Fig.1.10). Another family of GTPases involved in MAPK activation are the Rho-GTPases (e.g. Rac, RhoA, Cdc42). The guanine nucleotide exchange factor (GEF) for those GTPases is Vav which can be recruited to the BCR by BLNK [145]. Rac1 and Cdc42 have been shown to be involved in MAPK activation, especially the JNK and p38 pathways [146] by activating MEKK-1, MEK4 and MEK7 [147]. Once activated, the three sub-classes of MAPKs can phosphorylate various different substrates including phospholipases, cytoskeletal proteins and transcription factors as well as the MK (MAPK activated protein kinases) family of proteins (formerly known as MAPKAP kinases) [143].

1.5.3.1 The ERK1/ERK2 MAP kinase pathway

ERK1/2 are ubiquitiously expressed at varying levels in different tissues and cells, with multiple stimuli activating the ERK1/2 cascade such as serum, growth factors, cytokines, stress as well as some ligands for G protein-coupled receptors (GPCRs) [144]. Initiation of signalling by these stimuli leads to activation of small GTP-binding proteins such as Ras or Rap followed by activation of ERK1/2-specific MAPKKK, such as various Raf isoforms, Mos, MEKK1-3 and Tpl-2 [148]. Thus, following BCR ligation, ERK can be

activated in a Ras and Raf-1-dependent manner. Firstly, the adaptor transducer, Shc is recruited to the phosphorylated ITAMs of Igα/Igβ where upon Syk-mediated phosphorylation, Shc is able to recruit Grb2-Sos complexes [149] (Fig.1.9). Sos is a GEF which catalyses the exchange of GDP for GTP on Ras leading to its activation. Similarly, BLNK is another adaptor protein that is able to recruit the Grb2-Sos complex therefore representing an additional pathway of Ras activation other than via Shc recruitment [150]. The next step in the signalling cascade is the derepression of Raf by activated Ras thereby inducing its kinase activity [151]. The targets of Raf, and other ERK1/2 specific-MAPKKKs, are MEK1 and 2 [152,153], dual-specific threonine/tyrosine kinases, which are in turn activated by phosphorylation of two serine or threonine residues in their activation loop [148]. MEK1/2 then activates ERK1/2 by phosphorylation of the TEY motif thereby allowing ERK1/2 to phosphorylate and activate its relevant downstream targets which have been shown to include signal transducers such as protein kinases like RSK1-3 (90 kD ribosomal S6 kinase), MAPKAPkinase-2, or MAP kinase-interacting kinase (Mnk) 1/2, membrane or cytoplasmic proteins such as cytosolic phospholipase A_2 ($cPLA_2$), Ral-GDS (Ral-guanine nucleotide dissociation stimulator) or heat shock factor transcription factor 1 (hsp1) as well as the transcription factors c-Jun, c-Fos, ATF-2 and Elk-1 (reviewed in [144]). A more in depth overview of the relevance of ERK MAP kinase signalling in B cells can be found in Chapter 3.

1.5.3.2 The p38 MAP kinase pathway

The p38 MAP kinase family consists of the four related proteins p38α, p38β, p38γ (formerly ERK6 or SAPK3) and p38δ (SAPK4). Like the other members of the MAPK family, p38 molecules are activated downstream of a kinase cascade consisting of several MAPKKKs such as MEKK1-4, MLK2/3 (mixed lineage kinase), DLK (dual leucine zipper-bearing kinase), ASK1 (activator of S-phase kinase), Tpl2 and Tak1 (TGFβ-activated kinase 1), which in turn activate MAPKK such as MEK3 and 6, as well as MEK4. MEK3 and 6 specifically activate p38 whereas MEK4 is able to phosphorylate and activate p38 and JNK [154]. Some of the known targets of p38 are $cPLA_2$, p53, the transcription factors ATF1, EF2A, Elk-1, NF-κB and Ets-1 as well as MKs such as MSK1/2 (mitogen- and stress-activated protein kinase), MNK1/2, and MK2/3 [143]. p38 plays a critical role in the regulation of immunity as exemplified by the fact that p38 is activated downstream of inflammatory mediators such as cytokines, chemokines or LPS [155]. Furthermore, it is involved in the regulation of T cell differentiation and apoptosis as well as many functional responses in macrophages and neutrophils such as respiratory burst and chemotaxis [155]. By contrast, in B cells p38 does not seem to play such an important role as the

major MAPK activated by BCR signalling appears to be ERK. Nevertheless, p38 is involved in signalling pathways initiated by the ligation of other important receptors on B cells such as CD40, IL-4 receptor or BAFF receptor. Thus, in the case of CD40 p38 activation seems to be mediated downstream by NF-κB, whereas p38 signalling via the IL-4 receptor is mediated by STAT6 (signal transducer and activator of transcription 6) [156]. IL-4 together with CD40 stimulates the proliferation of B cells and induces the expression of MHC II as well as class-switching to IgG1 and IgE [156]. Thus, p38 plays an important role in regulating in T_H2-type humoral immune responses.

1.5.3.3 The JNK MAP kinase pathway

The JNK family of proteins consists of three isoforms – JNK1, JNK2 and JNK3 however, due to alternative splicing mechanisms these three isoforms yield a total of 12 different possible JNK proteins [157]. Similarly to the above-described pathways for ERK and p38 activation, JNK is also activated by consecutive phosphorylation of upstream MAPKKKs and MAPKKs. Some of the known MAPKKKs for JNK are MEKK1-4, MLK1-3, DLK, Tpl2, ASK and Tak which phosphorylate MEK4 and MEK7 [158]. The exact mechanisms activating the MAPKKKs are not fully elucidated yet, but adaptor proteins such as Crk or TRAFs (TNF-receptor associated factor), as well as small GTP-binding proteins like Rho appear to be involved [159]. One of the major substrates of JNK is the molecule that gave it its name, c-Jun which together with c-Fos forms the active transcription factor AP-1. JNK phosphorylates c-Jun thereby increasing its activity and possibly also its stability [160,161]. Further targets of JNK include the transcription factors ATF-2, Elk-1, p53 and NFAT4 and the anti-apoptotic molecule Bcl-x_L [159]. The functional outcome of JNK activity varies depending on numerous factors such as cell type and activation of other signalling cascades. For example, JNK has been implicated in induction of apoptosis [162] as well as survival [163], depending on the cell type and context. Indeed, in the human B cell line B104 it was shown to be linked to apoptosis downstream of BCR ligation [164] whereas it was found to be activated downstream of positive signalling in naïve B cells [165]. Similarly, whilst JNK was found to be activated by apoptotic signalling via the BCR in the murine immature B cell line WEHI-231, JNK activation was more pronounced downstream of CD40-mediated rescue signal in such cells [166]. As the functional outcome of JNK activation in these experiments was not always analysed, these studies left unanswered questions about the function of JNK in B cells some of which have since been addressed by animal models using mice deficient for JNK or its upstream regulators. For example, studies using T cells from JNK-deficient mice indicated that this kinase is not necessary for effective IL-2 production or proliferation; on

the contrary, lack of JNK actually increased the levels of IL-2 and proliferation. JNK however was found to be necessary for the production of the T_H1 effector cytokine IFNγ and JNK-deficiency consequently impaired the T_H1 differentiation of T cells *in vitro* due to the lack of IFNγ-mediated suppression of T_H2 differentiating cytokines [167]. By contrast, T cells lacking MEK4, the upstream activator of JNK, but potentially also that of p38, displayed impaired proliferation upon CD28 costimulation [168]. Moreover, MEK7-deficient T and B cells showed increased proliferation downstream of growth factor or antigen-receptor stimulation [169]. These studies therefore emphasise the complexity of JNK signalling and its' multiple roles in T and B cell signalling and demonstrate the need for further investigation to reconcile the contradictory results.

1.5.4 Integration of signalling cascades

The major signalling cascades utilised by B cells downstream of the BCR are not simply activated in a linear fashion but interact at many levels, regulating each other by cross-talk. Thus, activation of Ras downstream of the BCR can activate ERK [170] and PI3 kinase signalling [171]. Interestingly, these two pathways seem to be further connected at several additional levels. For example, PI3 kinase can positively and negatively regulate the Ras/Raf cascade. Thus, PI3 kinase can potentially activate Raf through a p21-activated kinase (PAK)-dependent mechanism thereby influencing ERK activation downstream of Raf [172] whilst on the other hand PI3 kinase can inhibit ERK signalling by inducing the phosphorylation of Raf in an Akt-dependent manner [173]. Moreover, PI3 kinase itself can be negatively regulated by ERK-mediated phosphorylation of GAB1 [174], thereby potentially connecting these two pathways by a complex series of positive and negative feedback loops. In addition, PKCξ is recruited via its PH domain to the plasma membrane where it gets activated by Ras [130] and then phosphorylates NF-κB, thereby enhancing its transcriptional activity [131]. Further emphasising the link between PI3 kinase and survival, PLCγ2 is another major signalling pathway downstream of BCR-ligation and it is also connected to both the PI3 kinase and ERK cascades. Thus, it has been shown in various studies that full initiation of calcium signalling depends on PI3 kinase activity [94]. As mentioned before, this partial dependency of PLCγ2 activation on PI3 kinase is due to the recruitment of Btk to the plasma membrane by PI-(3,4,5)-P_3 via its PH domain [122]. The ERK cascade is also linked to PLCγ2 as evidenced by the finding that deletion of PLCγ2 downregulates ERK activation [175]. One potential point of signal integration between ERK and PLCγ2 could be the activation of PKCβ2 and PKCθ by PLCγ2-dependent mechanisms such as production of DAG and initiation of calcium signalling. This is because PKCβ2 and PKCθ have recently been implicated in

phosphorylation and activation of RasGRP3, a GEF for Ras. Furthermore, RasGRP3 itself can be activated by DAG-binding, challenging the typical linear model of PLCγ2 activation followed by production of DAG and activation of PKC and its downstream targets. Therefore, RasGRP3 activation, through downstream activation of Ras, potentially links DAG production, PKC activation and the ERK pathway [176].

A major integrative junction of BCR signalling lies in the regulation of transcription factors as evidenced by reports that the three major signalling pathways activated by the BCR are all involved in the regulation of various transcription factors such as Elk-1, ATF, NF-κB, NFAT and AP-1. For example, NF-κB is an important transcription factor in B cells as it regulates survival and studies using various different knock-out mice for relevant signalling molecules such as the PI3 kinase subunit p85α, Btk, BLNK, PLCγ all showed impaired activation of NF-κB indicating that optimal activation of NF-κB requires both PI3 kinase and PLCγ signalling [131,177]. Similarly, AP-1 is another important transcription factor which is regulated by more than one BCR-dependent signalling cascade. For example, AP-1 comprises a family of transcription factors consisting of dimers comprising various combinations of two subunits of the Jun, Fos and ATF family of proteins. Depending on the precise subunits, AP-1 dimers can induce various cellular responses such as proliferation or apoptosis. Thus, in B cells it was shown that both JNK and ERK are needed for AP-1 dependent transcription of miR-155, and its primary transcript, B-cell integration cluster (BIC) which is involved in B-cell maturation and antibody production in response to antigen [178,179]. Moreover, AP-1 dependent upregulation of the cyclin D levels necessary for survival and proliferation requires integrated signalling via several transcription factors in B cells. This is because c-Jun which regulates expression of cyclin D1, is itself regulated by stable Jun/Fos AP-1 dimers, which are promoted by the ability of ERK to induce Fos upregulation via activation of Elk-1 [178]. Elk-1 is a member of the Ets family of transcription factors which can be regulated by all three MAPK cascades as well as calcium signalling [180]. Thus, phosphorylation of Elk-1 by ERK, JNK or p38 leads to the activation of Elk-1 which in turn can regulate the expression of its target genes such as c-Fos [180] which is able to regulate c-Jun expression, emphasising the complexity and the multiple levels of signal integration downstream of the BCR.

1.5.5 Co-receptors on B cells

The BCR is not the only receptor regulating B cell activity. B cells express additional receptors such as CD19, CD40 and FcγRIIb which can positively or negatively influence the function and outcome of signalling by modulating signalling thresholds downstream of the BCR.

1.5.5.1 CD19

CD19 is a transmembrane glycoprotein that is expressed by B cells from the early pre-B cell stage onwards until it is downregulated upon plasma cell differentiation [181,182]. During follicular B cell development, upregulation of CD19 can be detected at the mature B cell stage and B-1 B cells generally express higher levels of CD19 relative to follicular B cells [182]. Although CD19 levels seem to be developmentally regulated they do not however seem to be influenced by activation by stimuli such as LPS, anti-IgM or IL-4 [181,183]. On the surface of B cells, CD19 can be found in a complex with CD21 and CD81 (Fig.1.11) and this complex is an important mediator of B cell activation, as CD19-deficient B cells display reduced activation upon BCR ligation. This is because the CD19/CD21(CR2)/CD81 complex binds to soluble fragments of complement proteins such as C3b and C3d which bind to pathogen surfaces. Thus, B cells expressing BCR specific for antigens of such pathogens can be activated by the simultaneous binding of antigen to the BCR and engagement of the CD19 co-receptor complex through binding of C3 fragments [184]. Thus, although development of B cells *per se* does not seem to be affected by lack of CD19, B cell proliferation, expansion and differentiation are severely compromised in CD19-deficient mice. Furthermore, the humoral response and germinal centre formation in CD19-deficient mice is reduced as well [182,185,186] due to the increased signalling threshold in the absence of CD19-signalling. Costimulation of B cells by BCR and CD19 due to the presence of complement-targeted pathogens therefore provides a mechanism for enhancing B cell responses.

Signalling downstream of CD19 is initiated by Lyn-mediated phosphorylation of tyrosines in its' cytoplamic tail which creates SH2 binding sites allowing the recruitment and activation of various signalling molecules [187] such as Lyn (and other phosphotyrosine kinases), the GEF protein Vav as well as the PI3 kinase regulatory subunit p85. CD19 activation thereby amplifies the signalling initiated by BCR by enhancing activation of PLCγ2 by PTKs [187], the PI3 kinase pathway by localising p85 to the membrane [188] and recruitment of Vav [189] to potentially activate MAPK pathways via Rac1 or Cdc42. Moreover, such Vav-dependent activation of Rho can also stimulate phosphatidylinositol-4-phosphate-5-kinase which produces PI-(4,5)-P_2 thereby maintaining the levels of substrate required for prolonged PLCγ activation [89].

1.5.5.2 CD40

CD40 is a glycoprotein expressed not only by B cells but also by dendritic cells and monocytes as well as endothelial and epithelial cells [190]. Its ligand, CD154 (CD40L) is

mainly expressed on activated T_H cells, but it is also found on a small population of CTL cells, γδ T cells as well as mast cells, basophils and eosinophils. Furthermore, CD40L expression can be induced in B cells, NK cells, macrophages and dendritic cells under certain conditions, for example on phorbol ester/ionomycin-stimulated human B cells [190]. The important role of CD40-CD40L interaction was originally perceived due to studies in humans showing that the immune deficiency X-linked hyper-IgM syndrome can be caused by mutations in the gene encoding CD40L. Patients suffering from X-linked hyper-IgM syndrome display elevated levels of IgM in their circulation accompanied by reduced expression of class-switched isotypes such as IgG [191]. Further confirmation came from animal models with induced mutations or deletions of the CD40 or CD40L gene, showing similar deficient immune responses as seen in humans [190]. These deficiencies reflect that CD40 plays a pivotal role in B cells by activating their proliferation, differentiation and antibody production as well as rescuing B cells from apoptosis. It is involved in induction of class-switching, selection and maturation of memory cells and can regulate the differentiation of plasma cells [190].

CD40 is part of the TNF-receptor-family and signals through TRAFs. Several TRAFs (TRAF 1, 2, 3, 5 and 6) as well as JAK3 have been found to associate with CD40. Recruitment and activation of the different TRAF molecules initiates varying signalling outcomes such as activation of NF-κB, PI3 kinase, MAPKs and PLCγ2 [192] (Fig.1.12). Thus, TRAF2 is involved in activation of NF-κB [193], whereas TRAF6 links to ERK activation in both a Ras-dependent and -independent manner [194]. TRAF3, on the other hand, has been found to be important both for p38 and JNK activation downstream of CD40 in a human B cell line [195]. CD40 signalling is generally considered to be important for regulating survival and proliferation of B cells although it can transduce apoptotic signals in some human B cell lymphoma cell lines. Consistent with this, it induces the NF-κB-dependent upregulation of anti-apoptotic Bcl-2 family members such as Bcl-x_L and Bcl-2, thereby inhibiting the induction of apoptosis and actively promoting cell cycle progress by reducing the levels of the Cdk inhibitor, p27. Moreover, the expression and activation of Cdk4 (cyclin-dependent kinase) and Cdk6 are upregulated by CD40 signalling allowing cells to escape growth arrest from G1 and drive entry into S phase. c-Myc, another NF-κB-regulated protein, has also been shown to be upregulated upon CD40 ligation further supporting its role in promoting cell cycle progression [196]. Additionally, NF-κB-dependent upregulation of FLIP (FLICE-like inhibitory protein), an inhibitor of apoptosis, further strengthens the “survival” programme induced by CD40 [197].

1.5.5.3 FcγRIIb

FcγRIIb is a low affinity receptor for the Fc portion of IgG. Cross-linking the BCR and FcγRIIb inhibits BCR-mediated activation and proliferation of B cells by inhibiting BCR coupling to calcium mobilisation, Akt and MAPK activation [73]. This inhibitory mechanism, which reflects cognate immune complex-mediated co-ligation of the BCR and FcγRIIb, is widely believed to be important in the homeostatic regulation of B cell responses as it ensures that B cell responses are switched off as soon as enough antibodies to deal with the pathogen are circulating. That such FcγRIIb-mediated signalling is important in the downregulation of cognate antibody responses was finally proven with the analysis of FcγRIIb knockout mice which showed augmented antibody production in reaction to immunisation with immune complexes when compared to FcγRIIb-expressing mice [198].

FcγRIIb belongs to the family of Fcγ receptors which bind to the Fc portion of IgG. In the murine system there are four classes of Fcγ receptors: FcγRI, FcγRII, FcγRIII and FcγRIV. These different sub-classes of Fcγ differ in their binding affinities. For example, FcγRIV preferentially binds IgG2b whereas FcγRIIb has highest affinity for IgG1 [199]. FcγRI is a high affinity receptor whereas FcγRIIa and FcγRIIIa are of lower affinity and only able to bind IgG if it is present in immune complexes [199] (Table 1.1). FcγRIIb is widely expressed on cells such as macrophages, neutrophils and mast cells but it is the only Fcγ receptor expressed on murine B cells [199]. Recently, there have been studies postulating expression of FcγRIIa, an activating Fcγ receptor containing an ITAM, on the surface of peripheral human B cells and B leukemia cells [200,201]. However, as detection was carried out with antibodies against the extracellular domain, which is very similar in FcγRIIa and FcγRIIb, these proposed findings have still to be confirmed.

Whilst most other Fcγ receptors stimulate activating signals, FcγRIIb is an inhibitory receptor, both in humans and in mice. FcγRIIb comprises a single chain glycoprotein that contains an immuno-receptor tyrosine based inhibition motif (ITIM) domain, defined by the consensus sequence I/V/L/SxYxxL/V, in its cytoplasmic tail. This ITIM was shown to be indispensable for the inhibitory function of FcγRIIb, which is dependent on the phosphorylation of the ITIM-tyrosine upon BCR/FcγRIIb co-ligation. Recently however, new evidence has suggested that there is a second docking motif which might be necessary for recruitment of the 5' inositol phosphatase SHIP (SH2 domain containing inositol 5' phosphatase), the key molecule required for FcγRIIb-mediated negative signalling. This motif is located in the C-terminal region of FcγRIIb and also needs to be tyrosine-phosphorylated to be activated. This motif does not directly bind SHIP, but recruits the adapter molecules Grb2 and Grap (Grb2-like accessory protein) which help stabilise the binding between SHIP and the ITIM [202]. Human B cells also express

FcγRIIb which like the mouse homologue, recruits SHIP upon tyrosine-phosphorylation of its ITIM. Moreover, and again similar to the mouse receptor, the C-terminal region is also needed to ensure optimal SHIP phosphorylation and activation although the phospho-tyrosine-motif has not been detected in the human receptor [203].

At the proximal signalling level the co-ligation of BCR and FcγRIIb induces Lyn to tyrosine-phosphorylate the ITIM in the cytoplasmic portion of FcγRIIb (Fig.1.13). The importance of Lyn in this process is supported by studies showing that knocking-out Lyn in mice increases BCR-mediated induction of MAPK cascades and proliferation [204]. The main signal transducer recruited to the phosphorylated ITIM is SHIP and, as stated above, this was found to be indispensable for negative regulation carried out by FcγRIIb [205]. SHIP signalling affects PI3 kinase, Ras-ERK MAP kinase and calcium-dependent signalling [206,207]. For example, the downregulation of PI3 kinase activated signalling cascades by SHIP is due to its ability to convert PI-(3,4,5)-P_3 to PI-(3,4)-P_2. This counteracts PI3 kinase which produces the PI-(3,4,5)-P_3 required for many PH-domain mediated signals such as Akt [208]. Recent studies indicating that PI-(3,4)-P_2 generation could also lead to Akt activation made it very unlikely, however, that SHIP was the only mechanism for Akt deactivation. Thus, the finding that PTEN is also activated by FcγRIIb and BCR co-ligation potentially provided an additional regulatory molecule to ensure that BCR signalling is effectively abrogated [209]. This is because PTEN, which is a 3' inositol phosphatase, directly antagonises the effects of PI3 kinase by decreasing the levels of both PI-(3,4,5)-P_3 and PI-(3,4)-P_2 available for recruiting PH-domain containing signal transducers and therefore further reduces Akt activation.

The influence FcγRIIb signalling has on the mobilisation of calcium within cells is less well understood. Inositol-(1,3,4,5)-tetraphosphate (IP_4) is also a potential target for dephosphorylation by SHIP and IP_4 is known to be an activator of membrane Ca^{2+} channels [210]. Reduction of the IP_4 concentration may therefore disturb the calcium flux through these channels changing its distribution pattern in the cell [211]. Calcium is an important second messenger whose concentration determines the activation of molecules like calmodulin/calcineurin and consequently the transcription factor NFAT [212]. Alternatively, SHIP/PTEN mediated PI-(3,4,5)-P_3 degradation not only prevents Akt from associating with the membrane but also Btk and PLCγ which are required for sustained coupling of the BCR to an increase in intracellular calcium levels. This might therefore present a second mechanism by which SHIP and/or PTEN suppress calcium mobilisation after BCR/FcγRIIb co-ligation.

As illustrated above, the ERK MAP kinase pathway is a key proliferative signalling cascade initiated upon BCR activation. Upon BCR stimulation Shc and Grb2/Sos form a

complex, enabling Sos to exchange GDP for GTP on Ras, thereby activating it. Ras in consequence recruits Raf to the membrane resulting in its activation and leading to phosphorylation and activation of MEK1/2, the immediate upstream regulator of ERK1/2. SHIP directly competes for Shc binding, sequestering it from interacting with Sos/Grb2 and hence inhibiting the activation of Ras downstream signalling [213]. In addition, SHIP uses a second mechanism to decrease ERK MAPK signalling via the recruitment and activation of p62 Dok which interacts with RasGAP (Ras GTPase activating protein) to enhance the GTPase activity of Ras and render Ras inactive [214]. Additionally, BCR/FcγRIIb ligation recruits PAC-1 (phosphatase of activated cells-1), an ERK-specific dual specificity phosphatase, inducing dephosphorylation and thereby inactivation of previously activated ERK, thereby further reducing active ERK levels in the cell [209].

Interestingly, the induction of apoptosis upon FcγRIIb ligation in the absence of BCR involvement (non-cognate immune complexes) appears to induce signalling pathways independent of the ITIM sequence. Indeed, such apoptotic signals can be blocked by the recruitment of SHIP that normally occurs upon BCR/FcγRIIb colligation [215]. These ITIM-independent signaling mechanisms have been partially elucidated and shown to be dependent on the depolarisation of the mitochondrial membrane with resultant release of cytochrome C and activation of caspases 3 and 9. Moreover, under these conditions, FcγRIIb needs to be tyrosine phosphorylated to recruit two c-Abl family kinases, c-Abl and Arg, to couple to this apoptotic pathway, in an as yet to be defined manner [216]. It is thought that this ITIM/SHIP-independent pathway induced by ligation of FcγRIIb by non-cognate immune complexes, plays a role in the maintenance of peripheral tolerance. However, the *in vivo* relevance of this process, which is only seen in B cells, has yet to be elucidated.

Thus, FcγRIIb is a negative regulator of B cell responses playing an important role in downregulating ongoing immune responses after the successful removal of the pathogen. Such downregulation of the immune response is necessary to maintain the balance between the beneficial and detrimental effects of the inflammatory process and maintain B cell homeostasis.

1.6 The role of ubiquitination in cell signalling

Ubiquitin is a small molecule of only 76 amino acids, which can be attached to proteins thereby influencing their stability, localisation and function. The best characterised

function of posttranslational modification by ubiquitin is the targeting of proteins for degradation by the proteasome. In this way, ubiquitination plays a crucial role in the regulation of cell cycle progression, proliferation and signal transduction. Recently, however, it has become apparent that ubiquitination, dependent on the length of the ubiquitin chain and specific linkages between ubiquitin molecules, can influence cellular processes independently of proteasomal degradation.

1.6.1 Linking ubiquitin to target proteins

Linking ubiquitin to its target protein is a three-step process. The first step is the activation of a C-terminal glycine residue of ubiquitin. This step is carried out by an enzyme called E1 and uses up energy in the form of ATP. E1 then binds to activated ubiquitin via a thiolester linkage, releasing AMP in the process (Fig.1.14). Consequently, activated ubiquitin is transferred from E1 to an E2 ubiquitin-conjugating enzyme, the next enzyme in the cascade. This enzyme then forms a complex with an E3 ubiquitin ligase and the target protein whereby the activated ubiquitin gets transferred to an ε-amino group of a lysine of the substrate protein [217]. Depending on the E3 ligase, this last step either involves direct transfer of ubiquitin from E2 to the substrate, or transfer via E3 to the target protein [217]. The specificity of the ubiquitination system is conferred by E3 ligases, as these enzymes govern the recruitment of ubiquitin-loaded E2 enzymes to their specific target proteins [217].

Both mono- and poly-ubiquitination exist and these distinct modifications most likely control differential functional outcomes. Furthermore, several residues in proteins can be tagged by mono-ubiquitination, a process termed multi-ubiquitination [218]. Generally, poly-ubiquitination, by linkage of multiple ubiquitins via their lysine 48 residues, targets proteins for degradation by the 26S proteasome complex [219] leading to the release of peptides and re-usable ubiquitin. Linkages of ubiquitin molecules to each other on residues other than lysine 48 have been classified as atypical and have been shown to have several different functional effects. Thus, poly-ubiqutiniation via lysine 63 has been implicated in the regulation of the NF-κB pathway as well as receptor endocytosis and DNA repair [220]. The differential outcomes of the various ubiquitin-modifications is most likely due to binding of proteins containing different forms of ubiquitin binding domains (UBDs) which are thought to be able to preferentially bind to specific forms of ubiquitin linkages. Although these poly-ubiquitin chains are all made up of the same subunit, ubiquitin, the linkage seems to influence the confirmation of the chain, explaining how UBDs can distinguish between lysine 48 and lysine 63 mediated linkage [220]. Likewise, recent studies suggest an important role for the other form of ubiquitination, mono-

ubiquitination, in receptor endocytosis and histone modification [221]. Thus, Cbl has been shown to mono-ubiquitinate receptor tyrosine kinases targeting them to the lysosomal compartment and thereby regulating activation of signalling downstream of RTK dependent receptors [222]. Adding another layer of complexity to the ubiquitination system are DUBs (deubiquitinating enzymes) which can remove ubiquitin from proteins making ubiquitination a reversible process [223]. For example, in murine lymphocytes, cytokine stimulation leads to the upregulation of several DUBs indicating that these enzymes might play a role in the responses initiated by cytokine stimulation [224].

1.6.2 E3 ligases and their role in the immune system

There are many studies implicating various E3 ligases in signalling regulating the responses of immune cells such as T and B cells. Among the E3 ligases associated with the immune system, Itch and Cbl are probably the best studied. Initial interest in the E3 ligase Itch arose after the finding that Itch-deficient mice develop a late onset type of autoimmune disease [225]. More detailed anlysis of these mice indicated a role of Itch in T cell biology as Itch-deficient T cells were found to be hyperresponsive concerning proliferation and IL-2 production upon engagement of CD3. It was then found that Itch ubiquitinates JunB and c-Jun leading to their degradation and hence lack of Itch leads to increased stability of these transcription factors, production of AP-1 and consequent production of IL-2 and T cell proliferation [226]. The physiological outcome of Itch deficiency in T cells is therefore a reduced sensitivity of $Itch^{-/-}$ T_H2 cells to the induction of tolerance [227].

The Cbl family of E3 ligases has been reported to play multiple roles in cellular signalling although some of these appear to depend on the adaptor protein function of Cbl and are independent of its' E3 ubiquitin ligase activity. For example, a major ubiquitin-dependent function of Cbl is the downregulation of RTKs downstream of several immunoregulatory receptors such as CSF-1, stem cell factor (kit) and macrophage-stimulating protein (MSP) [228]. Similarly, Cbl can ubiquitinate non-receptor tyrosine kinases such as Syk, Fyn and Lyn and target them for degradation [228]. Consistent with this, mice lacking Cbl-b were shown to develop spontaneous autoimmune disease [229] and both T and B cells from these mice were found to be hyperresponsive to antigen-receptor stimulation [229,230]. Moreover, such Clb-b deficient T cells displayed a reduced need for CD28 costimulation for the production of IL-2 indicating that Cbl-b plays a role in the negative regulation of CD28 signalling [230]. A similar role for Cbl in the regulation of human T cell activation has recently also been demonstrated as lower levels of c-Cbl were shown to correlate with increased CD3/CD28-dependent activation [231].

Further important immunoregulatory signalling pathways which are regulated by ubiquitination-dependent processes are the Notch and NF-κB cascades. For example, Notch signalling is important in the development of T cells as well MZ B cell differentiation. Itch and c-Cbl are able to ubiquitinate Notch, which in case of c-Cbl leads to the lysosomal degradation of Notch resulting in the downregulation of Notch levels and hence signalling [232,233]. Likewise, ubiquitination plays multiple roles in the regulation of NF-κB signalling. The best known function of ubiquitination in the NF-κB pathway is probably the ubiquitination of IκB with a lysine 48 linked poly-ubiqutin chain which targets it for degradation via the proteasome. However, other forms of ubiquitination such as lysine 63-linked chains also play important roles. Thus, both NEMO, the regulatory subunit of IKK, and its activating kinase Tak1 require poly-ubiquitination via lysine 63-linked ubiquitin for their activation [234]. Similarly, RIP (receptor-interacting protein), another component of NF-κB signalling downstream of TNFα, is modified by a lysine 63-linked ubiquitin chain, protecting it from degradation [235]. Moreover, some reports have investigated the role of ubiquitination in regulation of B cell signalling, including modification of important molecules such as Igβ and Syk [236,237]. The role of ubiquitination and specific E3 ligases in B cell signalling is therefore addressed in more detail in Chapter 3.

1.7 Regulation of the cell cycle

The cell cycle constitutes a highly regulated sequence of events that orchestrates the processes underlying cell division. In order to divide, cells have to undergo a growth phase during which they increase their cytoplasmic volume followed by DNA duplication and mitosis. The cell cycle (Fig.1.15) is divided into four phases. After entering the cell cycle from the quiescent state (G0), cell growth takes place (G1 phase) before DNA replication (S phase) and another shorter growth phase (G2) after which the cells separate into two daughter cells (M phase), each inheriting a full set of chromosomes. To ensure that cells only proliferate in response to appropriate extrinsic and intrinsic signals, there are checkpoints at both the G1-S and G2-M boundaries. Overcoming these restriction points depends on the integrated signals the cells receive from their environment such as growth factor availability and cell culture density or alternatively, from signals created due to DNA damage.

The different phases of the cell cycle and entry into them are primarily regulated by the action of cyclin-dependent kinases (Cdk). Cdks are proline-directed kinases which require binding to cyclins for full activation [238] and each phase of the cell cycle is governed by different Cdk/cyclin complexes. Thus, the first cyclins to be expressed after

growth factor stimulation are the D-type cyclins [239] which form complexes with Cdk4 or Cdk6. Due to the constitutive expression of Cdk4 and Cdk6, regulation of these complexes therefore depends on cyclin D availability which is regulated both at the transcriptional and protein level [240,241]. The major target of the cyclin D/Cdk4/6 complex is the phosphorylation of Rb (Retinoblastoma) family proteins including Rb, p107 and p130 [242] (Fig.1.15). This is because hypophosphorylated Rb proteins bind to the transcription factor E2F thereby blocking its transactivation ability [243], whilst Cdk/cyclin D-mediated phosphorylation of Rb proteins at serine 780 leads to the release of E2F and its consequent binding to the family of DP proteins [244], allowing these complexes to act as transcriptional activators of genes such as cyclin E necessary for G1-S phase transition (reviewed in [245]). Indeed, cyclin E is upregulated in mid to late G1 phase [246] and the resultant cyclin E/Cdk2 complexes are required for the further hyperphosphorylation of Rb at serines 807/811 [247] that is necessary for complete S phase entry and initiation of DNA replication [248]. Moreover, additional targets of phosphorylation by the cyclin E/Cdk2 complex are the Cdk inhibitor (CKI) p27 and cyclin E itself, leading to their degradation, [249,250]. Cyclin A, an alternative partner for Cdk2, is then expressed at the G1/S boundary and is required for S phase transition and control of DNA replication [251,252]. The last cyclin/Cdk complex that requires to be activated before cell cycle completion consists of cyclin B1 and Cdc2 (Cdk1). Although Cyclin B1 gets upregulated in late S and G2 phases, the complexes remain inactive due to inhibitory phosphorylation [253]. This phosphorylation is removed by the phosphatase Cdc25 to allow activation of cyclin B1/Cdc2 complexes and M phase entry [253]. Cyclin B1/Cdc2 activity is needed for entry into M phase due to its phosphorylation of targets such as lamins, nuclear proteins and microtubule proteins that are necessary for the reorganisation of the cellular architecture [254]. Thus, phosphorylation of key target proteins regulate events such as the establishment of the bipolar spindle, breakdown of the nuclear lamina as well as cell rounding, processes essential to mitosis [254]. An associated and important function of cyclin B1/Cdc2 is the regulation of DNA replication, transcription and translation during M phase by phosphorylation of proteins regulating termination of these processes [255]. The sequential activation of cyclin/Cdk complexes therefore ensures correct entry and progression through the cell cycle. It is therefore not surprising that multiple regulatory mechanisms cooperate in order to guarantee their appropriate cell cycle control.

1.7.1 Regulation of cyclin/Cdk activity

Cyclin/Cdk activity is further regulated by a complex network of posttranslational modifications of the Cdks. For example, phosphorylation of cyclin/Cdks by Cdk activating

kinase (CAK; reviewed in [256]), which itself is a cyclin/Cdk complex composed of cyclin H and Cdk7 [257] (Fig.1.16), changes the confirmation of Cdks thereby allowing their full activation. Such CAK-mediated phosphorylation can be removed by the dual specificity serine/tyrosine phosphatase KAP (CDK associated phosphatase) leading to the inactivation of cyclin/Cdk complexes [258]. Moreover, whilst phosphorylation of inhibitory sites on Cdk2 and Cdc2 by serine/threonine kinases Wee1 and Myt1 provide additional mechanisms to abrogate CDK activity [259,260], these inhibitory modifications can be counteracted by phosphatases of the Cdc25 family such as Cdc25B which dephosphorylates and therefore activates Cdc2 [261]. Interestingly, Cdc25 phosphatases are themselves targets for activation by Cyclin/Cdk complexes creating a positive feedback loop [262].

Temporally regulated expression and degradation of CKI represents an additional layer of regulation. At present, seven CKI have been described and these can be divided into two families: the Ink4 family (p15, p16, p18 and p19) and the Cip/Kip family (p21, p27 and p57), reflecting their slightly different inhibitory mechanisms (Fig.1.16). Thus, whereas the Ink4 family proteins bind to Cdk4/6 to inhibit their binding to their cyclin partner, the Cip/Kip proteins have been shown to bind cyclin/Cdk complexes and directly inhibit their activity (reviewed in [263]). Like the cyclins and Cdks, CKI are regulated at the transcriptional, translational and posttranslational level, phosphorylation again being an important modification. For example, phosphorylation plays an important role in the inhibition of p27 which acts to regulate arrest of cells in G1. Thus, cyclin E/Cdk2 complexes phosphorylate p27 at threonine 187 thereby targeting it for ubiquitination and degradation by the proteasome [264].

Indeed, phosphorylation of other proteins involved in cell cycle regulation, such as cyclin D1 and E2F, targets them for ubiquitination by specific E3 ligases and consequent proteasome-mediated degradation. Thus, both, p27 and E2F are ubiquitinated by the SCF (Skp2) E3 ligase complex [264,265] and consistent with this, one of the mechanisms utilised by the transcription factor, c-Myc to promote cell cycle progress is the upregulation of Cul1 expression. Cul1 is part of the SCF complex and an increase of Cul1 and thereby SCF complexes increases the ubiquitination and degradation of p27, revealing another level of cell cycle control mediated through activation of E3 ligases [266].

1.7.2 c-Myc and its role in cell cycle regulation

c-Myc is a transcription factor which plays multiple roles in various cellular processes such as proliferation, differentiation, growth and adhesion (reviewed in [267]) and its importance has been underlined by many studies implicating an oncogenic role for c-Myc

in human cancers [268]. Functional c-Myc forms heterodimers with its binding partner Max through a basic-region/helix-loop-helix/leucin-zipper (bHLHZip) binding domain [269]. This domain acts not only as a protein-protein interaction platform but also as the DNA binding site for its canonical CACGTG responsive element sequence [270]. Max was found to be required not only for c-Myc binding to this canonical DNA sequence but also for binding to other non-canonical binding sites to which the complex is recruited by other proteins [271]. After binding to DNA, c-Myc/Max complexes can act as transcriptional activators or repressors depending on the co-factors involved [272]. Indeed, it has been estimated that c-Myc might be involved in the regulation of up to 15% of the genes in the genome [273], although to date, only a small percentage of the potential targets of c-Myc-mediated transcriptional regulation have been investigated. Nevertheless, it has been shown that the potential of c-Myc to drive proliferation is partly due to its ability to activate the transcription of genes such as Cdk4 and cyclin D2 and to repress the expression of cell cycle inhibitors such as p15, p27 and p21 [274-278].

1.8 Apoptosis

Cellular necrosis constitutes the accidental and passive death of cells resulting from environmental influences such as mechanical pressure, heat or toxins. By contrast, apoptosis is an actively induced and highly regulated mechanism of cell death that is a pivotal process in development as well as maintenance of cellular homeostasis in many organisms. Apoptosis is of special importance in the immune system as it regulates processes like negative and positive selection during lymphocyte development as well as removal of activated T and B cells at the end of an immune response. However, the majority of our understanding of this controlled cell death mechanism has come from studies using *Caenorhabditis elegans*, the organism in which the role of caspases (*c*ysteine-*asp*artic acid prote*ases)* was first discovered. Caspases are a family of cysteinyl aspartate proteases which are usually present in the cell in an inactive pro-caspase form. Cleavage of pro-caspases preferentially happens at the C-terminal end of a X-X-X-Asp motif leading to the activation of the caspase. Caspases themselves then cleave various substrates such as ICAD/DFF45, the inhibitor of caspase-actived DNAse (CAD), thereby activating this DNAse leading to fragmentation of genomic DNA, a hallmark of apoptosis [279,280]. Moreover, caspases cleave and thus inactivate PARP (poly(ADP-ribose) polymerase) and DNA-PK (DNA-dependent protein kinase), two molecules that usually act to maintain the integrity of genomic DNA. Caspases are also responsible for cleaving and activating pro-apoptotic Bcl-2 family members such as Bid thereby driving mitochondrial

disruption. Additionally, caspases contribute to the disassembly of the cytoskeleton by cleaving lamin, fodrin and gelsolin [280] with the overall outcome of caspase activation being the “orderly” disassembly of the cells. A major feature of the controlled break-down of cells is the creation of apoptotic bodies which are membrane bound cellular fragments that prevent plasma membrane breakdown and unwanted release of intracellular proteins. The apoptotic bodies are recognised and taken up by phagocytes such as macrophages or neutrophils without causing activation of these cells thereby averting unnecessary and potentially harmful inflammation [281].

Mammalian cells utilise two major apoptosis-inducing pathways: the extrinsic pathway through “death receptor” ligation or the intrinsic pathway functioning at the level of the mitochondria.

1.8.1 The extrinsic apoptotic pathway

The extrinsic pathway is initiated by ligation and signalling through so called “death receptors”. These include Fas (CD95) and its ligand FasL (CD178), the “death receptors” DR4 and 5 and their ligand TRAIL (TNF-related apoptosis inducing ligand) as well as the TNF-receptor and TNFα [279]. A feature that all of these death receptors share is the death domain (DD) [279] which recruits downstream effectors of the prototypic death receptor signalling pathways (Fig.1.17). For example, the initial event in Fas signalling is the binding of FasL to its receptor which induces the trimerisation of Fas molecules in the membrane. This in turn will lead to the recruitment of the DISC (death-inducing signalling complex), a multimeric complex consisting of Fas, the adaptor protein FADD (Fas-associated death domain) as well as inactive pro-caspase 8 [282]. FADD is a common adaptor protein shared amongst all the death receptor pathways which interacts with Fas through its DD. The binding of FADD to Fas initiates a conformational change which exposes the death effector domain (DED) of FADD allowing it to recruit pro-caspase 8 [282]. Following recruitment to the Fas receptor complex, pro-caspase 8 is activated by self-cleavage and in turn cleaves pro-caspases 3, 6 and 7. These effector caspases then execute the apoptosis process by cleaving their substrates including DNA repair enzymes, structural proteins as well as endonuclease inhibitors [279]. The other important substrate of caspase 8 is Bid, a pro-apoptotic member of the Bcl-2 family of proteins. Caspase 8 cleaves Bid creating the truncated form which can then translocate to the mitochondria and induce the intrinsic pathway of apoptosis [282]. This cross-regulation of the extrinsic and intrinsic pathway seems to be crucial in hepatocytes, but is apparently less important in lymphocytes [282].

The importance of apoptosis in the regulation of many pivotal processes such as cell homeostasis makes it necessary to tightly control its initiation. There are multiple levels of regulation in the “death receptor” signalling pathways including transcriptional regulation of Fas and FasL expression, expression of Fas isoforms lacking the transmembrane or DD domain and production of soluble FasL [279]. Another major regulatory mechanism is the expression of FLIP, an inhibitor of caspase 8 activation. FLIP displays a similar structure to caspase 8 and performs its inhibitory function by binding to the DISC complex thereby hampering its ability to recruit and activate caspase 8 [283].

It is known that B cells can express Fas on their surface and be killed by Fas-ligation induced apoptosis [284] but the physiological importance of Fas signalling in B cells depends on the maturation stage of the cells. Thus, whilst Fas does not seem to play a major role in developing B cells and negative selection of immature B cells [285], it is involved in the deletion of low affinity-BCR expressing B cells in the germinal centre reaction which have not successfully undergone affinity-maturation of their antigen receptors [286].

1.8.2 The intrinsic apoptotic pathway

The key event in the intrinsic pathway is the disruption of the mitochondrial outer membrane potential culminating in the permeabilisation of the mitochondria and this is termed MOMP (mitochondrial outer membrane permeabilization). It can be induced by various different events, such as viral infection, DNA damage or removal of growth factors and activation of this intrinsic pathway appears to be mainly regulated by the Bcl-2 family of proteins. This family consists of pro- and anti-apoptotic members which have been classified according to the number and combination of Bcl-2 homology (BH) domains in their structure. For example, the anti-apoptotic family members Bcl-x_L, Bcl-2, Bcl-w Mcl-1 and A1 share up to 4 BH domains (BH1-4) whereas the pro-apoptotic molecules of the “Bax, Bak” or “multi-BH domain’’ family (Bax, Bak and Bok) contain 3 BH domains. The other pro-apoptotic family are the BH3-only proteins (Bid, Bad, Bik, Hrk, Bim, Noxa, Puma and Bmf) which, as their name implies, only contain the BH3 domain (reviewed in [285]). The two pro-apoptotic molecules Bax and Bak are the major transducers of MOMP (Fig.1.18); how exactly these two molecules induce MOMP is still not fully elucidated yet, but it is thought that they might cause the formation of pores in the mitochondrial membrane. Ultimately, the leakage through the mitochondrial membrane will lead to the release of molecules usually retained in the space between the inner and outer mitochondrial membrane [285], the most important of these mediators are cytochrome C and DIABLO (also called Smac). Thus, upon release into the cytosol, cytochrome C binds

to APAF-1 (apoptotic peptidase activating factor 1) initiating formation of the apoptosome, a heptameric protein ring made up of cytochrome C and APAF-1 molecules, that activates pro-caspase 9 [287]. By contrast, the release of DIABLO constitutes an apoptosome-independent pathway leading to apoptosis in that DIABLO sequesters caspase inhibitors such as X-linked inhibitor of apoptosis proteins (XIAP), a family of proteins that bind and inhibit caspases such as caspase 9 and 3. Thus, through binding of DIABLO, XIAP will release the caspase it was bound to allowing it to be activated [285].

The precise events regulating activation of Bax and Bak are not fully known but there are currently two major models of the mechanisms involved (Fig.1.19). The first model suggests that Bax and Bak can directly interact with BH3-only proteins, which in turn activate Bax and Bak [288]. Alternatively, the second model argues that Bax and Bak are normally bound to anti-apoptotic Bcl-2 family members until induction of apoptosis and hence activation of BH3-only proteins leads to the displacement and activation of Bax and Bak [285]. What both models have in common is the need for the presence and activity of BH3-only proteins and this explains why the expression and activation of these proteins is highly regulated and only induced upon detection of apoptotic signals. For example, Noxa, Puma and Bim expression is upregulated downstream of DNA damage, growth factor deprivation and ER stress and the increase in expression of these molecules is achieved by the activation of transcription factors such as p53 or FOXO3A [289-293]. Post-translational modifications, proteolysis or release from complexes provide other additional important regulatory mechanisms controlling the activity of Bcl-2 family members [285]. Moreover, for example, upregulation of Bcl-x_L can protect WEHI-231 cells from BCR-induced apoptosis [294] and so in the end, the overall balance between pro- and anti-apoptotic signalling decides the fate of the cell.

1.8.3 Caspase-independent execution of apoptosis

Caspases and their role in the execution of apoptosis have long been the major focus, but in recent years it has become obvious that other proteases can play important roles in the final stages of apoptosis. The two classes discussed in this context are calpains and cathepsins. Calpains are calcium-dependent cysteine proteases that are active at neutral pH whereas cathepsins generally prefer an acidic environment, such as the lysosomes, for optimal function. However, upon activation of apoptotic signalling cathepsins have been found to be released into the cytosol. Thus, cathepsin D release into the cytosol precedes the oxidative stress-induced apoptosis of fibroblasts [295]. Moreover, another cathepsin isoform, cathepsin B was found to be released into the cytosol upon TNFα-mediated induction of apoptosis in hepatocytes [296]. Calpains and their precise

effector functions in apoptosis are still not well studied but some that are known include a role in cell fusion and motility by remodelling the cytoskeleton, degradation of cell cycle regulators, degradation of filamin, talin, and spectrin and modulation of signalling molecules such as PKC [297]. A role for calpains in apoptosis has been shown in many different cells and systems such as ionomycin-induced apoptosis of a human carcinoma cell line [298], dexamethasone-induced apoptosis in thymocytes [299], drug-induced death of HL-60 cells due to calpain-mediated cleavage of Bax [300] and radiation-induced apoptosis of the Burkitts' Lymphoma cell line BL30A [301]. Moreover, it seems that the calpain and caspase system are not necessarily exclusive to each other but rather seem to be cross-regulatory as shown by the inactivation of the calpain inhibitor calpastatin by caspases during Fas-induced apoptosis in Jurkat and U937 cells [302]. Calpain in turn is able to cleave pro-caspase 3 and 9 thereby activating them in a caspase-independent fashion [303].

Like calpains, cathepsins have been implicated in various systems of apoptosis in a range of cell types and in addition, cathepsin B has been shown to be able to induce chromatin condensation, a morphological feature of apoptosis in a cell-free system [304]. Thus, under conditions of TNFα-induced apoptosis of hepatocytes, cathepsin B was shown to be released from lysosomes in a caspase 8-dependent manner, resulting in cytochrome C release from mitochondria. Such cytochrome C release as well as caspase activation and resultant apoptosis were markedly reduced in cells from cathepsin B-deficient mice [296]. Likewise, inhibition of cathepsin B has been reported to reduce p53-induced apoptosis in myeloid leukemic cells [305] and it was similarly shown to be involved in the intrinsic apoptotic pathway induced by *Bacillus Calmette-Guérin* (attenuated *Mycobacterium bovis*) in cancer cell lines [306]. Moreover, studies in this laboratory have demonstrated the involvement of cathepsin B in BCR-induced apoptosis of WEHI-231 cells, although in this system cathepsin B, rather than caspases, seems to be the main executioner-protease [307]. Besides cathepsin B, another isoform, cathepsin D, has also displayed the potential to cleave molecules important in the last stages of apoptosis. Thus, in neutrophils cathepsin D cleaves and thereby activates caspase 8 under inflammatory conditions and might therefore play an important role in neutrophil apoptosis and hence resolution of inflammation [308].

1.9 Aims and Objectives

The core aim of this study was to characterise the differential signalling mechanisms underlying tolerance induction employed by B cells at distinct stages of development. In

particular, the primary objective was to investigate the signals that regulate commitment to, and rescue from, negative selection of immature B cells in the bone marrow (central tolerance). In addition, it was planned to compare these signals with those of a mechanism involved in peripheral tolerance: specifically, the homeostatic regulation of mature B cells provided by FcγRIIb-mediated negative feedback inhibition of B cell activation. Finally, it was proposed to investigate whether defects in the latter homeostatic mechanism of peripheral tolerance played a contributing role to the autoimmune responses of patients with autoimmune inflammatory diseases such as rheumatoid arthritis and systemic lupus erythematosus.

1.10 Figures and Tables

Figure 1.1 Structural features of antibodies

Antibodies consist of four chains, two heavy (55-70kD) and two light chains (~24kD) linked by disulphide bonds. Both heavy and light chains are composed of constant (C) and variable (V) regions which contain multiple immunoglobulin (Ig) domains. Antibodies can further be divided into their Fc and Fab regions. Antibody binding is conferred by the Fab region which contains the V regions of the heavy and light chains. These opposing regions create the antibody binding cleft, the site of antigen binding. The Fc portion binds to Fc-receptors which initiate signalling leading to various responses such as activation, inhibition or degranulation of various immune cells, depending on the cell class, antibody isotype as well as Fc-receptor isoforms.

There are five antibody isotypes: IgA, IgD, IgE, IgG and IgM. These isotypes differ concerning the number of Ig domains in their constant region as well as their ability to form multimeric structures. Each isotype has a defined set of functions increasing the versatility of B cell responses.

Figure 1.2 Somatic V(D)J recombination

Somatic recombination of immunoglobulin heavy and light chains differs slightly. Recombination of the heavy chain is achieved by two separate recombination events joining firstly the D and the J segments followed by joining the V segment to the D-J segment. Due to the lack of D segments, light chain rearrangement is achieved by a single recombination event which joins a V segment with a J segment.

Following somatic recombination the genes are transcribed and spliced to join up the parts encoding the variable region with the exons encoding the constant region. Finally, the RNA is translated into heavy or light chain proteins which are then assembled to yield functional antibodies.

Figure 1.3 Basic structure of the BCR

The BCR consists of an antigen-binding component – the membrane bound Ig molecule – and the signal-transducing units Igα and Igβ. The Ig molecule is made up of two heavy and light chains which are composed of constant and variable regions, the latter containing the so-called CDRs (complementarity-determining regions). CDRs are areas of high variabilty where most mutations occur during somatic hypermutation. The Ig molecule itself is not able to signal and therefore needs Igα and Igβ. Those proteins both contain ITAMs (immunoreceptor tyrosine-based activation motif), which confer their signalling ability.

Figure 1.4 B-2 B cell development

The development of B cells is characterised by changes in surface receptor expression and Ig gene rearrangement which allows the identification of different developmental stages. The first stage at which cells can be identified as being committmed to the B cell lineage is the pre-pro-B cells stage at which little or no immunoglobulin (Ig) rearrangement occurs. The transition from progenitor CLP (common lymphoid progenitor) to committed B cell is dependent on multiple transcription factors including Pax5, EBF and PU.1. Rearrangement of the heavy chain is first induced at the pre-pro B cell stage, but functional heavy chain is not expressed until the pre-B cells stage. Rearranged μ heavy chain is expressed on the surface in combination with λ5 and VpreB (surrogate light chain) to yield the pre-BCR. This receptor is associated with Igα and Igβ (CD79a/b) on the surface of the cell and signalling via the pre-BCR induces heavy chain allelic exclusion and initiates light chain rearrangement. Surface expression of functional μ heavy and light chain complexes (IgM) is a characteristic feature of the immature B cell stage. Up to this point, B cell development has been Ag-independent, however from the immature B cell stage onwards the clonal selection processes are Ag-dependent. Immature B cells which survive negative selection are released from the bone marrow into the circulation to migrate to the secondary lymphoid organs. The initiation of IgD expression on B cells indicates their development into transitional B cells which need BCR- and BAFF-dependent signalling to progress to their next developmental stage, mature naïve B cells. A mature B cell then has two main developmental possibilities after activation – becoming an antibody secreting plasma cell or a memory B cell.

Figure 1.5 Structure of the pre-BCR and BCR

At the pre-B cell stage rearranged μ heavy chain in combination with λ5 and VpreB (surrogate light chain) are expressed on the surface associated with Igα and Igβ compared to conventional light chains in the mature BCR. A functional pre-BCR is necessary to allow the B cells reach their next developmental stage. The association of the rearranged heavy chain with the surrogate light chain substitutes provides a mechanism to ensure that only B cells expressing a correctly folded heavy chain can develop any further.

Figure 1.6 The germinal centre reaction

During a T cell-dependent response naïve mature B cells will migrate from the T cell rich areas of secondary lymphoid organs into the follicular mantle **(1)** where they start forming the dark zone of the germinal centre. They undergo rapid proliferation, downregulate surface Ig expression and undergo somatic hypermutation **(2)**. After having mutated their Ig the cells stop dividing, express their new receptor and migrate into the light zone following a chemokine gradient **(3)**. Follicular dendritic cells in the light zone retain antigen and present it to all the B cells, but only centrocytes with high affinity receptors are selected and allowed to survive whereas low affinity or self-reactive BCR-expressing cells undergo apoptosis. The positively selected centrocytes interact with T_H cells thereby receiving CD40-mediated signals leading to isotype switching and development into either memory B cells or plasma cells **(4)**.

Figure 1.7 B cell development

B cells are divided into three subsets – follicular B cells, B-1 B cells and marginal zone (MZ) B cells. The development of these separate lineages has not been fully elucidated, but a general model has been proposed based on recent findings. Follicular B cells and MZ B cells, the so called B-2 B cells, both appear to originate from the same bone marrow precursor. The development of follicular and MZ B cells is thought to divide into the two subsets at the T2 transitional B cells stage. Follicular B cells will recirculate through lymph nodes and the spleen whereas MZ B cells are mainly sessile and stay in the marginal zone of the spleen. Separate B-1 B cell progenitors have recently been identified, placing this subset in its own developmental pathway diverging from B-2 B cells as early as the pro-B cell stage.

Figure 1.8 Tolerance checkpoints in B cell development

Activation of autoreactive B cells can play an important role in autoimmune diseases. In healthy humans these pathogenic cells are either absent or kept in an inactive state. Studies in humans and mice have found that self-reactive cells are depleted from the B cell pool at multiple points during the development. Thus, the percentage of autoreactive clones is reduced before cells enter the immature B cell stage and again after having left the bone marrow and hence before they develop into mature naïve cells. Not only are self-reactive B cells depleted but they are also prevented from entering certain developmental stages. Self-reactive B cells have been found to be excluded from the IgM^+ memory cell pool and the GC reaction. Moreover, these cells might not develop into plasma cells and even though autoreactive IgG^+ memory B cells are present in healthy humans, they are prevented from producing pathogenic autoantibodies.

Figure 1.9 BCR ligation initiates three major signalling cascades

Upon BCR ligation, three major signalling pathways are initiated: the PI3 kinase, PLCγ and MAP kinase pathways. PI3 kinase catalyses the phosphorylation of inositol lipids like PI, PI-(4)-P and PI-(4,5)-P_2 thereby producing PI-(3)-P, PI-(3,4)-P_2 and PI-(3,4,5)-P_3 (PIP_3), molecules normally present in the cell at very low levels and whose concentration increases after PI3 kinase activation. PIP_3 is able to recruit PH (pleckstrin homology) domain-containing proteins, such as PLCγ, Btk, Vav, PDK1/2 and Akt, to the membrane where they can be activated. PLCγ is recruited to the BCR-ITAMs, possibly by BLNK, to bring it into close proximity with Btk and Syk. This leads to PLCγ phosphorylation and activation and subsequent downstream signalling. PLCγ produces DAG and IP_3, two important second messengers that activate protein kinase C (PKC) and increase intracellular calcium levels, respectively. The ERK MAP kinase signalling cascade becomes activated due to the recruitment of Sos (son of sevenless), a guanine nucleotide exchange factor which catalyses the exchange of GDP for GTP on Ras leading to its activation. The next step in this signalling cascade is the derepression of Raf by activated Ras thereby inducing its kinase activity. Raf is a MAPKK and therefore able to phosphorylate MEK1/2 which in turn activate ERK1/2.

Figure 1.10 The MAPK signalling cascade

The MAP kinases (MAPK) are serine/threonine protein kinases which regulate multiple cellular responses including proliferation, apoptosis and differentiation. They can be separated into three groups: The extracellular signal-regulated kinases (ERK MAP kinase), the c-Jun N-terminal kinases (also known as stress activated protein kinases (JNK/SAPK) and the p38 MAP kinases. Activation of the MAP kinases is achieved by sequential activation of upstream kinases MAPKKK (MAPK kinase kinase) and MAPKK (MAPK kinase) ultimately leading to the phosphorylation of MAPKs on tyrosine and threonine residues located in a T-X-Y motif, the X being different in each MAPK group. Active MAPKs phosphorylate and thereby activate transcription factors such as Elk-1, c-Myc and c-Jun and numerous other cytoplasmic and nuclear substrates like $cPLA_2$. Another important class of proteins regulated by MAPK-dependent phosphorylation are the MAPK-activated protein kinases (MK) such as MAPKAPs and MNKs.

Figure 1.11 CD19 signalling

CD19 is expressed at the surface of B cells as a receptor complex together with CD21 and CD81. Binding of ligand to the CD21/CD81/CD19 receptor complex will lead to phosphorylation of tyrosine residues in CD19 allowing it to recruit and activate PI3 kinase as well as Vav which in turn induce Akt and PLCγ2 signalling. Therefore, CD19 contributes to the activating signals and hence lowers the signalling threshold of the BCR.

Figure 1.12 CD40 signalling in mature B cells

Ligation of CD40 with CD154 initiates the recruitment of TRAFs to the cytoplasmic portion of the receptor. TRAFs 2, 3, 5 and 6 can then activate multiple signalling pathways including the PLCγ2, PI3 kinase and MAPK pathways. The overall outcome of all these signals is the inhibition of apoptosis through NF-κB-dependent upregulation of Bcl-x_L and FLIP, and the initiation of cell cycle progression by downregulating levels of p27 and upregulating Cdk4/6.

Table 1.1 The family of Fcγ receptors

Murine and human cells express a variety of different activatory and inhibitory Fc receptors for the IgG subclass of antibodies. There are some major differences between Fcγ receptors expressed in mice and humans such as the lack of FcγRIIA and C in mice and the expression of FcγRIV on murine but not human cells. The expression of Fcγ receptors in mice and humans can be found on many cell lineages such as macrophages, neutrophils, eosinophils, B cells and NK cells.

Figure 1.13 BCR-mediated sigalling is inhibited by co-ligation of FcγRIIb

FcγRIIb is the low affinity receptor for the Fc portion of IgG. Cross-linking of BCR and FcγRIIb inhibits BCR-mediated activation and proliferation of B cells. At the proximal signalling level, the co-ligation of BCR and FcγRIIb induces Lyn to tyrosine-phosphorylate the ITIM in the cytoplasmic portion of FcγRIIb. The main signal transducer recruited to the phosphorylated ITIM is SHIP. SHP-1 and -2 are also recruited by FcγRIIb but do not appear to be essential for negative signalling. By contrast, SHIP signalling appears to effect negative signalling by dephosphorylating PIP_3 and consequently reducing recruitment of pro-survival and proliferation-promoting PH-domain containing proteins. Furthermore, FcγRIIb also recruits PTEN (inositol 3' phosphatase) to further antagonise PI3 kinase signalling. The ERK MAPK cascade is also inhibited by FcγRIIb signalling due to the direct inhibition of Shc/Gbr2 interaction by SHIP as well as recruitment of p62 Dok which activates RasGAP thereby reducing Ras activation. Additionally, BCR/FcγRIIb ligation recruits PAC-1, an ERK-specific dual phosphatase, inducing dephosphorylation and thereby inactivation of ERK. FcγRIIb signalling has also been found to decrease calcium signalling, but the underlying signalling mechanisms are not yet fully elucidated.

Figure 1.14 Ubiquitination and proteasomal degradation

Ubiquitination of target proteins consists of three major steps:

1. The initial activation of ubiquitin is catalysed by E1 enzymes in a process that requires energy in the form of ATP. The activated ubiquitin molecule is then transferred onto the E1 enzyme itself via a thioester linkage.
2. The ubiquitin is then transferred from E1 to the ubiquitin-conjugating enzyme E2 by trans-thio-esterification.
3. The last step in the process involves the E3 enzyme which functions as the substrate recognition unit of the complex. The E3 ligase forms a complex with E2-bound ubiquitin as well as the target protein allowing the transfer of ubiqutin to a lysine of the target protein.

If no further modification occurs the protein is classified as mono-ubiquitinated. But following this initial step the ubiquitin can also be linked to further ubiquitins creating poly-ubiquitination. The outcome of conventional polyubiqutination via lysine 48 is proteasome-dependent degradation of the protein whereas other forms of poly-ubiquitination (such as via lysine 63) or multi-monoubiquitination can target substrates for endocytosis and lysosomal degradation as well as influencing their signalling properties by changing their transduction interaction partners.

Figure 1.15 The cell cycle

The cell cycle consists of four major stages. Cells enter the cell cycle at the G1 phase and following growth and given the right signals, will enter S phase in which they will replicate their DNA, followed by another growth phase in the G2 phase. The last step is mitosis (M phase) and the division of the DNA and cellular contents between two daughter cells. The so called restriction point during arrest in G1 is mainly regulated by activation of cyclin/Cdk complexes which hyperphosphorylate the Retinoblastoma (Rb) proteins thereby releasing the transcription factor E2F. This will initiate transcription of genes necessary for entry and progress through S phase. Each stage of the cell cycle is highly regulated to stop damaged cells from entering the cell cycle and allowing the proper progression and completion of the previous stages before entry into the next one. One level of regulation is provided by the Ink and Cip/Kip cell cycle inhibitors which, by inhibiting cyclin/Cdk complexes, can stop progresssion of cells through the cell cycle at various stages.

Figure 1.16 Regulation of the cell cycle

(A) The cell cycle is divided into four phases. After entering the cell cycle from the quiescent state (G0) the cells' initial growth takes place during G1 phase. This is followed by DNA replication (S phase) and another shorter growth phase (G2) after which the cells separate into two daughter cells (M phase) with each inheriting a full set of chromosomes. Checkpoints at the G1-S boundary and G2-M boundary ensure that cells only progress through cell cycle and divide under appropriate conditions and in the absence of DNA damage. Such checkpoints involve regulation by Cdk/cyclin complexes.

(B) Activation of Cdk/cyclin complexes is regulated at multiple levels. Phosphorylation by CAK activates Cdks whereas Wee1 and Myt phosphorylate inhibitory sites on Cdk2 and Cdc2. Phosphatases of the Cdc25 family counteract Wee and Myt1 by dephosphorylating the inhibitory residues. The Cdk inhibitors are divided into two classes: The Ink4 family of proteins inhibit the assembly of cyclin D and Cdk4/6, the Cip/Kip family inhibitors block the activity of pre-assembled cyclin/Cdk complexes.

Figure 1.17 Extrinsic pathway of apoptosis - Fas/FasL signalling

Ligation of the Fas receptor by its ligand FasL induces the oligomerisation of Fas initiating the assembly of the DISC which consists of the Fas associated FADD proteins and consequently recruits pro-caspase 8. Interactions between Fas and FADD are via the proteins death domains (DD), whereas FADD recruits pro-caspase 8 using its death effector domain (DED). Following recruitment to this complex, pro-caspase 8 is then activated by autocleavage. FLIP is a specific inhibitor of DISC assembly due to its similar structure to pro-caspase 8, allowing it to compete for DED binding and thereby displacing pro-caspase 8. Active caspase 8 can activate effector caspases 3, 6 and 7 which in turn cleave multiple targets to induce the hallmark changes of apoptosis including chromatin condensation, nuclear shrinkage and cytoskeletal collapse. Caspase 8 also cleaves Bid to create active truncated Bid (tBid) which localises to the mitochondria thereby initiating the intrinsic mitochondrial apoptosis pathway.

Figure 1.18 Intrinsic/mitochondrial pathway of apoptosis

Pro-apoptotic stimuli induce the activation of Bax and Bak and these two pro-apoptotic Bcl-2 family members then lead to pore-formation at the mitochondria and initiation of mitochondrial outer membrane permeabilization (MOMP). Consequently, mitochondrial proteins, such as cytochrome C and DIABLO/Smac are released. In the cytoplasm cytochrome C can form complexes together with APAF-1. These oligomers, the so called apoptosome, activate pro-caspase 9 and subsequently effector caspases. One of the other molecules released from the mitochondria, DIABLO, carries out its pro-apoptotic function by blocking the binding of XIAP to caspases 3 and 9 thereby releasing them from inhibition and hence allowing them to cleave their substrates to induce disassembly of the major cellular structures required to induce apoptosis.

Figure 1.19 Models for the regulation of apoptosis by Bax-Bak Bcl-2 family proteins
Currently, the precise mechanism of apoptosis transduced by the Bax-Bak Bcl-2 family members is not known but there are two major models to explain their role in the regulation of mitochondrial stability and apoptosis. Model 1 proposes that apoptotic stimuli will lead to the upregulation of BH3-only proteins which will then be able to directly activate Bax and Bak, resulting in the disruption of the mitochondrial membrane and consequent generation of the apoptosome. In this model, the upregulation of BH3-only proteins and direct activation of Bax and Bak would be able to overcome the positive effects of anti-apoptotic Bcl-2 family members present in the cell. By contrast, Model 2 suggest that anti-apoptotic Bcl-2 family members are bound to Bax and Bak in viable cells thereby stopping them from being activated and translocated to the mitochondria. In this case, apoptotic signalling BH3-only proteins are upregulated and can then compete for binding to anti-apoptotic Bcl-2 proteins subsequently releasing Bax and Bak which can relocalise to the mitochondria and initiate the apoptotic process.

2 Materials and Methods

2.1 Cell culture reagents, antibodies and inhibitors

All cell culture reagents were purchased from Invitrogen Life Technologies. All other reagents were obtained from Sigma-Aldrich unless otherwise stated. For a full list of antibodies used, refer to Table 2.1, but to target particular receptors on murine B cells, the following antibodies were used as follows. For functional studies, AffiniPure $F(ab')_2$ fragments of goat anti-mouse IgM (H+L) antibodies (Jackson ImmunoResearch Laboratories) were used at 50 µg/ml to cross-link the BCR on mature B cells. By contrast, intact AffiniPure rabbit anti-mouse IgG+IgM (H+L) antibodies (Jackson ImmunoResearch Laboratories) were used at 75 µg/ml to cross-link the BCR and FcγRIIb on mature B cells. However, for Western Blotting studies, the BCR was ligated by a rat anti-mouse IgM (clone B7.6, made in house) mAb at 50 µg/ml, FcγRIIb was ligated by a rat anti-mouse FcγRIIb (clone 2.4G2, made in house) mAb at 50 µg/ml, and donkey anti-rat IgG (H+L) antibodies (Jackson ImmunoResearch Laboratories) at 75 µg/ml were used to cross-link the rat mAbs and hence the BCR and FcγRIIb. Blocking Fas/FasL interactions was achieved by adding 5 or 10 µg/ml armenian hamster anti-FasL (anti-CD178) antibody (BioLegend) to the cultures with armenian hamster IgG used as an isotype-specific control antibody (BioLegend). The rat anti-mouse IgM (clone B7.6) antibody was also used to cross-link the BCR on WEHI-231 cells at concentrations between 0.0001 and 10 µg/ml. To antagonise the anti-IgM-mediated growth arrest signal in WEHI-231 cells, rat anti-mouse CD40 (clone FGK 45, made in house) mAb was used at 10 µg/ml. Unless otherwise specified, cell signalling inhibitors were used at the following concentrations. The MEK-specific inhibitor PD98059 (Calbiochem) and the PI3 kinase-specific inhibitor LY294002 (Calbiochem) were used at previously established optimal concentrations (10 µM and 1 µM, respectively) [309,310]. Likewise, the Caspase-8 Inhibitor II (Z-IETD-FMK) (Calbiochem) was used at 10 µM whereas the proteasome inhibitor Z-Leu-Leu-Leu-al (MG132) (Sigma) was used at 0.5 µM.

2.2 Animals

Mice on a BALB/c background, were used to isolate primary splenic B cells. These mice were maintained at the Central Research Facility (CRF), University of Glasgow. The mouse model of Systemic Lupus Erythematosus, MRL/MpJ-*Fas*^{lpr}, and its' parental strain

MRL/MpJ, were kept at the Joint Research Facility (JRF), University of Glasgow and managed by Mairi McGrath, Dr. Angela Morton and myself.

2.3 WEHI-231 immature B cell line

The murine B cell lymphoma, WEHI-231 (obtained from ECACC) was cultured in RPMI-1640 medium supplemented with 5% foetal calf serum (FCS), 100 U/ml penicillin, 100 μg/ml streptomycin, 50 μM β-mercaptoethanol and 2 mM L-glutamine at 37°C in a 5% (v/v) CO_2 atmosphere at 95% humidity. WEHI-231.7 JM cells were transfected by electroporation with the pSFFV-Neo plasmid containing either the human *bcl-x*$_L$ gene ($BclX_L$ WEHI-231) or empty vector as control (Neo WEHI-231). Stable transfectants were selected for the acquisition of neomycin resistance by growth in the presence of the antibiotic G418 (500 μg/ml, Promega) and were a kind gift from Dr. C. B. Thompson (University of Pennsylvania). Stable transfectants were cultured in RPMI-1640 media supplemented with 5% FCS, 100 U/ml penicillin, 100 μg/ml streptomycin, 50 μM β-mercaptoethanol, 2 mM L-glutamine and 500 μg/ml G418 at 37°C in a 5% (v/v) CO_2 atmosphere at 95% humidity.

2.4 B cell purification from mouse spleens

Primary B cells were prepared from murine spleens using the anti-CD43-magnetic bead negative-selection method of Miltenyi Biotec. This method takes advantage of the fact that the CD43 antigen is expressed on nearly all leukocytes, except for immature and mature naive B cells. Negative selection of CD43-positive cells therefore removes all unwanted cells without manipulating the B cells themselves. To avoid non-specific labelling and increase survival of cells all procedures were carried out at 4℃.

Briefly, spleens were removed and washed in RPMI-1640 media and then dissociated through nitex. The resultant single cell suspension was centrifuged (450 *g*, 10 min, 4 °C) and the pellet resuspended in 9 ml of red blood cell removal buffer (0.168 M NH_4Cl, pH 7.2). The suspension was incubated on ice for 7 min to permit red blood cell lysis and lipid precipitation. The supernatant was removed, carefully layered over 1 ml FCS in a fresh tube and centrifuged again (450 *g*, 10 min, 4 °C). The pellet was resuspended in 9 ml dead cell removal buffer (20 mM HEPES, DPBS (8 mM Na_2HPO_4, 1.5 mM KH_2PO_4, 140 mM NaCl, 0.3 mM KCl, 0.7 mM $CaCl_2$, 0.5 mM $MgCl_2$, pH 7) supplemented with 0.12 M sorbitol and 20 mM glucose and filtered through dead cell removal columns (absorbent cotton wool

plugged, short-form, glass pasteur pipettes, wetted with 1 ml RPMI/5% FCS) into 1 ml FCS. The cells were centrifuged (450 *g*, 7 min, 4 °C) and resuspended in 50 ml ice-cold MACS buffer (phosphate buffered saline (PBS), 0.5% BSA, 2 mM EDTA) counted and pelleted again. The pellet was resuspended in ice-cold MACS buffer (2 x 10^8 cells/ml), incubated for 25 min at 4 ºC with anti-CD43 (Ly-48) beads (100 µl anti-$CD43^+$ beads/ 2 x 10^8 cells) and passed through a pre-separation filter. The cells were applied to a CS-type negative selection magnetic column (Miltenyi Biotec) in a strong magnetic field. Purified mature B cells (CD43-negative) were eluted from the column by washing with 50 ml ice-cold MACS buffer. The cells were centrifuged, the pellet resuspended in RPMI-1640 medium supplemented with 5% FCS, 100 U/ml penicillin, 100 µg/ml streptomycin, and 2 mM L-glutamine. Live B cells were then counted by trypan blue exclusion. To assess the purity of the purified B cells a small aliquot of cells was stained for B220 (CD45R) as described in section 2.9.1 and expression of this surface marker analysed by FACS (FACS Calibur, BD).

2.5 PBMC (peripheral blood mononuclear cells) purification and culture

Human peripheral blood samples were collected at the Rheumatology Clinic (Glasgow Royal Infirmary) and informed consent was obtained from patients and healthy controls prior to research use. Venous blood (10-25 ml) was collected in heparinised tubes and either used straight away or stored at 4℃ for a maximum of 12 h. PBMCs were isolated by Histopaque-1077 purification. In short, 9 ml blood diluted 1 in 2 with PBS was layered over 5 ml Histopaque in a 15 ml centrifuge tube. After 30 min centrifugation (430 *g*, 21℃) the opaque layer containing the PBMCs was transferred into a fresh tube and washed 3 times with PBS. PBMCs were cultured in RPMI-1640 media containing 5% FCS, 100 U/ml penicillin, 100 µg/ml streptomycin, 2 mM L-glutamine at 37℃ in a 5% (v/v) CO_2 atmosphere at 95% humidity. Cells were stimulated using the appropriate stimuli as indicated in the figure legends.

2.6 Purification of human B cells from peripheral blood

Several purification procedures were established in an attempt to ensure the enrichment of B cells from human peripheral blood without their activation. After purification, human B cells were cultured in RPMI-1640 media containing 5% FCS, 100 U/ml penicillin, 100 µg/ml streptomycin, 2 mM L-glutamine at 37℃ in a 5% (v/v) CO_2

atmosphere at 95% humidity. Cells were stimulated using the appropriate stimuli as indicated in the figure legends.

2.6.1 Positive selection of $CD19^+$ B cells using magnetic microbeads

The PBMC-pellet was resuspended in 80 µl MACS buffer (PBS containing 0.5% FCS, 2 mM EDTA) per 10^7 cells and incubated with 20 µl anti-CD19 microbeads (Miltenyi Biotec) for 15 min at 4°C. The cells were washed once with 1-2 ml MACS buffer and the pellet was resuspended in 500 µl MACS buffer (up to 10^8 cells). The cell suspension was filtered through pre-separation filters (Miltenyi Biotec) and loaded on the equilibrated positive selection column (MS column) followed by three wash steps with 500 µl MACS buffer. The cells were eluted by removing the column from the magnet and flushing with 1 ml MACS buffer. The purity (typically 85-95%) of the cells was assessed by staining with anti-CD20-PE antibody and FACS analysis (FACS Calibur, Becton Dickinson) (Fig 2.1).

2.6.2 Purification of B cells by negative selection using human B cell isolation kits

PBMCs were resuspended in 40µl MACS buffer (PBS containing 0.5% FCS, 2 mM EDTA) and incubated with 10 µl biotin-antibody cocktail consisting of either anti-CD2, -CD14, -CD16, -CD36, -CD43, and -CD235a antibodies (Human B cell Kit, Miltenyi Biotec) or anti-CD2, -CD14, -CD16, -CD27, -CD36, -CD43, and -CD235a antibodies (Naïve Human B cell Kit, Miltenyi Biotec) per 10^7 cells for 10 min at 4°C. After the addition of 30 µl MACS buffer and 20 µl anti-biotin microbeads per 10^7 cells the suspension was incubated for another 15 min at 4°C. The cells were then washed with 5-10 ml MACS buffer and the pellet was resuspended in 500 µl MACS buffer (up to 10^8 cells). The cell suspension was filtered through pre-separation filters (Miltenyi Biotec) and then loaded on an equilibrated LS-column and washed 3 times with 3 ml MACS buffer. The flow through was collected and the purity of the eluted cells was assessed by staining with anti-CD19-FITC and anti-CD20-PE antibodies and FACS analysis (Fig. 2.2). Only about 18% of the PBMC population are CD19-FITC positive cells before the purification. Although this percentage increased during the purification process (31.8% human B cell isolation kit, 52.5% naïve human B cell isolation kit) (Fig. 2.2), a high percentage of other cell classes (T cells and monocytes), as shown by anti-CD3 and anti-CD14 staining, could still be detected after one round of such B cell enrichment (Fig. 2.3).

2.6.3 High speed FACS sorting of $CD19^+$, $CD20^+$ B cells

Peripheral blood was collected by venipuncture in tubes with 200 µl heparin and PBMC were prepared as described above. PBMC were then either single-stained with anti-CD20-PE, anti-CD19-FITC for positive selection protocols or a mixture of anti-CD3-APC, anti-CD14-FITC and anti-CD56-PE for negative selection of T cells, monocytes and natural killer cells. The cells were stained in 100 µl FACS buffer (PBS containing 0.5% FCS, 2 mM EDTA) containing the antibodies (all at 1:50 dilution) for 15 min at room temperature. After two washes with 1 ml FACS buffer, the cells were subjected to FACS sorting using a FACSAria machine (BD). Positive selection of B cells proved superior in terms of purity of the B cells (~ 98.8% CD20-specific, ~99.3% CD19-specific) compared with that of populations obtained following negative selection of B cells (~87.8%) (Fig. 2.4). However, the B cells generated by all of the protocols showed low viability.

2.7 Purification of antibodies from hybridoma cell lines

Cells (B7.6 clone – rat IgG1; FGK45 clone – rat IgG2a, 2.4G2 clone – rat IgG2b) were cultured in RPMI-1640 medium supplemented with 10% FCS, 100 U/ml penicillin, 100 µg/ml streptomycin, 2 mM L-glutamine and 50 µM β-mercaptoethanol. The antibody-rich tissue culture supernatants were collected and the relevant Ab purified using protein G-sepharose columns filled with 1 ml protein G-sepharose beads (immunoglobulin capacity >20 mg/ml, Pierce) and washed with binding buffer (0.2 M $NaH_2PO_4.2H_2O$, 0.2 M $Na_2HPO_4.2H_2O$, pH 7.0). Tissue culture supernatant was loaded onto the column at 4^oC and the column was washed with binding buffer to elute unbound protein. Immunoglobulin was then eluted in 0.5 ml fractions using elution buffer (0.1 M glycine, pH 2.7) into tubes containing 0.5 ml 1M Tris base-HCl (pH 8) to raise the pH to neutral levels. The protein concentration of each fraction was determined using spectrophotometry to measure the absorbance at 280 nm (an optical density of 1.4 was approximately equivalent to 1 mg/ml of protein). The protein-rich fractions were pooled and dialysed exhaustively in PBS at 4℃. The resultant purified Abs were filter-sterili sed and stored at -20^oC.

2.8 Functional assays

2.8.1 DNA synthesis assay

To be able to divide, cells have to replicate their DNA. Thus, if cells are cultured in the presence of radio-labelled bases, such as thymidine, these are incorporated into their DNA with the levels of signal being proportional to the amount of DNA synthesised. The

most common label used to detect DNA synthesis is [^{3}H]-labeled thymidine which can be detected by scintillation counting. Thus, for the measurement of DNA synthesis, cells (10^5 cells/well human B cells, 5 x10^5 cells/well mature mouse B cells, 10^4 cells/well WEHI-231) were cultured in triplicate in round bottom microtitre plates in RPMI-1640 media supplemented with 2 mM L-glutamine , 1 mM sodium pyruvate, 1% nonessential amino acids, 50 μM β–mercaptoethanol, 100 U/ml penicillin, 100 μg/ml streptomycin, 5% FCS in the presence of the indicated stimuli at 37°C in a 5% (v/v) CO_2 atmosphere at 95% humidity. [^{3}H] thymidine (0.5 μCi/ well, Amersham) was added 4 (murine B cells) or 8 h (human B cells) before cell harvesting with an automated cell harvester (Perkin Elmer). Incorporated label was analyzed by liquid scintillation analysis (Microbeta Trilux, Perkin Elmer). Data are presented as cpm +/- SD.

2.9 FACS analysis

2.9.1 Staining for surface markers

Aliquots of cells (10^5-10^6 per sample) in 5 ml polystyrene tubes (Falcon, BD) were washed with 200 μl cold FACS buffer at 450 *g* for 5 min at 4℃. Cells were re-suspended in 200 μl Fc receptor (FcR) blocking buffer (anti-CD16/32, clone 2.4G2, hybridoma supernatant, 10% mouse serum, 0.1% sodium azide) containing the appropriate fluorochrome-conjugated or biotinylated primary Abs for 15-30 min in the dark at room temperature. Anti-CD16/32 binds to FcγRII/III and the immunoglobulin in mouse serum binds to FcγRI, and so the FcR blocking buffer blocks non-specific binding of Ab to such FcR-bearing cells. Details of the Ab clones, their specificities and isotype controls used are provided in Table 2.1. Cells were then washed with 1 ml FACS buffer as before and, where appropriate, biotinylated Abs were detected following incubation with fluorochrome-conjugated streptavidin (BD) for 15-30 min in the dark at room temperature. Finally, cells were washed again in FACS buffer re-suspended in 100-300 μl FACS buffer for analysis using a FACS Calibur (BD) and Flowjo software (version 8.8.6, TreeStar). Two or three-colour analysis was performed on a minimum of 10,000 events.

2.9.2 Cell cycle analysis by DNA content

Propidium iodide (PI) is a fluorescent dye that is able to intercalate into DNA in a stochiometric fashion enabling determination of the DNA content of cells. Thus, following permeabilisation of human B cells with 70% ethanol for 15 min on ice, cells were centrifuged and the pellet resuspended in 100 μl PI stain solution (PBS containing 0.5%

FCS, 2 mM EDTA, 50 µg/ml PI, 50 µg/ml RNAse A) and incubated at 4℃ for 30 min. FACS buffer (100 µl) was added and the cells filtered through nitex to remove clumps and analysed by FACS. However, due to strong autofluorescence after ethanol treatment, WEHI-231 cells and murine B cells were stained following a different protocol. Thus, these cells were harvested and washed twice in ice-cold FACS buffer before being resuspended in 200 µl PI stain (0.1% (w/v) sodium (tri) citrate, 0.1% (v/v) triton-X-100, 50 µg/ml PI, 50 µg/ml RNase A) for 45 min on ice. After addition of a further 200 µl of FACS buffer, cells were passed through nitex and analysed for PI fluorescence by FACS (FACS Calibur, BD).

Data were analysed by setting gates that identify the G0/G1 peak which represents 2n DNA, the cells that are in G2/M phase containing 4n DNA (double the fluorescence intensity) and the S phase located between the G0/G1 and G2/M peaks. Cells containing sub-diploid DNA show lower fluorescence than the G0/G1 peak and represent the apoptotic fraction (Fig.2.5).

2.9.3 $DiOC_6$ staining of mitochondrial potential

$DiOC_6$ is a cationic lipophilic dye that is incorporated into the mitochondrial membrane in a manner that is directly proportional to the mitochondrial membrane potential (MMP). Cells were stained in a solution of 2.5 µM $DiOC_6$ (Molecular Probes) in FACS buffer for 30 min at RT. Before analysis by FACS, the cells were washed twice with 1 ml FACS buffer and passed through nitex to remove cell clumps. The profiles obtained were used to set gates to divide cells into those with high (healthy) or low (apoptotic) MMP (Fig. 2.6).

2.9.4 CFSE staining of cell division

CFSE is a cell-permeable dye that becomes trapped inside cells following labelling and consequent binding to intracellular proteins. During each cell division therefore, the amount of cellular dye is halved and this can be detected as a shift to lower fluorescence intensity by FACS analysis Thus, each 50%-reduction of the fluorescence signal represents one division (Fig. 2.7). Briefly, prior to this analysis, cells (10^5/sample) were resuspended in PBS containing 0.1% BSA and loaded with 2.5 µM CFSE for 10 min at 37℃. The cells were then washed with 10 ml cold cu lture medium followed by a wash step with 10 ml warm medium followed by culture with the appropriate stimuli. The cells were analysed for CFSE-staining (intensity) by FACS analysis of cells in the FL-1 channel. The dilution of CFSE in the cells was then analysed using Flowjo software creating gates correlating with the number of cycles of proliferation (generations) the cells have undergone. As it has been found in this and other laboratories that murine B cells do not

generate discrete division peaks, the feasibility of the method was independently validated in this laboratory by Dr. Angela Morton utilising a T cell transfer model. Thus, *in vivo* antigen-stimulation of CFSE-labeled transferred T cells displayed CFSE dilution showing proliferation upon stimulation compared to unstimulated T cells (Fig. 2.7).

2.9.5 FACS-based caspase activation assay

This assay (BioVision) utilises a cell-permeable version of the pan-caspase inhibitor VAD-FMK conjugated to FITC which irreversibly binds to activated caspases and hence allows the detection of such activated caspase in cells. Briefly, cells were plated out (10^6 cells/well) with the appropriate treatments and incubated for up to 24 h. Cells were then transferred into FACS tubes and incubated with 1 µl FITC-VAD-FMK at 37°C/5% CO_2 for 45 min. The cells were then washed twice with 300 µl wash buffer (supplied by manufacturer) and the pellet was resuspended in 200 µl FACS buffer. The labelled cells were analysed by FACS by measuring the fluorescence intensity in the FL-1 channel.

2.10 Signalling assays

2.10.1 LSC (Laser Scanning Cytometry)

A key method for the *in situ* analysis of signalling pathways in immune cells has been established in this laboratory and involves Laser Scanning Cytometry (LSC) analysis of immunofluorescently-stained cytospins or tissue [311]. The use of LSC to analyse stained cells allows quantification and imaging of cell signalling molecules at the single cell level and within their physiological niche in tissue. Unlike FACS, which only allows detection of positive cells and their fluorescence intensity, the LSC also allows analysis of the subcellular localisation of the molecules. This can be very important especially for the analysis of signalling pathways as the localisation often determines the activity of a molecule.

2.10.1.1 LSC data collection

Detection of cytocentrifuged cells by LSC involves the use of analysis “contours” (Fig. 2.8A, figure reproduced with kind permission [312]). The primary contour, also called the threshold contour, is commonly set on cell nuclei which were stained with a dye that binds DNA, such as DAPI. To exclude detection of artefacts such as cell debris, the minimum detection area was set to 30 μm^2, allowing nuclei of 30 μm^2 or above to be scanned. In order to define the outer edge of the cell and hence allow the calculation of the total fluorescence within the cell, the integration contour was then set 10 pixels outside the

threshold contour (1 pixel equates to 0.5 µm). Furthermore, a peripheral contour was set between the threshold and integration contours enabling the detection of fluorescence emitted in the periphery of the cell (Fig. 2.8A). The background fluorescence outside the cells was measured by setting two background contours. This value was then automatically deducted from all measured fluorescence values.

Before scanning each batch of slides the detector gain voltages (PMTs) were adjusted in order to optimise fluorescence excitation with the maximum value of 75 for the number of saturated pixels. Furthermore, appropriate data collection protocol (.PRO) and display (.DPR) files were set up for each experiment [311]. The next step was to set the threshold value to a value between 5500 and 7500 fluorescence units to ensure the optimal detection of the cells as setting the threshold too high might exclude cells with low or medium DAPI staining from the analysis. A very low threshold, on the other hand, can lead to the erroneous detection of multiple cells as a single event (Fig. 2.8B, figure reproduced with kind permission [312]). Finally, the slide area was then scanned and the data file saved for analysis.

2.10.1.2 Cell cycle analysis by LSC

It has been shown previously that LSC can be used for the efficient examination of the cell cycle status of individual cells [313-315] as it determines both the content and concentration of DNA at the same time. Therefore, by plotting Max Pixel (the most highly fluorescent pixel value in the cell) against Integral (sum of all fluorescence in the cell) values of the nuclear staining, such as DAPI, the different cell cycle stages can easily be identified (Fig. 2.9, figure adapted with kind permission from [312]). This is because DAPI Max Pixel values correlate with concentration of the cellular chromatin (condensation) whereas the DAPI Integral value correlates with the absolute levels of DNA content. For example, cells in S phase (green gate) can be identified by their increased DNA content. However, cells in the other mitotic stages (G2/M phase) which also contain high amounts of DNA can be differentiated due to the higher level of chromatin condensation (max pixel; yellow gate). By contrast, cells arrested at the G1/G0 stage (red gate) of the cell cycle contain half the amount of DNA (2n DNA) compared to cells in G2/M (4n DNA) and can therefore be identified by the lower DNA content, as detected by lower DAPI Integral values. Cells undergoing apoptosis (blue gate) contain subdiploid DNA content due to their fragmented DNA placing them below cells in G1/G0 on the scattergram. New daughter cells (purple gate) represent cells which have recently undergone mitosis and can be identified due to their small nuclei with still highly condensed DNA. Representative images of cells in each stage of the cell cycle were captured using the xy re-location feature of

LSC to confirm that the cells in the various cell cycle gates were morphologically consistent with their cell cycle stage as detected on the scattergram [312] (Fig. 2.9).

2.10.1.3 Immunofluorescence staining

Cytospins were generated by centrifuging cells (0.75×10^5) onto glass slides at 40 *g* for 4 min. The following staining protocol was carried out at room temperature with incubation being performed in a darkened, humidified chamber. Firstly, the cells were fixed with 4% formaldehyde in PBS for 15 min and washed with PBS for 5 min, followed by incubation with permeabilisation buffer (2% FCS, 2 mM EDTA pH 8.0, 0.1% w/v saponin in PBS) for 5 min. Blocking of non-specific binding was performed after three washes with PBS (10 s each) with blocking/antibody-dilution buffer (PBS containing 1% BSA, 0.1% w/v saponin) for 10-15 min. The cells were then incubated with primary antibody (appropriate dilutions listed in Table 2.1) or the equivalent dilution of an appropriate IgG isotype/irrelevant antibody control for 30 min. Cells were then washed and incubated for 25 min with the appropriate HRP (horse radish peroxidase) - labeled anti-Ig antibody (diluted 1:100, Cell Signaling Technology, NEB) followed by another three washes with TNT buffer (100 mM Tris base, pH 7.5, 150 mM NaCl, 0.05% Tween-20) before Alexa Fluor® 488 tyramide (diluted 1:100, Invitrogen) was added for 10 min. After three washes with TNT buffer the cells were stained with 300 nM DAPI (in PBS, 0.1% saponin) for 4 min, washed with TNT buffer three times and left to air-dry for 5 min and covered with mounting medium (Vector). Pictures were acquired using a laser scanning microscope (Compucyte) and quantitatively analysed using Wincyte software version 3.6 (Compucyte).

2.10.2 WideScreen™ EpiTag™ ERK pathway assay

This assay allows simultaneous analysis of multiple signalling molecules and their phosphorylation status in a single sample. Briefly, the cells are lysed and the cellular proteins are extracted before digestion with proteases to create peptides. Antibodies specific for particular peptide epitopes are then used to detect molecules of interest. The principle of the assay is therefore the same as for other bead-array multiplex assays in that the different capture antibodies are bound on beads which emit fluorescence of distinct wavelengths and hence allow differentiation of beads coated with antibodies specific for the different target peptides. In addition, fluorescently labeled detection antibodies are used to label peptides bound to beads which are then analysed on a Bio-Plex (BioRad) machine. Thus, whilst the beads are recognised due to their specific emission, the intensity of bound detection antibody can also be measured to yield information on the amount of bound peptide relative to defined peptide standards and hence enabling the

absolute quantitation of protein in each sample.

The EpiTag™ assay (Merck) was used to detect phosphorylated B-Raf (p-B-RafS446) with ERK2 as the internal reference control protein. Phosphorylation at S446 stops auto-inhibition of B-Raf enhancing its activity [316]. The protocol was carried out using reagents supplied by the manufacturer and according to their instructions. Briefly, 0.5 x 10^7 cells/stimulation were cultured for the indicated time in the presence of appropriate stimuli. The cells were then washed twice with ice-cold PBS and lysed by the addition of 100 µl supplemented lysis reagent (lysis reagent, 1x phosphatase inhibitor cocktail, 0.5 U/µl benzonase nuclease) and incubation at room temperature for 5 mins with occasional vortexing. Subsequently, the samples were transferred to microcentrifuge tubes and incubated for an additional 20 min at 4°C. Following this incubation, 5 µl of each sample were set aside to perform quantitation of the total protein amount by BCA protein assay (Pierce) and the remainder of the sample was stored at -70°C until further use. The concentration of the samples was then adjusted to 1 mg/ml and 100 µl aliquots were digested as follows. Firstly, the lysates were denatured by the addition of 2 mM of the reducing agent TCEP (Tris(2-carboxyethyl)phosphine) and incubation at 95°C for 5 min before centrifugation of the sample at 12,000 *g* for 10 min and transfer of the supernatants into fresh tubes. Following alkylation of the supernatant by the addition of 10 mM α-Iodoacetamide (30 min at room temperature), proteins were digested with 5.7 mU Endopeptidase Lys-C at 37°C overnight. The samples were then adjusted to 400 µl by the addition of 287 µl Assay Diluent. The detection of p-B-Raf and ERK2-derived peptides was carried out by analysis on a Bio-Plex machine (BioRad) according to the manufacturer's instructions. Briefly, dilutions of the provided standard solutions were prepared by consecutive 1 in 3 dilutions in titration buffer (25% lysis reagent, 75% assay diluent). The provided filter plate was pre-wetted with 100 µl assay diluent per well and the liquid aspirated with a vacuum manifold. The capture beads were vortexed and 50 µl pipetted in each well followed by the addition of either 50 µl of the standard dilutions or 50 µl of the samples which had been further diluted 1 in 4 in titration buffer before addition to the plate. After 2 h incubation on a platform shaker the beads were washed three times with wash buffer and 100 µl Biotin-coupled detection antibody was added. The plate was then incubated for a further hour at room temperature on a platform shaker followed by three washes with wash buffer and the addition of 100 µl of Streptavidin-PE solution. The plate was incubated for 30 min at room temperature after which time the beads were washed three times with wash buffer and resuspended in 120 µl Assay diluent. Finally, 100 events per sample were acquired on a Bio-Plex (BioRad) machine on low gain RP1-setting.

2.11 PCR

2.11.1 mRNA isolation and reverse transcription

Total mRNA was isolated from purified B cells or WEHI-231 cells using an RNeasy Mini Kit (Qiagen) following the manufacturer's instructions and the mRNA was stored at -20℃ until further use. Optional DNAse I digestion was carried to digest possible genomic DNA impurities. To this end, DNAse I, amplification grade (Invitrogen), was used as per the manufacturer's instructions. In short, the RNA sample was digested at room temperature with 1 unit DNAse I for 15 min and then the enzyme was inactivated by addition of 2.5 mM EDTA and incubation at 65℃ for 10 min. Those pretreated samples were then used for reverse transcription with the Superscript II Reverse Transcriptase system (Invitrogen) to transcribe mRNA into cDNA following the manufacturer's instructions. Briefly, between 500 ng and 5 µg of mRNA were incubated with Oligo(dT) primers (500 µg/ml) and dNTP mix (10 mM each) at 65℃ for 5 min. After the addition of 0.1 M DTT and 5 x First Strand buffer, the mixture was heated for 5 min at 42℃ and 200 Units of Superscript enzyme were added. The reaction was carried out at 42℃ for 50 min followed by 15 min at 70℃ to inactivate the enzyme . Alternatively, DNAse-digested RNA was transcribed into cDNA using the "High Capacity cDNA Reverse Transcription Kit" (Applied Biosystems) following the manufacturer's instructions. Thus, between 500 ng and 5 µg of mRNA were incubated with random primers, 4 mM dNTPs and 50 units MultiScribe^{TM} Reverse Transcriptase for 10 min at 25℃ followed by 120 min at 37℃ and a final step at 85℃ for 5 s.

2.11.2 Real-time PCR by TaqMan®

Primers and probes (Table 2.2) were designed using PrimerExpress software (Applied Biosystems) and purchased from VH Bio. In some cases pre-designed primers/probe supplied in the form of Endogenous Control Kits or Taqman® Gene Expression Assays (Applied Biosystems) were used. TaqMan® real-time PCR was performed using a 2 x mastermix (Eurogentec) which contains dNTPs/dUTPs, Hot Gold Star enzyme, $MgCl_2$, UNG, stabilizers and the Rox passive reference. The probes contained a reporter dye (FAM) attached to the 5' end and a quencher dye (TAMRA) attached to the 3' end (Table 2.1). The PCR reactions were performed in the ABI-prism 7700 Sequence Detector or the 7900HT Fast Real-Time PCR System (Applied Biosystems). The reactions were performed in 10 µl total volume containing the 1 x mastermix, 200 nM primers and 900 nM probes. Amplification was performed using the

following conditions: 2 min at 50℃, 10 min at 95℃ , followed by a total of 45 two-temperature cycles (15 s at 95℃ and 1 min at 60℃) .

2.12 Western Blotting, ”pull-down”-based assays and subcellular fractionation

2.12.1 Whole cell lysates

Mature B cells or WEHI-231 cells (10^7 cells/stimulation) were stimulated as indicated. The cells were then washed in PBS and the reactions were terminated by the addition of 100 µl of ice-cold modified RIPA lysis buffer (50 mM Tris buffer, pH 7.4 containing 150 mM sodium chloride, 2% (v/v) NP 40, 0.25% (w/v) sodium deoxycholate, 1 mM EGTA, 10 mM sodium orthovanadate, 0.5 mM phenylmethylsulfonylfluoride, 10 µg/ml chymostatin, 10 µg/ml leupeptin, 10 µg/ml antipain, 10 µg/ml pepstatin A and 10 µg/ml aprotinin). After resuspending the pellet, the cells were solubilised for 30 min on ice before centrifugation of lysates at 16,000 *g* for 15 min. The resulting supernatants (whole cell lysate) were stored at -20^{o}C before being used for Western Blot analysis.

2.12.2 Nuclear extraction

An Active Motif Nuclear Extract kit was used to produce nuclear and cytosolic fractions. The protocol was followed as per the manufacturer’s instructions (overview in Fig.2.10). Briefly, cells (10^7) were incubated with the appropriate stimuli at 37°C in a 5% (v/v) CO_2 atmosphere at 95% humidity. Samples were washed with 5 ml of PBS containing phosphatase inhibitors to terminate any cellular reactions, and then centrifuged for 5 min at 400 *g*. The pellets were resuspended in 500 µl of hypotonic buffer by pipetting and then incubated on ice for 15 min. Following this, 25 µl of detergent (supplied with kit) was added and the samples were vortexed on the highest setting for 10 s. Samples were then centrifuged at 14,000 *g* for 30 s and the supernatant removed. This supernatant contains the cytosolic fraction and can be stored at -80 °C for further use. The pellet was then resuspended in 50 µl of complete lysis buffer (containing DTT and protease inhibitor cocktail) and vortexed for 10 s. The samples were then left on ice for 30 min and after a further vortexing centrifuged at 14,000 *g* for 10 min. The resultant supernatant contains the nuclear fraction and was stored at -80 °C.

2.12.3 Mitochondrial fractionation

An Active Motif Mitochondrial Fractionation kit was used to produce mitochondrial, nuclear and cytosolic fractions using a slightly modified version of the manufacturer’s

instructions as follows (overview in Fig.2.10). Briefly, cells (0.5-1 x 10^8) were incubated with the appropriate stimulations at 37°C in a 5% (v/v) CO_2 atmosphere at 95% humidity. To terminate reactions, samples were washed with 2 ml of PBS and centrifuged for 5 min at 400 *g*. The pellets were resuspended in 1 ml of ice cold 1x cytosolic buffer by pipetting and then incubated on ice for 15 min. Following this, the cell suspension was transferred to a pre-chilled homogeniser and lysed by the application of 40 strokes. The samples were then centrifuged at 400 *g* for 20 min to sediment cell debris, the supernatant transferred into a fresh tube and centrifuged at 800 *g* for 10 min. The supernatant, containing the mitochondria, was again centrifuged (8000 *g* for 20 min) after which the supernatant was transferred into a fresh tube (cytosolic fraction) and the pellet washed in 100 µl cytosolic buffer (8000 *g*, 10 min). The pellet was resuspended in 100 µl complete mitochondria lysis buffer, incubated on ice for 15 min and vortexed for 10 s to produce a solubilised mitochondrial fraction.

2.12.4 Subcellular fractionation

To obtain cytoplasmic, membrane/organelle, nuclear and cytoskeletal fractions a Cellular Protein Fractionation kit (Perkin Elmer) was used. This kit utilises different detergents to extract proteins from various subcellular compartments due to their differential solubility. The experiments were carried out as per the manufacturer's instructions except for slight changes of cell numbers and buffer volumes (overview in Fig.2.10). Briefly, cells (5 x 10^6) were incubated with appropriate stimulations at 37°C in a 5% (v/v) CO_2 atmosphere at 95% humidity. For some experiments, samples were counted again after harvesting and cell numbers were adjusted to match the sample with the lowest cell count. All buffers were supplemented with protease inhibitors immediately before use. Briefly, samples were washed with 2 ml of wash buffer twice (centrifuged at 400 *g* for 5-10 min) and the resulting pellet was resuspended in 200 µl ice-cold cytoplasmic buffer. The samples were then incubated at 4°C for 10 min on an orbital rotator. The insoluble fraction was pelleted by centrifugation at 1000 *g* for 10 min (4°C) and the supernatant transferred to a fresh tube (cytoplasmic fraction). The pellet was resuspended in 200 µl chilled membrane/organelle buffer and the samples were incubated for further 30 min at 4°C on an orbital rotator. The insoluble fraction was again collected by centrifugation (6000 *g*, 4°C) and the supernatant, representing the membrane/organelle-enriched fraction, was transferred to a fresh tube. To acquire the nuclear fraction, the insoluble material from the membrane/organelle enrichment was resuspended in 100 µl nuclear buffer followed by incubation at 4°C for 10 min on an orbital rotator. The cytoskeletal fraction was then

pelleted by centrifugation (6800 *g*, 10 min, 4°C) and the supernatant tranferred to a fresh tube (nuclear fraction). The cytoskeletal fraction was resuspended in 100 µl of cytoskeletal buffer.

2.12.5 Rap-1 activity assay

A Rap-1 activation kit (Upstate Biotechnology) was used to determine the activity of Rap-1 in WEHI-231 cell samples. Briefly, cells (1.25 x10^7) were harvested after stimulation and washed twice with cold TBS (50 mM Tris-HCl pH 7.4, 150 mM NaCl). Cells were incubated with 500 µl lysis buffer and the released DNA sheared by passing the lysate through a syringe needle. The lysate was cleared by centrifugation (5 min, 13,000 *g*) and 50 µl Ral-GDS-RBD (Ras-binding domain of the Ral guanine nucleotide dissociation stimulator) agarose slurry added. After 45 min incubation at 4℃ the beads were washed three times with 500 µl lysis buffer (30 s, 13,000 *g*). The agarose beads were then resuspended in 40 µl 2x reducing SDS-PAGE loading buffer (NuPAGE system, Invitrogen) and boiled for 5 min. Samples were analysed by SDS-PAGE gel electrophoresis followed by Western Blotting using anti-Rap-1 antibodies.

2.13 SDS-PAGE gel electrophoresis

The protein concentration of whole cell lysates or nuclear, cytoplasmic or mitochondrial fractions was assessed by either the BCA protein assay (Pierce) or the Bradford assay (BioRad). The BCA protein assay is more suited for whole cell lysates whereas the different detergents used for the cytoplasmic, nuclear and mitochondrial fractions made it necessary to use the Bradford assay. Equal protein amounts (whole cell lysates) or cell equivalents (using the Perkin Elmer Cellular Protein Fractionation kit) of samples were resolved using the XCell *SureLock* Mini-Cell kit with NuPAGE Novex high-performance pre-cast Bis-Tris gels and NuPAGE buffers and reagents (all supplied by Invitrogen). The appropriate volume of 4 x NuPAGE LDS (Lithium Dodecyl Sulfate) sample buffer and 10 x NuPAGE reducing agent were added prior to heating samples to 70^{o}C for 10 min and samples were resolved using NuPAGE Bis-Tris gels (10%, 12% or 4-12%) with NuPAGE MOPS or MES running buffer (supplemented with NuPAGE antioxidant) at 200 V for 50 min following the manufacturers instructions. The gel was then transferred onto a nitrocellulose membrane (Amersham) using NuPAGE transfer buffer with 20% (v/v) methanol at 30 V for at least 1 h.

2.14 Western Blotting

Following transfer, nitrocellulose membranes were washed once in TBS/Tween (0.5 M NaCl and 20 mM Tris pH7.5 with 0.1% (v/v) Tween-20) and blocked for 1 h in TBS/Tween containing 5% non-fat milk protein. Membranes were then incubated with the appropriate primary detection antibody overnight at 4^{o}C. All antibodies were diluted in TBS/Tween with 5% BSA. Following incubation with primary antibody, nitrocellulose membranes were washed (5 x 5 min) with TBS/Tween and incubated in the appropriate HRP-conjugated secondary antibody containing 5% non-fat milk protein for 1 h at room temperature. Nitrocellulose membranes were then washed (5 x 5 min) with TBS/Tween and protein bands were visualised using the ECL detection system. Nitrocellulose membranes were incubated in a mixture of equal volumes of ECL solution A (2.5 mM luminol, 0.4 mM p-coumaric acid and 100 mM Tris pH 8.5) and ECL solution B (0.002% hydrogen peroxide and 100 mM Tris pH8.5) for 1 min before exposing membranes to Kodak X-Ray film. Nitrocellulose membranes were sometimes stripped and re-probed with an alternative primary antibody. Membranes were stripped at room temperature for 1 h in stripping buffer (100 mM 2-mercaptoethanol, 2% SDS and 62.5 mM Tris pH 7). Nitrocellulose membranes were washed thoroughly in TBS/Tween and checked for residual signal before re-starting the Western Blotting protocol.

2.15 Cloning of Rap-1A WT, Rap-1A G12V and Rap-1A S17N into pcDNA3.1 (-) Zeo, pIRES2-AcGFP1 and pLVX-IRES-ZsGreen1 vectors

2.15.1 Transformation of chemically competent bacteria

One Shot® TOP10 competent *Escherichia coli* (*E. coli*; Invitrogen) cells were transformed with appropriate plasmids (Table 2.3) as per the manufacturer's instructions. Briefly, 0.1 - 0.5 µg plasmid or 5 µl ligation-reaction were added to 50 µl One Shot® cells and mixed by gentle tapping. Subsequently, the reactions were incubated on ice for 30 min. Following this incubation, the cells were heat-shocked at 42°C for 30 s before being placed on ice. Following the addition of 250 µl pre-warmed SOC media (2% (w/v) tryptone, 20 mM $MgSO_4$, 0.5% (w/v) yeast extract, 8.6 mM NaCl, 2.5 mM KCl, 20 mM glucose, Sigma), the vials were shaken at 3 *g* for 60 min at 37°C in an Innova 4400 incubator shaker (New Brunswick Scientific (UK) Ltd., St. Albans, Herts, UK). Each transformation was then spread on separate Luria broth (LB) agar plates containing 100 µg/ml ampicillin or 50 µg/ml kanamycin which were incubated at 37°C overnight.

2.15.2 PCR amplification of Rap-1A WT, Rap-1A G12V and RapS17N

In order to sub-clone Rap-1A WT, Rap-1A G12V and Rap-1A S17 into the pLVX-IRES-ZsGreen1 vector, the cDNA had to be amplified by PCR to introduce convenient restriction sites (Eco RI/Xba I). The pcDNA3.1 constructs (Missouri S&T cDNA Resource Center) were used as template DNA for the following PCR reaction. In short, 50 ng of the vector were mixed with Taq DNA Polymerase buffer (Invitrogen), 0.5 µM of the forward primer pcDNA3.1-Rap FW and the reverse primer pcDNA3.1-Rap RV (for sequence details see Table 2.3B), 0.2 mM dNTP mix (New England Biolabs), 1.5 mM $MgCl_2$ and 1.25 units of Taq DNA Polymerase (Invitrogen) and the volume adjusted with sterile dH_2O to 50 µl. Amplification was performed using the following conditions: 3 min at 95℃, followed by a total of 35 three-temperature cycles (30 s at 94℃, 30 s at 55℃ and 1 min at 72℃) and 10 min at 72℃. The PCR was then separate d on an agarose gel (1% (w/v) agarose in Tris-Acetate-EDTA (TAE) buffer with 667 ng/ml of the fluorescent DNA-intercalating dye, ethidium bromide). Subsequently, the appropriate PCR fragments were cut out of the gel and DNA was purified according to the manufacturer's instructions using a Gel Extraction Kit (Qiagen).

2.15.3 Restriction digest

The vectors (1 µg per reaction) or PCR-fragments (16.8 µl of the 50 µl PCR reaction) were digested by the addition of restriction enzyme buffer (Promega), 10 units of the appropriate restriction enzyme (see Table 2.3C), 0.2 µl BSA solution (Promega) and sterile dH_2O to a total volume of 20 µl per reaction. The digest was carried out at 37℃ for 1 h. Following this incubation, the digested DNA was separated on an agarose gel, as described above, and bands comprising either vector fragments or inserts were cut out and the DNA purified by gel extraction.

2.15.4 Ligation reaction

Appropriate vector fragments and inserts/PCR fragments (see Table 2.3C) were ligated in the following reaction: 5 µl digested vector and 12.6 µl digested insert/PCR fragment were mixed with T4 DNA ligase buffer (New England BioLabs), 160 units T4 DNA ligase (New England BioLabs) and incubated for 1 h at room temperature. Aliquots (5 µl) of this ligation reaction were then transformed into TOP10 *E.coli* as previously described and the bacteria were spread on LB agar plates containing 100 µg/ml ampicillin or 50 µg/ml kanamycin which were incubated at 37℃ overnig ht.

2.15.5 Screening for positive clones

To screen for bacteria expressing plasmids containing the desired inserts (Rap-1A WT, Rap-1A G12V and Rap-1A S17), single bacterial colonies were picked and used to inoculate 5 ml LB cultures containing 100 µg/ml ampicillin or 50 µg/ml kanamycin. The bacteria were allowed to grow over night at 37°C, shaking at 5 *g*. Following this incubation, the cells were centrifuged at 6000 *g* for 3 min and plasmid DNA was extracted using Plasmid Mini Kits (Qiagen). The plasmids were then digested with the appropriate restriction enzymes (see Table 2.3C), as described above. Finally, plasmids that harboured fragments of the desired size were chosen and the inserts sequenced (Geneservice). Plasmids with the correct sequence were then purified on a larger scale, as described below, and stored at -20°C until further use.

2.15.6 Purification of plasmid DNA

The plasmids were purified using HiSpeed Plasmid Midi Kits (Qiagen, Crawley, UK) as per the manufacturer's instructions. Briefly, single bacterial colonies were picked and used to inoculate a starter culture of 5 ml LB broth containing 100 µg/ml ampicillin or 50 µg/ml kanamycin. The cultures were incubated at 37°C with vigorous shaking (5 *g*) for 6-8 h before being diluted 1:500 in 100 ml LB broth containing ampicillin or kanamycin and cultured at 37°C with vigorous shaking for 16 h. The bacterial cells were then harvested by centrifugation at 6000 *g* at 4°C for 20 min and re-suspended in 6 ml buffer P1 (all buffers and components supplied with kit). To lyse the cultures, 6 ml of buffer P2 was added and the cultures were mixed gently and incubated at 37°C for 5 min followed by the addition of 6 ml chilled P3 buffer. Next, the cultures were mixed and poured immediately into the barrels of QIAfilter cartridges and incubated at room temperature for 10 min. The plungers were then inserted into the QIAfilter cartridges and the cultures were filtered into HiSpeed tips (previously equilibrated with 4 ml buffer QBT) and the HiSpeed tips were washed with 20 ml buffer QC before the relevant DNA was eluted with 5 ml buffer QF and collected in 15 ml tubes. DNA was then precipitated by addition of 3.5 ml isopropanol and incubation at room temperature for 5 min. This mixture was then filtered through a QIAprecipitator before the DNA was washed with 2 ml 70% ethanol. The membrane was then dried by forcing air through the QIAprecipitator and the DNA was eluted with 0.5 ml sterile dH_2O and collected into a 1.5 ml tube. To ensure a maximum yield the elution was repeated using the same filter and sample. Finally, the DNA concentration was determined by an Eppendorf BioPhotometer (Eppendorf).

2.16 Transfection of WEHI-231 cells

The relevant vectors (10 µg; see table 2.3A and Fig. 2.11-12 for information on the vectors) were digested with 10 units of *Pvu I* (pcDNA3.1/pcDNA3.1 Zeo-based vectors) or *Cla I* (pIRES2-AcGFP1-based vectors) (New England Biolabs) for 2 h at 37°C to linearise them. The DNA was then purified using a PCR purification kit (Qiagen) following the manufacturer's instructions and the linearised vector stored on ice until further use. For some experiments the vectors (5 µg) were used in a non-linearised form.

WEHI-231 cells were split 24 h prior to transfection. Before transfection the cells ($5x10^6$) were washed once with electroporation media (RPMI-1640 containing 20% FCS) and resuspended at a concentration of $2x10^7$ cells/ml. The linearised vector was cooled in a cuvette on ice for 5 min and then mixed with the cells followed by another incubation (10 min) on ice. Following optimisation, electroporation was carried out at 1000 µFarads and 140 V. After the cells had been left on ice for a further 10 min they were transferred into complete media (RPMI-1640, 2 mM L-glutamine, 100 U/ml penicillin, 100 µg/ml streptomycin, 20% FCS, 1% non-essential amino acids, 1 mM sodium pyruvate) and incubated for 48 h at 37°C to recover.

Alternatively, cells were transfected using the Nucleofector® Kit L (Amaxa). Briefly, cells ($2x10^6$) were washed once with complete media (RPMI-1640 , 2 mM L-glutamine , 100 U/ml penicillin, 100 µg/ml streptomycin, 5% FCS, 1% non-essential amino acids, 1 mM sodium pyruvate) and resuspended in 100 µl Nucleofector solution L. Following addition of 5 µg of the relevant vector, the cells were transferred into cuvettes (Amaxa) and electroporation was carried out using the advised pre-set programme (C-005) on the Nucleofector™ II (Amaxa). The cells were then transferred into complete media and incubated at 37°C for 48 h.

Irrespective of the protocol used for transfection the cells were washed through FCS once after the recovery phase and resuspended in complete media supplemented with varying concentrations of G418 (Promega) or Zeocin (Invitrogen) to select for neomycin- or zeocin-resistant gene expression.

2.17 Generation of lentiviral particles and transduction of HT-1080 cells

Lentiviral-based transduction can be used to stably introduce DNA into the genome of various cell types [317]. To this end, a lentiviral expression vector containing the gene of interest is co-transfected with plasmids expressing the packaging components needed for

the assembly of the virus. The cells used for the production of virions are a 293T-based packaging cell line (Lenti-X 293 T cells, Clontech) which produces infectious virions after transfection with the above-mentioned vectors and releases them into the supernatant which can then be used to transduce the target cells. In this study, pLVX-IRES-ZsGreen1 was chosen as the parental vector in which the gene of interest was inserted. This vector encodes the ZsGreen1 protein which, when excited by a 488 nm laser, fluoresces green and can be detected by FACS analysis (FL-1 channel). The gene of interest and the ZsGreen1 gene are connected by an IRES (internal ribosome entry site) sequence. Thus, both genes are transcribed as a single mRNA and then simply translated as separate proteins at the ribosome. ZsGreen1 therefore acts as a marker protein and expression of ZsGreen1 should directly correlate with the expression of the protein of interest.

2.17.1 Production of lentiviral particles in Lenti-X 293 T cells

Lenti-X 293 T cells were maintained in Dulbecco's Modified Eagle's Medium (DMEM) containing 4 mM L-glutamine, 4.5 g/L glucose, 1 mM sodium pyruvate, 1.5 g/L sodium bicarbonate, and 10% FCS. One day before transfection, the cells were washed once in DMEM media containing 10% tetracycline-free FCS and 4 x 10^6 cells were plated out in a 10 mm cell culture dish. The tetracycline-free FCS ensures the efficient production of virus-particles, as the packaging system utilises Tet-Off transactivation to drive high-level expression of the viral packaging proteins. Tetracycline present in the media would therefore reduce the expression of these proteins and potentially decrease viral titres. Transfection of Lenti-X 293 T cells was carried out 12-24 h after plating out the cells using the Lenti-X HT Packaging System (Clontech) and following the manufacturer's instructions. Briefly, 15 µl of the Lenti-X HT packaging mix (contains the plasmids encoding proteins needed for packaging), 3 µg of the various pLVX-IRES-ZsGreen1-based vectors (for vector information see Table 2.3) and sterile water (to make up the total volume to 438 µl) were mixed with 62 µl Lentiphos 1 solution and then 500 µl Lentiphos 2 solution was added drop-wise while vortexing. The solution was incubated at room temperature for 5 to 10 min to allow the formation of DNA precipitates. After this time the solution was added drop-wise to the Lenti-X 293 T cells which were then incubated at 37℃/5% CO_2 for 8-16 h. Following the replacement of the media, cells were left for an additional 48 h. The virus-containing supernatant was then harvested, aliquoted and stored at -80℃ until further use.

2.17.2 Transduction of HT-1080 cells with lentiviral particles

HT-1080 cells are a cell line which is easily transduced by lentiviruses. It can therefore be used to test the transduction efficiency of lentiviral particles produced by the Lenti-X 293 T packaging cell line. HT-1080 cells were grown in DMEM containing 2 mM L-glutamine, 4.5 g/L glucose, 1 mM sodium pyruvate, 1.5 g/L sodium bicarbonate, and 10% FCS. For transduction, HT-1080 cells (2×10^5 cells/well) were seeded into 6-well plates in 2 ml complete media 12 - 24 h before transduction with the virus-containing supernatants. The cells were then transduced by incubating them with 600 µl supernatant for 12 h. After replacing the media the cells were incubated for an additional 48 h after which they were analysed by FACS to detect ZsGreen1 expression.

Suppliers addresses

Abcam plc
332 Cambridge Science Park
Cambridge CB4 0FW

Active Motif
104 Avenue Franklin Roosevelt
Box 25
B-1330 Rixensart
Belgium

Alexis Biochemicals
c/o AXXORA (UK) Ltd.
P.O. Box 6757 Bingham
Nottingham NG13 8LS

Amaxa AG
Nattermannallee 1
50829 Cologne
Germany

Amersham/GE Healthcare UK Ltd
Amersham Place
Little Chalfont
Buckinghamshire HP7 9NA

Applied Biosystems
Lingley House
120 Birchwood Boulevard
Warrington WA3 7QH

BD Biosciences
21 Between Towns Road
Cowley
Oxford OX4 3LY

BioLegend distributed by
Cambridge BioScience Ltd.
24-25 Signet Court
Newmarket Road
Cambridge CB5 8LA

Bio-Rad Laboratories Ltd.
Bio-Rad House
Maxted Road
Hemel Hempstead
Hertfordshire HP2 7DX

BioVision distributed by
Cambridge BioScience Ltd.
24-25 Signet Court
Newmarket Road
Cambridge CB5 8LA

Calbiochem
c/o CN Biosciences
Boulevard Industrial Park
Padge Road
Beeston
Nottingham NG9 2JR

Cell Signaling Technology

New England Biolabs (UK) Ltd.
73 Knowl Piece,Wilbury Way
Hitchin
Hertfordshire SG4 OTY

Takara Bio Europe/Clontech
2 Avenue du President Kennedy
78100 Saint-Germain-en-Laye
France

CompuCyte Corporation
385 University Avenue,
Westwood
MA 02090, USA

ECACC

Health Protection Agency Culture Collections
Health Protection Agency
Centre for Emergency Preparedness and ResponsePorton Down
Salisbury
SP4 0JG

Eppendorf UK Limited
Endurance House
Chivers Way
Histon
Cambridge CB24 9ZR

Eurogentec Ltd.
Old Headmasters House
Unit 1, Building 1
Forest Business Centre
Fawley Road, Fawley
Southampton
Hampshire SO45 1FJ

Invitrogen Ltd

Fountain Drive
Inchinnan Business Park
Paisley PA4 9RF

Jackson Immunoresearch Laboratories

c/o Stratech Scientific Ltd.
Unit 7 Acorn Business Centre
Oaks Drive, Newmarket
Suffolk CB8 7SY

Kodak Ltd
Kodak House
Station Road
Hemel Hempstead
Herfortshire HP1 1JU

Merck Serono Ltd
Bedfont Cross
Stanwell Road
Feltham
Middlesex TW14 8NX

Miltenyi Biotec Ltd.
Almac House
Church Lane
Bisley
Surrey GU24 9DR

Pierce/Perbio Science UK Ltd.
Unit 9, Atley Way
North Nelson Industrial Estate
Cramlington
Northumberland NE231WA

PerkinElmer Life and Analytical Sciences
Via Tiepolo, 24
20052 Monza (Milano)
Italy

Promega UK Ltd
Delta House
Southampton Science Park
Southampton
Hampshire
SO16 7NS

QIAGEN Ltd.
QIAGEN House
Fleming Way
West Sussex RH10 9NQ

Santa Cruz Biotechnology Inc.
c/o Insight Biotechnology Limited
PO Box 520
Wembley HA9 7YN

Sigma-Aldrich Company Ltd
Fancy Rd
Poole
Dorset BH12 4QH

Vector Laboratories Ltd
Accent Park
Bakewell Road
Orton Southgate
Peterborough PE2 6XS

VH Bio Ltd.
Unit 11B Station Approach
Team Valley Trading Estate
Gateshead NE11 0ZF

Upstate
c/o Millipore Ltd.
Units 3&5 The Courtyards
Hatters Lane
Watford WD18 8YH

2.18 Figures and Tables

Table 2.1 Antibodies

(A) List of antibodies used for FACS based analysis

(B) List of antibodies used for the stimulation of cells

(C) List of antibodies used for Western Blotting

(D) List of antibodies used for Immunofluorescent staining

If applicable, optimised dilutions are listed.

Figure 2.1 Assessment of purity of $CD19^+$ MACS-sorted cells

To assess the purity of the enriched human B cell population, the cells were stained with anti-CD20-PE and analysed via FACS relative to an unstained sample. The percentage of $CD20^+$ cells was assessed by gating on live cells judging by their FSC/SSC distribution **(A)** followed by setting a gate on the CD20-expressing cells in the FL-2 channel **(B)**.

Figure 2.2 Assessment of B cells purified by negative selection using commercial B cell isolation kits

PBMCs **(A)** and cells purified by either the B cell isolation kit **(B)** or naïve B cell isolation kit **(C)** were stained for CD19 expression and analysed by FACS. The percentage of CD19-positive cells was assessed by gating on live cells judging by their FSC/SSC distribution as described in figure 2.1 followed by setting a gate on the CD19-expressing cells as detected in channel FL-1 by anti-CD19-FITC antibodies and by using unstained cells as a negative control.

Figure 2.3 T cell and monocyte contamination after B cell enrichment

B cells purified using the B cell isolation kit were stained for CD3 **(A)** or CD14 **(B)** expression and analysed by FACS. The percentage of $CD3^+$ or $CD14^+$ cells was assessed by gating on live cells judging by their FSC/SSC distribution as described in figure 2.1 followed by setting a gate on the CD3-APC (FL-4 channel) or CD14-FITC (FL-1 channel) expressing cells using unstained cells as a negative control.

Figure 2.4 Purification of B cells by high speed FACS sorting

Cells from a healthy individual were collected and PBMCs were purified by density centrifugation. The cells were stained with either anti-CD20-PE or anti-CD19-FITC and selected for fluorescence-positive cells. To purify B cells by negative selection, PBMCs were stained with anti-CD3-APC, anti-CD14-FITC and anti-CD56-PE and the unstained cells were selected. The purity of the CD20- **(A)**, CD19- **(B)** or negatively-selected cells **(C)** was assessed by staining for either CD20 or CD19 expression. Unstained cells were used to set the gates determining the percentage of CD20-PE positive cells detected in the FL-2 channel in the CD19-sorted population or the CD19-FITC positive cells (FL-1 channel) in the CD20-sorted and negatively selected populations.

Figure 2.5 FACS determination of cell cycle status by analysis of PI-stained cells

WEHI-231 cells were stained with PI and analysed by FACS using histograms for the FL-3 (**A**; linear) and FL-2 (**B**; log) fluorescence to gate on apoptotic cells (subdiploid DNA content), cells in G0/G1 phase of the cell cycle (2n DNA), cells in G2/M phase (4n DNA) or cells in S phase (DNA content between 2n and 4n).

Figure 2.6 Analysis of mitochondrial membrane potential (MMP) using $DiOC_6$ fluorescence

WEHI-231 cells were stained with $DiOC_6$ (2.5 µM) and analysed by FACS. Gates were set using FL-1 fluorescence histograms in order to identify populations of cells with high or low levels of $DiOC_6$ fluorescence. Anti-IgM treated WEHI-231 **(B)** cells show an increase in the percentage of cells expressing lower $DiOC_6$ fluorescence compared to untreated cells **(A)** indicating that these cells have dissipated their mitochondrial membrane potential which is an early sign of apoptosis.

Figure 2.7 Analysis of cellular proliferation using the cell division stain, CFSE

To assure the technical feasibility of CFSE dilution as a method for the detection of proliferation BALB/c recipients were immunised s.c. with OVA (100 µg) in 100 µl PBS/50% CFA 24 h after adoptive transfer of CFSE-labelled Ag-specific Tg TcR ($KJ1.26^+$) T cells. On day 5 after immunisation, inguinal lymph nodes were harvested from unimmunised **(A)** and immunised **(B)** mice and the CFSE staining in Ag-specific $CD4^+$ T cells was assessed by flow cytometry. Control mice (unimmunised) were injected s.c. with 100 µl PBS (Figure adapted with kind permission from [312]).

Purified human B cells were stained with CFSE before culturing them with $F(ab')_2$ anti-IgM/IgG for 48 h **(D)**. A sample of the cells before culture **(C)** was used to set multiple gates using FlowJo software. The gates were set to each represent one round of division starting with gate 0 representing undivided cells.

Figure 2.8 The principle of LSC cell detection

LSC analysis employs a series of contours **(A)** such as the threshold contour which is commonly set on nuclei. Furthermore, the integration and peripheral contours are used to define different parts of the cell. The integration contour is based on the size of the cell or detection of a cell surface marker, as it defines the outer edge of the cell. The inner peripheral contour is set one pixel out from the threshold contour and the outer peripheral contour is set one pixel in from the integration contour, allowing definition of the periphery of the cell. Detection of a cell is determined by the nuclear fluorescence it emits which has to be above a certain threshold set by the user **(B)**. The correct setting of the threshold is important as a high threshold enables to detect individual cells, whereas a low threshold might lead to the detection of multiple cells as one event. Figure taken with kind permission from [312].

Figure 2.9 Analysis of cell cycle progression by LSC

Nuclei of cytocentrifuged cells were stained with DAPI and analysis carried out by LSC by plotting the Max Pixel value (depicting chromatin condensation) along the x-axis and the Integral value (representing DNA content) along the y-axis of the scattergram. The plotted cells were then gated according to their xy-position on the scattergram, which allows identifying cells in S phase (green gate) by their increased DNA content. Moreover, cells in the other mitotic stages (G2/M phase) which also contain high amounts of DNA can be differentiated due to a higher level of chromatin condensation (yellow gate). Cells arrested at the G1/G0 phase (red gate) of the cell cycle contain half the amount of DNA (2n DNA) compared to cells in G2/M (4n DNA) and can therefore be identified by the lower DNA content, as detected by lower DAPI Integral values. Cells undergoing apoptosis (blue gate) contain subdiploid DNA content due to their fragmented DNA placing them below cells in G1/G0 on the scattergram. Representative images of cells validating each stage of the cell cycle were captured using the slide xy-re-location feature of LSC and are shown here. Figure adapted from [312].

Table 2.2 Primers and probes

The table shows the sequences of the primers and probes used for quantitative RT-PCR or TaqMan® real-time PCR and the covalently attached dyes and quenchers.

Figure 2.10 Protocols used for cellular fractionations

Three different commercially available kits were used to produce subcellular fractions.

(A) Nuclear fractionation (nuclear/cytosolic fractions) using a kit from Active Motif.

(B) Mitochondrial fractionation using a kit from Active Motif.

(C) Cytoplasmic, membrane/organelle, nuclear and cytoskeletal fractions were obtained utilising a Cellular Protein Fractionation kit from Perkin Elmer.

Table 2.3 Table of vectors used for transfection of WEHI-231

(A) List of vectors used in this study for the transfection of WEHI-231 B cells

(B) Primers used for the amplification of Rap-1 coding region from pcDNA3.1-based vectors

(C) Parental plasmids and cloning sites/enzymes used for the cloning of the listed constructs

Figure 2.11 Vector map of pcDNA3.1 (+) and pcDNA3.1 (-) Zeocin

(A) pcDNA3.1 (+) and **(B)** pcDNA3.1 (-) Zeocin both contain a human cytomegalovirus (CMV) promoter which permits high level expression of the gene of interest. They encode a multiple cloning sites (MCS) in forward or reverse orientation and pcDNA3.1 (+) harbours a neomycin resistance gene whereas pcDNA3.1 (-) Zeocin contains the gene encoding a zeocin resistance gene. These antibiotic resistance genes allow stable transfection of mammalian cells following selection by culturing with the antibiotics G418 or Zeocin, respectively. Expression of the resistance genes is controlled by the SV40 early promoter and the SV40 early polyadenylation signal. The presence of a pUC origin of replication allows replication and growth in *E. coli* and the ampicillin resistance gene enables selection of the plasmid in *E. coli*. Vector maps are courtesy of Invitrogen.

Figure 2.12 Vector map of pIRES2-AcGFP1 and pLVX-IRES-ZsGreen1

Both **(A)** pIRES2-AcGFP1 as well as **(B)** pLVX-IRES-ZsGreen1 contain a multiple cloning site (MCS) and an Internal Ribosomal Entry Site (IRES) of the *encephalomyocarditis virus* followed by green fluorescent protein (GFP) of *Aequorea coerulescens* or green fluorescent protein from Zoanthus sp (ZsGreen1), respectively. This allows the bicistronic expression of the gene of interest and the marker proteins GFP or ZsGreen1. High level expression of the gene of interest is ensured by the human cytomegalovirus (CMV) promoter. pIRES2-AcGFP1 harbours a neomycin resistance gene which allows stable transfection of mammalian cells following selection with the antibiotic G418. Expression of the resistance genes is controlled by the SV40 early promoter. pLVX-IRES-ZsGreen1 on the other hand does not encode a mammalian resistance gene. The presence of a pUC origin of replication in both vectors allows replication and growth in *E. coli* and the ampicillin or kanamycin resistance gene enables selection of the plasmid in *E. coli*. pLVX-IRES-ZsGreen1 is a HIV-based vector which has been optimised for the production of lentiviral particles. Thus, it contains the woodchuck hepatitis virus posttranscriptional regulatory element (WPRE) which promotes RNA processing events and nuclear export of viral RNA. Furthermore, the Rev-response element (RRE) increases viral titres by enhancing the transport of unspliced RNA from the nucleus. Vector maps are courtesy of Clontech.

3 Signalling involved in negative selection of immature B cells

3.1 Introduction

The immune system generates an extremely diverse repertoire of antigen-specific B cells. The drawback of this diversity is the potential to produce (cross)-reactivities against host components. Thus, because of their potential to initiate immune responses against self-molecules, B cell development and maturation is tightly regulated to ensure tolerance against self. For example, B cells have to undergo negative selection during the immature B cell stage which ensures the deletion of the majority of autoreactive clones in the bone marrow. Thus, whereas ligation of the BCR on mature B cells initiates activatory signals, on immature B cells it leads to either receptor editing, anergy or deletion by apoptosis [36]. However, the differential signalling mechanisms employed by mature and immature B cells to effect the distinct functional outcomes have still not been fully elucidated. Indeed, the majority of signals utilised downstream of the BCR in mature and immature B cells appear to be very similar. For example, as with mature B cells, the BCR of immature B cells can couple to the ERK MAPK, PI3 kinase and PLCγ pathways.

Nevertheless, it is possible that differences between BCR signalling in mature and immature B cells might reflect differential expression levels, kinetics or localisation of such signalling elements. Furthermore, there is increasing evidence that there are some major differences in the expression and/or nature of downstream mediators of the above mentioned pathways in mature and immature B cells. Thus, immature B cells express $cPLA_2$, a phospholipase which is not expressed by mature B cells [318] and hence, the ligation of the BCR leads to the activation of $cPLA_2$ and consequent induction of apoptosis in immature, but not mature, B cells. Similarly, another class of phospholipase, phospholipase D (PLD) is activated differentially in mature and immature B cells [319]. For example, in mature, but not immature, B cells BCR-ligation induces activation of a phosphatidyl-inositol specific PLD isoform which can create phosphatidic acid which is converted to DAG potentially feeding into the activation of PKC enzymes [319]. The lack of this activating PLD-dependent pathway in immature B cells might therefore contribute to their inability to proliferate upon BCR-ligation. Moreover, whilst the initiation of calcium mobilisation is not impaired in immature B cells, the hydrolysis of PIP_2 by PLCγ is reduced [320] also resulting in lower production of DAG than the levels required for the stronger activation of PKCs observed in mature B cells. Consistent with this, differential BCR-dependent activation of PKCs is thought to provide another crucial difference as defective PKC activation has been implicated in driving BCR-induced apoptosis of immature B cells [321,322]. For example, it was

shown that enforced activation of PKCβ can inhibit BCR-induced apoptosis of transitional immature B cells and that blocking PKCβ activation in mature follicular B cells makes them more prone to die by apoptosis after BCR-ligation [322]. Consistent with this, the downstream effector of PKCβ involved in the survival of immature B cells is thought to be NF-κB. Indeed, PKCs can activate NF-κB which in turn increases the expression of survival factors such as c-Myc, Bcl-x_L and Bcl-2 [131,323].

Moreover, c-Myc also plays an important role in the regulation of the cell cycle, specifically in the progression through G1 and into S phase. It is therefore not surprising that reduction of c-Myc was found to be linked to initiation of growth arrest and apoptosis in immature B cells or immature B cell lines such as the WEHI-231 lymphoma [324]. Furthermore, constitutive expression of c-Myc in B cells expressing an autoreactive BCR led to an increase of autoreactive clones appearing in the periphery of a double transgenic mouse model system. These mice express a transgene encoding a BCR specific for hen-egg lysozyme (HEL) as well as another transgene resulting in the ubiquitous expression of HEL thereby turning HEL into a neo self-antigen. In the absence of c-Myc overexpression the peripheral B cells in these mice are anergic due to constant exposure to the neo self-antigen HEL [325]. The increase of HEL-specific and hence autoreactive clones seen in mice overexpressing c-Myc therefore argues for a role of c-Myc in the regulation of negative selection in immature B cells [326].

Such differential BCR-signalling between mature and immature B cells might partly be due to a difference in the assembly of the initial BCR-related signalling complex. Indeed, in recent years many studies have revealed the importance of membrane organisation in signalling. These studies proposed that efficient assembly of signalling complexes at the membrane depends on so-called lipid rafts which are sterol- and sphingolipid-enriched domains. In mature B cells, BCR ligation leads to rapid localisation of the BCR into these lipid rafts and initiation of signalling [327]. Immature B cells however, were found to display a reduced ability to re-localise their BCR into lipid rafts upon antigenic stimulation [328] and this has been proposed to be due to lower levels of cholesterol in immature B cells [329]. Differential raft formation could therefore potentially influence the assembly of the signalling complex downstream of BCR-ligation thereby changing the signalling initiated at different stages of B cell development.

In addition to these intrinsic signalling differences, the bone marrow environment has also been identified as having an influence on the fate decisions of immature B cells. For example, the bone marrow was found to contain Thy-1^{dull} $DX5^{pos}$ cells which appear to be responsible for directing the response of autoreactive immature B cells towards receptor editing rather than apoptosis. Thus, lack of these cells increases the

number of immature B cells undergoing apoptosis in mixed bone marrow cultures compared to cultures containing this cell subset [330]. The lack of these cells in the periphery *in vivo* could therefore explain the preferential induction of receptor editing in the bone marrow compared to BCR-dependent induction of apoptosis, which is the predominant response of transitional immature cells in the periphery.

3.1.1 ERK MAP kinase signalling regulates proliferation and apoptosis in B cells

Activation of the ERK MAPK cascade is important in the regulation of mature B cell proliferation [331] and can be initiated by BCR-ligation and to a lesser extent by CD40 signalling [332]. However, activation of ERK has also been implicated in BCR-induced apoptosis and growth arrest by studies showing that cross-linking the BCR on WEHI-231 cells causes rapid upregulation of ERK activation [333]. Subsequently, work from this laboratory showed that ERK can play a dual role in determining functional responses of the immature B cell line, WEHI-231, linking it to apoptosis as well as proliferation. Thus, sustained cyclic activation of ERK was found to be necessary to maintain the spontaneous proliferation of WEHI-231 cells. By contrast, cross-linking of the antigen receptors on such WEHI-231 B cells stimulated a strong transient ERK activation (< 4h) but abrogated the cyclic activation of ERK, resulting in growth arrest and apoptosis [307,310]. The link between this strong transient ERK activation and apoptosis was provided by $cPLA_2$, a known substrate of ERK. Thus, upon BCR-ligation $cPLA_2$ is upregulated and activated by ERK-mediated phosphorylation, followed by its translocation to the mitochondria where it catalyses the production of arachidonic acid causing the mitochondrial membrane potential to dissipate [307] (Fig.3.1). Such disruption of mitochondrial integrity leads to loss of cellular ATP and initiation of an intrinsic mitochondrial apoptosis pathway which was found to be caspase-independent. Instead, the main executioner protease seems to be cathepsin B which is activated downstream of BCR-ligation. In confirmation of a role for this protease in such BCR-induced apoptosis, cell death could be prevented by the cathepsin B inhibitor EST [307].

The positive role for sustained cycling ERK activation in the survival and proliferation of WEHI-231 cells has been confirmed with several pieces of evidence. For example, BCR-induced as well as pharmacological (olomoucine) - induced growth arrest correlates with abrogation of the cyclic ERK activation [310]. Moreover, even in the presence of apoptotic BCR-signalling, CD40-ligation, a known rescue signal from growth arrest and apoptosis, re-instates the sustained cyclic activation of ERK. More direct evidence for a role of such ERK activation in CD40-mediated rescue from growth arrest was obtained by using pharmacological inhibition of ERK with MEK-specific

inhibitors PD98059 or UO126. Thus, inhibition of cyclic ERK activation downstream of CD40 ligation abrogated the ability of such signalling to rescue cells from BCR-induced growth arrest [310]. Finally, inhibition of ERK activation in otherwise untreated WEHI-231 cells reduced their spontaneous proliferation and increased levels of apoptosis indicating a role for ERK in the survival as well as the spontaneous proliferation of these cells [310].

3.1.2 The role of CD40 signalling

CD40 signalling plays a pivotal role in B cell biology regulating their proliferation, activation, survival and maturation-dependent effector functions such as class-switching and development of plasma cells [190]. Moreover, it has been shown that CD40 can rescue immature B cells from BCR-induced apoptosis and prevent spontaneous death of mature B cells [334]. Ligation of CD40 appears to antagonise BCR-mediated apoptosis by initiating signals which stabilise the mitochondrial membrane thereby avoiding ATP depletion and apoptosis [307]. A key mechanism is the CD40-dependent upregulation of anti-apoptotic Bcl-2 family members such as Bcl-x_L, Bcl-2 or A1 [335-338]. Previous work in our laboratory underpins the important role of Bcl-x_L in CD40-mediated rescue from apoptosis. For example, overexpression of Bcl-x_L in WEHI-231 cells was sufficient to mimic CD40 signalling in protecting these cells from BCR-induced apoptosis by preventing the dissipation of the mitochondrial membrane potential and subsequently activation of the executioner protease cathepsin B [294]. This protection from apoptosis was achieved by two Bcl-x_L-dependent mechanisms (Fig.3.1). Firstly, Bcl-x_L, by locating to the mitochondria itself, stabilises the mitochondrial membrane and secondly, it inhibits the translocation of $cPLA_2$ to the mitochondria. The finding that Bcl-x_L overexpression also protected cells from apoptosis induced by treatment with exogenous arachidonic acid (AA) implies that Bcl-x_L can stabilise the mitochondria in BCR-dependent apoptosis, at least in part, by counteracting the effects of AA produced by $cPLA_2$ [294].

As mentioned above, CD40 not only prevents BCR-induced apoptosis but also rescues WEHI-231 cells treated with anti-IgM from growth arrest and restores their proliferation [310]. However, in this case, overexpression of Bcl-x_L was not sufficient to mimic the effects of CD40-ligation. Indeed, BCR stimulation of Bcl-x_L-expressing WEHI-231 cells caused similar levels of growth arrest as seen in untransfected wild-type cells. These results, in conjunction with the need for (Bcl-x_L-independent) restoration of cyclic ERK activation for CD40-dependent rescue from growth arrest, implicated the existence of at least two independent pathways mediating rescue from apoptosis and growth arrest. Thus, CD40-mediated upregulation of Bcl-x_L is crucial in the prevention of apoptosis but does not affect growth arrest whereas the ERK-dependent pathway is

involved in rescue from BCR-dependent growth arrest but not apoptosis [294,310]. The exact mechanisms regulating CD40-dependent restoration of cyclic ERK have still to be delineated but preliminary data suggests that production of prostaglandins and leukotrienes is involved in proliferation of WEHI-231 cells. Thus, inhibitors of cycloxygenase 2 (Cox2) and lipoxygenase (Lox), the enzymes converting arachidonate to prostaglandins and leukotrienes, respectively, promote growth arrest. Interestingly, expression of PGE_2, a product of Cox2 which can potentially have growth promoting effects [339], is reduced upon BCR signalling and restored by CD40-ligation in WEHI-231 cells [294]. Additionally, pharmacological inhibition of Cox2 and Lox abrogated cyclic activation of ERK in CD40-stimulated WEHI-231 cells providing a more direct link between prostaglandin/leukotriene synthesis and CD40-mediated regulation of ERK levels [294]. Therefore, CD40-signalling might restore cyclic ERK activation and hence proliferation through a novel PGE_2-dependent pathway.

3.1.3 Regulation of ERK MAP kinase activation

The ERK MAPK cascade can be regulated by several mechanisms. For example, negative feedback regulation can act at multiple levels with ERK phosphorylating and thereby inhibiting some of its own upstream regulators such as MEK1/2 [340] and Raf [341]. In addition, ERK activation of the downstream serine/threonine kinase RSK2 leads to the phosphorylation of the Ras-GEF Sos, preventing it from interacting with Grb-2 and translocating to the plasma membrane, resulting in a consequent reduction of Ras activation [342]. Moreover, ERK can regulate some of its negative regulators, such as the dual-specificity phosphatase 1 (DUSP1, also known as MKP-1), a phosphatase which can dephosphorylate and hence inactivate ERK. Thus, ERK-mediated phosphorylation of DUSP1 contributes to its stabilisation [343] thereby creating another negative feedback loop causing downregulation of ERK activation. All these mechanisms might therefore contribute to avoiding uncontrolled ERK MAPK responses.

3.1.3.1 Scaffold proteins

An additional level of regulation is provided by scaffold proteins which are able to bind two or more components of the same signalling cascade bringing them into close contact. Therefore, these scaffold proteins can act to control the substrate specificity of a pathway, target the signalling complex to various subcellular localisations or link the cascade to a specific upstream regulator [344]. The best studied scaffold protein for the ERK cascaded is kinase suppressor of Ras (KSR) [345] which can bind Raf, MEK and ERK [344]. Depending on the expression levels of KSR, binding to ERK has been shown to have different outcomes. Thus, at optimal levels, KSR increases activation of

ERK whereas an excess of KSR over its ligands inhibits ERK [346,347]. The importance of KSR *in vivo* was confirmed by a study using KSR1-deficient T cells which showed a defect in their activation [348]. Another ERK-specific scaffold protein is MEK partner-1 (MP-1), a positive regulator of ERK which enhances the B-Raf-mediated phosphorylation of MEK1 [349].

3.1.3.2 MAPK phosphatases

A major mechanism of ERK inhibition is the direct dephosphorylation of the T-X-Y motif in the activation loop of the MAPKs. There are three types of phosphatases able to catalyse such dephosphorylation of MAPKs: tyrosine phosphatases, serine/threonine phosphatases and dual-specificity (threonine/tyrosine) phosphatases [350].

For example, upon activation by protein kinase A, the tyrosine protein phosphatase hematopoietic PTP (HePTP) can keep ERK1/2 in a dephosphorylated state causing reduced activity of ERK1/2 [351]. Indeed, HePTP has been shown to inhibit ERK1/2, as well as p38, following its activation downstream of the TCR [352]. Such dephosphorylation does not only influence ERK activity but also regulates its nuclear translocation. Hence, HePTP-dependent dephosphorylation of ERK2 inhibited its localisation to the nucleus in K562 myelogenous leukaemia cells [353]. Two other tyrosine phosphatases, PTP-SL and STEP were shown to have similar effects on ERK2 in Cos-7 and HEK-293 cells, inhibiting the activation and nuclear translocation of ERK2 by dephosphorylation [354].

Several serine/threonine protein phosphatases have been identified that regulate the activity of ERK, JNK and p38 by direct dephosphorylation or by targeting upstream activators of these MAPKs [355]. Protein phosphatase 2A (PP2A) is one such serine/threonine phosphatase involved in the regulation of the ERK pathway. It has been shown to influence ERK activation by interacting with its upstream modulators such as Shc, Raf-1 or MEK1/2. For example, PP2A can dephosphorylate and inhibit Raf-1 and MEK downstream of the PDGF receptor in NIH-3T3 cells leading to suppression of ERK [356]. Moreover, *in vitro* PP2A was shown to dephosphorylate not only MEK1/2 but also ERK1/2 itself [357] and in PC12 cells inactivation of the early transient ERK signal was achieved by PP2A-mediated dephosphorylation [358]. Overexpression of a dominant-negative form of PP2A in mouse brain caused an increase in MEK1/2 phosphorylation thereby providing an *in vivo* model confirming the activity of PP2A as an important regulator of the ERK MAPK cascade [358].

DUSP can dephosphorylate threonine and tyrosine residues and can therefore directly dephosphorylate the T-X-Y motif in MAPKs causing their inactivation [359]. Besides regulating the phosphorylation status of MAPK, some of these phosphatases

have also been implicated in determining the localisation of their targets, for example, MKP-3 was found to localise ERK1/2 in the cytoplasm [360].

MKPs, which can be regulated at both the transcriptional as well as their enzyme activity level, play an important role in feedback-type regulation of MAPKs [361]. For example, induction of MKP-1 and -2 expression is enhanced by ERK-dependent mechanisms resulting in downregulation of ERK activity by dephosphorylation of the TEY activation motif [361]. Similarly, ERK-mediated phosphorylation and thereby stabilisation of MKP-1 can also lead to reduced ERK activation [343]. However, there are also reports supporting the existence of positive feedback loops due to increased ERK-dependent degradation of dual-specificity phosphatases [362]. Dual-specificity phosphatases can regulate all three families of MAPK: ERK, JNK and p38. Indeed, each phosphatase has a different set of substrates allowing the selective inhibition of a defined subset of MAPKs and therefore responses in the cells [352]. For example, PAC-1 is a selective phosphatase for ERK and p38 whereas MKP-1 can interact with all three MAPKs and MKP-2 preferentially dephosphorylates ERK and JNK [363,364].

PAC-1 is of particular interest, as it is regulated in immune cells upon activation. It was identified originally as a mitogen-inducible gene in human T cells [365] and was consequentially found to be highly upregulated in activated immune system cells such as B and T cells [366] implicating a role for PAC-1 in the regulation of immune cells [367]. Interestingly, the upregulation of PAC-1 expression in activated immune cells depends on ERK, further underpinning the important role of negative feedback mechanisms in the MAPK cascades [365,366]. For example, ERK, which is activated by TCR-ligation in Jurkat cells, in turn increases expression of PAC-1 thereby terminating ERK activation [368]. Interestingly, p53 was recently identified as another transcriptional regulator of PAC-1, inducing an increase in its expression which was found to be necessary for p53-mediated apoptosis, possibly by inhibiting ERK activation [369]. A study using PAC-1-deficient mice has shown that this phosphatase may also play a role in regulating auto-immune responses. Perhaps surprisingly, lack of PAC-1 reduced the inflammatory responses in an antibody-mediated model for arthritis. This study therefore highlighted the complexity of the MAPK signalling network as PAC-1 deficiency increased the activity of JNK but subsequently reduced activation of ERK implicating the existence of regulatory cross-talk between the three MAPK pathways [367]. Thus, PAC-1 could be one of the major regulators of MAPK activation in immune system cells.

3.1.4 The role of ERK MAPK in cell cycle regulation

As stimulation with mitogens, which cause cell cycle progression and subsequently proliferation, is often associated with ERK activation it is therefore not

surprising that ERK has been implicated in the regulation of cell cycle. The initial link between ERK activation and cell cycle progression came from studies showing the correlation between ERK1/2 activation and induction of DNA synthesis [370]. More directly, inhibition of ERK1 by overexpressing an inactive mutant or ERK1-antisense RNA in fibroblasts reduced ERK activation causing decreased proliferation [371]. Similarly, pharmacological inhibition of MEK1/2, the upstream activators of ERK1/2, can reduce proliferation in many cell types such as fibroblasts, smooth muscle cells, hepatocytes and immune system cells including T and B cells [372,373]. Indeed, it was subsequently shown that ERK1/2 was active in G1 and its activity needed to be sustained until late G1 phase to guarantee entry into S phase [374].

At the molecular level activated ERK1/2 seems to have multiple functions impacting on the cell cycle including the control of transcription, translation and cell cycle regulators [372]. Thus, inhibition of ERK1/2 was found to reduce the phosphorylation of the translation initiation factor eIF4E which is a substrate of MNK1/2 suggesting that their ERK1/2 dependent activation might be involved in the regulation of translation [375-377]. Additionally, ERK1/2 could potentially also influence translation through modifying the mTOR signalling pathway which regulates ribosome biogenesis and initiation of translation [378]. mTor is regulated by inhibition through the tuberous sclerosis complex 1 (TSC1)/TSC2 heterodimer. Two studies have recently reported the involvement of ERK1/2 in regulating mTOR, either directly or indirectly through activation of RSK1 to phosphorylate TSC2 and thus reducing the inhibitory activity of the complex [379,380].

As mentioned above, ERK1/2 plays a crucial role in the transition from G1 to S phase. One of the known mechanisms by which ERK1/2 regulates this transition is the induction of cyclin D1 expression [372]. The mechanisms of this ERK1/2 – cyclin D1 signalling axis have not yet been fully delineated but it has been suggested to involve AP-1-dependent transcriptional upregulation of cyclin D1 [240,372]. Additionally, however, ERK has also been implicated in the regulation of the nuclear export of cyclin D1 mRNA to allow its translation at the ribosomes [381]. Finally, ERK1/2-mediated phosphorylation and stabilisation of c-Myc provides another link between cell survival and cell cycle progression and ERK1/2 activation.

3.1.5 Regulation of c-Myc expression

The importance of c-Myc in regulating processes such as proliferation and cell growth makes it necessary to tightly regulate its expression and activity. Thus, c-Myc is subject to regulation at the transcriptional, translational and post-translational level [382,383], the latter being the most extensively studied. For example, c-Myc protein

stability depends on its posttranslational modifications such as phosphorylation, ubiquitination and possibly acetylation (reviewed in [384]).

The role of phosphorylation was the first to be detected and characterised and is still the focus of much attention. In particular, two of the N-terminal phosphorylation sites at threonine 58 and serine 62 have been analysed in detail as it has been found that they influence c-Myc protein stability and possibly trans-activation potential [384-387] (Fig.3.2). For example, it has been shown by several groups that phosphorylation of T58 by glycogen synthase kinase 3 (GSK3) [388] renders c-Myc prone to ubiquitination by F-box protein Skp2 or Fbw7-containing SCF complex E3 ligases [389,390]. Whereas Fbw7-mediated ubiquitination of c-Myc is followed by its degradation by the proteasome, Skp2 signalling appears to play a more complex role in the regulation of c-Myc as it also influences its transactivation capacity. Indeed, Skp2 has been found to co-localise with c-Myc at its target promoters and increases its transcriptional activation possibly by recruiting proteasome subunits which were recently found to play a role in RNA polymerase II transcription [389]. By contrast, phosphorylation of S62 increases c-Myc stability through as yet unknown mechanisms and little is known about the kinases which carry out the phosphorylation [384]. Nevertheless, the consensus sequence surrounding S62 makes it a likely target for modification by proline directed kinases such as ERK MAPK which has been shown to phosphorylate c-Myc at position S62 *in vitro* [386]. It is of interest that T58 phosphorylation only occurs after prior phosphorylation at position S62 [386] further complicating the regulatory mechanisms underlying c-Myc stabilisation and degradation. The interaction of the c-Myc binding partner, Max with other bHLHZip – domain containing proteins such as Mad or Mnt provides another regulatory mechanism as these complexes act as transcriptional repressors being able to bind the same sequence as the c-Myc/Max complexes [391,392].

3.1.6 The small GTPase, Rap

Rap (Ras proximity) belongs to the Ras superfamily of small GTPase proteins which includes five subgroups: the Ras, Rho, Rab, Arf and Ran families [393]. Rap belongs to the Ras-like small G proteins which include the three Ras family members H-Ras, Ki-Ras, N-Ras and the five members of the Rap family: Rap-1A, Rap-1B, Rap-2A, Rap-2B, and Rap-2C [394]. The Rap-1 and Rap-2 isoforms are 60% identical and are mainly regulated by the same GEFs and RapGAPs but Rap-2 displays a lower sensitivity for RapGAPs allowing it to remain in an active state for longer. This has led to suggestions that Rap-1 and Rap-2, if activated in the same cell, might function as a molecular switch between fast (Rap-1) and slow (Rap-2) Rap activation/deactivation [395].

3.1.6.1 Regulation of Rap activity

Activation of Rap is achieved by the exchange of GDP for GTP which is carried out by GEF proteins including C3G, Epac1, Epac2, RasGRP2, PDZ (PSD-95/Dgl/ZO-1)-GEF1, PDZ-GEF2, CalDAG-GEF and PLCε (reviewed in [393]; Fig.3.3). Binding of GEF to Rap decreases its affinity for GDP and promotes its replacement by GTP, which is found in excess in the cell [394]. Binding of GTP induces a conformational change which exposes the effector binding loop allowing the recruitment of different Rap effectors. Different GEFs have been found to activate Rap downstream of a range of signals such as cytokines and chemokines, growth factors, cell adhesion molecules and antigen-receptors in B and T cells [396]. Moreover, activation of Rap can be achieved by different mechanisms depending on the expression of specific GEFs as well as the type of regulatory adaptor complex formed. For example, C3G (Crk SH3-domain-binding guanine-nucleotide releasing factor, where SH3 stands for Src homology region 3 domain), which is an ubiquitously expressed GEF in many cell types, is activated downstream of RTK (Fig.3.3). Thus, binding of C3G to its adaptor Crk allows recruitment to the plasma membrane where RTKs facilitate phosphorylation and hence activation of C3G on tyrosine 504 [397]. The phosphotyrosine docking sites needed for the recruitment of Crk/C3G can be provided by phosphorylation of scaffolding proteins such as Cbl, Cas or Gab1 [398-400]. The importance of the adaptor proteins and the complexes they form with Rap-1 downstream of RTK-induced signalling is emphasised by the fact that inhibition of complex formation blocks the activation of Rap-1 [400].

By contrast, CalDAG-GEF 1 is regulated by calcium binding whereas CalDAG-GEF 3 needs to bind DAG for activation. These RapGEFs therefore likely connect the PLC pathway with Rap activation [401]. Moreover, a recent addition to the RapGEF family of proteins, the Epac proteins, depend on cyclic AMP (cAMP) for activation and have thus been implicated in the transduction of signals through GPCRs [402]. Thus, different stimuli induce activation of Rap by initiating varied signals such as elevation of cAMP, calcium or phosphotyrosine kinase activity, all of which can cause the activation of different types of GEFs (Fig.3.3).

Inactivation of Rap is achieved by RapGAPs which enhance the intrinsic Rap GTPase activity leading to the hydrolysis of GTP to GDP and subsequent inactivation of Rap [403]. There are two major groups of RapGAPs: The RapGAP family (including RapGAP1 and 2) and the SPA-1 family of proteins (SPA-1, SPA-1-like (SPA-L) 1 (also called SPAR), SPA-L 2, and SPA-L 3) which all share the catalytic GAP-related domain (GRD) [396] (Fig.3.3). SPA-1 is the family member expressed most abundantly in lymphohematopoietic tissues whereas for example SPAR is more highly expressed in

epithelial tissues and brain [404,405]. RapGAPs do not need post-translational modifications such as phosphorylation to be activated as they are constitutively active and therefore expression levels appear to be the major determinant of their activity in the cell [396].

3.1.6.2 Functions of Rap

Rap has been implicated in a range of cellular responses including regulation of integrin expression and signalling, T cell anergy and neuronal cell differentiation [396]. Interestingly, activation of Rap can have distinct cellular effects depending on the cell type and/or stimuli. For example, Rap-1 was initially discovered as a factor that could suppress the K-Ras-mediated transformed phenotype of fibroblasts [406] which led to the initial hypothesis that Rap-1 antagonises Ras mediated signals by binding to Raf-1 and hence sequestering it away from Ras and consequently inhibiting Ras-mediated activation of ERK. Indeed, this seems to be the mechanism by which Rap-1 inhibits activation of ERK in *in vitro* anergised T cells. Thus, cross-linking of the TCR/CD3 complex in the absence of CD28 costimulation increases the recruitment and activation of Rap-1 at the TCR signalling complex whereas costimulation via CD28 blocks such Rap-1 activation [407,408]. Consistent with this, it has been shown subsequently by *in situ* immunofluorescence staining that upregulation of Rap-1 and reduction of ERK activation is also a hallmark of *in vivo* anergised antigen-specific T cells [409] and that T cells with an anergic phenotype *in vivo* display Rap-1 activation [410]. These studies therefore confirm the relevance of Rap-1-dependent inhibition of ERK activation in the regulation of T cell dependent immune responses.

By contrast, in neuronal cell lines, Rap-1 was found to activate the ERK pathway. It was shown that such activation of ERK was achieved in a B-Raf dependent manner [411]. Here Rap-1 binds and activates B-Raf, another Raf isoform known to effectively phosphorylate and thereby activate MEK1/2 and hence ERK1/2. Therefore, it is now thought that Rap-1 can either activate or inhibit the ERK cascade depending on cell type and expression of different Raf isoforms (Raf-1 or B-Raf). An interesting study by Dillon *et al* provides supporting evidence for this hypothesis in peripheral T cells which generally do not express B-Raf. In those cells Rap-1 functions as a negative regulator of ERK by binding Rap-1 and inhibiting Raf-1/Ras interactions. However, by creating mice expressing B-Raf in peripheral T cells, they showed that Rap-1 was then able to activate ERK in a B-Raf-dependent manner reducing the sensitivity of these cells towards induction of anergy [412].

Rap-1 is also involved in the regulation of integrin-mediated adhesion of various immune system cells such as lymphocytes and macrophages [413,414] by affecting the activity and clustering of integrins [415]. Indeed, in T cells Rap-1 is needed for the

activation of LFA-1 and synapse formation with antigen-loaded APCs [416,417]. Rap-1 utilises various effector proteins to achieve this regulation of integrins. For example, Rap-1 recruits RapL which in turn binds to the α-chain of the αLβ2 integrin, activating it and increasing its interaction with ICAM [415]. Alternatively, Rap-1-mediated recruitment of RacGEFs links Rap-1 to the control of cell spreading [415]. Thus, Rap-1 is a versatile signalling molecule which can regulate diverse cellular processes such as proliferation, differentiation or cellular adhesion depending on the cell type and expression of Rap-1-specific upstream or downstream regulatory molecules (Fig.3.3).

3.1.6.3 The role of Rap activation in B cells

Rap-1 and Rap-2 have been shown to be activated downstream of the BCR in B cells [418,419] and previous studies have indicated that Rap-1 can potentially regulate multiple signalling pathways including the ERK, p38 [420,421] and PI3 kinase/Akt pathways [422]. Interestingly, it has been suggested that, for example in chicken DT40 B cells, the B-Raf/Rap-dependent activation of ERK might be more important than the Raf-1/Ras cascade [170].

Rap-1A and Rap-1B deficient mice have been instrumental in further analysing the role of Rap in B cell development and activation. For example, Rap-1B was found to be the dominant form of Rap-1 in B cells [423] and Rap-1B-deficiency was shown to reduce the absolute number of pre-pro-B cells as well as immature B cells in the bone marrow. Similarly, in the periphery, numbers of MZ B cells were reduced as were mature follicular B cells in lymph nodes. Moreover, Rap-1B-deficient B cells were shown to display impaired adhesion and chemotaxis *in vivo* [424] as well as reduced SDF-1 (CXCL13)-induced migration and homing to lymph nodes [423]. These latter defects can be explained by the need for Rap for integrin activation and therefore adhesion. Indeed, Rap has not only been shown to be important for integrin activation but also for reorganisation of the actin cytoskeleton upon BCR and integrin-mediated stimulation [425]. Moreover, Rap is required for the BCR-ligation mediated formation of the immune-synapse as well as the F-actin-dependent extension of membrane processes upon BCR-ligation and cell spreading [426]. By contrast, proliferation of splenic B cells was not influenced by Rap-1B-deficiency thereby indicating that Rap-1B does not play a role in the expansion of mature B cells.

Unlike Rap-1B, Rap-1A does not seem to be crucial for T or B cell development but, similarly to Rap-1B, plays a role in adhesion of various cell types such as macrophages and chemotaxis of T, B and myeloid cells [427]. Taken together these studies show that Rap-1A and Rap-1B functions are partly redundant but some effects appear to be specific for one isoform or the other. Indeed, mice conditionally expressing a dominant-negative Rap-1 mutant Rap-1A17, which is able to inhibit all the

Rap family proteins, displayed a significant reduction of pre-B cells, immature and mature B cells [428] causing a more severe phenotype in these mice compared to mice deficient for single isoforms and hence indicating that more than one Rap protein may be involved in the regulation of development. Interestingly, Rap signalling also seems to be involved in the selection of the BCR repertoire of B cells. Thus, Ishida and colleagues have reported an increase of anti-dsDNA antibody-producing B-1a B cells as well as the development of lupus-like nephritis in mice deficient for the Rap-1-GAP, SPA-1. It seems that developing B cells with higher active Rap levels display a change in their V(D)J recombination and thereby receptor repertoire [429]. Thus, upregulation of Rap activity due to the lack of inhibition by SPA-1 increases the number of autoreactive B cells developing in these mice indicating a role for SPA-1 in the maintenance of tolerance.

3.1.7 The role of the Cbl family of E3 ubiquitin ligases in B cells

Ubiquitination of proteins involved in signalling cascades can influence their activity, protein stability and localisation and thereby change the signalling outcome downstream of various receptors [430] (see section 1.6). The members of the Cbl family of E3 ubiquitin ligases have been implicated in regulation of immune responses by influencing T and B cell signalling [431]. In mammals there are three Cbl isoforms: c-Cbl, Cbl-b and Cbl-c, but only c-Cbl and Cbl-b are expressed in haematopoietic cells [228]. Cbl proteins contain a tyrosine kinase-binding (TKB) domain [432] as well as a Zinc-binding RING finger domain which confers the E3 ubiquitin ligase activity of Cbl [433]. The TKB allows Cbl to bind to phospho-tyrosine residues in multiple PTKs and other signalling proteins [228]. Cbl itself is also tyrosine-phosphorylated by PTKs associated with the TCR, EGFR, IL-7, IL-4 and IL-2 receptors and this phosphorylation influences its adaptor function and E3 ligase activity [228].

There are two major mechanisms by which Cbl regulates receptor signalling. Firstly, Cbl can ubiquitinate receptors themselves such as the EGFR leading to internalisation and degradation of the receptor [434,435]. Additionally, Cbl ubiquitinates downstream signalling mediators such as Syk, Fyn, Lck and Lyn [228]. Generally ubiquitination will target the proteins for proteasomal degradation as seen for c-Cbl-mediated ubiquitination and degradation of Syk in B cells [236] (see Chapter 1, section 1.6). But in some cases ubiquitin-modification changes the capacity of proteins to interact with their usual binding partners. Thus, Cbl-b-dependent ubiquitination of the PI3 kinase subunit p85 does not induce degradation but inhibits its recruitment to CD28 or TCR [436,437]. Similarly, ubiquitination of CrkL, an adaptor protein involved in the recruitment of Rap, impairs the interaction with C3G [438]. Cbl therefore can potentially regulate various signalling pathways, some of which are known to be important in B

cells. Initial studies carried out in chicken B cells indeed showed that c-Cbl and Cbl-b regulate BCR signalling [439,440] and Cbl-b was found to downregulate Syk following BCR stimulation in a ubiquitination-dependent fashion [441]. A study by Kitaura *et al* has recently confirmed a role for c-Cbl and Cbl-b in the regulation of B cells *in vivo*. They used B cell-specific c-Cbl/Cbl-b-doubly-deficient mice to analyse the role of these proteins in B cell development and activation [442]. The c-Cbl/Cbl-b-deficient mice displayed major changes in B cell development leading to an increase of B cells in the periphery and reflecting an increase in T1, MZ as well as B-1 B cell numbers. Compared to wild-type littermates, the mice also expressed more IgM and detectable levels of anti-dsDNA and ANA antibodies and some animals developed SLE-like autoimmune disease [442]. This inability to regulate autoreactive B cells might be partly due to reduced ability of c-Cbl/Cbl-b-deficient B cells to be anergised resulting in increased levels of activated self-reactive B cells.

Similarly, both Cbl isoforms were shown to also play an important role in the negative regulation of T cell activation. Thus, T cells from mice deficient for Cbl-b produced IL-2 and proliferated upon stimulation via CD3 without any need for CD28 costimulation. Cbl-b was consequently found to be involved in the negative regulation of signalling through the TCR and CD28 by ensuring the need for CD28 costimulation to overcome a certain signalling threshold [230]. The decreased need for costimulation and subsequent hyperresponsiveness of these T cells made Cbl-b-deficient mice susceptible not only to the induction of autoimmune diseases such as experimental autoimmune encephalomyelitis [230] but also spontaneous autoimmune disease [229]. Mice deficient for both c-Cbl and Cbl-b in T cells also develop autoimmune disease due to hyperreactive T cells [443]. Thus, Cbl-mediated negative regulation of antigen-receptor signalling seems to influence pivotal processes including positive selection of T cells in the thymus, activation threshold of peripheral T cells as well as B cell tolerance mediated by anergy [431].

3.2 Aims

Negative selection of immature B cells expressing self-reactive specificities plays an important role in preventing the development of autoimmune diseases. It is therefore vital to characterise the signalling pathways that lead to the induction of growth arrest and apoptosis in immature B cells upon BCR stimulation.

The WEHI-231 B cell lymphoma expresses high levels of IgM as well as no/low levels of IgD, FcγR, and MHC class II on their surface, a phenotype similar to immature B cells. This cell line has therefore been used extensively as a model system for BCR-induced growth arrest and apoptosis of immature B cells [444,445]. Thus, cross-linking

of the BCR on WEHI-231 cells by treatment with anti-IgM antibodies leads to growth arrest in G1 phase of the cell cycle and apoptosis in a manner which models anergy and clonal deletion during negative selection of immature B cells in the bone marrow. Furthermore, and similarly to primary immature B cells, WEHI-231 cells can be rescued from growth arrest and apoptosis by T_H cell-derived signals such as ligation of the CD40 receptor [334]. WEHI-231 cells therefore represent an exploitable *in vitro* model for the dissection of signalling pathways underlying BCR-mediated negative selection which can then be translated and validated in primary immature B cells.

The specific aims and objectives of this investigation were:

- to investigate the signalling mechanisms regulating ERK activation in immature B cells and how these are modulated during BCR-mediated growth arrest and apoptosis and rescue via CD40 signalling. In particular, it was planned to focus on the roles of B-Raf, Rap-1 and SPA-1 in ERK signalling and consequent immature B cell fate.
- to characterise the downstream effectors of ERK, such as c-Myc, and to investigate their role in directing immature B cell fate.
- to further explore the role of other signalling pathways and regulatory mechanisms such as ubiquitination in BCR-induced growth arrest and apoptosis of WEHI-231 cells.

3.3 Results

3.3.1 Induction of growth arrest and apoptosis in WEHI-231 cells

In order to assess the negative selection response to BCR stimulation, WEHI-231 cells were stimulated with increasing concentrations of anti-mouse IgM antibody to mimic crosslinking of the BCR by high affinity/avidity antigen. Proliferation was assessed not only by determination of DNA synthesis using a [^{3}H] thymidine incorporation assay but also by analysis of the percentage of cells in the different cell cycle stages following quantitation of DNA content by PI staining. Thus, dose response experiments were performed that showed that increasing concentrations of anti-IgM repressed proliferation (Fig.3.4A). This growth arrest could be reversed by simultaneous treatment of the cells with agonistic anti-CD40 antibody (Fig.3.4B) as indicated by the restoration of proliferation.

Cell cycle analysis of living cells confirmed these results. Thus, treatment of WEHI-231 cells with anti-IgM for 48 or 72 hours dramatically decreased the percentage of cells in G2-M phase and S phase with a compensatory increase in the percentage of cells arrested in G1-G0 (Fig.3.5). However, analysis of all the cells in the culture revealed that G1-G0 arrest only partially accounted for the loss of proliferation as by 48-72 h there was also a dramatic increase in the percentage of cells with subdiploid DNA content, a hallmark of apoptosis (Fig.3.6).

Furthermore, it was shown that BCR-ligation led to the dissipation of the mitochondrial membrane potential (MMP), detected as a decrease of the percentage of cells with high $DiOC_6$ fluorescence intensity (Fig.3.6E). $DiOC_6$ is a dye that integrates into the mitochondrial membrane in a stoichiometric fashion correlating with the MMP. A decrease of the levels of $DiOC_6$-staining therefore indicates the disintegration of the cells MMP, a hallmark of the intrinsic apoptosis pathway. Both BCR-mediated growth arrest and apoptosis, as well as dissipation of the MMP, could be counteracted by the simultaneous stimulation of the cells with anti-CD40 antibody (Fig.3.5 and 3.6).

Collectively, therefore, these results showed that both growth arrest and apoptosis contributed to the decrease in proliferation of WEHI-231 cells following BCR ligation and that WEHI-231 immature cells provided an *in vitro* model not only for dissecting the BCR signals responsible for growth arrest and apoptosis during negative selection but also those directing rescue by CD40-mediated T_H-derived signals.

3.3.2 Regulation of ERK activation during BCR-mediated negative selection and rescue via CD40

Previous research in this laboratory has shown that differential ERK signals determine distinct important cell fate decisions of the immature B cell line WEHI-231.

Thus, depending on the strength and duration of ERK activation, WEHI-231 immature B cells can either survive and proliferate or undergo growth arrest and apoptosis [310]. Thus, as shown previously, cyclic activation of ERK accompanies the robust spontaneous proliferation of cultured WEHI-231 cells for up to at least 32 hours (Fig.3.7A). By contrast, stimulation of the cells with anti-IgM induced the transient upregulation of ERK phosphorylation during the first 2-4 hours after stimulation followed by a sustained downregulation for at least 32 hours (Fig.3.7B). This reduction of ERK activation was mirrored by that of its putative downstream effector of survival and proliferation, c-Myc, as expression of this protein also displayed an initial increase in the early phase of BCR stimulation followed by strong downregulation during the rest of the analysed time course. By contrast, simultaneous stimulation of the BCR and CD40 restored both the levels of activated ERK and c-Myc expression (Fig.3.7D) and the cyclic activation pattern seen in untreated cells (Fig.3.7A and D). Consistent with its anti-apoptotic effects, ligation of CD40 in the absence of BCR stimulation did not induce the early activation of ERK as seen after BCR-ligation but did generally tend to enhance ERK phosphorylation and c-Myc levels throughout the time course (Fig.3.7C).

To corroborate these data at the single cell level the activation of ERK, in terms of expression of dually-phosphorylated (T202/Y204) ERK, was imaged and quantitated by laser scanning cytometry. Image analysis showed that pERK showed a focused, punctate staining in the perinuclear region and, in agreement with the above Western Blot data and our previous studies [310], quantitative LSC analysis of the immunofluorescence staining of WEHI-231 cells treated with anti-IgM showed a reduction in the percentage of cells expressing pERK, as well as the level of pERK expressed in the cells at 48 h due to cross-linking of the BCR which was reversed upon CD40-mediated rescue from growth arrest (Fig.3.8). c-Myc expression detected by immunofluorescent staining was predominantly located, as expected, in the nucleus. Moreover, quantitative analysis by LSC showed that it was expressed in fewer cells and at a lower level after BCR-ligation, confirming the results demonstrated by Western Blotting (Fig.3.8). Moreover, mimicking T_H-cell help by ligation of CD40 restored the expression of c-Myc even in the presence of BCR-ligation (Fig.3.8).

3.3.3 Activation of ERK correlates with progression through the cell cycle

The cell cycle is controlled very tightly to ensure the timed entry and exit through cell cycle phases. Proteins regulating the cell cycle are therefore often expressed only during certain stages of the cell cycle and are downregulated once the next phase is entered. The correlation of protein expression and cell cycle stage can therefore indicate a positive or negative regulatory role of the analysed proteins. In order to

directly correlate protein expression levels with cell cycle stage, cells were cytocentrifuged and immunofluorescently stained and then analysed by LSC. The advantage of LSC analysis is that this method allows the direct correlation between cell cycle status and protein expression on a single cell basis. Firstly, to determine the different cell cycle phases in WEHI-231 cells, BCR- and/or CD40-stimulated cells were stained with DAPI to determine their DNA content and chromatin condensation (Fig.3.9). It was shown that such LSC-based analysis produced broadly similar results as FACS analysis of PI staining detecting an increase in cells arrested in G1 phase and a decrease of new daughter cells and cells in mitotic phases (G2/M and S phase) after treatment with anti-IgM at this time point (Fig.3.9C).

Activation of ERK has been shown to be important for the proliferation and survival of B cells [310] and it is known to be a prerequisite for G1/S phase transition and hence cell cycle progression in other cell systems such as fibroblasts [446]. The LSC-based analysis of cell cycle status was therefore utilised to investigate the possible correlation between pERK (active ERK) and cell cycle progression. Indeed, in confirmation of previous results [310], higher levels of ERK activation were found in cells in G2/M or S phase whereas lower levels of pERK were associated with growth arrested or apoptotic cells (Fig.3.10). Moreover, the percentage of pERK expressing cells was generally higher in mitotic cells compared to growth arrested/apoptotic cells (Fig.3.10). Interestingly, new daughter cells which represent cells having recently undergone mitosis, express relatively low levels of pERK, most likely due to their quiescent state (Fig.3.10). Taken together these results further confirm the connection between proliferation and ERK activation directly linking high levels of ERK activation with mitosis.

3.3.4 Rap/B-Raf signalling as a target of BCR-mediated negative selection?

It has been shown by this laboratory that whilst BCR signalling leads to the suppression of sustained, cycling ERK activation, activation of Ras, one of the major upstream regulators of the ERK cascade, was essentially unaffected [373]. Thus, downregulation of Ras activity did not appear to be the mechanism underlying BCR-mediated suppression of ERK activation. Interestingly, however, activation of MEK1, the ERK-specific MAPKK in BCR signalling, which is constitutively active in proliferating WEHI-231 cells, was found to display a cyclic pattern after BCR stimulation [447], suggesting that a Ras-independent pathway contributes to the full activation of the MEK/ERK cascade in spontaneously proliferating WEHI-231 immature B cells and that BCR-mediated downregulation of this pathway might be responsible for the suppression of ERK activity.

Since Rap-1 has also been reported to activate MEK via B-Raf [411], it was decided to investigate the potential of Rap-1/B-Raf signalling as targets in BCR-induced growth arrest. Rap-1 is a small GTPase and therefore only active if bound to GTP [422] and thus, Western Blotting using an anti-Rap-1 antibody detects Rap expression independent of its activation status. Nevertheless, to assess if all the components of the Rap/B-Raf cascade are expressed in WEHI-231 cells and to further examine any stimulation-induced changes, Rap, B-Raf and Raf-1 levels were detected by Western Blotting. Rap-1, B-Raf and Raf-1 were found to be expressed in WEHI-231 cells under all conditions tested and the levels of Rap-1 and Raf-1 did not appear to be substantially reduced by BCR-ligation or indeed correlate with the differential levels of pERK observed in control and BCR-stimulated WEHI-231 B cells (Fig.3.11A-D). Concerning Rap-1 expression, these results were further confirmed by LSC analysis of immunofluorescence staining of Rap-1 expression in individual cells showing no changes of the percentage or overall level of Rap-1 expression (Fig.3.11E). However, Raf-1 expression appeared to be upregulated by CD40 signalling, results perhaps consistent with the finding that ERK activation is generally found to be higher in these cells across the full time course. Rather unexpectedly, Rap-1 expression was found to be somewhat reduced in cells stimulated via the BCR and CD40 at later time points (Fig.3.11D). Most interestingly, however, was the finding that whilst B-Raf appeared to be highly expressed constitutively in control or CD40-stimulated WEHI-231 B cells, its expression appeared to be regulated in a cyclic manner in BCR-stimulated cells which was essentially reversed by CD40 signalling (Fig.3.11).

Next, the relative activities of these ERK pathway regulators were assessed under the various cell fate conditions. Firstly, preliminary studies using the EpiTag™ assay which detects phosphorylated B-Raf were performed. B-Raf is constitutively phosphorylated on serine 446 [448] and this phosphorylation is an indication of activation as it stops auto-inhibition of B-Raf by decreasing the binding of the regulatory and catalytic domain of B-Raf. Thus, even though this position is phosphorylated in the basal state, activation of receptors can enhance the phosphorylation of B-Raf at serine 446 to further increase the spontaneous activity of B-Raf [316]. Consistent with the proposal that BCR-signalling may abrogate Rap-1/B-Raf coupling to ERK, treatment with anti-IgM abrogates the expression of pB-Raf observed in control cells at 4 h. However, there were no significant differences at later time points indicating that this mechanism is likely to be insufficient to explain either the sustained cyclic levels of pERK in untreated WEHI-231 cells or the full BCR-mediated suppression of ERK and its' rescue afforded by CD40 signalling (Fig.3.11F).

To further analyse the impact of the different treatments on the potential activation of molecules involved in the Rap-1/ERK signalling cascade, levels of active

Rap-1 were determined. To this end a commercially available Rap-1 activity assay kit was used. The principle of this assay exploits the fact that GTP-Rap-1, but not GDP-Rap-1, is able to bind the Ras-binding domain of the Ral guanine nucleotide dissociation stimulator (RalGDS-RBD) [449] and hence only the active Rap-1 can be purified by binding to RalGDS-RBD-conjugated agarose beads and analysed by subsequent Western Blotting using an anti-Rap-1 antibody. Using this approach, stimulation of WEHI-231 cells with anti-IgM antibody was shown to substantially reduce the levels of active Rap-1 over the period where ERK activity is suppressed whereas simultaneous treatment with anti-CD40 could partially reverse this effect (Fig.3.12A-D). These results were confirmed by LSC analysis of immunofluorescence staining using a recombinant Ral-GDS-RBD-GST construct to track activated Rap in individual cells (Fig.3.12E). Here BCR stimulation of WEHI-231 cells was found to decrease overall expression levels as well as the percentage of cells expressing active Rap at high levels 24 hours post-stimulation (Fig.3.12F/G). Similar to the data acquired by Western Blotting, CD40-costimulation partially rescued the cells from downregulation of active Rap, slightly increasing the percentage of cells containing high levels of active Rap (Fig.3.12F/G). Taken together these results indicate that BCR-signalling in WEHI-231 cells decreases the levels of active Rap which could contribute to the observed reduced activation of MEK and hence ERK. CD40-ligation, which is known to re-establish cyclic ERK activation and proliferation in BCR-stimulated cells, was found to partially reverse the decrease of active Rap. This could be one of the mechanisms CD40 utilises to prevent growth arrest.

3.3.5 SPA-1 expression is regulated by BCR-mediated signalling

In order to shed some light on the possible mechanisms by which BCR-signalling could inactivate Rap-1, the role of the RapGAP, SPA-1, [405,450] was investigated. SPA-1 indeed appears to be upregulated both at the protein and at the transcriptional level in WEHI-231 cells after BCR stimulation (Fig.3.13A and D/E). Furthermore, anti-CD40 induces a significant downregulation of SPA-1 mRNA and protein levels and reverses the effects of BCR-ligation reducing SPA-1 levels even below the levels observed in untreated cells, findings perhaps consistent with the rescued levels of ERK activation found in these cells (Fig.3.13A and D/E). As previously reported, SPA-1 was mainly found in the nucleus and cytoplasm [451]. Its cytoplasmic localisation allows SPA-1 to regulate the activity of Rap whereas nuclear SPA-1 might carry out different, so far ill-defined, functions (Fig.3.13B).

Many of the negative regulators of the ERK MAPK cascade, such as MAPK phosphatases can be themselves regulated by feedback loops [452]. Therefore, in order to determine the effect of ERK activation on SPA-1 expression in spontaneously

proliferating WEH-231 B cells, these cells were treated with the pharmacological inhibitor of MEK, PD98059 (Fig.3.13C). Perhaps surprisingly, inhibition of sustained cycling ERK activation did not affect SPA-1 mRNA expression. Rather, inhibition of PI3 kinase appeared to mimic the effects of BCR-ligation concerning SPA-1 mRNA expression, as treatment of cells with a specific PI3 kinase inhibitor (LY294002) increased SPA-1 RNA levels (Fig.3.13D-E). No further increase in SPA-1 mRNA levels could be detected following co-culture of the cells with the MEK and PI3 kinase inhibitors.

Supporting evidence for a role for PI3 kinase in the regulation of SPA-1 expression was provided by experiments utilising WEHI-231 cells stably expressing RasV12, RasV12S35 and RasV12C40 [453] which are constitutively active Ras mutants either activating both the PI3 kinase and ERK cascades (RasV12), or selectively the ERK (RasV12S35) or PI3 kinase (RasV12C40) cascade [171,454].

Although, as previously mentioned, it had been shown by this laboratory that activation of Ras was not substantially modulated by BCR-ligation, overexpression of constitutively active Ras mutants which prevented BCR-mediated downregulation of ERK signalling was able to rescue WEHI-231 cells from growth arrest at least in the first 24 hours following BCR stimulation [373] (Fig.3.14) and as such provide a useful tool for the dissection of the role of differential effects of Ras activation.

Interestingly, although SPA-1 mRNA levels were essentially the same in empty vector control cells and all of the Ras-mutant cells at time zero, levels of SPA-1 mRNA were slightly lower in unstimulated cells transfected with either RasV12 or RasV12C40 compared to empty vector- or RasV12S35-transfected cells after 24 hours in culture (Fig.3.14C). Similarly, the increase of SPA-1 mRNA observed upon BCR-ligation was found to be reduced in cells transfected with either RasV12 or RasV12C40 compared to empty vector- or RasV12S35-transfected cells (Fig.3.14C). These results suggested that Ras-dependent PI3 kinase but not Ras-mediated ERK activation is efficient at suppression of SPA-1 transcription and supported the previous findings using pharmacological inhibition which showed pronounced effects of PI3 kinase but not ERK inhibition on SPA-1 mRNA levels (Fig.3.13D/E). Interestingly, expression of these Ras constructs was not effective at suppressing growth arrest at later timepoints (48 hours) [447], further supporting the hypothesis that Ras-independent signalling is a target of BCR-mediated growth arrest, especially during the later stages of the response.

Collectively, these results indicate that, in untreated and therefore proliferating WEHI-231 cells, PI3 kinase signalling suppresses the transcription of SPA-1 which could increase levels of active Rap and hence ERK. Consistent with this, BCR stimulation of immature B cells has been reported to reduce PI3 kinase signalling [455] and therefore, this could potentially lead to the loss of SPA-1 suppression and an

increase in SPA-1 levels. Thus, these elevated levels of SPA-1 might be partly responsible for the BCR-mediated downregulation of Rap and hence ERK.

3.3.6 PAC-1 mRNA expression is regulated by BCR-mediated signalling

PAC-1 is a DUSP which dephosphorylates ERK and thereby inactivates it [365,368]. It was previously shown to be upregulated at the protein level and recruited to ERK-containing complexes following BCR stimulation in WEHI-231 cells [310]. The mechanisms involved in such upregulation have not yet been defined and so the regulation of PAC-1 mRNA expression was therefore now examined in WEHI-231 cells. It was shown that anti-IgM stimulation appeared to increase the expression of PAC-1 mRNA in a cyclical manner with an early peak within 2 h followed by a later peak between 8-24 h (Fig.3.15). Similarly to that observed for SPA-1 expression, an inverse PAC-1 expression pattern was found in cells treated with either anti-CD40 (or indeed anti-IgM in combination with anti-CD40) as PAC-1 expression was downregulated in those cells to levels below those detected in untreated cells (Fig.3.15). As mentioned before, negative and positive feedback loops often modulate DUSP-mediated regulation of MAPK pathways. It was therefore perhaps not surprising to find that inhibition of PI3 kinase or, to a lesser extent, ERK increased the expression of PAC-1 at the mRNA level, to a similar extent as that observed following BCR-ligation (Fig.3.15). Interestingly, this enhancement was only apparent some 12-16 h after addition of inhibitors but functionally, this would mimic the period in which BCR signalling had also downregulated ERK activation. Whilst these data indicate that both ERK and PI3 kinase pathways can independently suppress the transcription of PAC-1, co-culture with both inhibitors appears to further enhance PAC-1 mRNA production suggesting that these may interact and perhaps even cross-regulate each other.

To potentially corroborate these data, PAC-1 mRNA expression levels were also investigated in the WEHI-231 B cell lines expressing the mutant constructs of RasV12. Here, PAC-1 mRNA expression was found to be comparable in all 4 lines at time zero, but was found to be lower in cells expressing any of the active forms of Ras compared to empty vector cells after 24 h of culture (Fig.3.15C). Moreover, and supportive of the pharmacological inhibitor data, cells transfected with any of the three Ras mutants displayed reduced upregulation of PAC-1 due to BCR-ligation (Fig.3.15C) confirming that Ras-mediated activation of either of the ERK and PI3 kinase pathways reduces the expression of PAC-1 and thereby enhances ERK signalling.

3.3.7 Differential subcellular localisation of Rap-1 and ERK

It is becoming increasingly evident that the functional outcome of signalling pathways is not only dependent on the expression levels and activation status of the proteins but also on their subcellular localisation as this determines the upstream and downstream interaction partners. Thus, preliminary experiments were carried out to investigate whether Rap-1, pERK and ERK signals were differentially localised in spontaneously proliferating cells in comparison to those undergoing BCR-mediated negative selection and rescue via CD40. Thus, the expression of Rap-1, pERK and ERK was further analysed in cytoplasmic, membrane/organelle (including mitochondrial), nuclear and cytoskeletal fractions (Fig.3.16).

At both timepoints analysed (1 and 24 hours) Rap-1 was most strongly expressed in the membrane/organelle fraction consistent with reports indicating it shuttles between the plasma membrane and endosomal membranes [456]. However, substantial amounts of Rap-1 could also be detected in the cytoplasmic and nuclear fraction both at the early and later timepoints. At the later timepoint (24 hours) Rap-1 was also found in the mitochondrial fraction and BCR-ligation appeared to increase the translocation of Rap-1 to the mitochondria (Fig.3.16C) where it has been shown previously to be able to influence mitochondrial function [457]. Interestingly, whilst Rap-1 expression in the membrane and cytoplasmic fractions appeared to be reduced in BCR-stimulated samples relative to those from spontaneously proliferating cells, it was found to be enhanced in the nuclear fractions under conditions of negative selection at 1 h suggesting that such differential localisation of this signalling element may contribute to the functional outcome of BCR-ligation. Moreover, for all conditions tested, whilst relatively higher levels of Rap-1 were detected in the nucleus compared to the cytoplasm at 1 h, an inverse pattern of Rap-1 expression in these cellular compartments was observed at 24 h. Similarly, localisation to the cytoskeleton could only be detected at the 1 h timepoint (Fig.3.16). Sustained Rap-1 signalling at later timepoints might therefore be originating from different subcellular compartments compared to the early signal (1 hour). This could potentially change the signalling outcome as it has been described before that activation of downstream effectors of the Rap-1 cascade depends on its localisation [458,459].

Activated ERK (pERK) was predominantly found in the cytoplasmic and nuclear fractions 1 hour after stimulation with low level expression of pERK1 but not pERK2 detected in the membrane/organelle fraction (Fig.3.16). The enhanced ERK activation routinely observed in BCR-stimulated cells at this time point (Fig.3.7) was reflected in all fractions analysed indicating that this was a global effect and not restricted to a particular location and/or group of downstream substrates. The selective activation of ERK1 observed in the membrane fractions (and in all but the cytoskeletal fraction

derived from spontaneously proliferating cells) was intriguing as essentially equivalent levels of ERK1 and ERK2 were expressed in these fractions indicating localisation-specific activation of this isoform (Fig.3.16). Moreover, given the relatively high expression of ERK1/2 protein in the cytoplasmic/cytoskeletal compared to the nuclear and membrane fractions, the ERK activation observed in the membrane and nuclear fractions under these conditions was particularly strong. The organelle/membrane fraction contains, amongst others, mitochondria and the expression of pERK in a purified mitochondrial fraction was therefore analysed. However, neither expression of ERK nor its activation was observed in this cellular compartment (Fig.3.16C). The membrane/organelle fraction further also contains endosomes. The importance of endocytosis as well as signalling from endosomes has been underlined by multiple studies [460,461]. For example, MEK partner-1 (MP-1) is a small scaffold protein which localises MEK/ERK to late endosomes where it binds to MEK1 and ERK1 thereby enhancing the activation of this pathway [349]. Interfering with the localisation of MP-1 to endosomes reduced the sustained activation of the ERK cascade rather than early signalling which appeared to take place at the membrane [349,462]. Thus, signalling from this compartment might provide an amplification mechanism to maintain high levels of ERK activation.

After 24 hours pERK was mostly found in the membrane/organelle and nuclear fractions whereas expression in the cytoplasm could not be detected anymore despite ERK protein still being strongly expressed in this fraction (Fig.3.16). Consistent with the whole cell lysate samples, pERK expression is highest in fractions from cells which had their BCR cross-linked in the presence of CD40 signalling but not in cells treated with anti-IgM only (Fig.3.16). Rather surprisingly, however, the high levels of ERK activation detected in whole cell lysates of spontaneously proliferating WEHI-231 cells were not found in any of the analysed subcellular fractions. It is possible that ERK activation in these cells, which is most likely initiated by growth factor signalling, takes place in a fraction of the cells which gets lost during the fractionation process. It would be of interest to identify the localisation of activated ERK in these spontaneously proliferating cells, as the reduced overall activation of ERK in BCR-stimulated cells could be due to the inability of ERK to localise to this, as yet not identified, cellular compartment. This might also reflect the other unexpected finding reputed above of the preferential activation of ERK1, rather than ERK2, in most compartments 1 hour after stimulation (Fig.3.16). This is in stark contrast to the favoured activation of ERK2 detected in whole cell lysates. Thus again, this discrepancy between the pattern found in whole cell lysates and the subcellular fractions might be due to the loss of a particular cellular compartment during the experimental procedure. These results are intriguing as ERK1 and ERK2, although they are highly homologous and can compensate for each other

concerning many ERK-dependent responses [463], carry out some non-overlapping functions [464,465]. The differential levels of activation of these two isoforms as well as their varying localisation could therefore indicate that ERK1/2 direct different signalling outcomes during BCR-mediated growth arrest and apoptosis.

Finally, detection of marker proteins such as VDAC-1 (marker protein for mitochondria – membrane/organelle fraction) and HDAC-1 (marker protein for nuclear fraction) was used to validate the subcellular fractionation. Thus, HDAC-1 although found to be weakly expressed in all fractions, was strongly enriched in the nuclear fraction, as expected (Fig.3.16). By contrast, VDAC-1 expression, a marker for mitochondria, was found to be enriched not only in the membrane/organelle fraction but also in the cytoskeletal fraction (Fig.3.16) possibly indicating carry over from the membrane/organelle fraction to the cytoskeletal fraction. Collectively, the data described in this section shows that subcellular fractionation and analysis by Western Blotting could provide a useful tool to identify interesting changes in the localisation of signal transducers under conditions of positive and negative signalling. However, a second method, such as immunofluorescent staining, should be used to confirm the biochemical data or clarify any inconsistencies.

3.3.8 Overexpression of Rap-1 in WEHI-231 cells

The data described above provides circumstantial evidence that Rap activity might contribute to ERK activation in spontaneously proliferating WEHI-231 cells. Thus, to directly address this, the effects of over-expressing different forms of HA-tagged Rap-1A (constitutively active/dominant negative forms) in WEHI-231 cells were assessed relative to empty vector controls.

The BCR-mediated growth arrest response of cells transfected with Rap-1A WT did not differ greatly from the response seen in cells expressing either the constitutively active form (Rap-1A G12V) or the dominant negative form (Rap-1A S17N) of the protein or indeed the empty vector control at 48 h. The rescue from anti-IgM induced growth arrest by stimulation of the CD40 signalling cascade was not differentially influenced by expression of any of these mutant proteins, but rather all of them prevented the full CD40-mediated rescue observed in the cells expressing the empty vector (Fig.3.17A).

WEHI-231 cells transfected with Bcl-x_L (WEHI-231- Bcl-x_L) are protected against BCR-induced apoptosis but not growth arrest [294]. These cells therefore provide a useful tool to study BCR-induced growth arrest independent of the apoptosis response, which is abrogated due to the overexpression of Bcl-x_L. Transfection of WEHI-231-Bcl-x_L cells with the constructs encoding the above mentioned forms of Rap-1A could therefore give further insight into the mechanisms regulating growth arrest

independently from apoptosis. Therefore, WEHI-231-Bcl-x_L cells were transfected with pcDNA3.1(-)Zeocin vectors encoding the previously described Rap-1A mutants. The pcDNA3.1(-)Zeocin vector encodes a resistance gene which allows the positive selection of successfully transfected cells in media containing the antibiotic Zeocin enabling selection of double-transfectants. Thus, after transfection with the above-mentioned vectors and positive selection in Zeocin-containing media, the functional responses such as anti-IgM induced growth arrest, CD40-mediated rescue from growth arrest as well as induction of apoptosis were analysed in the transfected cells. The cells expressing the Rap-constructs underwent growth arrest to a very similar extent as these containing the empty vector at 24 hours (Fig.3.17B). Moreover, in these WEHI-231 Bcl-x_L cells CD40-mediated rescue from BCR-induced growth arrest was not influenced by expression of Rap-1A or any of the Rap-1A mutants at 24 hours (Fig.3.17B). Moreover, analysis of the cell cycle stage of the cell populations showed only minor differences. Due to the overexpression of Bcl-x_L only a very small proportion of WEHI-231- Bcl-x_L cells undergo BCR-mediated apoptosis (Fig.3.18). Nevertheless, more of the cells transfected with Rap-1A WT, Rap-1A G12V and in particular Rap-1A S17N appeared to initiate apoptosis upon BCR-ligation compared to the empty vector-transfected control cells. However, none of the G0/G1 or mitotic responses observed in cells expressing the Rap constructs (Fig.3.18) indicated that Rap greatly influenced the responses of these cells to BCR stimulation.

To investigate the possibility that despite the selection procedures, inefficient transfection or expression of the molecules was the reason for the observed lack of changes of the response of transfected cells, expression of the HA-tag in WEHI-231-Bcl-x_L cells transfected with pcDNA3.1(-)Zeocin vectors, containing various forms of Rap, was assessed. Indeed, it was shown that even after selection in Zeocin containing media the expression of HA-tagged Rap-1A proteins could not be detected (Fig.3.19A). The positive signal detected in control fibroblast transfected with an HA-tagged PCKα construct further proved that the inability to detect the expression of HA-tagged proteins in the WEHI-231-Bcl-x_L cells was not due to a lack of antibody-binding or any other experimental difficulties (Fig.3.19A). Additionally, transfected WEHI-231-Bcl-x_L cells displayed the same levels of Rap-1 expression as empty control vector- or un-transfected cells further confirming the lack of overexpression of the transfected proteins (Fig.3.19A).

Due to these difficulties and to further assess the cause of the lack of expression it was decided to transfect WEHI-231 cells using pIRES2-AcGFP1-vectors encoding various forms of Rap-1A which should lead to the expression of the marker protein GFP upon successful transfection. Indeed, GFP-positive cells could be detected 24 h after transfection of WEHI-231 cells (Fig.3.19B). However, the efficiency of transfection

was very low. Furthermore, stability of transfected clones was an issue, as GFP-expression and hence expression of the genes of interest was found to be transient even in the presence of the selection antibiotic G418. Thus, expression of GFP declined rapidly and was lost by 11 days post-transfection (Fig.3.19B-C). To try and overcome the technical difficulties hindering stable transfection of WEHI-231 cells, various constructs, methods of transfection and selection conditions were tested (summarised in Fig.3.19C-ii/iii). However, stably transfected lines were not achieved under any of the tested conditions.

In view of the experimental problems in creating stable Rap-1A-expressing lines using conventional transfection methods, another method for creating stable clones, lentiviral transduction, was tested. Production of infective lentiviral particles was shown to be effective, as virus generated from transfected HEK293 T cells was able to transduce HT-1080 cells leading to the production of the marker protein ZsGreen1 which could be detected by FACS (Fig.3.20A). Furthermore, it was possible to detect high expression of the HA-tagged Rap-1A proteins in lysates of these transduced cells (Fig.3.20B). Lentiviral transfection therefore provides a promising method of choice for future experiments investigating Rap-1-dependent signals in WEHI-231 cells.

3.3.9 The role of the ERK cascade in the regulation of c-Myc

c-Myc is an important transcription factor involved in cell cycle progression and thereby cell proliferation. It is known that BCR cross-linking on the WEHI-231 B cell line leads to a transient induction of c-Myc mRNA and protein levels followed by a sustained downregulation [466,467]. By contrast, CD40 ligation, which is known to rescue WEHI-231 cells from growth arrest and apoptosis, was found to stabilise c-Myc levels [468]. In agreement with such results stimulation of WEHI-231 cells with anti-IgM resulted in downregulation of c-Myc protein levels within 4 hours reducing them to below baseline levels for at least 32 hours (Fig.3.21). By contrast, and in keeping with its ability to promote cell survival, CD40-ligation on its own enhanced c-Myc and ameliorated the downregulation of c-Myc induced by such BCR stimulation (Fig.3.21). Moreover, in unstimulated cells, c-Myc expression displayed a cyclic pattern over time, similar to previously observed with phosphorylated ERK (Fig.3.7). c-Myc expression therefore seems to mirror the pattern observed for phosphorylation and hence activation of ERK in either unstimulated, BCR- or BCR/CD40-stimulated WEHI-231 cells. Perhaps consistent with this, phosphorylation including that in response to ERK has been implicated as an important mechanism in the regulation of c-Myc protein levels. Thus, phosphorylation of the protein at residue serine 62 stabilises the protein, a mechanism that is probably used to promote c-Myc-driven progression through the cell cycle [469,470]. By contrast, phosphorylation of c-Myc on threonine 58 by GSK3 has

been shown to lead to the protein phosphatase 2A (PP2A)-dependent dephosphorylation of serine 62 which destabilises the protein leading to its ubiquitination and degradation by the proteasome [469]. In confirmation with the putative role the phosphorylation of these specific residues plays in the stabilisation of c-Myc, the stabilised form, pc-MycS62, was found to be downregulated by BCR-mediated inhibition of ERK (Fig.3.21). In order to furthermore address whether BCR-mediated downregulation of c-Myc and pc-MycS62 reflected GSK3-mediated phosphorylation of T58 followed by ubiquitination and degradation, the expression of pc-MycT58 was also analysed (Fig.3.22). At first sight, the finding that expression of this phosphorylated form of c-Myc was abrogated within 4-8 h of BCR stimulation was rather surprising but given that protein expression of c-Myc was not detectable in these cells suggests that c-Myc had already been degraded by this point and any such peak of T58 phosphorylation targeting c-Myc for ubiquitination would have occurred between 2-4 h. Consistent with this proposal, analysis of the profiles of pc-MycT58 expression in the spontaneously proliferating cells reveals that peaks of expression occurs prior to downregulation of c-Myc expression resulting in a cyclic pattern of c-Myc expression (Fig.3.22). These results were corroborated by analysis using an antibody that recognises c-Myc which is either dually-phosphorylated at Ser62 and Thr58 (pc-MycT58/S62) or phosphorylated at Thr58 but not at Ser62 alone and is therefore only able to detect c-Myc targeted for ubiquitination by Fbw7 [471] (Fig.3.22). Similarly, this antibody also detected major peaks of phosphorylated c-Myc prior to the general downregulation of c-Myc levels (Fig.3.22).

As it has been reported in other systems that ERK can regulate c-Myc stability by phosphorylating it at serine 62 [384,386], the potential role of ERK signalling in the regulation of c-Myc stability was assessed by treating spontaneously proliferating WEHI-231 cells with the MEK inhibitor, PD98059, which inhibits ERK activation and results in growth arrest and apoptosis of such cells [310,447]. Furthermore, LY294002, a specific PI3-Kinase inhibitor, was used in order to compare the effects of inhibiting this key regulator of c-Myc stability (by inhibition of GSK3 [388]) as it has previously been reported by the Harnett group and others that BCR-signalling suppresses PI3 kinase activity in WEHI-231 cells [373,455]. These data showed that repeated addition of the MEK inhibitor led to inhibition of ERK activation throughout the time course with substantial downregulation, comparable or greater than that seen following BCR-ligation observed at 2 h and from 8 h onwards (Fig.3.23). In general, inhibition of PI3 kinase was not effective at inhibiting early ERK activation but in agreement with previous findings [373] it inhibited ERK activation at later time points (>20 h) and therefore this may reflect induction of growth arrest and therefore secondary inactivation of ERK through unknown mechanisms (Fig.3.23). Consistent with their

proposed roles in stabilising c-Myc expression both inhibitors were also shown to reduce c-Myc expression (Fig.3.23 and 3.24A-D) and similar to BCR-ligation also reduced levels of pc-MycT58/S62 consistently (Fig.3.25A-D).

To determine if different stimulations not only changed the protein levels of c-Myc but also its subcellular localisation, nuclear and cytoplasmic fractions of WEHI-231 cells were prepared and tested for c-Myc expression. BCR- or CD40-ligation or the combination of both did not appear to lead to translocation of c-Myc or pc-MycT58/S62 into the cytoplasm as virtually no protein could be detected in the cytoplasm 4 hours after stimulation (Fig.3.24E and 3.25E). This indicates that c-Myc acts in the nucleus and that its activity is determined by its overall expression levels rather than translocation events. Corroboration of these Western Blot-based results was achieved by immunofluorescent staining which showed that both c-Myc and pc-MycS62 co-localised with the DAPI-stained nuclei (Fig.3.24/25F-i). Moreover, by analysing c-Myc expression using LSC, it was found that not only did BCR stimulation reduce the percentage of cells expressing c-Myc but it also reduced the overall expression level of c-Myc in these cells (Fig.3.24F). Additionally and in confirmation of Western Blotting-based assays, pharmacological inhibition of ERK and PI3 kinase also reduced the percentage of cells expressing c-Myc as well as their levels of c-Myc expression (Fig.3.24F). By contrast, CD40-mediated rescue from growth arrest was found to fully reverse the effects of BCR-ligation by enhancing the levels of c-Myc detected in cells and increasing the proportion of cells expressing c-Myc (Fig.3.24F). Similarly to the results described for c-Myc, the stabilised form of c-Myc, pc-MycS62, was found to be expressed by a smaller proportion of cells after BCR stimulation in comparison to untreated, proliferating WEHI-231 cells at 12 and 20 hours (Fig.3.25F). Moreover, the levels of pc-MycS62 expressed by such cells were found to be reduced upon induction of BCR-mediated growth arrest at the earlier timepoints. Although, at 32 hours the levels of pc-MycS62 in cells treated with anti-IgM were broadly equivalent to that of the control cultures (Fig.3.25F), this presumably reflects the cyclic nature of c-Myc expression in proliferating cells as indicated by the Western Blot analysis (Fig.3.7A). Pharmacological inhibition of ERK and PI3 kinase signalling was as effective at suppressing the expression of the stabilised form of c-Myc as BCR-ligation (Fig.3.25F), further confirming the important role of these cascades in stabilising c-Myc protein levels. Moreover, and in accordance with its ability to enhance the survival of WEHI-231 cells, CD40-ligation markedly increased the levels of pc-MycS62 detected (Fig.3.25F), restoring the expression of stabilised c-Myc in BCR-stimulated cells to levels detected in untreated, proliferating WEHI-231 cells (Fig.3.25F).

Due to its role in the regulation of proliferation and hence potential for oncogenic transformation of cells [472], c-Myc is highly regulated not just at the post-translational

but also at the transcriptional level. Thus, to determine if the BCR-mediated decrease of c-Myc observed at the protein level was partly due to a downregulation at the transcriptional level, c-Myc mRNA expression was determined in spontaneously proliferating WEHI-231 cells or anti-IgM and/or anti-CD40 stimulated cells. c-Myc mRNA expression was indeed found to follow a cyclical pattern in spontaneously proliferating WEHI-231 B cells, similar to those observed with the protein levels of c-Myc (Fig. 3.26A-i). Likewise, stimulation of BCR-signalling led to a transient increase of c-Myc expression peaking at around 2 hours after stimulation (Fig. 3.26A/B) followed by sustained downregulation of c-Myc mRNA levels over a period of 24 hours, which was reversed by activating the CD40 signalling cascade (Fig.3.26A/B). In contrast to their inhibitory effects on c-Myc protein expression (Fig.3.24), inhibitors of ERK and PI3 kinase did not however downregulate c-Myc mRNA levels to the same extent as treatment with anti-IgM, indicating that both the ERK and PI3 kinase signalling cascades acted to mainly regulate c-Myc at the post-translational rather than on a transcriptional level (Fig.3.26A-B). In confirmation of these findings, mRNA levels of c-Myc were also found not to be protected by the expression of the active Ras mutants (Fig.3.26C) which enhance the activation of the ERK and PI3 kinase signalling cascades. By contrast, overexpression of the active Ras mutants diminished the downregulation of c-Myc at the protein level after BCR-ligation (Fig.3.26D). These data therefore further support the idea that regulation of c-Myc downstream of ERK and PI3 kinase cascades seems to be mainly due to regulation at the protein level.

c-Myc is an important regulator of the cell cycle, as it controls the entry into S phase and consistent with this BCR-mediated growth arrest correlates with the reduction of c-Myc levels in WEHI-231 cells. Therefore, to prove the direct correlation between c-Myc levels and cell cycle status of cells, it was decided to utilise LSC analysis to gate on cells with different c-Myc or pc-MycS62 expression levels and determine their distribution in terms of cell cycle stage (Fig.3.27A). Thus, it was found that cells with very low c-Myc or pc-MycS62 expression levels were mostly apoptotic cells and cells arrested in G1 phase, whereas the cells with higher levels of c-Myc and c-Myc pSer62 expression were generally found to be in the mitotic G2/M phase of the cell cycle (Fig.3.27B/C). Although c-Myc expression is mainly needed to overcome the restriction point during G1 growth arrest, the finding that few cells in G0/G1 expressed c-Myc probably reflects that these are cells arrested in G0/G1 rather than transiting through the cell cycle. The relatively low levels of c-Myc/ pc-MycS62 detected in cells in the S phase (Fig.3.27B/C) on the other hand are not surprising as it has been shown before that progression through S phase is not hampered by the lack of c-Myc and that the need for elevated c-Myc expression is not as stringent during S phase [473,474]. Expression of c-Myc/c-Myc pSer62 was also found to be relatively low in freshly divided

new daughter cells (Fig.3.27B/C) which most likely reflects their resting state, as they have to induce growth prior to re-entering the cell cycle at the G1 phase.

As shown above, inhibition of the ERK and PI3 kinase cascades reduces the activation of ERK as well as the overall expression of c-Myc (Fig.3.23). In confirmation of previous results [310,373], such pharmacological inhibition of ERK or PI3 kinase gradually induced growth arrest of WEHI-231 cells between 12 and 32 hours after the addition of the inhibitors (Fig.3.28). Thus, both inhibitors increased the percentage of cells arrested in G0/G1 and diminished the proportion of cells in the mitotic phases of cell cycle (G2-M and S phase) in a similar manner to that following of BCR-ligation (Fig.3.28A). A more detailed analysis revealed that such effects on cell cycle progression directly correlated with the levels of c-Myc as well as its stabilised form c-Myc-pSer62. Thus, the higher the expression of c-Myc or pc-MycS62 in these populations of cells, the fewer cells were found in G0/G1 growth arrest (Fig.3.28B). Collectively, these data suggest that the direct correlation between growth arrest induced by the inhibition of ERK and PI3 kinase activation and reduced c-Myc expression indicates that BCR-mediated reduction of ERK and PI3 kinase signalling might contribute to growth arrest by abrogating c-Myc levels by interfering with c-Myc stabilisation.

3.3.10 The role of CTCF in BCR-induced growth arrest

The data presented so far suggests that BCR-mediated modulation of the ERK and PI3 kinase cascades regulates c-Myc levels mostly through post-translational modifications rather than transcriptional regulation. However, BCR-ligation was also found to inhibit c-Myc transcription and this is also likely to have contributed to the reduced protein expression observed. It was therefore decided to examine CTCF, a transcription factor that is known to repress transcription of the c-Myc gene [475] and has previously been shown to be upregulated after stimulating WEHI-231 cells with anti-IgM [476]. Consistent with this, CTCF overexpression has been shown to lead to the downregulation of c-Myc and upregulation of p19, p21, p27 and p53 and thereby to the induction of growth arrest [476].

Interestingly, given the previously demonstrated expression patterns of pERK and c-Myc (Fig.3.7), CTCF expression also appears to be regulated in a cyclical manner at both the mRNA and protein level in spontaneously proliferating cells (Fig.3.29). Moreover, expression at the protein level is enhanced throughout the time course following BCR-ligation and reduced by signalling via CD40 (Fig.3.29). Whilst the effects of BCR signalling were not replicated at the transcriptional level suggesting a role for stabilisation of CTCF protein expression, CD40 signalling did tend to suppress CTCF mRNA production. (Fig.3.29). Thus, increased expression of CTCF upon BCR-

ligation might contribute to the transcriptional repression of c-Myc. Like many other transcription factors, the activity of CTCF can be influenced by post-translational modifications such as phosphorylation. In the case of CTCF, phosphorylation at certain serines in its C-terminus attenuate its suppressive capacity [477]. It therefore remains to be determined if, rather than changing the overall level of CTCF, BCR-signalling might change CTCF activity more dramatically by changing its phosphorylation status.

3.3.11 BCR stimulation regulates expression and activation of key regulators of cell cycle control

Cell cycle progression of WEHI-231 cells has been reported to depend on the downregulation of inhibitors like p27 or p19 [335,476]. p27 especially seems to be crucial in the regulation of G1 growth arrest due to its ability to inhibit cyclin D/Cdk4/6 complexes as well as cyclin E/Cdk2 complexes thus hampering the entry into S phase [478]. Consistent with this, c-Myc induces the upregulation of an SCF-E3 ligase complex which ubiquitinates p27 thereby targeting it for degradation [479] and relieving such suppression of cyclin/Cdk activity. Moreover, c-Myc increases the expression of cyclins and hence further enhances the activity of cyclin/Cdk complexes [480]. Thus, BCR-mediated reduction of c-Myc levels could suppress cyclin/Cdk-mediated phosphorylation of Rb proteins and release of E2F which is necessary for S phase entry.

In confirmation of previous reports [481], p27 protein expression was shown to be increased within 16 h of BCR-ligation, and due to pharmacological inhibition of ERK as well as PI3 kinase pathways (Fig.3.30) correlating with the initiation of growth arrest induced by these stimuli/inhibitors. In confirmation of its pro-survival function, CD40-signalling reduced the expression of p27 and rescue from growth arrest achieved by CD40 costimulation correspondingly reduced the levels of p27 (Fig.3.30). Moreover, similarly to the pattern observed for pERK and c-Myc expression, p27 also seems to be expressed in a cyclical manner in spontaneously proliferating WEHI-231 cells. These data therefore indicate that in WEHI-231 cells p27 represents an important switch between proliferation and cell cycle arrest. BCR-mediated reduction of levels of activated ERK might be linked to increased p27 expression through multiple mechanisms. Thus, ERK has been shown to directly phosphorylate p27, targeting it for ubiquitination and degradation [482]. Additionally, c-Myc dependent regulation of p27 levels might be another mechanism linking activation of ERK and cell cycle progression. It is therefore proposed that BCR-mediated signalling increases the levels of p27 thereby reducing activation of cyclin/Cdk complexes. This will decrease the phosphorylation of Rb and hence ultimately lead to growth arrest.

p53 is another important cell cycle regulator which stops cells from dividing if there is for example, any damage to their DNA. The main mechanisms by which p53 achieves cell cycle arrest is the upregulation of p21, a cell cycle inhibitor which suppresses the activation of Cdk1 and Cdk2 [483]. Moreover, p53 plays an important role in regulation of apoptosis and was found to induce apoptosis by upregulating pro-apoptotic proteins such as Puma, Noxa and Bax, as well as directly interacting with Bcl-2 family members at the mitochondria [484-486]. Preliminary data by this group indicated that p53 might play a role in FcγRIIb-mediated apoptosis and or growth arrest in mature B cells [309]. Thus, p53 might also potentially regulate growth arrest/apoptosis at other B cell developmental stages, such as immature B cells. Therefore, the regulation of p53 downstream of BCR-signalling in the immature B cell line WEHI-231 was analysed. Due to its important role in the cell cycle it is highly regulated, especially at the protein level. Indeed, detection of protein levels of p53 showed an increase of the levels upon BCR-ligation at 24 hours and even more pronounced at 48 hours after stimulation (Fig.3.31A). This increase of p53 protein was counteracted by the simultaneous stimulation of CD40-signalling (Fig.3.31A). However, there were no significant changes at the mRNA level indicating that p53 expression under these conditions is mainly regulated at the protein level (Fig.3.31B).

Rb proteins and their binding partners, the E2F proteins, represent the principal regulatory element controlling entry into S phase [487]. Hyperphosphorylation of Rb disrupts the binding of Rb to E2F leading to the release of this transcription factor enabling it to trans-activate transcription of genes needed for cells to overcome the G1-restriction point [487] (see section 1.7). Phosphorylation of Rb proteins is a gradual process and phosphorylation at multiple positions is necessary to fully abrogate Rb binding to E2F. Cyclin D/Cdk4/6 complexes phosphorylate Rb at serine 780 during the earlier stages of G1 followed by phosphorylation of serines 807/811 by cyclin E/Cdk2 complexes [247,488]. Thus, the presence of hyperphosphorylated Rb proteins indicates the progression of a cell through G1/S transition. The ERK MAPK pathway appears to be involved at multiple stages in the control of Rb phosphorylation as ERK signalling can directly, as well as indirectly through its regulation of c-Myc, increase the expression of cyclin D and reduce levels of the cell cycle inhibitor p27 [482,489,490]. Activation of the ERK cascade can therefore enhance the activity of cyclin/Cdk complexes leading to the hyperphosphorylation of Rb proteins.

Thus, as predicted, phosphorylation of Rb on the serine residues 780 and 807/811 was found to be substantially reduced following BCR stimulation or pharmacological inhibition of the ERK and PI3-Kinase pathways (Fig.3.30). The expression of the other molecules involved in the proliferation and survival of WEHI-231 cells, such as pERK, c-Myc and p27, has been shown to be cyclical over time.

Thus, unsurprisingly, the expression of phosphorylated Rb followed a similar pattern indicating a connection between the mechanisms regulating pERK, c-Myc, p27 and Rb (Fig.3.30 and 3.32/33). CD40-mediated rescue from growth arrest not only restored the levels of phosphorylated Rb but it also enhanced it at the later timepoints (12 hours onwards), an effect also seen in cells solely stimulated through CD40 (Fig.3.30 and 3.32/33). However, at first sight, LSC analysis of pRbS780 expression only partially corroborated the Western Blotting data. Thus, although levels of pRbS780 were found to be increased due to CD40 signalling, the decrease of phosphorylated Rb upon BCR stimulation could not be detected by immunofluorescent staining as the percentage of pRbS780 expressing cells, as well as the expression intensity were found to be above the levels found in untreated, proliferating WEHI-231 cells (Fig.3.32E). However, this discrepancy may simply reflect the fact that Western Blotting for phosphorylated Rb allows analysis of not only the strength of the signal, but also of the relative distribution of the different pRb forms. Thus, phosphorylated Rb appears as multiple bands of increasing size reflecting the sequential hyperphosphorylation of Rb and it is mainly these higher molecular weight bands which are downregulated upon BCR-ligation (Fig.3.32A/B) and which may not be detected by LSC analysis which does not involve protein denaturation and cannot detect changes of protein size due to phosphorylation rather than overall expression differences. This problem however was not encountered concerning detection of pRb S807/811 as the BCR-mediated downregulation observed by Western Blotting analysis was also confirmed by LSC analysis of immunofluorescent staining (Fig.3.33E).Thus, a lower percentage of cells stimulated through the BCR expressed hyperphosphorylated RbS807/811 and the cells which expressed it did so at a reduced level (Fig.3.33Ei/ii). Moreover, in agreement with the results shown by Western Blotting, CD40 signalling not only efficiently increased the percentage of pRbS807/811-expressing cells as well as the level of expression but also prevented the BCR-mediated downregulation of pRbS807/811 (Fig.3.33Ei/ii).

As mentioned previously, phosphorylation of Rb plays a crucial role during G1/S transition, whereas hypophosphorylation will ultimately lead to growth arrest during G1. Thus, to confirm the direct correlation between cell cycle progress and phosphorylation of Rb proteins, cells stained for pRbS780 and pRbS807/811 were analysed concerning their cell cycle status. As expected, higher expression levels of pRbS780 as well as pRbS807/811 correlated with cells being located in the mitotic phases of the cell cycle (Fig.3.32/33F), whereas a higher percentage of cells expressing lower levels of hyperphosphorylated Rb were arrested in the G0/G1 phase of the cell cycle or undergoing apoptosis as detected by supdiploid DNA content (Fig.3.32/33F).

3.3.12 Ubiqitination and proteasomal degradation

Ubiquitination plays an important role in regulating many cellular processes including the cell cycle. Thus, phosphorylation of cell cycle regulators such as p27 and c-Myc at specific regulatory sites targets these proteins for ubiquitination followed by degradation [250,387]. Consistent with this, BCR-mediated growth arrest correlates with the downregulation of c-Myc as well as stabilisation and reduced degradation of p27 (Fig.3.28 and 3.30). Changes in the ubiquitination status of these crucial molecules could therefore reflect commitment to growth arrest and apoptosis of WEHI-231 cells. Indeed, preliminary data suggests that ubiquitination and expression of certain E3 ubiquitin ligases might play a role in directing both BCR-driven negative selection and CD40-mediated rescue. Firstly, when the global ubiquitination pattern of whole cell lysates of WEHI-231 cells treated with anti-IgM and/or anti-CD40 was examined, it was found that the pattern observed in anti-IgM treated cells differed markedly from cells stimulated with CD40 or untreated cells (Fig.3.34) as stimulation through the BCR strongly increased the total amount of ubiquitinated proteins (Fig.3.34B).

To further study whether these differential profiles are due to BCR-signalling pathways utilising ubiquitination to target key signalling elements for proteasomal degradation, the effect of a cell-permeable reversible proteasome inhibitor, MG132, was tested in WEHI-231 cells. Inhibition of the proteasome was found to induce growth arrest and apoptosis independent of any further stimulation, underlining the importance of proteasomal degradation in housekeeping functions needed for survival (Fig.3.34E-F). These non-specific effects of MG132 were found to strongly affect cells from around 8-12 hours after addition of the inhibitor and hence restricted the scope and timescale of analysis during these experiments. Thus, it was decided to mainly analyse timepoints before 20 hours or “trap” substrates of varying kinetics by restricting addition of MG132 to 1 hour before the cells were harvested.

Blocking proteasomal degradation by inhibiting the proteasome should lead to an accumulation of ubiquitinated proteins. Thus, as expected, treatment of the cells with an optimised dose of MG132 increased the level of ubiquitinated proteins as detected by Western Blotting (Fig.3.35). This analysis further showed that, at least in the first 12 h of culture, inhibition of the proteasome converted the profile seen in untreated cells to a phenotype more similar to that observed in cells stimulated via the BCR (Fig.3.35). These results perhaps suggest that in spontaneously proliferating cells there is a dynamic process of ubiquitination and degradation of negative regulatory elements that perhaps allows expression and activation of the cyclical signals promoting survival and proliferation. Moreover, the finding that many of the same bands appear to be ubiquitinated in control and BCR-treated cells, but to a lesser degree (Fig.3.35), may suggest that an additional level of regulation may be afforded by a dynamic balance of

E3 ligase-mediated ubiquitin-based targeting of positive signalling elements counteracted by de-ubiquitination. Thus, in the case of BCR-mediated negative selection, it is possible that this balance is skewed in favour of the ubiquitination system and downregulation of de-ubiquitination enzymes (DUBs).

Thus to assess the impact of the E3 ligase/DUB balance on negative selection of B cells, the effect of proteasome inhibition on p27 and c-Myc expression levels was examined. These elements were selected as BCR-mediated modulation of their protein stabilisation has been implicated by this study as a regulatory mechanism and both molecules have previously been shown to be regulated by ubiquitin-mediated degradation through the proteasome [250,387]. As indicated previously (Fig.3.7), whilst c-Myc expression exhibits a cyclical profile in spontaneously proliferating cells, its' expression is upregulated in the first 4 h following stimulation via the BCR before being profoundly downregulated, findings consistent with commitment of these cells to BCR-mediated growth arrest and apoptosis. Expression of c-Myc was found to be enhanced following proteasome inhibition in not only the negatively-selected but particularly the spontaneously proliferating WEHI-231 B cells, at least in the first 4 h following addition of MG132 (Fig.3.35). Moreover, inhibition of the proteasome partially inhibited the BCR-mediated downregulation of c-Myc levels even after 8 hours (Fig.3.35A). These results therefore suggested that the regulation of c-Myc protein stability under these conditions and at these early timepoints was achieved by the ubiquitin-proteasomal targeting mechanism through phosphorylation of threonine 58, as reported in other systems [387]. Accordingly, phosphorylation of c-Myc on threonine 58 was found to be strongly upregulated 2 hours after BCR-ligation (Fig.3.22B). Collectively, these results therefore indicate that a BCR-mediated increase of phosphorylation of this inhibitory position triggers ubiquitination and hence targeting of c-Myc to the proteasome followed by its degradation.

The cell cycle inhibitor p27 controls the stability of cyclin/Cdk complexes through directly binding these proteins [263]. Mitotic stimulation of cells induces signalling cascades which lead to the phosphorylation of p27 on threonine 187 by cyclin/Cdk kinases [250,491]. This facilitates the recognition and binding of p27 by the SCF E3-ubiquitin ligase complex thereby initiating the ubiquitination of p27 and finally degradation by the proteasome [479]. Apart from the earliest time point, inhibition of proteasomal degradation with MG132 only marginally increased p27 levels detected in spontaneously proliferating WEHI-231 cells (Fig.3.35). Moreover, inhibition of degradation had no major effects on the already enhanced levels of p27 in BCR-stimulated cells (Fig.3.35). Taken together these results indicate that decreased proteasomal degradation is not a major mechanism controlling the BCR-mediated increase of p27. Moreover, the suppression of p27 levels needed to allow WEHI-231

cells to spontaneously proliferate does not seem to reflect an increase of proteasomal degradation of p27. The increase of p27 levels observed after BCR-ligation is therefore more likely due to upregulation of p27 transcription, a mechanism which has been previously reported to play a major role in the induction of BCR-mediated growth arrest of WEHI-231 cells [481].

To further investigate the proposal that c-Myc is regulated by modification through ubiquitination, a specific ubiquitin-pull-down matrix was used. This method allows the extraction of ubiquitinated proteins which can then be analysed further by, for example, Western Blotting. Thus, c-Myc was found to be present in the fraction of ubiquitinated proteins (Fig.3.36A). At first sight it appeared that BCR-ligation did not increase the amount of ubiquitinated c-Myc, rather it seemed to reduce the levels of c-Myc. However, due to the late timepoint (24 hours) chosen for this analysis, this change seems to be due to the lower overall levels of c-Myc rather than ubiquitination-dependent changes of c-Myc levels, which appear to take place soon after BCR-ligation (2-8 hours) (Fig.3.35).

Ubiquitination seems to be involved in the regulation of many of the major signalling proteins regulating growth and survival of WEHI-231 cells. Therefore, it was decided to examine the effect of proteasomal inhibition on the dynamic regulation of ERK activation, one of the major pathways controlling the fate of WEHI-231 cells. Interestingly, ubiquitination and hence degradation of proteins seems not to be a major mechanism involved in the BCR-mediated reduction of ERK activation as MG132 did not substantially enhance or inhibit either the transient upregulation or subsequent downregulation of pERK (Fig.3.36B). Unexpectedly, the heightened activation of ERK usually observed at the later timepoints (8 hours) after costimulation of the BCR and CD40 was hampered by the inhibition of proteasomal degradation (Fig.3.36B-ii). Thus, these results might argue for the sustained presence of a negative regulator of the ERK cascade which under normal circumstances is targeted for degradation by the proteasome through CD40-mediated signalling thereby lifting the suppression and enhancing ERK signalling. Blocking proteasomal degradation could therefore hinder the degradation of this unknown negative regulator and stabilise it leading to the observed reduction of ERK activation.

Having established a connection between ubiquitination/proteasomal degradation and regulation of signalling pathways involved in BCR-mediated growth arrest, it was decided to analyse the expression of some E3 ubiquitin ligases previously implicated in the regulation of B cell responses (reviewed in [492]). Thus, preliminary experiments were carried out to examine the expression of Cbl-b, c-Cbl, Itch and Grail, all of which have been identified as negative regulators of B and/or T cell signalling [492]. Interestingly, it was observed that Cbl-b, an E3 ubiquitin ligase implicated in the

regulation of B cell and T cell signalling, was itself highly regulated by proteasome-dependent degradation as shown by an increase in Cbl-b levels in MG132-treated samples compared to untreated cells (Fig.3.37A). Moreover, analysis of expression of Cbl-b at the protein and mRNA levels indicated that Cbl-b was upregulated upon BCR-ligation at both the protein and mRNA levels whereas co-ligation of CD40 protected the cells from Cbl-b upregulation (Fig.3.37B/C). As previously mentioned, Cbl-b can influence BCR-signalling through different mechanisms. Hence, a BCR-mediated increase of Cbl-b could decrease Syk levels following its ubiquitination by Cbl-b [441]. Furthermore, Cbl-b could interfere with Rap-1 signalling as it has been shown to ubiquitinate adaptor proteins involved in recruiting Rap-1 [438]. The overall outcome of this BCR-mediated increase of Cbl-b levels could therefore potentially contribute to negative signalling induced by BCR-ligation.

These promising findings led us to analyse the expression of further E3 ubiquitin ligases implicated in regulation of immune cell signalling such as c-Cbl, Itch and Grail. Due to difficulties in qRT-PCR primer/probe design, mRNA expression data could only be acquired for c-Cbl but not for Itch or Grail. c-Cbl mRNA levels, similar to Cbl-b, were upregulated from 8 hours onwards after BCR-ligation (Fig.3.38A). This upregulation could again be prevented by simultaneous CD40 signalling. These changes in mRNA expression, however, did not fully translate into changes at the protein level although c-Cbl was most highly expressed in anti-IgM treated cells and this was suppressed by CD40-mediated signalling (Fig.3.38B). Similarly, analysis of the expression of Itch and Grail appeared to show degradation following co-ligation of the BCR and CD40 (Fig.3.38B). Indeed, Grail was found to be present in different forms (possible degradation products) and stimulation with anti-CD40 antibodies led to an increase in the smaller sized fragments detected (Fig.3.38B). It has been shown in T cells that degradation of Grail allows increased T cell proliferation and diminishes the induction of anergy. Thus, an increase of the levels of these E3 ligases due to upregulation or inhibition of their degradation could contribute to negative signalling mediated by the BCR in WEHI-231 cells.

3.4 Discussion

The adaptive immune system has evolved to allow recognition of and protection against an essentially infinite variety of pathogens. However, this generation of diversity in terms of the numbers of different antigen receptors also permits the creation of self-reactive specificities, necessitating the development of selection processes deleting self-reactive cells from the repertoire. In the case of B cells, this has led to the evolution of a number of checkpoints throughout development at which autoreactive cells are blocked from further progression and activation. Negative selection of self-reactive immature B cells in the bone marrow represents one of the major checkpoints and provides a mechanism of central tolerance. At this stage, strong BCR-mediated signals induce either receptor editing, anergy or apoptosis to drive clonal tolerance. Defects disturbing this checkpoint have been shown to increase the proportion of self-reactive B cells in the periphery, hence potentially increasing the risk of activating these cells and inducing autoimmune inflammation. Therefore, identifying the signals underlying negative selection might provide interesting information to counter the development of autoimmune disease by targeting the regulation of this mechanism. For example, in this chapter signals regulating the ERK MAPK cascade have been examined allowing further insight into the pathways utilised to induce BCR-mediated negative selection of immature B cells and hence potentially identify novel therapeutic targets.

3.4.1 Rap and the RapGAP SPA-1 are regulated by BCR-mediated signals

This laboratory has previously shown that sustained cyclic activation of ERK is necessary for proliferation of WEHI-231 cells (Fig.3.7) and BCR-mediated abrogation of this ERK signal induces growth arrest and apoptosis [310]. However, the signals linking ERK activation to cell survival and cell cycle progression were not fully elucidated in this model. Nevertheless, some of the pathways involved in the regulation of such ERK activation have been partly identified. These data indicated that downregulation of Ras activity due to BCR-ligation is not the only mechanism leading to reduced ERK activation. Thus, for example, whilst the Ras/Raf-1 pathway has been shown to couple to ERK activation in B cells, preliminary data showed that similar levels of Ras activation occurred in untreated and anti-IgM treated cells [373]. Perhaps consistent with this, other studies indicated that overexpression of Ras protected cells from growth arrest for up to 24 hours. After this time though, constitutively active Ras was not sufficient any more to prevent growth arrest and apoptosis [447]. Therefore,

other molecules which could potentially activate ERK downstream of the BCR were examined to identify their involvement in the induction of growth arrest.

Ras is the prototypical G protein activating the MEK/ERK signalling cascade, but it is not the only small GTPase involved in ERK signalling in B cells. Although initially identified as a potential activator of ERK in neuronal cells another GTPase, Rap, has been proposed to regulate ERK activation via a B-Raf-dependent pathway in B cells [411,493]. Thus, in chicken DT40 B cells B-Raf is the main MAPKKK regulating ERK phosphorylation and activation downstream of the BCR, indicating a role for Rap-dependent activation of ERK in mature B cells [170]. Here, Rap was also found to be regulated by BCR-ligation (Fig.3.12), in that BCR stimulation reduced the levels of activated Rap below the levels detected in untreated and hence proliferating WEHI-231 cells and such suppression of Rap activity correlates with the BCR-mediated reduction in cyclic ERK signalling. Interestingly, simultaneous engagement of CD40 reversed the negative effects of BCR-ligation partly restoring levels of active Rap (Fig.3.12). It has been reported that Ras and Rap-1 mediate transient and sustained activation of ERK, respectively. Thus, interfering with Rap-1 activation in PC12 cells causes the loss of sustained ERK activation usually seen upon stimulation with nerve growth factor. Blocking Ras activation on the other hand only affected the transient early activation of ERK [493]. Furthermore, computational simulations and experimental validations have further strengthened this model of a biphasic ERK activation dependent on the two different GTPases Ras and Rap [494]. It can be inferred that a similar system might be deployed to regulate ERK activation in WEHI-231 cells. Hence, the sustained ERK activation observed in spontaneously proliferating WEHI-231 cells would depend on Rap-1 rather than Ras activity.

The upstream regulators responsible for the activation of Rap in WEHI-231 cells have not been examined yet, but in order to identify the pathways involved it would be interesting to analyse the levels of Rap-specific GEFs such as C3G and the effects of BCR-ligation on their expression. For example, signalling through the BCR could potentially recruit proteins to interfere with the complexes formed by Rap, its GEFs and adaptor proteins such as CrkL, Cbl and Grb2. Indeed, this complex is a good candidate for recruitment and activation of Rap in B cells as it has been shown that these molecules interact upon BCR-mediated activation of Rap in mature B cells [495,496].

Interestingly, it has been shown in this chapter that BCR-ligation upregulates Cbl-b (Fig.3.37) which has been implicated in the regulation of C3G, CrkL and Rap complex formation and hence Rap activation. For example, it has been shown in T cells that Cbl-b can ubiquitinate CrkL and influence its ability to interact with its binding partner C3G. Thus, Rap activation was found to be enhanced in Cbl-b deficient T cells [438]. The observed BCR-mediated upregulation of Cbl-b expression in WEHI-231 cells

could therefore potentially be linked to reduced Rap activation. However, the subcellular localisation of Cbl-b and hence co-localisation with Rap or C3G and CrkL has not been examined in this study and it remains to be confirmed whether Cbl-b has a similar function in WEHI-231 cells as in T cells.

Rap activation is not only determined by interaction with GEFs but also by its negative regulators, RapGAPs. One of the best studied RapGAPs in lymphoid cells is SPA-1, making it a likely candidate for the regulation of Rap in the WEHI-231 system. Indeed, whilst SPA-1 was found to be upregulated at the mRNA and protein level by BCR-signalling, CD40-ligation actively suppressed expression of SPA-1 (Fig.3.13). Thus, negative signalling through the BCR upregulates signals leading to the inactivation of Rap such as SPA-1 and potentially, Cbl-b. Consistent with this, a crucial role for Rap signalling in the survival of immature B cells has recently been identified for the first time as an increased proportion of B cells from SPA-1-deficienct mice, which display high levels of Rap activation, showed signs of defects in receptor editing skewing their receptor repertoire towards auto-antigen-specificities ultimately leading to development of autoimmune disease in older SPA-1 deficient mice [429]. This study therefore emphasises the importance of regulated Rap/ERK signalling in immature B cells.

The elements and signalling cascades regulating BCR-mediated transcription of SPA-1 have not been fully elucidated, but SPA-1 was originally identified as a gene upregulated in lymphocytes upon IL-2, ConA as well as antigen receptor stimulation [405]. Moreover, preliminary data in this chapter indicated that negative feedback loops are likely to play a role in the regulation of SPA-1 in immature B cells. For example, it has been shown that PI3 kinase activity is likely to be involved in the suppression of SPA-1 transcription as inhibition of PI3 kinase increased the levels of SPA-1 mRNA to a similar extent as BCR-ligation (Fig.3.13). Consistent with this, overexpression of Ras molecules constitutively activating the PI3 kinase cascade and/or the ERK cascade were found to generally downregulate SPA-1 levels (Fig.3.14). These data imply that PI3 kinase signalling, which can be detected in proliferating, activated cells, negatively regulates SPA-1 and hence increases Rap activation, which in turn can activate ERK to induce signalling that further strengthens the pro-survival programme.

Another negative regulator of the ERK cascade, PAC-1, was also found to be transcriptionally regulated in a similar fashion to SPA-1. Thus, PAC-1 was found to be upregulated following inhibition of ERK and PI3 kinase signalling whilst overexpression of constitutively active Ras mutants acted to decrease the levels of PAC-1 (Fig.3.14/15), the latter finding being consistent with the ERK cascade being implicated in the regulation of PAC-1 mRNA levels in T cells [366]. However, whilst activation of T cells was found to induce sustained transcription of PAC-1 in an ERK-dependent

fashion, BCR-signalling only transiently upregulated PAC-1 transcription. Thus, BCR stimulation increased PAC-1 expression at the very early timepoint (2 h) (Fig.3.15) and it can be envisaged that this reflected the strong but transient ERK signal triggered by the BCR at this time. However, at the later timepoints, it is not clear what signals are responsible for PAC-1 transcription required for BCR-mediated downregulation of the sustained cyclic ERK activation. By contrast, the sustained cyclic moderate ERK signalling presumably reflects cycles of PAC-1 upregulation and decay.

In conclusion, positive signals such as PI3 kinase and ERK signalling appear to actively suppress the expression of negative regulators of the ERK cascade. On the other hand BCR-signalling acts to abrogate both these signalling cascades, releasing the transcriptional suppression of SPA-1 and PAC-1. These molecules therefore ensure the continuing inhibition of ERK signalling and in this way, the commitment of cells to growth arrest and apoptosis.

3.4.2 Subcellular localisation of signalling molecules

The localisation of signal transducers inside the cell can be as important as their levels of expression or activation status, due to the different potential interaction partners present in the various subcellular compartments. Analysis of the levels of Rap-1, activated ERK and SPA-1 showed that the cellular distribution of these signals indeed changes depending on the time points and stimuli analysed. For example, as expected, SPA-1 was mainly found in the nucleus and cytoplasm as previously observed [451]. Thus, cytoplasmic SPA-1 most likely regulates the activity of Rap whereas nuclear SPA-1 might carry out different, as yet unknown, functions. Relating to this, SPA-1 has recently been found in a complex with the chromatin binding protein Brd4 in the nucleus of HeLa cells [451]. Brd4 can influence assembly of transcription factor complexes and has been implicated in processes such as cell cycle control and DNA replication [497] suggesting that SPA-1, by binding Brd4 or potentially other nuclear proteins, could influence cellular processes independent of its RapGAP function.

Rap itself can also be found in different subcellular compartments as evidenced by its' presence in cytoplasmic, nuclear, membrane/organelle, cytoskeletal as well as mitochondrial fractions of WEHI-231 cells. However, Rap-1 levels and subcellular localisation were found to be similar in all the differently stimulated cell populations (Fig.3.16). Rather, the major change observed was in the localisation of Rap with time and hence cell fate status. Thus, independently of the various stimuli Rap expression was found to be diminished in the nuclear and cytoskeletal compartments following culture for 24 hours compared to the levels found at 1 hour. Rap isoforms have previously been found to localise to the ER [498], endosomes [499] and Golgi complex

[500] inducing different signalling outcomes depending on their localisation. For example, perinuclear activation of Rap by Epac does not result in the activation of the ERK cascade at this location as a result of C3G, as well as downstream components such as B-Raf, not being localised to this cellular compartment [458]. Interestingly, sustained Rap-1 and ERK activation in response to nerve growth factor stimulation has been observed at endosomes in PC12 cells rather than at the plasma membrane [459]. It is therefore possible that localisation of Rap to the endosomes could also reflect sustained Rap activation in the WEHI-231 system. Interestingly, given that Rap-1 was found in the mitochondrial fraction (Fig.3.16C), Rap-1 has also been found to localise to mitochondria in a renal tubular cell model of glucose induced apoptosis where it ameliorates mitochondrial dysfunction by interacting with Bcl-2 [457]. Whether Rap is activated at the mitochondria of WEHI-231 cells or interacts with Bcl-2 family members remains to be established. It should be borne in mind, moreover, that the general lack of change in Rap expression/subcellular localisation observed (Fig.3.16) might be due to the fact that detection of Rap-1 by Western Blotting does not differentiate between active and inactive Rap-1. Thus, immunofluorescent staining for Rap-1 activation in combination with subcellular marker proteins identifying organelles such as mitochondria, endosomes, plasma membrane or the nucleus would clarify if Rap-1 activation in various subcellular compartments is modulated due to BCR-ligation.

That it is likely that detection of active Rap would render different results from looking at Rap expression levels, is supported by the analysis of levels of activated ERK compared to those of ERK protein expression. Thus, although ERK expression as such does not change in the cytoplasmic or nuclear fraction, activation of ERK increases dramatically 1 hour after BCR-ligation (Fig.3.16). Even more striking is the altered distribution of activated ERK at the later timepoint as at 24 hours after BCR stimulation, hardly any activation can be detected in the cytoplasm whereas pERK is still present in the membrane/organelle and nuclear fractions (Fig.3.16).

In its inactive state ERK has been shown to be mainly localised in the cytoplasm where it is retained by various regulatory molecules, the major being MEK. Upon phosphorylation and hence activation, ERK can translocate to the nucleus whereas MEK stays in the cytoplasm [501]. The importance of such nuclear expression of activated ERK has been underpinned by the finding that growth factor induced DNA replication, as well as cFos activation, is blocked by the forced retention of ERK in the cytoplasm [502]. Although nuclear localisation seems to be the major pathway deployed to regulate ERK-mediated transcription, other downstream signalling cascades can be activated in different compartments of the cell. For example, β-arrestin was observed to associate with ERK retaining it in the cytoplasm and enhancing its activity. Thus, by preventing ERK from entering the nucleus [503], β-

arrestin complexing could provide a mechanism to potentially increase ERK activity in the cytoplasmic compartment, directing and allowing the phosphorylation and activation of cytoplasmic substrates such as $cPLA_2$ or MAPK-activated kinases. Indeed, this might be the case in the WEHI-231 cells as high levels of activated ERK were detected early on (1 h) in the cytoplasm of cells stimulated via the BCR (Fig.3.16), signalling which has previously been shown to be key to activating $cPLA_2$ and inducing apoptosis. BCR-signalling subsequently switches off sustained, cyclic ERK activation after this transient increase whereas simultaneous ligation of CD40 restores activation of ERK. Interestingly, the pool of activated ERK in the nucleus was diminished in BCR-stimulated cells after 24 hours of culture. Thus, whilst both negative (BCR) and positive (BCR and CD40) signalling can induce the strong upregulation of active ERK observed in the cytoplasm at early time points, only positive signalling allows the sustained nuclear activation of ERK which may act, at least in part, to overcome BCR-mediated negative signalling by inducing counteracting survival mechanisms partly dependent on the nuclear function of ERK. Moreover, although the strong cytoplasmic ERK activation appears to be prerequisite for activating the $cPLA_2$ apoptotic pathway, CD40 signalling blocks activation of $cPLA_2$ despite also inducing high ERK activation.

3.4.3 ERK-dependent regulation of c-Myc levels

ERK is known to regulate proliferation of various cell types by impacting on the regulation of the cell cycle. For example, cyclin D1 in a complex with its Cdk binding partner controls S phase entry and cyclin D1 upregulation is mediated by Fos-Jun transcription factors which in turn are activated by ERK [504]. Thus, increased levels of cyclin D1 therefore enhance the formation of active cyclin/Cdk complexes permitting the exit from G1 phase and hence cell cycle progression. Mitogenic signalling via the BCR in mature B cells induces cyclin D2 and to a lesser extent cyclin D3 expression rather than cyclin D1 [505] and B cells from cyclin D2-deficient mice displayed a lack of BCR-mediated proliferation confirming that this cyclin D isoform plays a crucial role in cell cycle progression [506]. Additionally, cyclin D2 has been shown, similarly to cyclin D1 in other cell types, to be regulated by ERK in mature B cells. Thus, inhibition of the MEK/ERK cascade blocked cyclin D2 expression and hence phosphorylation of Rb [490].

However, the exact mechanism connecting such ERK activation with cyclin D2 transcriptional regulation has not been experimentally determined. Nevertheless, there are a few possible candidates which could potentially link ERK and cyclin D2 transcription. For example, one of the transcription factors able to regulate cyclin D2 expression, STAT5 [507], has been shown in other cellular systems to be phosphorylated by ERK, increasing its activity [508]. Interestingly, cyclin D2 is also a

direct transcriptional target of c-Myc [480] as Myc/Max binding to its' promoter was shown to enhance cyclin D2 expression [274]. Perhaps consistent with a role for c-Myc in upregulating cyclin D2 in B cells, in this present study it was shown that pharmacological inhibition of ERK activation led to the downregulation of c-Myc protein levels (Fig.3.23-25). In WEHI-231 cells, this appeared to reflect ERK-mediated stabilisation of c-Myc protein levels rather than increase of c-Myc mRNA levels as c-Myc transcription was not influenced to the same extent by pharmacological inhibition of ERK activation as c-Myc protein levels. This is perhaps not surprising as ERK has been shown to regulate c-Myc activity by phosphorylating the serine 62 residue *in vitro* which, if modified, increases the protein stability [387]. Consistent with this, it has now been shown in this study that inhibition of ERK abrogated the levels of c-Myc phosphorylated on serine 62 hence potentially confirming the link of ERK-mediated phosphorylation with the stabilisation of c-Myc in intact cells. Therefore, ERK could be connected to the regulation of cell cycle progression by increasing the level of c-Myc which in turn enhances cyclin D2 expression. Unlike pharmacological inhibition of ERK, BCR-signalling was found to not only reduce the protein levels of c-Myc but also its mRNA levels. Ligation of the BCR might therefore induce additional ERK-independent pathways to regulate c-Myc mRNA levels. The transcription factor CTCF, a repressor of c-Myc transcription [475], has been shown to be upregulated downstream of BCR stimulation (Fig.3.29) and so the BCR-mediated increase of CTCF could contribute to the reduction of c-Myc mRNA levels.

Interestingly, pharmacological inhibition of PI3 kinase was also found to influence c-Myc expression (Fig.3.23), a finding that is consistent with the proposal that through the activation of Akt and inactivation of GSK3, PI3 kinase signalling can directly increase c-Myc protein stability by preventing the inhibitory phosphorylation of threonine 58. However, it is as yet not clear if this potential direct effect on c-Myc regulation is the only reason for reduced c-Myc levels upon inhibition of PI3 kinase signalling as ERK activation was found to be partly reduced in cells treated with the PI3 kinase inhibitor suggesting a link between these two cascades. It therefore remains to be determined whether diminished c-Myc expression is due to inhibition of PI3 kinase signalling or secondary abrogation of ERK activation. Independently of the inhibitor used, c-Myc mRNA levels were not decreased to the same extent as by BCR-ligation (Fig.3.26) indicating that both cascades, ERK as well as PI3 kinase, regulate c-Myc predominantly at the protein level by stabilisation mechanisms.

As mentioned before, c-Myc might provide one of the links between ERK activation and cell cycle progression as it plays an important role in the regulation of the cell cycle machinery. Therefore, by taking advantage of LSC, it was directly tested whether a correlation exists between expression levels of important cell cycle

regulators such as c-Myc and the cell cycle stage. Thus, cells were firstly analysed for the expression of various molecules of interest by Western Blotting to confirm that they are indeed regulated by BCR-ligation. Following this, immunofluorescent staining to link cell cycle stage with the expression level of the molecules of interest, showed that increasing levels of not only pERK, but also of its downstream effector c-Myc as well as the phosphorylated (Ser62) and hence stabilised form of c-Myc, were linked to cell cycle progression. For example, growth arrested cells, as well as apoptotic cells, displayed lower levels of pERK and c-Myc expression compared to cells found in the mitotic phases (G2/M and S phase) (Fig.3.10 and 3.27/28) of the cell cycle, findings consistent with reports that pERK and c-Myc expression is needed to overcome the restriction point and hence G1 growth arrest allowing successful entry into S phase [446,509]. Given that in WEHI-231 cells BCR stimulation suppresses sustained ERK activation which impacts on c-Myc protein stability, it is therefore perhaps not surprising to find a correlation between growth arrest/apoptosis and low levels of pERK/c-Myc expression. Proliferation on the other hand is linked to elevated levels of ERK activation and hence c-Myc levels confirming the need for WEHI-231 cells to upregulate c-Myc levels to enter into and successfully complete the cell cycle.

3.4.4 BCR-mediated regulation of the cell cycle

It has been established that ERK activation and c-Myc expression play a crucial role in determining the fate of WEHI-231 cells. How exactly the ERK/c-Myc cascade impacts on cell cycle progression was further examined by analysing downstream-effectors involved in cell cycle regulation. For example, p27 is a cell cycle inhibitor which acts on cyclin/Cdk complexes to reduce their activation [263]. p27 can be regulated by various means such as transcriptional upregulation or post-translational modifications including phosphorylation [278,510]. p27 provides another potential link between an increase of c-Myc levels and enhanced progress through the cell cycle due to the ability of c-Myc to influence the rate of degradation of p27. This is because components of the SCF-E3 ligase complex, which is responsible for p27 ubiquitination-mediated degradation, are upregulated by c-Myc [511]. Moreover, c-Myc can directly suppress p27 transcription, thereby further decreasing the overall levels of p27. Consistent with their effect on the induction of growth arrest, inhibitors of ERK or PI3 kinase activity mimicked BCR-signalling in increasing the protein levels of p27 (Fig.3.30), in a manner that correlated with the downregulation of c-Myc levels. In the case of BCR-ligation this might be partly due to increased transcription of p27 [481], however stabilisation of p27 due to reduced c-Myc levels in these cells might also play a role as indicated by partial rescue of p27 levels during inhibition of proteasomal degradation (Fig.3.35).

BCR-mediated upregulation of p53 (Fig.3.31) could represent another regulatory mechanism blocking the progress through the cell cycle as p53 signalling can enhance expression of p21, another cell cycle inhibitor regulating entry into S phase by blocking the activation of cyclin/Cdk complexes [512]. Alternatively, p53 could also target the putative ERK/c-Myc pathway by repressing c-Myc transcription [513,514]. For example, Mdm2 (murine double minute 2) is a ubiquitin ligase which binds to p53 and keeps it in an inactive state by binding and blocking its transactivation domain, as well as inducing p53 degradation [515,516]. Interestingly, it has been shown in hepatocytes that ERK is able to phosphorylate Mdm2 at serine 166 which increases Mdm2-dependent degradation of p53 [517]. Additionally, ERK signalling has been shown to induce the transcription of the Mdm2 gene as well as enhance the export of Mdm2 mRNA into the cytoplasm, thereby increasing its translation [518,519]. The reduced levels of active ERK in BCR-stimulated WEHI-231 cells could therefore lead to an increase in p53 and consequent downregulation of c-Myc by resulting in a decrease of Mdm2 expression and activation. Furthermore, the PI3 kinase-activated Akt also phosphorylates and activates Mdm2 at serine 166 [520] and therefore reduced levels of PI3 kinase activation, observed upon BCR-ligation, could further contribute to increased p53 levels. As well as being able to repress c-Myc transcription directly [513], p53 can also act to do this indirectly through upregulation of miR145 [514]. Taken together, BCR-mediated events such as an increase of p27 and p53 prevent cells from overcoming the G1 restriction point and induce growth arrest or pro-apoptotic pathways contributing to BCR-mediated negative signalling.

Mitotic stimulation of cells drives the transition through the G1 restriction point and entry into S phase with the major regulatory switch at this stage being the Rb/E2F module. In its hypophosphorylated state Rb is bound to E2F preventing this transcription factor from transactivating S phase genes [487]. Hyperphosphorylation of Rb by cyclin/Cdk kinase complexes modulates the binding capacity of Rb for E2F, ultimately leading to release of E2F [487]. The presence of hyperphosphorylated Rb is therefore generally a sign for progression through G1 phase. Hence, as might have been predicted, phosphorylated Rb proteins (Ser 807/811 as well as Ser 780) were found at higher levels in spontaneously proliferating WEHI-231 cells compared to those displayed by cells undergoing BCR-mediated growth arrest (Fig.3.32/33). As sustained ERK and c-Myc signalling likely feeds into the upregulation of cyclin D levels, the resultant activated cyclin/Cdk complexes would then phosphorylate Rb proteins contributing to the entry of WEHI-231 B cells into S phase. Stimulation of BCR-signalling, on the other hand, abrogates such ERK activation and c-Myc expression ultimately leading to reduced phosphorylation of Rb proteins and arrest in the G1 phase of cell cycle.

In line with its important role in cell cycle progress, hyperphosphorylation of Rb at Ser 780 as well as Ser 807/811 increased during the cell cycle with highest levels being detected in the mitotic phases (Fig.3.32/33). These regulatory sites on Rb are phosphorylated by different cyclin/Cdk complexes, thus, for example, cyclin D1/Cdk4 but not cyclinE/Cdk2 complexes are able to phosphorylate serine 780 [488]. However, there were no major differences in their pattern of expression as both forms of Rb were mainly found to be highly expressed in S and G2/M phases whereas hardly any cells arrested in G1 or undergoing apoptosis expressed hyperphosphorylated Rb (Fig.3.32/33). Thus, BCR-ligation on WEHI-231 cells induces growth arrest and apoptosis by abrogating cyclic activation of ERK resulting in reduced levels of c-Myc and potentially impacting on cyclin D2 levels and consequently diminished levels of hyperphosphorylated Rb leading to growth arrest due to insufficient release of E2F and induction of S phase genes.

3.4.5 Potential role for ubiquitination and E3 ubiquitin ligases in BCR-induced growth arrest

There are many ways of regulating protein levels and activity in a cell. Ubiquitination provides a mechanism allowing the cell to rapidly change the levels of protein present by targeting such molecules for degradation and thereby modulating signalling pathways in a quick and reversible manner. It was therefore examined whether ubiquitination plays a part in the pathways regulating the proliferative/growth arrest response of WEHI-231 cells. Indeed, initial experiments showed that the pattern of ubiquitinated protein expression by these cells changed following stimulation via the BCR suggesting that ubiquitination is indeed involved in BCR-mediated regulation of signal transducers (Fig.3.34). The availability of inhibitors of the proteasome makes it possible to analyse the contribution of ubiquitination-dependent proteasomal degradation to cellular responses and regulation of protein levels. However, WEHI-231 cells proved to be very sensitive to the toxic side effects of proteasome inhibitors making analysis of longer term signalling difficult. Nevertheless, preliminary results were still promising and provided some information on mechanisms regulating c-Myc levels in spontaneously proliferating WEHI-231 cells. Thus, protein levels of c-Myc were elevated in unstimulated WEHI-231 cells due the addition of MG132, a proteasomal inhibitor, indicating a dynamic regulation of c-Myc expression even in the absence of external stimuli such as BCR-ligation (Fig.3.35) and could explain the cyclic pattern of c-Myc expression observed in proliferating WEHI-231 B cells. Thus, stabilisation of c-Myc by post-translational mechanisms such as phosphorylation of serine 62 by ERK, as well as transcriptional upregulation, would therefore be counteracted by ubiquitin-mediated degradation allowing c-Myc to be maintained at a

steady-state level. This tight control of c-Myc levels is certainly very important, as mutated and hence de-regulated c-Myc has been detected in many tumours causing uncontrolled proliferation of cells [521].

The activation of ERK was also found to be potentially regulated by signalling involving regulatory mechanisms controlled by proteasomal degradation, as it was shown that CD40-mediated rescue of BCR-dependent abrogation of ERK activation could be partially prevented by inhibition of the proteasome (Fig.3.36) suggesting that such rescue might therefore depend on the degradation of a negative regulator. CD40-signalling is regulated by TRAF2, TRAF3 and TRAF6 and it has been shown in B cells that ubiquitination of TRAF3 is necessary to permit the CD40-mediated activation of JNK and p38 [522]. The CD40-dependent activation of ERK in B cells might therefore also rely on the ubiquitination of TRAF3 and consequently, proteasomal inhibition therefore might block ERK activation. Alternatively, a TRAF6-dependent pathway could be targeted by blocking the proteasome as in HEK293 cells, CD40-mediated activation of ERK is achieved through Ras-independent signalling by TRAF6 [194]. Consistent with this, TRAF6 needs to be auto-ubiquitinated to allow full NF-κB signalling [523]. As a side effect of inhibition of the proteasome is the rapid depletion of free ubiquitin [524], the reduced availability of ubiquitin could therefore hinder auto-ubiquitination of TRAF6 and hence reduce its activation and downstream signalling, potentially including the ERK cascade.

Ubiquitination is carried out by an array of enzymes called ubiquitin ligases. E1 and E2 ligases, the first two enzymes in the cascade are ubiquitously expressed in cells whereas E3 ubiquitin ligases confer the substrate specificity to the pathways (see section 1.6). In recent years, research has begun to unravel the various roles E3 ubiquitin ligases play in the immune system. These enzymes function as part of many cascades involved in the regulation of immune cells, such as NF-κB signalling [525] and have been shown to control events proximal to the antigen receptors of T and B cells [492]. The Cbl family of proteins have attracted special attention due to their role in TCR- and BCR-signalling and indeed, both c-Cbl and Cbl-b have been identified as regulators of signalling events controlling T and B cell activation and proliferation [431]. Interestingly, these molecules not only influence signalling pathways via their E3 ligase-mediated ability to ubiquitinate proteins, but also by functioning as adaptor molecules [526].

Data shown in this chapter indicates that Cbl-b and to a lesser extent c-Cbl are regulated by BCR-mediated signalling. Thus, cells stimulated through their BCR displayed enhanced levels of Cbl-b and c-Cbl compared to spontaneously proliferating WEHI-231 B cells (Fig.3.37/38). Cbl-b can potentially regulate BCR-signalling by multiple mechanisms such as its E3 ligase-mediated ubiquitination of adaptor

molecules involved in the activation of Rap. Furthermore, Cbl-b could dampen BCR-signalling by ubiquitination of Syk leading to its degradation [441]. Additionally, Cbl-b might also interfere with the PI3 kinase cascade as it has been shown in T cells that Cbl-b enhances the polyubiquitination of the PI3 kinase subunit p85 [436,437] and hence inhibits its activation by preventing p85 recruitment to CD28. Thus, Cbl-b could similarly contribute to the reduced levels of PI3 kinase signalling detected upon BCR-ligation [455]. Moreover, Cbl-b might negatively regulate Vav [527] as it has been shown that Cbl-b deficient T cells have increased Vav activity and that loss of Cbl-b can restore some of the functions of Vav1-deficient T cells [230]. Upon BCR-signalling Vav is recruited and acts as a GEF for the Rho-family of GTPases including Rac1, RhoA and Cdc42 [146], to influence various cellular functions such as rearrangement of the actin cytoskeleton, thereby regulating capping of the antigen receptor, and optimal calcium signalling as well as stimulation of PLCγ and PI3 kinase [146]. Cbl-b mediated suppression of Vav and its downstream signalling would therefore further contribute to the suppression of activation of WEHI-231 B cells upon BCR-ligation.

Itch and Grail are also E3 ubiquitin ligases which have been implicated in antigen receptor signalling [226,528]. Analysis of their expression levels displayed only minor changes upon BCR stimulation, however, degradation of Itch and Grail appeared to be increased upon CD40-signalling (Fig.3.38). Degradation of Grail has been shown to be regulated by otubain-1, a protein which can be transcriptionally upregulated by Akt/mTOR-mediated signalling [529]. Binding of otubain-1 is thought to allow auto-ubiquitination of Grail, targeting it for the proteasome and hence degradation. PI3 kinase-dependent effects in B cells have been shown to be partially mediated by mTOR signalling, as inhibition of mTOR with rapamycin induces growth arrest of B cells [530]. Moreover, mTOR levels are positively regulated by PI3 kinase signalling [531] and thus, CD40-mediated increased activity of Akt and hence mTOR would increase the expression of obutain-1 leading to Grail degradation. Although hardly any substrates for Grail have been identified yet, RhoGDI (Rho guanine dissociation inhibitor), has been shown to be ubiquitinated by Grail leading to the reduction of RhoA activity in T cells [532]. Interestingly, RhoA is involved in the regulation of PLCγ signalling and calcium mobilisation and hence proliferation of B cells [533]. Thus, CD40-mediated reduction of Grail levels could therefore contribute to the stabilisation of RhoA and calcium signalling further enhancing CD40-mediated pro-survival signals.

3.5 Figures

Figure 3.1 Signalling pathways regulating apoptosis in WEHI-231 cells

In WEHI-231 cells ligation of the BCR leads to a transient increase in ERK activation. Activated ERK in turn phosphorylates and activates $cPLA_2$ which translocates to the mitochondria. $cPLA_2$ catalyses the production of arachidonic acid at the mitochondria hence inducing dissipation of the mitochondrial membrane potential. Due to mitochondrial malfunction the cellular ATP levels will be depleted. The final step in this apoptotic pathway is the activation of executioner proteases such as cathepsin B. CD40 signalling is known to protect from BCR-mediated apoptosis. This protection is achieved by CD40-dependent activation and nuclear translocation of NF-κB. This transcription factor enhances the expression of pro-survival molecules such as c-Myc and Bcl-x_L. The anti-apoptotic Bcl-2 family member Bcl-x_L is crucial to the inhibition of apoptosis and overexpression of Bcl-x_L protects cells from BCR-mediated cell death. The anti-apoptotic function of Bcl-x_L in this model is bipartite: it inhibits the localisation of $cPLA_2$ to the mitochondria and it itself translocates to these organelles where it protects the integrity of the mitochondrial membrane.

Figure 3.2 Regulation of c-Myc protein levels

Phosphorylation is an important post-translational modification of c-Myc proteins determining their stability. Thus, phosphorylation of T58 by glycogen synthase kinase 3 (GSK3) renders c-Myc prone to ubiquitination followed by degradation by the proteasome. PI3 kinase signalling stabilises cyclic expression by inhibiting GSK3 and hence reduced phosphorylation of T58. Similarly, phosphorylation of S62 increases c-Myc stability through as yet unknown mechanisms. The consensus sequence surrounding S62 makes it a likely target for ERK MAP kinase which has indeed been shown to phosphorylate c-Myc at position S62 *in vitro.*

Figure 3.3 The Rap signalling cascade

Extracellular stimulation activates Rap GEFs by different mechanisms. For example, cAMP will activate Epacs, whilst calcium and DAG are needed for the activation of CalDAGGEFs and C3G is activated by protein tyrosine kinases (PTK). GEFs then catalyse the exchange of GDP for GTP hence activating Rap. Activated Rap has multiple functions depending on the cell type and upstream signalling involved. Thus, it can activate ERK through B-Raf dependent signals or inhibit it by sequestering Raf-1 away from Ras. The regulation of ERK and another MAPK, p38, makes Rap an important part of signals controlling proliferation and survival. Additionally, Rap has also been found to play a crucial role in regulating cell adhesion and motility through adaptor proteins such as RapL which can change integrin affinity and in turn signalling.

Figure 3.4 Ligation of the BCR on WEHI-231 induces growth arrest

(A) WEHI-231 cells (10^4 cells/well) were cultured in triplicate in round bottom microtitre plates in complete medium in the presence of increasing concentrations of anti-IgM antibody (0-10 µg/ml) for 48 h. **(B)** WEHI-231 cells (10^4 cells/well) were cultured in the presence of 10 µg/ml anti-IgM antibody, 10 µg/ml anti-CD40 or the combination of both for 48 h. Cells were harvested 4 h after the addition of [^{3}H] thymidine and the incorporated label analysed by liquid scintillation measurement. Data are represented as counts per minute (cpm) +/- standard deviation (SD) of triplicate values. Data are representative of at least five independent experiments. *** $p<0.001$

Figure 3.5 Ligation of the BCR on WEHI-231 cells induces growth arrest in G0/G1

WEHI-231 cells (10^5 cells/well) were cultured in complete medium in the presence of 10 µg/ml anti-IgM antibody, 10 µg/ml anti-CD40 or a combination of the aforementioned antibodies for 48 h. After this time the cells were harvested and analysed for DNA content by staining with PI to assess the percentage live cells in G1/G0 phase **(A)**, S phase **(B)** or G2/M phase **(C)** by excluding the subdiploid cells from the analysis. Cells stimulated with media only were included as a control. Data are representative of at least four independent experiments.

Figure 3.6 Ligation of the BCR on WEHI-231 cells induces growth arrest and apoptosis

(A-D) WEHI-231 cells (10^5 cells/well) were cultured in complete medium in the presence of 10 µg/ml anti-IgM antibody, 10µg/ml anti-CD40 or a combination of the aforementioned antibodies for 48 h. After this time the cells were harvested and analysed for DNA content by staining with PI to assess the percentage of subdiploid cells representing cells undergoing apoptosis **(A)**, cells in G1/G0 phase **(B)**, cells in S phase **(C)** or G2/M phase **(D)**. Cells stimulated with media only were included as a control.

(E) To determine changes of the mitochondrial membrane potential (MMP) cells (10^6 cells/ml) were stimulated with 10 µg/ml anti-IgM, 10 µg/ml anti-CD40 or 10 µg/ml anti-IgM in combination with anti-CD40. Cells were then stained with $DiOC_6$ and gates were set on $DiOC_6$-bright (high MMP) cells. Data are expressed as percentage of cells with high MMP. Data are representative of at least four independent experiments.

Figure 3.7 BCR stimulation reduces cyclic ERK activation and c-Myc expression levels

WEHI-231 cells (10^7 cells/stimulation) were stimulated with medium (untreated) **(A)**, 1 µg/ml anti-IgM **(B)**, 10 µg/ml anti-CD40 **(C)** or the combination of both **(D)** for 0-32 h, as indicated. Expression of pERK (T202/Y204), c-Myc and total ERK was assessed by SDS-PAGE gel electrophoresis followed by Western Blotting (15 µg protein/lane). This experiment is representative of at least three independent experiments.

Figure 3.8 BCR stimulation reduces pERK and c-Myc expression detected by immunofluorescent staining and LSC analysis

WEHI-231 cells (10^6 cells/well) were stimulated with 1 µg/ml anti-IgM, 10 µg/ml anti-CD40 or the combination of both for 48 h. Cells were cytocentrifuged, fixed, permeabilised and immunofluorescently stained for intracellular pERK (T202/Y204) or c-Myc expression. Expression of the molecules was analysed by LSC using DAPI-stained nuclei to contour on single cells. **(A)** Representative immunofluorescence pictures (unstimulated control cells) are shown. Data are presented as **(i)** percentage or **(ii)** fluorescence integral of pERK **(B)** or c-Myc **(C)** expressing cells. Cells stimulated with media were included as a control. This experiment is representative of at least two independent experiments.

Figure 3.9 Analysis of cell cycle progression of WEHI-231 cells after BCR-ligation by LSC

(A) Cells (unstimulated control cells) are gated on according to their Max Pixel value (chromatin concentration/condensation) along the x-axis and their Integral value (DNA content) along the y-axis (as described in section 2.10.1.2, Fig. 2.9) identifying them as cells with subdiploid DNA content (apoptotic cells), cells in G1-G0 phase, G2-M phase, S phase or as new daughter cells. The cell cycle status of WEHI-231 cells (10^6 cells/ml) stimulated with media **(B-i)**, 1 µg/ml anti-IgM **(B-ii)**, 10 µg/ml anti-CD40 **(B-iii)** or the combination of both antibodies **(B-iv)** for 32 h, was analysed following staining the nuclei with DAPI. The percentage of cells at different stages of the cell cycle was determined by LSC **(C)**. This experiment is representative of at least two independent experiments.

Figure 3.10 pERK expression correlates with cell cycle progress

WEHI-231 cells (10^6 cells/well) were cultured for 48 h. Cells were cytocentrifuged, fixed, permeabilised and fluorescently stained for intracellular pERK (T202/Y204) expression. Expression of pERK as well as DAPI staining was analysed by LSC. Cells with subdiploid DNA content (apoptotic cells), cells in G1-G0 phase, G2-M phase, S phase or new daughter cells (ND) were gated on as described in Figure 3.9. The pERK expression in each cell cycle stage was then analysed. **(A)** A dot plot depicting DAPI Max Pixel against DAPI Integral was used to gate on cells in different stages of the cell cycle. Separate histograms for the expression of pERK in each of these gates were then displayed. **(B)** Data are presented as pERK fluorescence integral of cells in each cell cycle stage or as **(C-i)** percentage of the cells that are pERK-expressing cells in each cell cycle stage or **(C-ii)** percentage of pERK-expressing cells in the total cell population that are in each cell cycle stage.

Figure 3.11 BCR ligation does not suppress the expression of Rap-1, B-Raf or Raf-1 in WEHI-231 cells

(A-D) WEHI-231 cells (10^7 cells/stimulation) were stimulated with medium (untreated) **(A)**, 1 µg/ml anti-IgM **(B)**, 10 µg/ml anti-CD40 **(C)** or the combination of both antibodies **(D)** for 0-32 h, as indicated. Expression of Rap-1, B-Raf, Raf-1, pERK and total ERK was assessed by SDS-PAGE gel electrophoresis followed by Western Blotting (15 µg protein/lane). This experiment is representative of at least two independent experiments.

(E) WEHI-231 cells (10^6 cells/well) were stimulated with 1 µg/ml anti-IgM, 10 µg/ml anti-CD40 or the combination of both for 48 h. Cells were cytocentrifuged, fixed, permeabilised and immunofluorescently stained for intracellular Rap-1 expression. Rap-1 expression was analysed by LSC using DAPI-stained nuclei to contour on single cells. Data are presented as **(i)** percentage of Rap-1 expressing cells or **(ii)** the Rap-1 fluorescence integral. This experiment is representative of at least two independent experiments.

(F) WEHI-231 cells (0.5 x 10^7 cells/stimulation) were stimulated with 1 µg/ml anti-IgM, 10 µg/ml anti-CD40 or the combination of both for 2, 4, 8 or 24 h and samples were prepared as per manufacturer's instructions. Unstimulated cells were included as a control (media). Expression of phospho-B-Raf (pS446) and ERK2 was detected on a Bio-Plex System (Bio-Rad). Data are displayed as the ratio of phospho-B-Raf (pS446)/ERK2 expression, +/- the range of duplicate values.

Figure 3.12 Downregulation of Rap-1 signalling following BCR stimulation

(A-D) WEHI-231 cells (1.25 x 10^7 cells/stimulation) were stimulated with medium (untreated) **(A)**, 1 µg/ml anti-IgM **(B)**, 10 µg/ml anti-CD40 **(C)** or the combination of both **(D)** for 4, 8 or 24 h, as indicated. Levels of active GTP-bound Rap-1 were detected using a Rap-1 activity assay. Active Rap-1 specifically binds to Ral GDS-RBD-agarose allowing to purify it and assess expression levels by Western Blotting. This experiment is representative of at least three independent experiments.

(E-G) WEHI-231 cells (10^6 cells/well) were stimulated with 1 µg/ml anti-IgM, 10 µg/ml anti-CD40 or the combination of both for 24 h. Cells were cytocentrifuged, fixed, permeabilised and immunofluorescently stained for active Rap-1 expression using GST-labelled recombinant Ral GDS-RBD or GST as a control **(E)**. Active Rap expression was analysed by LSC using DAPI-stained nuclei to contour on single cells. **(F)** Histograms are shown for cells stained with the GST control **(i)**, untreated cells **(ii)**, cells stimulated with 1 µg/ml anti-IgM **(iii)**, 10 µg/ml anti-CD40 **(iv)** or the combination of both antibodies **(v)**. **(G)** Data are presented as **(i)** Rap fluorescence integral or **(ii)** % of cells expressing Rap at high levels (gate is shown in **(F-ii)** to **(F-v)**). This experiment is representative of at least two independent experiments.

Figure 3.13 SPA-1 expression is regulated by BCR-mediated signalling

(A) WEHI-231 cells (10^7 cells/stimulation) were stimulated with medium, 1 µg/ml anti-IgM, 10 µg/ml anti-CD40 or the combination of both antibodies for 24 or 48 h, as indicated. Expression of SPA-1 and β-actin was assessed by SDS-PAGE gel electrophoresis followed by Western Blotting (45 µg protein/lane). This experiment is representative of at least three independent experiments.

(B) To determine SPA-1 expression in subcellular fractions and whole cell lysates, WEHI-231 cells (10^7 cells/well) were stimulated with 10 µg/ml anti-IgM, 10 µg/ml anti-CD40 or the combination of both antibodies for 24 h and nuclear and cytoplasmic fractions as well as whole cell lysates were prepared. Mitochondrial fractions were prepared after stimulating 1 x 10^8 cells/well as described above. Cells stimulated with medium were included as a control. Expression of SPA-1 was assessed by SDS-PAGE gel electrophoresis of these fractions followed by Western Blotting (25 µg protein/lane of nuclear, cytoplasmic and mitochondrial fractions, 80 µg protein/lane of whole cell lysates). Gel loading was as follows: *Lane 1* media, *Lane 2* anti-IgM, *Lane 3* anti-CD40, *Lane 4* anti-IgM+anti-CD40.

(C) WEHI 231 cells (10^7 cells/stimulation) were stimulated with media (untreated), 10 µM PD98059, 1 µM LY294002 or the combination of the two inhibitors for 0-32 h, as indicated. Expression of pERK and total ERK was assessed by SDS-PAGE gel electrophoresis followed by Western Blotting (15 µg protein/lane).

(D-E) WEHI-231 cells (10^6 cells/ml) were stimulated with medium, 1 µg/ml anti-IgM, 10 µg/ml anti-CD40 or the combination of both antibodies for 0-48 h, as indicated **(i)**. WEHI-231 cells were stimulated with 1 µg/ml anti-IgM, 10 µM PD98059, 1 µM LY294002 or the combination of the two inhibitors for 0-32 h **(ii)**. Whole mRNA was isolated and transcribed into cDNA. SPA-1 expression levels were detected by TaqMan® quantitative RT-PCR using HPRT as endogenous control. **(D)** Data are shown as mean % expression relative to HPRT +/- SD of triplicate values of a representative experiment. **(E)** Data shown are pooled from up to 4 experiments with individual time points representing the mean of SPA-1 expression relative to HPRT +/- SD of triplicate values in each independent experiment.

Figure 3.14 Expression of constitutively-active Ras mutants protects WEHI-231 cells from BCR-mediated growth arrest

(A) WEHI-231 cells (10^4 cells/well) expressing the empty pcDNA3.1 vector, pcDNA3.1-RasV12, or pcDNA3.1-RasV12 S35 vectors were stimulated with **(i)** increasing concentrations of anti-IgM antibody (0-10 µg/ml) or **(ii)** with 10 µg/ml anti-IgM antibody, 10µg/ml anti-CD40 or the combination of both for 24 h. Cells were harvested 4 h after the addition of [^{3}H] thymidine and incorporated label analysed by liquid scintillation measurement. **(B)** WEHI-231 cells (10^4 cells/well) containing the empty pcDNA3.1 vector, pcDNA3.1-RasV12, or pcDNA3.1-RasV12C40 vectors were cultured and proliferation assessed as in **(A)**. Data from individual experiments were normalised by expressing the mean [^{3}H] thymidine uptake values of treated cells as a percentage of those obtained with control cell cultures. The normalised values from 4 independent experiments were then pooled and expressed as means ± SEM.

(C) WEHI-231 cells transfected with empty pcDNA3.1 vector, pcDNA3.1-RasV12, pcDNA3.1-RasV12C40 and pcDNA3.1-RasV12S35 (10^6 cells/ml) were stimulated with 1 µg/ml anti-IgM or 10 µg/ml anti-CD40 and 1 µg/ml anti-IgM for 24 h. Cells stimulated in the presence of medium alone were included as a control. Whole mRNA was isolated and transcribed into cDNA. SPA-1 expression levels were detected by TaqMan® quantitative RT-PCR using HPRT as endogenous control. Data are shown as mean % expression relative to HPRT +/- SD of triplicate values.

Figure 3.15 BCR stimulation regulates PAC-1 mRNA levels

(A-B) WEHI-231 cells (10^6 cells/ml) were stimulated with medium, 1 µg/ml anti-IgM, 10 µg/ml anti-CD40 or the combination of both antibodies for 0-48 h, as indicated **(i)**. WEHI-231 cells (10^6 cells/ml) were stimulated with 1 µg/ml anti-IgM, 10 µM PD98059, 1 µM LY294002 or the combination of the two inhibitors for 0-32 h **(ii)**. Whole mRNA was isolated and transcribed into cDNA. PAC-1 expression levels were detected by TaqMan® quantitative RT-PCR using HPRT as endogenous control. **(A)** Data are shown as mean % expression relative to HPRT +/- SD of triplicate values of a representative experiment. **(B)** Data shown are pooled from up to 4 experiments with individual time points representing the mean of PAC-1 expression relative to HPRT +/- SD of triplicate values in each independent experiment.

(C) WEHI-231 cells transfected with empty pcDNA3.1 vector, pcDNA3.1-RasV12, pcDNA3.1-RasV12C40 and pcDNA3.1-RasV12S35 (10^6 cells/ml) were stimulated with 1 µg/ml anti-IgM or 10 µg/ml anti-CD40 and 1 µg/ml anti-IgM for 24 h. Cells stimulated in the presence of medium alone were included as a control. Whole mRNA was isolated and transcribed into cDNA. PAC-1 expression levels were detected by TaqMan® quantitative RT-PCR using HPRT as endogenous control. Data are shown as mean % expression relative to HPRT +/- SD of triplicate values.

Figure 3.16 Subcellular localisation of Rap-1 and pERK

To determine Rap-1, pERK and ERK expression in various subcellular localisations WEHI-231 cells (5 x 10^6 cells/well) were stimulated with media or 1 µg/ml anti-IgM or 10 µg/ml anti-CD40 in combination with 1 µg/ml anti-IgM for 1 h **(A)** or 24 h **(B)** and cytoplasmic, membrane/organelle, nuclear and cytoskeletal fractions were prepared following the manufacturer's instructions (Perkin Elmer, Cellular Protein fractionation Kit). Additionally, whole cell lysates were prepared at the same time. Cells stimulated with medium were included as a control. Expression of Rap-1, pERK, ERK as well as the marker protein VDAC-1 and HDAC-1 was assessed by SDS-PAGE gel electrophoresis followed by Western Blotting. Gel loading was as follows: *Lane 1* media, *Lane 2* anti-IgM, *Lane 3* anti-IgM+anti-CD40.

(C) The subcellular localisation of pERK, Rap-1 and ERK signals was furthermore analysed using a different protocol of fractionation. Here WEHI-231 cells (10^7 cells/well) were stimulated with 10 µg/ml anti-IgM, 10 µg/ml anti-CD40 or the combination of both for 24 h and nuclear and cytoplasmic fractions as well as whole cell lysates were prepared. Mitochondrial fractions were prepared after stimulating 10^8 cells/well as described above. Cells stimulated with medium were included as a control. Expression of pERK, Rap-1 and ERK was assessed by SDS-PAGE gel electrophoresis followed by Western Blotting (25 µg protein/lane of nuclear, cytoplasmic and mitochondrial fractions, 80 µg protein/lane of whole cell lysates). Gel loading was as follows: *Lane 1* media, *Lane 2* anti-IgM, *Lane 3* anti-CD40, *Lane 4* anti-IgM+anti-CD40.

Figure 3.17 Induction of growth arrest in WEHI-231 cells transfected with pcDNA3.1-Rap vectors

(A) WEHI-231 cells (10^4 cells/well) transfected with empty pcDNA3.1 vector, pcDNA3.1-Rap-1A WT, pcDNA3.1-Rap-1A G12V or pcDNA3.1-Rap-1A S17N were stimulated with rising concentration of anti-IgM antibody, as indicated, **(i)** or with 1 µg/ml anti-IgM or 1 µg/ml anti-IgM in combination with 10 µg/ml anti-CD40 **(ii)** and their DNA synthesis measured at 48 h. Cells were harvested 4 h after the addition of [^{3}H] thymidine and incorporated label was analysed by liquid scintillation measurement. Data represents counts per minute (cpm) as normalised to media values for each group +/- SD of triplicate values. This experiment is representative of at least two independent experiments.

(B) WEHI-231- Bcl-x_L cells (10^4 cells/well) transfected with either empty pcDNA3.1 Zeo vector, pcDNA3.1 Zeo-Rap-1A WT, pcDNA3.1 Zeo-Rap-1A G12V or pcDNA3.1 Zeo-Rap-1A S17N were stimulated with rising concentrations of anti-IgM antibody, as indicated **(i)** or 1 µg/ml anti-IgM or 1 µg/ml anti-IgM in combination with 10 µg/ml anti-CD40 **(ii)** and their DNA synthesis measured at 24 h. Cells were harvested 4 h after the addition of [^{3}H] thymidine and incorporated label was analysed by liquid scintillation measurement. Data represents counts per minute (cpm) as normalised to media values for each group +/- SD of triplicate values. This experiment is representative of at least two independent experiments.

Figure 3.18 Induction of growth arrest and apoptosis in WEHI-231 cells transfected with pcDNA3.1-Rap vectors

WEHI-231- Bcl-x_L cells (0.5 x 10^6 cells/well) transfected with either empty pcDNA3.1 Zeo vector, pcDNA3.1 Zeo-Rap-1A WT, pcDNA3.1 Zeo-Rap-1A G12V or pcDNA3.1 Zeo-Rap-1A S17N were stimulated with rising concentration of anti-IgM antibody (0-1 µg/ml) for 24 h, as indicated. The cell cycle stage was determined by staining the cells with PI followed by FACS analysis. Data are presented as percentage of subdiploid cells **(A)**, cells in G1/G0 **(B)** or cells in the mitotic phases (G2/M and S phase) **(C)** of cell cycle.

Figure 3.19 WEHI-231 cells were not stably transfected with pcDNA3.1-Rap constructs

(A) WEHI-231-Bcl-x_L cells (10^7 cells/stimulation) transfected with either empty pcDNA3.1 Zeo vector, pcDNA3.1 Zeo-Rap-1A WT, pcDNA3.1 Zeo-Rap-1A G12V or pcDNA3.1 Zeo-Rap-1A S17N were lysed with RIPA buffer and whole cell lysates prepared. MIEV and MIEV-PKCα-HA-tag transfected fibroblast-lysates were used as a negative or positive control for the HA-tag detection, respectively. Expression of HA-tag, Rap-1 and ERK was assessed by SDS-PAGE gel electrophoresis followed by Western Blotting (40 µg protein/lane). Gel loading was as follows : *Lane1* pcDNA3.1 Zeo-Rap-1A WT transfected cells, *Lane 2* pcDNA3.1 Zeo-Rap-1A G12V transfected cells, *Lane 3* pcDNA3.1 Zeo-Rap-1A S17N transfected cells, *Lane4* pcDNA3.1 Zeo (empty vector) transfected cells, *Lane5* untransfected cells *Lane 6* MIEV-transfected fibroblasts, *Lane 7* MIEV-PKCα-HA-tag transfected fibroblasts.

(B) WEHI-231 cells were transfected with empty pIRES2-AcGFP1 vector, pIRES2-AcGFP1-Rap-1A WT, pIRES2-AcGFP1-Rap-1A G12V, pIRES2-AcGFP1-Rap-1A S17N. **(i)** 24 h (Day 1) or **(ii)** 11 days after transfection cells were analysed for the expression of GFP. **(C-i)** Table summarising the percentage of GFP-positive cells detected 1, 5 or 11 days after transfection. **(C-ii)** Table summarising vectors, cells, concentrations of selection-antibiotic as well as methods of transfections tested during optimisation experiments. **(C-iii)** Table summarising experiments carried out to test conditions for the production of stably transfected clones.

Figure 3.20 HA-tagged Rap-1A WT, Rap-1A G12V and Rap-1A S17N are expressed in the a lentivirus-based transduction system

(A) HT-1080 cells were transduced or not with lentiviral particles encoding pLVX-IRES-ZsGreen1-Rap-1A WT, -Rap-1A G12V or -Rap-1A S17N and analysed by FACS to detect ZsGreen1 expression after 72 h. **(B)** The HT-1080 cells described in **(A)** above were lysed in RIPA buffer and the expression of the HA-tag or total ERK was assessed by SDS-PAGE gel electrophoresis followed by Western Blotting (60 µg protein/lane). Gel loading was as follows: *Lane1* untransduced cells, *Lane2* pLVX-IRES-ZsGreen1-Rap-1A WT, *Lane3* pLVX-IRES-ZsGreen1-Rap-1A G12V, *Lane4* pLVX-IRES-ZsGreen1-Rap-1A S17N.

Figure 3.21 BCR-mediated abrogation and CD40-dependent rescue of c-Myc expression

WEHI-231 cells (10^7 cells/stimulation) were stimulated with medium, 1 µg/ml anti-IgM, 10 µg/ml anti-CD40 or the combination of both antibodies for 0-32 h, as indicated. Expression of pERK, c-Myc phospho-c-MycS62, ERK and β-actin was assessed by SDS-PAGE gel electrophoresis followed by Western Blotting (15 µg protein/lane). Gel loading was as follows: *Lane1* media, *Lane2* anti-IgM, *Lane3* anti-CD40, *Lane4* anti-IgM+anti-CD40. These data are representative of at least two independent experiments.

Figure 3.22 Ligation of the BCR on WEHI-231 cells regulates the levels of c-Myc

WEHI-231 cells (10^7 cells/stimulation) were stimulated with medium (untreated) **(A)**, 1 µg/ml anti-IgM **(B)**, 10 µg/ml anti-CD40 **(C)** or the combination of both antibodies **(D)** for 0-32 h, as indicated. Expression of pERK, c-Myc, phospho-c-MycT58/S62, phospho c-MycT58 and total ERK was assessed by SDS-PAGE gel electrophoresis followed by Western Blotting (15-45 µg protein/lane). This experiment is representative of at least three independent experiments.

Figure 3.23 c-Myc expression is regulated by the ERK and PI3 kinase signalling

WEHI-231 cells (10^7 cells/stimulation) were stimulated with medium, 1 µg/ml anti-IgM, 10 µg/ml anti-CD40, the combination of both antibodies, 10 µM PD98059, 1 µM LY294002 or the combination of both inhibitors for 0-32 h, as indicated. Expression of pERK, c-Myc, ERK and β-actin was assessed by SDS-PAGE gel electrophoresis followed by Western Blotting (15 µg protein/lane). Gel loading was as follows: *Lane1* media, *Lane2* anti-IgM, *Lane3* anti-CD40, *Lane4* anti-IgM+anti-CD40, *Lane5* PD98059, *Lane6* LY294002, *Lane7* PD98059+ LY294002. These data are representative of at least two independent experiments.

Figure 3.24 c-Myc expression level is regulated by ERK and PI3 kinase signalling pathways

(A-D) WEHI-231 cells (10^7 cells/stimulation) were stimulated with medium (untreated) **(A)**, 10 µM PD98059 **(B)**, 1 µM LY294002 **(C)** or 10 µM PD98059 in combination with 1 µM LY294002 **(D)** for 0-32 h, as indicated. Expression of c-Myc, pERK and ERK was assessed by SDS-PAGE gel electrophoresis followed by Western Blotting (15 µg protein/lane). **(E)** To determine c-Myc expression in subcellular localisations WEHI-231 cells (10^7 cells/well) were stimulated with 1 µg/ml anti-IgM, 10 µg/ml anti-CD40 or the combination of both for 4 h and nuclear and cytoplasmic fractions were prepared. Cells stimulated with medium were included as a control. Expression of c-Myc was assessed by SDS-PAGE gel electrophoresis followed by Western Blotting (25 µg protein/lane). Gel loading was as follows: *Lane 1* 0 h, *Lane 2* media, *Lane 3* anti-IgM, *Lane 4* anti-CD40, *Lane 5* anti-IgM+anti-CD40. **(F)** WEHI-231 cells (10^6 cells/well) were stimulated with 1 µg/ml anti-IgM, 10 µg/ml anti-CD40, the combination of both, 10 µM PD98059, 1 µM LY294002 or the combination of the two inhibitors for 12, 20 or 32 h. Untreated cells were included as a control. Cells (0.75×10^5 cells/stain) were cytocentrifuged onto glass slides, fixed, permeabilised and immunofluorescently stained for intracellular c-Myc expression which was analysed by LSC using DAPI-stained nuclei to contour on single cells. **(i)** A representative image of CD40-stimulated cells is shown for the immunofluorescent staining. Data are presented as **(ii)** percentage of c-Myc expressing cells or **(iii)** fluorescence integral of the cells. This experiment is representative of at least two independent experiments.

Figure 3.25 c-Myc phosphorylation is regulated by ERK and PI3 kinase signalling pathways

(A-D) WEHI-231 cells (10^7 cells/stimulation) were stimulated with medium (untreated) **(A)**, 10 µM PD98059 **(B)**, 1 µM LY294002 **(C)** or 10 µM PD98059 in combination with 1 µM LY294002 **(D)** for 0-32 h, as indicated. Expression of phospho-c-MycT58/S62, pERK and ERK was assessed by SDS-PAGE gel electrophoresis followed by Western Blotting (15 µg protein/lane). **(E)** To determine phospho-c-MycT58/S62 expression in subcellular localisations WEHI-231 cells (10^7 cells/well) were stimulated with 1 µg/ml anti-IgM, 10 µg/ml anti-CD40 or the combination of both for 4 h and nuclear and cytoplasmic fractions were prepared. Cells stimulated with medium were included as a control. Expression of c-Myc was assessed by SDS-PAGE gel electrophoresis followed by Western Blotting (25 µg protein/lane). Gel loading was as follows: *Lane 1* 0 h, *Lane 2* media, *Lane 3* anti-IgM, *Lane 4* anti-CD40, *Lane 5* anti-IgM+anti-CD40. **(F)** WEHI-231 cells (10^6 cells/well) were stimulated with 1 µg/ml anti-IgM, 10 µg/ml anti-CD40, the combination of both, 10 µM PD98059, 1 µM LY294002 or the combination of the two inhibitors for 12, 20 or 32 h. Untreated cells were included as a control. Cells (0.75 x 10^5 cells/stain) were cytocentrifuged onto glass slides, fixed, permeabilised and immunofluorescently stained for intracellular phospho-c-MycS62 expression which was analysed by LSC using DAPI-stained nuclei to contour on single cells. **(i)** A representative image of CD40-stimulated cells is shown for the immunofluorescent staining. Data are presented as **(ii)** percentage of phospho-c-MycS62 expressing cells or **(iii)** phospho-c-MycS62 fluorescence integral of the cells. This experiment is representative of at least two independent experiments.

Figure 3.26 Transcriptional regulation of c-Myc expression

(A-B) WEHI-231 cells (10^6 cells/ml) were stimulated with medium, 1 µg/ml anti-IgM, 10 µg/ml anti-CD40 or the combination of both antibodies for 0-48 h, as indicated **(i)**. WEHI-231 cells were stimulated with 1 µg/ml anti-IgM, 10 µM PD98059, 1 µM LY294002 or the combination of the two inhibitors for 0-32 h **(ii)**. Whole mRNA was isolated and transcribed into cDNA. c-Myc expression levels were detected by TaqMan® quantitative RT-PCR using HPRT as endogenous control. **(A)** Data are shown as mean % expression relative to HPRT +/- SD of triplicate values of a representative experiment. **(B)** Data shown are pooled from up to 4 experiments with individual time points representing the mean of c-Myc expression relative to HPRT +/- SD of triplicate values in each independent experiment.

(C) WEHI-231 cells transfected with empty pcDNA3.1 vector, pcDNA3.1-RasV12, pcDNA3.1-RasV12C40 and pcDNA3.1-RasV12S35 (10^6 cells/ml) were stimulated with 1 µg/ml anti-IgM or 10 µg/ml anti-CD40 and 1 µg/ml anti-IgM for 8 h. Cells stimulated in the presence of medium alone were included as a control. Whole mRNA was isolated and transcribed into cDNA. c-Myc expression levels were detected by TaqMan® quantitative RT-PCR using HPRT as endogenous control. Data are shown as mean % expression relative to HPRT +/- SD of triplicate values.

(D) WEHI-231 cells or cells transfected with empty vector, pcDNA3.1-RasV12, pcDNA3.1-RasV12C40 and pcDNA3.1-RasV12S35 cells (0.5×10^7 cells/stimulation) were stimulated with 1 µg/ml anti-IgM or the combination of 1 µg/ml anti-IgM and 10 µg/ml anti-CD40 for 24 h. Expression of c-Myc and total ERK was assessed by SDS-PAGE gel electrophoresis followed by Western Blotting (35 µg protein/lane). Gel loading was as follows: *Lane 1* media, *Lane 2* anti-IgM, *Lane 3* anti-IgM+anti-CD40.

Figure 3.27 c-Myc expression level correlates with progression through the cell cycle

WEHI-231 cells (0.75 x 10^5 cells/stain) were analysed for expression of c-Myc or phospho-c-MycS62 and gates were set according to the intensity of the c-Myc or phospho-c-MycS62 signal. The cell cycle status of the population of cells of increasing expression of these markers was then assessed, identifying them as cells with subdiploid DNA content (apoptotic cells), cells in G1-G0 phase, G2-M phase, S phase or new daughter cells as previously described (section 2.10.1.2, Figure 2.9). **(A)** Representative histogram of CD40-stimulated cells (32 h) and cell cycle plots are shown. Data are presented as the percentage of cells in each cell cycle stage present in each region (fluorescence integral) of c-Myc **(B)** and phospho-c-MycS62 **(C)**.

Figure 3.28 Growth arrest correlates with reduced c-Myc expression and stabilisation

WEHI-231 cells (10^6 cells/well) were stimulated with 1 µg/ml anti-IgM, 10 µg/ml anti-CD40, the combination of both, 10 µM PD98059, 1 µM LY294002 or the combination of the two inhibitors for 12, 20 or 32 h. Untreated cells were included as a control. Cells (0.75 x 10^5 cells/stain) were cytocentrifuged onto glass slides, fixed, permeabilised and immunofluorescently stained for intracellular c-Myc and phospho-c-MycS62 expression as well as DAPI. **(A)** Cells were analysed by LSC to determine their cell cycle stage: G1-G0, S, G2-M phase and mitotic phases (S phase, G2-M phase and new daughter cells combined), as previously described (Figure 3.9). The data are presented as the percentage of cells in each cell cycle stage at 12, 20 and 32 h. **(B)** Furthermore, the correlation between the fluorescence integral (expression level) of **(i)** c-Myc or **(ii)** phospho-c-MycS62 detected in each of the differently stimulated samples described above (32 h) **(A)** and the percentage of cells in each cell cycle stage in those samples was analysed.

Figure 3.29 Regulation of CTCF expression upon BCR stimulation

WEHI-231 cells (10^7 cells/stimulation) were stimulated with medium (untreated) **(A)**, 1 µg/ml anti-IgM **(B)**, 10 µg/ml anti-CD40 **(C)** or the combination of anti-IgM and anti-CD40 **(D)** for 0-32 h, as indicated. Expression of CTCF and β-actin was assessed by SDS-PAGE gel electrophoresis followed by Western Blotting (45 µg protein/lane). This experiment is representative of at least two independent experiments.

(E) WEHI-231 cells (10^6 cells/ml) were stimulated with 1 µg/ml anti-IgM, 10 µg/ml anti-CD40 or the combination of both for 4-48 h, as indicated. Whole mRNA was isolated and transcribed into cDNA. CTCF expression levels were detected by TaqMan® quantitative RT-PCR using HPRT as endogenous control. Data are shown as mean % expression relative to HPRT +/- SD of triplicate values.

Figure 3.30 Regulation of phosphorylation of Rb and p27 expression in WEHI-231 B cells

WEHI-231 cells (10^7 cells/stimulation) were stimulated with medium, 1 µg/ml anti-IgM, 10 µg/ml anti-CD40, the combination of both antibodies, 10 µM PD98059, 1 µM LY294002 or the combination of the two inhibitors for 0-32 h, as indicated. Expression of pERK, phospho-RbS780, phospho-RbS807/811 and ERK was assessed by SDS-PAGE gel electrophoresis followed by Western Blotting (15 µg protein/lane). Gel loading was as follows: *Lane1* media, *Lane2* anti-IgM, *Lane3* anti-CD40, *Lane4* anti-IgM+anti-CD40, *Lane5* PD98059, *Lane6* LY294002, *Lane7* PD98059+LY294002. This experiment is representative of at least two independent experiments.

Figure 3.31 p53 expression is regulated downstream of BCR-ligation

(A) WEHI-231 cells (10^7 cells/well) were stimulated with 1 µg/ml anti-IgM, 10 µg/ml anti-CD40 antibody or the combination of both for 24 and 48 h and whole cell lysates were prepared. Cells stimulated with medium were included as a control. Expression of p53 was assessed by SDS-PAGE gel electrophoresis followed by Western Blotting (20 µg protein/lane).

(B) WEHI-231 cells (10^6 cells/ml) were stimulated with 1 µg/ml anti-IgM, 10 µg/ml anti-CD40 or the combination of both antibodies for 4-48 h, as indicated. Whole mRNA was isolated and transcribed into cDNA. p53 expression levels were detected by TaqMan® quantitative RT-PCR using HPRT as endogenous control. Data are shown as mean % expression relative to HPRT +/- SD of triplicate values.

Figure 3.32 Regulation of phospho-Rb Ser780 expression in WEHI-231 cells

(A-D) WEHI-231 cells (10^7 cells/stimulation) were stimulated with medium (untreated) **(A)**, 1 µg/ml anti-IgM **(B)**, 10 µg/ml anti-CD40 **(C)** or the combination of anti-IgM and anti-CD40 **(D)** for 0-32 h, as indicated. Expression of phospho-RbS780 and β-actin was assessed by SDS-PAGE gel electrophoresis followed by Western Blotting (15 µg protein/lane). This experiment is representative of at least three independent experiments.

(E) WEHI-231 (10^6 cells/ml) cells were stimulated with medium, 1 µg/ml anti-IgM, 10 µg/ml anti-CD40 or the combination of both for 32 h. Untreated cells were cytocentrifuged, fixed, permeabilised and stained for phospho-RbS780 expression. **(i)** A representative picture of the immunofluorescent staining of unstimulated cells is shown. Data are presented as **(ii)** percentage of cells expressing phospho-RbS780 or **(ii)** fluorescence integral of phospho-RbS780 staining.

(F) WEHI-231 cells (10^6 cells/ml) were stimulated as described above for 48 h. Cells were cytocentrifuged, fixed, permeabilised and stained for phospho-RbS780 expression as well as nuclear DNA content by DAPI staining. As described in Figure 3.27 cells were then gated according to the intensity of the phospho-RbS780 signal and their cell cycle status assessed, identifying them as cells with subdiploid DNA content (apoptotic cells), cells in G1-G0 phase, G2-M phase, S phase or new daughter cells as previously described (section 2.10.1.2, Figure 2.9). Data are presented as percentage of cells in each cell cycle stage present in each region (fluorescence integral).

Figure 3.33 Regulation of phospho-Rb Ser807/811 expression in WEHI-231 cells

(A-D) WEHI-231 cells (10^7 cells/stimulation) were stimulated with medium (untreated) **(A)**, 1 µg/ml anti-IgM **(B)**, 10 µg/ml anti-CD40 **(C)** or the combination of anti-IgM and anti-CD40 **(D)** for 0-32 h, as indicated. Expression of phospho-RbS807/811 and β-actin was assessed by SDS-PAGE gel electrophoresis followed by Western Blotting (15 µg protein/lane). This experiment is representative of at least three independent experiments.

(E) WEHI-231 (10^6 cells/ml) cells were stimulated with medium, 1 µg/ml anti-IgM, 10 µg/ml anti-CD40 or the combination of both for 32 h. Untreated cells were cytocentrifuged, fixed, permeabilised and stained for phospho-RbS807/811 expression. **(i)** A representative picture of the immunofluorescent staining of unstimulated cells is shown. Data are presented as **(ii)** percentage of cells expressing phospho-RbS807/811 or **(ii)** fluorescence integral of phospho-RbS807/811 staining after deduction of the fluorescence integral of the isotype-stained sample.

(F) WEHI-231 cells (10^6 cells/ml) were stimulated as described above for 48 h. Cells were cytocentrifuged, fixed, permeabilised and stained for phospho-pRbS807/811 expression as well as nuclear DNA content by DAPI staining. As described in Figure 3.27 cells were then gated according to the intensity of the phospho-RbS807/811 signal and their cell cycle status assessed, identifying them as cells with subdiploid DNA content (apoptotic cells), cells in G1-G0 phase, G2-M phase, S phase or new daughter cells as previously described (section 2.10.1.2, Figure 2.9). Data are presented as percentage of cells in each cell cycle stage present in each region (fluorescence integral).

Figure 3.34 BCR signalling modulates the protein-ubiquitination pattern in WEHI-231 cells

(A-D) WEHI-231 cells (10^7 cells/stimulation) were stimulated with medium (untreated) **(A)**, 1 µg/ml anti-IgM **(B)**, 10 µg/ml anti-CD40 **(C)** or the combination of anti-IgM and anti-CD40 **(D)** for 0-32 h, as indicated. Expression of ubiquitin or β-actin was assessed by SDS-PAGE gel electrophoresis followed by Western Blotting (45 µg protein/lane). Data are representative of at least two independent experiments.

(E) WEHI-231 cells (10^4 cells/well) were cultured in complete medium in the presence of 1 µg/ml anti-IgM antibody, 10 µg/ml anti-CD40 or the combination of both for 24 h. At 0, 8 and 16 h, 0.5 µM MG132 or DMSO control (%v/v) was added. Cells were harvested 4 h after the addition of [^{3}H] thymidine and the incorporated label analysed by liquid scintillation measurement. Data are represented as counts per minute (cpm) +/- SD of triplicate values.

(F) WEHI-231 cells (0.5 x 10^6 cells/well) were cultured in complete media -/+ DMSO control (%v/v) **(i)** or 0.5 µM MG132 **(ii)** for 24 h. Cells were harvested and stained with 7-AAD which specifically labels dead cells and then analysed by FACS. Representative dot plots indicating % 7-AAD$^+$ (dead) cells are shown.

Figure 3.35 Influence of proteasome inhibition on ubiquitinated-protein expression

WEHI-231 cells (10^7 cells/stimulation) were treated with medium, 1 µg/ml anti-IgM, 0.5 µM MG132 or the combination of anti-IgM and MG132 for **(A)** 2, 4, 8 h and **(B)** 12, 16 and 20 h, as indicated. MG132 (0.5 µM) was added to the cultures at 0, 8 and 16 h. Expression of ubiquitin, c-Myc, p27 or total ERK was assessed by SDS-PAGE gel electrophoresis followed by Western Blotting (35 µg protein/lane). Gel loading was as follows: *Lane 1* media, *Lane 2* media+MG132, *Lane 3* anti-IgM, *Lane 4* anti-IgM+MG132.

Figure 3.36 Regulation of c-Myc and pERK by ubiquitination and proteasomal degradation

(A) WEHI-231 cells (10^7 cells/stimulation) were stimulated with medium, 1 µg/ml anti-IgM, 10 µg/ml anti-CD40 or the combination of both antibodies for 24 h. One hour before harvesting, the cells were treated with 0.5 µM MG132 after which whole cell lysates were prepared. In order to pull-down ubiquitinated proteins 50 µg of each sample was treated with the Ubiqapture Q matrix (Biomol) as per the manufacturer's instructions. Ubiquitin and c-Myc expression was analysed in the samples before (25 µg protein/lane) and after ubiquitin-pull-down (25 µl/lane) by SDS-PAGE gel electrophoresis followed by Western Blotting. Gel loading was as follows: *Lane1* media, *Lane2* anti-IgM, *Lane3* anti-CD40, *Lane4* anti-IgM+anti-CD40.

(B) WEHI-231 cells (10^7 cells/stimulation) were pre-treated with 0.5 µM MG132 or DMSO vector control for 1 h and then stimulated with medium, 1 µg/ml anti-IgM or 1 µg/ml anti-IgM with 10 µg/ml anti-CD40 for 1, 2, 4 and 8 h and whole cell lysates were prepared. Expression of pERK or ERK was assessed by SDS-PAGE gel electrophoresis followed by Western Blotting (50 µg protein/lane). Gel loading was as follows: *Lane 1* media, *Lane 2* anti-IgM, *Lane3* anti-IgM+anti-CD40.

Figure 3.37 Expression of Cbl-b is regulated by BCR stimulation at both the protein and mRNA level

(A) WEHI-231 cells (10^7 cells/stimulation) were pre-treated with 0.5 µM MG132 or DMSO vector control for 1 h and then stimulated with medium, 1 µg/ml anti-IgM or 1 µg/ml anti-IgM and 10 µg/ml anti-CD40 for 8 h and whole cell lysates were prepared. Expression of Ubiquitin, Cbl-b or total ERK was assessed by SDS-PAGE gel electrophoresis followed by Western Blotting (50 µg protein/lane).

(B) WEHI-231 cells (10^7 cells/stimulation) were treated with medium, 1 µg/ml anti-IgM, 10 µg/ml anti-CD40 or the combination of both antibodies for 12 or 48 h. Expression of Cbl-b or ERK was assessed by SDS-PAGE gel electrophoresis followed by Western Blotting (90 µg protein/lane).

(C) WEHI-231 cells (10^6 cells/ml) were stimulated with 1 µg/ml anti-IgM, 10 µg/ml anti-CD40 or the combination of both for 0-48 h, as indicated. Whole mRNA was isolated and transcribed into cDNA. Cbl-b expression levels were detected by TaqMan® quantitative RT-PCR using HPRT as endogenous control. Data are shown as mean % expression relative to HPRT +/- SD of triplicate values. This experiment is representative of at least two independent experiments.

Figure 3.38 c-Cbl, Itch and Grail expression is influenced by BCR-ligation

(A) WEHI-231 cells (10^6 cells/ml) were stimulated with 1 µg/ml anti-IgM, 10 µg/ml anti-CD40 or the combination of both antibodies for 0-48 h, as indicated before mRNA was isolated and transcribed into cDNA. c-Cbl expression levels were detected by TaqMan® quantitative RT-PCR using HPRT as endogenous control. Data are shown as mean % expression relative to HPRT +/- SD of triplicate values. This experiment is representative of at least two independent experiments.

(B) WEHI-231 cells (10^7 cells/stimulation) were treated with medium, 1 µg/ml anti-IgM, 10 µg/ml anti-CD40 or the combination of the two for 48 h. Expression of c-Cbl, Itch, Grail or total ERK was assessed by SDS-PAGE gel electrophoresis followed by Western Blotting (90 µg protein/lane).

4 Signalling mechanisms underlying FcγRIIb mediated growth arrest and apoptosis

4.1 Introduction

4.1.1 Autoimmune disease

Autoimmunity is the result of inappropriate responses of the immune system to self-antigens and is therefore characterised by tissue damage caused by aberrant hyper-inflammatory processes. Over the last few decades the incidence of autoimmune diseases has risen dramatically, especially in the western/industrialised world and it is estimated that 4-5% of the human population suffer from some form of autoimmune disease. For example, in the United states about 90 people out of 100 000 per year will develop an autoimmune disease such as Grave's disease, rheumatoid arthritis, diabetes or uveitis [534].

Responses elicited against self-antigens can lead to damage of host tissue by a variety of mechanisms. For example, autoreactive B cells produce antibodies against molecules expressed by the host, which can be directly harmful by binding to surface proteins and interfering with their normal function as in Myasthenia gravis [535]. Similarly, in Grave's disease, the binding of the antibody to its antigen, the thyroid stimulating hormone receptor, leads to activation of the receptor cascade and consequent overproduction of the hormone [536]. Alternatively, if the autoantibody is specific for a surface antigen on circulating cells this may lead to the opsonisation of these cells followed by phagocytosis and initiation of Fc receptor-mediated macrophage activation, as seen in autoimmune thrombocytopenia purpura [537]. Another effector function of autoreactive antibodies can be the formation of immune complexes that, as seen in Systemic lupus erythematosus [538], can be deposited in small blood vessels in the kidney or in joints where they initiate complement activation and production of inflammatory mediators, leading to localised inflammation and aggravation of antigen release with consequent further production of immune complexes. However, B cells are not the only potentially harmful cells. For example, diseases like insulin-dependent diabetes mellitus are initiated by autoreactive T cells which mount responses against pancreatic β-cell antigen leading to the destruction of β-cells.

Genetic susceptibility is also a major contributor to the development of autoimmune diseases: indeed, it has been estimated that in rheumatoid arthritis about 60% of the susceptibility is caused by genetic factors [539]. For example, some HLA-alleles are very

strongly associated with the disease indicating that presentation of specific peptides that bind well to these HLA alleles plays a role in the disease development. Furthermore, various other genes encoding proteins with important regulatory functions in the immune system like PD-1, FcγRIIb, CD22, SHIP and CTLA-4 (reviewed in [540]) have been implicated in the development of different autoimmune diseases. Nevertheless, the multigenic nature of many of the common autoimmune diseases makes the identification of susceptibility genes very difficult because of the low penetrance and the very complex interaction of the various susceptibility loci with each other. Beside genetic susceptibility, environmental factors and their influence should not be underestimated as infections are known to aggravate autoimmune diseases, and habits like smoking have been linked to susceptibility to autoimmune diseases such as RA [541].

4.1.1.1 Rheumatoid arthritis (RA)

RA is a systemic, inflammatory autoimmune disease which mainly affects the joints leading to cartilage breakdown and bone destruction. Some patients also develop extra-articular manifestations such as vasculitis, pericarditis or glomerulonephritis which contribute to the increased risk of premature mortality in RA patients. The disease is defined as a symmetric polyarticular arthritis caused by chronic inflammation of the synovium. The inflammatory cell mass develops into the so-called pannus which invades articular structures leading to their destruction. RA primarily affects the small diarthrodial joints of the hands and feet. It occurs in about 0.5-1% of the population with the mean onset of the disease in the 5^{th} decade of life. As in SLE, there is a higher prevalence in women which suggests the involvement of hormones in the disease pathogenesis. Moreover, twin and family studies suggest a 60% genetic susceptibility for RA. Candidate genes shown in some studies to be linked to RA include HLA-DRB1, one of the genes encoding MHC II, PTPN22 which encodes Lyp, a negative regulator of T cell activity and CTLA-4, a negative costimulatory surface receptor on T cells [540]. However, as RA is thought to be a multigenic disease caused by the contribution of multiple low-penetrance susceptibility loci it will need much larger studies to prove any further linkages [540].

At the cellular level, the inflammation of the joint leads to massive infiltration of inflammatory cells such as T cells, B cells and macrophages. These cells can form organised structures which resemble germinal centres. In addition, hyperplasia of the synovial membrane is caused by increased proliferation of macrophage- and fibroblast-like synoviocytes, but the invading cells are not the only cause of destruction in the joint. Indeed, inflammation induces resident cells to produce degradative enzymes like

metalloproteinases, serine proteases and aggrecanases, all of which are able to digest extracellular matrix and thereby destroy joint structures (reviewed in [542]).

Production of autoantibodies is a major feature of RA with rheumatoid factor (RF – antibodies specific for the Fc portion of IgG) and ACPA (anti-citrunillated protein antibodies) representing the best studied specificities [543]. The exact role of these antibodies in pathogenesis of RA is still not fully elucidated yet but they can be detected in patients before disease onset [544] and it is therefore hypothesised that they might play a role in disease initiation. These antibodies are also detected in the synovium, the site of inflammation in RA, where they can form immune complexes with their antigens further enhancing inflammatory responses [545]. The efficacy of B-cell depleting therapies in RA has further confirmed the importance of B cells in RA pathogenesis [546].

4.1.1.2 Systemic lupus erythematosus (SLE)

Systemic lupus erythematosus is a systemic autoimmune disease characterised by the production of autoantibodies against various antigens such as double stranded (ds)-DNA, single stranded (ss)-DNA, snRNPs (small nuclear ribonucleoproteins), cardiolipin and phospholipids. The pathology of this disease varies widely between patients ranging from skin rash and joint pain to severe glomerulonephritis. There is a very high prevalence of the disease in women of childbearing age, the ratio of female to male patients being 8:1 at this age. After the menopause this ratio drops to 2:1 implicating a role for hormones in disease development, which is underlined by mouse studies showing that treatment with estrogen increases the number of autoreactive B cells escaping deletion [547]. SLE affects less people than other inflammatory autoimmune diseases such as RA, occurring only in 0.2% of the population (reviewed in [548]).

SLE patients produce very high levels of anti-nuclear antigen (ANA) autoantibodies and such antibody-producing B cells from some patients have been shown to be clonally expanded and to express somatically hypermutated and class-switched self-reactive antibodies, all signs of an antigen specific response. Furthermore peripheral B cells from SLE patients have been shown to be hyperactive with upregulated expression of costimulatory molecules such as CD154 and CD86 and increased activation of MAPKs [538,549,550]. The pathological role of such autoantibodies has not been definitively demonstrated but there is evidence that they contribute to tissue damage seen in SLE patients. Thus, self-reactive antibodies are able to form immune complexes with their antigen in the circulation and are deposited in organs like the kidney, the joints or vasculature. Deposition can lead to complement activation and hence induction of inflammatory processes accompanied by infiltration of inflammatory cells. In the absence

of regulation this inflammation produces a hyperresponse, initiating tissue destruction [538]. Moreover, the importance of B cells in disease progression has been underpinned recently by the efficacy of a B cell-depleting antibody, Rituximab, in the treatment of SLE [551].

4.1.2 Effector functions of B cells in autoimmunity

In the last few years it has become apparent that autoantibody production is not the only mechanism by which B cells can take part in harmful reactions against self. Thus, follicular B cells can also function as secondary APCs being very efficient at binding, internalising and processing antigen. That this APC capacity of B cells can play a major role in the development and maintenance of inflammation in autoimmune diseases has been illustrated by several findings. For example, a study by Takemura and colleagues [552] showed that the survival of human $CD4^+$ T cell clones from RA patients in SCID mice depended on the presence of CD20-positive B cells. Further support came from another model system in which mice that do not secrete antibody (mIgM-mice) were used to examine the role of B cells in a proteoglycan (PG) induced arthritis (PGIA) model and where it was found that B cell-deficient and mIgM-mice were both resistant to the development of arthritis [77]. This study showed that serum transfer of autoantibodies led to the development of transient, mild arthritis proving that antibodies do indeed play a pathogenic role in the PGIA model. However, T cells from mIgM-mice were not able to induce severe arthritis upon transfer into a healthy host indicating that these T cells are not properly primed as antigen-specific B cells were needed to prime T cells adequately to allow them to induce severe arthritis in the host animals. By contrast, the combination of transferring adequately primed T cells and pathogenic serum induced severe arthritis underlining the importance for T and B cell interactions in the pathology of such autoimmunity [77].

B cells might also contribute to autoimmune disease pathogenesis by the production of cytokines like IL-12 or IL-6 [553,554]. For example, the latter has been shown to play a role in diseases such as RA and juvenile idiopathic arthritis and indeed, anti-IL-6 treatment seems to be a promising treatment option in RA and other autoimmune diseases [555]. However, B cells do not only contribute to the aggravation of disease. The discovery of regulatory B cells has shown that these IL-10 producing cells can ameliorate autoimmune pathogenesis in disease models for Multiple sclerosis, inflammatory bowel disease, SLE as well as RA [82] (see section 1.4).

B-1 cells produce polyreactive antibodies including low-affinity self-reactive specificities, such as those found in increased numbers in some human diseases such as

Sjogren's syndrome. Moreover, there is some evidence that B-1 cells are able to produce high affinity antibodies against self-antigens [556] and such B-1 cells are found in increased numbers in the autoimmune strain NZB which develops lupus like disease [557] and they were found to produce autoantibodies in MRL/MpJ-*Fas*^{lpr} mice, another autoimmune-prone strain [558].

Some studies indicate that MZ B cells might play a pathogenic role in some autoimmune diseases where, for example in Grave's disease, cells with a MZ B cell phenotype have been found in infiltrates at the site of inflammation [559]. Additionally, MZ B cells have been found in increased number in lupus-prone autoimmune mice and these cells were shown to contribute to the production of anti-DNA antibodies [560,561]. Likewise, MZ B cells are similar to B-1 cells in that they are generally polyreactive with a restricted antibody diversity. MZ B cells mostly do not re-circulate and are found in the MZ of the spleen where, due to their location, they are able to react quickly to blood borne pathogens. After antigen-exposure, they rapidly migrate to lymphoid follicles and in this way are able to efficiently deliver systemic antigen to follicular dendritic cells [562]. Although in mice MZ B cells mainly take part in T-independent responses, in humans MZ B cells constitute a heterogenous population including cells with a memory phenotype displaying mutated V_H genes [563]. The production of autoantibodies may not be the only contribution of MZ B cells to the development of autoimmune disease. For example, MZ B cells are efficient APCs and can promote T cell activation, proliferation and cytokine production [564]. They could therefore also take part in the presentation of auto-antigen to T cells leading to their activation, thereby further enhancing the autoimmune response. It is not clear why high-affinity self-reactive B-1 and MZ B cells are produced and how tolerance is broken but it has been speculated that polyreactive/self-reactive B cells are generally recruited into the MZ and maybe also B-1 B cell compartment as means of keeping those B cells from any further diversification in order to prevent development of high-affinity self-reactivity [565]. A defect in the negative selection process that usually eliminates self-reactive clones could therefore lead to an increase in autoreactive cells which would be selected into the B-1 and MZ B cell compartment.

4.1.3 B cell tolerance and its role in autoimmunity

The immune system has to generate an extremely diverse repertoire of antigen-specific B and T cells to be able to combat all the pathogens a human being might encounter during a lifetime. The drawback to this diversity is the potential to produce reactivities against host components. Thus both T cells and B cells are negatively selected during their development by mechanisms which ensure that the vast majority of

autoreactive cells never reach the periphery (central tolerance). In addition, the immune system has developed homeostatic controls to ensure that immune responses are terminated after the clearance of pathogens as dysregulated responses lead to expanded pools of antigen-specific B lymphocytes which can persist in the periphery. Due to the relatively high frequency of such B cells recognising self-antigen with low-affinity this would increase the number of self-reactive B cells and therefore the chance for chronic activation of these clones. This is potentially a very dangerous situation and therefore normally regulated by a cascade of checkpoints ensuring not only that autoreactive cells are inactivated and/or deleted but also that there is homeostatic regulation of cells that recognise foreign antigen.

4.1.3.1 Defects in B cell tolerance observed in autoimmune disease

It has been postulated that in healthy humans, pathogenic autoreactive B cells are either absent or kept in an inactive state by central and/or peripheral tolerance checkpoints. Numerous studies in mice and humans have therefore tried to identify these checkpoints and potential defects affecting these checkpoints in individuals with autoimmune diseases. As stated in section 1.3, the major central tolerance checkpoint during B cell development is at the level of immature B cells (Fig 1.8) as in healthy humans this checkpoint reduces the initial percentage of self-reactive clones from 75 to 40% [71]. Using CD10 as a marker to distinguish between B cells newly emigrated from the bone marrow ($CD19^+IgM^+CD10^+CD27^-$) and mature naïve B cells ($CD19^+IgM^+CD10^-$ $CD27^-$), Yurasov *et al* [566] identified another checkpoint, which in healthy individuals removes some further 50% of the autoreactive B cells that have managed to escape central tolerance (Fig 1.8). Interestingly, this checkpoint seems to be non-functional in a subgroup of SLE patients and some patients with RA [566,567].

A later checkpoint has recently been identified that normally appears to act at the mature naïve B cell stage: thus, in healthy humans such autoreactive B cells which make up about 20% of the naïve population are not selected into the IgM^+ memory compartment [568] (Fig 1.8). To date, there have not been any follow-up studies determining whether this checkpoint is defective in patients with autoimmune disease. In addition to being excluded from the IgM^+ memory cell pool, such autoreactive mature naïve B cells might also be prevented from entering the GC reaction as it was shown that potentially autoreactive human B cells such as those specific for dsDNA and CD45 (9G4 B cells), which are present in normal healthy individuals, are excluded from the GC reaction [75] (Fig 1.8). Consequentially, these cells mainly display a naïve phenotype and do not take

part in the development of memory cells and IgG-production. However, the block of these self-reactive cells from IgG^+-memory cell development seems to be defective in some SLE patients as indicated by their higher prevalence (10-25 fold) of 9G4 IgG memory cells [75]. This defect in exclusion of 9G4 B cells does not seem to be a general mechanism involved in autoimmune diseases as patients with RA did not display an increased frequency of these cells in their IgG-memory compartment [75]. Moreover, this study only showed GC exclusion of one specific B cell clone and thus, it cannot be concluded that this mechanism applies to all autoreactive clones. It is therefore interesting that a recent study by Tiller and colleagues [569] has found that a higher percentage of IgG^+-memory B cells from healthy individuals express autoreactive BCRs compared to mature naïve B cells. The authors argue that the self-reactivity seen in those cells might be a by-product of affinity maturation and selection during the GC reaction leading to the enrichment of these clones [569]. It remains to be determined why these autoreactive memory cells do not induce disease in healthy individuals and it is therefore of interest to identify the mechanisms preventing these cells from being activated.

Finally, there are some animal studies which indicate that there may be an additional final checkpoint ensuring that autoreactive B cells do not produce pathogenic antibodies. One such model system uses mice expressing an anti-Sm (ribonucleoprotein) transgenic BCR to investigate the activity of these self-reactive B cells in the context of autoimmune and non-autoimmune prone backgrounds. For example, in normal mice, these autoreactive B cells were found to be unable to proceed past the pre-plasma cell stage to the plasma cell stage. By contrast, autoimmune prone mice exhibited a higher percentage of anti-Sm-producing B cells indicating deregulation of a checkpoint governing development of plasma cells [570] (Fig 1.8). The molecular mechanisms preventing such cells from further development in non-autoimmune prone mice are not known, but could involve repression of these cells by other cells such as DCs or regulatory T cells or indeed B cell intrinsic mechanisms such as anergy resulting from constant antigen exposure [570]. It has indeed been shown that TLR-4-activated myeloid DCs and macrophages can regulate B cell activation through the production of IL-6. Whereas IL-6 supports plasma cell differentiation in cells acutely exposed to antigen, it does not appear to be able to stimulate self-reactive cells which have been chronically exposed to antigen but rather acts to suppress antibody secretion by such self-reactive cells. These findings highlight that B cell tolerance is not solely a cell intrinsic process and hence emphasises the importance of other cells of the immune system in the regulation of self-reactive B cells.

Recent evidence has suggested that negative selection at these multiple maturation checkpoints is not the only mechanism controlling activation of self-reactive B cells,

however. For example, competition for survival factors as well as space in specific environmental niches might also influence the balance between healthy and autoreactive B cell survival. Thus, for example, in normal mice whilst high-affinity autoreactive B cells are arrested at the immature developmental stage and are also excluded from the B cell follicles in the spleen, lower-affinity autoreactive B cells of the same specificity are allowed to enter follicles. By contrast, in the absence of tolerant or low-affinity self-reactive B cells, high affinity self-reactive B cells could be detected in the follicles indicating that the exclusion of high affinity autoreactive B cells might be due to competition [571].

Probably the most important survival factor B cells compete for in the periphery is BAFF (B cell activating factor) which signals through the BAFF-receptor (BAFF-R). The need for BAFF-R signalling for survival first occurs at the transitional stage where it coincides with upregulation of expression of the BAFF-R [572]. The importance of BAFF was first shown using BAFF-R-deficient B cells which proliferated less and displayed impaired survival compared to wild-type B cells [33] and was further emphasised by the fact that BAFF-R-deficient B cells displayed a reduced lifespan which could be increased by administration of BAFF [573]. The survival-enhancing effect of BAFF signaling is achieved, at least in part, by the upregulation of anti-apoptotic Bcl-2 family members A1 and Bcl-x_L [573]. Thus, the reduced ability of high-affinity self-reactive cells to compete with low-affinity self reactive or non-self reactive cells might in part be due to an increased dependency on BAFF, as murine studies showed that elevated serum levels of BAFF were able to rescue autoreactive B cells which would normally be negatively selected at the transitional B cell stage [574]. It has been proposed that the higher dependency on BAFF of autoreactive B cells might reflect negative signalling via the BCR by self-antigen resulting in an increased threshold for positive signalling resulting from BAFF/BAFF-R interactions. This mechanism might have some relevance for human autoimmune diseases as certain SLE and RA patients have been found to express significantly elevated serum levels of BAFF [575] which might have resulted in an increased survival rate of self-reactive B cell clones in these patients.

4.1.4 Role of FcγRIIb in autoimmune disease

FcγRIIb is a low affinity receptor for the Fc portion of IgG (section 1.5.5.3). Cross-linking of BCR and FcγRIIb by immune complexes inhibits BCR-mediated activation and proliferation of B cells and thus provides an important homeostatic mechanism for terminating ongoing B cell responses [576]. Many studies have examined the implications of genetic modulation of FcγRIIb expression on immune responses and the development of autoimmune and/or inflammatory diseases. For example, depending on their different

genetic backgrounds, FcγRIIb-deficient mice were found to show an increased inflammatory response in immune complex alveolitis (Balb/C) [577], enhanced IgE-mediated anaphylactic responses (C57BL/6) [578] or increased susceptibility for induction of collagen-induced arthritis (CIA) (C57BL/6/129/SvJ hybrid) [579]. Other studies, using FcγRIIb$^{-/-}$ knockout mice on the C57BL/6 background showed that such mice develop spontaneous lupus-like disease with premature mortality [580]. By contrast, studies overexpressing FcγRIIb specifically on B cells showed that such mice displayed reduced antibody production in T-dependent immune responses as well as milder disease in the CIA model and lower levels of disease incidence in the MRL/MpJ-*Fas*^{lpr} model of SLE [581]. The mechanisms involved are not clear but it is likely that the lack of this receptor on B cells is the cause of the increased susceptibility for autoimmunity seen in these mice. Consistent with this, retroviral transfection of FcγRIIb$^{-/-}$ bone marrow cells with FcγRIIb and the transfer of these cells into an irradiated host can restore the normal phenotype with lower levels of autoantibodies, reduced immune complex deposition and inflammation in autoimmune prone strains [582].

More recent studies have tried to further elucidate the mechanisms that lead to lupus-like disease in such FcγRIIb knockout mice. Two independent studies found that deficiency in this receptor increases the levels of circulating RF [583] and anti-DNA autoantibodies [584] and that the number of anti-DNA specific plasma cells, which mostly expressed IgG antibodies, was increased [584]. Thus, expression of FcγRIIb might also play a role in controlling the expansion and activation of high affinity self-reactive B cells. Consistent with this, FcγRIIb-deficient mice, expressing a transgene-encoded heavy chain rendering their B cells specific for DNA, displayed an altered B cell repertoire comprising expansion and activation of high affinity anti-DNA B cell clones compared to that of FcγRIIb-expressing mice [585]. Moreover, it has also been proposed that FcγRIIb plays a role in the GC reaction by regulating the development of antibody-forming cells versus memory cells. Consistent with this, it was found that levels of FcγRIIb on GC B cells are increased compared with those on non-GC cells in wild-type mice and that this up-regulation is missing in autoimmune mice [586]. The disturbance of any, or a combination, of these functions could therefore influence the development and maintenance of autoimmune diseases.

There have not been many studies investigating the role of FcγRIIb in human autoimmune disease to date. However, Enyedy *et al* [587] have examined the FcγRIIb-associated inhibition of BCR signalling in B cells from SLE patients and found that they showed an increased intracytoplasmic calcium flux upon BCR stimulation relative to healthy volunteers. To investigate if this hyperreactivity was due to reduced FcγRIIb

signalling or expression, the effect of cross-linking BCR and FcγRIIb on B cells from SLE patients was tested. The inhibitory effect of FcγRIIb signalling on calcium flux upon BCR stimulation was reduced in SLE B cells, whilst the expression levels of FcγRIIb on the surface of these cells were found to be the same as on normal B cells indicating a defect in the signalling mechanisms. However, more recent studies, using newly developed FcγRIIb-specific antibodies, have looked in more detail at the expression of FcγRIIb by SLE patients [588] and have identified some major differences in B cell subsets. Thus, comparison between healthy controls and SLE patients showed that the upregulation of FcγRIIb expression on memory B cells and plasmablasts from peripheral blood was decreased in autoimmune patients leading to increased calcium signalling upon BCR-ligation. Interestingly, significantly more Afro-American patients showed this defect than patients of Caucasian background indicating involvement of a genetic component [588]. A reduction of FcγRIIb expression on memory and plasma cells could therefore be one of the mechanisms leading to hyperactive B cell responses and increased autoantibody production in patients with autoimmune diseases such as SLE. Interestingly, a polymorphism of FcγRIIb which changes the isoleucine at position 232 to a threonine was found to be associated with SLE in some racial groups such as Japanese patient cohorts [589]. This amino acid is in the transmembrane domain of FcγRIIb and the polymorphism reduces the signalling capability of FcγRIIb due to its exclusion from lipid rafts [590]. Taken together these studies therefore provide another link between reduced FcγRIIb signalling and an increased risk of developing SLE.

4.1.5 The role of toll-like receptor (TLR) signalling in B cells

It has become increasingly apparent that TLR signalling might not only play important roles in the innate immune system but also in regulating adaptive immune responses, including those of B cells. For example, recent data highlight the possibility that TLRs might act as a third signal for B cells to optimise their activation, isotype switching and terminal differentiation. Thus, proliferation of naïve human B cells was found to be prolonged after BCR stimulation in the context of T cell help, only in the presence of TLR ligands [37]. The possibility of self-reactive B cells with certain specificities such as anti-DNA or anti-RNA being activated by their antigen not only through the BCR but also via TLRs has led to the hypothesis that TLR signalling might contribute to the unwanted activation of autoreactive B cell clones. This is a realistic scenario especially in autoimmune diseases like SLE, which is characterised by the production of antibodies against potential TLR ligands, such as DNA. In addition to endogenous TLR ligands provided by the host itself, pathogens like bacteria or viruses might also induce activation

of such self-reactive B cells by providing costimulation via TLRs. This idea is supported by a chronic infection model in which Soulas and colleagues [591] used a transgenic RF (rheumatoid factor – antibodies specific for host IgG) - producing mouse model to examine the effect of chronic *Borrelia burgdorferi* infection on autoantibody production. They found that immune complexes of RF and *Borrelia burgdorferi* simultaneously stimulated the BCR (by the auto-antigen IgG) and TLR (*B. burgdorferi* antigen most likely through TLR1/2 by Pam3Cys-modified lipoproteins) and hence synergistically increased antibody production.

The hypothesis that TLRs play a role in the activation of autoreactive B cell clones was further strengthened by findings in MRL/MpJ-*Fas*^{lpr} mice, a strain prone to spontaneously developing lupus-like disease. Unlike their TLR9-expressing littermates, TLR9-deficient MRL/MpJ-*Fas*^{lpr} mice do not produce anti-DNA or anti-chromatin antibodies. Interestingly however, Sm, cardiolipin and phospholipid autoantibody responses were not influenced by TLR9 deficiency and the mice were not protected against disease development, indicating that the ability of TLRs to play a role in the induction of specific autoantibodies may depend on the nature of the antigen (TLR ligand or not) [592]. Similarly, another study found that FcγRIIb-deficient mice which normally develop lupus-like disease were protected if they did not express TLR9 and these mice also did not produce any anti-DNA antibodies [593]. This latter study also showed that MyD88/TLR9 is necessary to develop pathogenic IgG2a and IgG2b autoreactive antibodies by inducing T-bet expression in B cells. Indeed, lack of TLR9 prevented the class switch to IgG2a/b specifically in anti-DNA B cells but not in other B cell clones. Thus, TLR 9 signalling in combination with BCR-ligation can induce class-switching to IgG2a and IgG2b, but it is not necessary for class-switching *per se* [593].

Interestingly, in normal healthy individuals TLR engagement does not lead to the activation of autoreactive B cells and initiation of autoimmune disease, suggesting that there are normally potent mechanisms preventing stimulation of self-reactive B cells during an infection. Indeed, a mouse model widely used to study B cell anergy, the HEL/anti-HEL BCR double transgenic system has proved useful in the elucidation of the mechanisms that act to keep autoreactive B cells anergic even in the presence of TLR stimuli. For example, in the presence of the auto-antigen HEL, CpG (TLR9) stimulation of HEL-reactive B cells was not able to induce proliferation or plasma cell differentiation. Moreover, signalling by this self-antigen uncoupled the BCR from downstream calcineurin-dependent pathways thereby reducing proliferation, but led to constitutively elevated ERK activation which inhibited plasma cell differentiation [594]. These signals were reversible and removal of the self-antigen allowed stimulatory signalling through TLR9 [594]. These data therefore fit well with a recent report by Gauld *et al* [595] showing that constitutive

signalling is required to keep B cells in an anergic state. Here they used the Ars/A1 model for anergy, taking advantage of the fact that whilst B cells of these mice express an antibody specific for a self-antigen thought to be ssDNA, they also bind the hapten arsonate with slightly higher affinity than the self-antigen. Addition of excess hapten therefore displaces the bound self-antigen and terminates signalling due to the monovalent nature of the hapten which is not able to cross-link the BCR. Consistent with the findings in the HEL/anti-HEL model, anergic Ars/A1 B cells show reduced life-span, slightly increased basal levels of calcium, ERK and MAPK phosphorylation and activation marker expression. The increased life span of B cells resulting from the removal of auto-antigen from the BCR by hapten application correlated with a reduction of basal calcium levels and ERK phosphorylation back to normal levels and the capacity of these cells to upregulate CD86 and mobilise calcium upon stimulation with anti-IgM [595]. Collectively, these data indicate that constant antigen binding and signalling maintains B cells in an anergic state and thus, in normal individuals, B cell anergy induced by self-reactivity is not overcome by synergistic TLR signalling. In mice with autoimmune-prone background, or patients with autoimmune disease, this negative control mechanism might be defective allowing TLR signals to enhance activation and differentiation of self-reactive B cells and production of autoantibodies.

4.2 Aims

It is well established that co-ligation of the BCR and FcγRIIb results in inhibition of B cell growth and apoptosis with a consequent reduction in antibody production [209,596]. Recent studies using FcγRIIb-knockout mice have shown that this inhibitory receptor might play a role in suppressing the development of some autoimmune diseases like SLE, as deficiency can lead to the development of lupus-like disease [580]. However, the mechanisms underlying growth arrest and apoptosis downstream of BCR/FcγRIIb co-ligation have not yet been fully elucidated.

The specific aims of this chapter are therefore to:

- Characterise the key signals involved in growth arrest and apoptosis of B cells resulting from the cross-linking of BCR/FcγRIIb.
- Determine if FcγRIIb-mediated negative feedback inhibition is defective in MRL/MpJ-*Fas*^{lpr} mice.

- Characterise if similar signalling occurs in human B cells from healthy individuals and is defective in RA/SLE patients.

4.3 Results

4.3.1 Ligation of the BCR on mature B cells mediates survival and proliferation, whereas co-ligation with FcγRIIb induces growth arrest and apoptosis

The effects of BCR/FcγRIIb co-ligation were investigated in purified mature splenic B cells by using different forms of anti-Ig antibodies to mimic stimulation by free antigen and/or immune complexes. Thus, as a control, cells were cultured in media alone (designated **None** in the figures) and stimulation with $F(ab')_2$ fragments of anti-IgM was used to cross-link the BCR and induce mitogenic signals (designated **BCR** in the figures). By contrast, as stimulation with intact anti-IgM/IgG results in the generation of negative signals induced by co-ligation of the BCR and FcγRIIb [209], these antibodies were used in combination with $F(ab')_2$ fragments of anti-IgM to mimic the inhibition of antigen-driven mitogenic signals by immune complexes resulting in growth arrest and apoptosis [209] (designated **BCR+FcγRIIb** in the figures) (Fig.4.1). It should be noted that it is widely established that primary mature B cells cultured with media alone are prone to die in culture and hence results acquired with unstimulated cells reflect the spontaneous growth arrest and death of cells lacking survival signals in this time period. By contrast, cells provided with survival signals such as IL-4 survive but do not undergo proliferation [309].

Thus, as expected, the spontaneous levels of DNA synthesis of mature splenic B cells after 48 hours are very low if cells are left untreated (Fig.4.2A). By contrast, cross-linking the BCR induces mitogenic signalling as shown by the addition of $F(ab')_2$ fragments of anti-IgM therefore inducing substantial DNA synthesis (Fig.4.2A). These data are corroborated by cell cycle stage analysis (PI staining of DNA content) which demonstrated that the vast majority of the untreated cells were arrested in the G1 phase of cell cycle and only a very low number of cells were in the mitogenic phases of the cell cycle (S and G2/M phase) (Fig.4.2B-C). By contrast, ligation of the BCR reduced the percentage of cells arrested at the G1 stage and additionally promoted progress of cells into the S and G2/M phases of the cell cycle indicating proliferation of these cells (Fig.4.2B-C).

Cross-linking the FcγRIIb and BCR on the other hand is known to induce growth arrest and apoptosis in B cells [597]. Thus, as expected, co-ligation of FcγRIIb and BCR on purified splenic B cells reduced the levels of BCR-driven DNA synthesis compared to cells stimulated through their BCR alone (Fig.4.2A). This reduced proliferation is due to both growth arrest and apoptosis as there is a strong increase in the percentage of subdiploid cells in comparison to BCR-stimulated cells (Fig.4.2C). Additionally, BCR-mediated progression through the cell cycle was also inhibited by FcγRIIb co-ligation

shown by a reduction of cells in S and G2/M phase at 48 hours and indeed, analysis of the live cell gate revealed that there are proportionally more of this population in G0/G1 phase (Fig.4.2C-ii). Dissipation of the MMP is an early hallmark of apoptosis and consistent with this, ligation of the BCR protects the integrity of the mitochondria as shown by the strong $DiOC_6$ staining intensity (MMP-sensing dye) which directly correlates with higher and therefore more stable MMP compared to untreated cells at 48 h (Fig. 4.2D). Nevertheless, a proportion of these cells displayed lower MMP correlating with the cell cycle data showing that some BCR-stimulated cells were also undergoing growth arrest and/or or dying (Fig.4.2C). Similarly, untreated cells exhibited low MMP consistent with their status of G0/G1 arrest and consequent apoptosis. However, inhibition of BCR-driven signalling by co-ligation of the BCR with FcγRIIb resulted in the strongest reduction of MMP indicating that such FcγRIIb-mediated signals, at least in part, initiate apoptosis through dissipation of the MMP (Fig.4.2D).

4.3.2 Caspase-8 inhibition reduces FcγRIIb-induced apoptosis

It was shown by this laboratory that FcγRIIb-mediated apoptosis initiates the dissipation of the MMP and leads to the release of cytochrome C [309]. This mitochondrial-dependent apoptotic pathway seems to be induced, at least in part, by the FcγRIIb-mediated reduction of PI3 kinase-activity as inhibition of PI3 kinase induces apoptosis even in the presence of BCR-signalling [309]. PI3 kinase signalling, through activation of Akt, keeps the pro-apoptotic molecule Bad in an inactive state [598] and thus, reduced levels of activated Akt would therefore result in increased activation of Bad which in turn could sequester Bcl-x_L/Bcl-2 and stop them from protecting mitochondrial integrity [309]. The execution phase of such apoptosis did not appear to be dependent on caspases or any other executioner proteases such as cathepsin B or calpain as evidenced by the lack of effect on FcγRIIb-mediated apoptosis by the administration of pharmacological inhibitors against any of these proteases. Rather, the combination of such inhibitors and hence presumably inhibition of more than one of these executioner proteases, was sufficient to protect cells from BCR/FcγRIIb-mediated apoptosis [309] suggesting that concerted activation of these executioner proteases was required for apoptosis. Caspase 8 is an initiator caspase which is known to be able to initiate the intrinsic mitochondrial apoptotic pathway as well as the activation of executioner caspases such as caspase 3. As both dissipation of the MMP as well as activation of executioner proteases seems to play a role in FcγRIIb-induced apoptosis, caspase 8, which also controls both these pathways, might therefore be potentially involved in the regulation of this as yet undefined signalling

cascade. Therefore, a caspase 8-specific pharmacological inhibitor was used to analyse the effects of caspase 8 inhibition on FcγRIIb-mediated B cell responses (Fig. 4.3).

As shown above, cross-linking the BCR in the presence of negative signalling resulting from co-ligation of the BCR and FcγRIIb, strongly increased the percentage of apoptotic cells with subdiploid DNA content compared to that observed following mitogenic stimulation of the cells via the BCR (Fig.4.3A). This increase was efficiently blocked by the addition of a caspase 8 inhibitor which reduced the levels of apoptosis downstream of BCR/FcγRIIb ligation from 48% to 22% (Fig.4.3A). Caspase 8 inhibition also slightly reduced the percentage of untreated or BCR-stimulated cells undergoing apoptosis suggesting that caspase 8 played a general regulatory role in the apoptosis of mature B cells. As the caspase 8 inhibitor was shown to efficiently reduce FcγRIIb-mediated apoptosis almost to the levels observed in BCR-stimulated cells, it was further analysed whether this protection from apoptosis was due to increased stability of mitochondria. However, when caspase 8 activation was blocked, it was found that co-ligation of BCR and FcγRIIb still reduced the percentage of cells with high MMP to the same extent as seen in cells treated with DMSO as a control (Fig.4.3C/D). Furthermore, caspase 8 inhibition did not modulate the MMP in either untreated cells or BCR-stimulated cells (Fig.4.3B-E). It is therefore concluded that during spontaneous, BCR- or FcγRIIb-mediated apoptosis of mature B cells, dissipation of the MMP is a process induced upstream or in parallel with caspase 8 activation.

Consistent with these results, cleaved active caspase 8 was found at higher levels in cells after BCR/FcγRIIb co-ligation compared to these observed in untreated or BCR-stimulated cells, hence further confirming the association of caspase 8 with FcγRIIb-mediated apoptosis (Fig.4.4A). Moreover, although it is still somewhat controversial as to the exact role $cFLIP_L$ plays, as it has been shown to both inhibit and enhance apoptosis [599], $cFLIP_L$ has been proposed to be a major regulator of death receptor signalling involving caspase 8. For example, it has been suggested that $cFLIP_L$ may act as an inhibitor of caspase 8 activation when present at physiological levels, whereas overexpression of $cFLIP_L$ might drive apoptosis [599]. Perhaps consistent with this, preliminary results showed that whilst $cFLIP_L$ could be detected in untreated, BCR-stimulated as well as BCR/FcγRIIb costimulated cells, it was most highly expressed in cells in which the BCR and FcγRIIb were crosslinked (Fig.4.4B), indicating that this molecule may play some role in negative signalling during FcγRIIb-mediated apoptosis.

4.3.3 FcγRIIb-mediated regulation of p53 expression and localisation and induction of Noxa

These initial experiments established that caspase 8 is important in the regulation of FcγRIIb-mediated apoptosis. In order to shed some light on the downstream molecules involved in the apoptotic pathways utilised by FcγRIIb, it was decided to examine the role of known key regulators of apoptosis such as p53, a tumor suppressor which regulates growth arrest and apoptosis [600,601]. The main function of p53 is that of a transcription factor and as such it regulates genes important in the induction of growth arrest like the cell cycle inhibitor p21, or in apoptosis such as the pro-apoptotic BH3-only proteins Puma, Noxa [484] and Bax [485]. Interestingly, p53 has also recently been found to be able to initiate apoptosis by transcription-independent mechanisms. Thus, whilst for its role as a transcription factor p53 has to be localised in the nucleus where it is able to regulate transcription of its target genes, it was recently shown that p53 can translocate to the cytoplasm and mitochondria where it interacts with Bcl-2 family members. Thus, translocation of p53 to the mitochondria allows it to interact with Bcl-x_L and Bcl-2 liberating the pro-apoptotic Bax and Bak and inducing the intrinsic apoptosis pathway [486]. Furthermore, p53 was also shown to be capable of activating Bax in the absence of any other Bcl-2 family members [602]. Thus, to fully assess p53 activity it might therefore be important to analyse not only its overall expression levels but also its subcellular localisation.

To address the role of p53 in FcγRIIb-induced apoptosis its expression at the mRNA and protein levels downstream of BCR/FcγRIIb co-ligation was first analysed. Levels of p53 mRNA were found to be highest in untreated cells and suppressed by mitogenic stimulation through the BCR. Perhaps rather surprisingly, this reduction of p53 expression was partially reversed due to co-ligation of the FcγRIIb, remaining at considerably lower levels than in unstimulated cells (Fig.4.5A). To determine if these changes at the transcriptional level translated into protein expression, whole cell lysates were also analysed for p53 expression. At 48 h, p53 protein expression was indeed found to be suppressed by BCR signalling and this effect was not only reversed by FcγRIIb-co-ligation but p53 expression was strongly upregulated relative to the levels observed in naïve, untreated cells (Fig.4.5B). Collectively, these results suggest that p53 may play a role not only in driving FcγRIIb-mediated negative signalling but also in maintaining naïve cells in an inactive form. Moreover, as the profiles of p53 mRNA and protein expression were distinct, these results suggest that the upregulation of p53 observed in response to FcγRIIb signalling likely reflected predominantly protein stabilisation rather than *de novo* gene induction.

As stated above, the functional consequences of p53 activity are highly dependent on its localisation. In the nucleus, p53 functions mainly as a transcriptional regulator whereas in the cytoplasm and at the mitochondria it seems to be directly involved in regulating the balance between the activity of pro- and anti-apoptotic molecules. To determine the effects of BCR and/or FcγRIIb signalling on p53 localisation, subcellular fractions (cytoplasmic and nuclear) were prepared 48 hours after stimulation and the levels of p53 protein expression determined. In both the cytoplasmic as well as the nuclear fractions, p53 could only be detected in samples derived from cells undergoing FcγRIIb-mediated negative signalling (Fig.4.5C/D). Having established that p53 is indeed regulated by BCR and FcγRIIb signalling, the potential connection between p53 and caspase 8 was analysed by investigating the effects of caspase 8 inhibition on p53 expression and localisation. Inhibition of caspase 8 did not affect the protein levels of p53 detected in whole cell lysates in untreated cells or BCR-stimulated cells (Fig.4.5B) but did appear to slightly reduce p53 expression in cells stimulated via the BCR and FcγRIIb (Fig.4.5B). More striking effects of caspase 8 inhibition, however, could be detected in terms of the subcellular localisation of p53. Thus, whilst BCR/FcγRIIb-mediated signalling predominantly induced cytoplasmic p53 expression, inhibition of caspase 8 induced a striking re-localisation of p53 from the cytoplasm to the nucleus thereby strongly reducing the cytoplasmic levels of p53 (Fig.4.5C/D).

There are various potential effects of increased p53 activity. For example, increased p53 levels could enhance the transcription and hence protein levels of its targets such as Noxa [603], a pro-apoptotic BH3-only protein. Following transcriptional upregulation Noxa can translocate to mitochondria where it binds to anti-apoptotic Bcl-2 family members such as Mcl-1 but does not directly bind Bax [289,604]. Noxa-dependent apoptosis is therefore most likely initiated by indirect release of Bim and Bak from Mcl-1 allowing them to destabilise the mitochondria [605]. In melanoma cells Noxa has also been found to locate to the endoplasmic reticulum where it induces intracellular calcium release, but the relevance of this mitochondrial-independent pathway has yet to be analysed in other cellular systems [606]. Taken together these studies indicate that Noxa can play an important role in p53-dependent apoptosis. One of the functional outcomes of the increased levels of p53 detected upon ligation of BCR/FcγRIIb (Fig.4.5B) could therefore potentially be the upregulation of Noxa expression. It was therefore decided to analyse the regulation of Noxa in FcγRIIb-mediated apoptosis. Indeed, Noxa, which could not be detected in freshly isolated cells (0 h) was upregulated by cross-linking of the BCR and FcγRIIb at 24 and particularly, 48 hours (Fig.4.6A). Untreated cells also slightly upregulated the expression of Noxa over time, but not to the same extent as cells

stimulated through BCR/FcγRIIb ligation (Fig.4.6A). Noxa expression was below the detection limit in BCR-stimulated cells, indicating that BCR-signalling perhaps maintained suppression of upregulation of Noxa by reducing p53 expression (Fig.4.5B and 4.6A). Taken together these results suggest that FcγRIIb-mediated negative signalling induces p53 expression thereby increasing Noxa expression. Both Noxa, and also p53 itself, could translocate to the mitochondria and induce dissipation of the MMP by either interacting with Bcl-2 family proteins or through direct mechanisms [484,602].

4.3.4 Caspase 8 does not inhibit FcγRIIb-mediated activation of effector caspases

As described above, data from this laboratory suggested that that FcγRIIb-mediated apoptosis might depend on the concerted activation of multiple executioner proteases such as effector caspases, cathepsins and calpains [309]. Caspase 8 seems to play an important role in apoptosis induced by BCR/FcγRIIb co-ligation and it is known to activate caspase 3 [607]. Thus, it was investigated whether blocking of caspase 8 activity resulted in inhibition of BCR/FcγRIIb-mediated activation of caspase 3 subfamily caspases as evidenced by binding of the FITC-labelled pan-caspase inhibitor, VAD-FMK that can bind and inhibit ICE like proteases/group 1 proteases (including caspases 1, 4, 5) and, to a lesser extent, caspase 3 subfamily proteases (including caspases 2, 3, 6, 7, 9) [608]. Cells, which had been left untreated over the 24 h stimulation period, displayed high levels of caspase activation (Fig.4.6B-E) which were not influenced by mitogenic stimulation of cells through the BCR (Fig.4.6C-E). By contrast, co-ligation of BCR/FcγRIIb increased the level of FITC fluorescence detected after labelling of the cells with FITC-VAD-FMK indicating an increase in caspase activation (Fig.4.6C-E). Having established a role for caspase activation in the FcγRIIb-signalling pathway, the role of caspase 8 in the regulation of such caspase activity was assessed. Again taking advantage of the specific caspase 8 inhibitor, it was shown that caspase-8 inhibition did not increase or inhibit caspase activation in either untreated, BCR/FcγRIIb or BCR-ligated cells (Fig. 4.6C-E). The activity of calpain as well as cathepsin B was tested as well, but no activity could be detected. Collectively, these results suggest either that caspase 8 activity is not needed for the concerted activation of executioner caspases or perhaps that the combined protease inhibitors, which have been previously described to inhibit FcγRIIb-mediated apoptosis, might have been targeting caspase 8 activity.

4.3.5 Caspase 8 inhibition does not affect BCR/FcγRIIb induced growth arrest

The experiments described so far have established that caspase 8 plays a pivotal role in the regulation of BCR/FcγRIIb-induced apoptosis. Initial cell cycle data indicated that although caspase-8 inhibition reduced the level of subdiploid/apoptotic cells (Fig.4.3A-iv), it did not decrease the percentage of cells arrested in the G1 phase of the cell cycle in BCR/FcγRIIb-stimulated cells (Fig.4.7A/B). Indeed, more detailed analysis of the cell cycle stages showed that whilst cross-linking of the BCR and FcγRIIb in the presence of the caspase 8 inhibitor increased the percentage of live cells in G1 growth arrest (Fig.4.7A and B), it did not prevent the FcγRIIb-mediated suppression of BCR-mediated S-phase and G2-M phase progression (Fig.4.7C/D). Further corroboration of these results came from DNA synthesis experiments in which addition of the caspase 8 inhibitor did not influence proliferation of cells at 48 and 72 h, regardless of the stimuli used (Fig.4.7E/F). Thus, caspase 8 inhibition protected cells from apoptosis but was not able to restore cell cycle progression and proliferation, leading to an accumulation of growth arrested cells.

4.3.6 Effects of FcγRIIb-signalling on cell cycle regulation

Having established that cross-linking of the BCR and FcγRIIb results in growth arrest in the G1 phase of the cell cycle that ultimately leads to apoptosis, the effects of FcγRIIb-signalling on regulators of cell survival and cell cycle progression were analysed. c-Myc is an important regulator of the cell cycle [609] at multiple levels: for example, c-Myc promotes cell cycle progression by increasing the expression of cyclins and indirectly leading to degradation of p27 [610,611]. c-Myc itself is regulated at the transcriptional and protein level, therefore, firstly, to assess if c-Myc was regulated by BCR or BCR/FcγRIIb-signalling in mature B cells, c-Myc expression at the mRNA and protein levels were analysed. As expected, c-Myc mRNA levels were indeed found to be upregulated following mitogenic stimulation via the BCR, but this was transient returning to basal levels within 7 h (Fig.4.8A). By contrast, and consistent with the growth arrest-inducing effects of FcγRIIb-mediated signalling, simultaneous cross-linking of the BCR with FcγRIIb suppressed the BCR-mediated upregulation of c-Myc RNA levels, although the levels observed were still higher than those of untreated cells (Fig.4.8A). Reflecting the differential induction observed at the mRNA level, c-Myc protein expression at 24 h was higher in cells mitogenically stimulated via the BCR than in those stimulated via the BCR and FcγRIIb (Fig.4.8B). Moreover, c-Myc could not be detected at all in untreated cells at this time point, presumably reflecting the fact that these cells were spontaneously dying. Although c-Myc mRNA levels did not differ between untreated, BCR or BCR/FcγRIIb-stimulated

cells at 24 h, the differential protein levels observed not only probably represent the delayed kinetics of c-Myc regulation at the protein compared to RNA level (Fig.4.8B), but may also reflect the involvement of other regulatory mechanisms such as c-Myc protein stabilisation through phosphorylation.

The key step in the progression of cells through G1 phase and into S phase is governed by the hyperphosphorylation-status of Rb proteins [612]. Mitogenic stimuli can induce an increase in the activity of Cdk/cyclin complexes which phosphorylate Rb which in turn reduces the binding of Rb to E2F and releases E2F to induce the transcription of genes controlling the entry into S phase [613]. In order to examine the effect of BCR stimulation, as well as inhibitory FcγRIIb-signalling, on this major regulatory mechanism, the expression of hyperphosphorylated Rb (phospho-serine 807/811) was detected by Western Blotting. Levels of pRbS807/811 were found to be below the detection limit in untreated cells but were strongly upregulated upon BCR stimulation (Fig.4.8B) correlating with increased proliferation and cell cycle progression in these cells (Fig.4.2A/B). Co-ligation of the BCR with FcγRIIb reduced the levels of pRbS807/811, correlating with the observed reduced c-Myc expression (Fig.4.8B). Thus, FcγRIIb-signals, probably by reducing the activation of mitogenic pathways such as PI3 kinase or ERK, reduce the upregulation of c-Myc. This in turn could decrease the activation of Cdk/cyclin complexes by c-Myc which would explain the reduced levels of phosphorylated Rb.

The analysis of cell cycle progression and cellular proliferation (DNA synthesis) performed above suggested that caspase 8 signalling was not involved in the FcγRIIb-mediated regulation of growth arrest of B cells mitogenically stimulated via the BCR (Fig.4.7A). It was therefore not surprising to find that inhibition of caspase 8 did not restore the expression of c-Myc or pRbS807/811 observed in cells costimulated through the BCR and FcγRIIb to the levels found in cells mitogenically stimulated via the BCR (Fig.4.8B). Moreover, inhibition of caspase 8 did not have any effects on c-Myc or phospho-Rb expression in untreated or BCR-stimulated cells (Fig.4.8B).

4.3.7 Involvement of regulatory elements of the ERK MAPK cascade in FcγRIIb-mediated inhibitory effects

FcγRIIb-mediated negative feedback inhibition downregulates multiple signalling pathways including the ERK MAPK cascade. This cascade is important for survival and proliferation of mature B cells [331] with inhibition of ERK activation being shown to be linked to growth arrest and apoptosis [310], most likely by modulating cyclin D expression as well as c-Myc stability, as seen in immature WEHI-231 B cells (section 3.3.9). The downregulation of ERK MAPK signalling by FcγRIIb-ligation is therefore one of the major

mechanisms inducing growth arrest upon BCR/FcγRIIb co-ligation. This is consistent with the finding that the major effector recruited to FcγRIIb is SHIP, which reduces Ras activation by several mechanisms and thereby inhibits the activation of ERK [214,614]. It was shown previously by this laboratory that ERK activation is rapidly abrogated upon co-ligation of FcγRIIb within the first 5 minutes and, consistent with its important role in BCR-induced proliferation and survival, such inhibition is sustained for up to 96 hours [309,453]. FcγRIIb-signalling not only inhibits initiation of the ERK cascade, it also decreases ongoing activation of ERK, as it has been shown to recruit PAC-1, an ERK-specific MAP kinase phosphatase, thereby leading to dephosphorylation of previously activated ERK [209]. However, it has not been shown in these previous studies how PAC-1 was regulated by FcγRIIb-signalling, and hence it was investigated whether PAC-1 mRNA expression levels were influenced by BCR/FcγRIIb co-ligation. Thus, using Taqman RT-PCR to detect PAC-1 mRNA levels, it was shown that co-ligation of the BCR and FcγRIIb increased PAC-1 mRNA expression relative to that observed following mitogenic BCR signalling at all timepoints analysed (7-24 hours) (Fig.4.9A-ii). This could in turn lead to increased PAC-1 at the protein level and would further contribute to the FcγRIIb-mediated downregulation of ERK signalling.

It has been proposed that activation of the ERK MAPK cascade in B cells might not only depend on Ras activation, but potentially involves another small G protein, Rap which couples to the B-Raf/MEK pathway [411]. Indeed, in the DT40 chicken B cell line, B-Raf was found to be the major Raf-isoform involved in the activation of MEK and hence ERK phosphorylation [170]. SPA-1 is a Rap specific GTPase activating protein and therefore able to increase the intrinsic GTPase-activity of Rap leading to the inactivation of Rap [396]. It was therefore hypothesised that SPA-1 mediated inhibition of Rap-1 (and hence ERK) could also play a part in the FcγRIIb-mediated downregulation of ERK in mature B cells. Indeed, SPA-1 mRNA expression was found to be strongly reduced by BCR stimulation compared to levels observed in untreated cells at all timepoints analysed (3-24 hours) (Fig.4.9B-i). Thus, assuming that Rap is linked to the activation of ERK in mature B cells, reduction of SPA-1 expression would increase the levels of active Rap and hence enhance ERK activation. According to this hypothesis, FcγRIIb-mediated signalling would most likely increase the expression of SPA-1 to further strengthen the inhibition of ERK activation. Indeed, it was observed that BCR/FcγRIIb co-ligation enhanced SPA-1 expression between 3 and 24 hours after stimulation (Fig.4.9B-ii). Taken together, these results imply that FcγRIIb-signalling induces the transcription of genes which encode negative regulators of the ERK cascade. This would allow the sustained repression of ERK signals ensuring the commitment of cells to growth arrest and apoptosis.

4.3.8 FcγRIIb-dependent regulation of Fas/FasL expression

The results reported in section 4.3.2 suggested that caspase 8 is the major initiator caspase involved in FcγRIIb-induced apoptosis of mature B cells. Caspase 8 is best known, however, for its role in death receptor signalling. Thus, ligation of death receptors such as Fas leads to the assembly of the DISC complex which activates caspase 8 [615]. As B cells can express Fas and be killed by Fas/FasL-dependent apoptosis [284,616], it was therefore hypothesised that FcγRIIb-signalling might influence caspase 8 activation by enhancing Fas/FasL signalling by, for example, increasing Fas/FasL levels. Indeed, cell surface expression of Fas, detected by staining cells with a fluorochrome labelled anti-Fas antibody followed by FACS analysis, was found to be strongly enhanced following co-ligation of the BCR/FcγRIIb both in terms of the percentage of cells expressing Fas as well as an increase in the fluorescence intensity. Fas expression was also increased by BCR stimulation at 24 h (Fig.4.10A) but on much fewer cells and the increase in fluorescence intensity was minimal when compared to the levels detected after BCR/FcγRIIb co-ligation (Fig.4.10A/B), presumably reflecting the low percentage of BCR-stimulated cells undergoing apotosis at this time point (Fig.4.2). By contrast, no expression could be detected in unstimulated cells, suggesting that these cells dying by neglect do not employ a Fas/FasL death mechanism. These findings correlated with protein expression data acquired by Western Blotting. Again, expression of Fas was enhanced upon FcγRIIb-signalling at 24 h but it was below the detection limit in samples from untreated as well as BCR-stimulated cells (Fig.4.10C). Upregulation of Fas by FcγRIIb-mediated signals and hence increased Fas-death receptor signalling could therefore participate in the initiation of apoptosis by activating caspase 8.

Fas signalling is initiated by FasL binding. FasL can be expressed on other cells or on activated B cells themselves [617]. It is therefore possible that upregulation of FasL on B cells in our purified cultures could induce Fas/FasL-dependent apoptosis. Consistent with this, analysis of FasL protein expression showed that a decrease could be detected in BCR-stimulated cells when compared either to untreated cells or to cells in which FcγRIIb-signalling had been initiated (Fig.4.10C). Thus, BCR stimulation not only seems to increase Fas levels but also at the same time reduces FasL expression (Fig.4.10A and B). By contrast, in combination with the observed increase of Fas levels, the presence of high FasL expression in cells after BCR/FcγRIIb co-ligation would therefore allow the efficient induction of Fas/FasL-signalling followed by initiation of apoptosis in a caspase 8-dependent fashion.

As a major mechanism of modulating Fas/FasL signalling involves transcriptional regulation of their expression [618], Fas and FasL mRNA levels were analysed after BCR- or BCR/FcγRIIb co-ligation. Although Fas mRNA was generally found to be expressed at low levels at all timepoints analysed, the levels observed following co-ligation of BCR and FcγRIIb were higher than those seen in BCR-stimulated cells (Fig.4.11A). It was shown that protein levels of FasL had not changed much due to the different stimuli, at least at 24 hours (Fig.4.10C). To confirm that there were not any major changes at the mRNA level either, FasL expression was also analysed by quantitative RT-PCR. Consistent with this, the overall levels of FasL were found to be even lower than those of Fas, at all timepoints analysed (Fig.4.12A). Untreated cells had no detectable levels of FasL mRNA at 7 and 20 h, but slightly increased the expression at 24 h allowing detection of very low levels of FasL mRNA (Fig.4.12A). BCR stimulation induced detectable levels of FasL at all timepoints analysed, whereas ligation of the BCR and FcγRIIb did so only at 20 and 24 h (Fig.4.12A). Thus, similar to the situation for Fas, regulation at the transcriptional level does not seem to be the major mechanism controlling the protein levels of FasL in these cells.

To further dissect the role of caspase 8 in FcγRIIb-mediated cell death, the influence of caspase 8 inhibition on the BCR/FcγRIIb-mediated increase of Fas/FasL expression was analysed. Perhaps unsurprisingly, given that caspase 8 is located downstream of Fas/FasL signalling in the typical death receptor pathway, the lack of caspase 8 activity did not reduce the FcγRIIb-induced upregulation of Fas protein, detected by FACS staining or Western Blotting (Fig.4.10B/C). Moreover, caspase 8 inhibition also did not change the protein expression of FasL in combination with any of the stimulations used (Fig.4.10C). Similarly, caspase 8 inhibition also did not alter the expression of Fas or FasL at the mRNA level at 24 h (Fig.4.11/12B). In summary, Fas and FasL expression were regulated in a caspase 8-independent manner at both the mRNA and protein levels downstream of FcγRIIb-signalling.

4.3.9 The FcγRIIb-mediated apoptosis response is affected in B cells from MRL/MpJ-*Fas*^{lpr} mice

MRL/MpJ-*Fas*^{lpr} mice are a widely used animal model for SLE [619]. They are homozygous for a spontaneous mutation (*Fas*^{lpr}) in the Fas gene reducing the expression of Fas and hence show systemic autoimmunity, massive lymphadenopathy associated with aberrant proliferation of T cells, arthritis, and immune complex glomerulonephritis. Starting at about three months of age, levels of circulating immune complexes rise greatly in the MRL/MpJ-*Fas*^{lpr} mice but not in the MRL/MpJ parental strain [620]. The MRL/MpJ-

Fas^{lpr} model therefore provides the opportunity to analyse the role of Fas-mediated apoptosis downstream of FcγRIIb-signalling in B cells.

B cells from MRL/MpJ-*Fas*^{lpr} mice of varying age (9, 12, 16, 20 weeks old) were found to show a reduced inhibition of proliferation upon BCR/FcγRIIb co-ligation compared to cells from MRL/Mp mice or mice on Balb/C background (Fig.4.13A). This reduction of growth arrest was accompanied by a reduced ability of B cells from MRL/MpJ-*Fas*^{lpr} mice to undergo apoptosis upon cross-linking of BCR/FcγRIIb (Fig.4.13B) and examination of the changes in the MMP upon BCR/FcγRIIb co-ligation showed that the reduced increase in apoptosis observed in B cells from MRL/MpJ-*Fas*^{lpr} was at least in part due to failed induction of MMP dissipation. Thus, an increased percentage of B cells from MRL/MpJ-*Fas*^{lpr} mice displayed a high MMP after cross-linking of the BCR and FcγRIIb compared to B cells from MRL/MpJ mice (Fig.4.13C).

Overall, these experiments indicate that B cells defective for Fas-signalling have impaired FcγRIIb-dependent inhibitory responses. This implies that Fas/FasL-mediated signals play a role in FcγRIIb-induced apoptosis.

4.3.10 Inhibition of Fas/FasL signalling reduces FcγRIIb-mediated apoptosis

Given that Fas/FasL expression is differentially regulated by mitogenic BCR- and FcγRIIb-mediated negative signalling and that impaired expression of Fas, as observed in MRL/MpJ-*Fas*^{lpr} mice, was found to impact on the ability of B cells to be inhibited by FcγRIIb-dependent signals, these data strongly suggested that FcγRIIb-mediated apoptosis is linked to Fas/FasL signalling. To more directly prove a connection between these two events, Fas/FasL signalling was inhibited with blocking anti-FasL antibodies, which act to interfere with Fas/FasL binding, and the effects on FcγRIIb-mediated apoptosis analysed. Consistent with the above results, it was shown that inhibition of Fas-signalling decreased the percentage of subdiploid cells in BCR/FcγRIIb stimulated samples at 24 h (Fig.4.13D). Both concentrations of the blocking antibody tested were shown to be effective and the reduction of apoptosis was not a non-specific antibody-effect, as treatment with isotype control antibodies did not affect the response (Fig.4.13D). These preliminary findings suggest that upregulation of Fas followed by enhanced Fas-signalling and downstream activation of caspase 8 is indeed one of the major pathways inducing apoptosis downstream of BCR/FcγRIIb co-ligation.

4.3.11 Inhibitory FcγRIIb signalling affects proliferation of human peripheral B cells

Although the important role of FcγRIIb-mediated induction of growth arrest and apoptosis in the homeostatic regulation of B cell activation has been widely established in the murine immune system [73,576], the investigation of FcγRIIb-associated inhibitory mechanisms in human B cells has been less extensive. However, there are promising findings that FcγRIIb-mediated inhibition of BCR signalling is defective in B cells from SLE patients [587] and that plasmablasts and memory B cells from SLE patients express lower levels of FcγRIIb [588]. Moreover, a polymorphism of FcγRIIb which reduces its signalling capacity has been found to be associated with SLE in some racial groups [589]. Nevertheless, the effects of such reduced expression or signalling efficiency of FcγRIIb on B cell proliferation has not been examined in any of these studies. Thus, functional analysis of the FcγRIIb-mediated inhibitory response in human B cells from RA and SLE patients would therefore give further insight into potential defects in tolerance checkpoints in autoimmunity. It was therefore decided to compare the responses of peripheral B cells from healthy individuals and patients with RA and SLE, as both of these diseases involve autoantibody production and activation of autoreactive B cells. Hence, dysregulated B cell activation might be one of the underlying causes of both of these diseases.

Firstly, the proliferative capacity of human B cells (derived from peripheral blood) stimulated via the BCR or following co-ligation of FcγRIIb was assessed. As with the murine system, cells were treated with $F(ab)_2$ fragments of anti-human IgG+IgM antibodies to cross-link the BCR (designated **BCR** in the figures) or with intact anti-human IgG+IgM antibodies to co-ligate the BCR and FcγRIIb (designated **BCR + FcγRIIb** in the figures). Moreover, the inhibitory effect of FcγRIIb-mediated signalling upon mitogenic BCR stimulation was tested by treating cells with $F(ab)_2$ anti-human IgG+IgM in combination with intact anti-human IgG+IgM (designated **mitogenic BCR+ FcγRIIb** in the figures). Finally, unstimulated purified B cells (designated **None** in the figures) were included in the experiments. Similarly to murine B cells, unstimulated human B cells do not survive well in culture and slowly die by neglect.

CFSE staining and DNA synthesis were the methods chosen to detect proliferation in cultures. The comparison of [^{3}H]-labeled thymidine incorporation assays and CFSE staining indicated, however, that CFSE staining was not a suitable method to detect proliferation of purified human B cells as the data showed that the intensity of CFSE staining of purified B cells declined rapidly, having decreased within 4 hours even in the absence of stimuli suggesting that the cells were leaky to CFSE (Fig.4.14B-D). To confirm that CFSE analysis was indeed not a suitable assay to detect proliferation in such B cell

cultures, multiple experiments varying the incubation times, purification methods, stimuli and concentrations of antibodies, as well as FCS concentrations used for culture were carried out (data not shown). In confirmation with the data shown in Figure 4.14 these experiments yielded similar results, with no changes detectable between untreated cells or cells treated with different stimuli. By contrast, analysis of DNA synthesis by [^{3}H] thymidine incorporation indicated that BCR-stimulated cells did indeed proliferate significantly more than untreated cells at 48 hours (Fig.4.14A), indicating that this was the best assay to screen for FcγRIIb-mediated growth arrest in CD19$^+$-purified human B cells from the blood. Thus, following activation of BCR signalling, DNA synthesis increased whereas it was found to be reduced as a result of FcγRIIb/BCR co-ligation (Fig.4.14A). This confirmed that human B cells, similar to murine B cells, are sensitive to FcγRIIb-mediated growth arrest.

Further preliminary experiments were carried out in order to examine how long the purified human B cells could be cultured before their proliferative response started to decline, and to determine the optimal timepoint to detect the FcγRIIb-mediated growth arrest response. To this end, purified human B cells were stimulated as described before with BCR and BCR/FcγRIIb cross-linking antibodies, and the proliferation was measured after 48, 72 and 96 hours. Increased proliferation following BCR and BCR/FcγRIIb cross-linking could be detected at all timepoints (Fig.4.14A-ii). The inhibitory effect due to simultaneous BCR and FcγRIIb activation is most pronounced at 48 hours, but still detectable after 72 hours (Fig.4.14A-ii). Due to a decline of BCR-mediated proliferation at 96 hours there was no difference between the level of DNA synthesis between BCR and BCR/FcγRIIb stimulated cells at this timepoint. In consideration of these results, it was decided to routinely analyse B cell responses 48 hours after stimulation.

4.3.12 Correlation between growth inhibition, mitochondrial membrane potential and cell cycle status of human B cells

It has been shown in murine B cells that FcγRIIb-signalling not only induces growth arrest but also apoptosis [597]. Thus, to directly assess any correlation between growth inhibition and apoptosis in human B cells, their cell cycle status after BCR-ligation or BCR/FcγRIIb co-ligation was examined. Rather surprisingly, FcγRIIb co-ligation did not substantially increase the percentage of cells with subdiploid DNA content or arrested in G0/G1 relative to the levels observed in BCR-stimulated cells at this time point (Fig.4.15-ii). These effects were observed in a healthy control (Fig.4.15A) as well as three RA patients (Fig.4.15B) whose B cells displayed low, but detectable levels of FcγRIIb-mediated inhibition of BCR-induced DNA synthesis (Fig.4.15-i). Moreover, although the FcγRIIb-mediated reduction of cells observed in the mitotic phases of the cell cycle (G2/M

and S phase) fitted well with the growth arrest indicated by the DNA synthesis studies (Fig.4.15-i/iii), the percentage of B cells, particularly those of patients, cycling at 48 h was very low. This suggests that differential effects between the control and patient groups might be masked by culture exhaustion as indicated by the high levels of G0/G1 arrest and apoptosis in response to both mitogenic and negative feedback stimuli. Cell cycle analysis by PI staining of DNA content therefore represents a potentially useful tool for the examination of proliferation/apoptosis in human B cells, but it should preferentially be assessed at a range of time points and used in combination with additional methods such as DNA synthesis assays.

Apoptosis initiated by FcγRIIb-signalling has been shown to induce the dissipation of the MMP in murine B cells. To test whether mitochondrial disintegration was also a hallmark of FcγRIIb-mediated apoptosis in human B cells, their MMP was examined by $DiOC_6$ staining of mitochondria. This showed a trend towards a reduction of cells with high MMP and a corresponding increase of cells with low MMP upon FcγRIIb-signalling (Fig.4.15-iv). Collectively, it was shown that although BCR/FcγRIIb co-ligation on human B cells initiates similar functional responses as those observed with murine B cells, such as reduced proliferation, detected as a decrease of cells in the mitotic phases of the cell cycle as well as decreased DNA synthesis, these effects are much less pronounced. Moreover, it seems that disruption of the MMP and consequent apoptosis might play only a minor role in FcγRIIb-mediated negative feedback inhibition of human peripheral B cells. Rather surprisingly, it appeared that the patient samples were, if anything, more susceptible to growth arrest and apoptosis in response to both mitogenic and negative feedback signalling, suggesting that such circulating cells may not be directly comparable to murine splenic B cells.

4.3.13 Some patients with RA and SLE show a defect in FcγRIIb inhibitory signalling

Having established that FcγRIIb-mediated signalling inhibited BCR-driven proliferation of purified human B cells from a healthy control subject (Fig.4.14A), it was investigated whether B cells from patients with autoimmune disease are refractory to such homeostatic regulation. Analysis of B cell responses from a panel of patients and normal subjects showed that there was no significant difference between the responses of control cells and those derived from patients with RA or SLE. However, closer analysis suggested that whilst the B cells from all the healthy controls showed normal inhibitory responses, albeit of varying strength, a small percentage of RA and SLE patients showed decreased FcγRIIb-mediated inhibitory capacity (Fig.4.16). Some patients whose samples were

analysed for inhibition of growth arrest through FcγRIIb-mediated signalling did not suffer from RA or SLE, but from other autoimmune disease or a combination of diseases including Connective tissue disease, Sjogrens's syndrome or Psoriatic arthritis (Fig.4.16). The data acquired from these patients was therefore grouped separately. Similar to the other patient cohorts, no significant differences were found between the responses of B cells from healthy controls and patients, again confirming that reduced FcγRIIb-mediated inhibitory responses are not a general feature of autoimmune disease.

Although it was possible that the inhibitory defects observed in a small percentage of RA and SLE patients might reflect a long lasting defect, it was also possible that this defect might be due to their specific immune-status at the time of analysis. Thus, the B cells of two patients who showed defective inhibitory responses were tested again six months later to determine whether the refractoriness of their B cells to FcγRIIb-mediated signalling was indicative of a stable phenotype. However, whilst the B cells of one of the RA patients were again refractory to inhibition (Fig.4.17A), the B cells from the other patient with RA responded more normally (Fig.4.17B). These differential responses indicate that the responsiveness of B cells to inhibitory signaling by FcγRIIb might indeed change over time due to as yet unidentified influences. Thus, to confirm any correlation between immune status or different treatments and effective FcγRIIb-mediated inhibition of B cells, a study with more patients and more detailed information on the status of the patient would be needed.

4.3.14 Patients with autoimmune disease display changes in the expression of FcγRIIb isoforms

Human FcγRIIb encodes three transcripts, FcγRIIb1, FcγRIIb2 and FcγRIIb3, which arise by alternative splicing mechanisms. FcγRIIb isoforms are widely expressed by cells of haematopoetic origin, with preferential expression of FcγRIIb1 on B cells and FcγRIIb2 on myeloid cells. The mature forms of FcγRIIb1 and FcγRIIb3 are identical but they differ in their peptide leader sequences [621]. FcγRIIb3 lacks the information required for surface expression, encoded on the S2 exon, and is thus not expressed. FcγRIIb2 is capable of mediating rapid IgG endocytosis by means of clathrin-coated vesicles. However, due to an insertion of 19 amino acids in the cytoplasmic tail, FcγRIIb1 is not able to mediate receptor internalisation as the insertion disturbs the cytoskeletal attachment domain (Fig.4.18) [622].

Thus, FcγRIIb1 and FcγRIIb2 expression dictates the threshold for BCR signalling whereas FcγRIIb2 may be the isoform predominantly utilised by B cells for antigen uptake and processing. By downregulating expression of FcγRIIb1, whilst keeping FcγRIIb2 levels

constant, an autoreactive B cell might remain responsive to stimulation by immune complexes and costimulatory T cell help. CD40 ligand-expressing, activated T cells, in conjunction with T cell derived IL-4, will induce proliferation, antibody production and isotype switching by B cells in addition to overcoming the inhibitory effects of FcγRIIb1.

Examination of FcγRIIb1/2 mRNA expression levels in PBMCs from healthy controls as well as patients suffering from RA or SLE showed that the mRNA levels of both FcγRIIb1 and 2 are significantly reduced in PBMCs from RA, but not SLE, patients compared to healthy controls (Fig.4.19). This suggests that, as indicated by the B cell functional studies, the B cells from at least some patients may be refractory to FcγRIIb-mediated negative feedback inhibition. Moreover, analysis of the ratio of FcγRIIb1/FcγRIIb2 levels in control and patient cohorts indicated that the FcγRIIb1/2 RNA expression ratio is significantly decreased in both the RA and SLE patient groups relative to control subjects. This might be important, as the two isoforms differ in their capacity to endocytose bound IgG and these data might indicate that the cells from patients are more efficient at auto-antigen-presentation and T cell activation than those of healthy individuals (Fig.4.19E/F) [623].

This analysis of FcγRIIb1/2 expression levels was carried out on PBMCs which contain multiple cell types such as B and T cells, monocytes as well as natural killer cells. The observed differences of FcγRIIb1/2 expression levels and ratio between healthy controls and patients might therefore theoretically be due to changes in any of these cell types. Thus, to assess the overall contribution of FcγRIIb1/2 expressed by B cells, preliminary experiments were carried out to determine the transcript levels in different cell preparations. Purification of B cells enriched the levels of FcγRIIb1 or FcγRIIb2 transcripts detected 50- or 20-fold compared to levels found in non-B cells (PBMCs after B cells were negatively selected), respectively (Fig.4.20A). Indeed, and as expected, $CD3^+$-purified T cells were found to express negligible levels of either FcγRIIb1 or FcγRIIb2 (Fig.4.20B). Interestingly, purified B cells displayed a different pattern of FcγRIIb1/2 expression compared to PBMCs or non-B cells, as they expressed higher levels of FcγRIIb1 compared to FcγRIIb2 (Fig.4.20B). The recent development of anti-human FcγRIIb-specific antibodies made it possible to also detect the protein expression of FcγRIIb by FACS. Thus, it was shown that around 17% of human PBMCs express FcγRIIb on their surface and that almost all B cells express it at relatively high levels (Fig.4.20C). CD11b-positive cells which includes monocytic cells as well as granulocytes, natural killer cells and B-1 B cells are the other major cell class expressing FcγRIIb on the surface, albeit at generally lower levels than B cells (Fig.4.20C). Most of the CD11b/FcγRIIb-expressing cells were found to be relatively large cells judging by their forward and side scatter

characteristics on the FACS (data not shown), and therefore most likely represent monocytes or granulocytes. A small proportion of the cells though is smaller and less granular and hence might be natural killer or B-1 B cells. It would therefore be of interest to carry out further studies examining the contribution of the different cell types in peripheral blood towards the significant change of isoform expression observed in SLE and RA patients.

4.4 Discussion

During B cell development harmful self-reactive clones are deleted at various stages of development, with negative selection of immature B cells in the bone marrow representing a major checkpoint. Nevertheless, a considerable proportion of autoreactive cells escapes this mechanism and is released into the periphery. Further checkpoints in the periphery therefore ensure the removal or inactivation of these cells at later stages. FcγRIIb is an inhibitory receptor which influences the threshold for B cell activation by transducing negative signals. This receptor is important in sustaining homeostasis of B cells ensuring that activated B cells are removed from the system in a timely manner once an infection is under control, hence avoiding an overreaction of the immune system. Due to this function, FcγRIIb seems to play an important regulatory function in preventing autoimmune disease by reducing activation of a large pool of potentially weakly self-reactive B cells.

4.4.1 FcγRIIb-mediated apoptosis is caspase 8 dependent

FcγRIIb signalling plays an important role in the downregulation of B cell responses by negatively regulating BCR-dependent proliferation in mature B cells (Fig.4.2). Besides growth arrest, BCR/FcγRIIb co-ligation was also shown to induce apoptosis [624] which was found to lead to the disruption of the mitochondrial membrane potential (Fig.4.2). Previous findings in this laboratory indicated that the apoptotic pathway induced by FcγRIIb-mediated signals led to the release of cytochrome C from mitochondria as well as upregulation of pro-apoptotic Bcl-2 family members [309]. However, activation of the classical executioner protease of the intrinsic pathway, caspase 3, was only slightly increased upon cross-linking of BCR/FcγRIIb, and inhibition of this protease had only marginal effects on the levels of apoptosis observed suggesting that caspase 3 activation was not sufficient for such cell death. Likewise, whilst inhibition of calpain or cathepsin B executioner protease activities also failed to block FcγRIIb-mediated apoptosis, by contrast, combined inhibition of executioner caspase, calpain and cathepsin B activities prevented FcγRIIb-mediated apoptosis [309]. It was therefore unlikely that the caspase-dependent intrinsical mitochondrial pathway was the only contributor to FcγRIIb-mediated apoptosis of B cells. As another major pathway of apoptosis is the caspase 8-mediated death receptor signalling pathway, it was decided to examine the role of caspase 8 in FcγRIIb-dependent apoptosis. The results presented in this chapter showed that in mature B cells caspase 8 is indeed crucial for the induction of cell death downstream of BCR/FcγRIIb co-ligation, as inhibition of this initiator caspase reduced the percentage of

cells undergoing apoptosis (Fig.4.3). Although dissipation of the MMP was a hallmark of apoptosis observed in mature B cells due to cross-linking of the BCR and FcγRIIb, inhibition of caspase 8 did not rescue the cells from disruption of the MMP (Fig. 4.3). Activation of caspase 8 might therefore be downstream of the disruption of mitochondrial function or indeed represent a parallel contributing apoptotic pathway.

The precise signalling events downstream of caspase 8 in FcγRIIb-mediated apoptosis have not been elucidated yet, but the major effects of caspase 8 inhibition suggested that caspase 8 might orchestrate the activation of multiple executioner proteases such as caspase 3, calpain and cathepsin B. Caspase 3 is a well known substrate for caspase 8, and caspase 3 activation occurs downstream of caspase 8 in various models of apoptosis [607]. Previous findings showed that caspase 3 was slightly upregulated by BCR/FcγRIIb co-ligation [309], but the level of caspase activation, as determined by the binding of a pan-caspase reagent, was found not to be significantly changed by caspase 8 inhibition (Fig.4.6). Although these data suggest that caspase 8 is not essential for the FcγRIIb-mediated activation of these caspases, changes in the executioner caspases 3/6 might be masked by other caspases such as caspase 1/2.

There is some evidence in the literature that cathepsin B and calpain could also be activated downstream of caspase 8. For example, caspase 8 dependent cleavage of Bid has been found to be involved in a TNFα-dependent apoptosis pathway which induces lysosomal permeabilisation and consequent release of cathepsin B in a rat hepatoma cell line [625]. Moreover, in a cellular model for Alzheimer's disease involving Amyloid beta peptide-dependent cell death of the neuronal cell line PC12, calpastatin was cleaved by caspase 8, leading to calpain activation [626]. Similarly, calpains were found to be involved in Fas-dependent apoptosis of $CD8^+$ T cells [627] and as caspase 8 activation is known to be downstream of Fas signalling, it therefore suggests itself that calpain activation might be caspase 8-dependent in this system. The cascades involved in apoptosis are further complicated by the fact that calpains and cathepsin can also be part of positive feedback loops in that both enzymes have been shown to activate caspases such as capase 8 [628] whilst caspase 3 and 7 can in turn cleave and inactivate the calpain inhibitor calpastatin [629,630]. Caspase 8 could therefore represent the major switch potentially integrating all these signals.

4.4.2 FcγRIIb-signalling leads to p53 upregulation and translocation

Interestingly, p53 expression was found to be enhanced at both the transcriptional and protein levels upon BCR/FcγRIIb co-ligation (Fig.4.5). p53 is a major regulator of growth arrest and apoptosis acting predominantly as a transcription factor, for example, to

increase gene expression of p21, Bax or Fas [485,631]. However, p53 can also induce apoptosis by translocating to the cytoplasm or the mitochondria where it interacts with Bcl-2 family members [486]. It is therefore interesting that p53 was mainly found in the cytoplasm of cells following co-ligation of the BCR and FcγRIIb and that caspase 8 inhibition reduced the levels of p53 found in the cytoplasm by seemingly sequestering it in the nucleus (Fig.4.5C/D). Caspase 8 might therefore be involved in the regulation of p53 localisation by, for example, degrading proteins involved in the nuclear retention mechanism of p53. Hence, this would allow p53 to localise to the cytoplasm where it could potentially bind to and activate pro-apoptotic Bcl-2 members to induce mitochondrial destabilisation and drive FcγRIIb-mediated, p53-dependent apoptosis of B cells. There have been many studies examining the regulation of caspase 8 by p53. For example, p53 can upregulate Fas expression and thereby potentially activate caspase 8 [631]. Moreover, in tumor cells p53 was found to directly increase caspase 8 mRNA and protein levels, thereby rendering these cells sensitive to induction of apoptosis [632]. Additionally, a cleavage product of caspase 8 (DEDa) can induce p53-dependent transcription of caspase 8 thereby creating a positive feedback loop [633]. On the other hand, caspase 8-mediated cleavage of Bid might be one of the mechanisms involved in p53-dependent apoptosis [634]. Moreover, caspase 8 not only seems to play a role in p53-mediated apoptosis that is dependent on the transcription factor-function of p53, but it has also been found to be involved in a transcription-independent form of p53-mediated apoptosis [635]. Collectively, these studies show that caspase 8 activity can be regulated by p53 and hence plays an important role in p53-mediated apoptotic pathways in some systems.

As mentioned above, a major function of p53 is that of a transcription factor. Besides the above mentioned targets, p53 can also upregulate Noxa and Puma, two pro-apoptotic Bcl-2 family members [484]. BCR/FcγRIIb co-ligation increased Noxa protein levels (Fig.4.6), implying that p53 could promote FcγRIIb-mediated apoptosis by the more classical transcription-dependent, as well as transcription-independent, mechanisms. In addition to regulating the apoptotic response downstream of BCR/FcγRIIb co-ligation, p53 could also potentially influence FcγRIIb-mediated growth arrest. For example, PAC-1 which can de-activate ERK was found to be transcriptionally upregulated by BCR/FcγRIIb co-ligation (Fig.4.9A), and whilst the mechanisms responsible for this increase are as yet unknown, p53 has been shown to regulate PAC-1 expression [369]. ERK itself might be involved in the regulation of p53, as it has been shown by this group that p53 activity is increased due to the pharmacological inhibition of ERK [309]. p53 therefore represents an interesting candidate for the regulation of multiple pathways involved in FcγRIIb-mediated

growth arrest and apoptosis but further studies are needed to define the connection between caspase 8 and p53.

4.4.3 Caspase 8 is not involved in FcγRIIb-dependent growth arrest response

Previous studies in this laboratory have identified ERK as an important regulator of proliferation and apoptosis in B cells [310]. In mature B cells ERK was shown to be induced by mitogenic signals through the BCR and this activation was found to be reduced by simultaneous FcγRIIb-signalling [623]. Moreover, inhibition of ERK mimicked the growth arrest-inducing effects of FcγRIIb [309]. Many signalling events leading to decreased ERK activation downstream of BCR/FcγRIIb co-ligation have been identified. These include the direct competition of SHIP for Shc binding and hence reduced Ras activation, as well as events further downstream such as PAC-1 recruitment [209,213,614,636]. In this study we identified further potential regulatory events, namely the transcriptional upregulation of PAC-1 and SPA-1 (Fig.4.9). PAC-1 can directly inactivate ERK by dephosphorylation [368] and SPA-1 could contribute to decreased ERK levels through the inhibition of the Rap/B-Raf pathway. The FcγRIIb-dependent increase of both of these molecules could therefore influence growth arrest by downregulation of ERK activation.

This study has shown that caspase 8 is a major regulator of FcγRIIb-mediated apoptosis. Even though multiple caspases, including caspase 8, have been implicated in the regulation of apoptosis-independent events such as cell cycle entry/progression and hence proliferation [637] the results obtained in this study did not support a role for caspase 8 in FcγRIIb-mediated growth arrest. Thus, inhibition of caspase 8 did not influence the levels of DNA synthesis of either untreated, BCR- or BCR/FcγRIIb-stimulated cells (Fig.4.7). Moreover, although caspase 8 inhibition efficiently prevented apoptosis, it could not re-instate cycling in BCR/FcγRIIb co-ligated cells leading to an accumulation of cells arrested in G1 phase (Fig.4.7). Another sign of growth arrest is the reduction of positive regulators of the cell cycle and, in confirmation with the previously mentioned results, caspase 8 inhibition was not able to prevent the FcγRIIb-mediated downregulation of c-Myc or hyperphosphorylated Rb levels. FcγRIIb-signalling therefore seems to initiate separate signalling pathways regulating apoptosis (caspase 8-dependent) and growth arrest (caspase 8-independent).

4.4.4 FcγRIIb-mediated apoptosis depends on Fas/FasL signalling

Caspase 8 is known to be activated downstream of death receptors such as Fas [282]. Thus, as it was shown in this study that caspase 8 is crucial for FcγRIIb-mediated

apoptosis, Fas/FasL signalling provided an interesting candidate for the upstream regulation of caspase 8. Indeed, preliminary results indicated that Fas and to a lower extent FasL are upregulated due to BCR/FcγRIIb ligation at both the RNA and protein level (Fig.4.10-12). Subsequently, FcγRIIb-mediated apoptosis was found to be reduced due to inhibition of Fas signalling with anti-FasL blocking antibodies confirming the involvement of this death receptor cascade (Fig.4.13D). Thus, FcγRIIb-signalling might upregulate Fas which, due to the presence of FasL in these B cells, can induce death receptor signalling and hence caspase 8 activation.

Further support for this hypothesis comes from the MRL/MpJ-*Fas*^{lpr} mouse model. These mice are on an autoimmune background (MRL/MpJ strain) and developed a spontaneous mutation in the gene encoding Fas and hence do not express normal levels of Fas. Subsequently, Fas/FasL induced apoptosis is defective in these mice leading to the accumulation of immune cells and development of lupus-like disease [638]. MRL/MpJ-*Fas*^{lpr} mice express high levels of self-reactive pathogenic antibodies such as anti-DNA antibodies that contribute to the disease by forming immune complexes which can be deposited in the kidney and hence have the potential to induce glomerunephritis [638]. The massive production of self-reactive antibodies indicates a breach of tolerance in these mice, allowing autoreactive B cells to be activated. Defects in FcγRIIb-mediated homeostasis of activated B cells could therefore potentially play a role in the accumulation of self-reactive cells in this model. Indeed, purified splenic B cells from MRL/MpJ-*Fas*^{lpr} mice displayed reduced levels of inhibition of DNA synthesis upon BCR/FcγRIIb co-ligation indicating a defect in the growth arrest response of these mice (Fig.4.13A). Moreover, their apoptotic response also seemed to be reduced as indicated by reduced percentages of subdiploid cells as well as increased numbers of cells with high MMP (Fig.4.13B/C). The reduced potential of these cells to undergo FcγRIIb-mediated apoptosis might be due to the inability of these cells to signal through Fas/FasL due to the disruptive mutation in the Fas gene. It can therefore be hypothesised that the lack of Fas expression in B cells from MRL/MpJ-*Fas*^{lpr} mice affects their ability to apoptose due to inhibitory signals downstream of BCR/FcγRIIb co-ligation, hence making them insensitive to negative regulation. This in turn could lead to an increase of activated B cells, including self-reactive clones. Fas/FasL signalling might therefore be an important part of the signals controlling FcγRIIb-dependent homeostatic regulation of mature B cells in these mice.

4.4.5 A small proportion of B cells from RA and SLE patients display a defect in FcγRIIb-mediated growth arrest

Homeostatic regulation of B cells is crucial in the human immune system as dysregulated activation of weakly self-reactive cells has been implicated in the pathology of autoimmune diseases such as SLE and RA. The important role of FcγRIIb in the regulation of B cell responses and hence autoimmunity has been firmly established in the murine system [73]. Dissection of the role of FcγRIIb in the human system is obviously more complicated. There have been few studies examining the connection between dysregulation of FcγRIIb-dependent responses and autoimmune disease in humans. However, it was shown that FcγRIIb-expression is indeed reduced on plasma and memory B cells from SLE patients [588]. Nevertheless, these studies did not address the functional outcome of these lower FcγRIIb levels. Here it was investigated whether mature B cells from patients with autoimmune disease (RA and SLE) displayed defective growth arrest responses upon BCR/FcγRIIb co-ligation. Generally, the FcγRIIb-mediated growth arrest response of human B cells did not seem to be as strong as that of murine B cells (Fig.4.14). This might be due to the expression of FcγRIIa in the human system, an activating Fcγ receptor which is not present in mice [576]. Human B cells might therefore express both FcγRIIa and FcγRIIb which would compete for binding to IgG and thus, positive signals through FcγRIIa would reduce the inhibitory FcγRIIb-response. Even though the growth arrest response in human B cells was not as pronounced as in the murine system, B cells from healthy individuals all displayed an intact inhibitory response upon BCR/FcγRIIb co-ligation (Fig.4.16).

Interestingly, a small proportion of patients displayed little or no inhibition of proliferation upon FcγRIIb ligation (Fig.4.16). The differences between the healthy control and RA or SLE cohorts were not statistically significant though, due to the majority of patients still displaying a normal response. Thus although FcγRIIb-mediated regulation of proliferation of mature peripheral B cells might not be a major disease-driving mechanism in most patients, it might contribute to the disease in some. It remains to be seen if more detailed analysis of responses of plasma cells and memory cells, the developmental stages which were found to display reduced expression of FcγRIIb in SLE patients, would render clearer results as the percentage of these cells in B cells purified from blood is very low, and any changes in their response to inhibitory signalling might therefore be overlooked due to their small numbers.

4.4.6 Patients with autoimmune disease display changed FcγRIIb-isoform expression pattern

The B cell numbers achieved by purification from patient blood were usually not sufficient to carry out functional studies as well as analyse FcγRIIb protein levels by FACS or isolate RNA to examine FcγRIIb mRNA expression. This would have been interesting to allow the correlation between reduced FcγRIIb-mediated inhibitory responses and expression of the receptor. Moreover, changes in the expression of the different FcγRIIb isoforms, FcγRIIb1 and FcγRIIb2, could potentially influence the response of B cells due to the lack of endocytic capacity of FcγRIIb1 [622]. Thus, higher expression of FcγRIIb2 could increase antigen uptake and hence presentation to T cells. Therefore, to gain some insight into the regulation of FcγRIIb in peripheral immune cells, transcriptional regulation of this receptor was analysed in PBMCs from patients and healthy controls, as analysis in purified B cells from a bigger panel of patients was not feasible. Interestingly, expression of both FcγRIIb1 and FcγRIIb2 was found to be downregulated in PBMCs from RA patients (Fig.4.19). This was not the case for PBMCs from SLE patients, as no significant differences were found between the patients and the healthy controls concerning either FcγRIIb1 and FcγRIIb2 mRNA expression (Fig.4.19). A small proportion of RA patients displayed a reduced growth arrest response upon BCR/FcγRIIb co-ligation and, although there was no statistically significant difference, there was a noticeable trend for more RA patients showing this defect compared to either healthy controls or SLE patients. This seems to correlate with the FcγRIIb RNA expression data, which showed that PBMCs from RA patients, but not cells from SLE patients, express reduced levels of FcγRIIb1. For future experiments it would therefore be interesting to obtain information about FcγRIIb RNA levels and the extent of growth arrest of purified B cells from the same patient to identify a potential correlation.

The most striking change between the RA/SLE patient cohorts and the healthy patients was the reduction of the FcγRIIb1/FcγRIIb2 ratio (Fig.4.19). The cause of this phenomenon was a relative increase of FcγRIIb2 levels in patients compared to healthy controls. As discussed before, this change of relative levels of FcγRIIb1 and FcγRIIb2 could tip the balance between antigen uptake and presentation and inhibitory signalling towards an increased ability of cells to present antigen. In an autoimmune-prone setting this could increase the presentation of self-antigen by autoreactive B cells, followed by activation of autoreactive T cells and thereby create an amplification loop.

4.4.7 Concluding remarks

In conclusion, it has been demonstrated that BCR/FcγRIIb co-ligation results in growth arrest and apoptosis. The signalling pathways underlying apoptosis have been further elucidated and it has been shown that caspase 8 is the major initiator caspase involved. Moreover, FcγRIIb was found to stimulate expression of Fas and its ligand FasL and signalling through this death receptor presumably activates caspase 8. Inhibition of Fas/FasL signalling and caspase 8 activation were both sufficient to block apoptosis, underscoring the crucial role these signals play. Furthermore, this study has clearly demonstrated that p53 is regulated by FcγRIIb-dependent mechanisms inducing its upregulation and translocation. Thus, various scenarios can be envisaged, as p53 can achieve the initiation of the apoptotic programme by different pathways. p53 could increase Fas and caspase 8 expression, thereby initiating as well as propagating this signalling axis. Additionally, it might trigger apoptosis by enhancing the expression of pro-apoptotic molecules such as Noxa or by translocating to the mitochondria and hence interaction with pro- and anti-apoptotic molecules at this interface. The growth arrest response has not been examined in detail in this study, but some progress has been made towards fully elucidating the signals involved. Thus, another level of negative regulation of the ERK MAPK pathway has been identified to be transcriptional upregulation of PAC-1 and SPA-1. Furthermore, FcγRIIb-mediated growth arrest was found to be linked to the reduction of positive regulatory elements of the cell cycle, including c-Myc and hyperphosphorylated Rb (Fig.4.21).

The ultimate goal of immunological research is to apply findings to the human immune system and support development of disease treatments. This study therefore set out to begin to translate some of the findings acquired in the murine system to humans. Encouragingly, it was demonstrated that human B cells, like their murine counterparts, undergo growth arrest and apoptose upon BCR/FcγRIIb co-ligation. Furthermore, it was shown that the B cells of a proportion of patients exhibit a defective inhibitory response, indicating that FcγRIIb-mediated negative signalling is affected in these patients. Furthermore, major differences between RA patients and healthy controls were found concerning the expression of FcγRIIb isoforms. It is therefore concluded that this inhibitory receptor could be one of the many contributing factors towards development or propagation of autoimmune diseases.

4.5 Figures

Figure 4.1 Diagram of stimulations

Antibodies were used to mimic stimulation of B cells by free antigen and/or immune complexes. Stimulation with $F(ab')_2$ fragments of anti-IgM cross-links the BCR and induces mitogenic signals (designated **BCR**). By contrast, as stimulation with intact anti-IgM/IgG results in the generation of negative signals induced by co-ligation of the BCR and FcγRIIb, these antibodies were used in combination with $F(ab')_2$ fragments of anti-IgM to mimic the inhibition of antigen-driven mitogenic signals by immune complexes resulting in growth arrest and apoptosis (designated **BCR+FcγRIIb**).

Figure 4.2 BCR/FcγRIIb co-ligation induces growth arrest and apoptosis

Purified mature mouse B cells (10^6 cells/ml) were stimulated for 48 h in the presence of 50 µg/ml $F(ab')_2$ anti-mouse IgM (BCR) or 50 µg/ml $F(ab')_2$ anti-mouse IgM in combination with 75 µg/ml anti-mouse IgG+IgM (BCR+FcγRIIb), as indicated. Cells stimulated in the presence of medium alone were included as a control (None).

(A) DNA synthesis was assessed by pulsing the cells with 0.5 µCi/well [^{3}H] thymidine for the last 6 h of culture and measurement of incorporated label using a liquid scintillation counter. Data are shown as counts per minute (cpm) +/- standard deviation (SD) of triplicate values. *** $p<0.001$

(B) DNA content was determined by propidium iodide (PI) staining followed by FACS analysis. A representative histogram is shown and data are presented as **(C-i)** mean percentage of all cells in each cell cycle stage or as **(C-ii)** mean percentage of live cells (excluding cells with subdiploid DNA content) in each cell cycle stage (+/- range of duplicate values).

(D) For the assessment of the mitochondrial membrane potential the cells were stained with $DiOC_6$ and analysed by FACS. A representative histogram is shown and data are presented as the mean percentage of cells with high or low membrane potential (+/- range of duplicate values).

Data are representative of at least three independent experiments.

Figure 4.3 Caspase 8 inhibition reduces FcγRIIb-mediated apoptosis

Purified mature splenic B cells (10^6 cells/ml) were stimulated for 48 h in the presence of 50 µg/ml $F(ab')_2$ anti-mouse IgM (BCR) or 50 µg/ml $F(ab')_2$ anti-mouse IgM in combination with 75 µg/ml anti-mouse IgG+IgM (BCR+FcγRIIb), as indicated. Furthermore, cells were treated with a caspase 8 inhibitor or DMSO as a control. Cells stimulated in the presence of medium alone were included as a control (None). **(A)** DNA content was determined by propidium iodide (PI) staining followed by FACS analysis. Representative FACS histogram plots are shown for media **(A-i)**, $F(ab')_2$ anti-mouse IgM stimulated cells **(A-ii)** or cells treated with $F(ab')_2$ anti-mouse IgM in combination with anti-mouse IgG+IgM **(A-iii)**. Data represents the mean percentage of subdiploid cells (+/- range of duplicate values) **(A-iv)**.
For the assessment of the mitochondrial membrane potential the cells were stained with $DiOC_6$ and analysed by FACS, representative histograms are shown in **(B)** and **(C)**. Data are expressed as the mean percentage of cells with **(D)** high or **(E)** low membrane potential (+/- range of duplicate values). Data are representative of at least three independent experiments.

Figure 4.4 Expression of caspase 8 and cFLIP

To determine caspase 8 **(A)** and cFLIP **(B)** expression in whole cell lysates, purified mature splenic B cells (10^7 cells/well) were stimulated with 50 µg/ml $F(ab')_2$ anti-mouse IgM (BCR) or 50 µg/ml $F(ab')_2$ anti-mouse IgM in combination with 75 µg/ml anti-mouse IgG+IgM (BCR+FcγRIIb) for 24 or 48 h and whole cell lysates were prepared. Cells stimulated with medium were included as a control (None). Expression of caspase 8 was assessed by SDS-PAGE gel electrophoresis followed by Western Blotting.

Gel loading was as follows: *Lane 1* None, *Lane 2* BCR, *Lane 3* BCR+FcγRIIb.

Figure 4.5 p53 expression is upregulated by BCR/FcγRIIb co-ligation

(A) Purified mature splenic B cells (10^6 cells/ml) were stimulated for 3, 7, 20 or 24 h in the presence of 50 µg/ml $F(ab')_2$ anti-mouse IgM (BCR) or 50 µg/ml $F(ab')_2$ anti-mouse IgM in combination with 75 µg/ml anti-mouse IgG+IgM (BCR+FcγRIIb). Whole mRNA was isolated and transcribed into cDNA. p53 expression levels were detected by TaqMan® quantitative RT-PCR using GAPDH as endogenous control. Data are shown as mean % expression relative to GAPDH, as indicated, +/- SD of triplicate values.

(B-D) For the detection of p53 protein levels purified mature splenic B cells (10^7 cells) were stimulated for 48 h in the presence of 50 µg/ml $F(ab')_2$ anti-mouse IgM (BCR) or 50 µg/ml $F(ab')_2$ anti-mouse IgM in combination with B7.6 anti-IgM to ligate the BCR (50 µg/ml), 2.4G2 IgG to ligate FcγRIIb (50 µg/ml) and 75 µg/ml Donkey anti- Rat IgG to crosslink the B7.6 and 24G.2 Abs and hence coligate the BCR and FcγRIIb (BCR+FcγRIIb). Furthermore, cells were treated with caspase 8 inhibitor or DMSO as a control. Cells stimulated in the presence of medium alone were included as a control (None). After 48 h **(B)** whole cell lysates or **(C)** nuclear and **(D)** cytoplasmic fractions were prepared and expression of p53 was assessed by SDS-PAGE gel electrophoresis followed by Western Blotting. Gel loading was as follows: *Lane 1* +DMSO, *Lane 2* + caspase 8 inhibitor.

Figure 4.6 Noxa expression and effector caspase activation are increased by FcγRIIb-mediated signalling

(A) To determine Noxa expression in whole cell lysates, purified mature splenic B cells (10^7 cells/well) were stimulated with 50 µg/ml $F(ab')_2$ anti-mouse IgM (BCR) or 50 µg/ml $F(ab')_2$ anti-mouse IgM in combination with 75 µg/ml anti-mouse IgM (BCR+FcγRIIb) for 24 or 48 h and whole cell lysates were prepared. Cells stimulated with medium were included as a control (None). Expression of Noxa was assessed by SDS-PAGE gel electrophoresis followed by Western Blotting. Gel loading was as follows: *Lane 1* None, *Lane 2* BCR, *Lane 3* BCR+FcγRIIb.

(B-E) For the assessment of caspase activation cells (10^6 cells/ml) were stimulated as described above. Furthermore, cells were treated with caspase 8 inhibitor or DMSO as a control. After 24 h the cells were labeled with FITC-VAD-FMK and analysed by FACS. Representative histograms are shown of the **(B)** unlabeled control cells as well as **(C)** treated and labelled cells. Data are shown as either **(D)** the percentage of cells positive for FITC-expression or **(E)** as MFI. Data are representative of at least two independent experiments.

Figure 4.7 Caspase 8 inhibition does not affect FcγRIIb-dependent growth arrest

Murine purified splenic B cells (10^6 cells/ml) were stimulated for 48 h in the presence of 50 µg/ml $F(ab')_2$ anti-mouse IgM (BCR) or 50 µg/ml $F(ab')_2$ anti-mouse IgM in combination with 75 µg/ml anti-mouse IgG+IgM (BCR+FcγRIIb), as indicated. Furthermore, cells were treated with caspase 8 inhibitor or DMSO as a control. Cells stimulated in the presence of medium alone were included as a control (None). DNA content was determined by propidium iodide (PI) staining followed by FACS analysis. **(A)** Data are displayed as the percentage of cells in the different phases of cell cycle after stimulation with 50 µg/ml $F(ab')_2$ anti-mouse IgM in combination with 75 µg/ml anti-mouse IgG+IgM (BCR+FcγRIIb) in the presence or absence of caspase 8 inhibitor, as indicated. **(B)** % of cells in G1-G0 phase, **(C)** % cells in S phase, **(D)** % of cells in G2-M phase of cell cycle. Data represents each cell cycle stage expressed as the mean percentage of the total number of live cells (excluding cells with subdiploid DNA content) analysed (+/- range of duplicate values).

(E-F) To assess DNA synthesis by analysis of labelled thymidine incorporation additional cells were stimulated for **(E)** 48 or **(F)** 72 h as described above. Proliferation was assessed by pulsing the cells with 0.5 µCi/well [^{3}H] thymidine for 6 h and measurement of incorporated label using a liquid scintillation counter. Data are shown as counts per minute (cpm) +/- SD of triplicate values. Data are representative of at least three independent experiments.

Figure 4.8 Proteins involved in cell cycle control are not regulated by caspase 8

(A) Mature purified splenic B cells (10^6 cells/ml) were stimulated for 3, 7, 20 or 24 h in the presence of 50 µg/ml $F(ab')_2$ anti-mouse IgM (BCR) or 50 µg/ml $F(ab')_2$ anti-mouse IgM in combination with 75 µg/ml anti-mouse IgG+IgM (BCR+FcγRIIb). Whole mRNA was isolated and transcribed into cDNA. c-Myc expression levels were detected by TaqMan® quantitative RT-PCR using GAPDH as endogenous control. Data are shown as mean % expression relative to GAPDH +/- SD of triplicate values.

(B) Cells were stimulated for 24 h with 50 µg/ml $F(ab')_2$ anti-mouse IgM (BCR) or a combination of 50 µg/ml $F(ab')_2$ anti-mouse IgM, 50 µg/ml rat anti-mouse IgM, 50 µg/ml rat anti-mouse FcγRIIb and 75 µg/ml donkey anti-rat IgG (H+L) antibodies (BCR+FcγRIIb) and whole cell lysates prepared. Expression of c-Myc, phospho-RbS807/811 or β-actin was assessed by SDS-PAGE gel electrophoresis followed by Western Blotting (15 µg protein/lane). Gel loading was as follows: *Lane 1* +DMSO, *Lane 2* + caspase 8 inhibitor.

Figure 4.9 BCR/FcγRIIb cross-linking regulates SPA-1 and PAC-1 mRNA expression
Purified mature splenic B cells (10^6 cells/ml) were stimulated for 3, 7, 20 or 24 h in the presence of 50 µg/ml $F(ab')_2$ anti-mouse IgM (BCR) or 50 µg/ml $F(ab')_2$ anti-mouse IgM in combination with 75 µg/ml anti-mouse IgG+IgM (BCR+FcγRIIb). Whole mRNA was isolated and transcribed into cDNA. **(A)** PAC-1 and **(B)** SPA-1 expression levels were detected by TaqMan® quantitative RT-PCR using GAPDH as an endogenous control. Data are shown as mean % expression relative to GAPDH, as indicated, +/- SD of triplicate values.

Figure 4.10 Co-ligation of BCR/FcγRIIb induces Fas expression

Purified mature splenic B cells (10^6 cells/ml) were stimulated for 48 h in the presence of 50 µg/ml $F(ab')_2$ anti-mouse IgM (BCR) or 50 µg/ml $F(ab')_2$ anti-mouse IgM in combination with 75 µg/ml anti-mouse IgG+IgM (BCR+FcγRIIb), as indicated. Furthermore, cells were treated with caspase 8 inhibitor or DMSO as a control. Cells stimulated in the presence of medium alone were included as a control (None). Extracellular expression of Fas (CD95) was detected by staining with a Fas-specific antibody. **(A)** Representative histograms are shown and **(B)** data are expressed as **(i)** mean percentage of $B220^+$ cells expressing Fas or **(ii)** MFI (+/- range of duplicate values). Data are representative of at least two independent experiments.

(C) Cells were stimulated with 50 µg/ml $F(ab')_2$ anti-mouse IgM (BCR) or a combination of 50 µg/ml $F(ab')_2$ anti-mouse IgM, 50 µg/ml rat anti-mouse IgM, 50 µg/ml rat anti-mouse FcγRIIb and 75 µg/ml donkey anti-rat IgG (H+L) antibodies (BCR+FcγRIIb) for 24 h and whole cell lysates were prepared. Expression of Fas, FasL or β-actin was assessed by SDS-PAGE gel electrophoresis followed by Western Blotting (15 µg/lane). Gel loading was as follows: *Lane 1* +DMSO, *Lane 2* + caspase 8 inhibitor.

Figure 4.11 Caspase 8 is not involved in the regulation of Fas mRNA levels

(A) Purified mature splenic B cells (10^6 cells/ml) were stimulated for 3, 7, 20 or 24 h in the presence of 50 µg/ml $F(ab')_2$ anti-mouse IgM (BCR) or 50 µg/ml $F(ab')_2$ anti-mouse IgM in combination with 75 µg/ml anti-mouse IgG+IgM (BCR+FcγRIIb).

(B) Cells were treated for 24 h as described above in the presence or absence of 10 µM caspase 8 Inhibitor or DMSO as control. Whole mRNA was isolated and transcribed into cDNA and Fas (CD95) expression levels were detected by TaqMan® quantitative RT-PCR using GAPDH as an endogenous control. Data are shown as mean % expression relative to GAPDH +/- SD of triplicate values.

Figure 4.12 FasL mRNA expression is not influenced by caspase 8 activation

(A) Purified mature splenic B cells (10^6 cells/ml) were stimulated for 3, 7, 20 or 24 h in the presence of 50 µg/ml $F(ab')_2$ anti-mouse IgM (BCR) or 50 µg/ml $F(ab')_2$ anti-mouse IgM in combination with 75 µg/ml anti-mouse IgG+IgM (BCR+FcγRIIb).

(B) Cells were treated for 24 h as described above in the presence or absence of 10 µM caspase 8 Inhibitor or DMSO as control. Whole mRNA was isolated and transcribed into cDNA and FasL (CD178) expression levels were detected by TaqMan® quantitative RT-PCR using GAPDH as endogenous control. Data are shown as mean % expression relative to GAPDH +/- SD of triplicate values.

Figure 4.13 FcγRIIb-dependent growth arrest and apoptosis are reduced in MRL/MpJ-*Fas*^{lpr} mice and inhibition of Fas/FasL signalling prevents FcγRIIb-mediated apoptosis

Purified mature splenic B cells were stimulated for 48 h in the presence of 50 µg/ml F(ab')$_2$ anti-mouse IgM (BCR) or 50 µg/ml F(ab')$_2$ anti-mouse IgM in combination with 75 µg/ml anti-mouse IgG+IgM (BCR+FcγRIIb), as indicated. Cells stimulated in the presence of medium alone were included as a control (None).

(A) DNA synthesis was assessed by pulsing the cells (5 x 10^5 cells/well) with 0.5 µCi/well [^{3}H] thymidine for 6 h of culture and measurement of incorporated label using a liquid scintillation counter (**A-i**; 17 wks old MRL/MpJ, **A-ii**; 12 wks old MRL/MpJ-*Fas*^{lpr}). **(A-iii)** The data represents values from experiments using B cells from Balb/C mice, MRL/MpJ mice and pooled values for B cells from 9, 12, 16 and 20 week old MRL/MpJ-*Fas*^{lpr} mice. *** p<0.001, ** p<0.01, * p<0.05

(B) DNA content was determined by propidium iodide (PI) staining followed by FACS analysis. Data are shown as the percentage of subiploid cells (**B-i**; 17 wks old MRL/MpJ, **B-ii**; 12 wks old MRL/MpJ-*Fas*^{lpr}). **(B-iii)** Data represents subdiploid cells (normalised against values from BCR-stimulated cells) and is expressed as a ratio of the MRL/MpJ control cells. The values from experiments using B cells from 9, 12, 16 and 20 week old MRL/MpJ-*Fas*^{lpr} mice were pooled.

(C) The dissipation of the MMP was assessed by staining cells with $DiOC_6$ and data are expressed as the percentage of cells with high MMP (**C-i**; 17 wks old MRL/MpJ, **C-ii**; 12 wks old MRL/MpJ-*Fas*^{lpr}). **(C-iii)** Data represents cells with high $DiOC_6$ fluorescence (normalised against values from BCR-stimulated cells) and is expressed as a ratio of the MRL/MpJ control cells. The values from experiments using B cells from 9, 12, 16 and 20 week old MRL/MpJ-*Fas*^{lpr} mice were pooled.

(D) Purified mature splenic B cells (10^6 cells/well) were stimulated as described above. Furthermore, cells were treated with 5 or 10 µg/ml armenian hamster IgG as a control or 5 or 10 µg/ml anti-FasL blocking antibody. Cells stimulated in the presence of medium alone were included as a control (None). For the assessment of cell cycle status cells were stained with PI and analysed by FACS. Data are shown as the % subdiploid cells after treatment with BCR+FcγRIIb. Data are representative of at least two independent experiments.

Figure 4.14 Proliferation analysis of purified peripheral B cells by [^{3}H] thymidine incorporation and CFSE labelling

Purified peripheral B cells ($CD19^+$-selected) from a healthy control were subjected to proliferation analysis. The cells (10^5 cells/well) were stimulated for **(A-i)** 4, 24, 48 or **(A-ii)** 48, 72 or 96 h in the presence of 50 µg/ml $F(ab')_2$ anti-human IgG+IgM (BCR), 75 µg/ml anti-human IgG+IgM (BCR+FcγRIIb) or the combination of both (mitogenic BCR+FcγRIIb), as indicated. Cells stimulated in the presence of medium alone were included as a control (None). DNA synthesis was assessed by pulsing the cells with 0.5 µCi/well [^{3}H] thymidine for the last 8 h of culture (for 4 h for the 4 h timepoint) followed by measurement of incorporated label using a liquid scintillation counter. **(A)** Data are shown as counts per minute (cpm) +/- SD of triplicate values. *** $p<0.001$, BCR against BCR+FcγRIIb, BCR against mitogenic BCR+FcγRIIb

(B-D) To analyse proliferation by a different method, cells were stained with CFSE after $CD19^+$-purification and harvested after the indicated times followed by FACS analysis. The data are shown as the percentage of all cells analysed and the number of divisions they have undergone (**B** – 4 h, **C** – 24 h, **D** – 48 h).

Figure 4.15 Correlation between proliferation, cell cycle stages and apoptosis

Purified peripheral B cells ($CD19^+$-selected) from a **(A)** healthy control and **(B)** three RA patients were subjected to proliferation analysis. The cells (10^5 cells/well) were stimulated for 48 h in the presence of 50 µg/ml F(ab')2 anti-human IgG+IgM (BCR) or 50 µg/ml $F(ab')_2$ anti-human IgG+IgM in combination with 75 µg/ml anti-human IgG+IgM (mitogenic BCR+FcγRIIb), as indicated. Cells stimulated in the presence of medium alone were included as a control (None). **(i)** DNA synthesis was assessed by pulsing the cells with 0.5 µCi/well for the last 8 h of culture and measurement of incorporated label using a liquid scintillation counter. Data are shown as counts per minute (cpm) +/- SD of triplicate values (data from the three patients was pooled). **(ii)** DNA content was determined by propidium iodide (PI) staining followed by FACS analysis. Data represents each cell cycle stage expressed as a percentage of the total number of cells analysed or **(iii)** the percentage of cells in the mitotic phases of the cell cycle. **(iv)** For the assessment of the mitochondrial membrane potential the cells were stained with $DiOC_6$ and analysed by FACS. Data are shown as percentage of cells with high or low membrane potential. **(B)** The data from the three patients was pooled.

Figure 4.16 Inhibition of proliferation after BCR/FcγRIIb cross-linking is reduced in some patients suffering from autoimmune disease

Purified peripheral B cells ($CD19^+$ selected) from 12 healthy controls and 16 RA patients, 10 SLE patients as well as 9 patients with other autoimmune diseases (Sjogren's syndrome, Connective tissue disease, Dermatomyositis, Psoriatic arthritis) were tested for their inhibitory capacity upon BCR/FcγRIIb cross-linking. The data are shown as %-inhibition of DNA synthesis upon stimulation with $F(ab')_2$+Intact anti-IgG+IgM (the BCR response represents 100%).

Figure 4.17 Proliferation analysis of purified peripheral B cells from recalled patients with RA

Purified peripheral B cells ($CD19^+$-selected) from two different patients with RA who had been tested before, were subjected to proliferation analysis. The cells (10^5 cells/well) were stimulated for 48 h in the presence of 50 µg/ml $F(ab')_2$ anti-human IgG+IgM (BCR) or 50 µg/ml $F(ab')_2$ anti-human IgG+IgM in combination with 75 µg/ml anti-human IgG+IgM (mitogenic BCR+FcγRIIb), as indicated. Cells stimulated in the presence of medium alone were included as a control (None). DNA synthesis was assessed by pulsing the cells with 0.5 µCi/well [^{3}H] thymidine for the last 8 h of culture and measurement of incorporated label using a liquid scintillation counter. Data are shown as counts per minute (cpm) +/- SD of triplicate values. **(A)** Patient 72 **(i)** first experiment, **(ii)** recall experiment. **(B)** Patient 66 **(i)** first experiment, **(ii)** recall experiment.

Figure 4.18 Differences in the function of the two FcγRIIb isoforms FcγRIIb1 and FcγRIIb2

(A) Separate exons encode the transmembrane and cytoplasmic domains of FcγRIIb; thus several isoforms can be created by alternative splicing of mRNA transcripts. Human FcγRIIb encodes three transcripts, FcγRIIb1, FcγRIIb2 and FcγRIIb3, which arise by alternative splicing mechanisms. The mature forms of FcγRIIb1 and FcγRIIb3 are identical but differences in their peptide leader sequences prevent the expression of FcγRIIb3.

(B) Upon IgG binding, FcγRIIb2 is capable of mediating rapid endocytosis by means of clathrin-coated vesicles allowing antigen processing and presentation on MHC II. However, an insertion of 19 amino acids in the cytoplasmic tail of FcγRIIb1 disrupts the cytoskeletal attachment domain responsible for modulating receptor internalisation. Thus, FcγRIIb1 mainly carries out the inhibitory functions described in this chapter.

Figure 4.19 FcγRIIb1/FcγRIIb2 expression of PBMCs from patients with RA or SLE and healthy controls

Total RNA was extracted from PBMCs from patients with RA **(left panel)** or SLE **(right panel)** or healthy controls and reverse transcribed. Expression levels of FcγRIIb1 **(A-B)** and FcγRIIb2 **(C-D)** were assessed by TaqMan® quantitative RT-PCR and the FcγRIIb1/FcγRIIb2 ratio calculated **(E-F)**. Individual mRNA levels are expressed as a percentage relative to HPRT mRNA levels. Some of the data were acquired by Kirsty Brown and used with her permission. *** $p<0.001$, ** $p<0.01$, * $p<0.05$

Figure 4.20 Expression of FcγRIIb in cells of the immune system

Total RNA was extracted from either purified peripheral B cells, B cell-depleted PBMCs (Non-B cells) **(A)**, whole PBMCs, purified T cells or T cell-depleted PBMCs (Non-T cells) **(B)**. Whole mRNA was then transcribed into cDNA and FcγRIIb1/FcγRIIb2 RNA expression levels were detected by TaqMan® quantitative RT-PCR using β-actin as endogenous control. Data are shown as % expression relative to β-actin.

(C) PBMCs from a healthy control were stained with anti-FcγRIIb, anti-CD19, anti-CD11b antibodies or relevant isotype controls. Data are shown as representative histograms of FcγRIIb-positive cells as well as plots showing CD19/FcγRIIb or CD11b/FcγRIIb double-positive cells.

Figure 4.21 FcγRIIb signalling reduces cell cycle progression/proliferation

Co-ligation of the BCR and FcγRIIb reduces the strength of BCR-mediated signalling by reducing the activation of various signalling cascades including the ERK MAPK pathway. This is achieved by, for example, reducing the activation of Ras/Raf through the recruitment of p62 Dok. Furthermore, another level of negative regulation of the ERK MAPK pathway has been identified to be transcriptional upregulation of PAC-1 and SPA-1. PAC-1 dephosphorylates and thereby inactivates ERK, whereas SPA-1 decreases the levels of active Rap. Furthermore, FcγRIIb-mediated growth arrest was found to be linked to reduction of positive regulatory elements of the cell cycle, including c-Myc and hyperphosphorylated Rb which could be partially due to the reduced levels of ERK activation observed upon BCR/FcγRIIb co-ligation.

5 General Discussion

The immune system has evolved to protect the host from invading pathogens. Thus, the mammalian immune system consists of highly specialised tissues and cells that orchestrate the defense against different pathogens such as viruses, bacteria and parasites. B cells and the antibodies they produce are a major part of the protective mechanisms of the immune system. The large number of BCR specificities necessary to recognise and mount responses against the numerous pathogen antigens that the host is likely to encounter in a lifetime is best achieved by random recombination events. The side effect of this efficient mechanism, however, is the potential creation of self-reactive antigen receptors. Hence the evolution of negative selection events which ensure that autoreactive B cells are removed from the repertoire has generally provided the solution to this problem. In addition, homeostatic mechanisms have developed in which B cell responses in the periphery are tightly regulated and efficiently switched off upon successful removal of the pathogens by inhibitory feedback mechanisms such as those depending on interactions between immune complexes and FcγRIIb. Thus, co-ligation of this receptor with the BCR by the engagement of antigen-antibody immune-complexes allows the cell to sense the balance between free and antibody-bound antigen. As, in the event of a succesful immune response against pathogens, the majority of antigen will be present in immune complexes rather than free monomeric antigen, simultaneous signalling via FcγRIIb and the BCR desensitises the activatory signalling cascades allowing the B cell response to be switched off.

Perturbations in the checkpoints controlling negative selection or in the homeostatic balance between activation and termination of responses due to changes in the expression of FcγRIIb, can therefore potentially increase the chances of survival and activation of self-reactive B cell clones or indeed an expanded pool of pathogen-specific B cells that are weakly cross-reactive with self-antigens. Such an increase in autoreactive cells might therefore lead to the initiation of autoantibody production and hence autoimmune diseases such as RA and SLE. Thus the eventual outcome of the core aims of this thesis, to identify and dissect the key signalling pathways underlying BCR-mediated negative selection of immature B cells as well as those underpinning inhibitory FcγRIIb signalling, could therefore shed light on the mechanisms permitting the progression of autoimmune disorders and provide information to further the development of targeted therapies.

5.1 Immature B cell signalling

In confirmation of previous evidence [310], the activation of the MAPK ERK1/2 was found to be crucial for the survival of WEHI-231 cells. The WEHI-231 B cell lymphoma, which exhibits the phenotype ($sIgM^{+}$, $sIgD^{-/low}$, $Fc\gamma R^{low}$, Fas^{low}, MHC class II^{low}) of immature B cells, has been widely used as a model for the dissection of the signalling mechanisms controlling BCR-mediated negative selection of immature B cells and their rescue by T cell-derived and survival factors. Previous studies from this laboratory [310] suggested that whilst a strong transient BCR-stimulated spike of ERK activation (1-4 h) correlated with induction of apoptosis in WEHI-231 B cells, maintenance of sustained, yet cycling activation of the MAPK, ERK1/2 was crucial for the survival and proliferation of WEHI-231 cells. Indeed, the abrogation of such sustained ERK activation is one of the major signalling events leading to BCR-mediated growth arrest and apoptosis of WEHI-231 B cells [310]. The mechanisms involved were not fully delineated but these earlier studies suggested that in addition to partially suppressing activation of MEK1/2, the upstream regulator of ERK1/2, BCR signalling also resulted in termination of ongoing ERK signalling by recruitment of the ERK MAPK phosphatase, PAC-1. Rather surprisingly, however, given the desensitisation of MEK activity, it was found that Ras activation was not suppressed by such BCR-signalling.

This study has now confirmed and extended these previous findings to show that the reduction of such MEK and ERK activation coincides with the downmodulation of the Rap-1/B-Raf signalling pathway. Thus, ligation of the BCR diminished the levels of active Rap-1 in the cells (Fig.3.12). These findings are intriguing as Rap-1/B-Raf signalling has been shown in various models, including B cells, to activate the ERK cascade [411]. In B cells, Rap-1B is the dominant form of Rap-1 [423], and Rap-1B-deficiency impacts on B cell development reducing the number of immature B cells in the bone marrow [423], consistent with the proposal that such Rap-1-mediated ERK activation promotes immature B cell survival. However, both isoforms of Rap, Rap-1 and Rap-2, which share 60% homology and are mainly regulated by the same activators/inhibitors, have been shown to be activated upon BCR-ligation in WEHI-231 B cells [418,419]. Nevertheless, such Rap-1 activation is maximal within the first 1-4 hours [373,418] and hence perhaps correlates with the coupling of the BCR to the strong, transient spike of apoptotic ERK signalling [310,373]. Interestingly, although Rap-1 and Rap-2 seem to carry out similar functions, they differ in their interaction with RapGAPs. Thus, Rap-2 has lower sensitivity to deactivation by RapGAPs and therefore remains active for longer providing a more long-lasting Rap signal [395]. It would therefore be interesting to analyse the relative amounts

and subcellular localisation of active Rap-1 and Rap-2 after BCR-ligation or in spontaneously proliferating WEHI-231 cells to determine if both forms of Rap are needed for the activation of ERK, and if indeed inhibition of both forms is necessary to achieve abrogation of the ERK signal.

WEHI-231 cells also express two isoforms of Raf, B-Raf and Raf-1, both of which can interact with Rap. However, binding of Rap to Raf-1 and B-Raf is thought to induce very different signals. Thus, whilst Rap/B-Raf has been found to mainly activate the ERK cascade [411], Rap/Raf-1 interaction has been shown to inhibit ERK activation sequestering Raf-1 away from Ras [408]. Indeed, it has been reported previously, that in chicken B cells, B-Raf rather than Raf-1 is the major upstream regulator of the ERK cascade [170]. Interestingly, the forced expression of B-Raf in peripheral T cells transformed Rap-1 into an activator of the ERK cascade whereas in normal peripheral T cells, which express little or no B-Raf, Rap-1 generally signals to inhibit ERK activation by sequestering Raf-1 [412]. The relative amounts of B-Raf and Raf-1 or characterisation of which isoform is generally found complexed with Rap-1 has not been addressed in this study. It would therefore be of interest to determine how cells, such as WEHI-231 cells, which express both isoforms regulate the binding and activation of one or the other Raf isoform.

Rap signalling can be regulated by various mechanisms including modulation of the levels of specific GEFs (responsible for their activation) or RapGAPS (proteins that increase the intrinsic GTPase activity of Rap leading to its deactivation) that act to homeostatically regulate Rap activity [393]. As the precise mechanisms regulating Rap activity after BCR-ligation in WEHI-231 cells have not been identified, this study therefore contributed to the dissection of these signalling pathways by establishing a potential role for SPA-1. Thus, BCR-ligation was found to upregulate SPA-1 whereas CD40-mediated positive signals actively suppressed SPA-1 expression (Fig.3.13) suggesting that the reduction of Rap signalling observed due to BCR-ligation could therefore be partly achieved by an increase in SPA-1 levels (Fig.5.1). The biological importance of SPA-1 mediated suppression of Rap-1 in immature B cells has been recently confirmed as SPA-1 deficient B cells showed signs of skewed receptor editing creating higher numbers of auto-antigen specific B cells [429]. Thus, the Rap-1/SPA-1 signalling module seems to play a crucial role in regulating tolerance checkpoints in developing B cells.

Although Rap-1 has been found to be important in the regulation of ERK activation, more recently its role in the regulation of adhesion and migration has been a major research focus [639]. Thus, in B cells Rap was found to be essential for the spreading response and immune synapse formation upon antigen encounter [426]. Thus, the

possibility that the reduction of Rap activity in WEHI-231 cells also influences cell-cell interactions or migration and adhesion, processes which could also affect BCR-signalling, can not be excluded. Moreover, these functions might explain why Rap is activated via the BCR at early time points (< 4 h). Further studies to dissect these separate effects of Rap might provide insight into the relative roles of Rap signalling in immature and mature B cells. Indeed, studies to address the differential roles of Rap were initiated by attempting to analyse the effects of over-expressing dominant negative or constitutively active Rap mutants on the regulation of the ERK cascade and consequent functional outcomes of WEHI-231 B cells. However, technical difficulties hampered the transfection and selection of stable clones and hence further studies examining the effects of forced Rap expression are therefore still needed to confirm the role of Rap in ERK signalling. Alternatively, primary immature B cells from SPA-1-deficient mice would provide another tool to dissect the effects of Rap overexpression. As mentioned above, these mice display defects in their B cell development as well as negative selection processes [429]. The analysis of BCR-mediated responses in SPA-1-deficient immature B cells would therefore potentially yield information on the role of SPA-1 and Rap-1 in the negative selection process.

The experiments analysing SPA-1 expression following BCR ligation revealed additional layers of regulation involving PI3 kinase- and ERK-mediated negative feedback loops (Fig.5.1). For example, PI3 kinase signalling was found to hamper the transcription of SPA-1 as well as PAC-1 mRNA, whereas the ERK cascade only regulated the expression of PAC-1, but had no influence on SPA-1 levels (Fig.3.14/15). The inhibition of these negative regulators therefore strengthens the survival programme of positively stimulated cells by stabilising or even increasing the activity of ERK. These findings are not unexpected as other regulatory elements of the ERK cascade, such as DUSPs, have previously been shown to be regulated by negative feedback inhibition [361]. The elements controlling SPA-1 and PAC-1 RNA expression, especially downstream of PI3 kinase and ERK signalling have not been identified in this study and it would therefore be of interest to determine these factors.

The functional outcome of ERK activation does not solely depend on the strength of the signal but also on its timing. As stated above, previous studies in this laboratory have not only confirmed the importance of sustained ERK signalling for proliferation of WEHI-231 cells but also demonstrated that strong but transient ERK activation, following BCR ligation, induces apoptosis [310]. These distinct effects of temporally regulated signals could be further influenced by the location of the activated ERK signal. For example, depending on the type of cell, GT1-7 cells or HEK293 cells, treatment with gonadotropin-releasing hormone was found to induce a transient or sustained ERK signal, respectively,

which influenced the functional outcome of such ERK activation. Thus, whilst the transient signal did not allow the translocation of active ERK to the nucleus, sustained signalling did [640], suggesting that the duration of the ERK signal might determine downstream signalling by dictating differential localisation of activated ERK. Indeed, in this present study it was shown that the transient ERK signal induced by the ligation of the BCR was reflected by reduced expression of activated ERK in the nucleus when compared to that resulting from the sustained signal in cells rescued from BCR-mediated growth arrest by CD40 (Fig.3.16). Thus the strength, duration and localisation (cytoplasmic versus nuclear) of ERK activation might influence the balance between pro-survival and apoptotic ERK signalling.

Relating to this, the results in Chapter 3 implicate c-Myc as the major downstream effector of sustained cycling ERK signalling in survival and proliferation of WEHI-231 B cells and presumably reflect the ability of c-Myc to enhance cell cycle progression by various mechanisms such as increasing the transcription of cyclin D genes or the suppression of p27 expression [274,278]. With respect to the mechanisms involved, pharmacological inhibition of the ERK pathway supported the notion that ERK is involved in the stabilisation of c-Myc protein levels as abrogating ERK signalling reduced the expression of c-Myc protein but hardly affected its' transcriptional levels (Fig.3.23-25). The stabilisation of c-Myc expression therefore provides a link between ERK signalling and proliferation and survival of WEHI-231 cells (Fig.5.2). Further support for the importance of activated ERK as well as c-Myc for cell cycle progression and proliferation came from the experiments utilising LSC analysis to directly correlate the expression and activation of molecules of interest with cell cycle stage on a single cell basis. Thus in confirmation of their known roles in cell cycle progression, this analysis revealed that both ERK and c-Myc expression levels were found to be highest in mitotic cells and severely diminished in growth arrested and apoptotic cells (Fig.3.10 and 3.27). Thus, sustained activation of ERK induces stable levels of c-Myc and hence enables cells to overcome the G1 restriction point and enter mitosis.

Both ERK and c-Myc have been implicated in the induction of cyclin expression [274,372] and hence the enhanced activation of cyclin D/Cdk complexes and consequent hyperphosphorylation of Rb resulting in the release of the E2F transcription factor required for induction of S-phase genes [245]. Consistent with this, the reduced levels of c-Myc (achieved by the abrogation of ERK activation secondary to either BCR-ligation or pharmacological inhibition) correlated with increased levels of the cyclin/Cdk inhibitor, p27 (Fig.3.30) and severely compromised levels of hyperphosphorylated Rb (Fig.3.30 and 3.32/33).

CD40-dependent proliferation requires the induction of cyclin D/Cdk complexes to progress through the G1/S transition [336] and the importance of this is indicated by studies in which forced expression of E2F can protect Bcl-x_L-overexpressing WEHI-231 cells from BCR-driven growth arrest [641]. CD40-mediated rescue from growth arrest appears to be achieved by sustaining ERK activation [310,373] and hence c-Myc levels, thereby inducing hyperphosphorylation of Rb proteins and release of E2F via the induction of cyclin/Cdk complexes (Fig.5.2). Indeed, CD40 signalling reverses BCR-mediated upregulation of the cell cycle inhibitor p27 and likely overcomes the suppression of E2F by inducing Rb hyperphosphorylation (Fig.3.30 and 3.32/33).

The ubiquitination of proteins is important in many cellular processes and signalling pathways. It plays a major role in the regulation of cellular protein levels by targeting proteins for degradation by the proteasome. Interestingly, many of the proteins involved in cell cycle regulation, including c-Myc and p27, can be targeted for ubiquitination and proteasomal degradation. It was therefore hypothesised that ubiquitination would be an important process in BCR-mediated signalling leading to growth arrest. Indeed, c-Myc as well as p27 were found to be regulated by proteasomal degradation and inhibition of the proteasome partially protected these molecules from degradation especially in spontaneously proliferating WEHI-231 cells (Fig.3.35). These findings are preliminary and more in depth studies of the role of ubiquitination might provide a more detailed insight into the role of this modification in the signalling leading to growth arrest or survival.

Consistent with this, E3 ligases, the enzymes carrying out the transfer of ubiquitin to target proteins, have been implicated in T cell anergy by, for example, determining the signalling threshold and need for costimulation for T cell priming [229]. Some of these E3 ubiquitin ligases, such as the Cbl family of proteins, have also been found to regulate B cell responses [229], where in the majority of cases these enzymes appear to function as negative regulators of B cell signalling [431]. Indeed, in this present study, the expression of the E3 ubiqutin ligase Cbl-b was found to be regulated by BCR-signalling as ligation of the BCR increased the levels of Cbl-b (Fig.3.37), indicating a role for this E3 ligase in negative signalling induced by the BCR. Interestingly, Cbl-b has been implicated in the regulation of Rap activation by influencing C3G, Crk and Rap complex formation and in T cells, Cbl-b mediated ubiquitination of Crk reduced the activation of Rap [438]. Grb2/C3G/Crk/Cbl complexes have also been found to be recruited to the BCR in B cells and hence Cbl-b might inihibit Rap activation in these cells as well (Fig.5.2) [495]. Constructs encoding wild-type or a dominant negative form of Cbl-b are available in this laboratory and thus transfection of WEHI-231 cells with these constructs might provide

further insight into the role these molecules play in BCR-mediated growth arrest and apoptosis in immature WEHI-231 B cells.

5.2 FcγRIIb signalling in mature B cells

FcγRIIb-mediated suppression of immune responses is known to be important for the maintenance of B cell homeostasis as indicated by the findings that FcγRIIb-deficient animals exhibit increased inflammatory responses and enhanced susceptibility to autoimmune disorders [577,579,580]. FcγRIIb-signalling acts, at least in part, by reducing the antigen-driven activation of B cells resulting in growth arrest and apoptosis [309]. Such apoptosis reflects the dissipation of the mitochondrial membrane potential and ultimately the release of cytochrome C and apoptosis [309]. Similar to other types of apoptosis induced in B cells, such as that observed in germinal centre B cells [642], execution of FcγRIIb-mediated apoptosis did not appear to depend on effector caspases (3,6 or 9) or even a single type of protease but rather seemed to involve simultaneous activation of multiple executioner proteases including caspases, cathepsins and calpains [309].

The study presented in Chapter 4 extended these findings by shedding light on the role of caspase 8, and the signals controlling it, in this process. Thus, caspase 8 was found to be crucial for the induction of FcγRIIb-dependent apoptosis as pharmacological inhibition of caspase 8 reduced the levels of apoptosis dramatically (Fig.4.3). As caspase 8 is the major initiator caspase utilised during death receptor signalling, it was hypothesised that FcγRIIb might induce the expression and consequent autocrine signalling of death receptors and their ligands, such as Fas/FasL. Indeed, Fas and FasL were found to be upregulated due to BCR/FcγRIIb ligation at both the mRNA and protein level. Importantly, FcγRIIb-mediated apoptosis was reduced due to inhibition of Fas signalling (Fig.4.13). Consistent with this, B cells from MRL/MpJ-*Fas*^{lpr} mice, a strain harbouring a deleterious mutation of the Fas gene, displayed defective growth arrest and apoptotic responses upon inhibitory BCR/FcγRIIb co-ligation. Collectively, therefore, these results suggest that Fas/FasL death receptor signalling might be involved in controlling FcγRIIb-dependent homeostatic regulation of mature B cells.

The downstream effector mechanisms are not yet clear but p53, which is a major regulator of growth arrest and apoptosis, is an important candidate signal. For example, in its function as a transcription factor, it can result in growth arrest and apoptosis by increasing gene expression of p21, Bax or Fas [485,631]. Moreover, it has recently been shown to transduce apoptotic signalling in a transcription-independent manner by translocating to the cytoplasm or the mitochondria where it interacts with anti-apoptotic

Bcl-2 family members and hence induces the release of pro-apoptotic Bcl-2 proteins such as Bax [486]. Consistent with a key role for p53, signalling resulting from BCR/FcγRIIb co-ligation regulates the expression levels as well as the localisation of p53 (Fig.4.5). Of particular interest, it was found that inhibition of caspase 8 prevented p53 from translocating from the nuclear to the cytoplasmic/mitochondrial compartments suggesting that caspase 8 plays a role in allowing p53 to localise to the cytoplasm where it could potentially bind to and activate pro-apoptotic Bcl-2 members and hence induce mitochondrial destabilisation. Additionally, p53 has been implied in the transcriptional regulation of caspase 8 [632,643] which could create a positive feedback loop between p53 and caspase 8. Moreover, the expression of one of the pro-apoptotic downstream targets of p53, the BH3-only Bcl-2 family member Noxa, was also found to be increased by FcγRIIb-mediated signals further confirming the involvement of p53 and suggesting that a signalling axis including Fas/FasL, caspase 8, p53 and Noxa, may be induced by FcγRIIb-signalling.

Although the results of this study have provided a model based on such Fas/FasL signalling for fully dissecting the mechanisms underlying apoptosis induced by co-ligation of BCR and FcγRIIb (Fig.5.3), there are still many unanswered questions. For example, it will be of interest not only to determine the mechanisms regulating the expression of Fas/FasL downstream of BCR/FcγRIIb co-ligation, but also to elucidate how the regulation of p53 and its' subcellular localisation impact on B cell responses.

5.3 FcγRIIb-mediated inhibition in human B cells

B cells participate in the immune response through various functions such as antibody production, antigen-presentation and cytokine production and hence influence the responses of other cells including T cells. Thus, de-regulated and excessive B cell activation may increase the likelihood of developing autoimmunity. Mechanisms controlling B cell homeostasis such as inhibitory FcγRIIb-signalling therefore might play a crucial role in determining the threshold for B cell activation and autoantibody production in autoimmune diseases such as RA and SLE. Indeed, the pathology of these diseases have been shown to be linked to antibody production and B cell depletion has proven beneficial in many cases [551]. Moreover, a polymorphism of FcγRIIb which reduces its signalling capacity [590] has been found to be associated with SLE in some racial groups such as Japanese patients [589]. Thus, FcγRIIb provides a candidate which could potentially regulate B cell activation in the human system in the context of autoimmune disease.

Interestingly, therefore, in this study it was shown that cells from a small proportion of RA and SLE patients displayed little or no inhibition of BCR-driven proliferation upon FcγRIIb ligation *in vitro* (Fig.4.16), although, overall, the differences between the healthy control and RA or SLE cohorts were not statistically significant. However, only small cohorts of patients were studied, thus investigations of FcγRIIb expression in B cells from larger cohorts of patients, potentially from varying ethnic backgrounds, may provide statistically significant data to support a role for FcγRIIb function in the dysregulation of B cell responses in RA or SLE patients in certain populations. Indeed, it has previously been shown that de-regulation of FcγRIIb expression on memory and plasma B cells is more apparent in SLE patients with African-American background [588]. Thus, if the defects of the inhibitory response observed in this study correlate with overall expression levels of FcγRIIb they could also be more obvious and statistically significant in populations of other ethnic backgrounds. Nevertheless, the results presented in Chapter 4 indicate that FcγRIIb-mediated regulation of proliferation of mature peripheral B cells is not a dominant disease-driving mechanism. However, there is a possibility that changes in FcγRIIb-signalling might contribute to the disease in some patients. Consistent with the theory that FcγRIIb expression is important for maintenance of self-tolerance, FcγRIIb1 and FcγRIIb2 were found to be downregulated in PBMCs from RA patients. However, the most striking change between the RA/SLE patient cohorts and the healthy patients was the reduction of the FcγRIIb1/FcγRIIb2 ratio (Fig.4.19) due to a relative increase of FcγRIIb2 levels in patients compared to healthy controls. This change could influence the balance between antigen uptake and presentation and inhibitory signalling towards increased ability of cells to present antigen. In an autoimmune prone setting this could increase the presentation of self-antigen by autoreactive B cells which in turn could activate autoreactive T cells thus perpetuating auto-inflammatory responses.

The results described in Chapter 4 therefore support a role for FcγRIIb in human autoimmune disease. However, there are many areas which are still unexplored such as the mechanisms regulating the differential expression of FcγRIIb1 and FcγRIIb2. Furthermore, it would be of interest to identify the contribution of the various cell types making up the PBMC compartment (B cells, monocytes, dendritic cells) towards the changes seen in FcγRIIb1/FcγRIIb2 expression. More detailed studies analysing a potential correlation between expression levels of FcγRIIb and changes in the inhibitory function of B cells would also contribute to further dissecting the function of this receptor in human B cells. Finally, examination of B cells in the location of the auto-inflammatory response such as the joint in RA patients would be of even more interest, as circulating B cells might not necessarily represent the status of tissue-resident B cells actively involved

in inflammation. Thus, the evidence of a role for FcγRIIb in the negative regulation of inappropriately activated B cells might provide necessary information for potential therapeutic intervention during autoimmune inflammatory diseases.

5.4 Figures

Figure 5.1 Regulation of the ERK cascade in WEHI-231 B cells

Cross-linking of the BCR on WEHI-231 cells reduces ERK signalling by multiple mechanisms. Thus, BCR-ligation suppresses the activation of the Rap/B-Raf pathway which is most likely achieved by the upregulation of SPA-1 levels but might also involve the increased expression and recruitment of the E3 ubiquitin ligase Cbl-b. The formation of the adaptor complex consisting of C3G, Grb2 and Crk can be inhibited by Cbl-b-dependent ubiquitination of Crk. C3G is a GEF for Rap and reduced recruitment and formation of this complex therefore reduces the activation of Rap. SPA-1 and the ERK-specific phosphatase PAC-1 were both found to be regulated by negative feedback loops involving ERK and PI3 kinase signalling. Hence, abrogation of ERK/PI3 kinase signalling induced the increase of SPA-1 and PAC-1 mRNA transcription by as yet unknown transcription factors. BCR-mediated downregulation of ERK ultimately leads to the reduction of c-Myc levels and growth arrest.

Figure 5.2 Cell cycle regulation by the ERK/c-Myc cascade

Activated ERK phosphorylates c-Myc on serine 62 which stabilises nuclear c-Myc. c-Myc and ERK itself facilitate the G1/S transition by inducing cyclin D gene expression. Moreover, c-Myc reduces the levels of p27 by inhibiting its transcription and increasing the expression of the SCF E3 ubiquitin ligase complex. This complex ubiquitinates phosphorylated p27 leading to its degradation by the proteasome. Finally, active cyclin/Cdk complexes phosphorylate Rb proteins and hence induce the release of the E2F transcription factor to transactivate the expression of S phase genes. The lack of ERK activation due to BCR-ligation reduces c-Myc stabilisation and hence protein levels thereby contributing to increased levels of p27 and reduced activation of cyclin/Cdk complexes. Rb therefore remains in its hypophosphorylated state, inhibiting the release of E2F and hence G1/S phase transition.

Figure 5.3 Model for FcγRIIb-mediated apoptosis

BCR/FcγRIIb co-ligation results in dissipation of the MMP and apoptosis. FcγRIIb-signalling increases the expression of Fas and its ligand FasL and signalling through this death receptor can activate caspase 8 which was shown to be the major initiator caspase involved in FcγRIIb-mediated apoptosis. Furthermore, p53 is upregulated by FcγRIIb-dependent mechanisms and in turn could increase Fas and caspase 8 expression at the transcriptional level, thereby initiating as well as propagating this signalling axis. Additionally, p53 could trigger apoptosis by enhancing expression of pro-apoptotic molecules such as Noxa or by translocating to the mitochondria itself and hence interacting with pro- and anti-apoptotic molecules at this interface.

6 References

1. Reth M: **B cell antigen receptors**. *Curr Opin Immunol* 1994, **6**:3-8.
2. Baumgarth N, Tung JW, Herzenberg LA: **Inherent specificities in natural antibodies: a key to immune defense against pathogen invasion**. *Springer Semin Immunopathol* 2005, **26**:347-362.
3. Kantor AB, Herzenberg LA: **Origin of murine B cell lineages**. *Annu Rev Immunol* 1993, **11**:501-538.
4. Haas KM, Poe JC, Steeber DA, Tedder TF: **B-1a and B-1b cells exhibit distinct developmental requirements and have unique functional roles in innate and adaptive immunity to S. pneumoniae**. *Immunity* 2005, **23**:7-18.
5. Alugupalli KR, Leong JM, Woodland RT, Muramatsu M, Honjo T, Gerstein RM: **B1b lymphocytes confer T cell-independent long-lasting immunity**. *Immunity* 2004, **21**:379-390.
6. Lopes-Carvalho T, Kearney JF: **Development and selection of marginal zone B cells**. *Immunol Rev* 2004, **197**:192-205.
7. Kondo M, Weissman IL, Akashi K: **Identification of clonogenic common lymphoid progenitors in mouse bone marrow**. *Cell* 1997, **91**:661-672.
8. Busslinger M: **Transcriptional control of early B cell development**. *Annu Rev Immunol* 2004, **22**:55-79.
9. Li YS, Wasserman R, Hayakawa K, Hardy RR: **Identification of the earliest B lineage stage in mouse bone marrow**. *Immunity* 1996, **5**:527-535.
10. Bain G, Robanus Maandag EC, te Riele HP, Feeney AJ, Sheehy A, Schlissel M, Shinton SA, Hardy RR, Murre C: **Both E12 and E47 allow commitment to the B cell lineage**. *Immunity* 1997, **6**:145-154.
11. Lin H, Grosschedl R: **Failure of B-cell differentiation in mice lacking the transcription factor EBF**. *Nature* 1995, **376**:263-267.
12. Spanopoulou E, Roman CA, Corcoran LM, Schlissel MS, Silver DP, Nemazee D, Nussenzweig MC, Shinton SA, Hardy RR, Baltimore D: **Functional immunoglobulin transgenes guide ordered B-cell differentiation in Rag-1-deficient mice**. *Genes Dev* 1994, **8**:1030-1042.
13. Reichman-Fried M, Hardy RR, Bosma MJ: **Development of B-lineage cells in the bone marrow of scid/scid mice following the introduction of functionally rearranged immunoglobulin transgenes**. *Proc Natl Acad Sci U S A* 1990, **87**:2730-2734.
14. Gellert M: **V(D)J recombination: RAG proteins, repair factors, and regulation**. *Annu Rev Biochem* 2002, **71**:101-132.
15. Nagata K, Nakamura T, Kitamura F, Kuramochi S, Taki S, Campbell KS, Karasuyama H: **The Ig alpha/Igbeta heterodimer on mu-negative proB cells is competent for transducing signals to induce early B cell differentiation**. *Immunity* 1997, **7**:559-570.
16. Kouro T, Nagata K, Takaki S, Nisitani S, Hirano M, Wahl MI, Witte ON, Karasuyama H, Takatsu K: **Bruton's tyrosine kinase is required for signaling the CD79b-mediated pro-B to pre-B cell transition**. *Int Immunol* 2001, **13**:485-493.
17. Pelanda R, Braun U, Hobeika E, Nussenzweig MC, Reth M: **B cell progenitors are arrested in maturation but have intact VDJ recombination in the absence of Ig-alpha and Ig-beta**. *J Immunol* 2002, **169**:865-872.
18. Karasuyama H, Kudo A, Melchers F: **The proteins encoded by the VpreB and lambda 5 pre-B cell-specific genes can associate with each other and with mu heavy chain**. *J Exp Med* 1990, **172**:969-972.
19. Karasuyama H, Rolink A, Melchers F: **Surrogate light chain in B cell development**. *Adv Immunol* 1996, **63**:1-41.
20. Galler GR, Mundt C, Parker M, Pelanda R, Martensson IL, Winkler TH: **Surface mu heavy chain signals down-regulation of the V(D)J-recombinase machinery in the absence of surrogate light chain components**. *J Exp Med* 2004, **199**:1523-1532.
21. Keenan RA, De Riva A, Corleis B, Hepburn L, Licence S, Winkler TH, Martensson IL: **Censoring of autoreactive B cell development by the pre-B cell receptor**. *Science* 2008, **321**:696-699.
22. Neuberger MS: **Antigen receptor signaling gives lymphocytes a long life**. *Cell* 1997, **90**:971-973.

23. Benschop RJ, Cambier JC: **B cell development: signal transduction by antigen receptors and their surrogates**. *Curr Opin Immunol* 1999, **11**:143-151.
24. Nemazee D, Buerki K: **Clonal deletion of autoreactive B lymphocytes in bone marrow chimeras**. *Proc Natl Acad Sci U S A* 1989, **86**:8039-8043.
25. Sandel PC, Monroe JG: **Negative selection of immature B cells by receptor editing or deletion is determined by site of antigen encounter**. *Immunity* 1999, **10**:289-299.
26. Tiegs SL, Russell DM, Nemazee D: **Receptor editing in self-reactive bone marrow B cells**. *J Exp Med* 1993, **177**:1009-1020.
27. Lang J, Jackson M, Teyton L, Brunmark A, Kane K, Nemazee D: **B cells are exquisitely sensitive to central tolerance and receptor editing induced by ultralow affinity, membrane-bound antigen**. *J Exp Med* 1996, **184**:1685-1697.
28. Julien S, Soulas P, Garaud JC, Martin T, Pasquali JL: **B cell positive selection by soluble self-antigen**. *J Immunol* 2002, **169**:4198-4204.
29. Allman DM, Ferguson SE, Lentz VM, Cancro MP: **Peripheral B cell maturation. II. Heat-stable antigen(hi) splenic B cells are an immature developmental intermediate in the production of long-lived marrow-derived B cells**. *J Immunol* 1993, **151**:4431-4444.
30. Allman D, Lindsley RC, DeMuth W, Rudd K, Shinton SA, Hardy RR: **Resolution of three nonproliferative immature splenic B cell subsets reveals multiple selection points during peripheral B cell maturation**. *J Immunol* 2001, **167**:6834-6840.
31. Merrell KT, Benschop RJ, Gauld SB, Aviszus K, Decote-Ricardo D, Wysocki LJ, Cambier JC: **Identification of anergic B cells within a wild-type repertoire**. *Immunity* 2006, **25**:953-962.
32. Niiro H, Clark EA: **Regulation of B-cell fate by antigen-receptor signals**. *Nat Rev Immunol* 2002, **2**:945-956.
33. Harless SM, Lentz VM, Sah AP, Hsu BL, Clise-Dwyer K, Hilbert DM, Hayes CE, Cancro MP: **Competition for BLyS-mediated signaling through Bcmd/BR3 regulates peripheral B lymphocyte numbers**. *Curr Biol* 2001, **11**:1986-1989.
34. Smith SH, Cancro MP: **Cutting edge: B cell receptor signals regulate BLyS receptor levels in mature B cells and their immediate progenitors**. *J Immunol* 2003, **170**:5820-5823.
35. Sasaki Y, Derudder E, Hobeika E, Pelanda R, Reth M, Rajewsky K, Schmidt-Supprian M: **Canonical NF-kappaB activity, dispensable for B cell development, replaces BAFF-receptor signals and promotes B cell proliferation upon activation**. *Immunity* 2006, **24**:729-739.
36. Monroe JG: **Balancing signals for negative selection and activation of developing B lymphocytes**. *Clin Immunol* 2000, **95**:S8-13.
37. Ruprecht CR, Lanzavecchia A: **Toll-like receptor stimulation as a third signal required for activation of human naive B cells**. *Eur J Immunol* 2006, **36**:810-816.
38. Jacob J, Kelsoe G: **In situ studies of the primary immune response to (4-hydroxy-3-nitrophenyl)acetyl. II. A common clonal origin for periarteriolar lymphoid sheath-associated foci and germinal centers**. *J Exp Med* 1992, **176**:679-687.
39. Wykes M, Pombo A, Jenkins C, MacPherson GG: **Dendritic cells interact directly with naive B lymphocytes to transfer antigen and initiate class switching in a primary T-dependent response**. *J Immunol* 1998, **161**:1313-1319.
40. MacLennan IC, Toellner KM, Cunningham AF, Serre K, Sze DM, Zuniga E, Cook MC, Vinuesa CG: **Extrafollicular antibody responses**. *Immunol Rev* 2003, **194**:8-18.
41. McHeyzer-Williams MG, McLean MJ, Lalor PA, Nossal GJ: **Antigen-driven B cell differentiation in vivo**. *J Exp Med* 1993, **178**:295-307.
42. Jacob J, Kelsoe G, Rajewsky K, Weiss U: **Intraclonal generation of antibody mutants in germinal centres**. *Nature* 1991, **354**:389-392.
43. Paus D, Phan TG, Chan TD, Gardam S, Basten A, Brink R: **Antigen recognition strength regulates the choice between extrafollicular plasma cell and germinal center B cell differentiation**. *J Exp Med* 2006, **203**:1081-1091.
44. Allen CD, Ansel KM, Low C, Lesley R, Tamamura H, Fujii N, Cyster JG: **Germinal center dark and light zone organization is mediated by CXCR4 and CXCR5**. *Nat Immunol* 2004, **5**:943-952.
45. Kawabe T, Naka T, Yoshida K, Tanaka T, Fujiwara H, Suematsu S, Yoshida N, Kishimoto T, Kikutani H: **The immune responses in CD40-deficient mice: impaired immunoglobulin class switching and germinal center formation**. *Immunity* 1994, **1**:167-178.

46. Grammer AC, Bergman MC, Miura Y, Fujita K, Davis LS, Lipsky PE: **The CD40 ligand expressed by human B cells costimulates B cell responses**. *J Immunol* 1995, **154**:4996-5010.
47. Kehry MR: **CD40-mediated signaling in B cells. Balancing cell survival, growth, and death**. *J Immunol* 1996, **156**:2345-2348.
48. Takahashi Y, Ohta H, Takemori T: **Fas is required for clonal selection in germinal centers and the subsequent establishment of the memory B cell repertoire**. *Immunity* 2001, **14**:181-192.
49. Martinez-Valdez H, Guret C, de Bouteiller O, Fugier I, Banchereau J, Liu YJ: **Human germinal center B cells express the apoptosis-inducing genes Fas, c-myc, P53, and Bax but not the survival gene bcl-2**. *J Exp Med* 1996, **183**:971-977.
50. Dent AL, Shaffer AL, Yu X, Allman D, Staudt LM: **Control of inflammation, cytokine expression, and germinal center formation by BCL-6**. *Science* 1997, **276**:589-592.
51. Phan TG, Paus D, Chan TD, Turner ML, Nutt SL, Basten A, Brink R: **High affinity germinal center B cells are actively selected into the plasma cell compartment**. *J Exp Med* 2006, **203**:2419-2424.
52. Blink EJ, Light A, Kallies A, Nutt SL, Hodgkin PD, Tarlinton DM: **Early appearance of germinal center-derived memory B cells and plasma cells in blood after primary immunization**. *J Exp Med* 2005, **201**:545-554.
53. Lin KI, Angelin-Duclos C, Kuo TC, Calame K: **Blimp-1-dependent repression of Pax-5 is required for differentiation of B cells to immunoglobulin M-secreting plasma cells**. *Mol Cell Biol* 2002, **22**:4771-4780.
54. Shapiro-Shelef M, Lin KI, McHeyzer-Williams LJ, Liao J, McHeyzer-Williams MG, Calame K: **Blimp-1 is required for the formation of immunoglobulin secreting plasma cells and pre-plasma memory B cells**. *Immunity* 2003, **19**:607-620.
55. Lin Y, Wong K, Calame K: **Repression of c-myc transcription by Blimp-1, an inducer of terminal B cell differentiation**. *Science* 1997, **276**:596-599.
56. Shaffer AL, Lin KI, Kuo TC, Yu X, Hurt EM, Rosenwald A, Giltnane JM, Yang L, Zhao H, Calame K, et al.: **Blimp-1 orchestrates plasma cell differentiation by extinguishing the mature B cell gene expression program**. *Immunity* 2002, **17**:51-62.
57. Ozaki K, Spolski R, Ettinger R, Kim HP, Wang G, Qi CF, Hwu P, Shaffer DJ, Akilesh S, Roopenian DC, et al.: **Regulation of B cell differentiation and plasma cell generation by IL-21, a novel inducer of Blimp-1 and Bcl-6**. *J Immunol* 2004, **173**:5361-5371.
58. Schliephake DE, Schimpl A: **Blimp-1 overcomes the block in IgM secretion in lipopolysaccharide/anti-mu F(ab')2-co-stimulated B lymphocytes**. *Eur J Immunol* 1996, **26**:268-271.
59. Hauser AE, Debes GF, Arce S, Cassese G, Hamann A, Radbruch A, Manz RA: **Chemotactic responsiveness toward ligands for CXCR3 and CXCR4 is regulated on plasma blasts during the time course of a memory immune response**. *J Immunol* 2002, **169**:1277-1282.
60. Manz RA, Lohning M, Cassese G, Thiel A, Radbruch A: **Survival of long-lived plasma cells is independent of antigen**. *Int Immunol* 1998, **10**:1703-1711.
61. Tangye SG, Avery DT, Deenick EK, Hodgkin PD: **Intrinsic differences in the proliferation of naive and memory human B cells as a mechanism for enhanced secondary immune responses**. *J Immunol* 2003, **170**:686-694.
62. Montecino-Rodriguez E, Leathers H, Dorshkind K: **Identification of a B-1 B cell-specified progenitor**. *Nat Immunol* 2006, **7**:293-301.
63. Hardy RR, Hayakawa K: **A developmental switch in B lymphopoiesis**. *Proc Natl Acad Sci U S A* 1991, **88**:11550-11554.
64. Martin F, Kearney JF: **B1 cells: similarities and differences with other B cell subsets**. *Curr Opin Immunol* 2001, **13**:195-201.
65. Tung JW, Mrazek MD, Yang Y, Herzenberg LA: **Phenotypically distinct B cell development pathways map to the three B cell lineages in the mouse**. *Proc Natl Acad Sci U S A* 2006, **103**:6293-6298.
66. Pillai S, Cariappa A, Moran ST: **Marginal zone B cells**. *Annu Rev Immunol* 2005, **23**:161-196.
67. Srivastava B, Quinn WJ, 3rd, Hazard K, Erikson J, Allman D: **Characterization of marginal zone B cell precursors**. *J Exp Med* 2005, **202**:1225-1234.
68. Lam KP, Rajewsky K: **B cell antigen receptor specificity and surface density together determine B-1 versus B-2 cell development**. *J Exp Med* 1999, **190**:471-477.

69. Diz R, McCray SK, Clarke SH: **B cell receptor affinity and B cell subset identity integrate to define the effectiveness, affinity threshold, and mechanism of anergy**. *J Immunol* 2008, **181**:3834-3840.
70. Allman D, Pillai S: **Peripheral B cell subsets**. *Curr Opin Immunol* 2008, **20**:149-157.
71. Wardemann H, Yurasov S, Schaefer A, Young JW, Meffre E, Nussenzweig MC: **Predominant autoantibody production by early human B cell precursors**. *Science* 2003, **301**:1374-1377.
72. Cambier JC, Gauld SB, Merrell KT, Vilen BJ: **B-cell anergy: from transgenic models to naturally occurring anergic B cells?** *Nat Rev Immunol* 2007, **7**:633-643.
73. Tarasenko T, Dean JA, Bolland S: **FcgammaRIIB as a modulator of autoimmune disease susceptibility**. *Autoimmunity* 2007, **40**:409-417.
74. Pugh-Bernard AE, Silverman GJ, Cappione AJ, Villano ME, Ryan DH, Insel RA, Sanz I: **Regulation of inherently autoreactive VH4-34 B cells in the maintenance of human B cell tolerance**. *J Clin Invest* 2001, **108**:1061-1070.
75. Cappione A, 3rd, Anolik JH, Pugh-Bernard A, Barnard J, Dutcher P, Silverman G, Sanz I: **Germinal center exclusion of autoreactive B cells is defective in human systemic lupus erythematosus**. *J Clin Invest* 2005, **115**:3205-3216.
76. Yurasov S, Hammersen J, Tiller T, Tsuiji M, Wardemann H: **B-cell tolerance checkpoints in healthy humans and patients with systemic lupus erythematosus**. *Ann N Y Acad Sci* 2005, **1062**:165-174.
77. O'Neill SK, Shlomchik MJ, Glant TT, Cao Y, Doodes PD, Finnegan A: **Antigen-specific B cells are required as APCs and autoantibody-producing cells for induction of severe autoimmune arthritis**. *J Immunol* 2005, **174**:3781-3788.
78. Cariappa A, Boboila C, Moran ST, Liu H, Shi HN, Pillai S: **The recirculating B cell pool contains two functionally distinct, long-lived, posttransitional, follicular B cell populations**. *J Immunol* 2007, **179**:2270-2281.
79. Gonzalez M, Mackay F, Browning JL, Kosco-Vilbois MH, Noelle RJ: **The sequential role of lymphotoxin and B cells in the development of splenic follicles**. *J Exp Med* 1998, **187**:997-1007.
80. Harris DP, Haynes L, Sayles PC, Duso DK, Eaton SM, Lepak NM, Johnson LL, Swain SL, Lund FE: **Reciprocal regulation of polarized cytokine production by effector B and T cells**. *Nat Immunol* 2000, **1**:475-482.
81. Liu Q, Liu Z, Rozo CT, Hamed HA, Alem F, Urban JF, Jr., Gause WC: **The role of B cells in the development of CD4 effector T cells during a polarized Th2 immune response**. *J Immunol* 2007, **179**:3821-3830.
82. Mizoguchi A, Bhan AK: **A case for regulatory B cells**. *J Immunol* 2006, **176**:705-710.
83. Mauri C, Gray D, Mushtaq N, Londei M: **Prevention of arthritis by interleukin 10-producing B cells**. *J Exp Med* 2003, **197**:489-501.
84. Parekh VV, Prasad DV, Banerjee PP, Joshi BN, Kumar A, Mishra GC: **B cells activated by lipopolysaccharide, but not by anti-Ig and anti-CD40 antibody, induce anergy in CD8+ T cells: role of TGF-beta 1**. *J Immunol* 2003, **170**:5897-5911.
85. Bayry J, Lacroix-Desmazes S, Kazatchkine MD, Hermine O, Tough DF, Kaveri SV: **Modulation of dendritic cell maturation and function by B lymphocytes**. *J Immunol* 2005, **175**:15-20.
86. Evans JG, Chavez-Rueda KA, Eddaoudi A, Meyer-Bahlburg A, Rawlings DJ, Ehrenstein MR, Mauri C: **Novel suppressive function of transitional 2 B cells in experimental arthritis**. *J Immunol* 2007, **178**:7868-7878.
87. Mizoguchi A, Mizoguchi E, Takedatsu H, Blumberg RS, Bhan AK: **Chronic intestinal inflammatory condition generates IL-10-producing regulatory B cell subset characterized by CD1d upregulation**. *Immunity* 2002, **16**:219-230.
88. Cambier JC: **Antigen and Fc receptor signaling. The awesome power of the immunoreceptor tyrosine-based activation motif (ITAM)**. *J Immunol* 1995, **155**:3281-3285.
89. Campbell KS: **Signal transduction from the B cell antigen-receptor**. *Curr Opin Immunol* 1999, **11**:256-264.
90. DeFranco AL, Richards JD, Blum JH, Stevens TL, Law DA, Chan VW, Datta SK, Foy SP, Hourihane SL, Gold MR, et al.: **Signal transduction by the B-cell antigen receptor**. *Ann N Y Acad Sci* 1995, **766**:195-201.

91. Cushley W, Harnett MM: **Cellular signalling mechanisms in B lymphocytes**. *Biochem J* 1993, **292 (Pt 2)**:313-332.
92. Wymann MP, Pirola L: **Structure and function of phosphoinositide 3-kinases**. *Biochim Biophys Acta* 1998, **1436**:127-150.
93. Franke TF, Kaplan DR, Cantley LC, Toker A: **Direct regulation of the Akt proto-oncogene product by phosphatidylinositol-3,4-bisphosphate**. *Science* 1997, **275**:665-668.
94. Falasca M, Logan SK, Lehto VP, Baccante G, Lemmon MA, Schlessinger J: **Activation of phospholipase C gamma by PI 3-kinase-induced PH domain-mediated membrane targeting**. *Embo J* 1998, **17**:414-422.
95. Alessi DR, James SR, Downes CP, Holmes AB, Gaffney PR, Reese CB, Cohen P: **Characterization of a 3-phosphoinositide-dependent protein kinase which phosphorylates and activates protein kinase Balpha**. *Curr Biol* 1997, **7**:261-269.
96. Aagaard-Tillery KM, Jelinek DF: **Phosphatidylinositol 3-kinase activation in normal human B lymphocytes**. *J Immunol* 1996, **156**:4543-4554.
97. Okkenhaug K, Vanhaesebroeck B: **PI3K in lymphocyte development, differentiation and activation**. *Nat Rev Immunol* 2003, **3**:317-330.
98. Donahue AC, Fruman DA: **PI3K signaling controls cell fate at many points in B lymphocyte development and activation**. *Semin Cell Dev Biol* 2004, **15**:183-197.
99. Deane JA, Trifilo MJ, Yballe CM, Choi S, Lane TE, Fruman DA: **Enhanced T cell proliferation in mice lacking the p85beta subunit of phosphoinositide 3-kinase**. *J Immunol* 2004, **172**:6615-6625.
100. Alcazar I, Cortes I, Zaballos A, Hernandez C, Fruman DA, Barber DF, Carrera AC: **p85beta phosphoinositide 3-kinase regulates CD28 coreceptor function**. *Blood* 2009, **113**:3198-3208.
101. Garcia Z, Silio V, Marques M, Cortes I, Kumar A, Hernandez C, Checa AI, Serrano A, Carrera AC: **A PI3K activity-independent function of p85 regulatory subunit in control of mammalian cytokinesis**. *EMBO J* 2006, **25**:4740-4751.
102. Ji H, Rintelen F, Waltzinger C, Bertschy Meier D, Bilancio A, Pearce W, Hirsch E, Wymann MP, Ruckle T, Camps M, et al.: **Inactivation of PI3Kgamma and PI3Kdelta distorts T-cell development and causes multiple organ inflammation**. *Blood* 2007, **110**:2940-2947.
103. Okkenhaug K, Patton DT, Bilancio A, Garcon F, Rowan WC, Vanhaesebroeck B: **The p110delta isoform of phosphoinositide 3-kinase controls clonal expansion and differentiation of Th cells**. *J Immunol* 2006, **177**:5122-5128.
104. Patton DT, Garden OA, Pearce WP, Clough LE, Monk CR, Leung E, Rowan WC, Sancho S, Walker LS, Vanhaesebroeck B, et al.: **Cutting edge: the phosphoinositide 3-kinase p110 delta is critical for the function of CD4+CD25+Foxp3+ regulatory T cells**. *J Immunol* 2006, **177**:6598-6602.
105. Thomas MS, Mitchell JS, DeNucci CC, Martin AL, Shimizu Y: **The p110gamma isoform of phosphatidylinositol 3-kinase regulates migration of effector CD4 T lymphocytes into peripheral inflammatory sites**. *J Leukoc Biol* 2008, **84**:814-823.
106. Martin AL, Schwartz MD, Jameson SC, Shimizu Y: **Selective regulation of CD8 effector T cell migration by the p110 gamma isoform of phosphatidylinositol 3-kinase**. *J Immunol* 2008, **180**:2081-2088.
107. Rodriguez-Borlado L, Barber DF, Hernandez C, Rodriguez-Marcos MA, Sanchez A, Hirsch E, Wymann M, Martinez AC, Carrera AC: **Phosphatidylinositol 3-kinase regulates the CD4/CD8 T cell differentiation ratio**. *J Immunol* 2003, **170**:4475-4482.
108. Tsukamoto K, Hazeki K, Hoshi M, Nigorikawa K, Inoue N, Sasaki T, Hazeki O: **Critical roles of the p110 beta subtype of phosphoinositide 3-kinase in lipopolysaccharide-induced Akt activation and negative regulation of nitrite production in RAW 264.7 cells**. *J Immunol* 2008, **180**:2054-2061.
109. Leverrier Y, Okkenhaug K, Sawyer C, Bilancio A, Vanhaesebroeck B, Ridley AJ: **Class I phosphoinositide 3-kinase p110beta is required for apoptotic cell and Fcgamma receptor-mediated phagocytosis by macrophages**. *J Biol Chem* 2003, **278**:38437-38442.
110. Guillermet-Guibert J, Bjorklof K, Salpekar A, Gonella C, Ramadani F, Bilancio A, Meek S, Smith AJ, Okkenhaug K, Vanhaesebroeck B: **The p110beta isoform of phosphoinositide 3-kinase signals downstream of G protein-coupled receptors and is functionally redundant with p110gamma**. *Proc Natl Acad Sci U S A* 2008, **105**:8292-8297.

111. Fruman DA, Snapper SB, Yballe CM, Davidson L, Yu JY, Alt FW, Cantley LC: **Impaired B cell development and proliferation in absence of phosphoinositide 3-kinase p85alpha**. *Science* 1999, **283**:393-397.
112. Donahue AC, Hess KL, Ng KL, Fruman DA: **Altered splenic B cell subset development in mice lacking phosphoinositide 3-kinase p85alpha**. *Int Immunol* 2004, **16**:1789-1798.
113. Jou ST, Carpino N, Takahashi Y, Piekorz R, Chao JR, Wang D, Ihle JN: **Essential, nonredundant role for the phosphoinositide 3-kinase p110delta in signaling by the B-cell receptor complex**. *Mol Cell Biol* 2002, **22**:8580-8591.
114. Okkenhaug K, Bilancio A, Farjot G, Priddle H, Sancho S, Peskett E, Pearce W, Meek SE, Salpekar A, Waterfield MD, et al.: **Impaired B and T cell antigen receptor signaling in p110delta PI 3-kinase mutant mice**. *Science* 2002, **297**:1031-1034.
115. Al-Alwan MM, Okkenhaug K, Vanhaesebroeck B, Hayflick JS, Marshall AJ: **Requirement for phosphoinositide 3-kinase p110delta signaling in B cell antigen receptor-mediated antigen presentation**. *J Immunol* 2007, **178**:2328-2335.
116. Reif K, Okkenhaug K, Sasaki T, Penninger JM, Vanhaesebroeck B, Cyster JG: **Cutting edge: differential roles for phosphoinositide 3-kinases, p110gamma and p110delta, in lymphocyte chemotaxis and homing**. *J Immunol* 2004, **173**:2236-2240.
117. Beitz LO, Fruman DA, Kurosaki T, Cantley LC, Scharenberg AM: **SYK is upstream of phosphoinositide 3-kinase in B cell receptor signaling**. *J Biol Chem* 1999, **274**:32662-32666.
118. Suire S, Hawkins P, Stephens L: **Activation of phosphoinositide 3-kinase gamma by Ras**. *Curr Biol* 2002, **12**:1068-1075.
119. Inabe K, Ishiai M, Scharenberg AM, Freshney N, Downward J, Kurosaki T: **Vav3 modulates B cell receptor responses by regulating phosphoinositide 3-kinase activation**. *J Exp Med* 2002, **195**:189-200.
120. Park H, Wahl MI, Afar DE, Turck CW, Rawlings DJ, Tam C, Scharenberg AM, Kinet JP, Witte ON: **Regulation of Btk function by a major autophosphorylation site within the SH3 domain**. *Immunity* 1996, **4**:515-525.
121. Rawlings DJ, Scharenberg AM, Park H, Wahl MI, Lin S, Kato RM, Fluckiger AC, Witte ON, Kinet JP: **Activation of BTK by a phosphorylation mechanism initiated by SRC family kinases**. *Science* 1996, **271**:822-825.
122. Clayton E, Bardi G, Bell SE, Chantry D, Downes CP, Gray A, Humphries LA, Rawlings D, Reynolds H, Vigorito E, et al.: **A crucial role for the p110delta subunit of phosphatidylinositol 3-kinase in B cell development and activation**. *J Exp Med* 2002, **196**:753-763.
123. Bae YS, Cantley LG, Chen CS, Kim SR, Kwon KS, Rhee SG: **Activation of phospholipase C-gamma by phosphatidylinositol 3,4,5-trisphosphate**. *J Biol Chem* 1998, **273**:4465-4469.
124. Barker SA, Lujan D, Wilson BS: **Multiple roles for PI 3-kinase in the regulation of PLCgamma activity and Ca2+ mobilization in antigen-stimulated mast cells**. *J Leukoc Biol* 1999, **65**:321-329.
125. Vanhaesebroeck B, Alessi DR: **The PI3K-PDK1 connection: more than just a road to PKB**. *Biochem J* 2000, **346 Pt 3**:561-576.
126. Duronio V: **The life of a cell: apoptosis regulation by the PI3K/PKB pathway**. *Biochem J* 2008, **415**:333-344.
127. Khwaja A: **Akt is more than just a Bad kinase**. *Nature* 1999, **401**:33-34.
128. Gardai SJ, Hildeman DA, Frankel SK, Whitlock BB, Frasch SC, Borregaard N, Marrack P, Bratton DL, Henson PM: **Phosphorylation of Bax Ser184 by Akt regulates its activity and apoptosis in neutrophils**. *J Biol Chem* 2004, **279**:21085-21095.
129. Ozes ON, Mayo LD, Gustin JA, Pfeffer SR, Pfeffer LM, Donner DB: **NF-kappaB activation by tumour necrosis factor requires the Akt serine-threonine kinase**. *Nature* 1999, **401**:82-85.
130. Diaz-Meco MT, Lozano J, Municio MM, Berra E, Frutos S, Sanz L, Moscat J: **Evidence for the in vitro and in vivo interaction of Ras with protein kinase C zeta**. *J Biol Chem* 1994, **269**:31706-31710.
131. Moscat J, Diaz-Meco MT, Rennert P: **NF-kappaB activation by protein kinase C isoforms and B-cell function**. *EMBO Rep* 2003, **4**:31-36.
132. Kurosaki T, Maeda A, Ishiai M, Hashimoto A, Inabe K, Takata M: **Regulation of the phospholipase C-gamma2 pathway in B cells**. *Immunol Rev* 2000, **176**:19-29.

133. Kurosaki T: **Molecular mechanisms in B cell antigen receptor signaling**. *Curr Opin Immunol* 1997, **9**:309-318.
134. Jacobson MD: **Apoptosis: Bcl-2-related proteins get connected**. *Curr Biol* 1997, **7**:R277-281.
135. Schievella AR, Regier MK, Smith WL, Lin LL: **Calcium-mediated translocation of cytosolic phospholipase A2 to the nuclear envelope and endoplasmic reticulum**. *J Biol Chem* 1995, **270**:30749-30754.
136. Mathiasen IS, Sergeev IN, Bastholm L, Elling F, Norman AW, Jaattela M: **Calcium and calpain as key mediators of apoptosis-like death induced by vitamin D compounds in breast cancer cells**. *J Biol Chem* 2002, **277**:30738-30745.
137. Mellor H, Parker PJ: **The extended protein kinase C superfamily**. *Biochem J* 1998, **332 (Pt 2)**:281-292.
138. Guo B, Su TT, Rawlings DJ: **Protein kinase C family functions in B-cell activation**. *Curr Opin Immunol* 2004, **16**:367-373.
139. Leitges M, Schmedt C, Guinamard R, Davoust J, Schaal S, Stabel S, Tarakhovsky A: **Immunodeficiency in protein kinase cbeta-deficient mice**. *Science* 1996, **273**:788-791.
140. Caamano J, Hunter CA: **NF-kappaB family of transcription factors: central regulators of innate and adaptive immune functions**. *Clin Microbiol Rev* 2002, **15**:414-429.
141. Miyamoto A, Nakayama K, Imaki H, Hirose S, Jiang Y, Abe M, Tsukiyama T, Nagahama H, Ohno S, Hatakeyama S, et al.: **Increased proliferation of B cells and auto-immunity in mice lacking protein kinase Cdelta**. *Nature* 2002, **416**:865-869.
142. Akira S, Hirano T, Taga T, Kishimoto T: **Biology of multifunctional cytokines: IL 6 and related molecules (IL 1 and TNF)**. *FASEB J* 1990, **4**:2860-2867.
143. Roux PP, Blenis J: **ERK and p38 MAPK-activated protein kinases: a family of protein kinases with diverse biological functions**. *Microbiol Mol Biol Rev* 2004, **68**:320-344.
144. Pearson G, Robinson F, Beers Gibson T, Xu BE, Karandikar M, Berman K, Cobb MH: **Mitogen-activated protein (MAP) kinase pathways: regulation and physiological functions**. *Endocr Rev* 2001, **22**:153-183.
145. Fu C, Turck CW, Kurosaki T, Chan AC: **BLNK: a central linker protein in B cell activation**. *Immunity* 1998, **9**:93-103.
146. DeFranco AL: **The complexity of signaling pathways activated by the BCR**. *Curr Opin Immunol* 1997, **9**:296-308.
147. Harnett MM, Katz E, Ford CA: **Differential signalling during B-cell maturation**. *Immunol Lett* 2005, **98**:33-44.
148. Rubinfeld H, Seger R: **The ERK cascade: a prototype of MAPK signaling**. *Mol Biotechnol* 2005, **31**:151-174.
149. Harmer SL, DeFranco AL: **Shc contains two Grb2 binding sites needed for efficient formation of complexes with SOS in B lymphocytes**. *Mol Cell Biol* 1997, **17**:4087-4095.
150. Kelly ME, Chan AC: **Regulation of B cell function by linker proteins**. *Curr Opin Immunol* 2000, **12**:267-275.
151. Geyer M, Wittinghofer A: **GEFs, GAPs, GDIs and effectors: taking a closer (3D) look at the regulation of Ras-related GTP-binding proteins**. *Curr Opin Struct Biol* 1997, **7**:786-792.
152. Crews CM, Alessandrini A, Erikson RL: **The primary structure of MEK, a protein kinase that phosphorylates the ERK gene product**. *Science* 1992, **258**:478-480.
153. Wu J, Harrison JK, Vincent LA, Haystead C, Haystead TA, Michel H, Hunt DF, Lynch KR, Sturgill TW: **Molecular structure of a protein-tyrosine/threonine kinase activating p42 mitogen-activated protein (MAP) kinase: MAP kinase kinase**. *Proc Natl Acad Sci U S A* 1993, **90**:173-177.
154. Brancho D, Tanaka N, Jaeschke A, Ventura JJ, Kelkar N, Tanaka Y, Kyuuma M, Takeshita T, Flavell RA, Davis RJ: **Mechanism of p38 MAP kinase activation in vivo**. *Genes Dev* 2003, **17**:1969-1978.
155. Ono K, Han J: **The p38 signal transduction pathway: activation and function**. *Cell Signal* 2000, **12**:1-13.
156. Cook R, Wu CC, Kang YJ, Han J: **The role of the p38 pathway in adaptive immunity**. *Cell Mol Immunol* 2007, **4**:253-259.
157. Zhang W, Liu HT: **MAPK signal pathways in the regulation of cell proliferation in mammalian cells**. *Cell Res* 2002, **12**:9-18.
158. Kyriakis JM, Avruch J: **Mammalian mitogen-activated protein kinase signal transduction pathways activated by stress and inflammation**. *Physiol Rev* 2001, **81**:807-869.

159. Barr RK, Bogoyevitch MA: **The c-Jun N-terminal protein kinase family of mitogen-activated protein kinases (JNK MAPKs)**. *Int J Biochem Cell Biol* 2001, **33**:1047-1063.
160. Hibi M, Lin A, Smeal T, Minden A, Karin M: **Identification of an oncoprotein- and UV-responsive protein kinase that binds and potentiates the c-Jun activation domain**. *Genes Dev* 1993, **7**:2135-2148.
161. Musti AM, Treier M, Bohmann D: **Reduced ubiquitin-dependent degradation of c-Jun after phosphorylation by MAP kinases**. *Science* 1997, **275**:400-402.
162. Davis RJ: **Signal transduction by the JNK group of MAP kinases**. *Cell* 2000, **103**:239-252.
163. Lamb JA, Ventura JJ, Hess P, Flavell RA, Davis RJ: **JunD mediates survival signaling by the JNK signal transduction pathway**. *Mol Cell* 2003, **11**:1479-1489.
164. Graves JD, Draves KE, Craxton A, Saklatvala J, Krebs EG, Clark EA: **Involvement of stress-activated protein kinase and p38 mitogen-activated protein kinase in mIgM-induced apoptosis of human B lymphocytes**. *Proc Natl Acad Sci U S A* 1996, **93**:13814-13818.
165. Healy JI, Dolmetsch RE, Timmerman LA, Cyster JG, Thomas ML, Crabtree GR, Lewis RS, Goodnow CC: **Different nuclear signals are activated by the B cell receptor during positive versus negative signaling**. *Immunity* 1997, **6**:419-428.
166. Sutherland CL, Heath AW, Pelech SL, Young PR, Gold MR: **Differential activation of the ERK, JNK, and p38 mitogen-activated protein kinases by CD40 and the B cell antigen receptor**. *J Immunol* 1996, **157**:3381-3390.
167. Dong C, Yang DD, Tournier C, Whitmarsh AJ, Xu J, Davis RJ, Flavell RA: **JNK is required for effector T-cell function but not for T-cell activation**. *Nature* 2000, **405**:91-94.
168. Nishina H, Bachmann M, Oliveira-dos-Santos AJ, Kozieradzki I, Fischer KD, Odermatt B, Wakeham A, Shahinian A, Takimoto H, Bernstein A, et al.: **Impaired CD28-mediated interleukin 2 production and proliferation in stress kinase SAPK/ERK1 kinase (SEK1)/mitogen-activated protein kinase kinase 4 (MKK4)-deficient T lymphocytes**. *J Exp Med* 1997, **186**:941-953.
169. Sasaki T, Wada T, Kishimoto H, Irie-Sasaki J, Matsumoto G, Goto T, Yao Z, Wakeham A, Mak TW, Suzuki A, et al.: **The stress kinase mitogen-activated protein kinase kinase (MKK)7 is a negative regulator of antigen receptor and growth factor receptor-induced proliferation in hematopoietic cells**. *J Exp Med* 2001, **194**:757-768.
170. Brummer T, Shaw PE, Reth M, Misawa Y: **Inducible gene deletion reveals different roles for B-Raf and Raf-1 in B-cell antigen receptor signalling**. *Embo J* 2002, **21**:5611-5622.
171. Rodriguez-Viciana P, Warne PH, Dhand R, Vanhaesebroeck B, Gout I, Fry MJ, Waterfield MD, Downward J: **Phosphatidylinositol-3-OH kinase as a direct target of Ras**. *Nature* 1994, **370**:527-532.
172. Sun H, King AJ, Diaz HB, Marshall MS: **Regulation of the protein kinase Raf-1 by oncogenic Ras through phosphatidylinositol 3-kinase, Cdc42/Rac and Pak**. *Curr Biol* 2000, **10**:281-284.
173. Guan KL, Figueroa C, Brtva TR, Zhu T, Taylor J, Barber TD, Vojtek AB: **Negative regulation of the serine/threonine kinase B-Raf by Akt**. *J Biol Chem* 2000, **275**:27354-27359.
174. Yu CF, Liu ZX, Cantley LG: **ERK negatively regulates the epidermal growth factor-mediated interaction of Gab1 and the phosphatidylinositol 3-kinase**. *J Biol Chem* 2002, **277**:19382-19388.
175. Hashimoto A, Okada H, Jiang A, Kurosaki M, Greenberg S, Clark EA, Kurosaki T: **Involvement of guanosine triphosphatases and phospholipase C-gamma2 in extracellular signal-regulated kinase, c-Jun NH2-terminal kinase, and p38 mitogen-activated protein kinase activation by the B cell antigen receptor**. *J Exp Med* 1998, **188**:1287-1295.
176. Teixeira C, Stang SL, Zheng Y, Beswick NS, Stone JC: **Integration of DAG signaling systems mediated by PKC-dependent phosphorylation of RasGRP3**. *Blood* 2003, **102**:1414-1420.
177. Suzuki H, Matsuda S, Terauchi Y, Fujiwara M, Ohteki T, Asano T, Behrens TW, Kouro T, Takatsu K, Kadowaki T, et al.: **PI3K and Btk differentially regulate B cell antigen receptor-mediated signal transduction**. *Nat Immunol* 2003, **4**:280-286.
178. Shaulian E, Karin M: **AP-1 in cell proliferation and survival**. *Oncogene* 2001, **20**:2390-2400.
179. Yin Q, Wang X, McBride J, Fewell C, Flemington E: **B-cell receptor activation induces BIC/miR-155 expression through a conserved AP-1 element**. *J Biol Chem* 2008, **283**:2654-2662.

180. Yordy JS, Muise-Helmericks RC: **Signal transduction and the Ets family of transcription factors**. *Oncogene* 2000, **19**:6503-6513.
181. Sato S, Ono N, Steeber DA, Pisetsky DS, Tedder TF: **CD19 regulates B lymphocyte signaling thresholds critical for the development of B-1 lineage cells and autoimmunity**. *J Immunol* 1996, **157**:4371-4378.
182. Sato S, Steeber DA, Jansen PJ, Tedder TF: **CD19 expression levels regulate B lymphocyte development: human CD19 restores normal function in mice lacking endogenous CD19**. *J Immunol* 1997, **158**:4662-4669.
183. Boyd AW, Anderson KC, Freedman AS, Fisher DC, Slaughenhoupt B, Schlossman SF, Nadler LM: **Studies of in vitro activation and differentiation of human B lymphocytes. I. Phenotypic and functional characterization of the B cell population responding to anti-Ig antibody**. *J Immunol* 1985, **134**:1516-1523.
184. Carroll MC: **The complement system in regulation of adaptive immunity**. *Nat Immunol* 2004, **5**:981-986.
185. Engel P, Zhou LJ, Ord DC, Sato S, Koller B, Tedder TF: **Abnormal B lymphocyte development, activation, and differentiation in mice that lack or overexpress the CD19 signal transduction molecule**. *Immunity* 1995, **3**:39-50.
186. Sato S, Steeber DA, Tedder TF: **The CD19 signal transduction molecule is a response regulator of B-lymphocyte differentiation**. *Proc Natl Acad Sci U S A* 1995, **92**:11558-11562.
187. Poe JC, Hasegawa M, Tedder TF: **CD19, CD21, and CD22: multifaceted response regulators of B lymphocyte signal transduction**. *Int Rev Immunol* 2001, **20**:739-762.
188. Weng WK, Jarvis L, LeBien TW: **Signaling through CD19 activates Vav/mitogen-activated protein kinase pathway and induces formation of a CD19/Vav/phosphatidylinositol 3-kinase complex in human B cell precursors**. *J Biol Chem* 1994, **269**:32514-32521.
189. Fujimoto M, Fujimoto Y, Poe JC, Jansen PJ, Lowell CA, DeFranco AL, Tedder TF: **CD19 regulates Src family protein tyrosine kinase activation in B lymphocytes through processive amplification**. *Immunity* 2000, **13**:47-57.
190. van Kooten C, Banchereau J: **CD40-CD40 ligand**. *J Leukoc Biol* 2000, **67**:2-17.
191. Schneider LC: **X-linked hyper IgM syndrome**. *Clin Rev Allergy Immunol* 2000, **19**:205-215.
192. Dallman C, Johnson PW, Packham G: **Differential regulation of cell survival by CD40**. *Apoptosis* 2003, **8**:45-53.
193. Rothe M, Sarma V, Dixit VM, Goeddel DV: **TRAF2-mediated activation of NF-kappa B by TNF receptor 2 and CD40**. *Science* 1995, **269**:1424-1427.
194. Kashiwada M, Shirakata Y, Inoue JI, Nakano H, Okazaki K, Okumura K, Yamamoto T, Nagaoka H, Takemori T: **Tumor necrosis factor receptor-associated factor 6 (TRAF6) stimulates extracellular signal-regulated kinase (ERK) activity in CD40 signaling along a ras-independent pathway**. *J Exp Med* 1998, **187**:237-244.
195. Grammer AC, Swantek JL, McFarland RD, Miura Y, Geppert T, Lipsky PE: **TNF receptor-associated factor-3 signaling mediates activation of p38 and Jun N-terminal kinase, cytokine secretion, and Ig production following ligation of CD40 on human B cells**. *J Immunol* 1998, **161**:1183-1193.
196. Harnett MM: **CD40: a growing cytoplasmic tale**. *Sci STKE* 2004, **2004**:pe25.
197. Rothstein TL, Wang JK, Panka DJ, Foote LC, Wang Z, Stanger B, Cui H, Ju ST, Marshak-Rothstein A: **Protection against Fas-dependent Th1-mediated apoptosis by antigen receptor engagement in B cells**. *Nature* 1995, **374**:163-165.
198. Wernersson S, Karlsson MC, Dahlstrom J, Mattsson R, Verbeek JS, Heyman B: **IgG-mediated enhancement of antibody responses is low in Fc receptor gamma chain-deficient mice and increased in Fc gamma RII-deficient mice**. *J Immunol* 1999, **163**:618-622.
199. Ravetch JV, Bolland S: **IgG Fc receptors**. *Annu Rev Immunol* 2001, **19**:275-290.
200. Rabinovitch N, Gelfand EW: **Expression of functional activating and inhibitory Fcgamma receptors on human B cells**. *Int Arch Allergy Immunol* 2004, **133**:285-294.
201. Gamberale R, Fernandez-Calotti P, Sanjurjo J, Arrossagaray G, Avalos JS, Geffner J, Giordano M: **Signaling capacity of FcgammaRII isoforms in B-CLL cells**. *Leuk Res* 2005, **29**:1277-1284.
202. Isnardi I, Lesourne R, Bruhns P, Fridman WH, Cambier JC, Daeron M: **Two distinct tyrosine-based motifs enable the inhibitory receptor FcgammaRIIB to cooperatively recruit the**

inositol phosphatases SHIP1/2 and the adapters Grb2/Grap. *J Biol Chem* 2004, **279**:51931-51938.
203. Isnardi I, Bruhns P, Bismuth G, Fridman WH, Daeron M: **The SH2 domain-containing inositol 5-phosphatase SHIP1 is recruited to the intracytoplasmic domain of human FcgammaRIIB and is mandatory for negative regulation of B cell activation**. *Immunol Lett* 2006, **104**:156-165.
204. Chan VW, Meng F, Soriano P, DeFranco AL, Lowell CA: **Characterization of the B lymphocyte populations in Lyn-deficient mice and the role of Lyn in signal initiation and down-regulation**. *Immunity* 1997, **7**:69-81.
205. Liu Q, Oliveira-Dos-Santos AJ, Mariathasan S, Bouchard D, Jones J, Sarao R, Kozieradzki I, Ohashi PS, Penninger JM, Dumont DJ: **The inositol polyphosphate 5-phosphatase ship is a crucial negative regulator of B cell antigen receptor signaling**. *J Exp Med* 1998, **188**:1333-1342.
206. Aman MJ, Lamkin TD, Okada H, Kurosaki T, Ravichandran KS: **The inositol phosphatase SHIP inhibits Akt/PKB activation in B cells**. *J Biol Chem* 1998, **273**:33922-33928.
207. Bolland S, Pearse RN, Kurosaki T, Ravetch JV: **SHIP modulates immune receptor responses by regulating membrane association of Btk**. *Immunity* 1998, **8**:509-516.
208. Damen JE, Liu L, Rosten P, Humphries RK, Jefferson AB, Majerus PW, Krystal G: **The 145-kDa protein induced to associate with Shc by multiple cytokines is an inositol tetraphosphate and phosphatidylinositol 3,4,5-triphosphate 5-phosphatase**. *Proc Natl Acad Sci U S A* 1996, **93**:1689-1693.
209. Brown KS, Blair D, Reid SD, Nicholson EK, Harnett MM: **FcgammaRIIb-mediated negative regulation of BCR signalling is associated with the recruitment of the MAPkinase-phosphatase, Pac-1, and the 3'-inositol phosphatase, PTEN**. *Cell Signal* 2004, **16**:71-80.
210. Luckhoff A, Clapham DE: **Inositol 1,3,4,5-tetrakisphosphate activates an endothelial Ca(2+)-permeable channel**. *Nature* 1992, **355**:356-358.
211. Coggeshall KM: **Inhibitory signaling by B cell Fc gamma RIIb**. *Curr Opin Immunol* 1998, **10**:306-312.
212. Dolmetsch RE, Lewis RS, Goodnow CC, Healy JI: **Differential activation of transcription factors induced by Ca2+ response amplitude and duration**. *Nature* 1997, **386**:855-858.
213. Tridandapani S, Kelley T, Cooney D, Pradhan M, Coggeshall KM: **Negative signaling in B cells: SHIP Grbs Shc**. *Immunol Today* 1997, **18**:424-427.
214. Tamir I, Stolpa JC, Helgason CD, Nakamura K, Bruhns P, Daeron M, Cambier JC: **The RasGAP-binding protein p62dok is a mediator of inhibitory FcgammaRIIB signals in B cells**. *Immunity* 2000, **12**:347-358.
215. Pearse RN, Kawabe T, Bolland S, Guinamard R, Kurosaki T, Ravetch JV: **SHIP recruitment attenuates Fc gamma RIIB-induced B cell apoptosis**. *Immunity* 1999, **10**:753-760.
216. Tzeng SJ, Bolland S, Inabe K, Kurosaki T, Pierce SK: **The B cell inhibitory Fc receptor triggers apoptosis by a novel c-Abl family kinase-dependent pathway**. *J Biol Chem* 2005, **280**:35247-35254.
217. Hershko A, Ciechanover A: **The ubiquitin system**. *Annu Rev Biochem* 1998, **67**:425-479.
218. Mukhopadhyay D, Riezman H: **Proteasome-independent functions of ubiquitin in endocytosis and signaling**. *Science* 2007, **315**:201-205.
219. Coux O, Tanaka K, Goldberg AL: **Structure and functions of the 20S and 26S proteasomes**. *Annu Rev Biochem* 1996, **65**:801-847.
220. Ikeda F, Dikic I: **Atypical ubiquitin chains: new molecular signals. 'Protein Modifications: Beyond the Usual Suspects' review series**. *EMBO Rep* 2008, **9**:536-542.
221. Hicke L: **Protein regulation by monoubiquitin**. *Nat Rev Mol Cell Biol* 2001, **2**:195-201.
222. Haglund K, Sigismund S, Polo S, Szymkiewicz I, Di Fiore PP, Dikic I: **Multiple monoubiquitination of RTKs is sufficient for their endocytosis and degradation**. *Nat Cell Biol* 2003, **5**:461-466.
223. Hochstrasser M: **Ubiquitin, proteasomes, and the regulation of intracellular protein degradation**. *Curr Opin Cell Biol* 1995, **7**:215-223.
224. Baek KH: **Conjugation and deconjugation of ubiquitin regulating the destiny of proteins**. *Exp Mol Med* 2003, **35**:1-7.
225. Hustad CM, Perry WL, Siracusa LD, Rasberry C, Cobb L, Cattanach BM, Kovatch R, Copeland NG, Jenkins NA: **Molecular genetic characterization of six recessive viable alleles of the mouse agouti locus**. *Genetics* 1995, **140**:255-265.

226. Liu YC: **The E3 ubiquitin ligase Itch in T cell activation, differentiation, and tolerance**. *Semin Immunol* 2007, **19**:197-205.
227. Venuprasad K, Elly C, Gao M, Salek-Ardakani S, Harada Y, Luo JL, Yang C, Croft M, Inoue K, Karin M, et al.: **Convergence of Itch-induced ubiquitination with MEKK1-JNK signaling in Th2 tolerance and airway inflammation**. *J Clin Invest* 2006, **116**:1117-1126.
228. Swaminathan G, Tsygankov AY: **The Cbl family proteins: ring leaders in regulation of cell signaling**. *J Cell Physiol* 2006, **209**:21-43.
229. Bachmaier K, Krawczyk C, Kozieradzki I, Kong YY, Sasaki T, Oliveira-dos-Santos A, Mariathasan S, Bouchard D, Wakeham A, Itie A, et al.: **Negative regulation of lymphocyte activation and autoimmunity by the molecular adaptor Cbl-b**. *Nature* 2000, **403**:211-216.
230. Chiang YJ, Kole HK, Brown K, Naramura M, Fukuhara S, Hu RJ, Jang IK, Gutkind JS, Shevach E, Gu H: **Cbl-b regulates the CD28 dependence of T-cell activation**. *Nature* 2000, **403**:216-220.
231. Brembilla NC, Weber J, Rimoldi D, Pradervand S, Schutz F, Pantaleo G, Ruegg C, Quadroni M, Harshman K, Doucey MA: **c-Cbl expression levels regulate the functional responses of human central and effector memory CD4 T cells**. *Blood* 2008, **112**:652-660.
232. Jehn BM, Dittert I, Beyer S, von der Mark K, Bielke W: **c-Cbl binding and ubiquitin-dependent lysosomal degradation of membrane-associated Notch1**. *J Biol Chem* 2002, **277**:8033-8040.
233. Qiu L, Joazeiro C, Fang N, Wang HY, Elly C, Altman Y, Fang D, Hunter T, Liu YC: **Recognition and ubiquitination of Notch by Itch, a hect-type E3 ubiquitin ligase**. *J Biol Chem* 2000, **275**:35734-35737.
234. Haglund K, Dikic I: **Ubiquitylation and cell signaling**. *EMBO J* 2005, **24**:3353-3359.
235. Silverman N, Maniatis T: **NF-kappaB signaling pathways in mammalian and insect innate immunity**. *Genes Dev* 2001, **15**:2321-2342.
236. Rao N, Ghosh AK, Ota S, Zhou P, Reddi AL, Hakezi K, Druker BK, Wu J, Band H: **The non-receptor tyrosine kinase Syk is a target of Cbl-mediated ubiquitylation upon B-cell receptor stimulation**. *EMBO J* 2001, **20**:7085-7095.
237. Zhang M, Veselits M, O'Neill S, Hou P, Reddi AL, Berlin I, Ikeda M, Nash PD, Longnecker R, Band H, et al.: **Ubiquitinylation of Ig beta dictates the endocytic fate of the B cell antigen receptor**. *J Immunol* 2007, **179**:4435-4443.
238. Solomon MJ, Glotzer M, Lee TH, Philippe M, Kirschner MW: **Cyclin activation of p34cdc2**. *Cell* 1990, **63**:1013-1024.
239. Matsushime H, Roussel MF, Ashmun RA, Sherr CJ: **Colony-stimulating factor 1 regulates novel cyclins during the G1 phase of the cell cycle**. *Cell* 1991, **65**:701-713.
240. Albanese C, Johnson J, Watanabe G, Eklund N, Vu D, Arnold A, Pestell RG: **Transforming p21ras mutants and c-Ets-2 activate the cyclin D1 promoter through distinguishable regions**. *J Biol Chem* 1995, **270**:23589-23597.
241. Diehl JA, Cheng M, Roussel MF, Sherr CJ: **Glycogen synthase kinase-3beta regulates cyclin D1 proteolysis and subcellular localization**. *Genes Dev* 1998, **12**:3499-3511.
242. Kato J, Matsushime H, Hiebert SW, Ewen ME, Sherr CJ: **Direct binding of cyclin D to the retinoblastoma gene product (pRb) and pRb phosphorylation by the cyclin D-dependent kinase CDK4**. *Genes Dev* 1993, **7**:331-342.
243. Ikeda MA, Jakoi L, Nevins JR: **A unique role for the Rb protein in controlling E2F accumulation during cell growth and differentiation**. *Proc Natl Acad Sci U S A* 1996, **93**:3215-3220.
244. Helin K, Wu CL, Fattaey AR, Lees JA, Dynlacht BD, Ngwu C, Harlow E: **Heterodimerization of the transcription factors E2F-1 and DP-1 leads to cooperative trans-activation**. *Genes Dev* 1993, **7**:1850-1861.
245. Ohtani K: **Implication of transcription factor E2F in regulation of DNA replication**. *Front Biosci* 1999, **4**:D793-804.
246. Geng Y, Eaton EN, Picon M, Roberts JM, Lundberg AS, Gifford A, Sardet C, Weinberg RA: **Regulation of cyclin E transcription by E2Fs and retinoblastoma protein**. *Oncogene* 1996, **12**:1173-1180.
247. Lundberg AS, Weinberg RA: **Functional inactivation of the retinoblastoma protein requires sequential modification by at least two distinct cyclin-cdk complexes**. *Mol Cell Biol* 1998, **18**:753-761.

248. Koff A, Giordano A, Desai D, Yamashita K, Harper JW, Elledge S, Nishimoto T, Morgan DO, Franza BR, Roberts JM: **Formation and activation of a cyclin E-cdk2 complex during the G1 phase of the human cell cycle**. *Science* 1992, **257**:1689-1694.
249. Clurman BE, Sheaff RJ, Thress K, Groudine M, Roberts JM: **Turnover of cyclin E by the ubiquitin-proteasome pathway is regulated by cdk2 binding and cyclin phosphorylation**. *Genes Dev* 1996, **10**:1979-1990.
250. Vlach J, Hennecke S, Amati B: **Phosphorylation-dependent degradation of the cyclin-dependent kinase inhibitor p27**. *Embo J* 1997, **16**:5334-5344.
251. Pines J, Hunter T: **Human cyclin A is adenovirus E1A-associated protein p60 and behaves differently from cyclin B**. *Nature* 1990, **346**:760-763.
252. Cardoso MC, Leonhardt H, Nadal-Ginard B: **Reversal of terminal differentiation and control of DNA replication: cyclin A and Cdk2 specifically localize at subnuclear sites of DNA replication**. *Cell* 1993, **74**:979-992.
253. O'Farrell PH: **Triggering the all-or-nothing switch into mitosis**. *Trends Cell Biol* 2001, **11**:512-519.
254. Smits VA, Medema RH: **Checking out the G(2)/M transition**. *Biochim Biophys Acta* 2001, **1519**:1-12.
255. Papst PJ, Sugiyama H, Nagasawa M, Lucas JJ, Maller JL, Terada N: **Cdc2-cyclin B phosphorylates p70 S6 kinase on Ser411 at mitosis**. *J Biol Chem* 1998, **273**:15077-15084.
256. Kaldis P: **The cdk-activating kinase (CAK): from yeast to mammals**. *Cell Mol Life Sci* 1999, **55**:284-296.
257. Fisher RP, Morgan DO: **A novel cyclin associates with MO15/CDK7 to form the CDK-activating kinase**. *Cell* 1994, **78**:713-724.
258. Hannon GJ, Casso D, Beach D: **KAP: a dual specificity phosphatase that interacts with cyclin-dependent kinases**. *Proc Natl Acad Sci U S A* 1994, **91**:1731-1735.
259. Mueller PR, Coleman TR, Kumagai A, Dunphy WG: **Myt1: a membrane-associated inhibitory kinase that phosphorylates Cdc2 on both threonine-14 and tyrosine-15**. *Science* 1995, **270**:86-90.
260. Parker LL, Piwnica-Worms H: **Inactivation of the p34cdc2-cyclin B complex by the human WEE1 tyrosine kinase**. *Science* 1992, **257**:1955-1957.
261. Honda R, Ohba Y, Nagata A, Okayama H, Yasuda H: **Dephosphorylation of human p34cdc2 kinase on both Thr-14 and Tyr-15 by human cdc25B phosphatase**. *FEBS Lett* 1993, **318**:331-334.
262. Hoffmann I, Draetta G, Karsenti E: **Activation of the phosphatase activity of human cdc25A by a cdk2-cyclin E dependent phosphorylation at the G1/S transition**. *Embo J* 1994, **13**:4302-4310.
263. Vidal A, Koff A: **Cell-cycle inhibitors: three families united by a common cause**. *Gene* 2000, **247**:1-15.
264. Tsvetkov LM, Yeh KH, Lee SJ, Sun H, Zhang H: **p27(Kip1) ubiquitination and degradation is regulated by the SCF(Skp2) complex through phosphorylated Thr187 in p27**. *Curr Biol* 1999, **9**:661-664.
265. Marti A, Wirbelauer C, Scheffner M, Krek W: **Interaction between ubiquitin-protein ligase SCFSKP2 and E2F-1 underlies the regulation of E2F-1 degradation**. *Nat Cell Biol* 1999, **1**:14-19.
266. O'Hagan RC, Ohh M, David G, de Alboran IM, Alt FW, Kaelin WG, Jr., DePinho RA: **Myc-enhanced expression of Cul1 promotes ubiquitin-dependent proteolysis and cell cycle progression**. *Genes Dev* 2000, **14**:2185-2191.
267. Adhikary S, Eilers M: **Transcriptional regulation and transformation by Myc proteins**. *Nat Rev Mol Cell Biol* 2005, **6**:635-645.
268. Herold S, Herkert B, Eilers M: **Facilitating replication under stress: an oncogenic function of MYC?** *Nat Rev Cancer* 2009, **9**:441-444.
269. Blackwood EM, Luscher B, Eisenman RN: **Myc and Max associate in vivo**. *Genes Dev* 1992, **6**:71-80.
270. Blackwell TK, Kretzner L, Blackwood EM, Eisenman RN, Weintraub H: **Sequence-specific DNA binding by the c-Myc protein**. *Science* 1990, **250**:1149-1151.
271. Blackwell TK, Huang J, Ma A, Kretzner L, Alt FW, Eisenman RN, Weintraub H: **Binding of myc proteins to canonical and noncanonical DNA sequences**. *Mol Cell Biol* 1993, **13**:5216-5224.

272. Mao DY, Watson JD, Yan PS, Barsyte-Lovejoy D, Khosravi F, Wong WW, Farnham PJ, Huang TH, Penn LZ: **Analysis of Myc bound loci identified by CpG island arrays shows that Max is essential for Myc-dependent repression**. *Curr Biol* 2003, **13**:882-886.
273. Dang CV, O'Donnell KA, Zeller KI, Nguyen T, Osthus RC, Li F: **The c-Myc target gene network**. *Semin Cancer Biol* 2006, **16**:253-264.
274. Bouchard C, Dittrich O, Kiermaier A, Dohmann K, Menkel A, Eilers M, Luscher B: **Regulation of cyclin D2 gene expression by the Myc/Max/Mad network: Myc-dependent TRRAP recruitment and histone acetylation at the cyclin D2 promoter**. *Genes Dev* 2001, **15**:2042-2047.
275. Hermeking H, Rago C, Schuhmacher M, Li Q, Barrett JF, Obaya AJ, O'Connell BC, Mateyak MK, Tam W, Kohlhuber F, et al.: **Identification of CDK4 as a target of c-MYC**. *Proc Natl Acad Sci U S A* 2000, **97**:2229-2234.
276. Seoane J, Le HV, Massague J: **Myc suppression of the p21(Cip1) Cdk inhibitor influences the outcome of the p53 response to DNA damage**. *Nature* 2002, **419**:729-734.
277. Staller P, Peukert K, Kiermaier A, Seoane J, Lukas J, Karsunky H, Moroy T, Bartek J, Massague J, Hanel F, et al.: **Repression of p15INK4b expression by Myc through association with Miz-1**. *Nat Cell Biol* 2001, **3**:392-399.
278. Yang W, Shen J, Wu M, Arsura M, FitzGerald M, Suldan Z, Kim DW, Hofmann CS, Pianetti S, Romieu-Mourez R, et al.: **Repression of transcription of the p27(Kip1) cyclin-dependent kinase inhibitor gene by c-Myc**. *Oncogene* 2001, **20**:1688-1702.
279. Xu G, Shi Y: **Apoptosis signaling pathways and lymphocyte homeostasis**. *Cell Res* 2007, **17**:759-771.
280. Nicholson DW: **Caspase structure, proteolytic substrates, and function during apoptotic cell death**. *Cell Death Differ* 1999, **6**:1028-1042.
281. Edinger AL, Thompson CB: **Death by design: apoptosis, necrosis and autophagy**. *Curr Opin Cell Biol* 2004, **16**:663-669.
282. Strasser A, Jost PJ, Nagata S: **The many roles of FAS receptor signaling in the immune system**. *Immunity* 2009, **30**:180-192.
283. Irmler M, Thome M, Hahne M, Schneider P, Hofmann K, Steiner V, Bodmer JL, Schroter M, Burns K, Mattmann C, et al.: **Inhibition of death receptor signals by cellular FLIP**. *Nature* 1997, **388**:190-195.
284. Krammer PH: **CD95's deadly mission in the immune system**. *Nature* 2000, **407**:789-795.
285. Youle RJ, Strasser A: **The BCL-2 protein family: opposing activities that mediate cell death**. *Nat Rev Mol Cell Biol* 2008, **9**:47-59.
286. Guzman-Rojas L, Sims-Mourtada JC, Rangel R, Martinez-Valdez H: **Life and death within germinal centres: a double-edged sword**. *Immunology* 2002, **107**:167-175.
287. Shi Y: **Mechanical aspects of apoptosome assembly**. *Curr Opin Cell Biol* 2006, **18**:677-684.
288. Green DR, Kroemer G: **The pathophysiology of mitochondrial cell death**. *Science* 2004, **305**:626-629.
289. Oda E, Ohki R, Murasawa H, Nemoto J, Shibue T, Yamashita T, Tokino T, Taniguchi T, Tanaka N: **Noxa, a BH3-only member of the Bcl-2 family and candidate mediator of p53-induced apoptosis**. *Science* 2000, **288**:1053-1058.
290. Nakano K, Vousden KH: **PUMA, a novel proapoptotic gene, is induced by p53**. *Mol Cell* 2001, **7**:683-694.
291. Yu J, Zhang L, Hwang PM, Kinzler KW, Vogelstein B: **PUMA induces the rapid apoptosis of colorectal cancer cells**. *Mol Cell* 2001, **7**:673-682.
292. Dijkers PF, Medema RH, Lammers JW, Koenderman L, Coffer PJ: **Expression of the pro-apoptotic Bcl-2 family member Bim is regulated by the forkhead transcription factor FKHR-L1**. *Curr Biol* 2000, **10**:1201-1204.
293. Puthalakath H, O'Reilly LA, Gunn P, Lee L, Kelly PN, Huntington ND, Hughes PD, Michalak EM, McKimm-Breschkin J, Motoyama N, et al.: **ER stress triggers apoptosis by activating BH3-only protein Bim**. *Cell* 2007, **129**:1337-1349.
294. Katz E, Lord C, Ford CA, Gauld SB, Carter NA, Harnett MM: **Bcl-(xL) antagonism of BCR-coupled mitochondrial phospholipase A(2) signaling correlates with protection from apoptosis in WEHI-231 B cells**. *Blood* 2004, **103**:168-176.
295. Roberg K, Johansson U, Ollinger K: **Lysosomal release of cathepsin D precedes relocation of cytochrome c and loss of mitochondrial transmembrane potential during apoptosis induced by oxidative stress**. *Free Radic Biol Med* 1999, **27**:1228-1237.

296. Guicciardi ME, Deussing J, Miyoshi H, Bronk SF, Svingen PA, Peters C, Kaufmann SH, Gores GJ: **Cathepsin B contributes to TNF-alpha-mediated hepatocyte apoptosis by promoting mitochondrial release of cytochrome c**. *J Clin Invest* 2000, **106**:1127-1137.
297. Goll DE, Thompson VF, Li H, Wei W, Cong J: **The calpain system**. *Physiol Rev* 2003, **83**:731-801.
298. Gil-Parrado S, Fernandez-Montalvan A, Assfalg-Machleidt I, Popp O, Bestvater F, Holloschi A, Knoch TA, Auerswald EA, Welsh K, Reed JC, et al.: **Ionomycin-activated calpain triggers apoptosis. A probable role for Bcl-2 family members**. *J Biol Chem* 2002, **277**:27217-27226.
299. Squier MK, Miller AC, Malkinson AM, Cohen JJ: **Calpain activation in apoptosis**. *J Cell Physiol* 1994, **159**:229-237.
300. Wood DE, Thomas A, Devi LA, Berman Y, Beavis RC, Reed JC, Newcomb EW: **Bax cleavage is mediated by calpain during drug-induced apoptosis**. *Oncogene* 1998, **17**:1069-1078.
301. Waterhouse NJ, Finucane DM, Green DR, Elce JS, Kumar S, Alnemri ES, Litwack G, Khanna K, Lavin MF, Watters DJ: **Calpain activation is upstream of caspases in radiation-induced apoptosis**. *Cell Death Differ* 1998, **5**:1051-1061.
302. Porn-Ares MI, Samali A, Orrenius S: **Cleavage of the calpain inhibitor, calpastatin, during apoptosis**. *Cell Death Differ* 1998, **5**:1028-1033.
303. Wolf BB, Goldstein JC, Stennicke HR, Beere H, Amarante-Mendes GP, Salvesen GS, Green DR: **Calpain functions in a caspase-independent manner to promote apoptosis-like events during platelet activation**. *Blood* 1999, **94**:1683-1692.
304. Vancompernolle K, Van Herreweghe F, Pynaert G, Van de Craen M, De Vos K, Totty N, Sterling A, Fiers W, Vandenabeele P, Grooten J: **Atractyloside-induced release of cathepsin B, a protease with caspase-processing activity**. *FEBS Lett* 1998, **438**:150-158.
305. Lotem J, Sachs L: **Differential suppression by protease inhibitors and cytokines of apoptosis induced by wild-type p53 and cytotoxic agents**. *Proc Natl Acad Sci U S A* 1996, **93**:12507-12512.
306. Sandes E, Lodillinsky C, Cwirenbaum R, Arguelles C, Casabe A, Eijan AM: **Cathepsin B is involved in the apoptosis intrinsic pathway induced by Bacillus Calmette-Guerin in transitional cancer cell lines**. *Int J Mol Med* 2007, **20**:823-828.
307. Katz E, Deehan MR, Seatter S, Lord C, Sturrock RD, Harnett MM: **B cell receptor-stimulated mitochondrial phospholipase A2 activation and resultant disruption of mitochondrial membrane potential correlate with the induction of apoptosis in WEHI-231 B cells**. *J Immunol* 2001, **166**:137-147.
308. Conus S, Perozzo R, Reinheckel T, Peters C, Scapozza L, Yousefi S, Simon HU: **Caspase-8 is activated by cathepsin D initiating neutrophil apoptosis during the resolution of inflammation**. *J Exp Med* 2008, **205**:685-698.
309. Carter NA: **Dissection of the differential mechanisms of apoptosis used during B cell maturation**. Glasgow: University of Glasgow: 2006.
310. Gauld SB, Blair D, Moss CA, Reid SD, Harnett MM: **Differential roles for extracellularly regulated kinase-mitogen-activated protein kinase in B cell antigen receptor-induced apoptosis and CD40-mediated rescue of WEHI-231 immature B cells**. *J Immunol* 2002, **168**:3855-3864.
311. Grierson AM, Mitchell P, Adams CL, Mowat AM, Brewer JM, Harnett MM, Garside P: **Direct quantitation of T cell signaling by laser scanning cytometry**. *J Immunol Methods* 2005, **301**:140-153.
312. Morton AM: **Investigation of T cell signalling events regulating immunity and tolerance in vivo**. Glasgow: University of Glasgow: 2007.
313. Bedner E, Li X, Gorczyca W, Melamed MR, Darzynkiewicz Z: **Analysis of apoptosis by laser scanning cytometry**. *Cytometry* 1999, **35**:181-195.
314. Kawasaki M, Sasaki K, Satoh T, Kurose A, Kamada T, Furuya T, Murakami T, Todoroki T: **Laser scanning cytometry (LCS) allows detailed analysis of the cell cycle in PI stained human fibroblasts (TIG-7)**. *Cell Prolif* 1997, **30**:139-147.
315. Luther E, Kamentsky LA: **Resolution of mitotic cells using laser scanning cytometry**. *Cytometry* 1996, **23**:272-278.
316. Mason CS, Springer CJ, Cooper RG, Superti-Furga G, Marshall CJ, Marais R: **Serine and tyrosine phosphorylations cooperate in Raf-1, but not B-Raf activation**. *EMBO J* 1999, **18**:2137-2148.

317. Ausubel FM, Brent, R., Kingdom, R. E., Moore, D. M., Seidman, J. G., Smith, J. A., Struhl, K. (Ed): *Current Protocols in Molecular Biology* New York: John Wiley & Sons; 1995.
318. Gilbert JJ, Stewart A, Courtney CA, Fleming MC, Reid P, Jackson CG, Wise A, Wakelam MJ, Harnett MM: **Antigen receptors on immature, but not mature, B and T cells are coupled to cytosolic phospholipase A2 activation: expression and activation of cytosolic phospholipase A2 correlate with lymphocyte maturation**. *J Immunol* 1996, **156**:2054-2061.
319. Gilbert JJ, Pettitt TR, Seatter SD, Reid SD, Wakelam MJ, Harnett MM: **Antagonistic roles for phospholipase D activities in B cell signaling: while the antigen receptors transduce mitogenic signals via a novel phospholipase D activity, phosphatidylcholine-phospholipase D mediates antiproliferative signals**. *J Immunol* 1998, **161**:6575-6584.
320. Yellen AJ, Glenn W, Sukhatme VP, Cao XM, Monroe JG: **Signaling through surface IgM in tolerance-susceptible immature murine B lymphocytes. Developmentally regulated differences in transmembrane signaling in splenic B cells from adult and neonatal mice**. *J Immunol* 1991, **146**:1446-1454.
321. Monroe JG, Dorshkind K: **Fate decisions regulating bone marrow and peripheral B lymphocyte development**. *Adv Immunol* 2007, **95**:1-50.
322. King LB, Norvell A, Monroe JG: **Antigen receptor-induced signal transduction imbalances associated with the negative selection of immature B cells**. *J Immunol* 1999, **162**:2655-2662.
323. Gugasyan R, Grumont R, Grossmann M, Nakamura Y, Pohl T, Nesic D, Gerondakis S: **Rel/NF-kappaB transcription factors: key mediators of B-cell activation**. *Immunol Rev* 2000, **176**:134-140.
324. Fischer G, Kent SC, Joseph L, Green DR, Scott DW: **Lymphoma models for B cell activation and tolerance. X. Anti-mu-mediated growth arrest and apoptosis of murine B cell lymphomas is prevented by the stabilization of myc**. *J Exp Med* 1994, **179**:221-228.
325. Goodnow CC, Crosbie J, Adelstein S, Lavoie TB, Smith-Gill SJ, Brink RA, Pritchard-Briscoe H, Wotherspoon JS, Loblay RH, Raphael K, et al.: **Altered immunoglobulin expression and functional silencing of self-reactive B lymphocytes in transgenic mice**. *Nature* 1988, **334**:676-682.
326. Refaeli Y, Field KA, Turner BC, Trumpp A, Bishop JM: **The protooncogene MYC can break B cell tolerance**. *Proc Natl Acad Sci U S A* 2005, **102**:4097-4102.
327. Gupta N, DeFranco AL: **Lipid rafts and B cell signaling**. *Semin Cell Dev Biol* 2007, **18**:616-626.
328. Sproul TW, Malapati S, Kim J, Pierce SK: **Cutting edge: B cell antigen receptor signaling occurs outside lipid rafts in immature B cells**. *J Immunol* 2000, **165**:6020-6023.
329. Karnell FG, Brezski RJ, King LB, Silverman MA, Monroe JG: **Membrane cholesterol content accounts for developmental differences in surface B cell receptor compartmentalization and signaling**. *J Biol Chem* 2005, **280**:25621-25628.
330. Sandel PC, Gendelman M, Kelsoe G, Monroe JG: **Definition of a novel cellular constituent of the bone marrow that regulates the response of immature B cells to B cell antigen receptor engagement**. *J Immunol* 2001, **166**:5935-5944.
331. Richards JD, Dave SH, Chou CH, Mamchak AA, DeFranco AL: **Inhibition of the MEK/ERK signaling pathway blocks a subset of B cell responses to antigen**. *J Immunol* 2001, **166**:3855-3864.
332. Kashiwada M, Kaneko Y, Yagita H, Okumura K, Takemori T: **Activation of mitogen-activated protein kinases via CD40 is distinct from that stimulated by surface IgM on B cells**. *Eur J Immunol* 1996, **26**:1451-1458.
333. Lee JR, Koretzky GA: **Extracellular signal-regulated kinase-2, but not c-Jun NH2-terminal kinase, activation correlates with surface IgM-mediated apoptosis in the WEHI 231 B cell line**. *J Immunol* 1998, **161**:1637-1644.
334. Choi MS, Boise LH, Gottschalk AR, Quintans J, Thompson CB, Klaus GG: **The role of bcl-XL in CD40-mediated rescue from anti-mu-induced apoptosis in WEHI-231 B lymphoma cells**. *Eur J Immunol* 1995, **25**:1352-1357.
335. Hirai H, Adachi T, Tsubata T: **Involvement of cell cycle progression in survival signaling through CD40 in the B-lymphocyte line WEHI-231**. *Cell Death Differ* 2004, **11**:261-269.

336. Ishida T, Kobayashi N, Tojo T, Ishida S, Yamamoto T, Inoue J: **CD40 signaling-mediated induction of Bcl-XL, Cdk4, and Cdk6. Implication of their cooperation in selective B cell growth**. *J Immunol* 1995, **155**:5527-5535.
337. Merino R, Grillot DA, Simonian PL, Muthukkumar S, Fanslow WC, Bondada S, Nunez G: **Modulation of anti-IgM-induced B cell apoptosis by Bcl-xL and CD40 in WEHI-231 cells. Dissociation from cell cycle arrest and dependence on the avidity of the antibody-IgM receptor interaction**. *J Immunol* 1995, **155**:3830-3838.
338. Craxton A, Chuang PI, Shu G, Harlan JM, Clark EA: **The CD40-inducible Bcl-2 family member A1 protects B cells from antigen receptor-mediated apoptosis**. *Cell Immunol* 2000, **200**:56-62.
339. Fujino H, Xu W, Regan JW: **Prostaglandin E2 induced functional expression of early growth response factor-1 by EP4, but not EP2, prostanoid receptors via the phosphatidylinositol 3-kinase and extracellular signal-regulated kinases**. *J Biol Chem* 2003, **278**:12151-12156.
340. Eblen ST, Slack-Davis JK, Tarcsafalvi A, Parsons JT, Weber MJ, Catling AD: **Mitogen-activated protein kinase feedback phosphorylation regulates MEK1 complex formation and activation during cellular adhesion**. *Mol Cell Biol* 2004, **24**:2308-2317.
341. Dougherty MK, Muller J, Ritt DA, Zhou M, Zhou XZ, Copeland TD, Conrads TP, Veenstra TD, Lu KP, Morrison DK: **Regulation of Raf-1 by direct feedback phosphorylation**. *Mol Cell* 2005, **17**:215-224.
342. Douville E, Downward J: **EGF induced SOS phosphorylation in PC12 cells involves P90 RSK-2**. *Oncogene* 1997, **15**:373-383.
343. Brondello JM, Pouyssegur J, McKenzie FR: **Reduced MAP kinase phosphatase-1 degradation after p42/p44MAPK-dependent phosphorylation**. *Science* 1999, **286**:2514-2517.
344. Ramos JW: **The regulation of extracellular signal-regulated kinase (ERK) in mammalian cells**. *Int J Biochem Cell Biol* 2008, **40**:2707-2719.
345. Claperon A, Therrien M: **KSR and CNK: two scaffolds regulating RAS-mediated RAF activation**. *Oncogene* 2007, **26**:3143-3158.
346. Denouel-Galy A, Douville EM, Warne PH, Papin C, Laugier D, Calothy G, Downward J, Eychene A: **Murine Ksr interacts with MEK and inhibits Ras-induced transformation**. *Curr Biol* 1998, **8**:46-55.
347. Yu W, Fantl WJ, Harrowe G, Williams LT: **Regulation of the MAP kinase pathway by mammalian Ksr through direct interaction with MEK and ERK**. *Curr Biol* 1998, **8**:56-64.
348. Nguyen A, Burack WR, Stock JL, Kortum R, Chaika OV, Afkarian M, Muller WJ, Murphy KM, Morrison DK, Lewis RE, et al.: **Kinase suppressor of Ras (KSR) is a scaffold which facilitates mitogen-activated protein kinase activation in vivo**. *Mol Cell Biol* 2002, **22**:3035-3045.
349. Schaeffer HJ, Catling AD, Eblen ST, Collier LS, Krauss A, Weber MJ: **MP1: a MEK binding partner that enhances enzymatic activation of the MAP kinase cascade**. *Science* 1998, **281**:1668-1671.
350. Keyse SM: **Protein phosphatases and the regulation of mitogen-activated protein kinase signalling**. *Curr Opin Cell Biol* 2000, **12**:186-192.
351. Saxena M, Williams S, Tasken K, Mustelin T: **Crosstalk between cAMP-dependent kinase and MAP kinase through a protein tyrosine phosphatase**. *Nat Cell Biol* 1999, **1**:305-311.
352. Saxena M, Mustelin T: **Extracellular signals and scores of phosphatases: all roads lead to MAP kinase**. *Semin Immunol* 2000, **12**:387-396.
353. Pettiford SM, Herbst R: **The protein tyrosine phosphatase HePTP regulates nuclear translocation of ERK2 and can modulate megakaryocytic differentiation of K562 cells**. *Leukemia* 2003, **17**:366-378.
354. Tarrega C, Blanco-Aparicio C, Munoz JJ, Pulido R: **Two clusters of residues at the docking groove of mitogen-activated protein kinases differentially mediate their functional interaction with the tyrosine phosphatases PTP-SL and STEP**. *J Biol Chem* 2002, **277**:2629-2636.
355. Krishna M, Narang H: **The complexity of mitogen-activated protein kinases (MAPKs) made simple**. *Cell Mol Life Sci* 2008, **65**:3525-3544.
356. Bhalla US, Ram PT, Iyengar R: **MAP kinase phosphatase as a locus of flexibility in a mitogen-activated protein kinase signaling network**. *Science* 2002, **297**:1018-1023.

357. Sontag E, Fedorov S, Kamibayashi C, Robbins D, Cobb M, Mumby M: **The interaction of SV40 small tumor antigen with protein phosphatase 2A stimulates the map kinase pathway and induces cell proliferation**. *Cell* 1993, **75**:887-897.
358. Kins S, Kurosinski P, Nitsch RM, Gotz J: **Activation of the ERK and JNK signaling pathways caused by neuron-specific inhibition of PP2A in transgenic mice**. *Am J Pathol* 2003, **163**:833-843.
359. Kondoh K, Nishida E: **Regulation of MAP kinases by MAP kinase phosphatases**. *Biochim Biophys Acta* 2007, **1773**:1227-1237.
360. Karlsson M, Mathers J, Dickinson RJ, Mandl M, Keyse SM: **Both nuclear-cytoplasmic shuttling of the dual specificity phosphatase MKP-3 and its ability to anchor MAP kinase in the cytoplasm are mediated by a conserved nuclear export signal**. *J Biol Chem* 2004, **279**:41882-41891.
361. Brondello JM, Brunet A, Pouyssegur J, McKenzie FR: **The dual specificity mitogen-activated protein kinase phosphatase-1 and -2 are induced by the p42/p44MAPK cascade**. *J Biol Chem* 1997, **272**:1368-1376.
362. Lin YW, Chuang SM, Yang JL: **ERK1/2 achieves sustained activation by stimulating MAPK phosphatase-1 degradation via the ubiquitin-proteasome pathway**. *J Biol Chem* 2003, **278**:21534-21541.
363. Chu Y, Solski PA, Khosravi-Far R, Der CJ, Kelly K: **The mitogen-activated protein kinase phosphatases PAC1, MKP-1, and MKP-2 have unique substrate specificities and reduced activity in vivo toward the ERK2 sevenmaker mutation**. *J Biol Chem* 1996, **271**:6497-6501.
364. Matsuguchi T, Musikacharoen T, Johnson TR, Kraft AS, Yoshikai Y: **A novel mitogen-activated protein kinase phosphatase is an important negative regulator of lipopolysaccharide-mediated c-Jun N-terminal kinase activation in mouse macrophage cell lines**. *Mol Cell Biol* 2001, **21**:6999-7009.
365. Rohan PJ, Davis P, Moskaluk CA, Kearns M, Krutzsch H, Siebenlist U, Kelly K: **PAC-1: a mitogen-induced nuclear protein tyrosine phosphatase**. *Science* 1993, **259**:1763-1766.
366. Grumont RJ, Rasko JE, Strasser A, Gerondakis S: **Activation of the mitogen-activated protein kinase pathway induces transcription of the PAC-1 phosphatase gene**. *Mol Cell Biol* 1996, **16**:2913-2921.
367. Jeffrey KL, Brummer T, Rolph MS, Liu SM, Callejas NA, Grumont RJ, Gillieron C, Mackay F, Grey S, Camps M, et al.: **Positive regulation of immune cell function and inflammatory responses by phosphatase PAC-1**. *Nat Immunol* 2006, **7**:274-283.
368. Ward Y, Gupta S, Jensen P, Wartmann M, Davis RJ, Kelly K: **Control of MAP kinase activation by the mitogen-induced threonine/tyrosine phosphatase PAC1**. *Nature* 1994, **367**:651-654.
369. Yin Y, Liu YX, Jin YJ, Hall EJ, Barrett JC: **PAC1 phosphatase is a transcription target of p53 in signalling apoptosis and growth suppression**. *Nature* 2003, **422**:527-531.
370. Meloche S, Seuwen K, Pages G, Pouyssegur J: **Biphasic and synergistic activation of p44mapk (ERK1) by growth factors: correlation between late phase activation and mitogenicity**. *Mol Endocrinol* 1992, **6**:845-854.
371. Pages G, Lenormand P, L'Allemain G, Chambard JC, Meloche S, Pouyssegur J: **Mitogen-activated protein kinases p42mapk and p44mapk are required for fibroblast proliferation**. *Proc Natl Acad Sci U S A* 1993, **90**:8319-8323.
372. Meloche S, Pouyssegur J: **The ERK1/2 mitogen-activated protein kinase pathway as a master regulator of the G1- to S-phase transition**. *Oncogene* 2007, **26**:3227-3239.
373. Gauld SB: **Differential roles of ERK-MAPKinase in WEHI-231 cell apoptosis and growth**. Glasgow: University of Glasgow: 2000.
374. Yamamoto T, Ebisuya M, Ashida F, Okamoto K, Yonehara S, Nishida E: **Continuous ERK activation downregulates antiproliferative genes throughout G1 phase to allow cell-cycle progression**. *Curr Biol* 2006, **16**:1171-1182.
375. Flynn A, Proud CG: **Insulin and phorbol ester stimulate initiation factor eIF-4E phosphorylation by distinct pathways in Chinese hamster ovary cells overexpressing the insulin receptor**. *Eur J Biochem* 1996, **236**:40-47.
376. Morley SJ, McKendrick L: **Involvement of stress-activated protein kinase and p38/RK mitogen-activated protein kinase signaling pathways in the enhanced phosphorylation of initiation factor 4E in NIH 3T3 cells**. *J Biol Chem* 1997, **272**:17887-17893.

377. Ueda T, Watanabe-Fukunaga R, Fukuyama H, Nagata S, Fukunaga R: **Mnk2 and Mnk1 are essential for constitutive and inducible phosphorylation of eukaryotic initiation factor 4E but not for cell growth or development**. *Mol Cell Biol* 2004, **24**:6539-6549.
378. Wullschleger S, Loewith R, Hall MN: **TOR signaling in growth and metabolism**. *Cell* 2006, **124**:471-484.
379. Ma L, Chen Z, Erdjument-Bromage H, Tempst P, Pandolfi PP: **Phosphorylation and functional inactivation of TSC2 by Erk implications for tuberous sclerosis and cancer pathogenesis**. *Cell* 2005, **121**:179-193.
380. Roux PP, Ballif BA, Anjum R, Gygi SP, Blenis J: **Tumor-promoting phorbol esters and activated Ras inactivate the tuberous sclerosis tumor suppressor complex via p90 ribosomal S6 kinase**. *Proc Natl Acad Sci U S A* 2004, **101**:13489-13494.
381. Topisirovic I, Ruiz-Gutierrez M, Borden KL: **Phosphorylation of the eukaryotic translation initiation factor eIF4E contributes to its transformation and mRNA transport activities**. *Cancer Res* 2004, **64**:8639-8642.
382. Jones TR, Cole MD: **Rapid cytoplasmic turnover of c-myc mRNA: requirement of the 3' untranslated sequences**. *Mol Cell Biol* 1987, **7**:4513-4521.
383. Kelly K, Cochran BH, Stiles CD, Leder P: **Cell-specific regulation of the c-myc gene by lymphocyte mitogens and platelet-derived growth factor**. *Cell* 1983, **35**:603-610.
384. Vervoorts J, Luscher-Firzlaff J, Luscher B: **The ins and outs of MYC regulation by posttranslational mechanisms**. *J Biol Chem* 2006, **281**:34725-34729.
385. Henriksson M, Bakardjiev A, Klein G, Luscher B: **Phosphorylation sites mapping in the N-terminal domain of c-myc modulate its transforming potential**. *Oncogene* 1993, **8**:3199-3209.
386. Lutterbach B, Hann SR: **Hierarchical phosphorylation at N-terminal transformation-sensitive sites in c-Myc protein is regulated by mitogens and in mitosis**. *Mol Cell Biol* 1994, **14**:5510-5522.
387. Hann SR: **Role of post-translational modifications in regulating c-Myc proteolysis, transcriptional activity and biological function**. *Semin Cancer Biol* 2006, **16**:288-302.
388. Gregory MA, Qi Y, Hann SR: **Phosphorylation by glycogen synthase kinase-3 controls c-myc proteolysis and subnuclear localization**. *J Biol Chem* 2003, **278**:51606-51612.
389. von der Lehr N, Johansson S, Wu S, Bahram F, Castell A, Cetinkaya C, Hydbring P, Weidung I, Nakayama K, Nakayama KI, et al.: **The F-box protein Skp2 participates in c-Myc proteosomal degradation and acts as a cofactor for c-Myc-regulated transcription**. *Mol Cell* 2003, **11**:1189-1200.
390. Welcker M, Orian A, Jin J, Grim JE, Harper JW, Eisenman RN, Clurman BE: **The Fbw7 tumor suppressor regulates glycogen synthase kinase 3 phosphorylation-dependent c-Myc protein degradation**. *Proc Natl Acad Sci U S A* 2004, **101**:9085-9090.
391. Ayer DE, Kretzner L, Eisenman RN: **Mad: a heterodimeric partner for Max that antagonizes Myc transcriptional activity**. *Cell* 1993, **72**:211-222.
392. Hurlin PJ, Queva C, Eisenman RN: **Mnt, a novel Max-interacting protein is coexpressed with Myc in proliferating cells and mediates repression at Myc binding sites**. *Genes Dev* 1997, **11**:44-58.
393. Bos JL, Rehmann H, Wittinghofer A: **GEFs and GAPs: critical elements in the control of small G proteins**. *Cell* 2007, **129**:865-877.
394. Raaijmakers JH, Bos JL: **Specificity in Ras and Rap signaling**. *J Biol Chem* 2009, **284**:10995-10999.
395. Ohba Y, Mochizuki N, Matsuo K, Yamashita S, Nakaya M, Hashimoto Y, Hamaguchi M, Kurata T, Nagashima K, Matsuda M: **Rap2 as a slowly responding molecular switch in the Rap1 signaling cascade**. *Mol Cell Biol* 2000, **20**:6074-6083.
396. Minato N, Kometani K, Hattori M: **Regulation of immune responses and hematopoiesis by the Rap1 signal**. *Adv Immunol* 2007, **93**:229-264.
397. Ichiba T, Hashimoto Y, Nakaya M, Kuraishi Y, Tanaka S, Kurata T, Mochizuki N, Matsuda M: **Activation of C3G guanine nucleotide exchange factor for Rap1 by phosphorylation of tyrosine 504**. *J Biol Chem* 1999, **274**:14376-14381.
398. Barber DL, Mason JM, Fukazawa T, Reedquist KA, Druker BJ, Band H, D'Andrea AD: **Erythropoietin and interleukin-3 activate tyrosine phosphorylation of CBL and association with CRK adaptor proteins**. *Blood* 1997, **89**:3166-3174.
399. Kirsch KH, Georgescu MM, Hanafusa H: **Direct binding of p130(Cas) to the guanine nucleotide exchange factor C3G**. *J Biol Chem* 1998, **273**:25673-25679.

400. Sakkab D, Lewitzky M, Posern G, Schaeper U, Sachs M, Birchmeier W, Feller SM: **Signaling of hepatocyte growth factor/scatter factor (HGF) to the small GTPase Rap1 via the large docking protein Gab1 and the adapter protein CRKL**. *J Biol Chem* 2000, **275**:10772-10778.
401. Kawasaki H, Springett GM, Toki S, Canales JJ, Harlan P, Blumenstiel JP, Chen EJ, Bany IA, Mochizuki N, Ashbacher A, et al.: **A Rap guanine nucleotide exchange factor enriched highly in the basal ganglia**. *Proc Natl Acad Sci U S A* 1998, **95**:13278-13283.
402. Bos JL: **Epac: a new cAMP target and new avenues in cAMP research**. *Nat Rev Mol Cell Biol* 2003, **4**:733-738.
403. Daumke O, Weyand M, Chakrabarti PP, Vetter IR, Wittinghofer A: **The GTPase-activating protein Rap1GAP uses a catalytic asparagine**. *Nature* 2004, **429**:197-201.
404. Pak DT, Yang S, Rudolph-Correia S, Kim E, Sheng M: **Regulation of dendritic spine morphology by SPAR, a PSD-95-associated RapGAP**. *Neuron* 2001, **31**:289-303.
405. Hattori M, Tsukamoto N, Nur-e-Kamal MS, Rubinfeld B, Iwai K, Kubota H, Maruta H, Minato N: **Molecular cloning of a novel mitogen-inducible nuclear protein with a Ran GTPase-activating domain that affects cell cycle progression**. *Mol Cell Biol* 1995, **15**:552-560.
406. Kitayama H, Sugimoto Y, Matsuzaki T, Ikawa Y, Noda M: **A ras-related gene with transformation suppressor activity**. *Cell* 1989, **56**:77-84.
407. Boussiotis VA, Freeman GJ, Berezovskaya A, Barber DL, Nadler LM: **Maintenance of human T cell anergy: blocking of IL-2 gene transcription by activated Rap1**. *Science* 1997, **278**:124-128.
408. Reedquist KA, Bos JL: **Costimulation through CD28 suppresses T cell receptor-dependent activation of the Ras-like small GTPase Rap1 in human T lymphocytes**. *J Biol Chem* 1998, **273**:4944-4949.
409. Morton AM, McManus B, Garside P, Mowat AM, Harnett MM: **Inverse Rap1 and phospho-ERK expression discriminate the maintenance phase of tolerance and priming of antigen-specific CD4+ T cells in vitro and in vivo**. *J Immunol* 2007, **179**:8026-8034.
410. Li L, Greenwald RJ, Lafuente EM, Tzachanis D, Berezovskaya A, Freeman GJ, Sharpe AH, Boussiotis VA: **Rap1-GTP is a negative regulator of Th cell function and promotes the generation of CD4+CD103+ regulatory T cells in vivo**. *J Immunol* 2005, **175**:3133-3139.
411. Vossler MR, Yao H, York RD, Pan MG, Rim CS, Stork PJ: **cAMP activates MAP kinase and Elk-1 through a B-Raf- and Rap1-dependent pathway**. *Cell* 1997, **89**:73-82.
412. Dillon TJ, Karpitski V, Wetzel SA, Parker DC, Shaw AS, Stork PJ: **Ectopic B-Raf expression enhances extracellular signal-regulated kinase (ERK) signaling in T cells and prevents antigen-presenting cell-induced anergy**. *J Biol Chem* 2003, **278**:35940-35949.
413. Reedquist KA, Ross E, Koop EA, Wolthuis RM, Zwartkruis FJ, van Kooyk Y, Salmon M, Buckley CD, Bos JL: **The small GTPase, Rap1, mediates CD31-induced integrin adhesion**. *J Cell Biol* 2000, **148**:1151-1158.
414. Schmidt A, Caron E, Hall A: **Lipopolysaccharide-induced activation of beta2-integrin function in macrophages requires Irak kinase activity, p38 mitogen- activated protein kinase, and the Rap1 GTPase**. *Mol Cell Biol* 2001, **21**:438-448.
415. Bos JL: **Linking Rap to cell adhesion**. *Curr Opin Cell Biol* 2005, **17**:123-128.
416. Katagiri K, Hattori M, Minato N, Irie S, Takatsu K, Kinashi T: **Rap1 is a potent activation signal for leukocyte function-associated antigen 1 distinct from protein kinase C and phosphatidylinositol-3-OH kinase**. *Mol Cell Biol* 2000, **20**:1956-1969.
417. Katagiri K, Hattori M, Minato N, Kinashi T: **Rap1 functions as a key regulator of T-cell and antigen-presenting cell interactions and modulates T-cell responses**. *Mol Cell Biol* 2002, **22**:1001-1015.
418. McLeod SJ, Ingham RJ, Bos JL, Kurosaki T, Gold MR: **Activation of the Rap1 GTPase by the B cell antigen receptor**. *J Biol Chem* 1998, **273**:29218-29223.
419. Christian SL, Lee RL, McLeod SJ, Burgess AE, Li AH, Dang-Lawson M, Lin KB, Gold MR: **Activation of the Rap GTPases in B lymphocytes modulates B cell antigen receptor-induced activation of Akt but has no effect on MAPK activation**. *J Biol Chem* 2003, **278**:41756-41767.
420. Sawada Y, Nakamura K, Doi K, Takeda K, Tobiume K, Saitoh M, Morita K, Komuro I, De Vos K, Sheetz M, et al.: **Rap1 is involved in cell stretching modulation of p38 but not ERK or JNK MAP kinase**. *J Cell Sci* 2001, **114**:1221-1227.
421. Tamada M, Sheetz MP, Sawada Y: **Activation of a signaling cascade by cytoskeleton stretch**. *Dev Cell* 2004, **7**:709-718.

422. Stork PJ: **Does Rap1 deserve a bad Rap?** *Trends Biochem Sci* 2003, **28**:267-275.
423. Chu H, Awasthi A, White GC, 2nd, Chrzanowska-Wodnicka M, Malarkannan S: **Rap1b regulates B cell development, homing, and T cell-dependent humoral immunity**. *J Immunol* 2008, **181**:3373-3383.
424. Chen Y, Yu M, Podd A, Wen R, Chrzanowska-Wodnicka M, White GC, Wang D: **A critical role of Rap1b in B-cell trafficking and marginal zone B-cell development**. *Blood* 2008, **111**:4627-4636.
425. Tse KW, Dang-Lawson M, Lee RL, Vong D, Bulic A, Buckbinder L, Gold MR: **B cell receptor-induced phosphorylation of Pyk2 and focal adhesion kinase involves integrins and the Rap GTPases and is required for B cell spreading**. *J Biol Chem* 2009.
426. Lin KB, Freeman SA, Zabetian S, Brugger H, Weber M, Lei V, Dang-Lawson M, Tse KW, Santamaria R, Batista FD, et al.: **The rap GTPases regulate B cell morphology, immune-synapse formation, and signaling by particulate B cell receptor ligands**. *Immunity* 2008, **28**:75-87.
427. Li Y, Yan J, De P, Chang HC, Yamauchi A, Christopherson KW, 2nd, Paranavitana NC, Peng X, Kim C, Munugalavadla V, et al.: **Rap1a null mice have altered myeloid cell functions suggesting distinct roles for the closely related Rap1a and 1b proteins**. *J Immunol* 2007, **179**:8322-8331.
428. Katayama Y, Sekai M, Hattori M, Miyoshi I, Hamazaki Y, Minato N: **Rap signaling is crucial for the competence of IL-7 response and the development of B-lineage cells**. *Blood* 2009.
429. Ishida D, Su L, Tamura A, Katayama Y, Kawai Y, Wang SF, Taniwaki M, Hamazaki Y, Hattori M, Minato N: **Rap1 signal controls B cell receptor repertoire and generation of self-reactive B1a cells**. *Immunity* 2006, **24**:417-427.
430. Fang S, Weissman AM: **A field guide to ubiquitylation**. *Cell Mol Life Sci* 2004, **61**:1546-1561.
431. Huang F, Gu H: **Negative regulation of lymphocyte development and function by the Cbl family of proteins**. *Immunol Rev* 2008, **224**:229-238.
432. Meng W, Sawasdikosol S, Burakoff SJ, Eck MJ: **Structure of the amino-terminal domain of Cbl complexed to its binding site on ZAP-70 kinase**. *Nature* 1999, **398**:84-90.
433. Joazeiro CA, Wing SS, Huang H, Leverson JD, Hunter T, Liu YC: **The tyrosine kinase negative regulator c-Cbl as a RING-type, E2-dependent ubiquitin-protein ligase**. *Science* 1999, **286**:309-312.
434. Levkowitz G, Waterman H, Zamir E, Kam Z, Oved S, Langdon WY, Beguinot L, Geiger B, Yarden Y: **c-Cbl/Sli-1 regulates endocytic sorting and ubiquitination of the epidermal growth factor receptor**. *Genes Dev* 1998, **12**:3663-3674.
435. Mosesson Y, Shtiegman K, Katz M, Zwang Y, Vereb G, Szollosi J, Yarden Y: **Endocytosis of receptor tyrosine kinases is driven by monoubiquitylation, not polyubiquitylation**. *J Biol Chem* 2003, **278**:21323-21326.
436. Fang D, Liu YC: **Proteolysis-independent regulation of PI3K by Cbl-b-mediated ubiquitination in T cells**. *Nat Immunol* 2001, **2**:870-875.
437. Fang D, Wang HY, Fang N, Altman Y, Elly C, Liu YC: **Cbl-b, a RING-type E3 ubiquitin ligase, targets phosphatidylinositol 3-kinase for ubiquitination in T cells**. *J Biol Chem* 2001, **276**:4872-4878.
438. Shao Y, Elly C, Liu YC: **Negative regulation of Rap1 activation by the Cbl E3 ubiquitin ligase**. *EMBO Rep* 2003, **4**:425-431.
439. Yasuda T, Tezuka T, Maeda A, Inazu T, Yamanashi Y, Gu H, Kurosaki T, Yamamoto T: **Cbl-b positively regulates Btk-mediated activation of phospholipase C-gamma2 in B cells**. *J Exp Med* 2002, **196**:51-63.
440. Yasuda T, Maeda A, Kurosaki M, Tezuka T, Hironaka K, Yamamoto T, Kurosaki T: **Cbl suppresses B cell receptor-mediated phospholipase C (PLC)-gamma2 activation by regulating B cell linker protein-PLC-gamma2 binding**. *J Exp Med* 2000, **191**:641-650.
441. Sohn HW, Gu H, Pierce SK: **Cbl-b negatively regulates B cell antigen receptor signaling in mature B cells through ubiquitination of the tyrosine kinase Syk**. *J Exp Med* 2003, **197**:1511-1524.
442. Kitaura Y, Jang IK, Wang Y, Han YC, Inazu T, Cadera EJ, Schlissel M, Hardy RR, Gu H: **Control of the B cell-intrinsic tolerance programs by ubiquitin ligases Cbl and Cbl-b**. *Immunity* 2007, **26**:567-578.

443. Naramura M, Jang IK, Kole H, Huang F, Haines D, Gu H: **c-Cbl and Cbl-b regulate T cell responsiveness by promoting ligand-induced TCR down-modulation**. *Nat Immunol* 2002, **3**:1192-1199.
444. Hasbold J, Klaus GG: **Anti-immunoglobulin antibodies induce apoptosis in immature B cell lymphomas**. *Eur J Immunol* 1990, **20**:1685-1690.
445. Scott DW, Tuttle J, Livnat D, Haynes W, Cogswell JP, Keng P: **Lymphoma models for B-cell activation and tolerance. II. Growth inhibition by anti-mu of WEHI-231 and the selection and properties of resistant mutants**. *Cell Immunol* 1985, **93**:124-131.
446. Villanueva J, Yung Y, Walker JL, Assoian RK: **ERK activity and G1 phase progression: identifying dispensable versus essential activities and primary versus secondary targets**. *Mol Biol Cell* 2007, **18**:1457-1463.
447. Ford CA: **Differential regulation of Erk-MAPK in the control of survival and proliferation of immature B cells**. Glasgow: University of Glasgow: 2004.
448. Tran NH, Wu X, Frost JA: **B-Raf and Raf-1 are regulated by distinct autoregulatory mechanisms**. *J Biol Chem* 2005, **280**:16244-16253.
449. Herrmann C, Horn G, Spaargaren M, Wittinghofer A: **Differential interaction of the ras family GTP-binding proteins H-Ras, Rap1A, and R-Ras with the putative effector molecules Raf kinase and Ral-guanine nucleotide exchange factor**. *J Biol Chem* 1996, **271**:6794-6800.
450. Kurachi H, Wada Y, Tsukamoto N, Maeda M, Kubota H, Hattori M, Iwai K, Minato N: **Human SPA-1 gene product selectively expressed in lymphoid tissues is a specific GTPase-activating protein for Rap1 and Rap2. Segregate expression profiles from a rap1GAP gene product**. *J Biol Chem* 1997, **272**:28081-28088.
451. Farina A, Hattori M, Qin J, Nakatani Y, Minato N, Ozato K: **Bromodomain protein Brd4 binds to GTPase-activating SPA-1, modulating its activity and subcellular localization**. *Mol Cell Biol* 2004, **24**:9059-9069.
452. Owens DM, Keyse SM: **Differential regulation of MAP kinase signalling by dual-specificity protein phosphatases**. *Oncogene* 2007, **26**:3203-3213.
453. Blair D: **Signalling mechanisms regulating proliferation and apoptosis in immature and mature B cells**. Glasgow: University of Glasgow: 2004.
454. Rodriguez-Viciana P, Warne PH, Vanhaesebroeck B, Waterfield MD, Downward J: **Activation of phosphoinositide 3-kinase by interaction with Ras and by point mutation**. *EMBO J* 1996, **15**:2442-2451.
455. Banerji L, Glassford J, Lea NC, Thomas NS, Klaus GG, Lam EW: **BCR signals target p27(Kip1) and cyclin D2 via the PI3-K signalling pathway to mediate cell cycle arrest and apoptosis of WEHI 231 B cells**. *Oncogene* 2001, **20**:7352-7367.
456. Bivona TG, Wiener HH, Ahearn IM, Silletti J, Chiu VK, Philips MR: **Rap1 up-regulation and activation on plasma membrane regulates T cell adhesion**. *J Cell Biol* 2004, **164**:461-470.
457. Sun L, Xie P, Wada J, Kashihara N, Liu FY, Zhao Y, Kumar D, Chugh SS, Danesh FR, Kanwar YS: **Rap1b GTPase ameliorates glucose-induced mitochondrial dysfunction**. *J Am Soc Nephrol* 2008, **19**:2293-2301.
458. Wang Z, Dillon TJ, Pokala V, Mishra S, Labudda K, Hunter B, Stork PJ: **Rap1-mediated activation of extracellular signal-regulated kinases by cyclic AMP is dependent on the mode of Rap1 activation**. *Mol Cell Biol* 2006, **26**:2130-2145.
459. Wu C, Lai CF, Mobley WC: **Nerve growth factor activates persistent Rap1 signaling in endosomes**. *J Neurosci* 2001, **21**:5406-5416.
460. Kolch W: **Coordinating ERK/MAPK signalling through scaffolds and inhibitors**. *Nat Rev Mol Cell Biol* 2005, **6**:827-837.
461. Kholodenko BN: **MAP kinase cascade signaling and endocytic trafficking: a marriage of convenience?** *Trends Cell Biol* 2002, **12**:173-177.
462. Teis D, Wunderlich W, Huber LA: **Localization of the MP1-MAPK scaffold complex to endosomes is mediated by p14 and required for signal transduction**. *Dev Cell* 2002, **3**:803-814.
463. Lefloch R, Pouyssegur J, Lenormand P: **Single and combined silencing of ERK1 and ERK2 reveals their positive contribution to growth signaling depending on their expression levels**. *Mol Cell Biol* 2008, **28**:511-527.

464. Vantaggiato C, Formentini I, Bondanza A, Bonini C, Naldini L, Brambilla R: **ERK1 and ERK2 mitogen-activated protein kinases affect Ras-dependent cell signaling differentially**. *J Biol* 2006, **5**:14.
465. Fremin C, Ezan F, Boisselier P, Bessard A, Pages G, Pouyssegur J, Baffet G: **ERK2 but not ERK1 plays a key role in hepatocyte replication: an RNAi-mediated ERK2 knockdown approach in wild-type and ERK1 null hepatocytes**. *Hepatology* 2007, **45**:1035-1045.
466. Levine RA, McCormack JE, Buckler A, Sonenshein GE: **Transcriptional and posttranscriptional control of c-myc gene expression in WEHI 231 cells**. *Mol Cell Biol* 1986, **6**:4112-4116.
467. Wu M, Arsura M, Bellas RE, FitzGerald MJ, Lee H, Schauer SL, Sherr DH, Sonenshein GE: **Inhibition of c-myc expression induces apoptosis of WEHI 231 murine B cells**. *Mol Cell Biol* 1996, **16**:5015-5025.
468. Schauer SL, Wang Z, Sonenshein GE, Rothstein TL: **Maintenance of nuclear factor-kappa B/Rel and c-myc expression during CD40 ligand rescue of WEHI 231 early B cells from receptor-mediated apoptosis through modulation of I kappa B proteins**. *J Immunol* 1996, **157**:81-86.
469. Yeh E, Cunningham M, Arnold H, Chasse D, Monteith T, Ivaldi G, Hahn WC, Stukenberg PT, Shenolikar S, Uchida T, et al.: **A signalling pathway controlling c-Myc degradation that impacts oncogenic transformation of human cells**. *Nat Cell Biol* 2004, **6**:308-318.
470. Dominguez-Sola D, Dalla-Favera R: **PINning down the c-Myc oncoprotein**. *Nat Cell Biol* 2004, **6**:288-289.
471. Sears R, Nuckolls F, Haura E, Taya Y, Tamai K, Nevins JR: **Multiple Ras-dependent phosphorylation pathways regulate Myc protein stability**. *Genes Dev* 2000, **14**:2501-2514.
472. Junttila MR, Westermarck J: **Mechanisms of MYC stabilization in human malignancies**. *Cell Cycle* 2008, **7**:592-596.
473. Karn J, Watson JV, Lowe AD, Green SM, Vedeckis W: **Regulation of cell cycle duration by c-myc levels**. *Oncogene* 1989, **4**:773-787.
474. Mateyak MK, Obaya AJ, Adachi S, Sedivy JM: **Phenotypes of c-Myc-deficient rat fibroblasts isolated by targeted homologous recombination**. *Cell Growth Differ* 1997, **8**:1039-1048.
475. Filippova GN, Fagerlie S, Klenova EM, Myers C, Dehner Y, Goodwin G, Neiman PE, Collins SJ, Lobanenkov VV: **An exceptionally conserved transcriptional repressor, CTCF, employs different combinations of zinc fingers to bind diverged promoter sequences of avian and mammalian c-myc oncogenes**. *Mol Cell Biol* 1996, **16**:2802-2813.
476. Qi CF, Martensson A, Mattioli M, Dalla-Favera R, Lobanenkov VV, Morse HC, 3rd: **CTCF functions as a critical regulator of cell-cycle arrest and death after ligation of the B cell receptor on immature B cells**. *Proc Natl Acad Sci U S A* 2003, **100**:633-638.
477. Klenova EM, Chernukhin IV, El-Kady A, Lee RE, Pugacheva EM, Loukinov DI, Goodwin GH, Delgado D, Filippova GN, Leon J, et al.: **Functional phosphorylation sites in the C-terminal region of the multivalent multifunctional transcriptional factor CTCF**. *Mol Cell Biol* 2001, **21**:2221-2234.
478. Slingerland J, Pagano M: **Regulation of the cdk inhibitor p27 and its deregulation in cancer**. *J Cell Physiol* 2000, **183**:10-17.
479. Carrano AC, Eytan E, Hershko A, Pagano M: **SKP2 is required for ubiquitin-mediated degradation of the CDK inhibitor p27**. *Nat Cell Biol* 1999, **1**:193-199.
480. Coller HA, Grandori C, Tamayo P, Colbert T, Lander ES, Eisenman RN, Golub TR: **Expression analysis with oligonucleotide microarrays reveals that MYC regulates genes involved in growth, cell cycle, signaling, and adhesion**. *Proc Natl Acad Sci U S A* 2000, **97**:3260-3265.
481. Wu M, Bellas RE, Shen J, Yang W, Sonenshein GE: **Increased p27Kip1 cyclin-dependent kinase inhibitor gene expression following anti-IgM treatment promotes apoptosis of WEHI 231 B cells**. *J Immunol* 1999, **163**:6530-6535.
482. Kawada M, Yamagoe S, Murakami Y, Suzuki K, Mizuno S, Uehara Y: **Induction of p27Kip1 degradation and anchorage independence by Ras through the MAP kinase signaling pathway**. *Oncogene* 1997, **15**:629-637.
483. Abbas T, Dutta A: **p21 in cancer: intricate networks and multiple activities**. *Nat Rev Cancer* 2009, **9**:400-414.

484. Villunger A, Michalak EM, Coultas L, Mullauer F, Bock G, Ausserlechner MJ, Adams JM, Strasser A: **p53- and drug-induced apoptotic responses mediated by BH3-only proteins puma and noxa**. *Science* 2003, **302**:1036-1038.
485. Miyashita T, Reed JC: **Tumor suppressor p53 is a direct transcriptional activator of the human bax gene**. *Cell* 1995, **80**:293-299.
486. Mihara M, Erster S, Zaika A, Petrenko O, Chittenden T, Pancoska P, Moll UM: **p53 has a direct apoptogenic role at the mitochondria**. *Mol Cell* 2003, **11**:577-590.
487. Sun A, Bagella L, Tutton S, Romano G, Giordano A: **From G0 to S phase: a view of the roles played by the retinoblastoma (Rb) family members in the Rb-E2F pathway**. *J Cell Biochem* 2007, **102**:1400-1404.
488. Kitagawa M, Higashi H, Jung HK, Suzuki-Takahashi I, Ikeda M, Tamai K, Kato J, Segawa K, Yoshida E, Nishimura S, et al.: **The consensus motif for phosphorylation by cyclin D1-Cdk4 is different from that for phosphorylation by cyclin A/E-Cdk2**. *EMBO J* 1996, **15**:7060-7069.
489. Bouchard C, Thieke K, Maier A, Saffrich R, Hanley-Hyde J, Ansorge W, Reed S, Sicinski P, Bartek J, Eilers M: **Direct induction of cyclin D2 by Myc contributes to cell cycle progression and sequestration of p27**. *EMBO J* 1999, **18**:5321-5333.
490. Piatelli MJ, Doughty C, Chiles TC: **Requirement for a hsp90 chaperone-dependent MEK1/2-ERK pathway for B cell antigen receptor-induced cyclin D2 expression in mature B lymphocytes**. *J Biol Chem* 2002, **277**:12144-12150.
491. Muller D, Bouchard C, Rudolph B, Steiner P, Stuckmann I, Saffrich R, Ansorge W, Huttner W, Eilers M: **Cdk2-dependent phosphorylation of p27 facilitates its Myc-induced release from cyclin E/cdk2 complexes**. *Oncogene* 1997, **15**:2561-2576.
492. Liu YC: **Ubiquitin ligases and the immune response**. *Annu Rev Immunol* 2004, **22**:81-127.
493. York RD, Yao H, Dillon T, Ellig CL, Eckert SP, McCleskey EW, Stork PJ: **Rap1 mediates sustained MAP kinase activation induced by nerve growth factor**. *Nature* 1998, **392**:622-626.
494. Sasagawa S, Ozaki Y, Fujita K, Kuroda S: **Prediction and validation of the distinct dynamics of transient and sustained ERK activation**. *Nat Cell Biol* 2005, **7**:365-373.
495. Smit L, van der Horst G, Borst J: **Sos, Vav, and C3G participate in B cell receptor-induced signaling pathways and differentially associate with Shc-Grb2, Crk, and Crk-L adaptors**. *J Biol Chem* 1996, **271**:8564-8569.
496. Ichiba T, Kuraishi Y, Sakai O, Nagata S, Groffen J, Kurata T, Hattori S, Matsuda M: **Enhancement of guanine-nucleotide exchange activity of C3G for Rap1 by the expression of Crk, CrkL, and Grb2**. *J Biol Chem* 1997, **272**:22215-22220.
497. Wu SY, Chiang CM: **The double bromodomain-containing chromatin adaptor Brd4 and transcriptional regulation**. *J Biol Chem* 2007, **282**:13141-13145.
498. Beranger F, Tavitian A, de Gunzburg J: **Post-translational processing and subcellular localization of the Ras-related Rap2 protein**. *Oncogene* 1991, **6**:1835-1842.
499. Uechi Y, Bayarjargal M, Umikawa M, Oshiro M, Takei K, Yamashiro Y, Asato T, Endo S, Misaki R, Taguchi T, et al.: **Rap2 function requires palmitoylation and recycling endosome localization**. *Biochem Biophys Res Commun* 2009, **378**:732-737.
500. Pizon V, Desjardins M, Bucci C, Parton RG, Zerial M: **Association of Rap1a and Rap1b proteins with late endocytic/phagocytic compartments and Rap2a with the Golgi complex**. *J Cell Sci* 1994, **107 (Pt 6)**:1661-1670.
501. Burack WR, Shaw AS: **Live Cell Imaging of ERK and MEK: simple binding equilibrium explains the regulated nucleocytoplasmic distribution of ERK**. *J Biol Chem* 2005, **280**:3832-3837.
502. Brunet A, Roux D, Lenormand P, Dowd S, Keyse S, Pouyssegur J: **Nuclear translocation of p42/p44 mitogen-activated protein kinase is required for growth factor-induced gene expression and cell cycle entry**. *EMBO J* 1999, **18**:664-674.
503. Tohgo A, Pierce KL, Choy EW, Lefkowitz RJ, Luttrell LM: **beta-Arrestin scaffolding of the ERK cascade enhances cytosolic ERK activity but inhibits ERK-mediated transcription following angiotensin AT1a receptor stimulation**. *J Biol Chem* 2002, **277**:9429-9436.
504. Balmanno K, Cook SJ: **Sustained MAP kinase activation is required for the expression of cyclin D1, p21Cip1 and a subset of AP-1 proteins in CCL39 cells**. *Oncogene* 1999, **18**:3085-3097.

505. Solvason N, Wu WW, Kabra N, Wu X, Lees E, Howard MC: **Induction of cell cycle regulatory proteins in anti-immunoglobulin-stimulated mature B lymphocytes**. *J Exp Med* 1996, **184**:407-417.
506. Solvason N, Wu WW, Parry D, Mahony D, Lam EW, Glassford J, Klaus GG, Sicinski P, Weinberg R, Liu YJ, et al.: **Cyclin D2 is essential for BCR-mediated proliferation and CD5 B cell development**. *Int Immunol* 2000, **12**:631-638.
507. Martino A, Holmes JHt, Lord JD, Moon JJ, Nelson BH: **Stat5 and Sp1 regulate transcription of the cyclin D2 gene in response to IL-2**. *J Immunol* 2001, **166**:1723-1729.
508. Pircher TJ, Petersen H, Gustafsson JA, Haldosen LA: **Extracellular signal-regulated kinase (ERK) interacts with signal transducer and activator of transcription (STAT) 5a**. *Mol Endocrinol* 1999, **13**:555-565.
509. Heikkila R, Schwab G, Wickstrom E, Loke SL, Pluznik DH, Watt R, Neckers LM: **A c-myc antisense oligodeoxynucleotide inhibits entry into S phase but not progress from G0 to G1**. *Nature* 1987, **328**:445-449.
510. Vervoorts J, Luscher B: **Post-translational regulation of the tumor suppressor p27(KIP1)**. *Cell Mol Life Sci* 2008, **65**:3255-3264.
511. Keller UB, Old JB, Dorsey FC, Nilsson JA, Nilsson L, MacLean KH, Chung L, Yang C, Spruck C, Boyd K, et al.: **Myc targets Cks1 to provoke the suppression of p27Kip1, proliferation and lymphomagenesis**. *EMBO J* 2007, **26**:2562-2574.
512. Gartel AL, Serfas MS, Tyner AL: **p21--negative regulator of the cell cycle**. *Proc Soc Exp Biol Med* 1996, **213**:138-149.
513. Ho JS, Ma W, Mao DY, Benchimol S: **p53-Dependent transcriptional repression of c-myc is required for G1 cell cycle arrest**. *Mol Cell Biol* 2005, **25**:7423-7431.
514. Sachdeva M, Zhu S, Wu F, Wu H, Walia V, Kumar S, Elble R, Watabe K, Mo YY: **p53 represses c-Myc through induction of the tumor suppressor miR-145**. *Proc Natl Acad Sci U S A* 2009, **106**:3207-3212.
515. Momand J, Zambetti GP, Olson DC, George D, Levine AJ: **The mdm-2 oncogene product forms a complex with the p53 protein and inhibits p53-mediated transactivation**. *Cell* 1992, **69**:1237-1245.
516. Haupt Y, Maya R, Kazaz A, Oren M: **Mdm2 promotes the rapid degradation of p53**. *Nature* 1997, **387**:296-299.
517. Malmlof M, Roudier E, Hogberg J, Stenius U: **MEK-ERK-mediated phosphorylation of Mdm2 at Ser-166 in hepatocytes. Mdm2 is activated in response to inhibited Akt signaling**. *J Biol Chem* 2007, **282**:2288-2296.
518. Phelps M, Phillips A, Darley M, Blaydes JP: **MEK-ERK signaling controls Hdm2 oncoprotein expression by regulating hdm2 mRNA export to the cytoplasm**. *J Biol Chem* 2005, **280**:16651-16658.
519. Ries S, Biederer C, Woods D, Shifman O, Shirasawa S, Sasazuki T, McMahon M, Oren M, McCormick F: **Opposing effects of Ras on p53: transcriptional activation of mdm2 and induction of p19ARF**. *Cell* 2000, **103**:321-330.
520. Mayo LD, Donner DB: **A phosphatidylinositol 3-kinase/Akt pathway promotes translocation of Mdm2 from the cytoplasm to the nucleus**. *Proc Natl Acad Sci U S A* 2001, **98**:11598-11603.
521. Prochownik EV: **c-Myc: linking transformation and genomic instability**. *Curr Mol Med* 2008, **8**:446-458.
522. Matsuzawa A, Tseng PH, Vallabhapurapu S, Luo JL, Zhang W, Wang H, Vignali DA, Gallagher E, Karin M: **Essential cytoplasmic translocation of a cytokine receptor-assembled signaling complex**. *Science* 2008, **321**:663-668.
523. Lamothe B, Besse A, Campos AD, Webster WK, Wu H, Darnay BG: **Site-specific Lys-63-linked tumor necrosis factor receptor-associated factor 6 auto-ubiquitination is a critical determinant of I kappa B kinase activation**. *J Biol Chem* 2007, **282**:4102-4112.
524. Patnaik A, Chau V, Wills JW: **Ubiquitin is part of the retrovirus budding machinery**. *Proc Natl Acad Sci U S A* 2000, **97**:13069-13074.
525. Skaug B, Jiang X, Chen ZJ: **The role of ubiquitin in NF-kappaB regulatory pathways**. *Annu Rev Biochem* 2009, **78**:769-796.
526. Schmidt MH, Dikic I: **The Cbl interactome and its functions**. *Nat Rev Mol Cell Biol* 2005, **6**:907-918.

527. Bustelo XR, Crespo P, Lopez-Barahona M, Gutkind JS, Barbacid M: **Cbl-b, a member of the Sli-1/c-Cbl protein family, inhibits Vav-mediated c-Jun N-terminal kinase activation**. *Oncogene* 1997, **15**:2511-2520.
528. Lin JT, Lineberry NB, Kattah MG, Su LL, Utz PJ, Fathman CG, Wu L: **Naive CD4 t cell proliferation is controlled by mammalian target of rapamycin regulation of GRAIL expression**. *J Immunol* 2009, **182**:5919-5928.
529. Soares L, Seroogy C, Skrenta H, Anandasabapathy N, Lovelace P, Chung CD, Engleman E, Fathman CG: **Two isoforms of otubain 1 regulate T cell anergy via GRAIL**. *Nat Immunol* 2004, **5**:45-54.
530. Grumont RJ, Strasser A, Gerondakis S: **B cell growth is controlled by phosphatidylinosotol 3-kinase-dependent induction of Rel/NF-kappaB regulated c-myc transcription**. *Mol Cell* 2002, **10**:1283-1294.
531. Fruman DA: **Phosphoinositide 3-kinase and its targets in B-cell and T-cell signaling**. *Curr Opin Immunol* 2004, **16**:314-320.
532. Su L, Lineberry N, Huh Y, Soares L, Fathman CG: **A novel E3 ubiquitin ligase substrate screen identifies Rho guanine dissociation inhibitor as a substrate of gene related to anergy in lymphocytes**. *J Immunol* 2006, **177**:7559-7566.
533. Saci A, Carpenter CL: **RhoA GTPase regulates B cell receptor signaling**. *Mol Cell* 2005, **17**:205-214.
534. Cooper GS, Stroehla BC: **The epidemiology of autoimmune diseases**. *Autoimmun Rev* 2003, **2**:119-125.
535. Gilhus NE: **Autoimmune myasthenia gravis**. *Expert Rev Neurother* 2009, **9**:351-358.
536. Weetman AP: **Graves' disease**. *N Engl J Med* 2000, **343**:1236-1248.
537. Stasi R, Evangelista ML, Stipa E, Buccisano F, Venditti A, Amadori S: **Idiopathic thrombocytopenic purpura: current concepts in pathophysiology and management**. *Thromb Haemost* 2008, **99**:4-13.
538. Fairhurst AM, Wandstrat AE, Wakeland EK: **Systemic lupus erythematosus: multiple immunological phenotypes in a complex genetic disease**. *Adv Immunol* 2006, **92**:1-69.
539. MacGregor AJ, Lanchbury J, Rigby AS, Kaprio J, Snieder H: **Using twin studies to label disease as genetic or environmental is inappropriate**. *BMJ* 2002, **324**:1100-1101.
540. Worthington J: **Investigating the genetic basis of susceptibility to rheumatoid arthritis**. *J Autoimmun* 2005, **25 Suppl**:16-20.
541. Liao KP, Alfredsson L, Karlson EW: **Environmental influences on risk for rheumatoid arthritis**. *Curr Opin Rheumatol* 2009, **21**:279-283.
542. Firestein GS: **Evolving concepts of rheumatoid arthritis**. *Nature* 2003, **423**:356-361.
543. Nishimura K, Sugiyama D, Kogata Y, Tsuji G, Nakazawa T, Kawano S, Saigo K, Morinobu A, Koshiba M, Kuntz KM, et al.: **Meta-analysis: diagnostic accuracy of anti-cyclic citrullinated peptide antibody and rheumatoid factor for rheumatoid arthritis**. *Ann Intern Med* 2007, **146**:797-808.
544. Rantapaa-Dahlqvist S, de Jong BA, Berglin E, Hallmans G, Wadell G, Stenlund H, Sundin U, van Venrooij WJ: **Antibodies against cyclic citrullinated peptide and IgA rheumatoid factor predict the development of rheumatoid arthritis**. *Arthritis Rheum* 2003, **48**:2741-2749.
545. Hochberg MC, Silman AJ, Smolen JS, Weinblatt ME, Weisman MH (Ed): *Rheumatoid arthritis* Philadelphia: Mosby Elsevier; 2009.
546. Sibilia J, Gottenberg JE, Mariette X: **Rituximab: a new therapeutic alternative in rheumatoid arthritis**. *Joint Bone Spine* 2008, **75**:526-532.
547. Grimaldi CM, Jeganathan V, Diamond B: **Hormonal regulation of B cell development: 17beta-estradiol impairs negative selection of high-affinity DNA-reactive B cells at more than one developmental checkpoint**. *J Immunol* 2006, **176**:2703-2710.
548. Kotzin BL: **Systemic lupus erythematosus**. *Cell* 1996, **85**:303-306.
549. Grammer AC, Fischer R, Lee O, Zhang X, Lipsky PE: **Flow cytometric assessment of the signaling status of human B lymphocytes from normal and autoimmune individuals**. *Arthritis Res Ther* 2004, **6**:28-38.
550. Folzenlogen D, Hofer MF, Leung DY, Freed JH, Newell MK: **Analysis of CD80 and CD86 expression on peripheral blood B lymphocytes reveals increased expression of CD86 in lupus patients**. *Clin Immunol Immunopathol* 1997, **83**:199-204.
551. Leandro MJ, Edwards JC, Cambridge G: **Clinical outcome in 22 patients with rheumatoid arthritis treated with B lymphocyte depletion**. *Ann Rheum Dis* 2002, **61**:883-888.

552. Takemura S, Klimiuk PA, Braun A, Goronzy JJ, Weyand CM: **T cell activation in rheumatoid synovium is B cell dependent**. *J Immunol* 2001, **167**:4710-4718.
553. Schultze JL, Michalak S, Lowne J, Wong A, Gilleece MH, Gribben JG, Nadler LM: **Human non-germinal center B cell interleukin (IL)-12 production is primarily regulated by T cell signals CD40 ligand, interferon gamma, and IL-10: role of B cells in the maintenance of T cell responses**. *J Exp Med* 1999, **189**:1-12.
554. McInnes IB, Schett G: **Cytokines in the pathogenesis of rheumatoid arthritis**. *Nat Rev Immunol* 2007, **7**:429-442.
555. Mima T, Nishimoto N: **Clinical value of blocking IL-6 receptor**. *Curr Opin Rheumatol* 2009, **21**:224-230.
556. Mantovani L, Wilder RL, Casali P: **Human rheumatoid B-1a (CD5+ B) cells make somatically hypermutated high affinity IgM rheumatoid factors**. *J Immunol* 1993, **151**:473-488.
557. Mohan C, Morel L, Yang P, Wakeland EK: **Accumulation of splenic B1a cells with potent antigen-presenting capability in NZM2410 lupus-prone mice**. *Arthritis Rheum* 1998, **41**:1652-1662.
558. Watanabe N, Ikuta K, Nisitani S, Chiba T, Honjo T: **Activation and differentiation of autoreactive B-1 cells by interleukin 10 induce autoimmune hemolytic anemia in Fas-deficient antierythrocyte immunoglobulin transgenic mice**. *J Exp Med* 2002, **196**:141-146.
559. Segundo C, Rodriguez C, Garcia-Poley A, Aguilar M, Gavilan I, Bellas C, Brieva JA: **Thyroid-infiltrating B lymphocytes in Graves' disease are related to marginal zone and memory B cell compartments**. *Thyroid* 2001, **11**:525-530.
560. Schuster H, Martin T, Marcellin L, Garaud JC, Pasquali JL, Korganow AS: **Expansion of marginal zone B cells is not sufficient for the development of renal disease in NZBxNZW F1 mice**. *Lupus* 2002, **11**:277-286.
561. Wither JE, Paterson AD, Vukusic B: **Genetic dissection of B cell traits in New Zealand black mice. The expanded population of B cells expressing up-regulated costimulatory molecules shows linkage to Nba2**. *Eur J Immunol* 2000, **30**:356-365.
562. Martin F, Kearney JF: **B-cell subsets and the mature preimmune repertoire. Marginal zone and B1 B cells as part of a "natural immune memory"**. *Immunol Rev* 2000, **175**:70-79.
563. Spencer J, Perry ME, Dunn-Walters DK: **Human marginal-zone B cells**. *Immunol Today* 1998, **19**:421-426.
564. Attanavanich K, Kearney JF: **Marginal zone, but not follicular B cells, are potent activators of naive CD4 T cells**. *J Immunol* 2004, **172**:803-811.
565. Viau M, Zouali M: **B-lymphocytes, innate immunity, and autoimmunity**. *Clin Immunol* 2005, **114**:17-26.
566. Yurasov S, Wardemann H, Hammersen J, Tsuiji M, Meffre E, Pascual V, Nussenzweig MC: **Defective B cell tolerance checkpoints in systemic lupus erythematosus**. *J Exp Med* 2005, **201**:703-711.
567. Samuels J, Ng YS, Coupillaud C, Paget D, Meffre E: **Impaired early B cell tolerance in patients with rheumatoid arthritis**. *J Exp Med* 2005, **201**:1659-1667.
568. Tsuiji M, Yurasov S, Velinzon K, Thomas S, Nussenzweig MC, Wardemann H: **A checkpoint for autoreactivity in human IgM+ memory B cell development**. *J Exp Med* 2006, **203**:393-400.
569. Tiller T, Tsuiji M, Yurasov S, Velinzon K, Nussenzweig MC, Wardemann H: **Autoreactivity in human IgG+ memory B cells**. *Immunity* 2007, **26**:205-213.
570. Culton DA, O'Conner BP, Conway KL, Diz R, Rutan J, Vilen BJ, Clarke SH: **Early preplasma cells define a tolerance checkpoint for autoreactive B cells**. *J Immunol* 2006, **176**:790-802.
571. Huang H, Kearney JF, Grusby MJ, Benoist C, Mathis D: **Induction of tolerance in arthritogenic B cells with receptors of differing affinity for self-antigen**. *Proc Natl Acad Sci U S A* 2006, **103**:3734-3739.
572. Stadanlick JE, Cancro MP: **BAFF and the plasticity of peripheral B cell tolerance**. *Curr Opin Immunol* 2008, **20**:158-161.
573. Hsu BL, Harless SM, Lindsley RC, Hilbert DM, Cancro MP: **Cutting edge: BLyS enables survival of transitional and mature B cells through distinct mediators**. *J Immunol* 2002, **168**:5993-5996.

574. Lesley R, Xu Y, Kalled SL, Hess DM, Schwab SR, Shu HB, Cyster JG: **Reduced competitiveness of autoantigen-engaged B cells due to increased dependence on BAFF**. *Immunity* 2004, **20**:441-453.
575. Zhang J, Roschke V, Baker KP, Wang Z, Alarcon GS, Fessler BJ, Bastian H, Kimberly RP, Zhou T: **Cutting edge: a role for B lymphocyte stimulator in systemic lupus erythematosus**. *J Immunol* 2001, **166**:6-10.
576. Nimmerjahn F, Ravetch JV: **Fcgamma receptors as regulators of immune responses**. *Nat Rev Immunol* 2008, **8**:34-47.
577. Clynes R, Maizes JS, Guinamard R, Ono M, Takai T, Ravetch JV: **Modulation of immune complex-induced inflammation in vivo by the coordinate expression of activation and inhibitory Fc receptors**. *J Exp Med* 1999, **189**:179-185.
578. Ujike A, Ishikawa Y, Ono M, Yuasa T, Yoshino T, Fukumoto M, Ravetch JV, Takai T: **Modulation of immunoglobulin (Ig)E-mediated systemic anaphylaxis by low-affinity Fc receptors for IgG**. *J Exp Med* 1999, **189**:1573-1579.
579. Yuasa T, Kubo S, Yoshino T, Ujike A, Matsumura K, Ono M, Ravetch JV, Takai T: **Deletion of fcgamma receptor IIB renders H-2(b) mice susceptible to collagen-induced arthritis**. *J Exp Med* 1999, **189**:187-194.
580. Bolland S, Ravetch JV: **Spontaneous autoimmune disease in Fc(gamma)RIIB-deficient mice results from strain-specific epistasis**. *Immunity* 2000, **13**:277-285.
581. Brownlie RJ, Lawlor KE, Niederer HA, Cutler AJ, Xiang Z, Clatworthy MR, Floto RA, Greaves DR, Lyons PA, Smith KG: **Distinct cell-specific control of autoimmunity and infection by FcgammaRIIb**. *J Exp Med* 2008, **205**:883-895.
582. McGaha TL, Sorrentino B, Ravetch JV: **Restoration of tolerance in lupus by targeted inhibitory receptor expression**. *Science* 2005, **307**:590-593.
583. Moll T, Nitschke L, Carroll M, Ravetch JV, Izui S: **A critical role for Fc gamma RIIB in the induction of rheumatoid factors**. *J Immunol* 2004, **173**:4724-4728.
584. Fukuyama H, Nimmerjahn F, Ravetch JV: **The inhibitory Fcgamma receptor modulates autoimmunity by limiting the accumulation of immunoglobulin G+ anti-DNA plasma cells**. *Nat Immunol* 2005, **6**:99-106.
585. Venkatesh J, Kawabata D, Kim S, Xu X, Chinnasamy P, Paul E, Diamond B, Grimaldi CM: **Selective regulation of autoreactive B cells by FcgammaRIIB**. *J Autoimmun* 2009, **32**:149-157.
586. Rahman ZS, Manser T: **Failed up-regulation of the inhibitory IgG Fc receptor Fc gamma RIIB on germinal center B cells in autoimmune-prone mice is not associated with deletion polymorphisms in the promoter region of the Fc gamma RIIB gene**. *J Immunol* 2005, **175**:1440-1449.
587. Enyedy EJ, Mitchell JP, Nambiar MP, Tsokos GC: **Defective FcgammaRIIb1 signaling contributes to enhanced calcium response in B cells from patients with systemic lupus erythematosus**. *Clin Immunol* 2001, **101**:130-135.
588. Mackay M, Stanevsky A, Wang T, Aranow C, Li M, Koenig S, Ravetch JV, Diamond B: **Selective dysregulation of the Fc{gamma}IIB receptor on memory B cells in SLE**. *J Exp Med* 2006.
589. Kyogoku C, Dijstelbloem HM, Tsuchiya N, Hatta Y, Kato H, Yamaguchi A, Fukazawa T, Jansen MD, Hashimoto H, van de Winkel JG, et al.: **Fcgamma receptor gene polymorphisms in Japanese patients with systemic lupus erythematosus: contribution of FCGR2B to genetic susceptibility**. *Arthritis Rheum* 2002, **46**:1242-1254.
590. Floto RA, Clatworthy MR, Heilbronn KR, Rosner DR, MacAry PA, Rankin A, Lehner PJ, Ouwehand WH, Allen JM, Watkins NA, et al.: **Loss of function of a lupus-associated FcgammaRIIb polymorphism through exclusion from lipid rafts**. *Nat Med* 2005, **11**:1056-1058.
591. Soulas P, Woods A, Jaulhac B, Knapp AM, Pasquali JL, Martin T, Korganow AS: **Autoantigen, innate immunity, and T cells cooperate to break B cell tolerance during bacterial infection**. *J Clin Invest* 2005, **115**:2257-2267.
592. Christensen SR, Kashgarian M, Alexopoulou L, Flavell RA, Akira S, Shlomchik MJ: **Toll-like receptor 9 controls anti-DNA autoantibody production in murine lupus**. *J Exp Med* 2005, **202**:321-331.
593. Ehlers M, Fukuyama H, McGaha TL, Aderem A, Ravetch JV: **TLR9/MyD88 signaling is required for class switching to pathogenic IgG2a and 2b autoantibodies in SLE**. *J Exp Med* 2006, **203**:553-561.

594. Rui L, Vinuesa CG, Blasioli J, Goodnow CC: **Resistance to CpG DNA-induced autoimmunity through tolerogenic B cell antigen receptor ERK signaling**. *Nat Immunol* 2003, **4**:594-600.
595. Gauld SB, Benschop RJ, Merrell KT, Cambier JC: **Maintenance of B cell anergy requires constant antigen receptor occupancy and signaling**. *Nat Immunol* 2005, **6**:1160-1167.
596. Heyman B: **Feedback regulation by IgG antibodies**. *Immunol Lett* 2003, **88**:157-161.
597. Nimmerjahn F, Ravetch JV: **Fcgamma receptors: old friends and new family members**. *Immunity* 2006, **24**:19-28.
598. Datta SR, Dudek H, Tao X, Masters S, Fu H, Gotoh Y, Greenberg ME: **Akt phosphorylation of BAD couples survival signals to the cell-intrinsic death machinery**. *Cell* 1997, **91**:231-241.
599. Budd RC, Yeh WC, Tschopp J: **cFLIP regulation of lymphocyte activation and development**. *Nat Rev Immunol* 2006, **6**:196-204.
600. Green DR, Kroemer G: **Cytoplasmic functions of the tumour suppressor p53**. *Nature* 2009, **458**:1127-1130.
601. Riley T, Sontag E, Chen P, Levine A: **Transcriptional control of human p53-regulated genes**. *Nat Rev Mol Cell Biol* 2008, **9**:402-412.
602. Chipuk JE, Kuwana T, Bouchier-Hayes L, Droin NM, Newmeyer DD, Schuler M, Green DR: **Direct activation of Bax by p53 mediates mitochondrial membrane permeabilization and apoptosis**. *Science* 2004, **303**:1010-1014.
603. Shibue T, Takeda K, Oda E, Tanaka H, Murasawa H, Takaoka A, Morishita Y, Akira S, Taniguchi T, Tanaka N: **Integral role of Noxa in p53-mediated apoptotic response**. *Genes Dev* 2003, **17**:2233-2238.
604. Day CL, Smits C, Fan FC, Lee EF, Fairlie WD, Hinds MG: **Structure of the BH3 domains from the p53-inducible BH3-only proteins Noxa and Puma in complex with Mcl-1**. *J Mol Biol* 2008, **380**:958-971.
605. Han J, Goldstein LA, Hou W, Rabinowich H: **Functional linkage between NOXA and Bim in mitochondrial apoptotic events**. *J Biol Chem* 2007, **282**:16223-16231.
606. Hassan M, Alaoui A, Feyen O, Mirmohammadsadegh A, Essmann F, Tannapfel A, Gulbins E, Schulze-Osthoff K, Hengge UR: **The BH3-only member Noxa causes apoptosis in melanoma cells by multiple pathways**. *Oncogene* 2008, **27**:4557-4568.
607. Stennicke HR, Jurgensmeier JM, Shin H, Deveraux Q, Wolf BB, Yang X, Zhou Q, Ellerby HM, Ellerby LM, Bredesen D, et al.: **Pro-caspase-3 is a major physiologic target of caspase-8**. *J Biol Chem* 1998, **273**:27084-27090.
608. Hara H, Friedlander RM, Gagliardini V, Ayata C, Fink K, Huang Z, Shimizu-Sasamata M, Yuan J, Moskowitz MA: **Inhibition of interleukin 1beta converting enzyme family proteases reduces ischemic and excitotoxic neuronal damage**. *Proc Natl Acad Sci U S A* 1997, **94**:2007-2012.
609. Obaya AJ, Mateyak MK, Sedivy JM: **Mysterious liaisons: the relationship between c-Myc and the cell cycle**. *Oncogene* 1999, **18**:2934-2941.
610. Chandramohan V, Mineva ND, Burke B, Jeay S, Wu M, Shen J, Yang W, Hann SR, Sonenshein GE: **c-Myc represses FOXO3a-mediated transcription of the gene encoding the p27(Kip1) cyclin dependent kinase inhibitor**. *J Cell Biochem* 2008, **104**:2091-2106.
611. Mateyak MK, Obaya AJ, Sedivy JM: **c-Myc regulates cyclin D-Cdk4 and -Cdk6 activity but affects cell cycle progression at multiple independent points**. *Mol Cell Biol* 1999, **19**:4672-4683.
612. Beijersbergen RL, Bernards R: **Cell cycle regulation by the retinoblastoma family of growth inhibitory proteins**. *Biochim Biophys Acta* 1996, **1287**:103-120.
613. Pardee AB, Li CJ, Reddy GP: **Regulation in S phase by E2F**. *Cell Cycle* 2004, **3**:1091-1094.
614. Tridandapani S, Pradhan M, LaDine JR, Garber S, Anderson CL, Coggeshall KM: **Protein interactions of Src homology 2 (SH2) domain-containing inositol phosphatase (SHIP): association with Shc displaces SHIP from FcgammaRIIb in B cells**. *J Immunol* 1999, **162**:1408-1414.
615. Medema JP, Scaffidi C, Kischkel FC, Shevchenko A, Mann M, Krammer PH, Peter ME: **FLICE is activated by association with the CD95 death-inducing signaling complex (DISC)**. *EMBO J* 1997, **16**:2794-2804.
616. Nagata S: **Apoptosis by death factor**. *Cell* 1997, **88**:355-365.

617. Hahne M, Renno T, Schroeter M, Irmler M, French L, Bornard T, MacDonald HR, Tschopp J: **Activated B cells express functional Fas ligand**. *Eur J Immunol* 1996, **26**:721-724.
618. Sharma K, Wang RX, Zhang LY, Yin DL, Luo XY, Solomon JC, Jiang RF, Markos K, Davidson W, Scott DW, et al.: **Death the Fas way: regulation and pathophysiology of CD95 and its ligand**. *Pharmacol Ther* 2000, **88**:333-347.
619. Cohen PL, Eisenberg RA: **Lpr and gld: single gene models of systemic autoimmunity and lymphoproliferative disease**. *Annu Rev Immunol* 1991, **9**:243-269.
620. Hewicker M, Kromschroder E, Trautwein G: **Detection of circulating immune complexes in MRL mice with different forms of glomerulonephritis**. *Z Versuchstierkd* 1990, **33**:149-156.
621. Brooks DG, Qiu WQ, Luster AD, Ravetch JV: **Structure and expression of human IgG FcRII(CD32). Functional heterogeneity is encoded by the alternatively spliced products of multiple genes**. *J Exp Med* 1989, **170**:1369-1385.
622. Daeron M: **Fc receptor biology**. *Annu Rev Immunol* 1997, **15**:203-234.
623. Brown KS: **FcγRIIb: Signalling aspects and implications for autoimmune disease** Glasgow: University of Glasgow: 2001.
624. Carter NA, Harnett MM: **Dissection of the signalling mechanisms underlying FcgammaRIIB-mediated apoptosis of mature B-cells**. *Biochem Soc Trans* 2004, **32**:973-975.
625. Werneburg N, Guicciardi ME, Yin XM, Gores GJ: **TNF-alpha-mediated lysosomal permeabilization is FAN and caspase 8/Bid dependent**. *Am J Physiol Gastrointest Liver Physiol* 2004, **287**:G436-443.
626. Vaisid T, Kosower NS, Elkind E, Barnoy S: **Amyloid beta peptide toxicity in differentiated PC12 cells: calpain-calpastatin, caspase, and membrane damage**. *J Neurosci Res* 2008, **86**:2314-2325.
627. Estaquier J, Tanaka M, Suda T, Nagata S, Golstein P, Ameisen JC: **Fas-mediated apoptosis of CD4+ and CD8+ T cells from human immunodeficiency virus-infected persons: differential in vitro preventive effect of cytokines and protease antagonists**. *Blood* 1996, **87**:4959-4966.
628. Vaisid T, Barnoy S, Kosower NS: **Calpain activates caspase-8 in neuron-like differentiated PC12 cells via the amyloid-beta-peptide and CD95 pathways**. *Int J Biochem Cell Biol* 2009.
629. Ruiz-Vela A, Gonzalez de Buitrago G, Martinez AC: **Implication of calpain in caspase activation during B cell clonal deletion**. *EMBO J* 1999, **18**:4988-4998.
630. Kato M, Nonaka T, Maki M, Kikuchi H, Imajoh-Ohmi S: **Caspases cleave the amino-terminal calpain inhibitory unit of calpastatin during apoptosis in human Jurkat T cells**. *J Biochem* 2000, **127**:297-305.
631. Muller M, Wilder S, Bannasch D, Israeli D, Lehlbach K, Li-Weber M, Friedman SL, Galle PR, Stremmel W, Oren M, et al.: **p53 activates the CD95 (APO-1/Fas) gene in response to DNA damage by anticancer drugs**. *J Exp Med* 1998, **188**:2033-2045.
632. Ehrhardt H, Hacker S, Wittmann S, Maurer M, Borkhardt A, Toloczko A, Debatin KM, Fulda S, Jeremias I: **Cytotoxic drug-induced, p53-mediated upregulation of caspase-8 in tumor cells**. *Oncogene* 2008, **27**:783-793.
633. Yao Z, Duan S, Hou D, Heese K, Wu M: **Death effector domain DEDa, a self-cleaved product of caspase-8/Mch5, translocates to the nucleus by binding to ERK1/2 and upregulates procaspase-8 expression via a p53-dependent mechanism**. *EMBO J* 2007, **26**:1068-1080.
634. Fischer B, Coelho D, Dufour P, Bergerat JP, Denis JM, Gueulette J, Bischoff P: **Caspase 8-mediated cleavage of the pro-apoptotic BCL-2 family member BID in p53-dependent apoptosis**. *Biochem Biophys Res Commun* 2003, **306**:516-522.
635. Ding HF, Lin YL, McGill G, Juo P, Zhu H, Blenis J, Yuan J, Fisher DE: **Essential role for caspase-8 in transcription-independent apoptosis triggered by p53**. *J Biol Chem* 2000, **275**:38905-38911.
636. Tridandapani S, Chacko GW, Van Brocklyn JR, Coggeshall KM: **Negative signaling in B cells causes reduced Ras activity by reducing Shc-Grb2 interactions**. *J Immunol* 1997, **158**:1125-1132.
637. Arechiga AF, Bell BD, Leverrier S, Weist BM, Porter M, Wu Z, Kanno Y, Ramos SJ, Ong ST, Siegel R, et al.: **A Fas-associated death domain protein/caspase-8-signaling axis**

promotes S-phase entry and maintains S6 kinase activity in T cells responding to IL-2. *J Immunol* 2007, **179**:5291-5300.
638. Kimura M, Ogata Y, Shimada K, Wakabayashi T, Onoda H, Katagiri T, Matsuzawa A: **Nephritogenicity of the lprcg gene on the MRL background**. *Immunology* 1992, **76**:498-504.
639. Hattori M, Minato N: **Rap1 GTPase: functions, regulation, and malignancy**. *J Biochem* 2003, **134**:479-484.
640. Shah BH, Farshori MP, Jambusaria A, Catt KJ: **Roles of Src and epidermal growth factor receptor transactivation in transient and sustained ERK1/2 responses to gonadotropin-releasing hormone receptor activation**. *J Biol Chem* 2003, **278**:19118-19126.
641. Lam EW, Choi MS, van der Sman J, Burbidge SA, Klaus GG: **Modulation of E2F activity via signaling through surface IgM and CD40 receptors in WEHI-231 B lymphoma cells**. *J Biol Chem* 1998, **273**:10051-10057.
642. van Eijk M, de Groot C: **Germinal center B cell apoptosis requires both caspase and cathepsin activity**. *J Immunol* 1999, **163**:2478-2482.
643. Liedtke C, Groger N, Manns MP, Trautwein C: **The human caspase-8 promoter sustains basal activity through SP1 and ETS-like transcription factors and can be up-regulated by a p53-dependent mechanism**. *J Biol Chem* 2003, **278**:27593-27604.

Publications

1: Wallmann J, Proell M, Stepanoska T, Hantusch B, Pali-Schöll I, **Thalhamer T**, Thalhamer J, Jensen-Jarolim E, Hartl A. *A mimotope gene encoding the major IgE epitope of allergen Phl p 5 for epitope-specific immunization*. Immunol Lett. 2009 Jan 29;122(1):68-75.

2: **Thalhamer T**, McGrath MA, Harnett MM. *MAPKs and their relevance to arthritis and inflammation*. Rheumatology (Oxford). 2008 Apr;47(4):409-14.

3: Harnett MM, Kean DE, Boitelle A, McGuiness S, **Thalhamer T**, Steiger CN, Egan C,Al-Riyami L, Alcocer MJ, Houston KM, Gracie JA, McInnes IB, Harnett W. *The phosphorycholine moiety of the filarial nematode immunomodulator ES-62 is responsible for its anti-inflammatory action in arthritis*. Ann Rheum Dis. 2008 Apr;67(4):518-23.

4: Wallner M, Stöcklinger A, **Thalhamer T**, Bohle B, Vogel L, Briza P, Breiteneder H, Vieths S, Hartl A, Mari A, Ebner C, Lackner P, Hammerl P, Thalhamer J, Ferreira F. *Allergy multivaccines created by DNA shuffling of tree pollen allergens*. J Allergy Clin Immunol. 2007 Aug;120(2):374-80.

5: Bauer R, Scheiblhofer S, Kern K, Gruber C, Stepanoska T, **Thalhamer T**, Hauser-Kronberger C, Alinger B, Zoegg T, Gabler M, Ferreira F, Hartl A, Thalhamer J, Weiss R. *Generation of hypoallergenic DNA vaccines by forced ubiquitination: preventive and therapeutic effects in a mouse model of allergy*. J Allergy Clin Immunol. 2006 Jul;118(1):269-76.

6: Anderson EJ, McGrath MA, **Thalhamer T**, McInnes IB. *Interleukin-12 to interleukin 'infinity': the rationale for future therapeutic cytokine targeting*. Springer Semin Immunopathol. 2006 Jun;27(4):425-42.

Figure 1.1

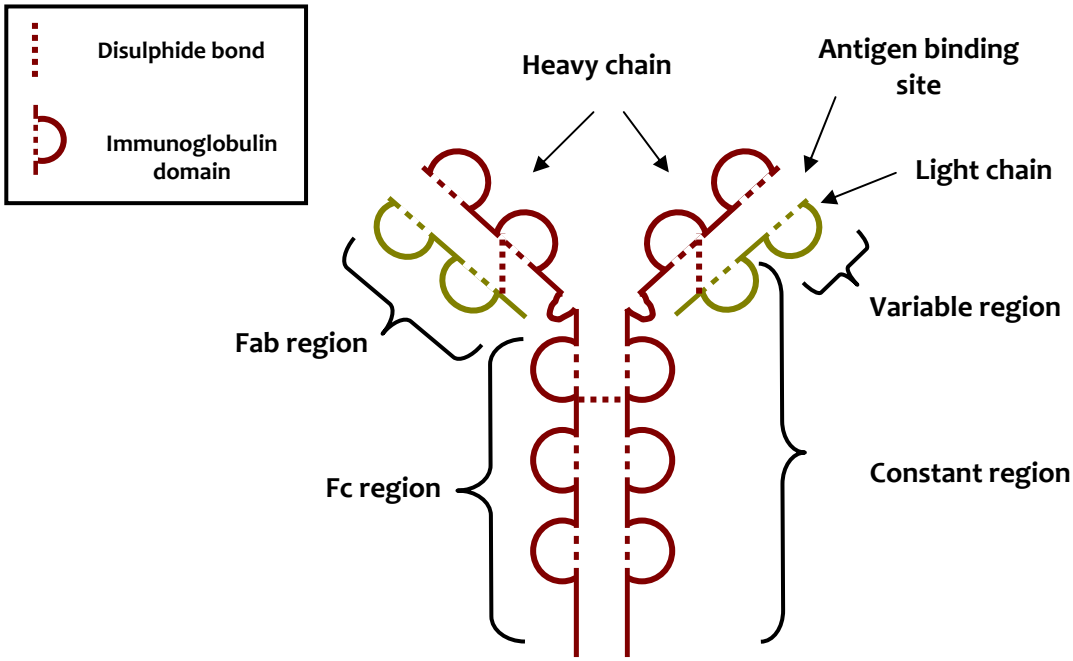

Isotype	Secreted form	Functions
IgA	monomer, dimer or trimer 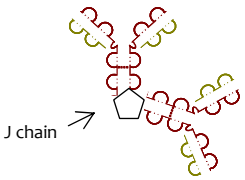	**Mucusal immunity** Secretion into lumen of gastrointestinal and respiratory tract
IgD	None	Antigen receptor on naïve B cells
IgE		**Immunity against large parasites** IgE-mediated release of cytotoxic granules-content by granulocytes
IgG		• Opsonisation of pathogens • Activation of complement pathway • Antibody-dependent cell-mediated cytotoxicity • Neutralising pathogens and their toxins
IgM	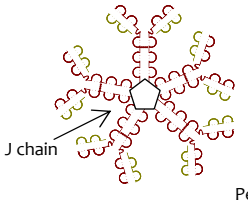 Pentamer	Activation of complement pathway

Figure 1.2

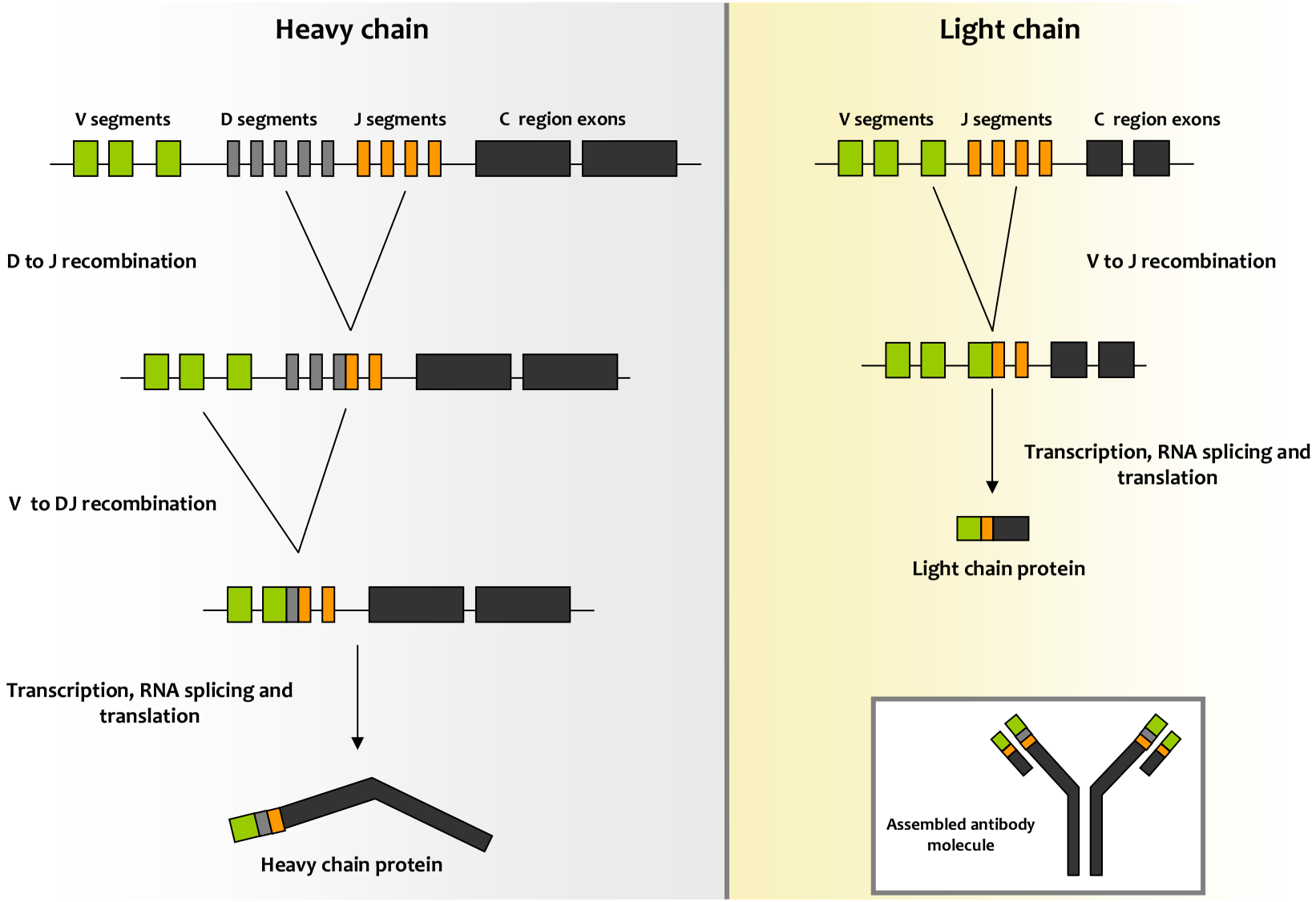
Heavy chain
V segments
D segments
J segments
C region exons
D to J recombination
V to DJ recombination
Transcription, RNA splicing and translation
Heavy chain protein
Light chain
V segments
J segments
C region exons
V to J recombination
Transcription, RNA splicing and translation
Light chain protein
Assembled antibody molecule

Figure 1.3

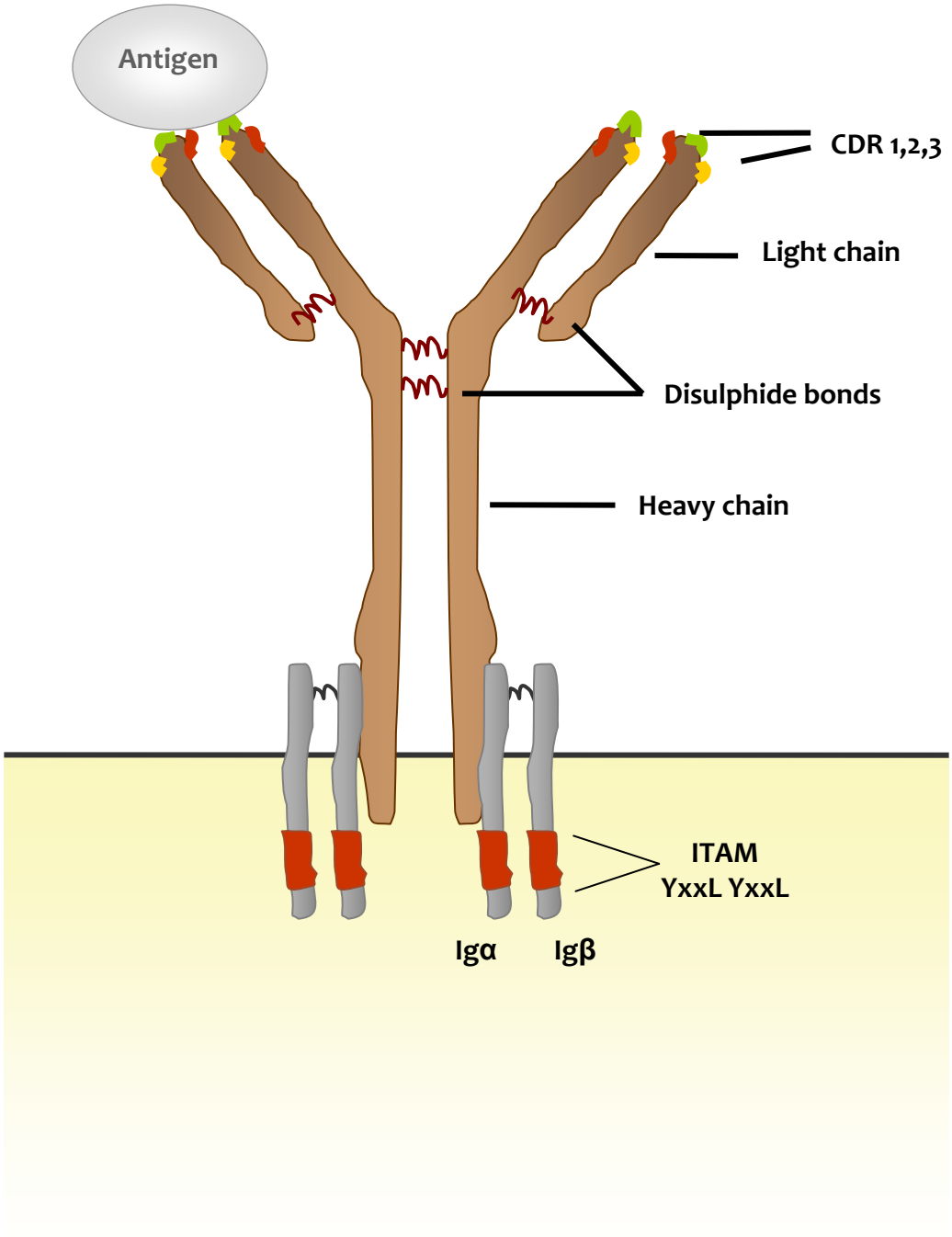
Antigen
CDR 1,2,3
Light chain
Disulphide bonds
Heavy chain
ITAM
YxxL YxxL
Igα
Igβ

Figure 1.4

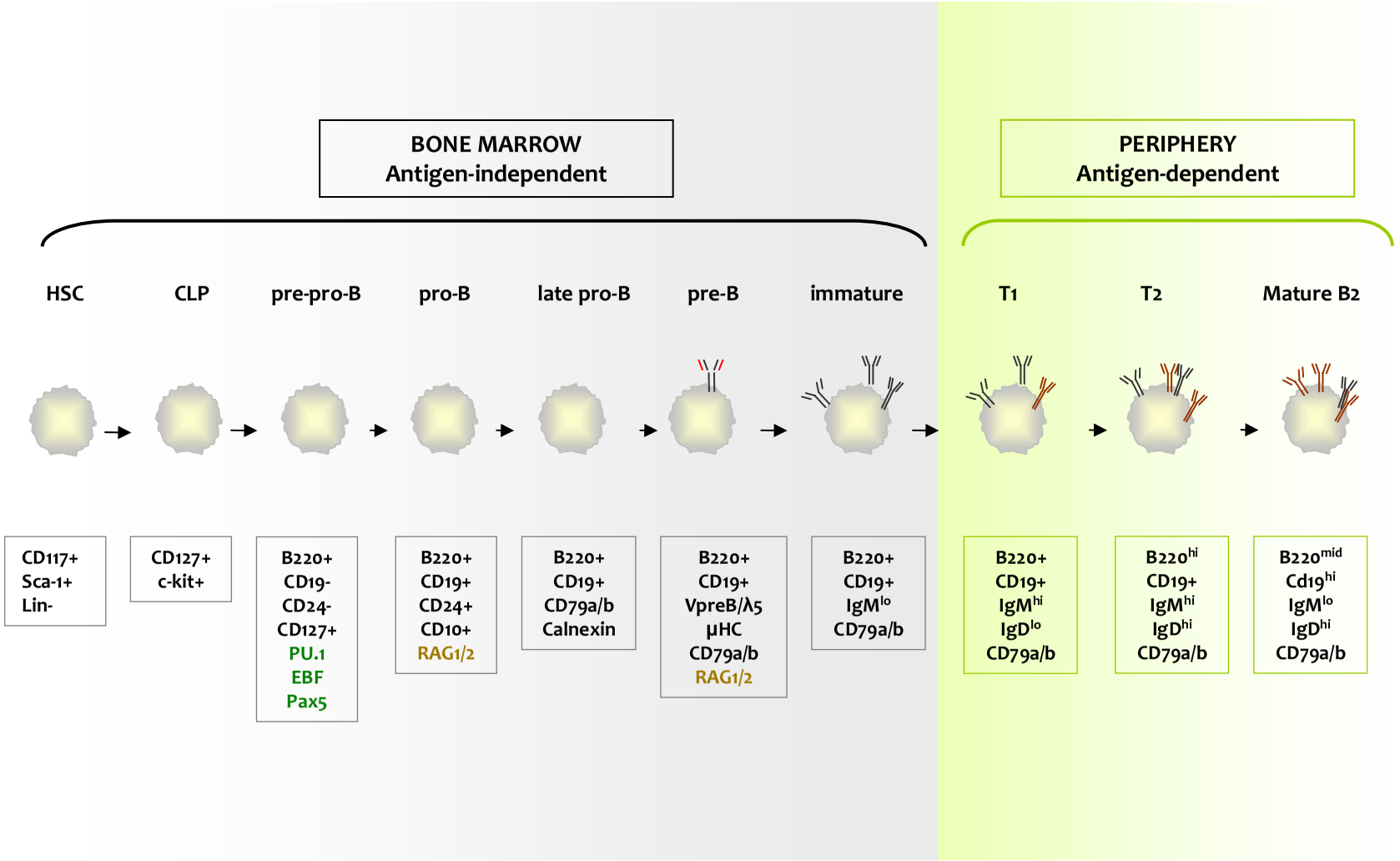
BONE MARROW
Antigen-independent
PERIPHERY
Antigen-dependent
HSC
CLP
pre-pro-B
pro-B
late pro-B
pre-B
immature
T1
T2
Mature B2
CD117+
Sca-1+
Lin-
CD127+
c-kit+
B220+
CD19-
CD24-
CD127+
PU.1
EBF
Pax5
B220+
CD19+
CD24+
CD10+
RAG1/2
B220+
CD19+
CD79a/b
Calnexin
B220+
CD19+
VpreB/λ5
μHC
CD79a/b
RAG1/2
B220+
CD19+
IgM^{lo}
CD79a/b
B220+
CD19+
IgM^{hi}
IgD^{lo}
CD79a/b
B220^{hi}
CD19+
IgM^{hi}
IgD^{hi}
CD79a/b
B220^{mid}
Cd19^{hi}
IgM^{lo}
IgD^{hi}
CD79a/b

Figure 1.5

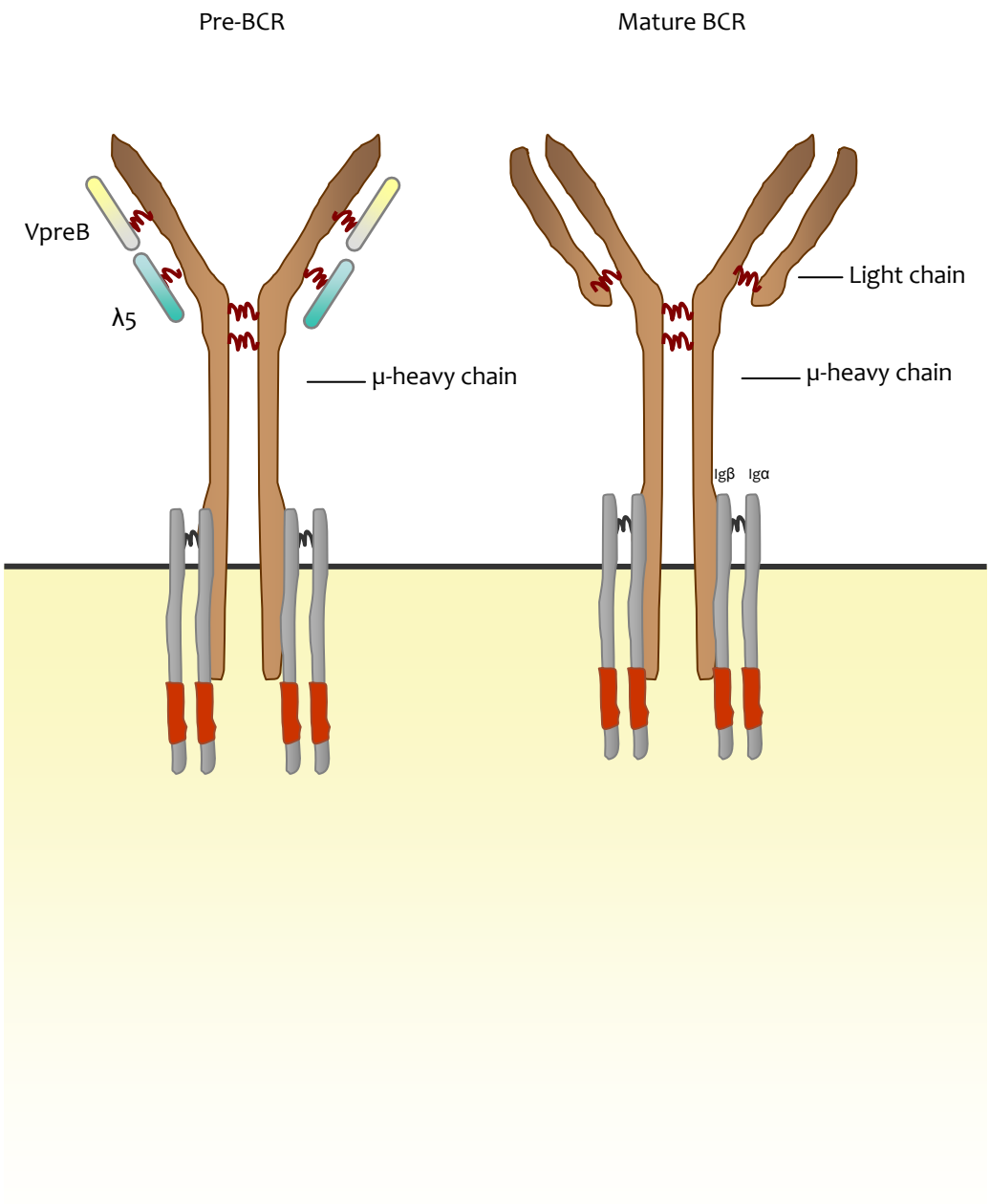
Pre-BCR
Mature BCR
VpreB
λ5
μ-heavy chain
Light chain
μ-heavy chain
Igβ
Igα

Figure 1.6

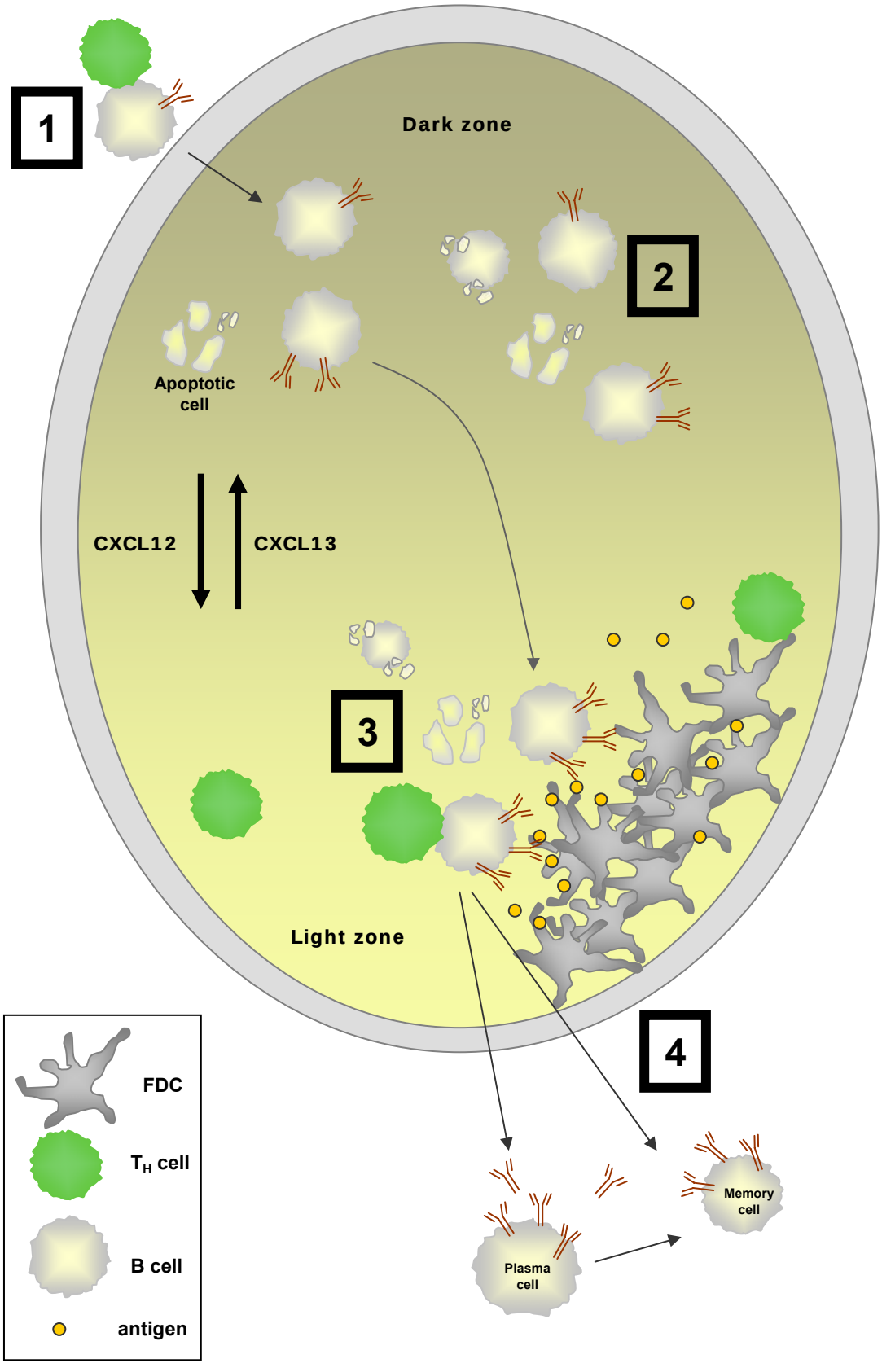
1
Dark zone
2
Apoptotic cell
CXCL12
CXCL13
3
Light zone
4
Memory cell
Plasma cell
FDC
T_H cell
B cell
antigen

Figure 1.7

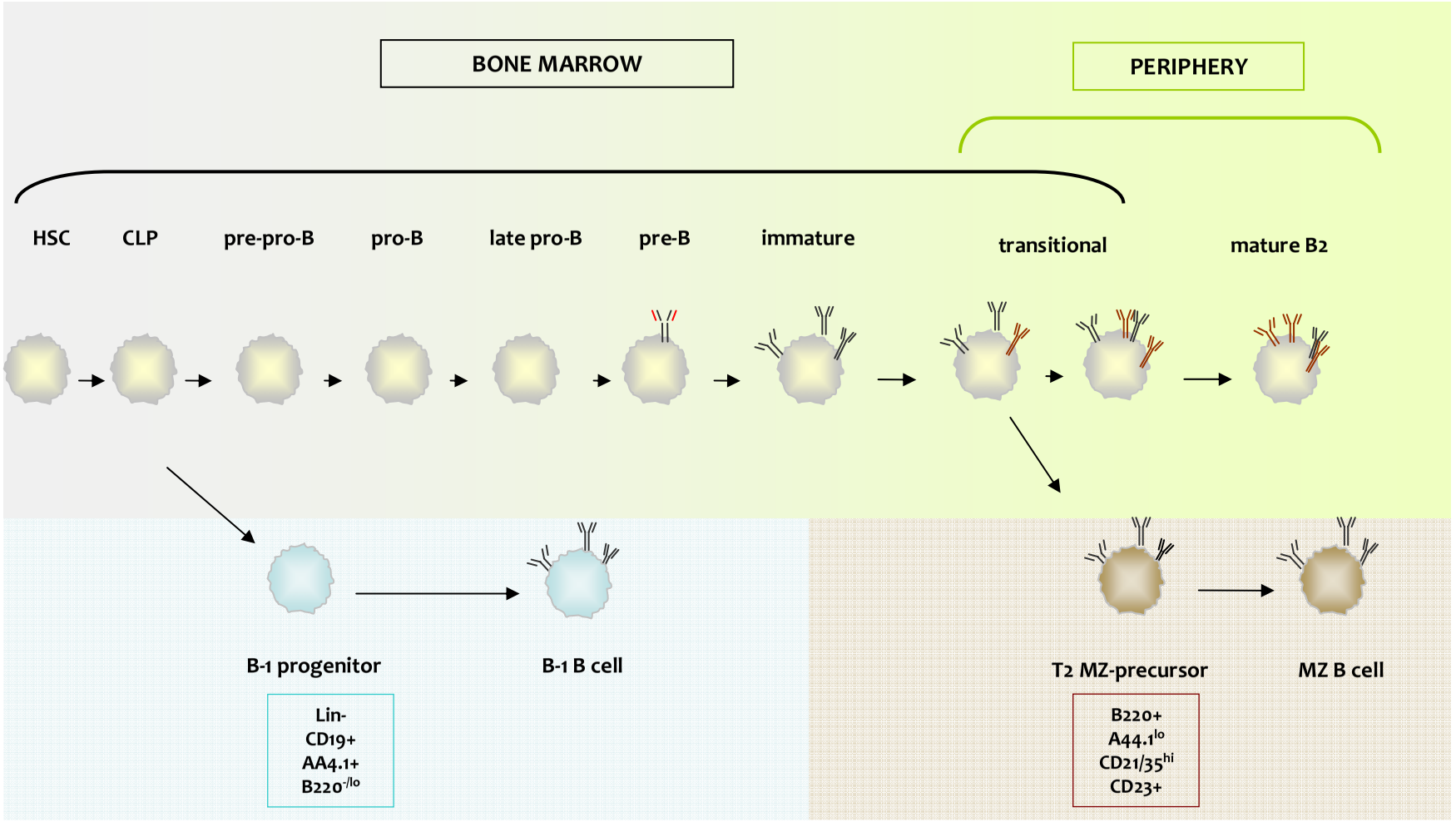
BONE MARROW
PERIPHERY
HSC
CLP
pre-pro-B
pro-B
late pro-B
pre-B
immature
transitional
mature B2
B-1 progenitor
B-1 B cell
Lin-
CD19+
AA4.1+
B220-/lo
T2 MZ-precursor
MZ B cell
B220+
A44.1lo
CD21/35hi
CD23+

Figure 1.8

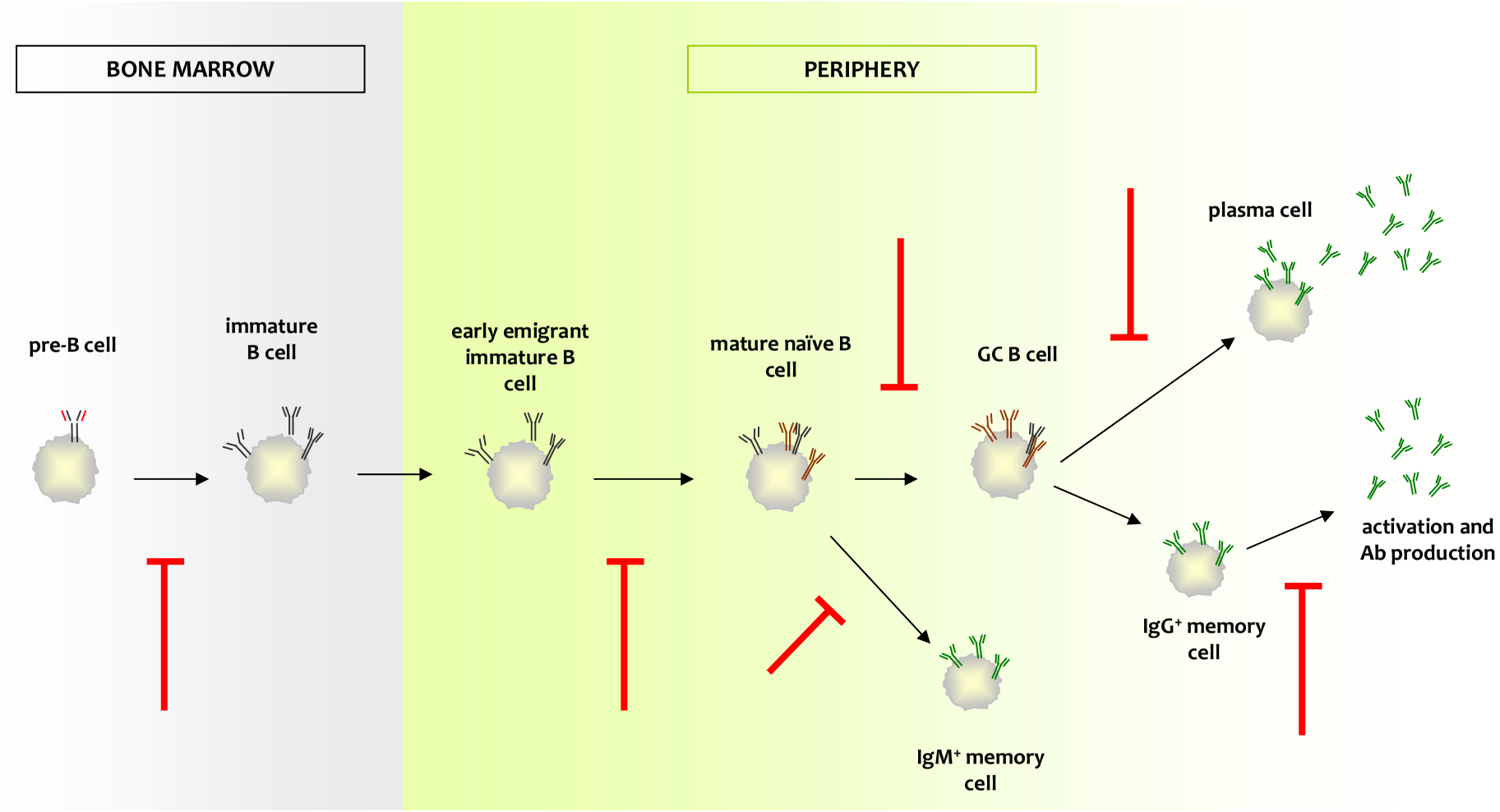
BONE MARROW
PERIPHERY
pre-B cell
immature B cell
early emigrant immature B cell
mature naïve B cell
GC B cell
plasma cell
activation and Ab production
IgG+ memory cell
IgM+ memory cell

Figure 1.9

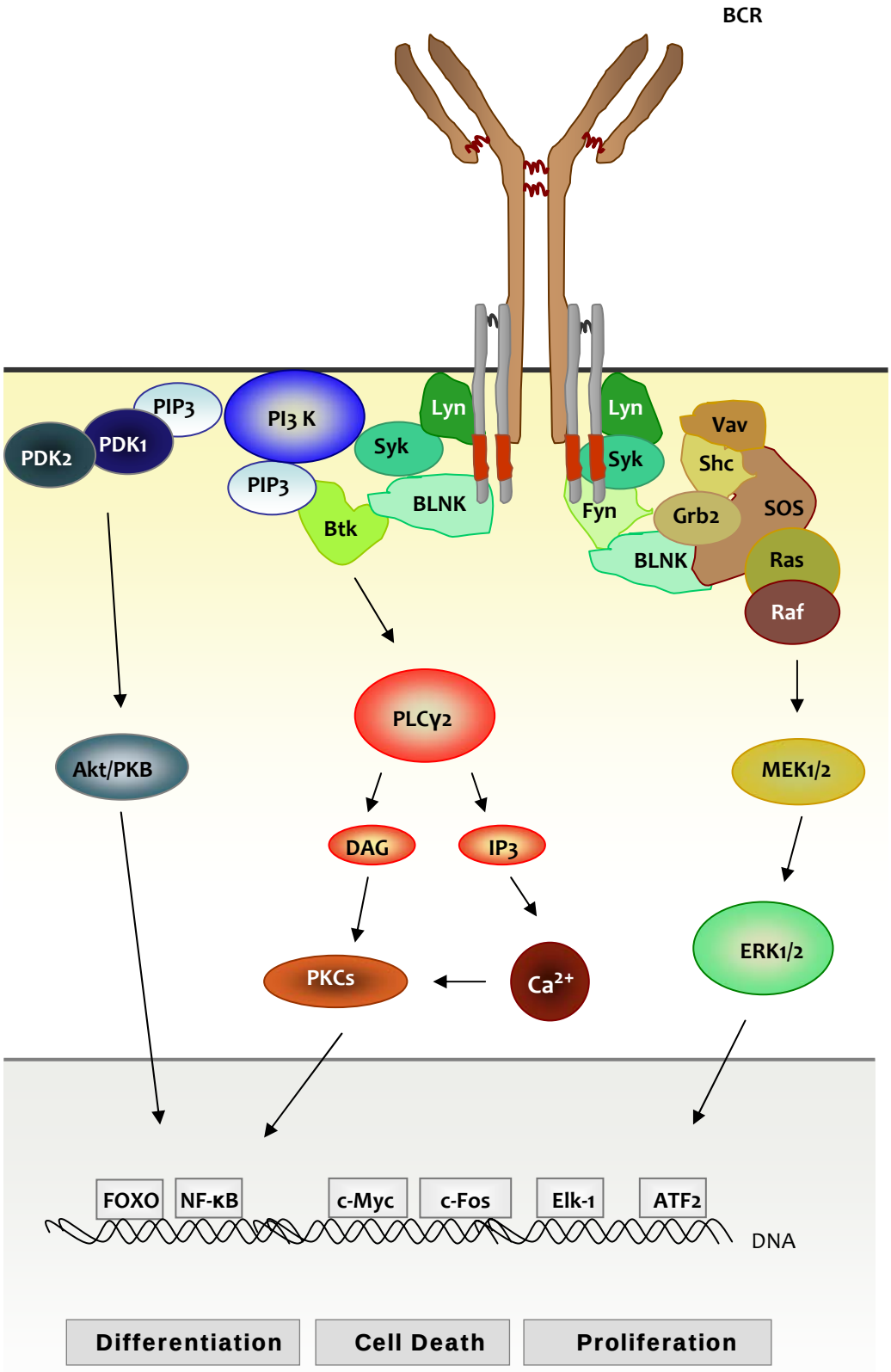
BCR
PIP3
PDK2
PDK1
PI3 K
PIP3
Syk
Lyn
Lyn
Syk
Vav
Shc
BLNK
Btk
Fyn
Grb2
SOS
BLNK
Ras
Raf
PLCγ2
Akt/PKB
MEK1/2
DAG
IP3
ERK1/2
PKCs
Ca2+
FOXO
NF-κB
c-Myc
c-Fos
Elk-1
ATF2
DNA
Differentiation
Cell Death
Proliferation

Figure 1.10

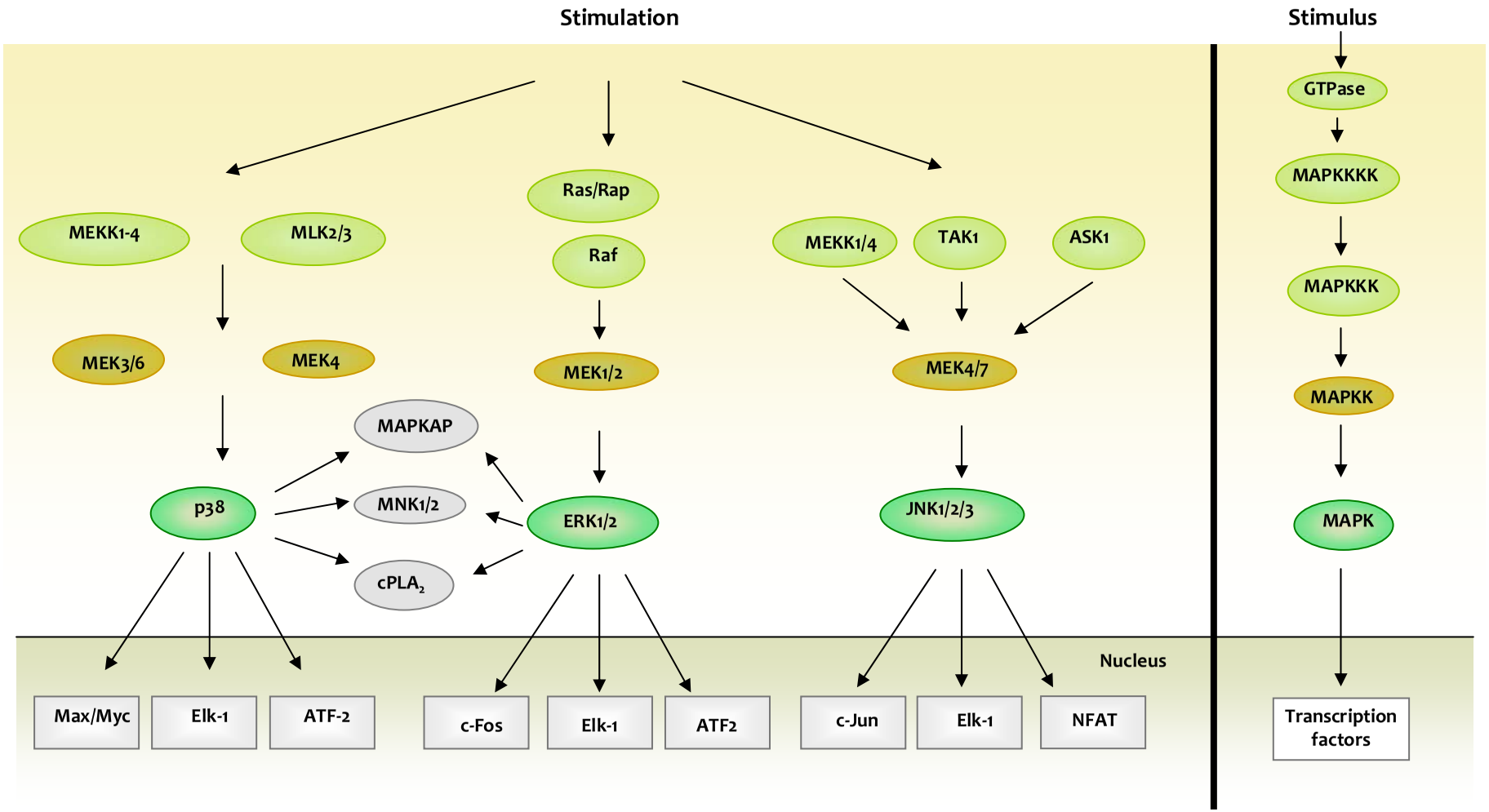
Stimulation
Stimulus
GTPase
MAPKKKK
MAPKKK
MAPKK
MAPK
Ras/Rap
Raf
MEK1/2
ERK1/2
MEKK1-4
MLK2/3
MEK3/6
MEK4
p38
MAPKAP
MNK1/2
cPLA2
MEKK1/4
TAK1
ASK1
MEK4/7
JNK1/2/3
Nucleus
Max/Myc
Elk-1
ATF-2
c-Fos
Elk-1
ATF2
c-Jun
Elk-1
NFAT
Transcription factors

Figure 1.11

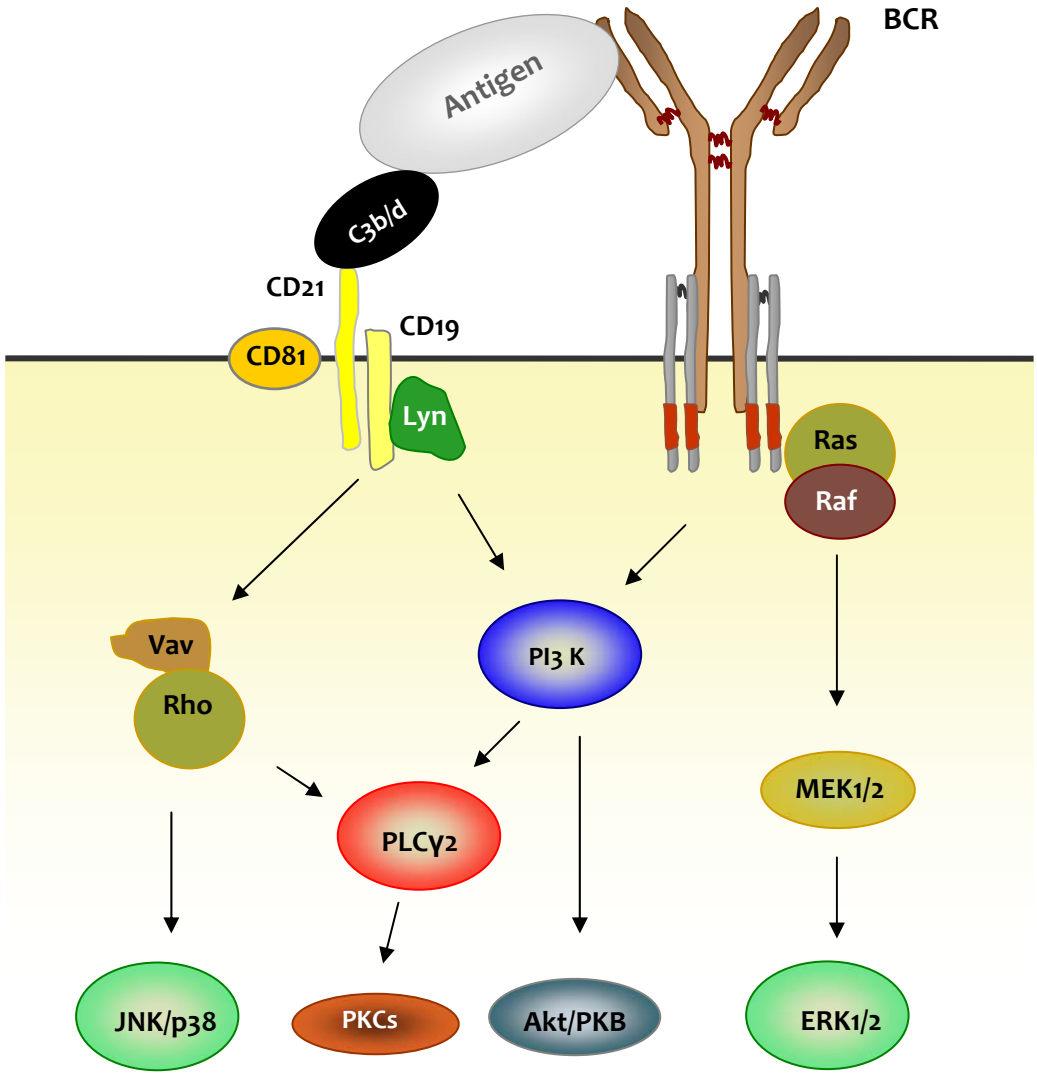
BCR
Antigen
C3b/d
CD21
CD19
CD81
Lyn
Ras
Raf
Vav
Rho
PI3 K
PLCγ2
MEK1/2
JNK/p38
PKCs
Akt/PKB
ERK1/2

Figure 1.12

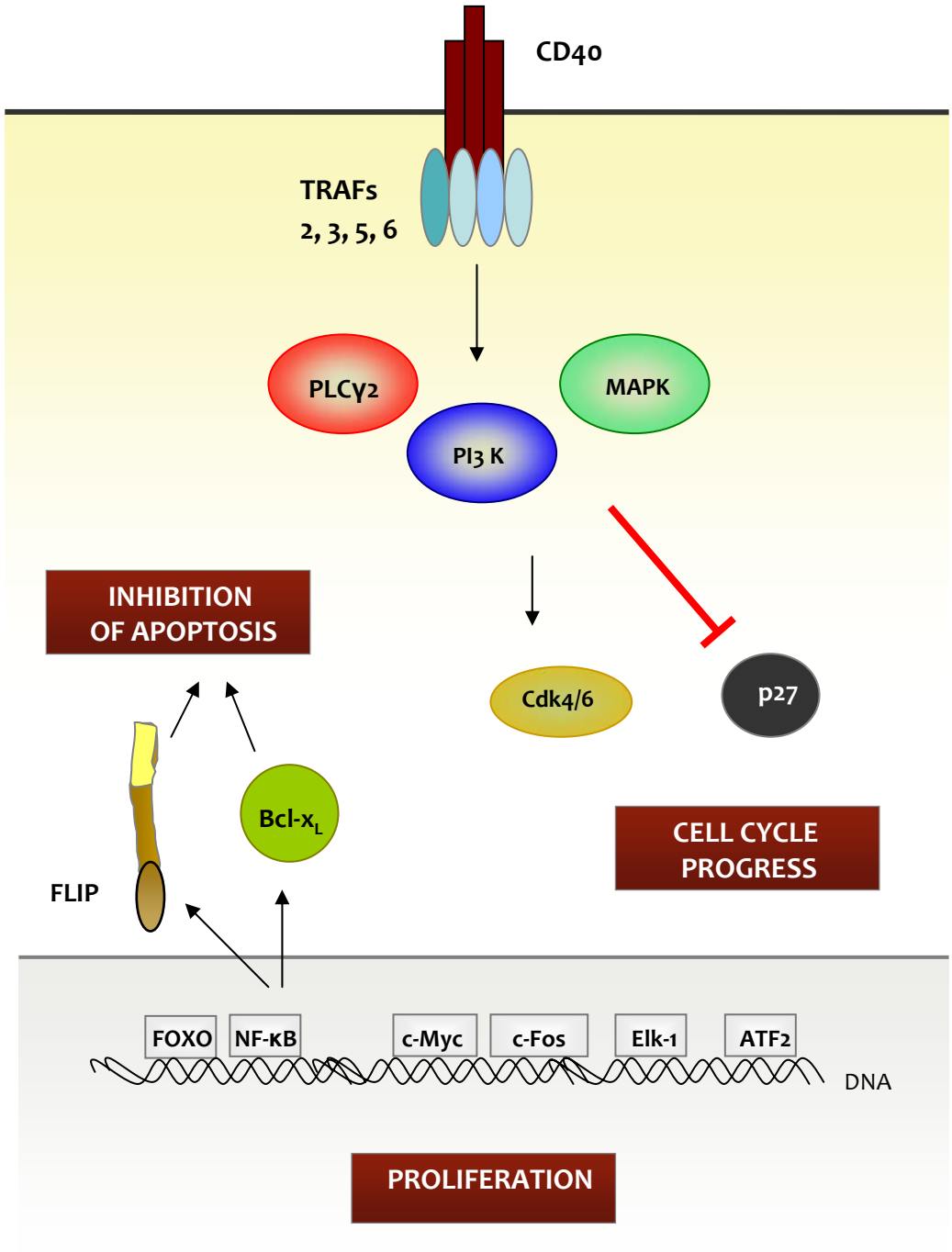
CD40
TRAFs
2, 3, 5, 6
PLCγ2
MAPK
PI3 K
INHIBITION
OF APOPTOSIS
Cdk4/6
p27
Bcl-xL
FLIP
CELL CYCLE
PROGRESS
FOXO
NF-κB
c-Myc
c-Fos
Elk-1
ATF2
DNA
PROLIFERATION

Table 1.1

Murine

Receptor	FcγRI	FcγRIII	FcγRIV	FcγRIIB
Affinity	High	low/ medium		low/ medium
Signalling	activatory			inhbitory
Expression	Macrophage Monocyte Neutrophil DC			B cell Macrophage Basophil Neutrophil Eosinophil DC

Human

Receptor	FcγRI	FcγRIIA	FcγRIIC	FcγRIIIA	FcγRIIIB	FcγRIIB
Affinity	High	low/ medium				low/ medium
Signalling	activatory					inhbitory
Expression	Macrophage Neutrophil Eosinophil DC		NK cell	Macrophage Monocyte DC	Neutrophil Eosinophil	B cell Macrophage Basophil Neutrophil Eosinophil DC

Figure 1.13

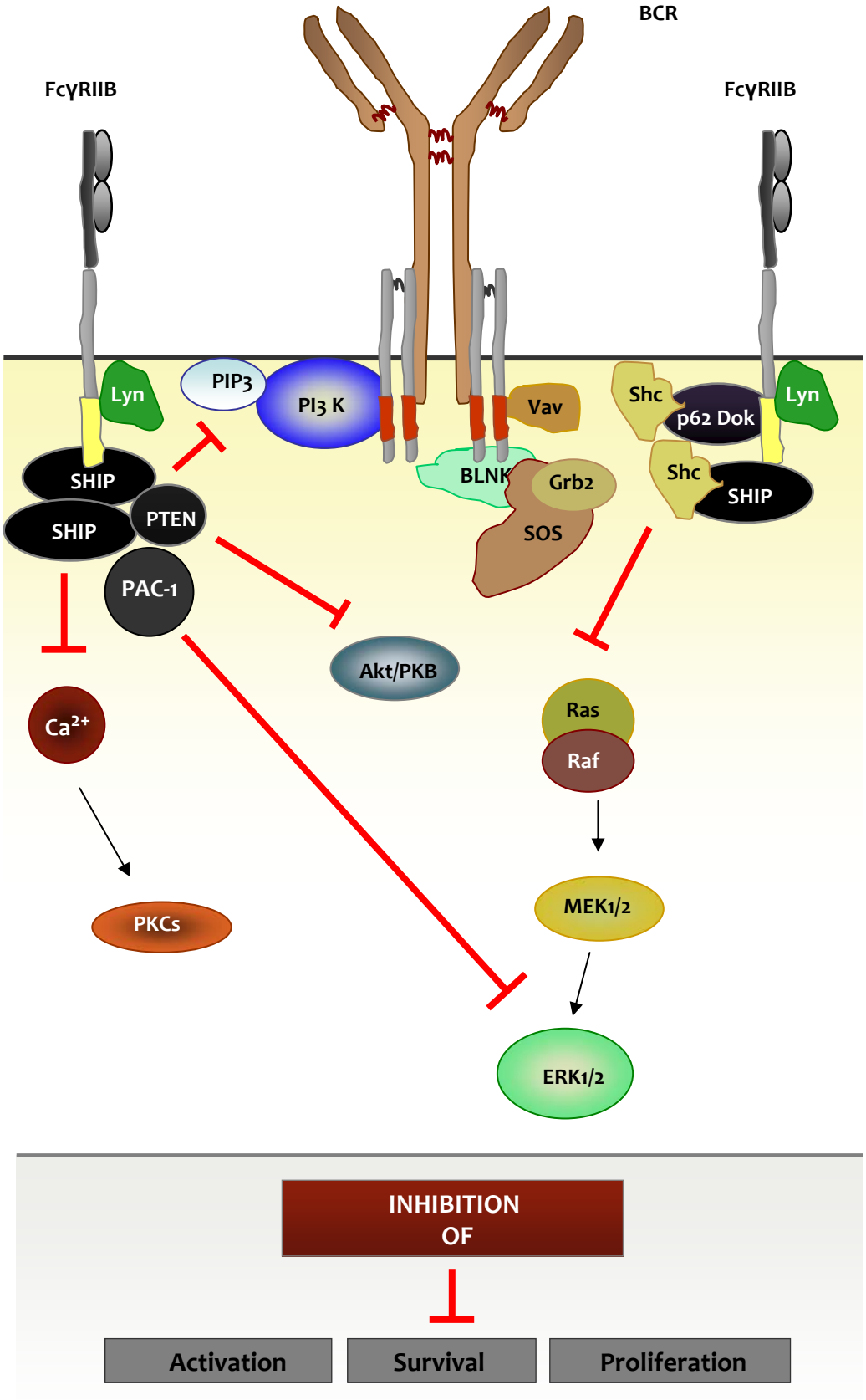
BCR
FcγRIIB
FcγRIIB
Lyn
PIP3
PI3 K
Vav
Shc
p62 Dok
Lyn
SHIP
BLNK
Grb2
Shc
SHIP
SHIP
PTEN
SOS
PAC-1
Akt/PKB
Ca2+
Ras
Raf
PKCs
MEK1/2
ERK1/2
INHIBITION OF
Activation
Survival
Proliferation

Figure 1.14

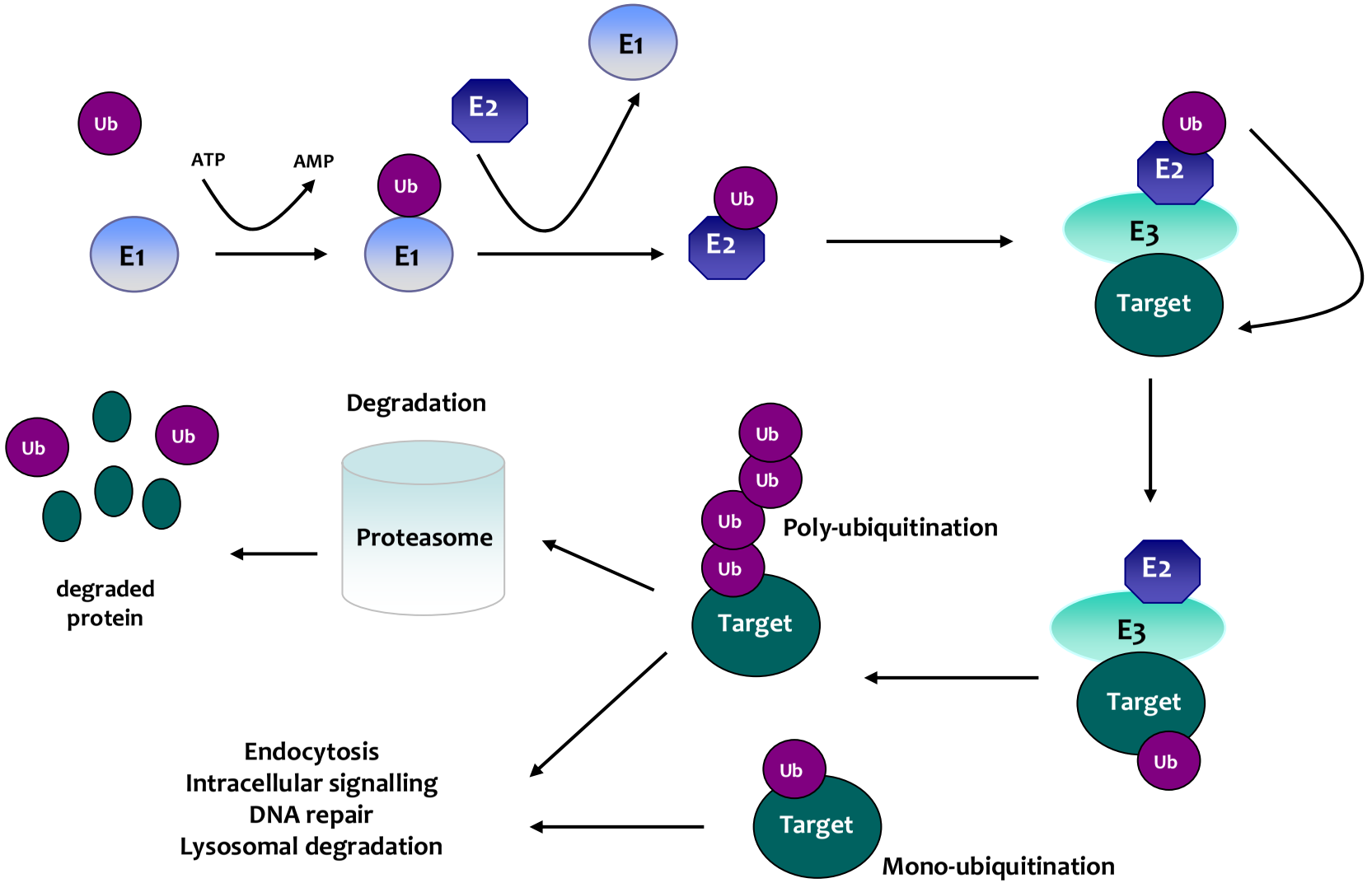
Ub
ATP
AMP
E1
E1
E2
Ub
E1
Ub
E2
Ub
E2
E3
Target
Degradation
Ub
Ub
Proteasome
degraded
protein
Ub
Ub
Ub
Ub
Poly-ubiquitination
Target
E2
E3
Target
Ub
Endocytosis
Intracellular signalling
DNA repair
Lysosomal degradation
Ub
Target
Mono-ubiquitination

Figure 1.15

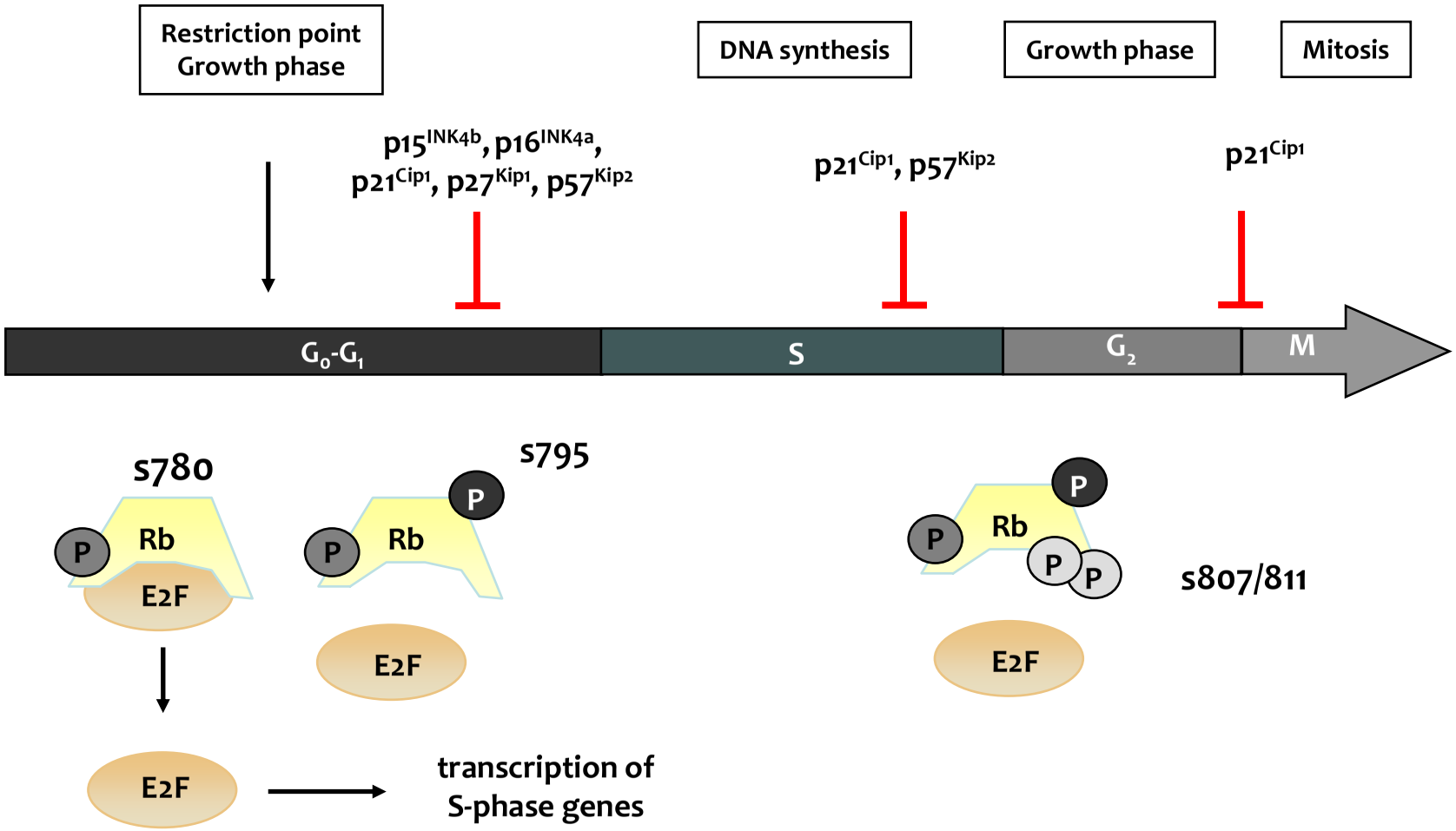
Restriction point
Growth phase
DNA synthesis
Growth phase
Mitosis
p15INK4b, p16INK4a,
p21Cip1, p27Kip1, p57Kip2
p21Cip1, p57Kip2
p21Cip1
G0-G1
S
G2
M
s780
s795
P
Rb
E2F
s807/811
transcription of
S-phase genes

Figure 1.16

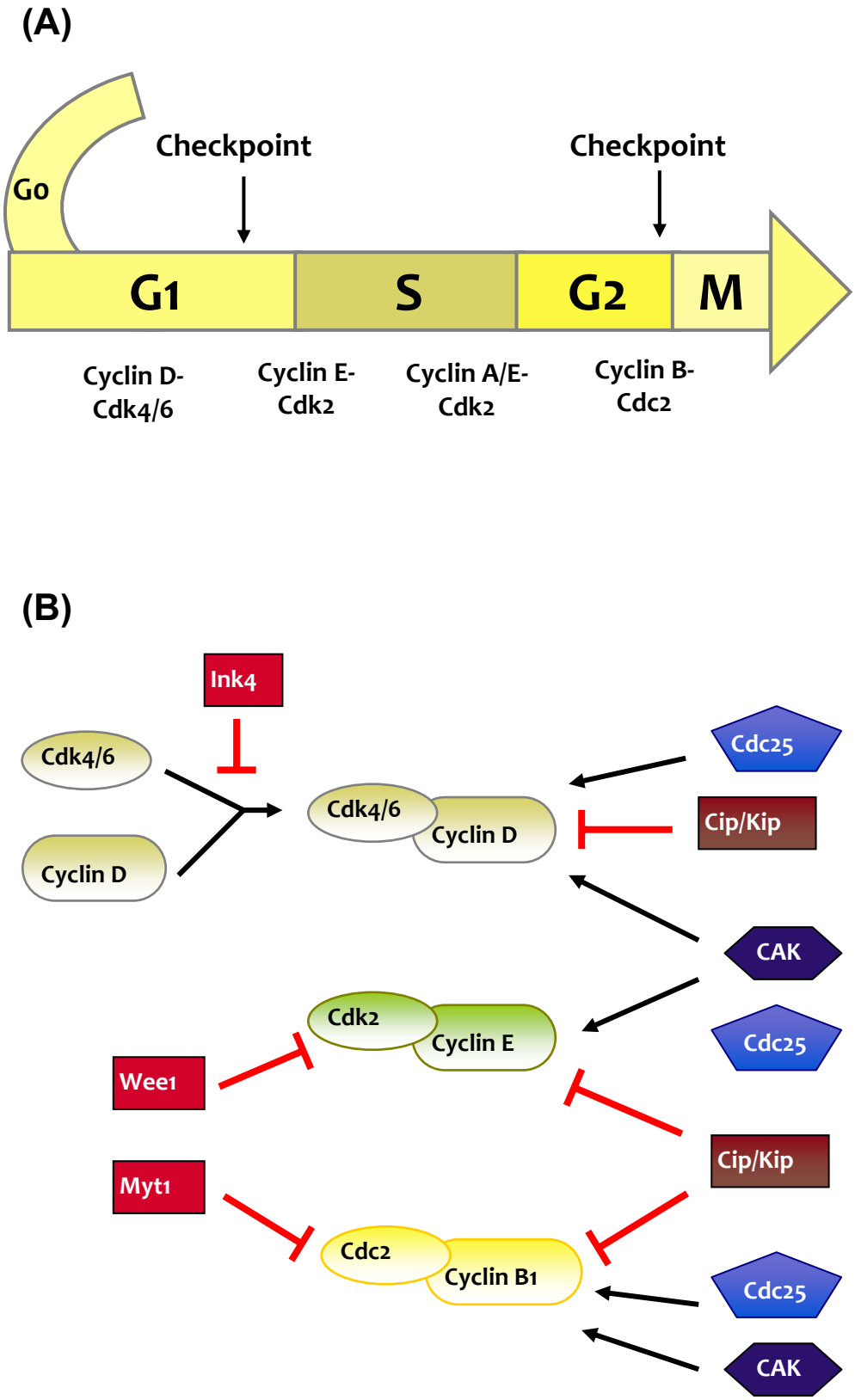
(A)
Go
Checkpoint
Checkpoint
G1
S
G2
M
Cyclin D-Cdk4/6
Cyclin E-Cdk2
Cyclin A/E-Cdk2
Cyclin B-Cdc2
(B)
Ink4
Cdk4/6
Cyclin D
Cdk4/6
Cyclin D
Cdc25
Cip/Kip
CAK
Cdk2
Cyclin E
Cdc25
Wee1
Cip/Kip
Myt1
Cdc2
Cyclin B1
Cdc25
CAK

Figure 1.17

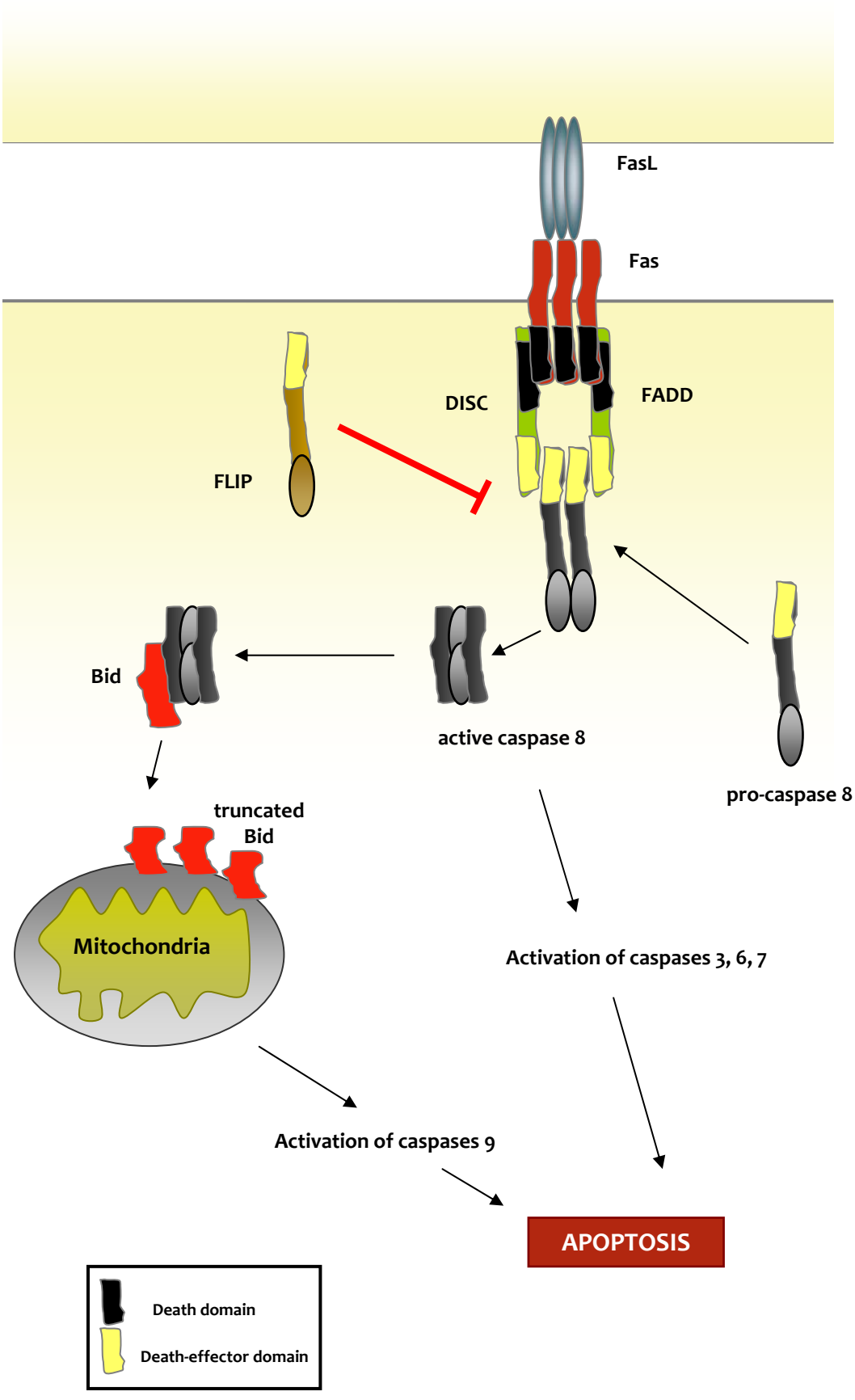
FasL
Fas
DISC
FADD
FLIP
Bid
active caspase 8
pro-caspase 8
truncated
Bid
Mitochondria
Activation of caspases 3, 6, 7
Activation of caspases 9
APOPTOSIS
Death domain
Death-effector domain

Figure 1.18

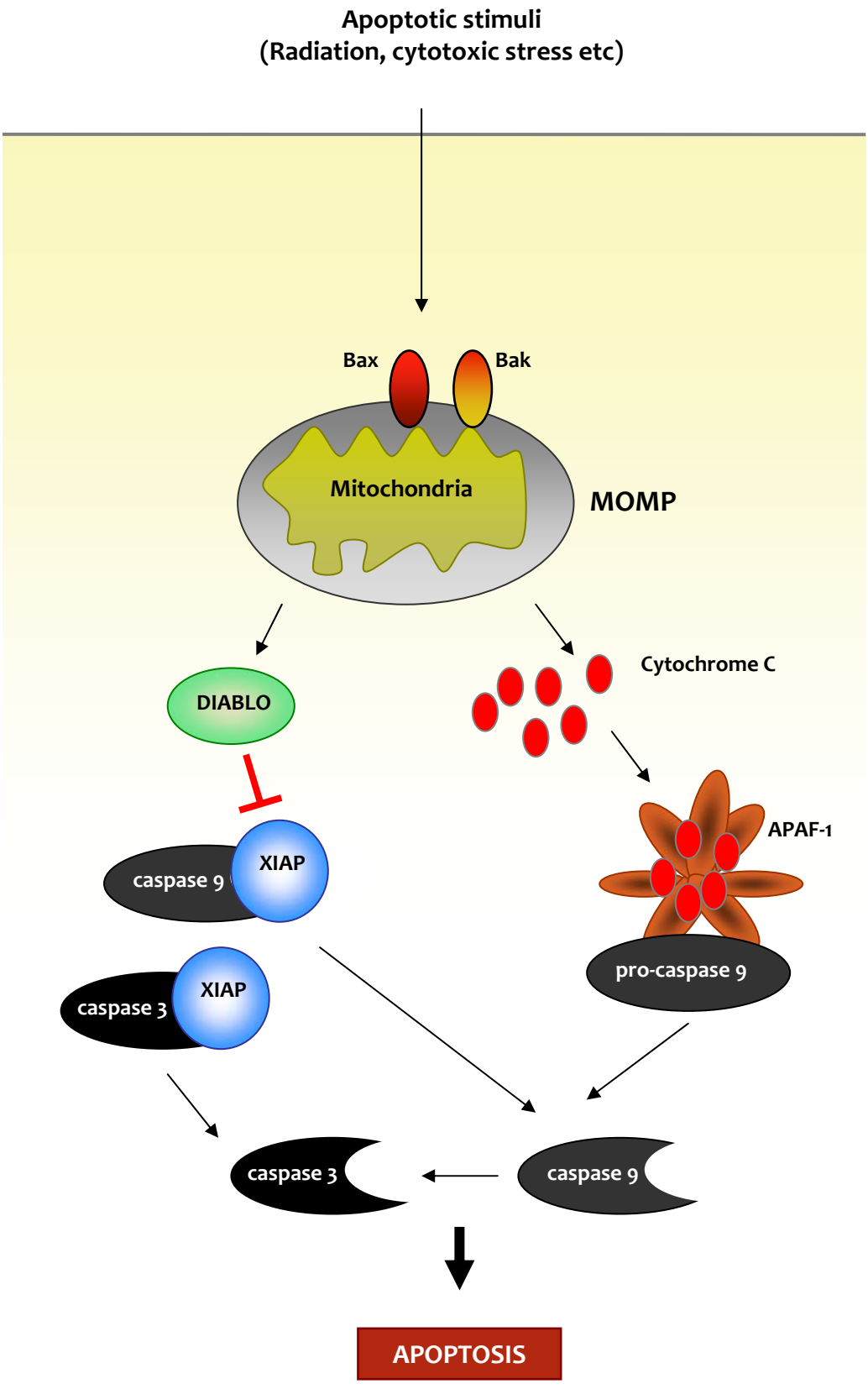
Apoptotic stimuli
(Radiation, cytotoxic stress etc)
Bax
Bak
Mitochondria
MOMP
DIABLO
Cytochrome C
XIAP
caspase 9
APAF-1
pro-caspase 9
XIAP
caspase 3
caspase 3
caspase 9
APOPTOSIS

Figure 1.19

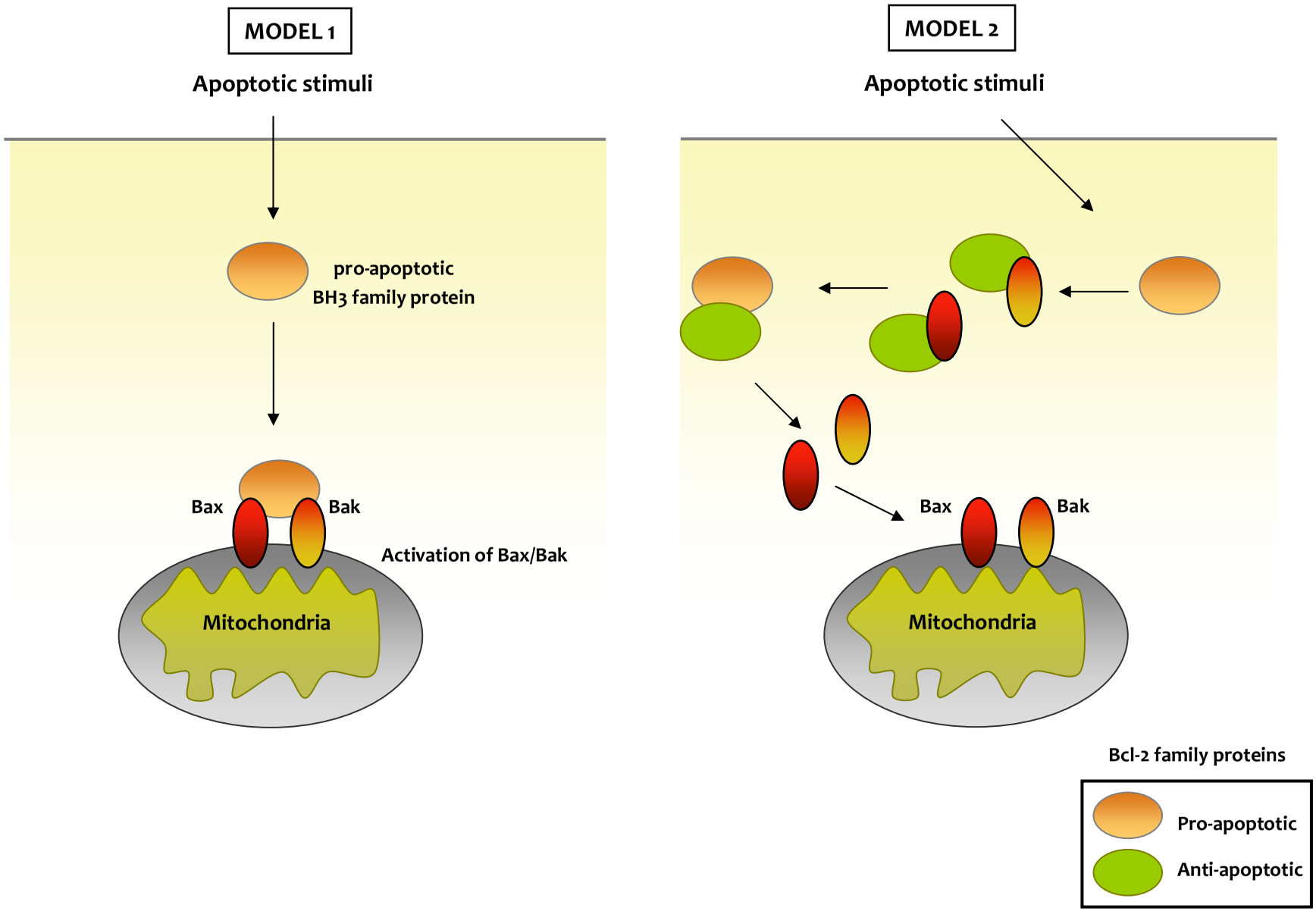
MODEL 1
Apoptotic stimuli
pro-apoptotic
BH3 family protein
Bax
Bak
Activation of Bax/Bak
Mitochondria
MODEL 2
Apoptotic stimuli
Bax
Bak
Mitochondria
Bcl-2 family proteins
Pro-apoptotic
Anti-apoptotic

Table 2.1

(A) FACS

Specificity of antibody	Reactivity	Isotype	Clone	Conjugated	Manufacturer
CD3	Human	Mouse IgG1	UCHT1	APC	BD Pharmingen
CD11b	Human	Mouse IgG1	ICRF44 (44)	APC	BD Pharmingen
CD14	Human	Mouse IgG2a	M5E2	FITC	BD Pharmingen
CD19	Human	Mouse IgG1	HIB19	APC/FITC	BD Pharmingen
CD20	Human	Mouse IgG2b	2H7	PE	BD Pharmingen
CD32B	Human	Human chimeric mouse	ch2B6N297Q	AF488	MacroGenics
CD56	Human	Mouse IgG1	B159	PE	BD Pharmingen
Isotype controls			Clone	Conjugated	Manufacturer
Mouse IgG1			MOPC-21	AF488/APC/FITC/PE	BD Pharmingen
Mouse IgG2b			27-35	PE	BD Pharmingen
Mouse IgG2a			G155-178	FITC	BD Pharmingen
Specificity of antibody	Reactivity	Isotype	Clone	Conjugated	Manufacturer
B220	Mouse	Rat IgG2a	RA3-6B2	FITC	BD Pharmingen
CD95 (Fas)	Mouse	Hamster IgG	Jo2	Biotin	BD Pharmingen
Isotype controls				Conjugated	Manufacturer
Rat IgG2a				FITC	BD Pharmingen
Hamster IgG				Biotin	BD Pharmingen
Secondary reagents	Reactivity	Isotype	Clone	Conjugated	Manufacturer
Streptavidin APC			554067	APC	BD Pharmingen

(B) Antibodies used for stimulation

Specificity of antibody	Host	Clone	Manufacturer
anti-mouse IgM	Rat	B7.6	made in house
anti-mouse CD40	Rat	FGK45	made in house
anti-mouse FcγRII	Rat	24G2	made in house
anti-mouse FasL	Armenian Hamster	MFL3	BioLegend
Armenian Hamster IgG	Armenian Hamster	HTK888	BioLegend
anti-mouse IgG+IgM (H+L)	Rabbit	315-005-044	Jackson ImmunoResearch
F(ab')2 anti-mouse IgM	Goat	115-006-020	Jackson ImmunoResearch
anti-human IgG+IgM (H+L)	Rabbit	309-005-107	Jackson ImmunoResearch
F(ab')2 anti-human IgG+IgM	Goat	109-006-127	Jackson ImmunoResearch
anti-rat IgG (H+L)	Donkey	712-005-150	Jackson ImmunoResearch

Table 2.1

(C) Western Blotting

Specificity of antibody	Host	Clone/ID	Dilution	Manufacturer
β-Actin	Mouse	sc-47778	1:5000	Santa Cruz
Caspase-8	Mouse	Clone 1G12	1:1000	Alexis Biochemicals
Cbl-b	Rabbit	sc-1705	1:1000	Santa Cruz
c-Cbl	Mouse	Clone 17	1:1000	BD Transduction Laboratories
FLIP, C-terminus	Rabbit	06-864	1:1000	Upstate
c-Myc	Rabbit	9402	1:1000	Cell Signaling Technology
c-Myc pThr58	Rabbit	ab28842	1:1000	Abcam
c-Myc Ser62	Rabbit	ab51156	1:1000	Abcam
c-Myc pThr58/Ser62	Rabbit	9401	1:1000	Cell Signaling Technology
CTCF	Rabbit	sc-28198	1:1000	Santa Cruz
Fas (CD95)	Mouse	Clone 13	1:2500	BD Transduction Laboratories
FasL (CD178)	Mouse	Clone 33	1:1000	BD Transduction Laboratories
Grail	Rat	Clone H11-744	1:150	BD Pharmingen
HDAC-1	Rabbit	sc-7872	1:1000	Santa Cruz
HA tag	Rat	Clone 3F10	1:1000	Roche
Itch	Mouse	32/Itch	1:500	BD Transduction Laboratories
Noxa	Rabbit	ab13687	1:500	Abcam
p27	Rabbit	sc-776	1:1000	Santa Cruz
p53	Rabbit	sc-6243	1:1000	Santa Cruz
p42/44 (ERK)	Rabbit	9102	1:1000	Cell Signaling Technology
p42/44 (ERK) pThr202/Tyr204	Rabbit	9101	1:1000	Cell Signaling Technology
Rap1	Rabbit	sc-65	1:1000	Santa Cruz
B-Raf	Rabbit	sc-9002	1:1000	Santa Cruz
Raf-1	Rabbit	sc-133	1:1000	Santa Cruz
Rb pSer780	Rabbit	9307	1:1000	Cell Signaling Technology
Rb pSer807/811	Rabbit	9308	1:1000	Cell Signaling Technology
SPA-1	Mouse	3/SPA-1	1:250	BD Transduction Laboratories
Ubiquitin	Mouse	Clone P4D1	1:1000	Cell Signaling Technology
VDAC-1	Rabbit	4866	1:1000	Cell Signaling Technology
Secondary antibodies	**Host**	**Clone/ID**	**Dilution**	**Manufacturer**
anti-rabbit-HRP	Goat	7074	1:2000	Cell Signaling Technology
anti-mouse-HRP	Horse	7076	1:2000	Cell Signaling Technology
anti-rat-HRP	Goat	7077	1:2000	Cell Signaling Technology

(D) Immunofluorescent staining

Primary antibodies	Host	Clone/ID	Dilution	Manufacturer
p42/44 (ERK) pThr202/Tyr204	Rabbit	9101	1:50	Cell Signaling Technology
c-Myc	Rabbit	9402	1:50	Cell Signaling Technology
c-Myc Ser62	Rabbit	ab51156	1:500	Abcam
Rap-1	Rabbit	sc-65	1:100	Santa Cruz
RalGSD-RBD	recombinant E.coli	Z02039	1:5000	GenScript/Bioquote Ltd.
Rb pSer780	Rabbit	9307	1:500	Cell Signaling Technology
Rb pSer807/811	Rabbit	9308	1:50	Cell Signaling Technology
Isotype control			**Dilution**	**Manufacturer**
Rabbit IgG			appropriate	Sigma
Secondary antibodies	**Host**	**Clone/ID**	**Dilution**	**Manufacturer**
anti-GST	Rabbit	2622	1:100	Cell Signaling Technology
anti-rabbit-HRP	Goat	7074	1:100	Cell Signaling Technology

Figure 2.1

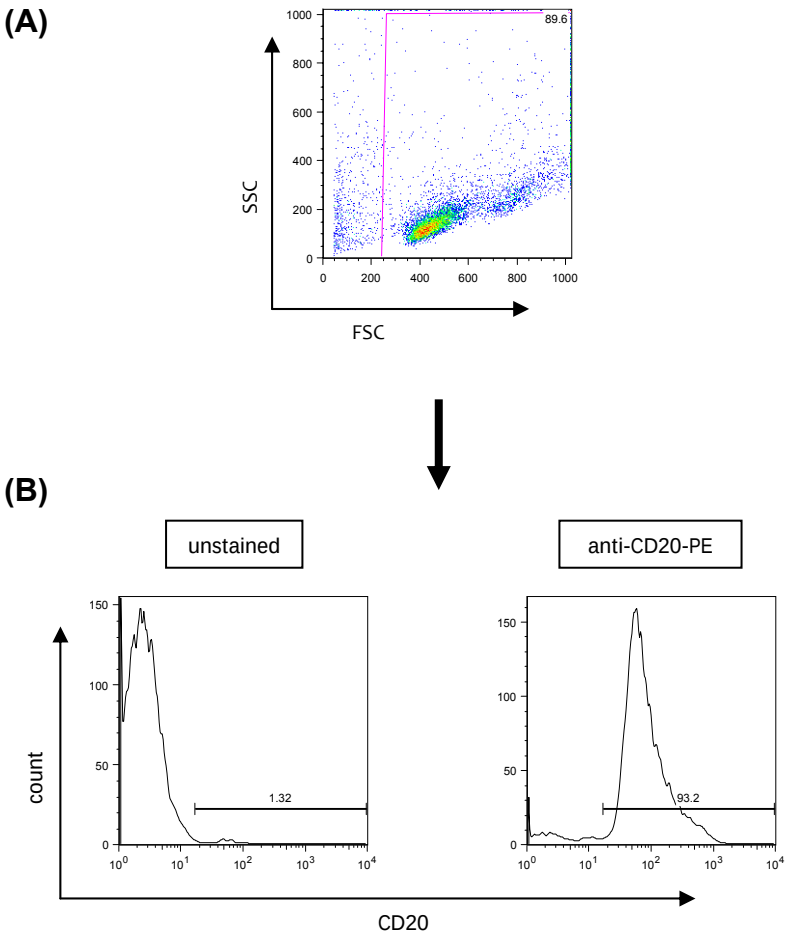

Figure 2.2

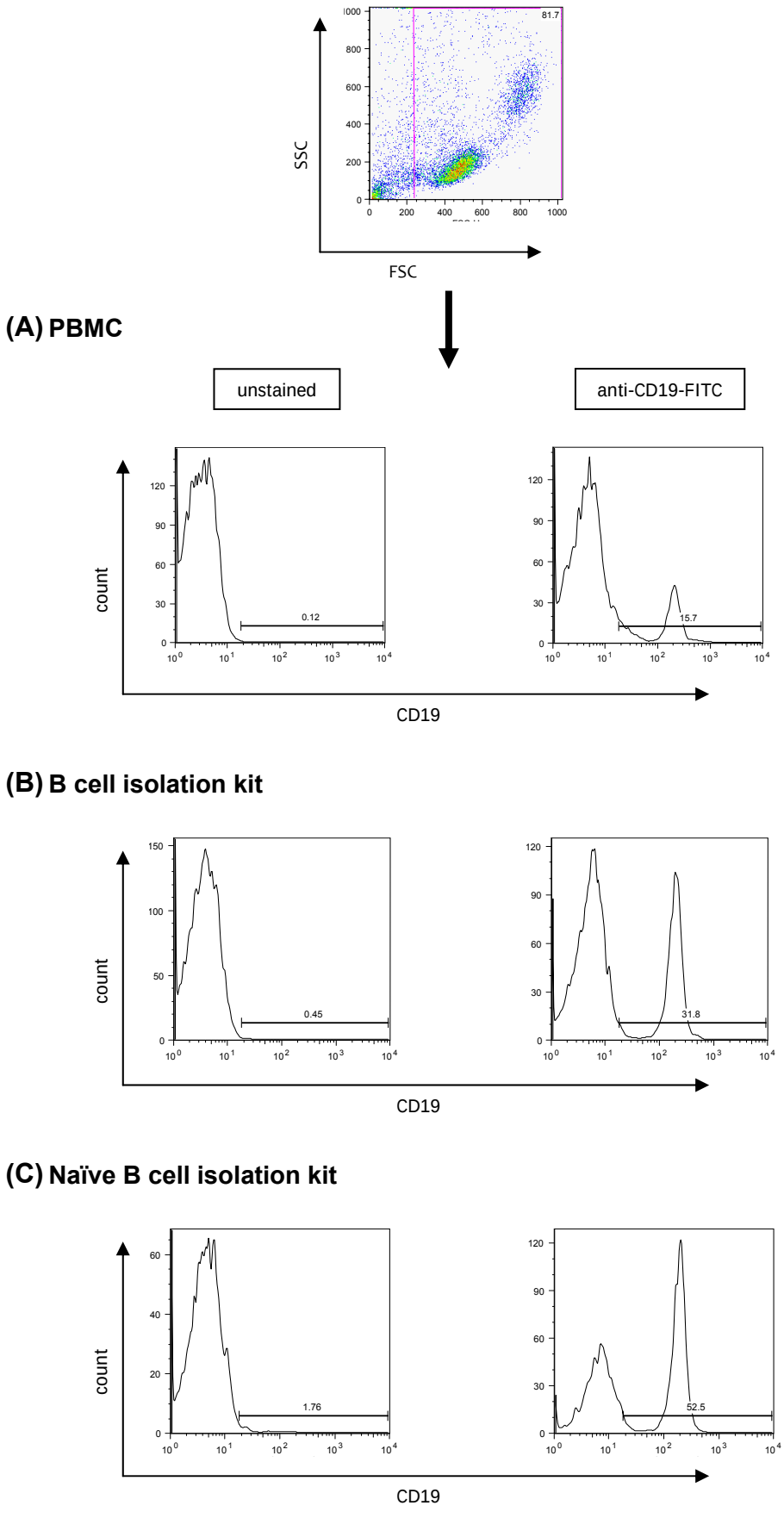
81.7
SSC
FSC
(A) PBMC
unstained
anti-CD19-FITC
0.12
15.7
count
CD19
(B) B cell isolation kit
0.45
31.8
count
CD19
(C) Naïve B cell isolation kit
1.76
52.5
count
CD19

Figure 2.3

(A) CD3 – T cells

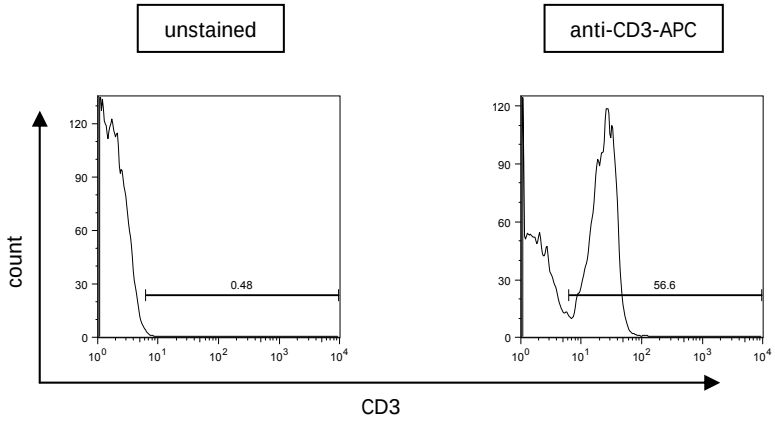

(B) CD14 - monocytes

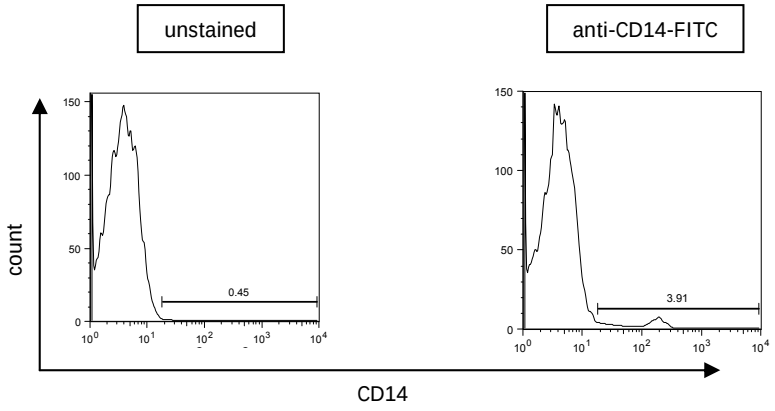

Figure 2.4

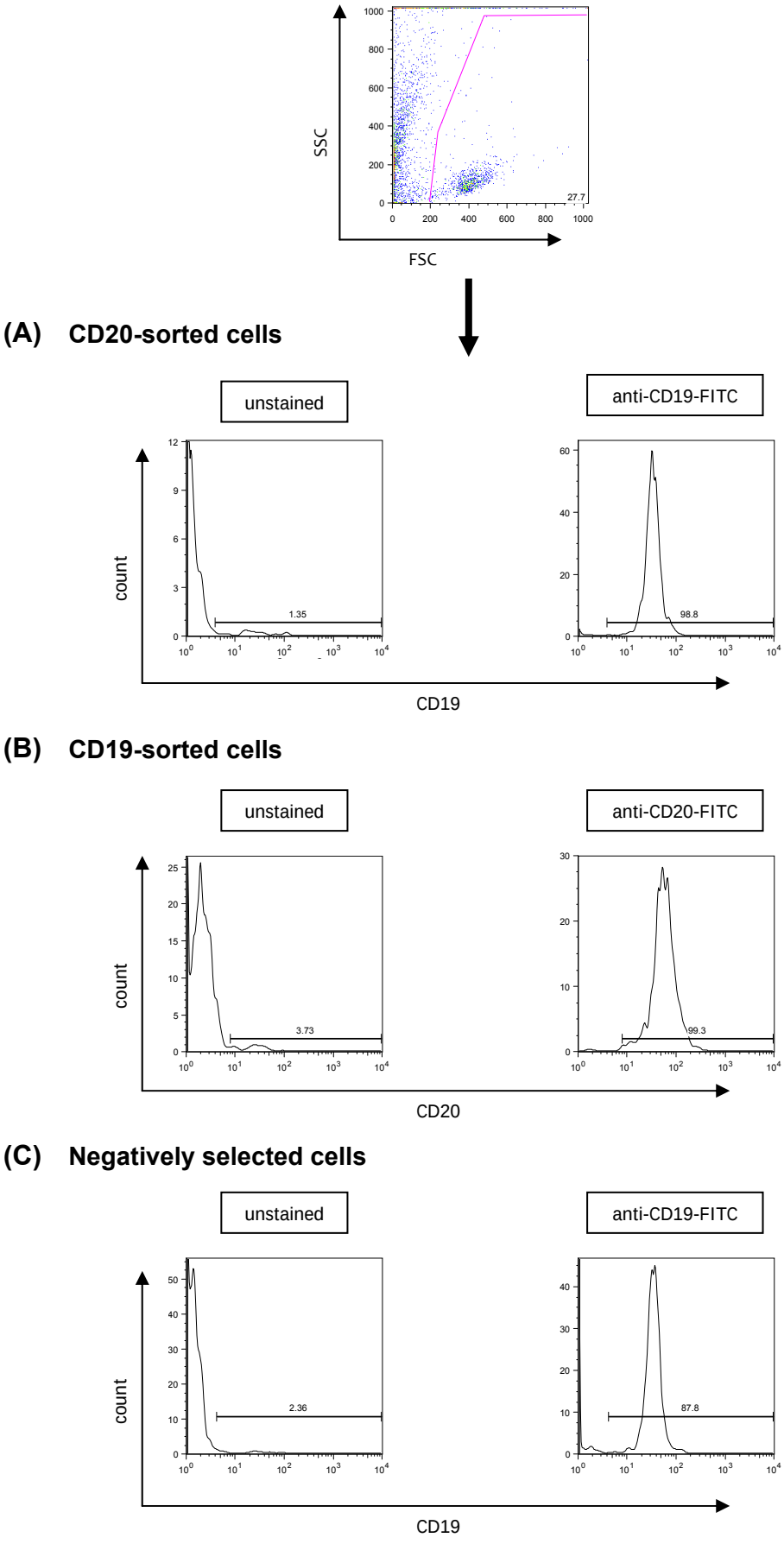
SSC
FSC
27.7
(A) CD20-sorted cells
unstained
anti-CD19-FITC
count
1.35
98.8
CD19
(B) CD19-sorted cells
unstained
anti-CD20-FITC
count
3.73
99.3
CD20
(C) Negatively selected cells
unstained
anti-CD19-FITC
count
2.36
87.8
CD19

Figure 2.5

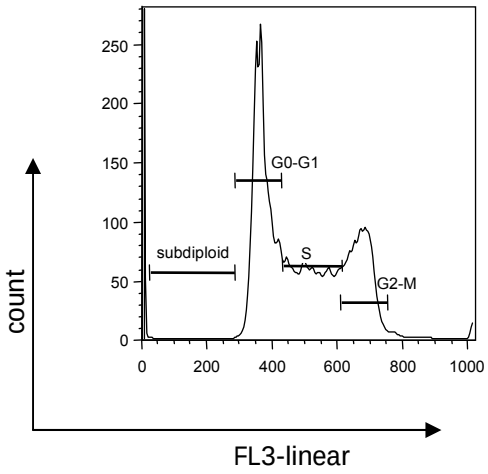
250
200
150
100
50
0
G0-G1
subdiploid
S
G2-M
0
200
400
600
800
1000
count
FL3-linear

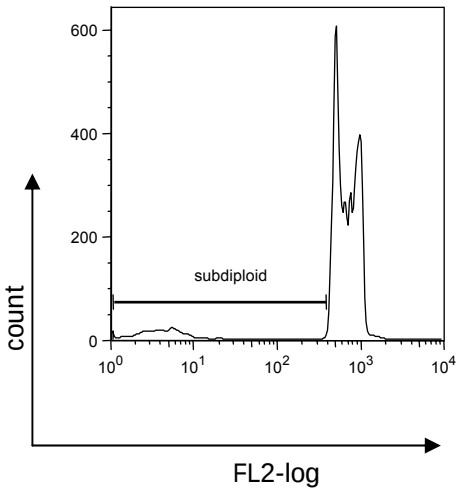
600
400
200
0
subdiploid
10^0
10^1
10^2
10^3
10^4
count
FL2-log

Figure 2.6

(A) untreated

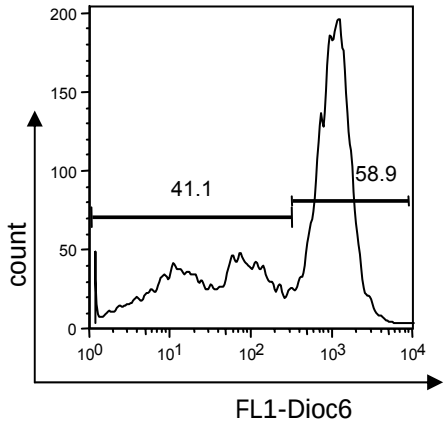

(B) anti-IgM

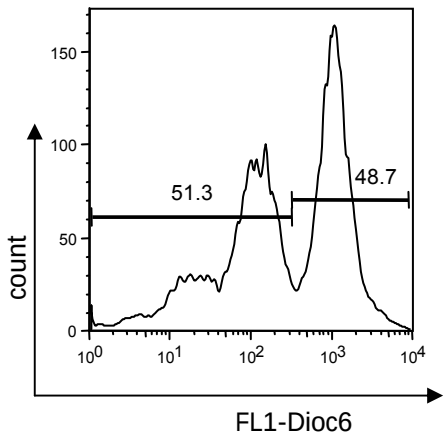

Figure 2.7

(A) Murine lymph node cells- unimmunised mice

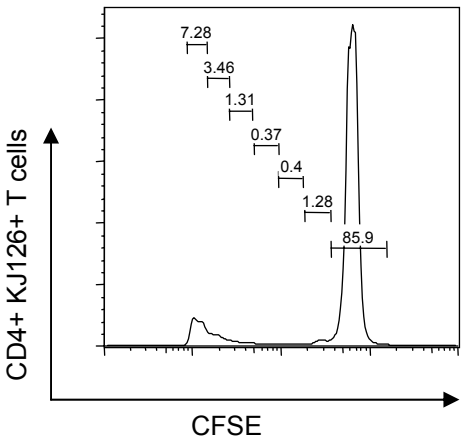

(B) Murine lymph node cells- immunised mice

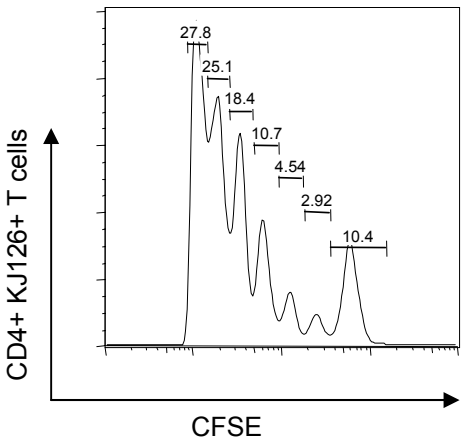

(C) Untreated human B cells– before culture

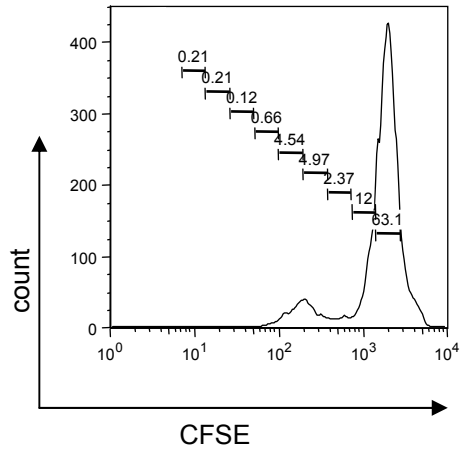

(D) Human B cells stimulated with F(ab')2 anti-IgM/IgG for 48 hrs

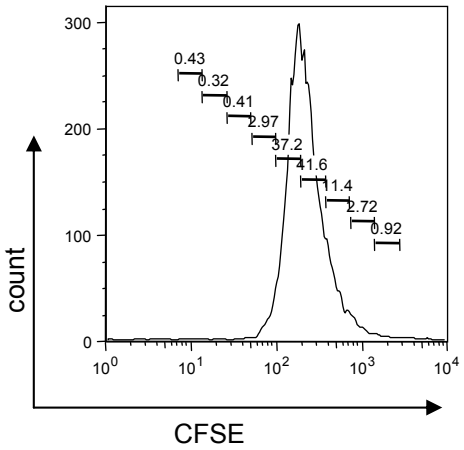

Figure 2.8

(A)

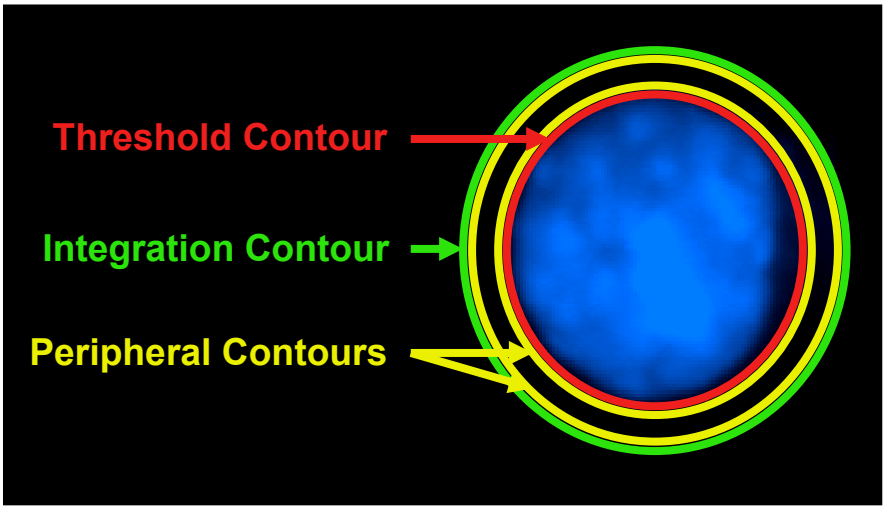
Threshold Contour
Integration Contour
Peripheral Contours

(B)

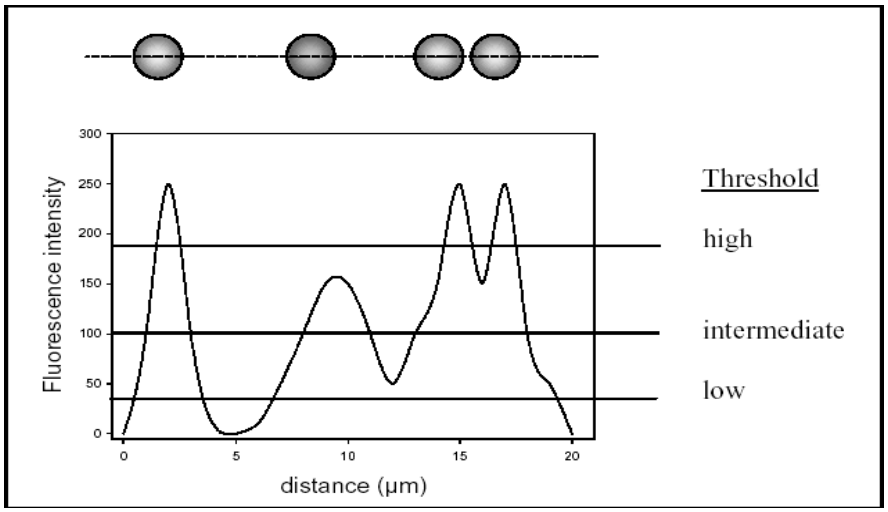
Fluorescence intensity
300
250
200
150
100
50
0
0
5
10
15
20
distance (μm)
Threshold
high
intermediate
low

Figure 2.9

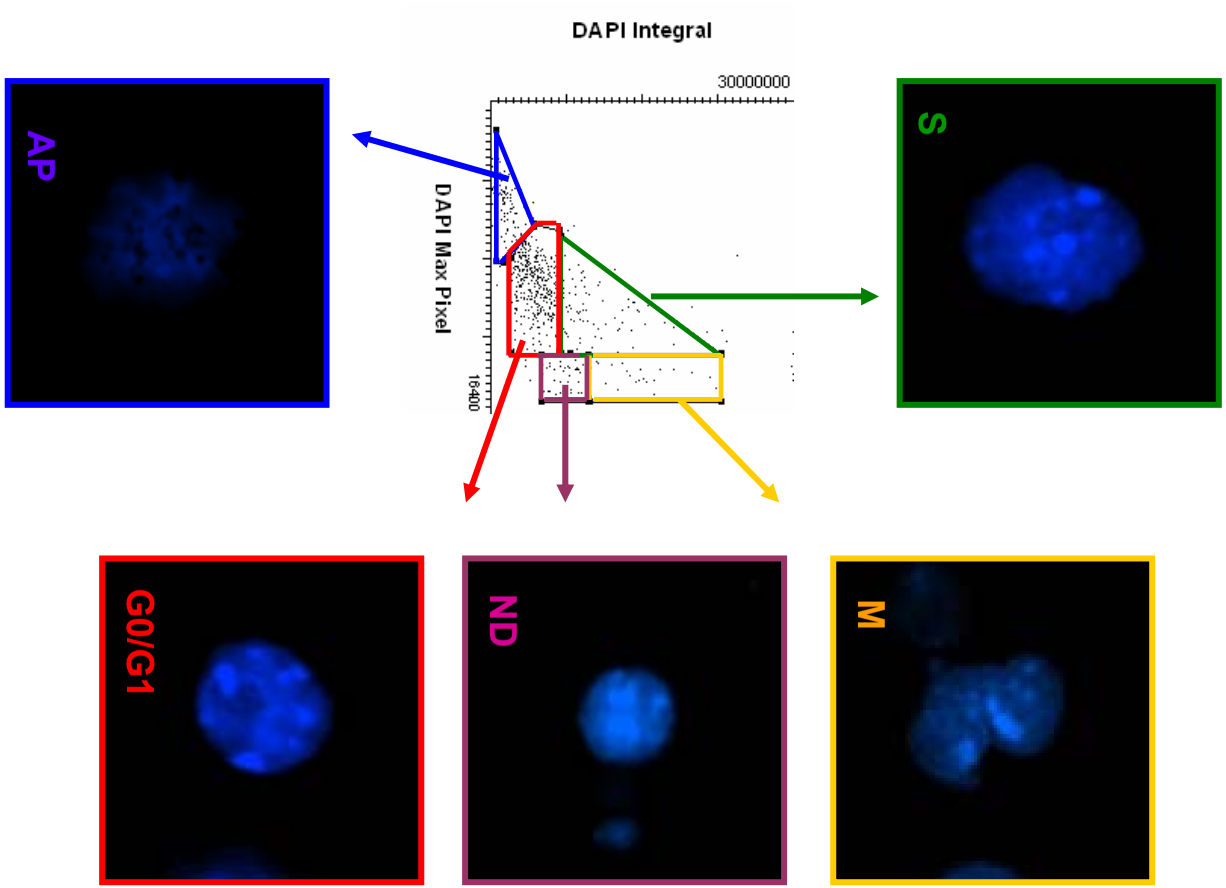

Table 2.2

Primers human	Sequence
FcγRIIb1 fw	5' ggccttgatctactgcaggaa 3'
FcγRIIb1 fw	5' gggcgggtctctcccatttc 3'
FcγRIIb2 fw	5' tgctgctgtagtggccttga 3'
FcγRIIb2 rv	5' ccccaactttgtcagcctcat 3'
Probes human	
FcγRIIb1	FAM - 5' cggatttcagctctcccaggataccct 3' - TAMRA
FcγRIIb2	FAM - 5' aggaaaaagcggatttcagccaatcccacta 3' - TAMRA
HPRT	Kit (AB Applied Biosystems)
β-Actin	Kit (AB Applied Biosystems)
Primers murine	
Cbl-b fw	5' tgtgcacttcgtgccttacc 3'
Cbl-b rv	5' tgggctccgttccttttatct 3'
c-Cbl fw	5' tgatccttggaatgggagaga 3'
c-Cbl rv	5' ttccatttgtgagggcaatg 3'
cMyc fw	5' agctgaagcgcagctttttt 3'
cMyc rv	5' gtaggcggtggctttttga 3'
CTCF fw	5' ttgtagacaggagcggcacat 3'
CTCF rv	5' gctgtttctggcggaaggt 3'
p53 fw	5' aagacgtgccctgtgcagtt 3'
p53 rv	5' acctccgtcatgtgctgtga 3'
PAC-1 fw	5' gctggatctctcgctcag 3'
PAC-1 rv	5' ccccgacgttgcttaacaaa 3'
SPA-1 fw	5' tcctgaggaagcgtcatatcg 3'
SPA-1 rv	5' ctggaagtgagagcggattgt 3'
Probes murine	
Cbl-b	FAM - 5' ccaaggctgccccttctgtcgc 3' - TAMRA
c-Cbl	FAM - 5' ttgaccaatcggcactcgcttcc 3' - TAMRA
cMyc	FAM - 5' ccctgcgtgaccagatccctgaat 3' - TAMRA
CTCF	FAM - 5' atcatgcacaagcgcactcacacg 3' - TAMRA
GAPDH	Kit (AB Applied Biosystems)
p53	FAM - 5' tggtcagcgccacacctcca 3' - TAMRA
PAC-1	FAM - 5' caccatctgcctggcatacctgattca 3' - TAMRA
SPA-1	FAM - 5' caacgatattgtgaccatcgtgttccagg 3' - TAMRA
Fas	Taqman gene expression assay (Applied Biosystems - Mm01204974_m1)
FasL	Taqman gene expression assay (Applied Biosystems - Mm00438864_m1)

Figure 2.10

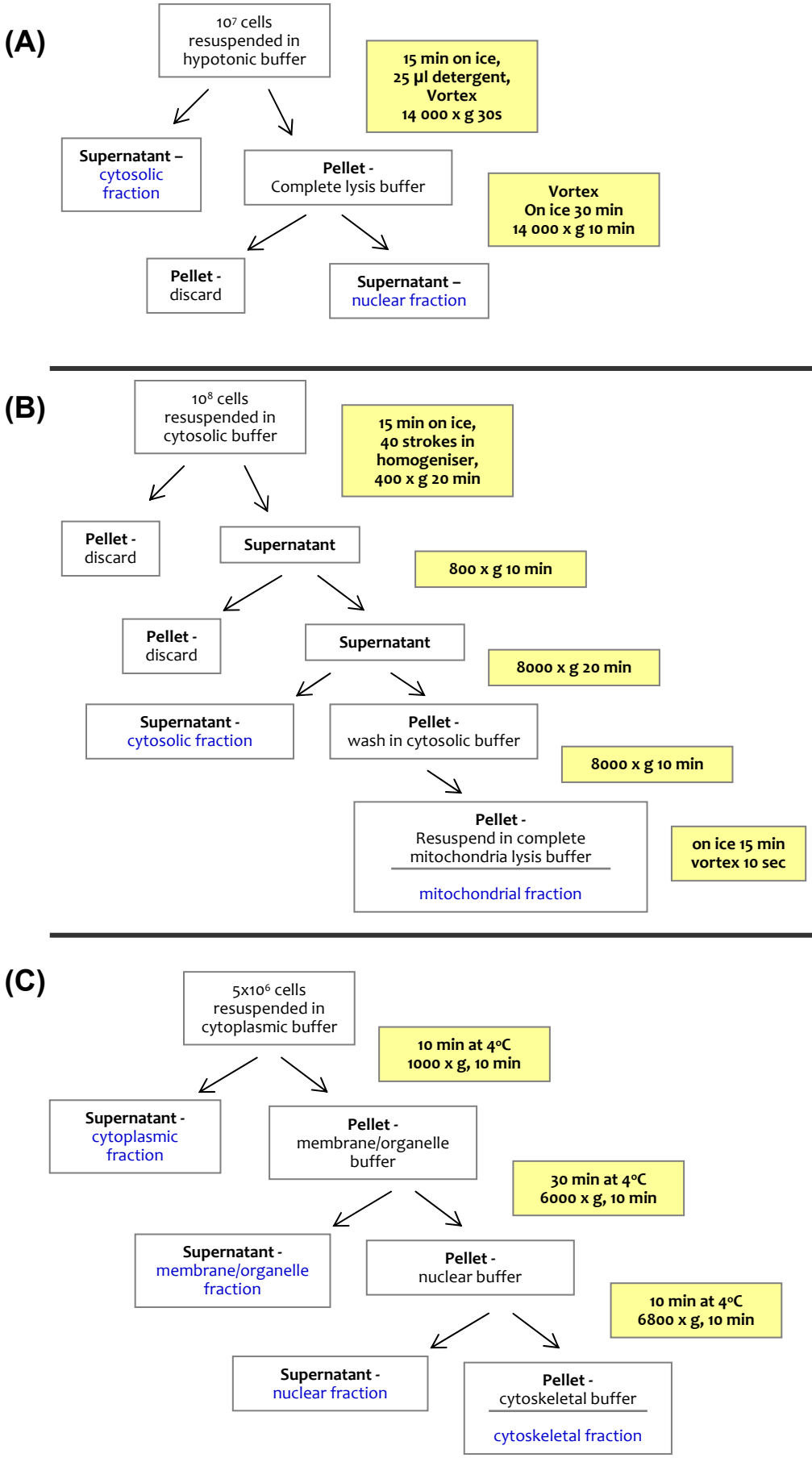
(A)
10⁷ cells resuspended in hypotonic buffer
15 min on ice, 25 µl detergent, Vortex 14 000 x g 30s
Supernatant – cytosolic fraction
Pellet - Complete lysis buffer
Vortex On ice 30 min 14 000 x g 10 min
Pellet - discard
Supernatant – nuclear fraction
(B)
10⁸ cells resuspended in cytosolic buffer
15 min on ice, 40 strokes in homogeniser, 400 x g 20 min
Pellet - discard
Supernatant
800 x g 10 min
Pellet - discard
Supernatant
8000 x g 20 min
Supernatant - cytosolic fraction
Pellet - wash in cytosolic buffer
8000 x g 10 min
Pellet - Resuspend in complete mitochondria lysis buffer
mitochondrial fraction
on ice 15 min vortex 10 sec
(C)
5x10⁶ cells resuspended in cytoplasmic buffer
10 min at 4°C 1000 x g, 10 min
Supernatant - cytoplasmic fraction
Pellet - membrane/organelle buffer
30 min at 4°C 6000 x g, 10 min
Supernatant - membrane/organelle fraction
Pellet - nuclear buffer
10 min at 4°C 6800 x g, 10 min
Supernatant - nuclear fraction
Pellet - cytoskeletal buffer
cytoskeletal fraction

Table 2.3

(A) Vectors

Vector	Inserted via restriction sites	Supplier
pcDNA™3.1 (+)		Invitrogen
pcDNA™3.1/Zeo (-)		Invitrogen
pIRES2-AcGFP1		Clontech
pLVX-IRES-ZsGreen1		Clontech
pcDNA™3.1 (+) - Rap1A WT		Missouri S&T cDNA Resource Center
pcDNA™3.1 (+) - Rap1A G12V		Missouri S&T cDNA Resource Center
pcDNA™3.1 (+) - Rap1A S17N		Missouri S&T cDNA Resource Center
pcDNA™3.1/Zeo (-) - Rap1A WT	Nhe I/Xho I	
pcDNA™3.1/Zeo (-) - Rap1A G12V	Nhe I/Xho I	
pcDNA™3.1/Zeo (-) - Rap1A S17N	Nhe I/Xho I	
pIRES2-AcGFP1 - Rap1A WT	Nhe I/Xho I	
pIRES2-AcGFP1 - Rap1A G12V	Nhe I/Xho I	
pIRES2-AcGFP1 - Rap1A S17N	Nhe I/Xho I	
pLVX-IRES-ZsGreen1 - Rap1A WT	Eco RI/Xba I	
pLVX-IRES-ZsGreen1 - Rap1A G12V	Eco RI/Xba I	
pLVX-IRES-ZsGreen1 - Rap1A S17N	Eco RI/Xba I	

(B) Primers

Primers	Sequence
pcDNA3.1-Rap FW (Eco RI)	5' gagagaattcgctggctagcgtttaaactta 3'
pCDNA3.1-Rap RV (Xba I)	5' gagatctagataaacgggccctctagactc 3'

(C) Cloning strategy

Final construct	Parental plasmid for vector	Parental plasmid for insert	Restriction enzymes
pcDNA™3.1/Zeo (-) - Rap1A WT	pcDNA™3.1/Zeo (-)	pcDNA™3.1 (+) - Rap1A WT	Nhe I/Xho I
pcDNA™3.1/Zeo (-) - Rap1A G12V	pcDNA™3.1/Zeo (-)	pcDNA™3.1 (+) - Rap1A G12V	Nhe I/Xho I
pcDNA™3.1/Zeo (-) - Rap1A S17N	pcDNA™3.1/Zeo (-)	pcDNA™3.1 (+) - Rap1A S17N	Nhe I/Xho I
pIRES2-AcGFP1 - Rap1A WT	pIRES2-AcGFP1	pcDNA™3.1 (+) - Rap1A WT	Nhe I/Xho I
pIRES2-AcGFP1 - Rap1A G12V	pIRES2-AcGFP1	pcDNA™3.1 (+) - Rap1A G12V	Nhe I/Xho I
pIRES2-AcGFP1 - Rap1A S17N	pIRES2-AcGFP1	pcDNA™3.1 (+) - Rap1A S17N	Nhe I/Xho I
pLVX-IRES-ZsGreen1 - Rap1A WT	pLVX-IRES-ZsGreen1	pcDNA™3.1 (+) - Rap1A WT - PCR fragment	Eco RI/Xba I
pLVX-IRES-ZsGreen1 - Rap1A G12V	pLVX-IRES-ZsGreen1	pcDNA™3.1 (+) - Rap1A G12V - PCR fragment	Eco RI/Xba I
pLVX-IRES-ZsGreen1 - Rap1A S17N	pLVX-IRES-ZsGreen1	pcDNA™3.1 (+) - Rap1A S17N - PCR fragment	Eco RI/Xba I

Figure 2.11

(A) pcDNA3.1 (+)

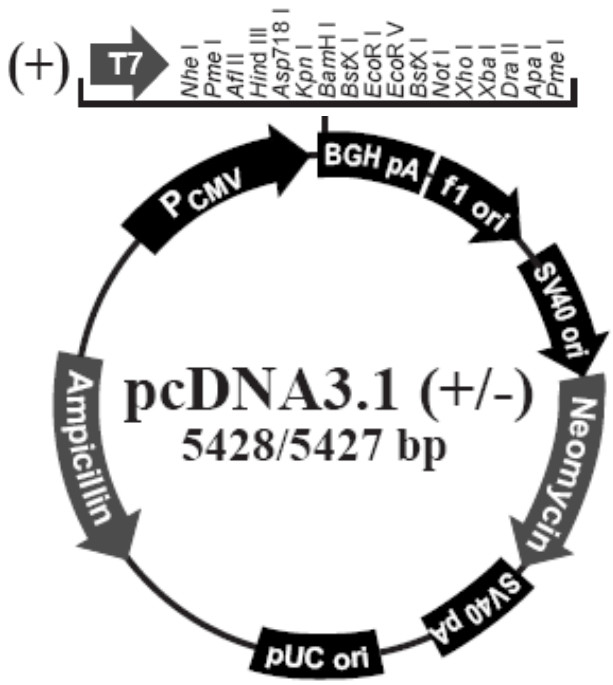

(B) pcDNA3.1/Zeo (-)

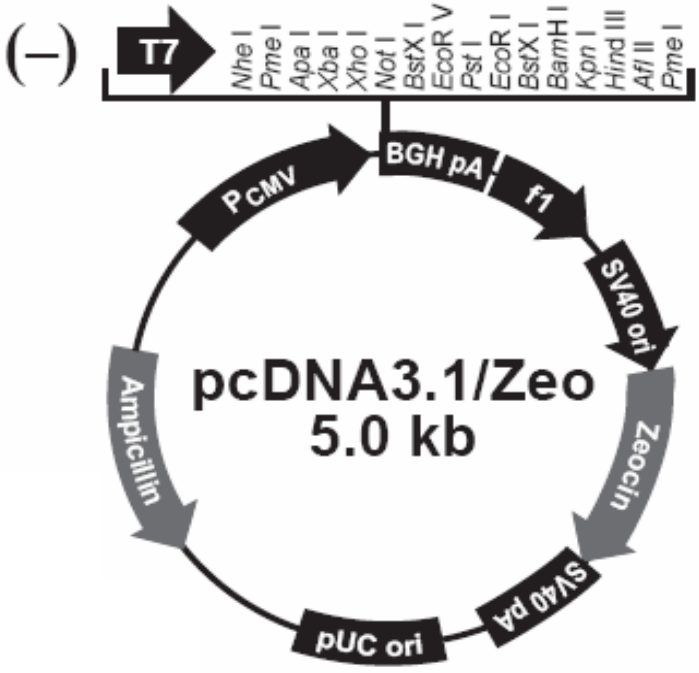

Figure 2.12

(A) pIRES2-AcGFP1

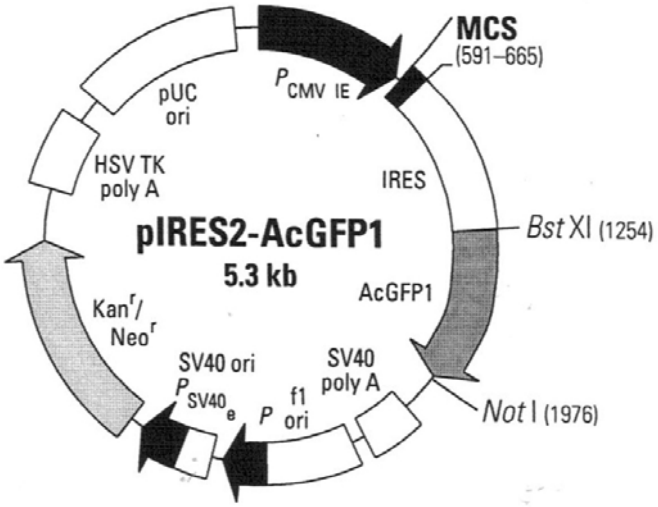

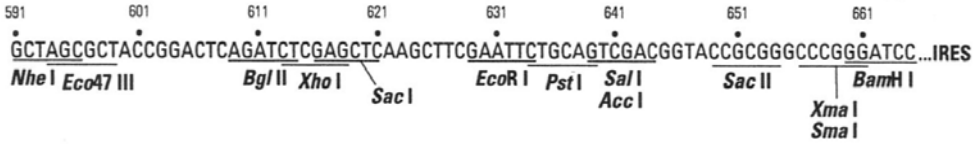

(B) pLVX-IRES-ZsGreen1

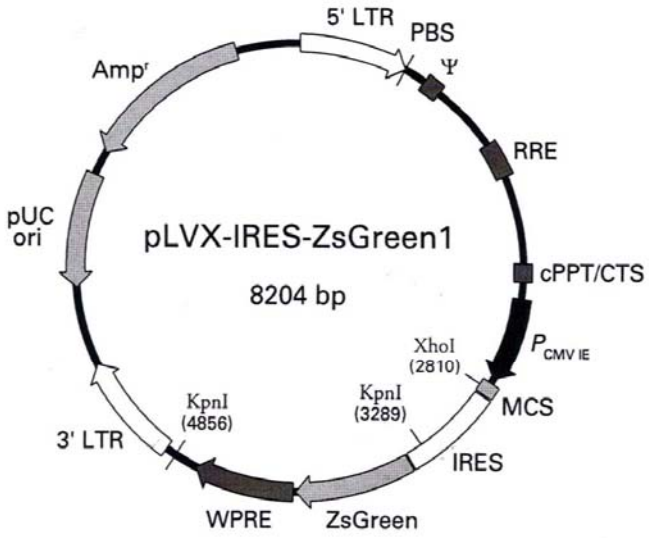

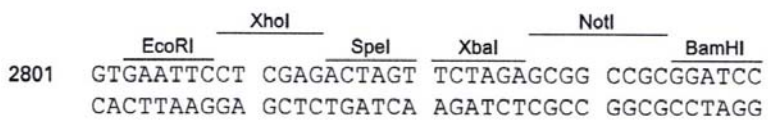

Figure 3.1

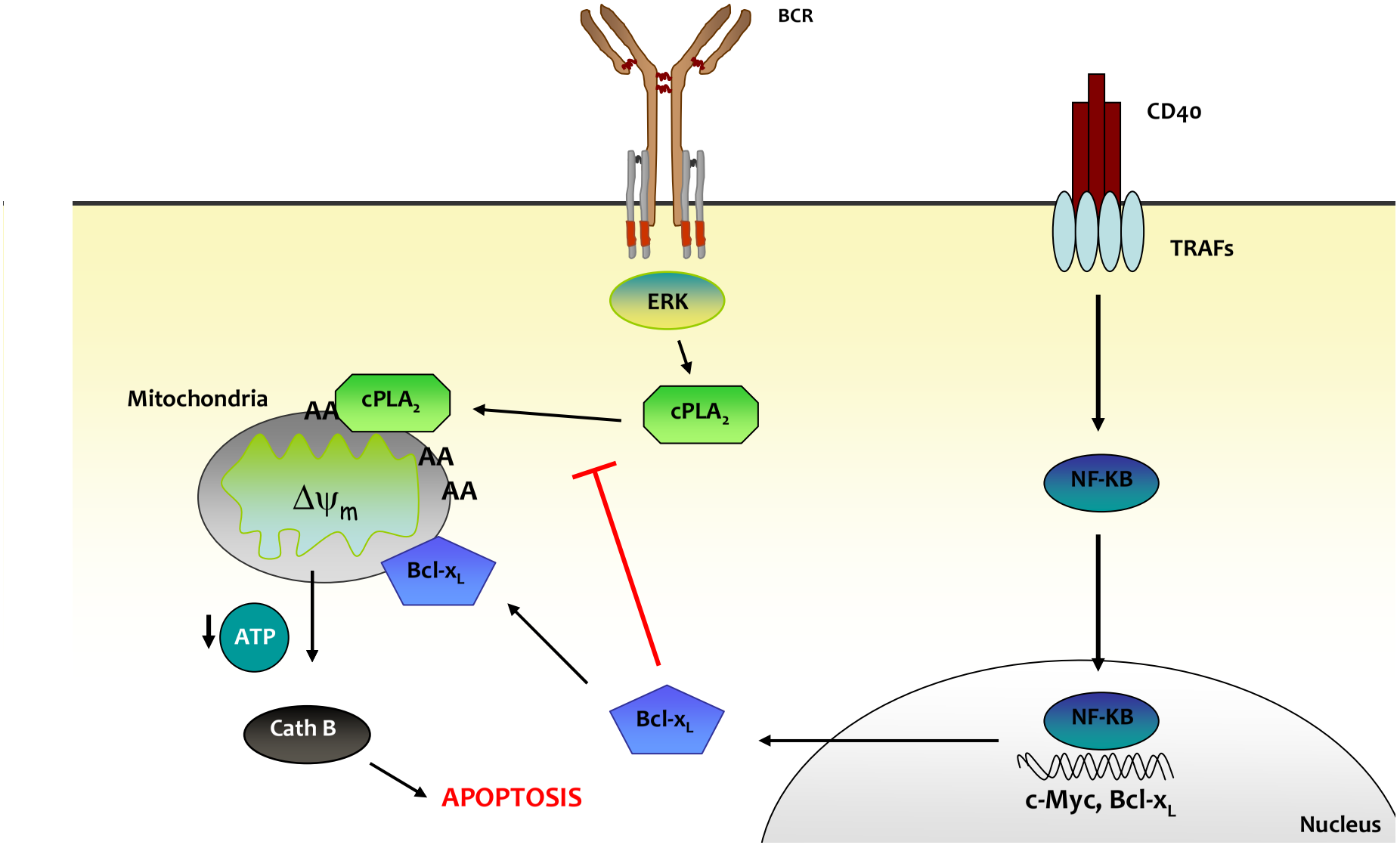
BCR
CD40
TRAFs
ERK
cPLA2
cPLA2
Mitochondria
AA
AA
AA
ΔΨm
Bcl-xL
ATP
Cath B
APOPTOSIS
NF-KB
Bcl-xL
NF-KB
c-Myc, Bcl-xL
Nucleus

Figure 3.2

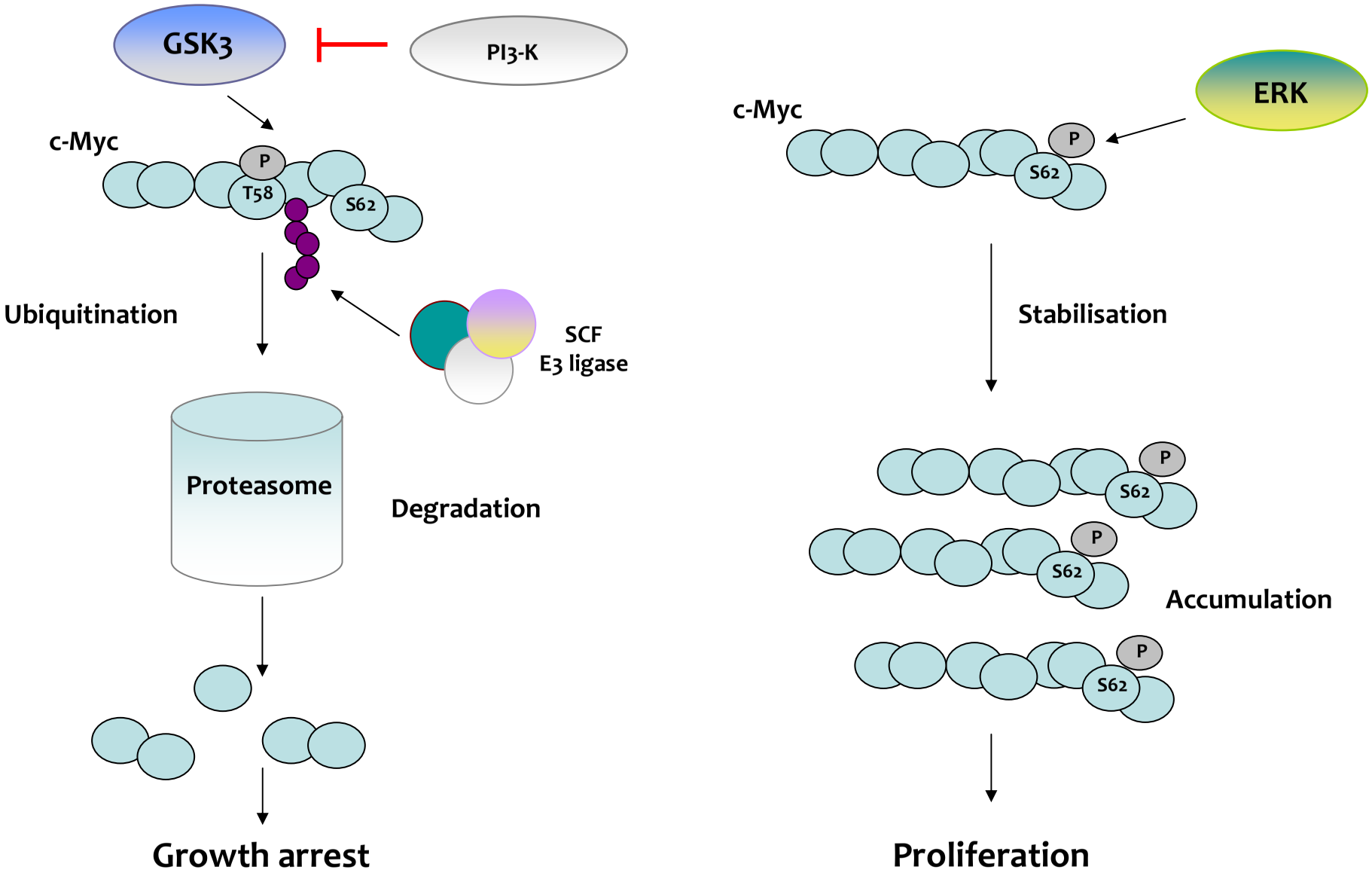
GSK3
PI3-K
c-Myc
P
T58
S62
Ubiquitination
SCF
E3 ligase
Proteasome
Degradation
Growth arrest
c-Myc
ERK
P
S62
Stabilisation
P
S62
P
S62
Accumulation
P
S62
Proliferation

Figure 3.3

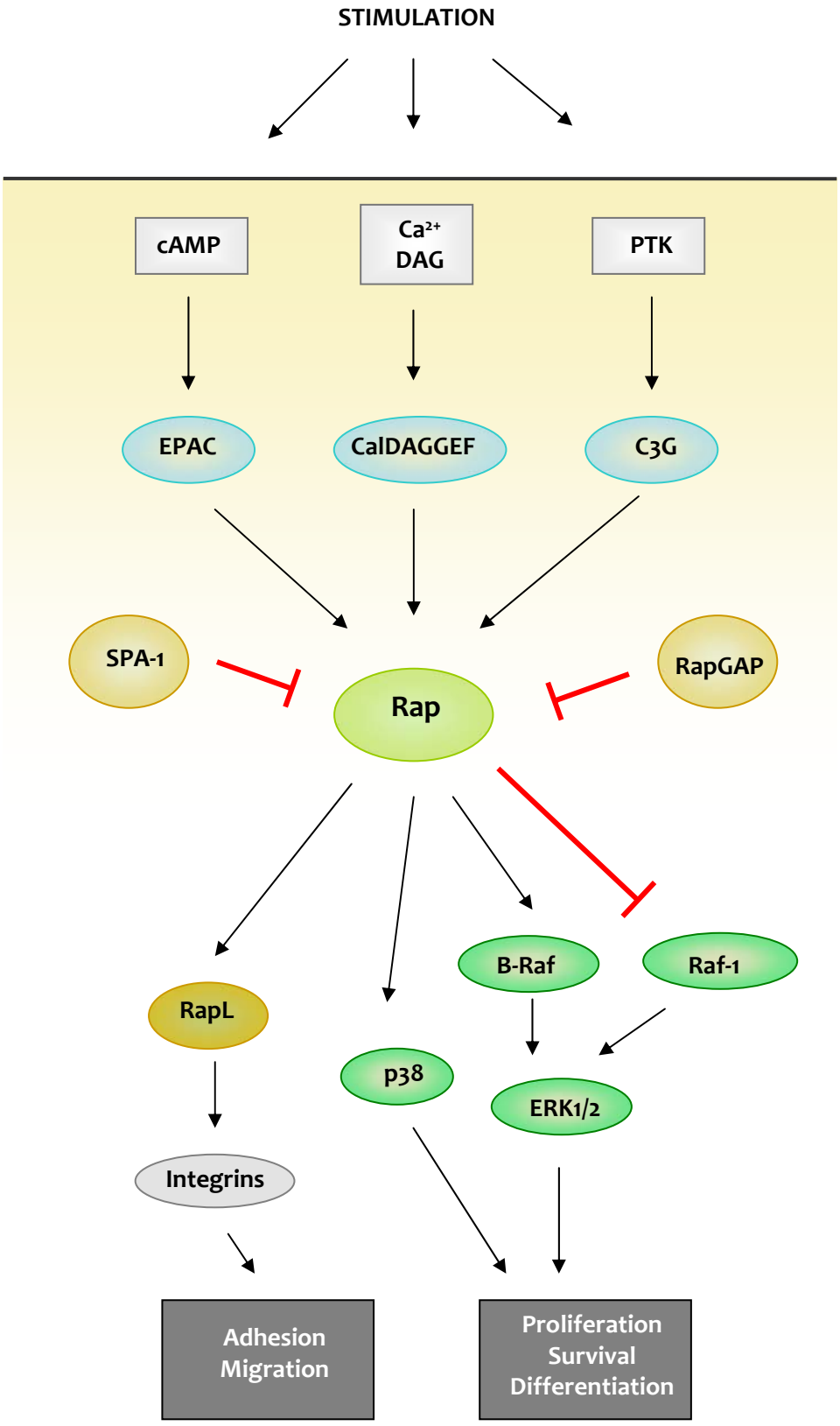
STIMULATION
cAMP
Ca2+
DAG
PTK
EPAC
CalDAGGEF
C3G
SPA-1
Rap
RapGAP
RapL
B-Raf
Raf-1
p38
ERK1/2
Integrins
Adhesion
Migration
Proliferation
Survival
Differentiation

Figure 3.4

(A)

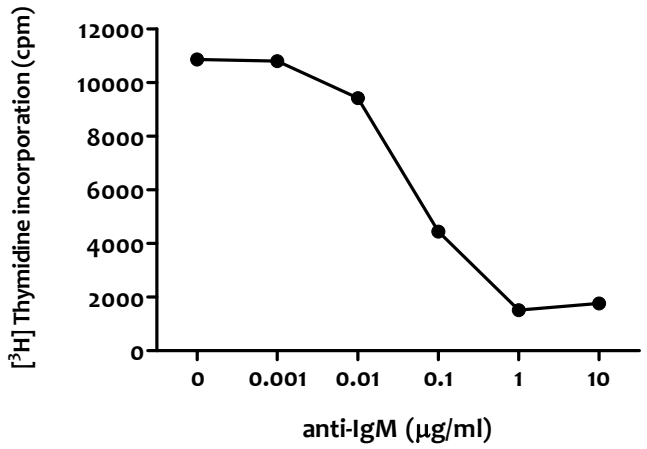
[3H] Thymidine incorporation (cpm)
12000
10000
8000
6000
4000
2000
0
0
0.001
0.01
0.1
1
10
anti-IgM (µg/ml)

(B)

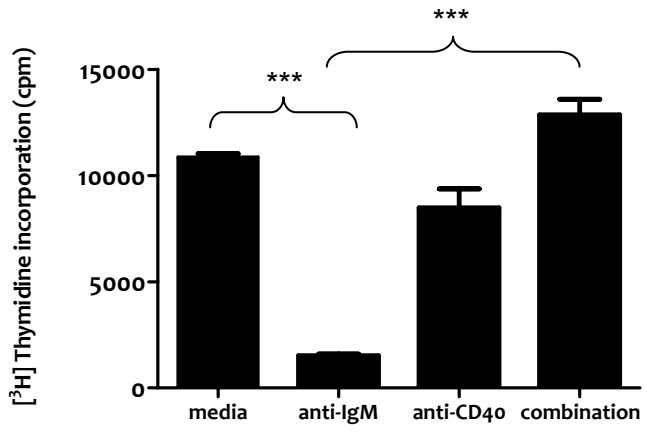
[3H] Thymidine incorporation (cpm)
15000
10000
5000
0
***
***
media
anti-IgM
anti-CD40
combination

Figure 3.5

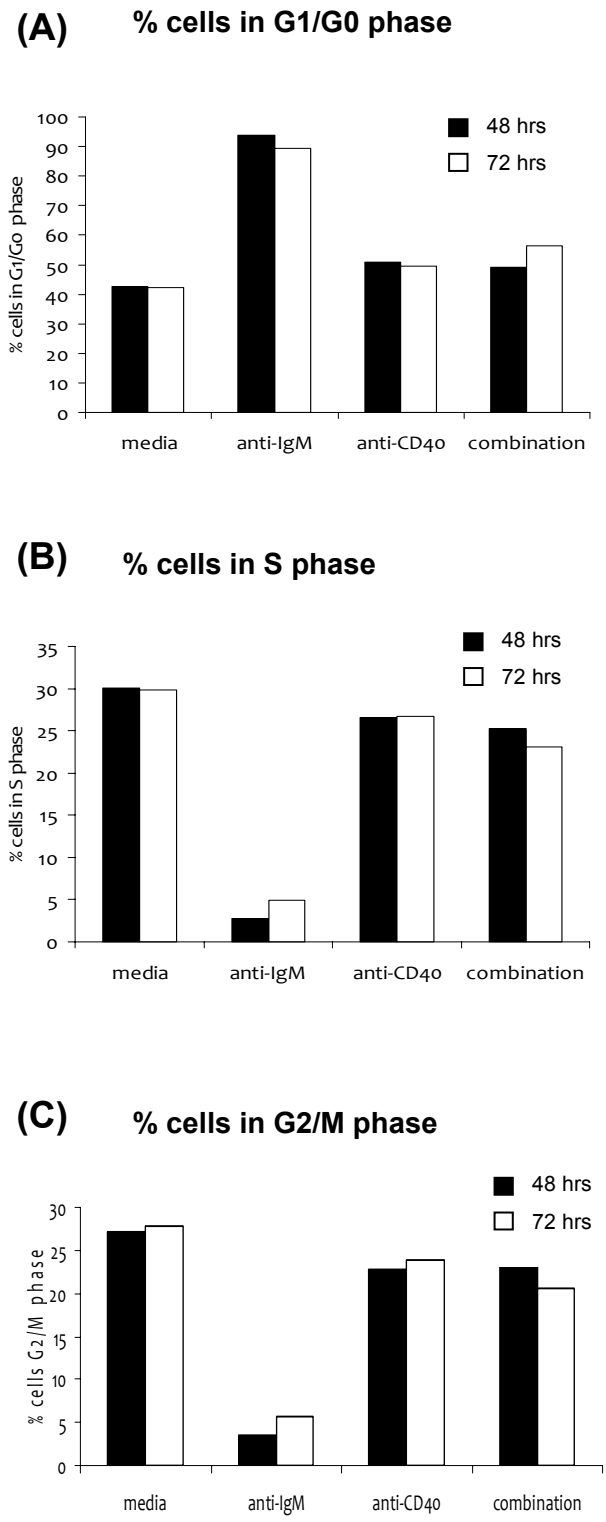
(A)
% cells in G1/G0 phase
% cells in G1/Go phase
100
90
80
70
60
50
40
30
20
10
0
48 hrs
72 hrs
media
anti-IgM
anti-CD40
combination
(B)
% cells in S phase
% cells in S phase
35
30
25
20
15
10
5
0
48 hrs
72 hrs
media
anti-IgM
anti-CD40
combination
(C)
% cells in G2/M phase
% cells G2/M phase
30
25
20
15
10
5
0
48 hrs
72 hrs
media
anti-IgM
anti-CD40
combination

Figure 3.6

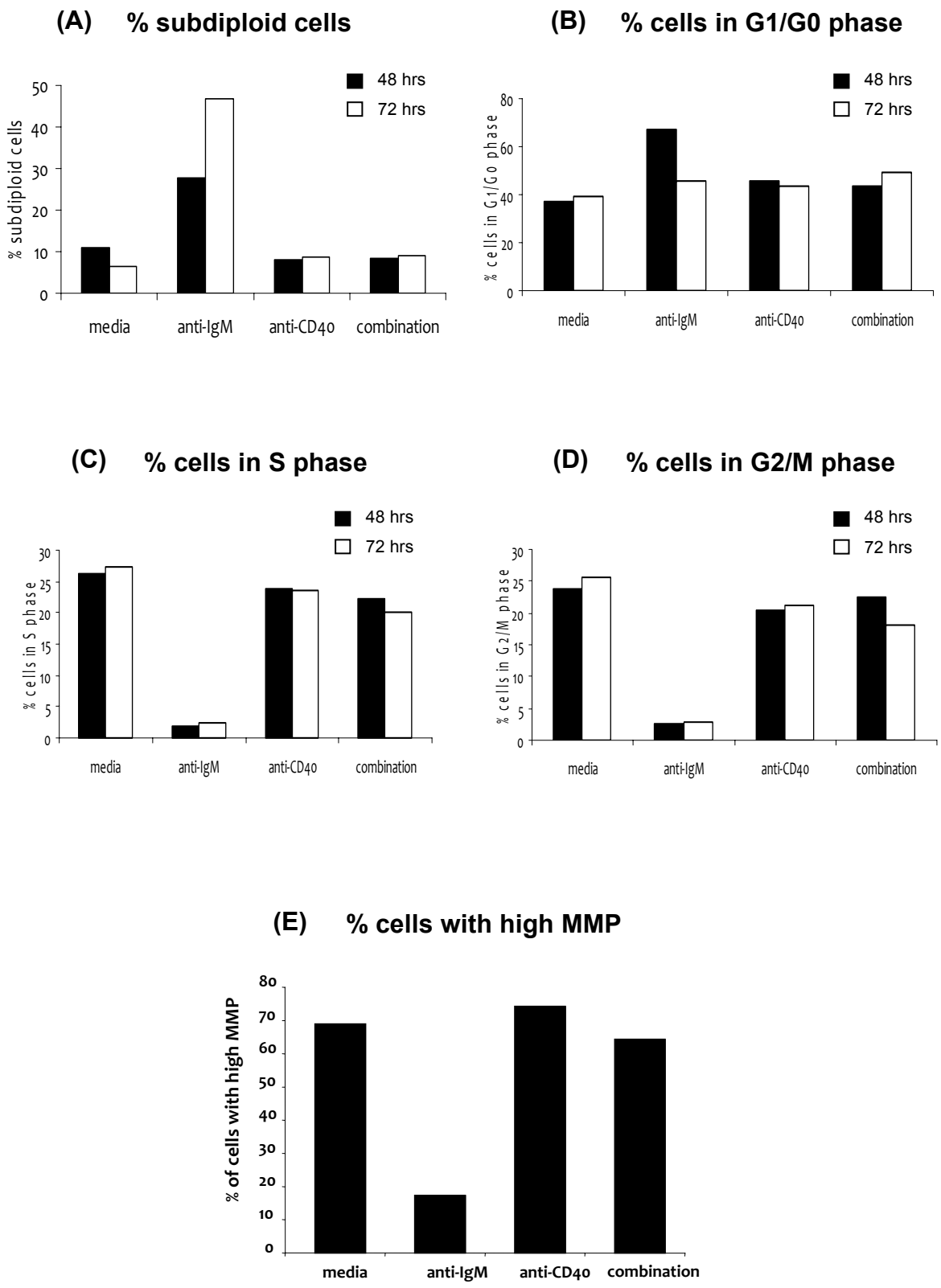
(A) % subdiploid cells
% subdiploid cells
48 hrs
72 hrs
media
anti-IgM
anti-CD40
combination
(B) % cells in G1/G0 phase
% cells in G1/Go phase
(C) % cells in S phase
% cells in S phase
(D) % cells in G2/M phase
% cells in G2/M phase
(E) % cells with high MMP
% of cells with high MMP

Figure 3.7

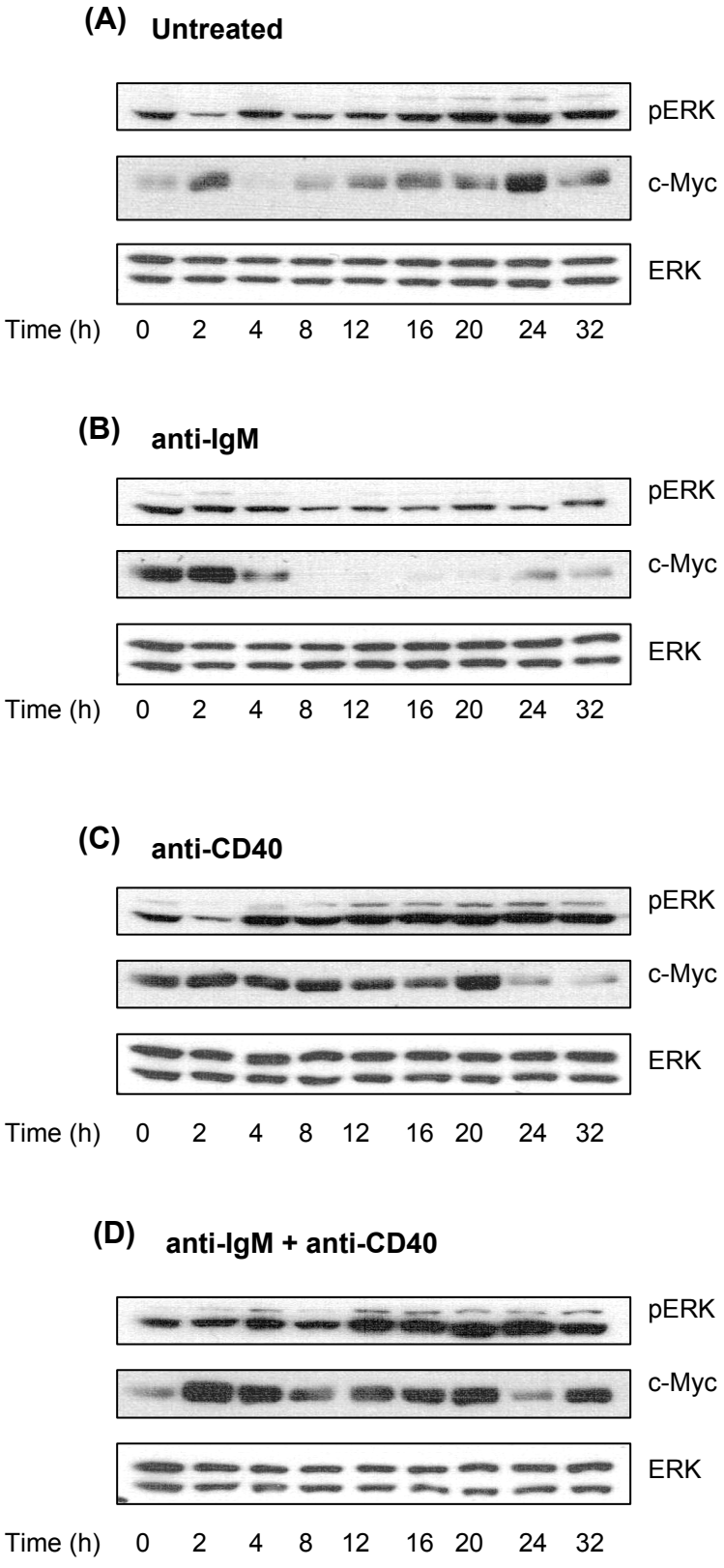
(A) Untreated
pERK
c-Myc
ERK
Time (h) 0 2 4 8 12 16 20 24 32
(B) anti-IgM
pERK
c-Myc
ERK
Time (h) 0 2 4 8 12 16 20 24 32
(C) anti-CD40
pERK
c-Myc
ERK
Time (h) 0 2 4 8 12 16 20 24 32
(D) anti-IgM + anti-CD40
pERK
c-Myc
ERK
Time (h) 0 2 4 8 12 16 20 24 32

Figure 3.8

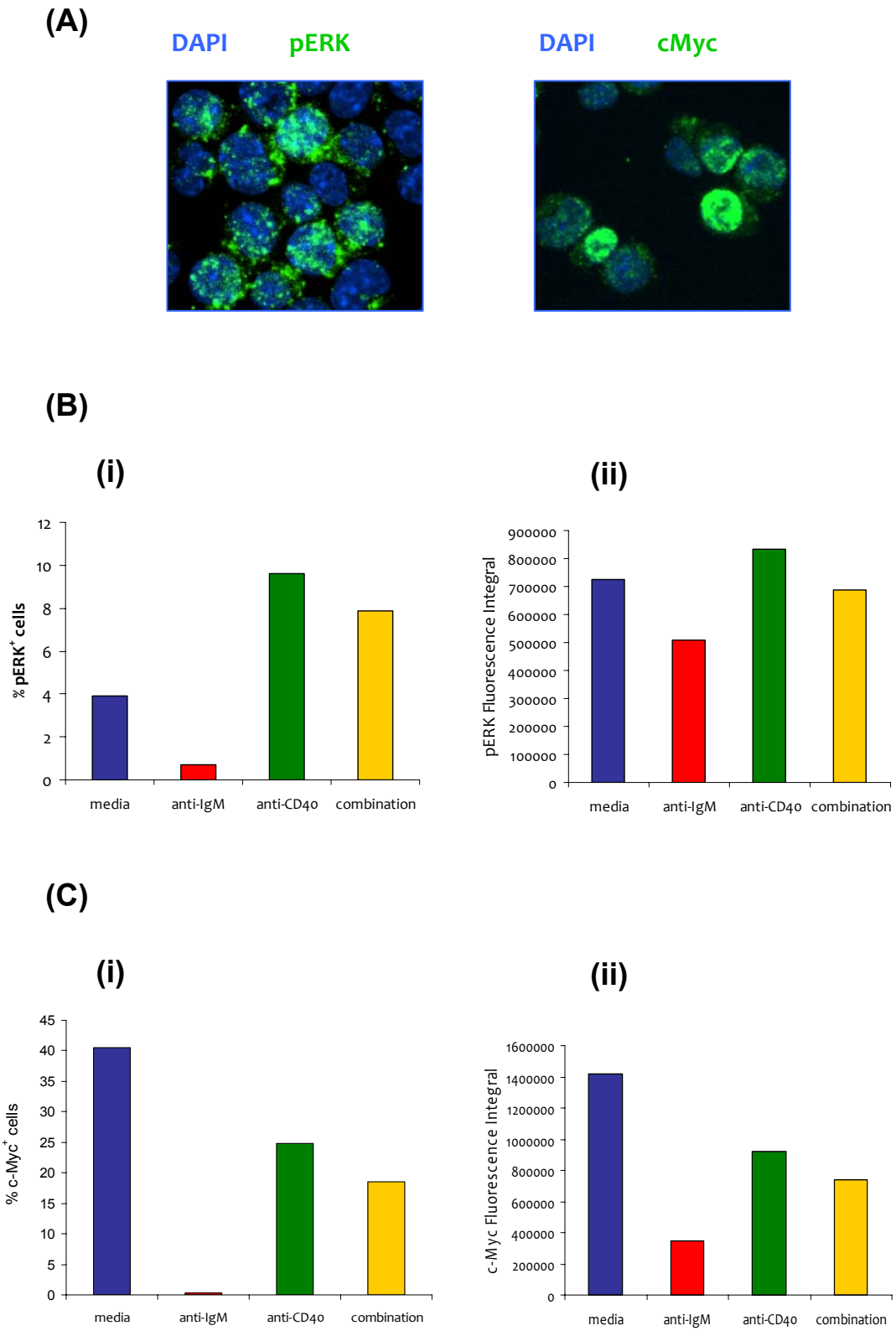
(A)
DAPI
pERK
DAPI
cMyc
(B)
(i)
% pERK+ cells
0
2
4
6
8
10
12
media
anti-IgM
anti-CD40
combination
(ii)
pERK Fluorescence Integral
0
100000
200000
300000
400000
500000
600000
700000
800000
900000
media
anti-IgM
anti-CD40
combination
(C)
(i)
% c-Myc+ cells
0
5
10
15
20
25
30
35
40
45
media
anti-IgM
anti-CD40
combination
(ii)
c-Myc Fluorescence Integral
0
200000
400000
600000
800000
1000000
1200000
1400000
1600000
media
anti-IgM
anti-CD40
combination

Figure 3.9

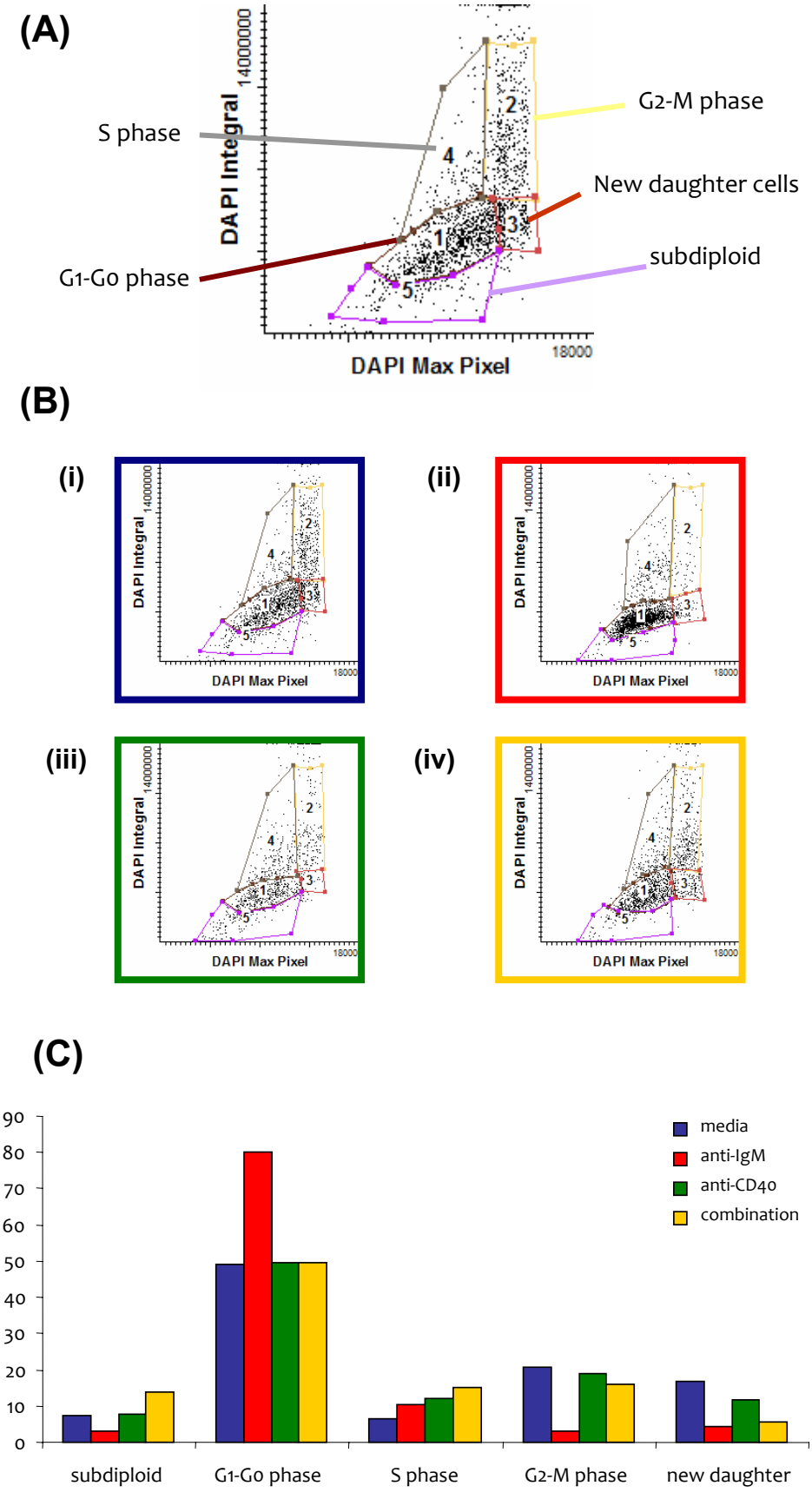
(A)
S phase
G2-M phase
New daughter cells
G1-Go phase
subdiploid
DAPI Integral
DAPI Max Pixel
14000000
18000
(B)
(i)
(ii)
(iii)
(iv)
(C)
% cells
media
anti-IgM
anti-CD40
combination
subdiploid
G1-Go phase
S phase
G2-M phase
new daughter

Figure 3.10

(A)

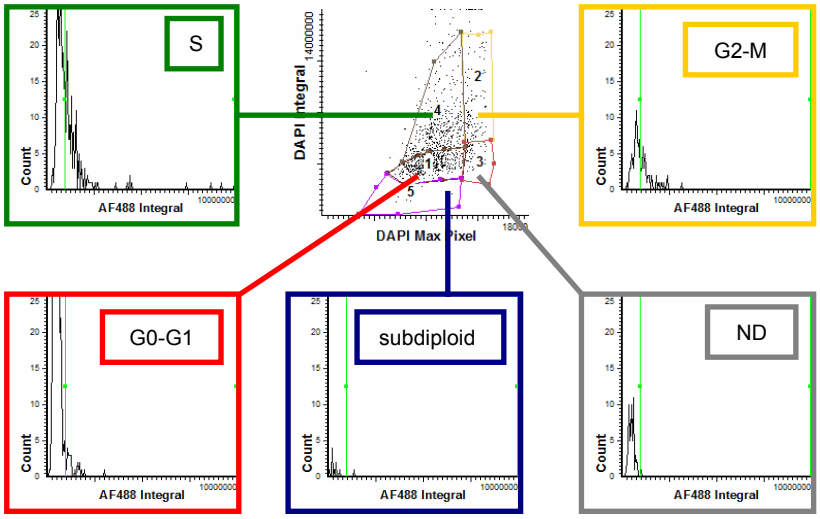

(B)

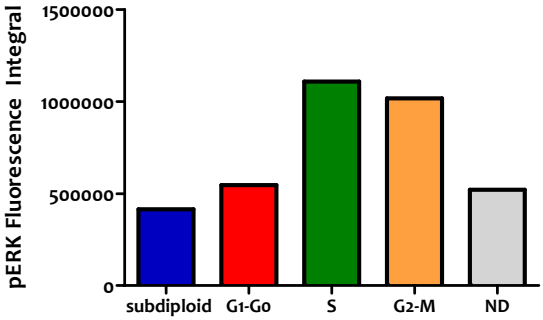

(C)

(i)

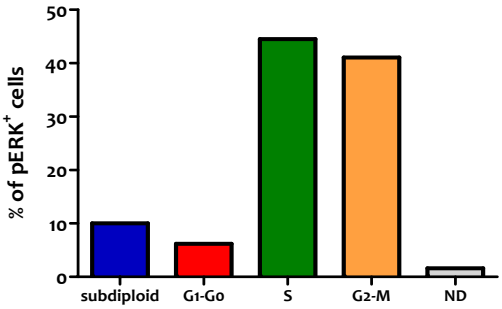

(ii)

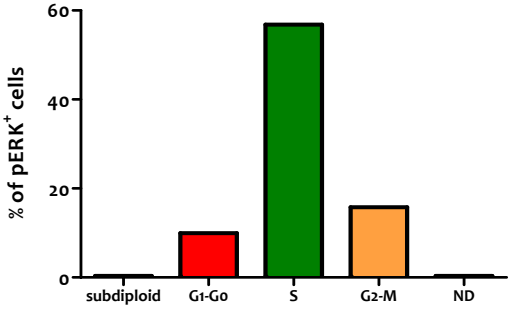

Figure 3.11

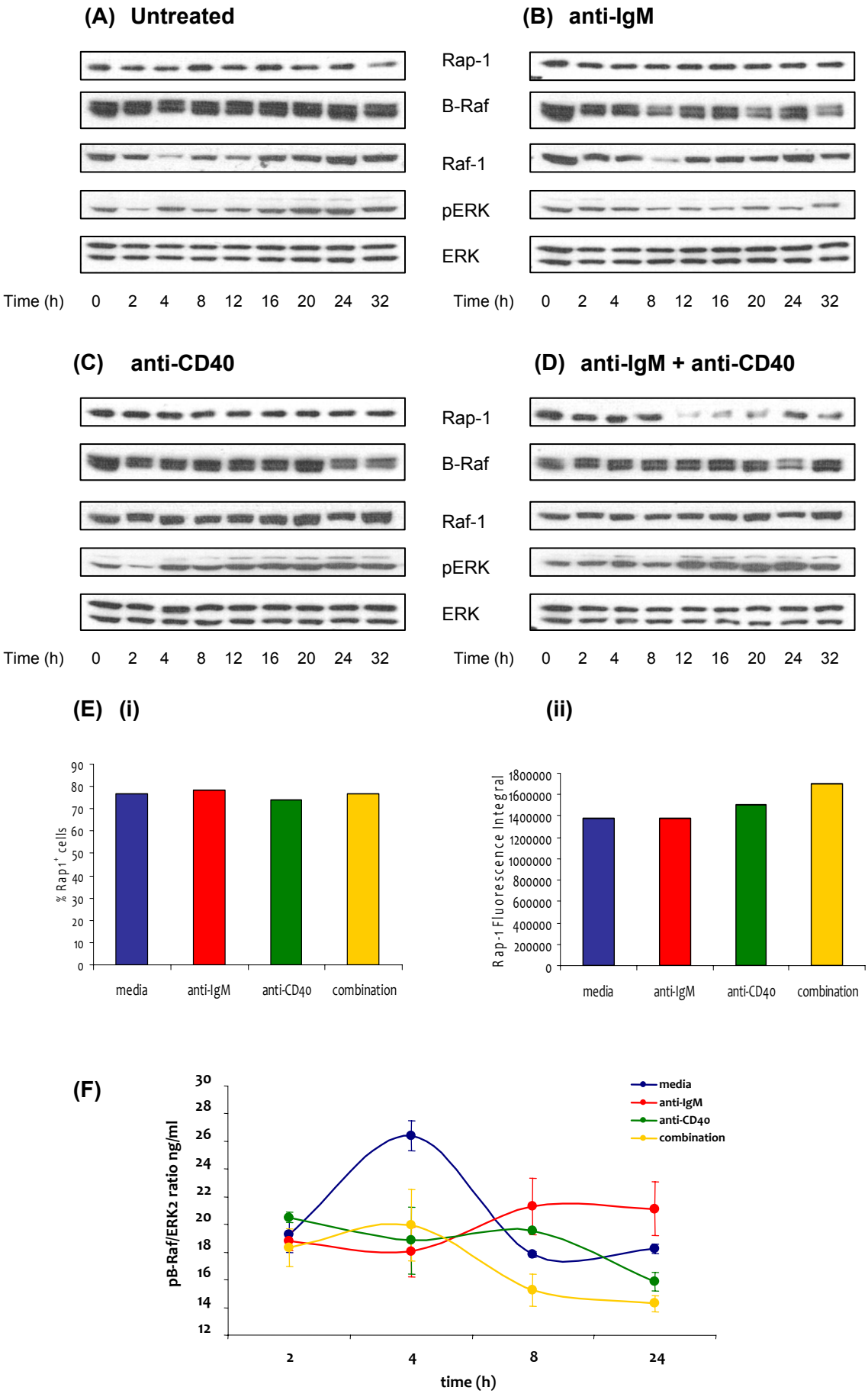
(A) Untreated
(B) anti-IgM
Rap-1
B-Raf
Raf-1
pERK
ERK
Time (h) 0 2 4 8 12 16 20 24 32
(C) anti-CD40
(D) anti-IgM + anti-CD40
(E) (i)
(ii)
% Rap1+ cells
Rap-1 Fluorescence Integral
media
anti-IgM
anti-CD40
combination
(F)
pB-Raf/ERK2 ratio ng/ml
time (h)

Figure 3.12

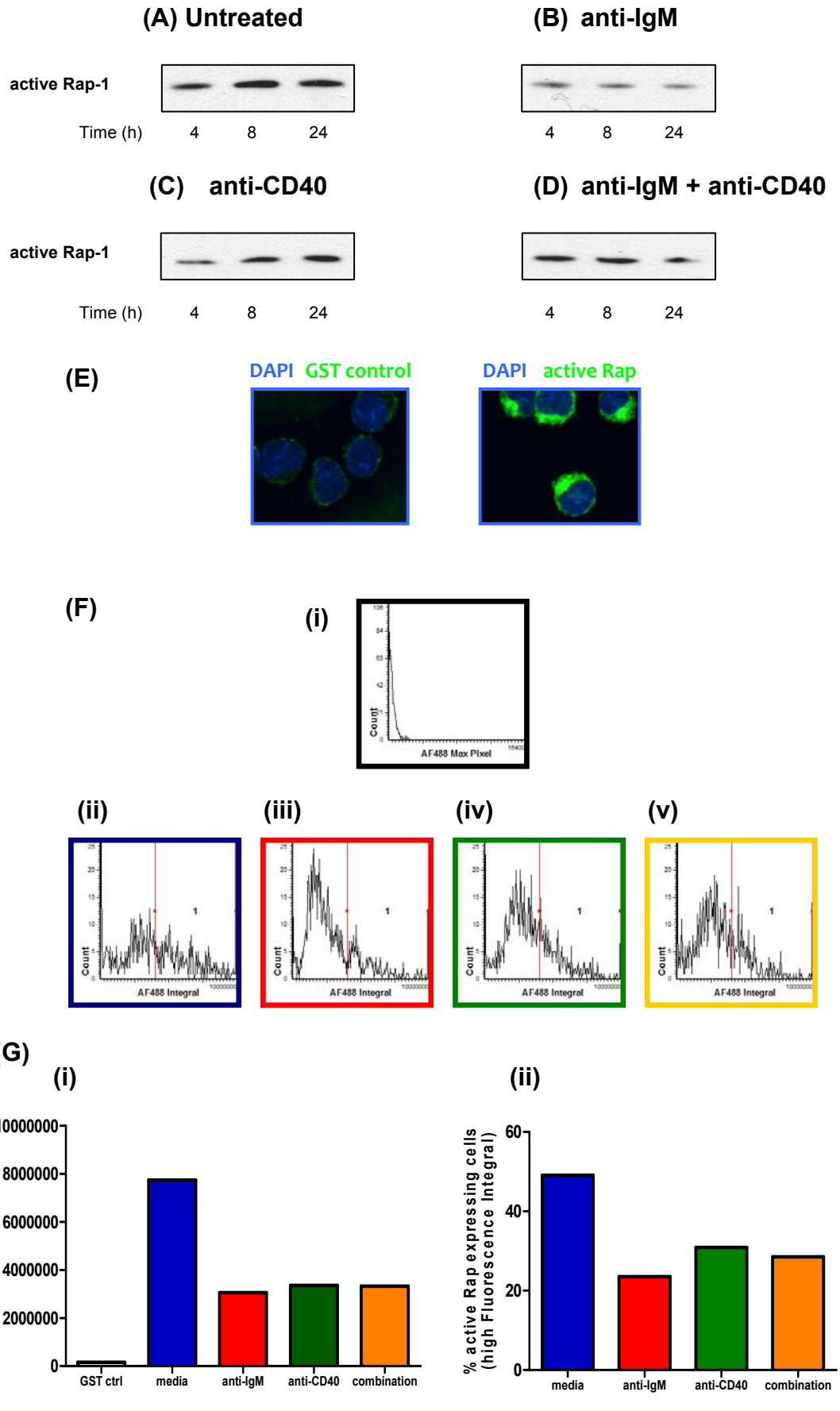
(A) Untreated
(B) anti-IgM
active Rap-1
Time (h) 4 8 24
4 8 24
(C) anti-CD40
(D) anti-IgM + anti-CD40
active Rap-1
Time (h) 4 8 24
4 8 24
(E)
DAPI GST control
DAPI active Rap
(F)
(i)
Count
AF488 Max Pixel
(ii)
(iii)
(iv)
(v)
Count
AF488 Integral
(G)
(i)
active Rap Fluorescence Integral
10000000
8000000
6000000
4000000
2000000
0
GST ctrl
media
anti-IgM
anti-CD40
combination
(ii)
% active Rap expressing cells (high Fluorescence Integral)
60
40
20
0
media
anti-IgM
anti-CD40
combination

Figure 3.13

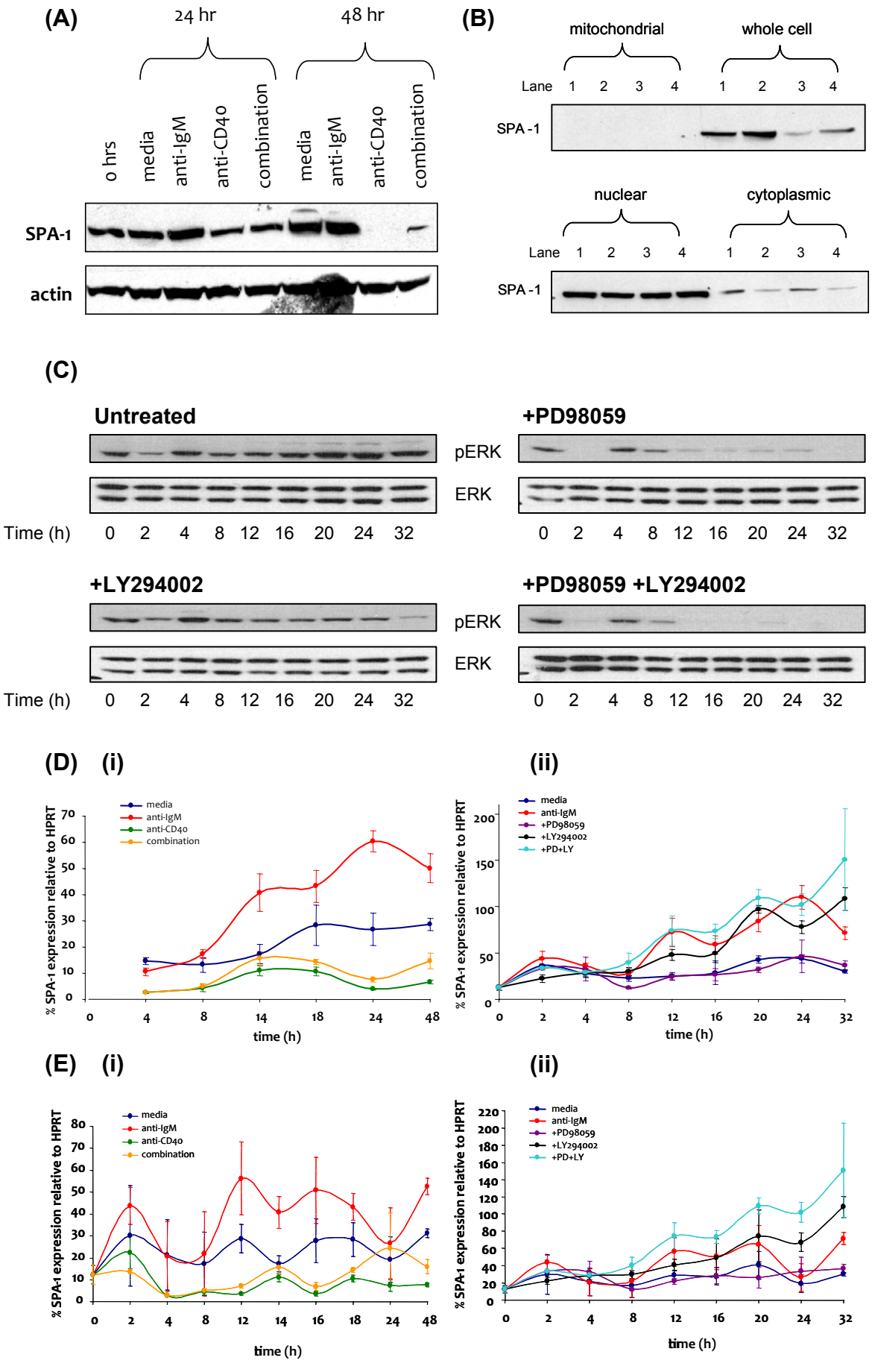
(A)
24 hr
48 hr
0 hrs
media
anti-IgM
anti-CD40
combination
media
anti-IgM
anti-CD40
combination
SPA-1
actin
(B)
mitochondrial
whole cell
Lane 1 2 3 4 1 2 3 4
SPA-1
nuclear
cytoplasmic
Lane 1 2 3 4 1 2 3 4
SPA-1
(C)
Untreated
+PD98059
pERK
ERK
Time (h) 0 2 4 8 12 16 20 24 32
0 2 4 8 12 16 20 24 32
+LY294002
+PD98059 +LY294002
pERK
ERK
Time (h) 0 2 4 8 12 16 20 24 32
0 2 4 8 12 16 20 24 32
(D) (i)
(ii)
media
anti-IgM
anti-CD40
combination
% SPA-1 expression relative to HPRT
time (h)
media
anti-IgM
+PD98059
+LY294002
+PD+LY
% SPA-1 expression relative to HPRT
time (h)
(E) (i)
(ii)
media
anti-IgM
anti-CD40
combination
% SPA-1 expression relative to HPRT
time (h)
media
anti-IgM
+PD98059
+LY294002
+PD+LY
% SPA-1 expression relative to HPRT
time (h)

Figure 3.14

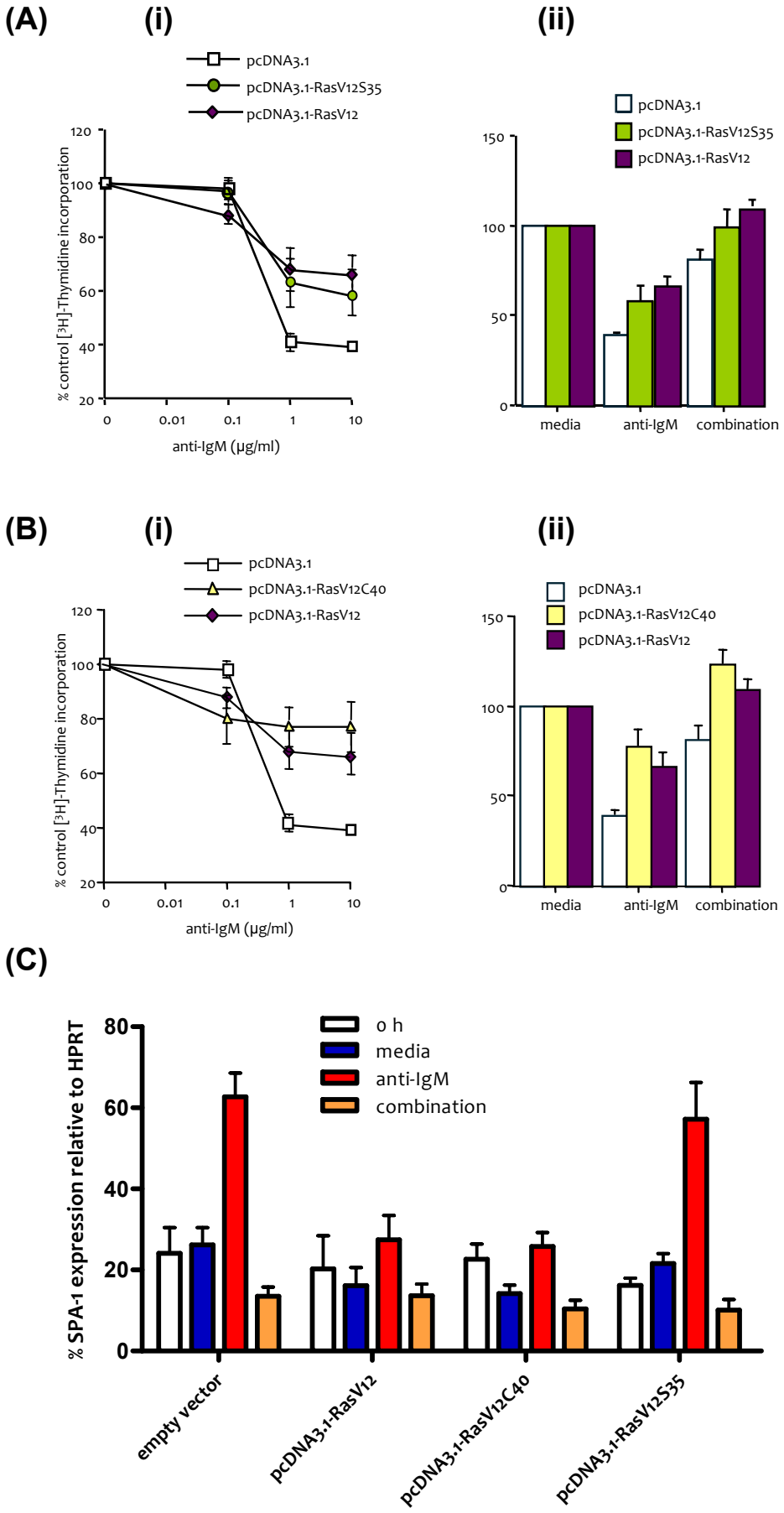
(A)
(i)
pcDNA3.1
pcDNA3.1-RasV12S35
pcDNA3.1-RasV12
% control [3H]-Thymidine incorporation
anti-IgM (µg/ml)
(ii)
media
anti-IgM
combination
(B)
(i)
pcDNA3.1
pcDNA3.1-RasV12C40
pcDNA3.1-RasV12
(ii)
(C)
% SPA-1 expression relative to HPRT
o h
media
anti-IgM
combination
empty vector
pcDNA3.1-RasV12
pcDNA3.1-RasV12C40
pcDNA3.1-RasV12S35

Figure 3.15

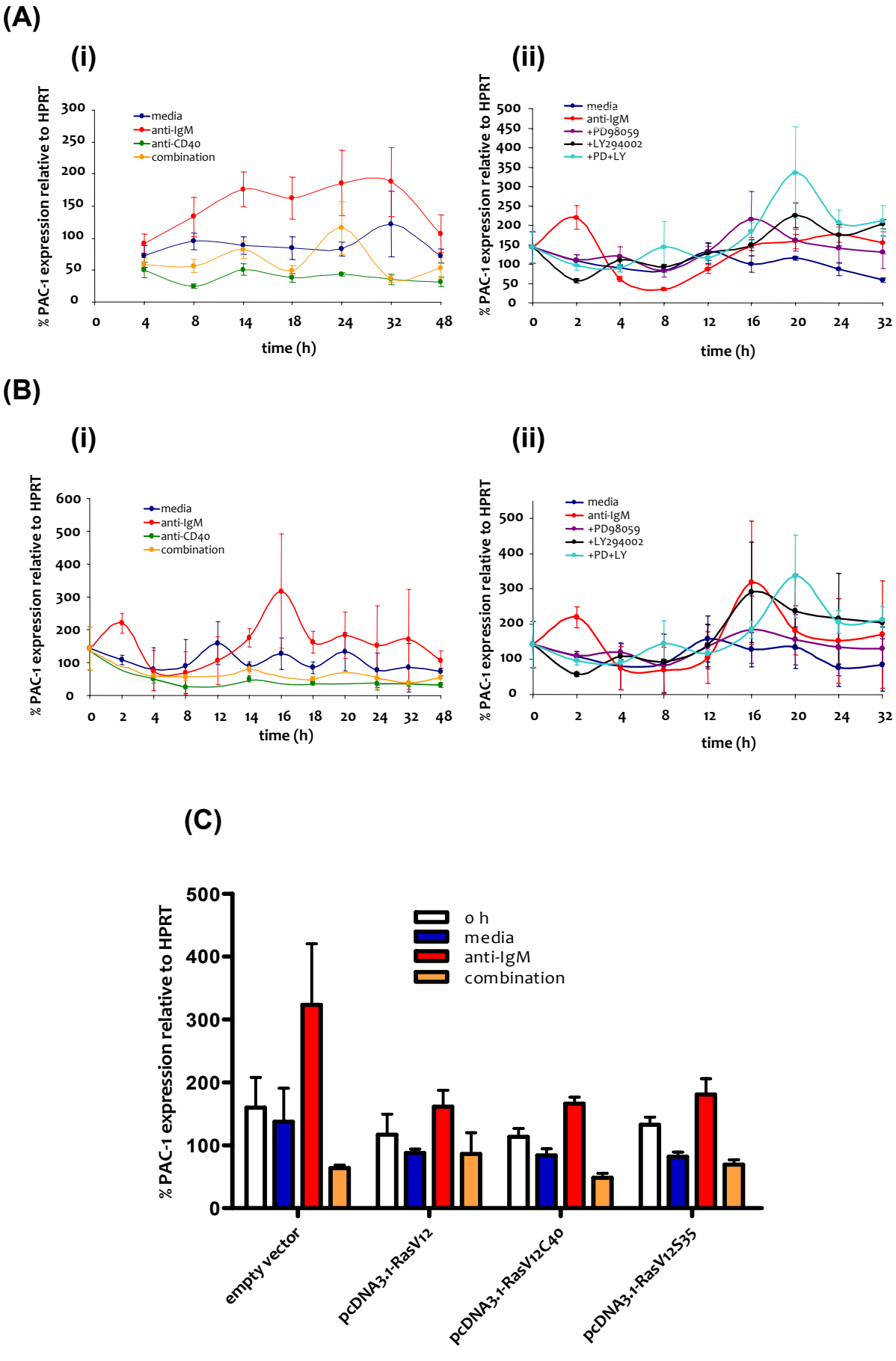
(A)
(i)
% PAC-1 expression relative to HPRT
media
anti-IgM
anti-CD40
combination
time (h)
(ii)
% PAC-1 expression relative to HPRT
media
anti-IgM
+PD98059
+LY294002
+PD+LY
time (h)
(B)
(i)
% PAC-1 expression relative to HPRT
media
anti-IgM
anti-CD40
combination
time (h)
(ii)
% PAC-1 expression relative to HPRT
media
anti-IgM
+PD98059
+LY294002
+PD+LY
time (h)
(C)
% PAC-1 expression relative to HPRT
o h
media
anti-IgM
combination
empty vector
pcDNA3.1-RasV12
pcDNA3.1-RasV12C40
pcDNA3.1-RasV12S35

Figure 3.16

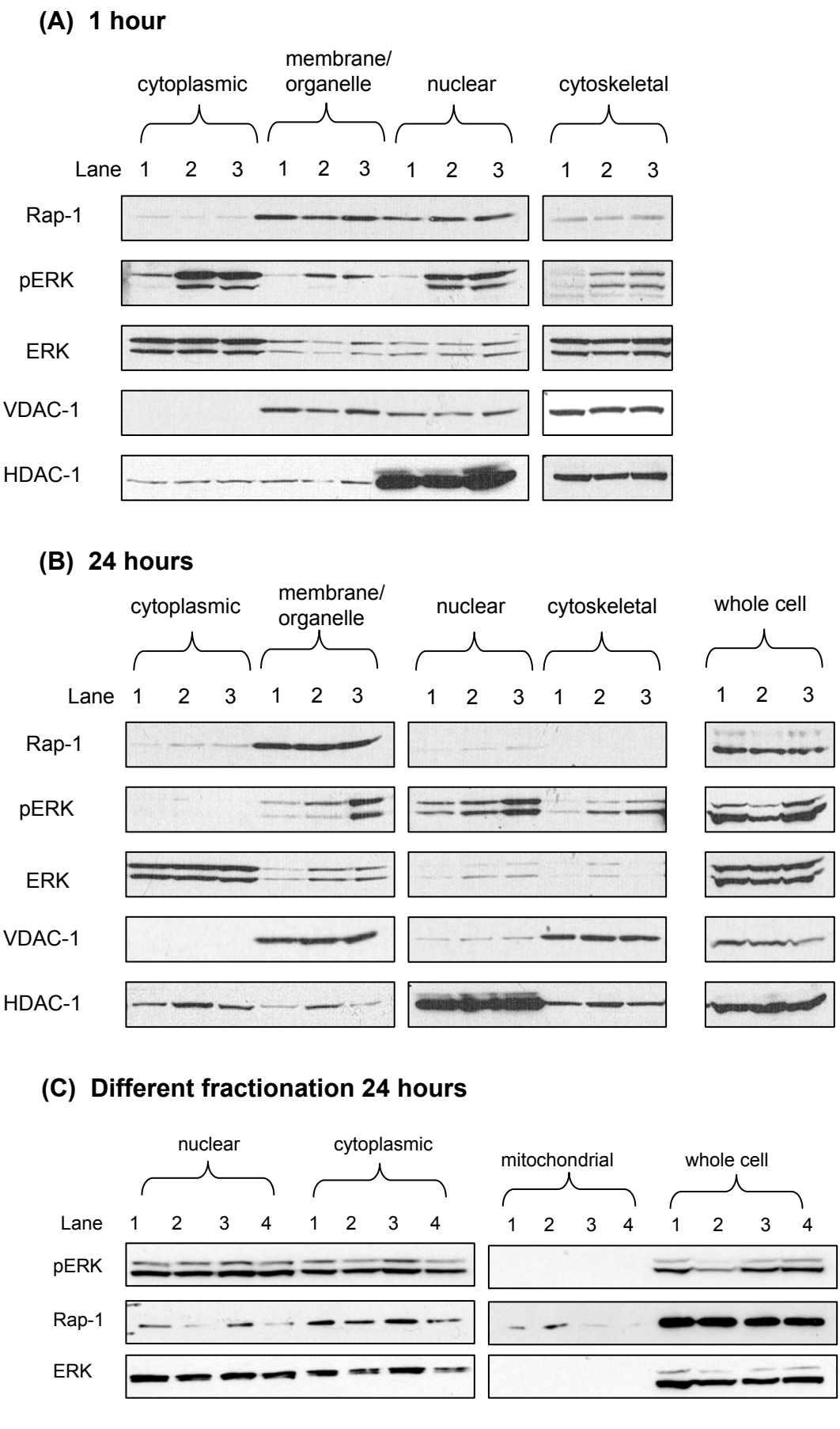
(A) 1 hour
cytoplasmic
membrane/ organelle
nuclear
cytoskeletal
Lane 1 2 3 1 2 3 1 2 3 1 2 3
Rap-1
pERK
ERK
VDAC-1
HDAC-1
(B) 24 hours
cytoplasmic
membrane/ organelle
nuclear
cytoskeletal
whole cell
Lane 1 2 3 1 2 3 1 2 3 1 2 3 1 2 3
Rap-1
pERK
ERK
VDAC-1
HDAC-1
(C) Different fractionation 24 hours
nuclear
cytoplasmic
mitochondrial
whole cell
Lane 1 2 3 4 1 2 3 4 1 2 3 4 1 2 3 4
pERK
Rap-1
ERK

Figure 3.17

(A)

(i)

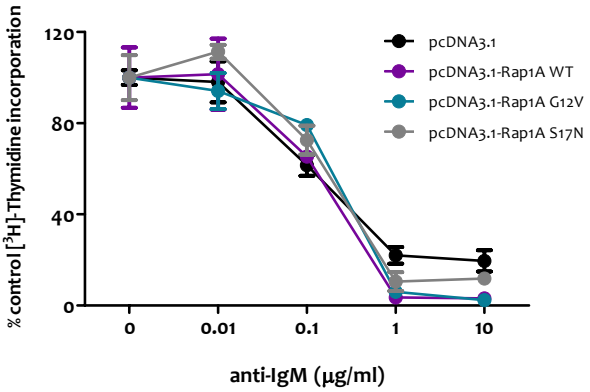

(ii)

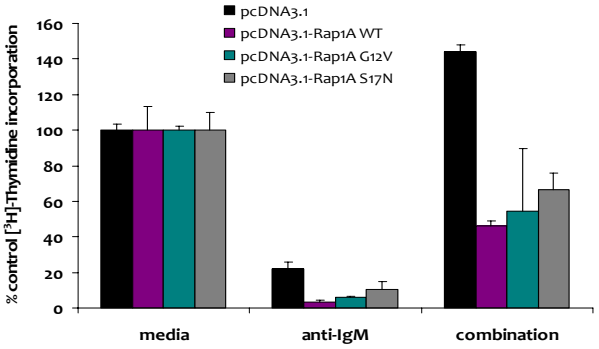

(B)

(i)

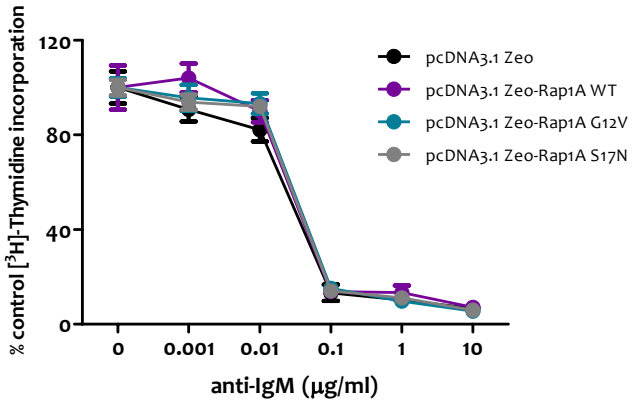

(ii)

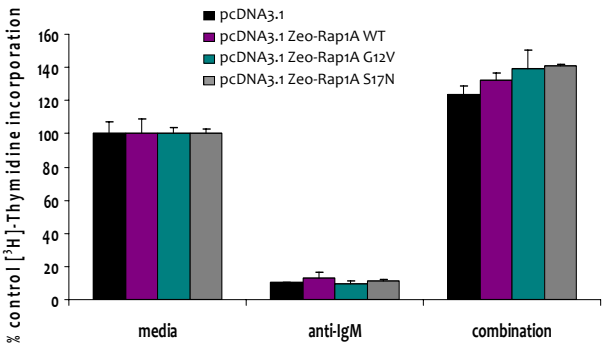

Figure 3.18

(A) % subdiploid cells

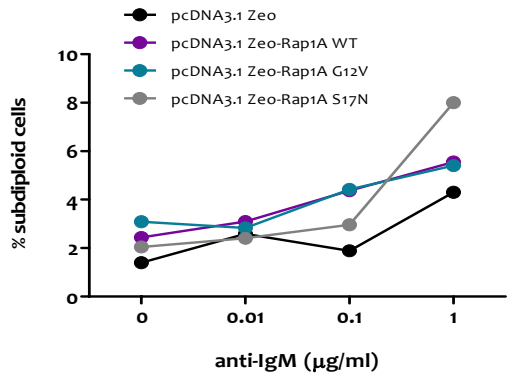

(B) % cells in G1/G0 phase

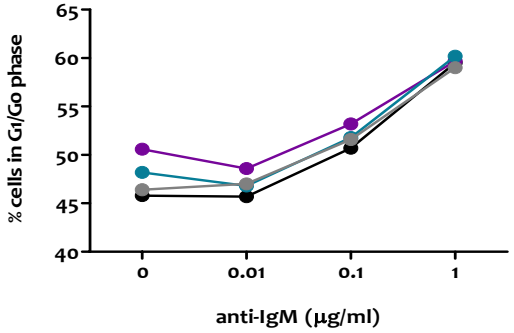

(C) % cells in mitotic phases

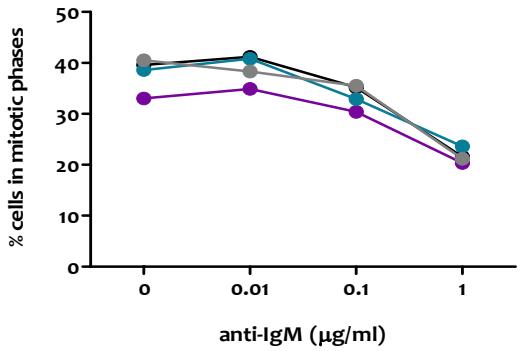

Figure 3.19

(A)

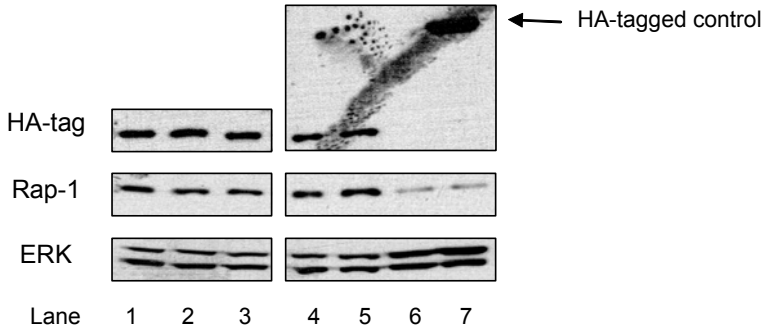

(B) (i) Day 1

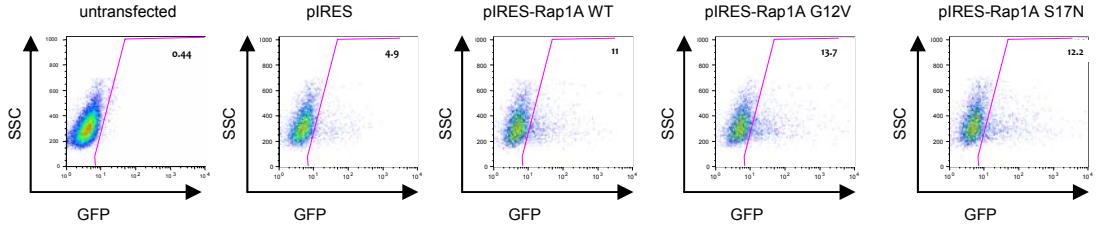

(ii) Day 11

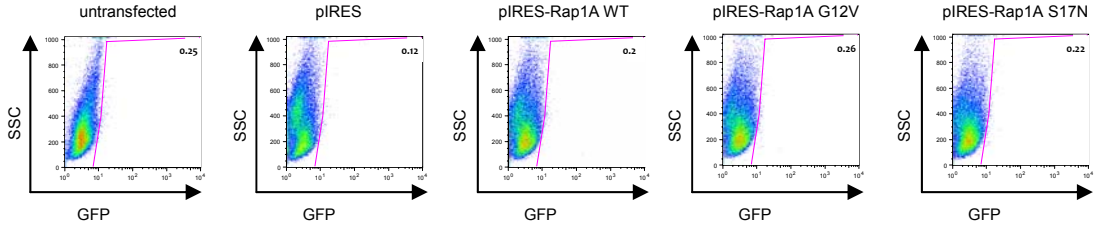

(C)

(i)

	day 1	day 5	day 11
pIRES-GFP	4.9	1.74	0.12
pIRES-GFP-Rap1A WT	13.7	11.8	0.2
pIRES-GFP-Rap1A G12V	12.2	15.4	0.26
pIRES-GFP-Rap1A S17N	11	15.8	0.22

(ii)

vectors used	cells used	selection conditions	method of transfection
pcDNA3.1(+)	WEHI 231	150-1000 µg/ml G418	Gene Pulser Xcell Electroporation System (BioRad)
pcDNA3.1(-)Zeo	WEHI 231-Bcl-xl	50-500 µg/ml Zeocin	Amaxa Nucleofector System (Amaxa/Lonza)
pIRES2-AcGFP1			MP-100 Microporator (Labtech)

(iii)

	vectors used	cells used	selection conditions	linearised/not linearised	method of transfection
1	pcDNA3.1(+)	WEHI 231	500 µg/ml G418	linearised	Amaxa Nucleofector System (Amaxa/Lonza)
2	pcDNA3.1(+)	WEHI 231	250 then 500 µg/ml G418	linearised	Amaxa Nucleofector System (Amaxa/Lonza)
3	pcDNA3.1(+) Zeo	WEHI 231-Bcl-xl	200 µg/ml Zeocin	linearised	Amaxa Nucleofector System (Amaxa/Lonza)
4	pIRES2-AcGFP1	WEHI 231-Bcl-xl	500 µg/ml G418	not linearised	Amaxa Nucleofector System (Amaxa/Lonza)
5	pIRES2-AcGFP1	WEHI 231	300 µg/ml G418	not linearised	Amaxa Nucleofector System (Amaxa/Lonza)
6	pIRES2-AcGFP1	WEHI 231	300 then 500 µg/ml G418	not linearised	Amaxa Nucleofector System (Amaxa/Lonza)
7	pIRES2-AcGFP1	WEHI 231	300-1000 µg/ml G418	not linearised	Amaxa Nucleofector System (Amaxa/Lonza)
8	pIRES2-AcGFP1	WEHI 231	500 then 600 µg/ml G418	linearised	Amaxa Nucleofector System (Amaxa/Lonza)
9	pcDNA3.1(+) Zeo	WEHI 231-Bcl-xl	200 µg/ml Zeocin	linearised	Amaxa Nucleofector System (Amaxa/Lonza)

Figure 3.20

(A)

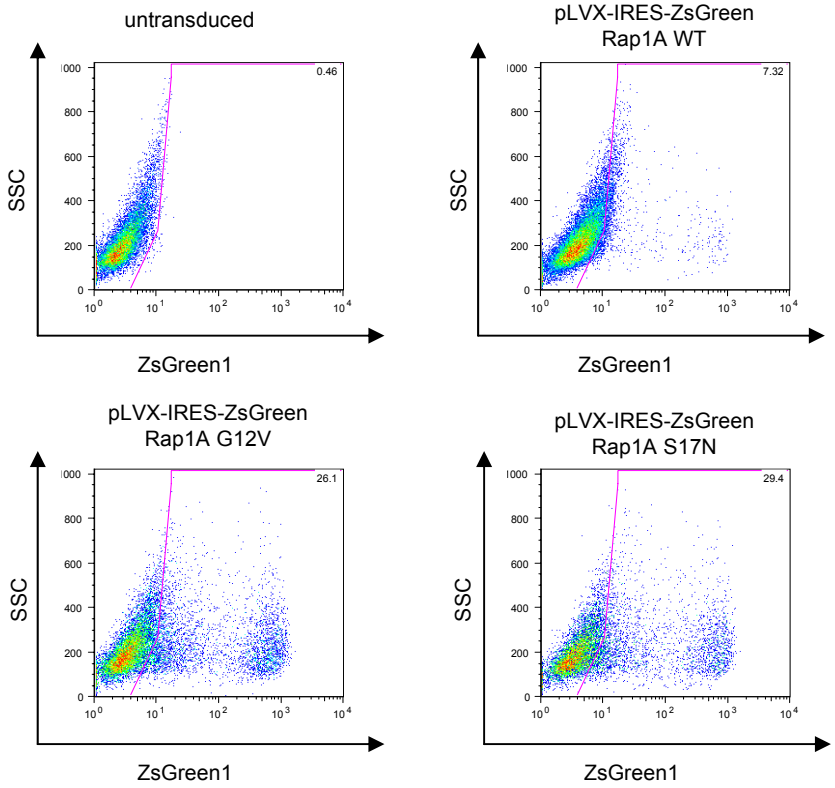

(B)

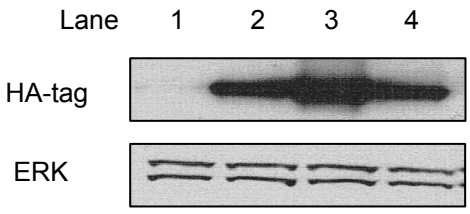

Figure 3.21

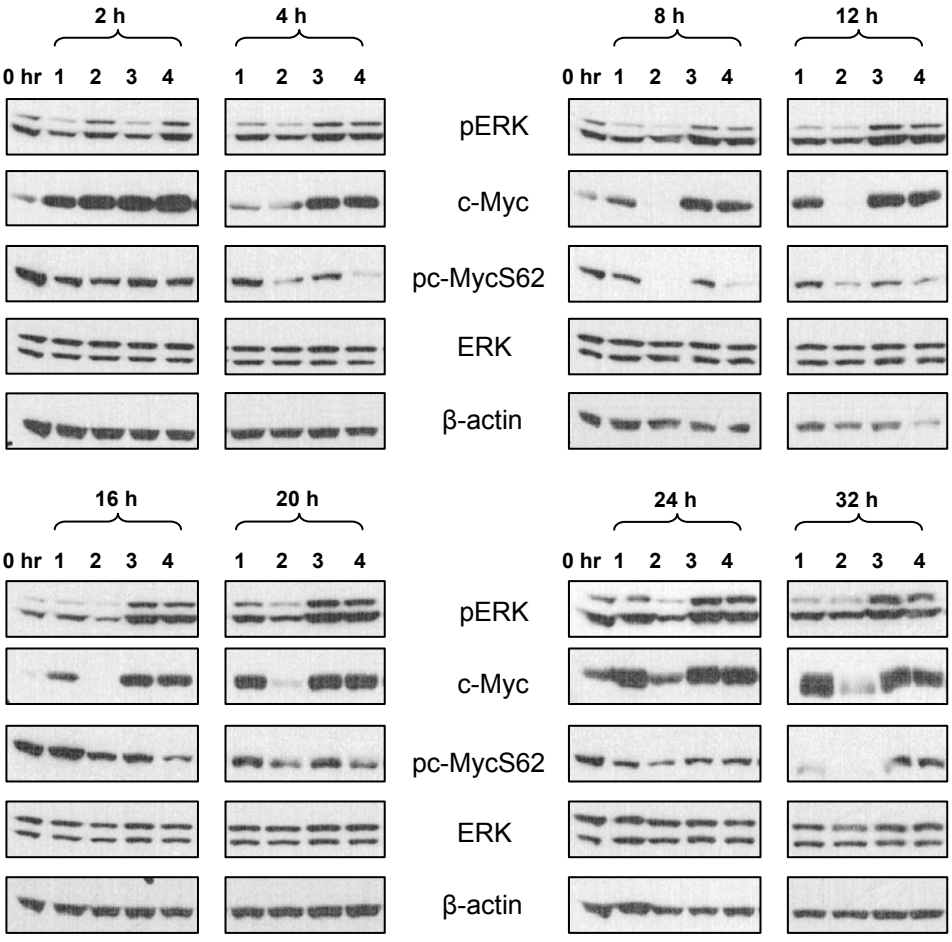
2 h
4 h
8 h
12 h
0 hr 1 2 3 4
1 2 3 4
0 hr 1 2 3 4
1 2 3 4
pERK
c-Myc
pc-MycS62
ERK
β-actin
16 h
20 h
24 h
32 h
0 hr 1 2 3 4
1 2 3 4
0 hr 1 2 3 4
1 2 3 4
pERK
c-Myc
pc-MycS62
ERK
β-actin

Figure 3.22

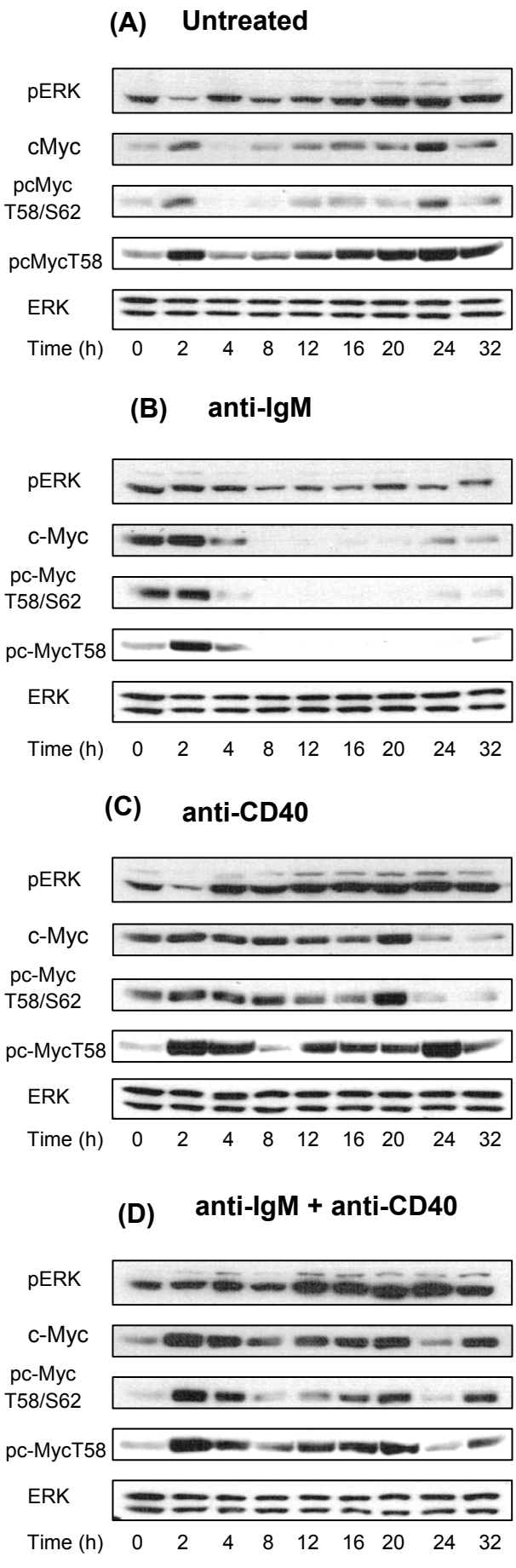
(A) Untreated
pERK
cMyc
pcMyc T58/S62
pcMycT58
ERK
Time (h) 0 2 4 8 12 16 20 24 32
(B) anti-IgM
pERK
c-Myc
pc-Myc T58/S62
pc-MycT58
ERK
Time (h) 0 2 4 8 12 16 20 24 32
(C) anti-CD40
pERK
c-Myc
pc-Myc T58/S62
pc-MycT58
ERK
Time (h) 0 2 4 8 12 16 20 24 32
(D) anti-IgM + anti-CD40
pERK
c-Myc
pc-Myc T58/S62
pc-MycT58
ERK
Time (h) 0 2 4 8 12 16 20 24 32

Figure 3.23

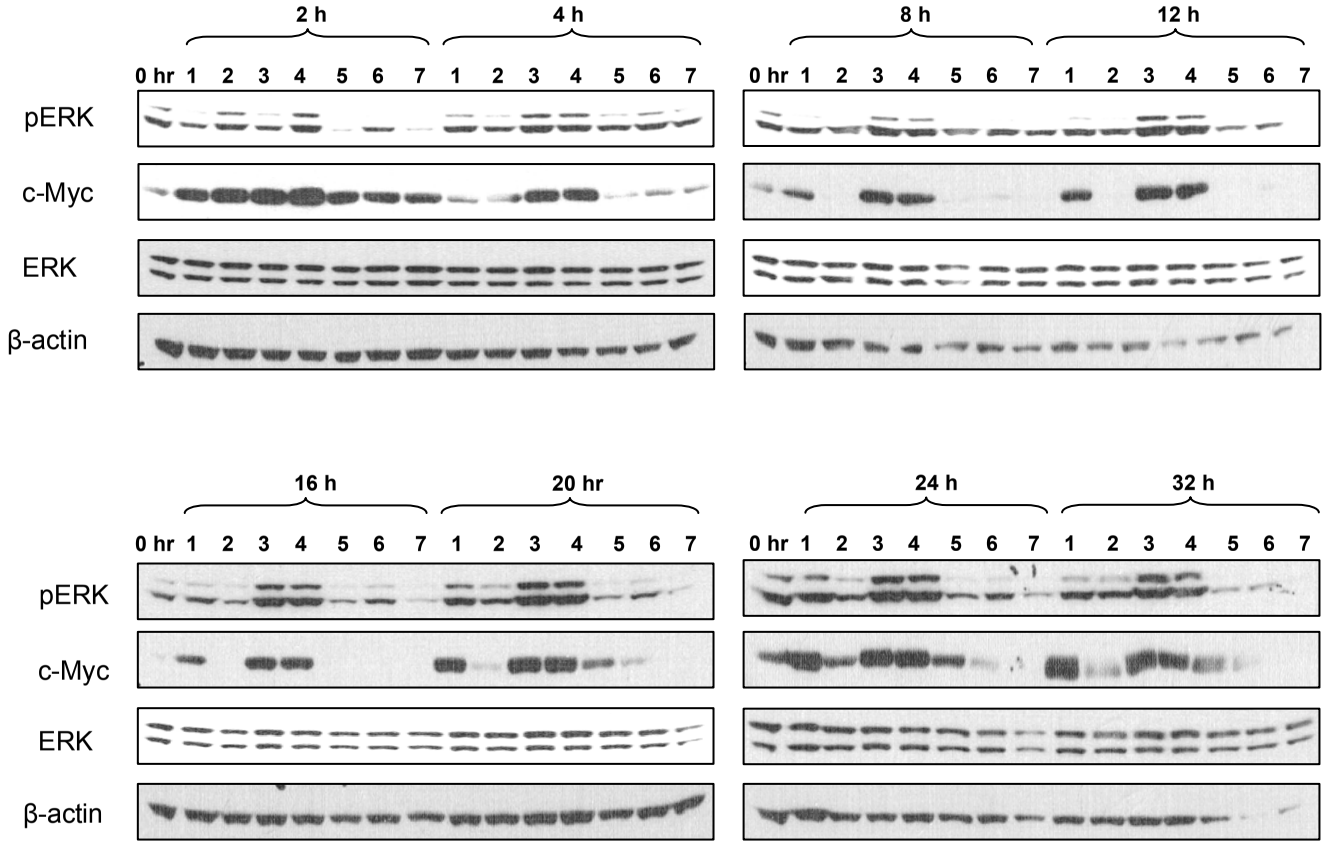
2 h
4 h
8 h
12 h
0 hr 1 2 3 4 5 6 7 1 2 3 4 5 6 7
pERK
c-Myc
ERK
β-actin
16 h
20 hr
24 h
32 h

Figure 3.24

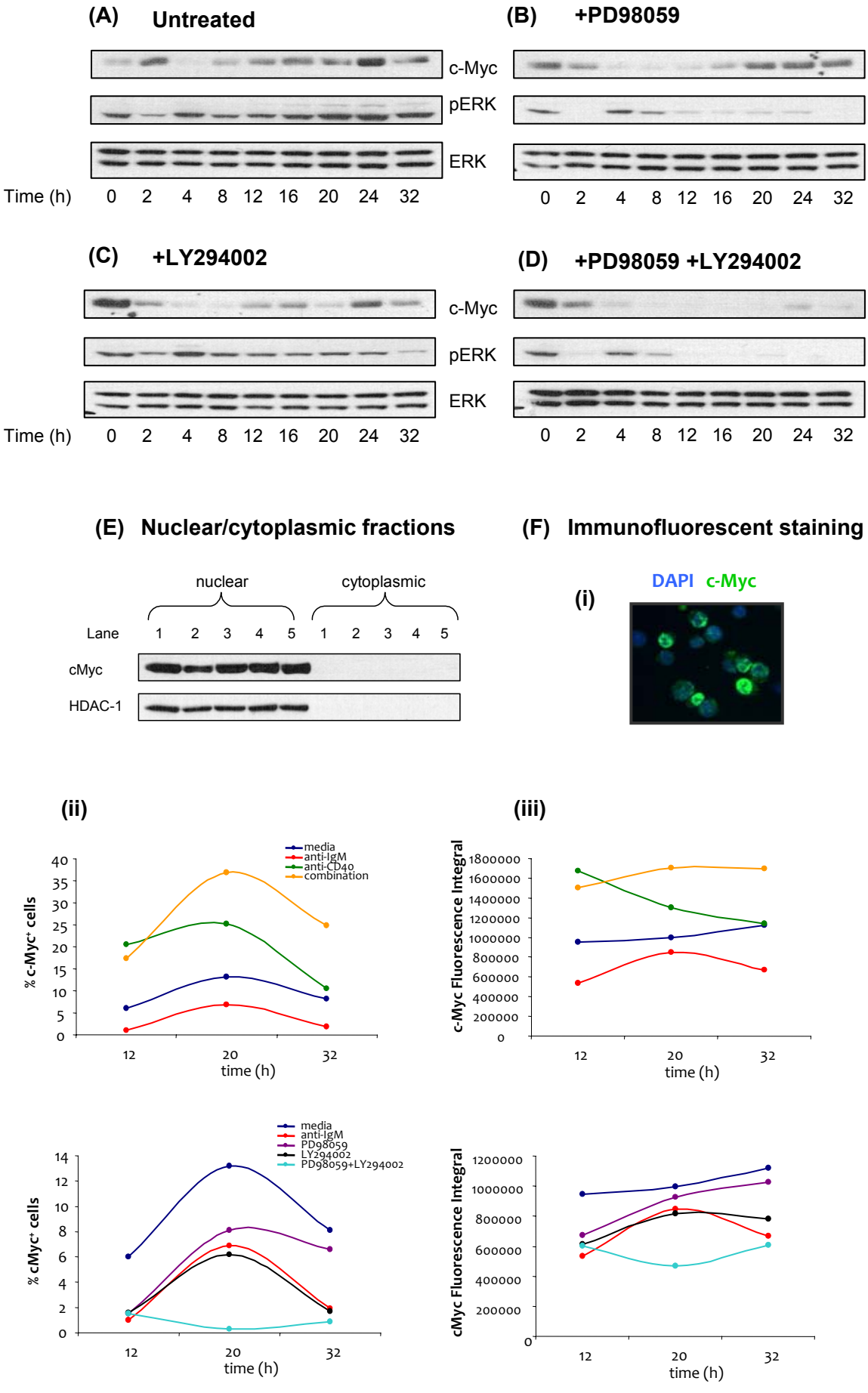
(A) Untreated
(B) +PD98059
(C) +LY294002
(D) +PD98059 +LY294002
c-Myc
pERK
ERK
Time (h) 0 2 4 8 12 16 20 24 32
(E) Nuclear/cytoplasmic fractions
nuclear
cytoplasmic
Lane 1 2 3 4 5 1 2 3 4 5
cMyc
HDAC-1
(F) Immunofluorescent staining
(i)
DAPI c-Myc
(ii)
media
anti-IgM
anti-CD40
combination
% c-Myc+ cells
time (h)
(iii)
c-Myc Fluorescence Integral
time (h)
media
anti-IgM
PD98059
LY294002
PD98059+LY294002
% cMyc+ cells
time (h)
cMyc Fluorescence Integral
time (h)

Figure 3.25

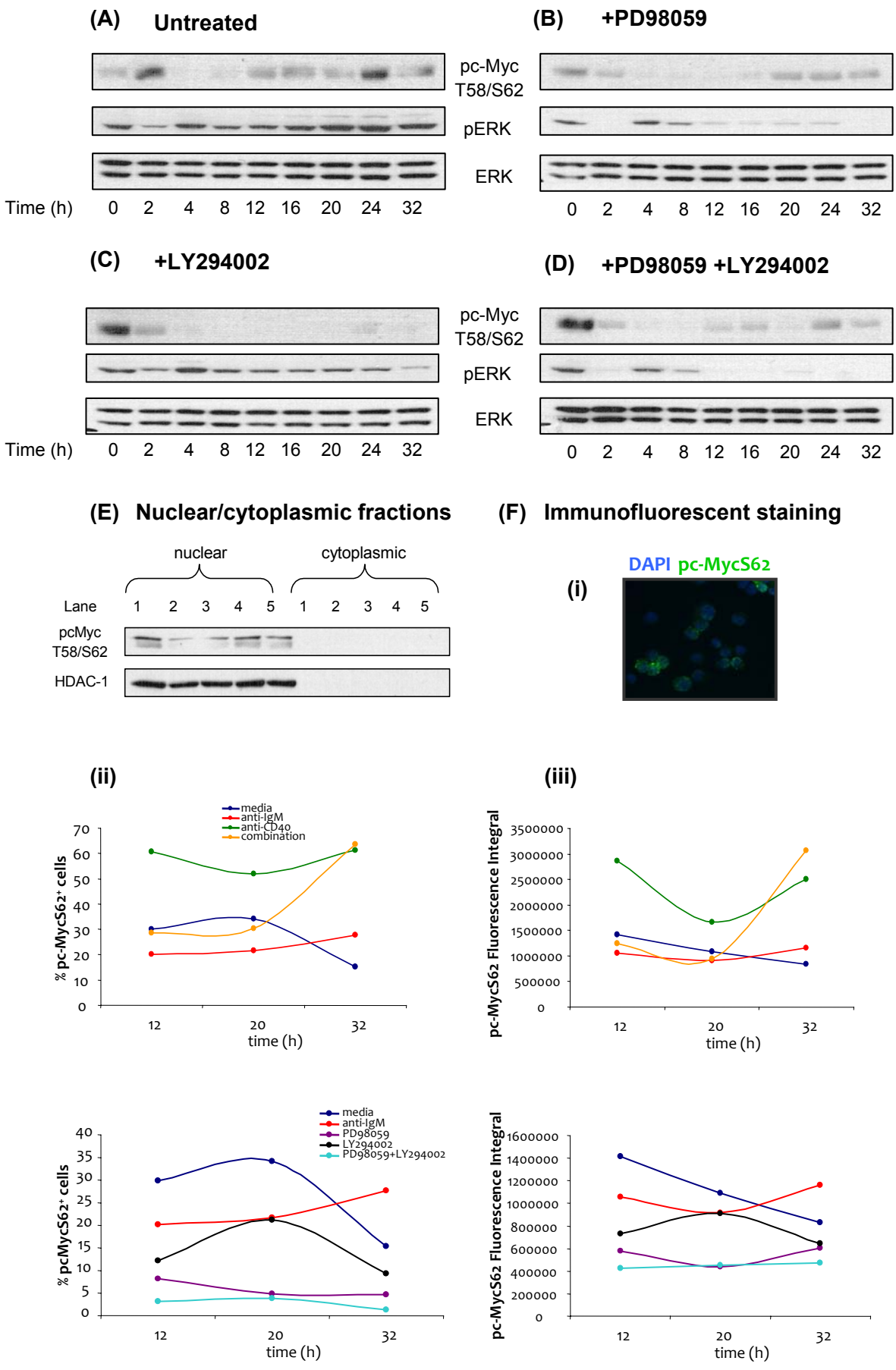
(A) Untreated
(B) +PD98059
(C) +LY294002
(D) +PD98059 +LY294002
pc-Myc T58/S62
pERK
ERK
Time (h) 0 2 4 8 12 16 20 24 32
(E) Nuclear/cytoplasmic fractions
nuclear
cytoplasmic
Lane 1 2 3 4 5 1 2 3 4 5
pcMyc T58/S62
HDAC-1
(F) Immunofluorescent staining
(i)
DAPI pc-MycS62
(ii)
media
anti-IgM
anti-CD40
combination
% pc-MycS62+ cells
time (h)
(iii)
pc-MycS62 Fluorescence Integral
time (h)
media
anti-IgM
PD98059
LY294002
PD98059+LY294002
% pcMycS62+ cells
time (h)
pc-MycS62 Fluorescence Integral
time (h)

Figure 3.26

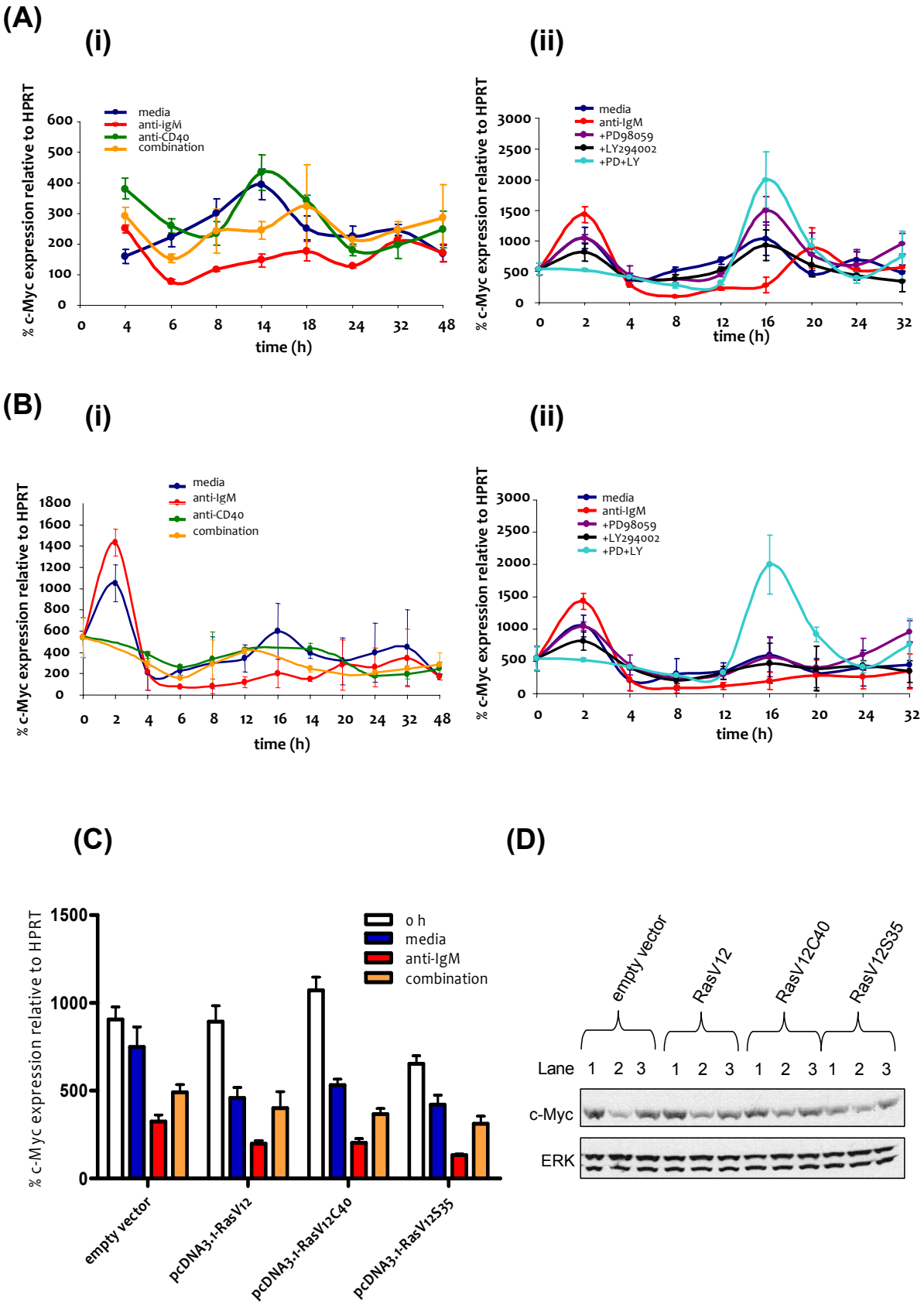
(A)
(i)
% c-Myc expression relative to HPRT
media
anti-IgM
anti-CD40
combination
time (h)
(ii)
% c-Myc expression relative to HPRT
media
anti-IgM
+PD98059
+LY294002
+PD+LY
time (h)
(B)
(i)
% c-Myc expression relative to HPRT
media
anti-IgM
anti-CD40
combination
time (h)
(ii)
% c-Myc expression relative to HPRT
media
anti-IgM
+PD98059
+LY294002
+PD+LY
time (h)
(C)
% c-Myc expression relative to HPRT
0 h
media
anti-IgM
combination
empty vector
pcDNA3.1-RasV12
pcDNA3.1-RasV12C40
pcDNA3.1-RasV12S35
(D)
empty vector
RasV12
RasV12C40
RasV12S35
Lane 1 2 3 1 2 3 1 2 3 1 2 3
c-Myc
ERK

Figure 3.27

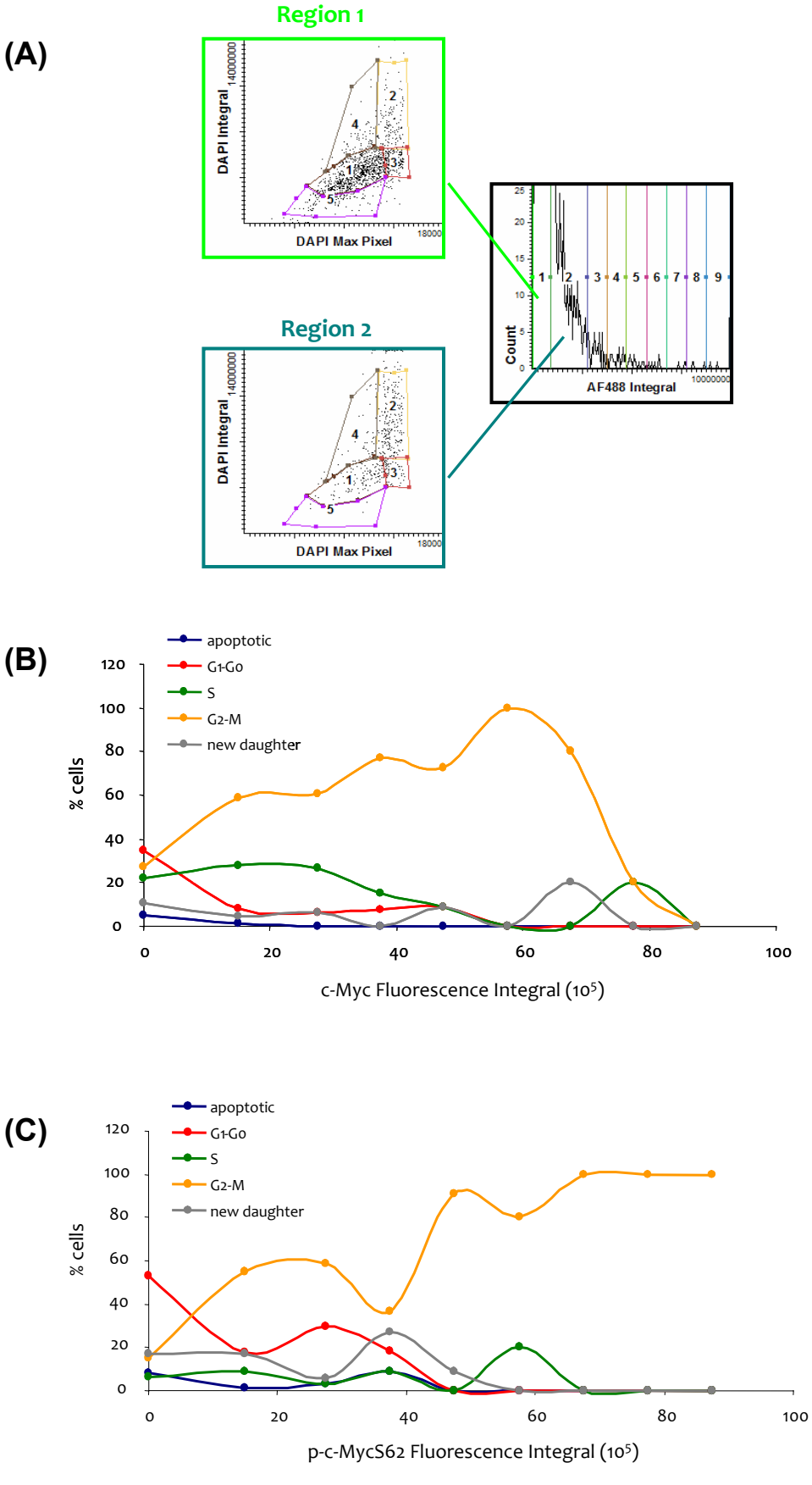
(A)
Region 1
DAPI Integral
DAPI Max Pixel
Region 2
DAPI Integral
DAPI Max Pixel
Count
AF488 Integral
(B)
apoptotic
G1-Go
S
G2-M
new daughter
% cells
c-Myc Fluorescence Integral (10⁵)
(C)
apoptotic
G1-Go
S
G2-M
new daughter
% cells
p-c-MycS62 Fluorescence Integral (10⁵)

Figure 3.28

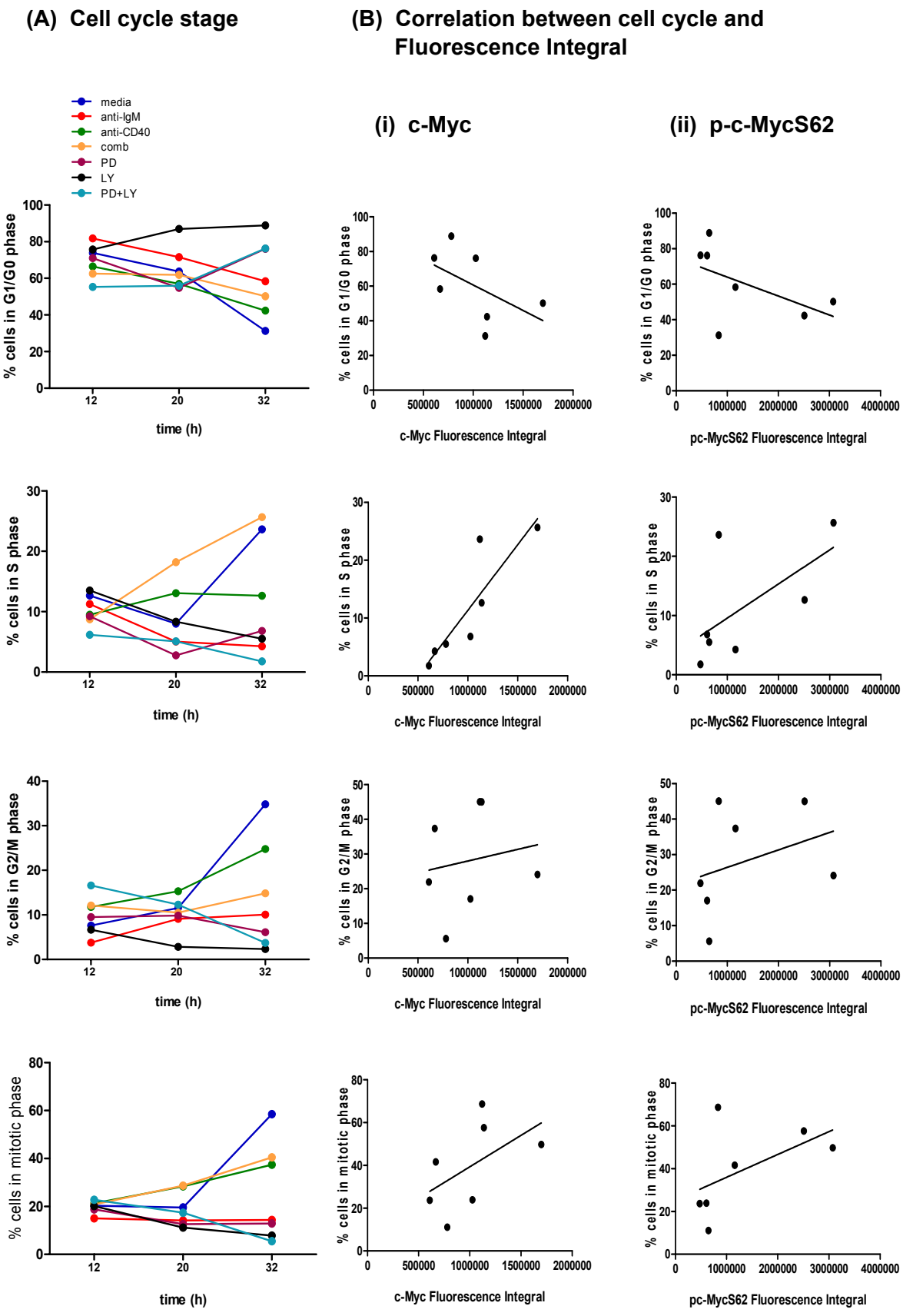
(A) Cell cycle stage
(B) Correlation between cell cycle and Fluorescence Integral
(i) c-Myc
(ii) p-c-MycS62
media
anti-IgM
anti-CD40
comb
PD
LY
PD+LY
% cells in G1/G0 phase
% cells in S phase
% cells in G2/M phase
% cells in mitotic phase
time (h)
c-Myc Fluorescence Integral
pc-MycS62 Fluorescence Integral

Figure 3.29

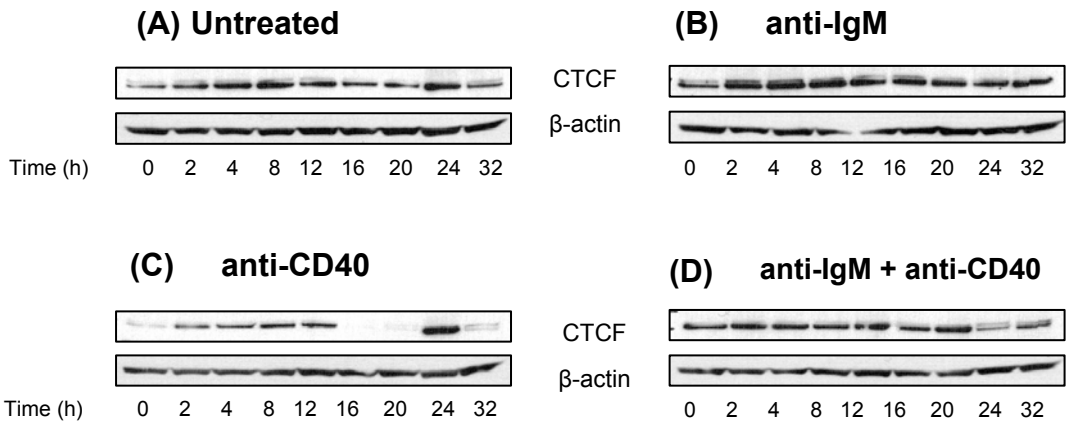
(A) Untreated
(B) anti-IgM
CTCF
β-actin
Time (h)
0 2 4 8 12 16 20 24 32
(C) anti-CD40
(D) anti-IgM + anti-CD40
CTCF
β-actin
Time (h)
0 2 4 8 12 16 20 24 32

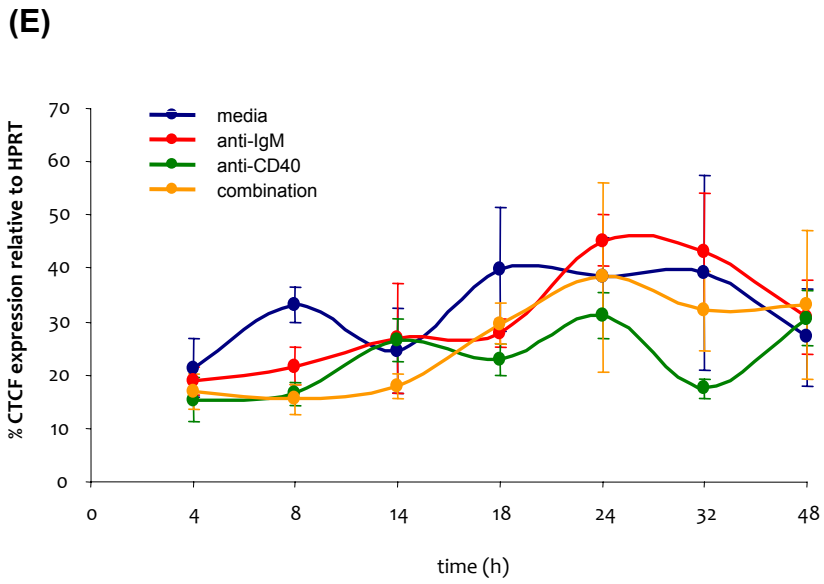
(E)
media
anti-IgM
anti-CD40
combination
% CTCF expression relative to HPRT
0
10
20
30
40
50
60
70
0
4
8
14
18
24
32
48
time (h)

Figure 3.30

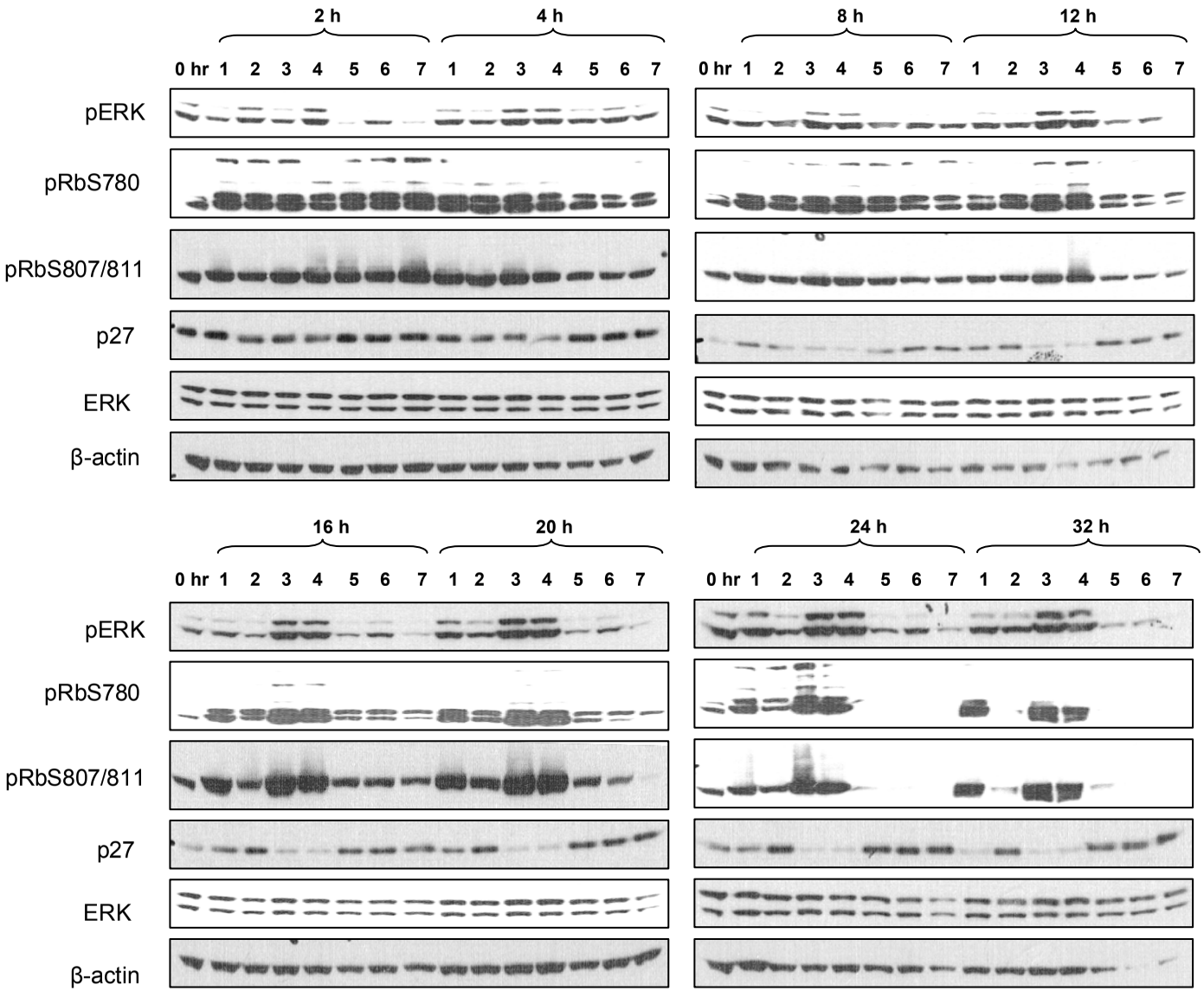
2 h
4 h
8 h
12 h
16 h
20 h
24 h
32 h
0 hr 1 2 3 4 5 6 7 1 2 3 4 5 6 7
pERK
pRbS780
pRbS807/811
p27
ERK
β-actin

Figure 3.31

(A)

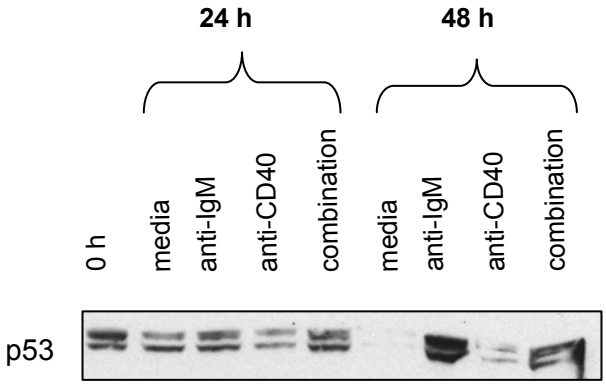

(B)

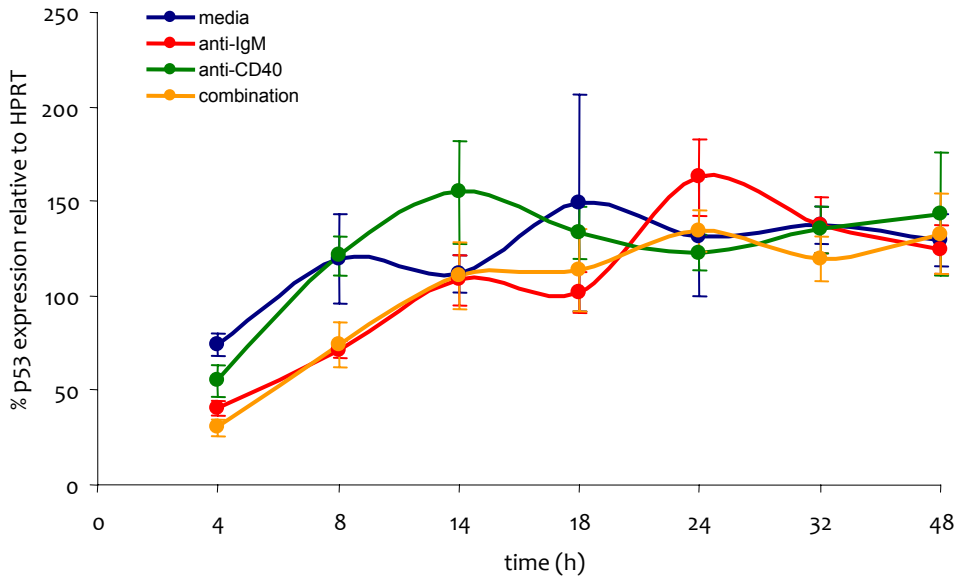

Figure 3.32

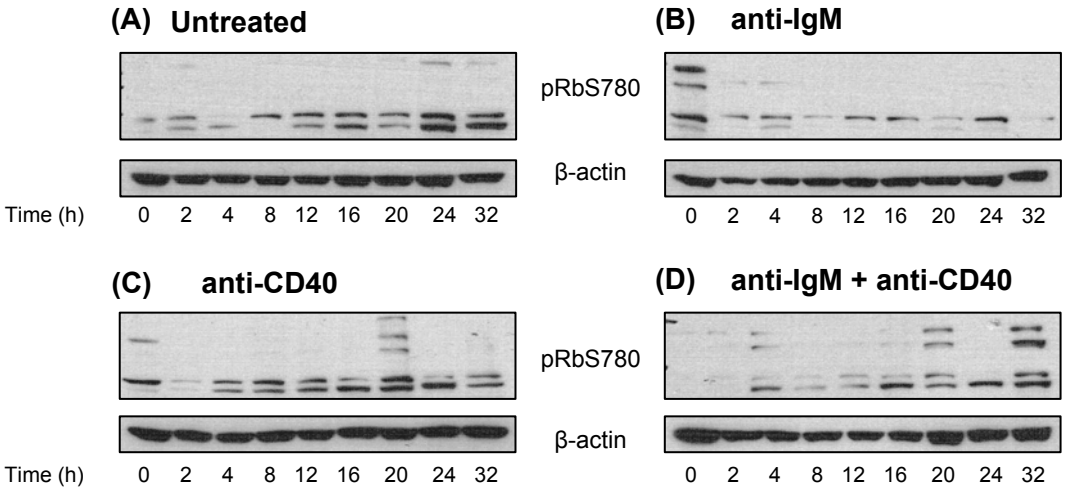
(A) Untreated
(B) anti-IgM
pRbS780
β-actin
Time (h)
0 2 4 8 12 16 20 24 32
(C) anti-CD40
(D) anti-IgM + anti-CD40

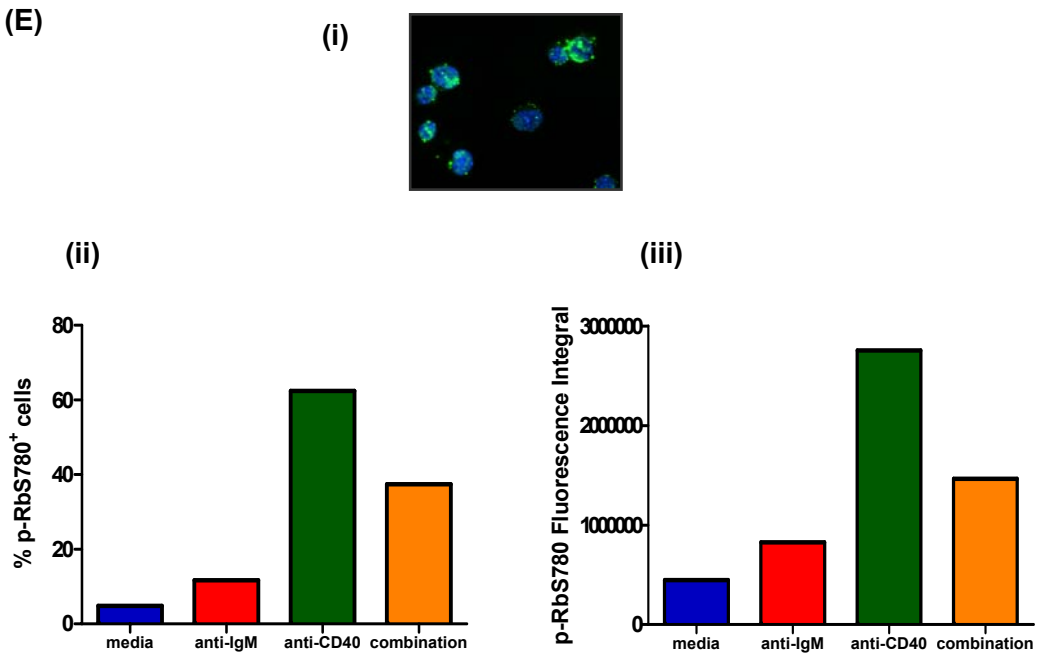
(E)
(i)
(ii)
(iii)
% p-RbS780+ cells
p-RbS780 Fluorescence Integral
media
anti-IgM
anti-CD40
combination

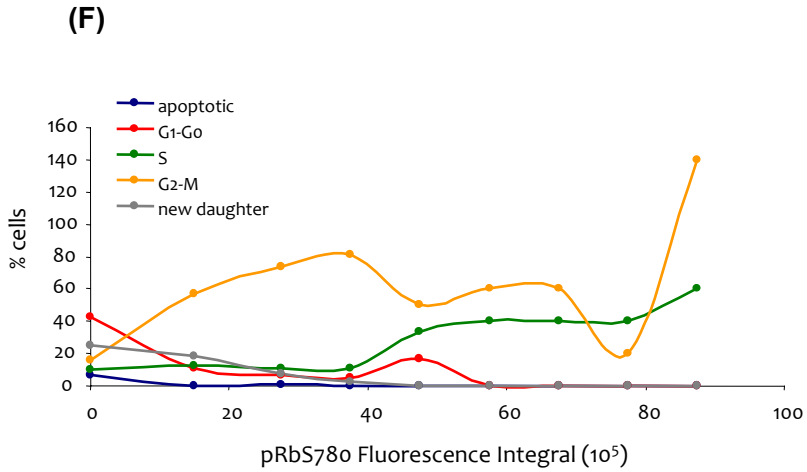
(F)
apoptotic
G1-Go
S
G2-M
new daughter
% cells
pRbS780 Fluorescence Integral (10⁵)

Figure 3.33

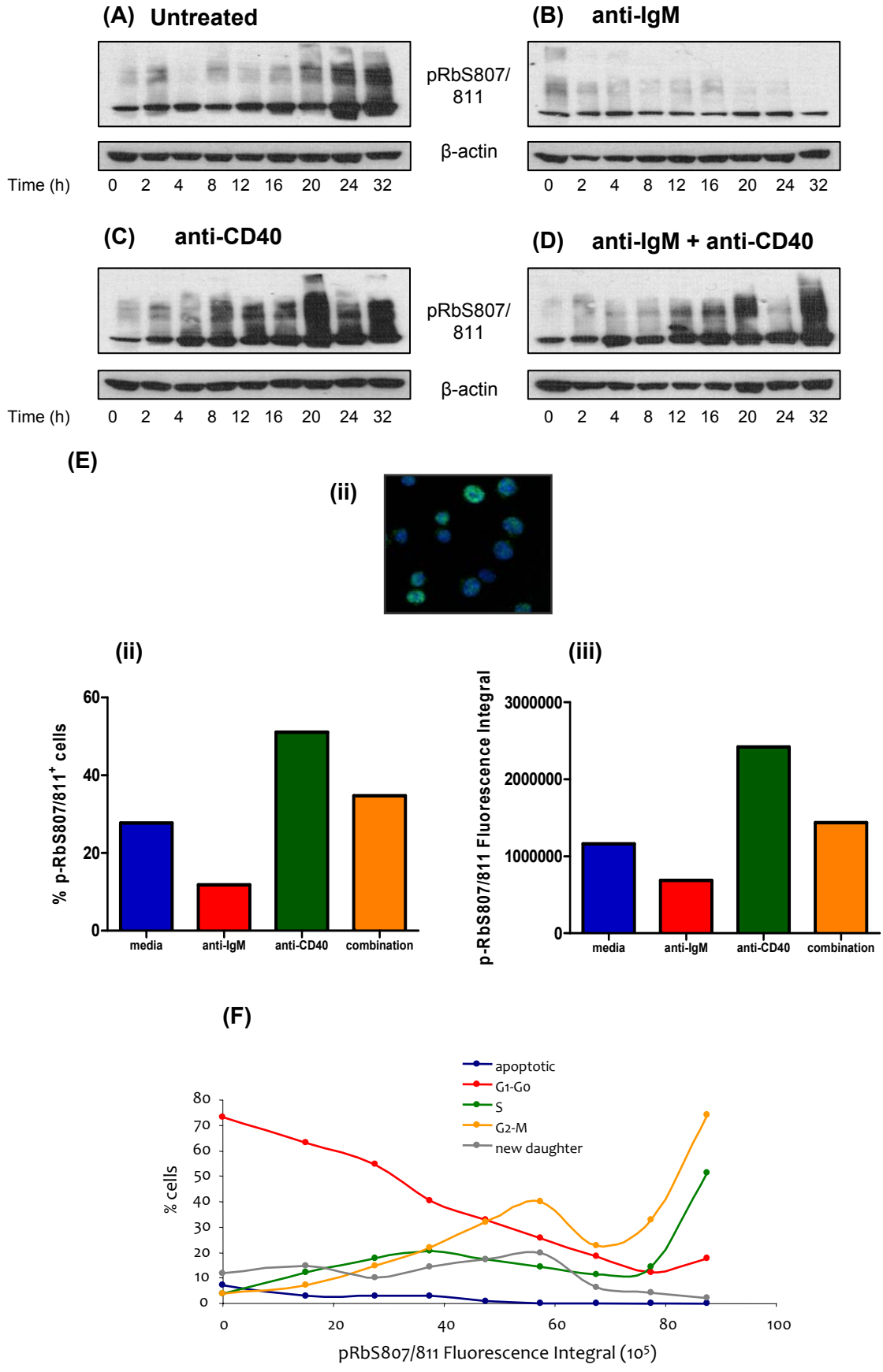
(A) Untreated
(B) anti-IgM
pRbS807/811
β-actin
Time (h)
0 2 4 8 12 16 20 24 32
(C) anti-CD40
(D) anti-IgM + anti-CD40
(E)
(ii)
(ii)
% p-RbS807/811+ cells
media
anti-IgM
anti-CD40
combination
(iii)
p-RbS807/811 Fluorescence Integral
(F)
apoptotic
G1-Go
S
G2-M
new daughter
% cells
pRbS807/811 Fluorescence Integral (10^5)

Figure 3.34

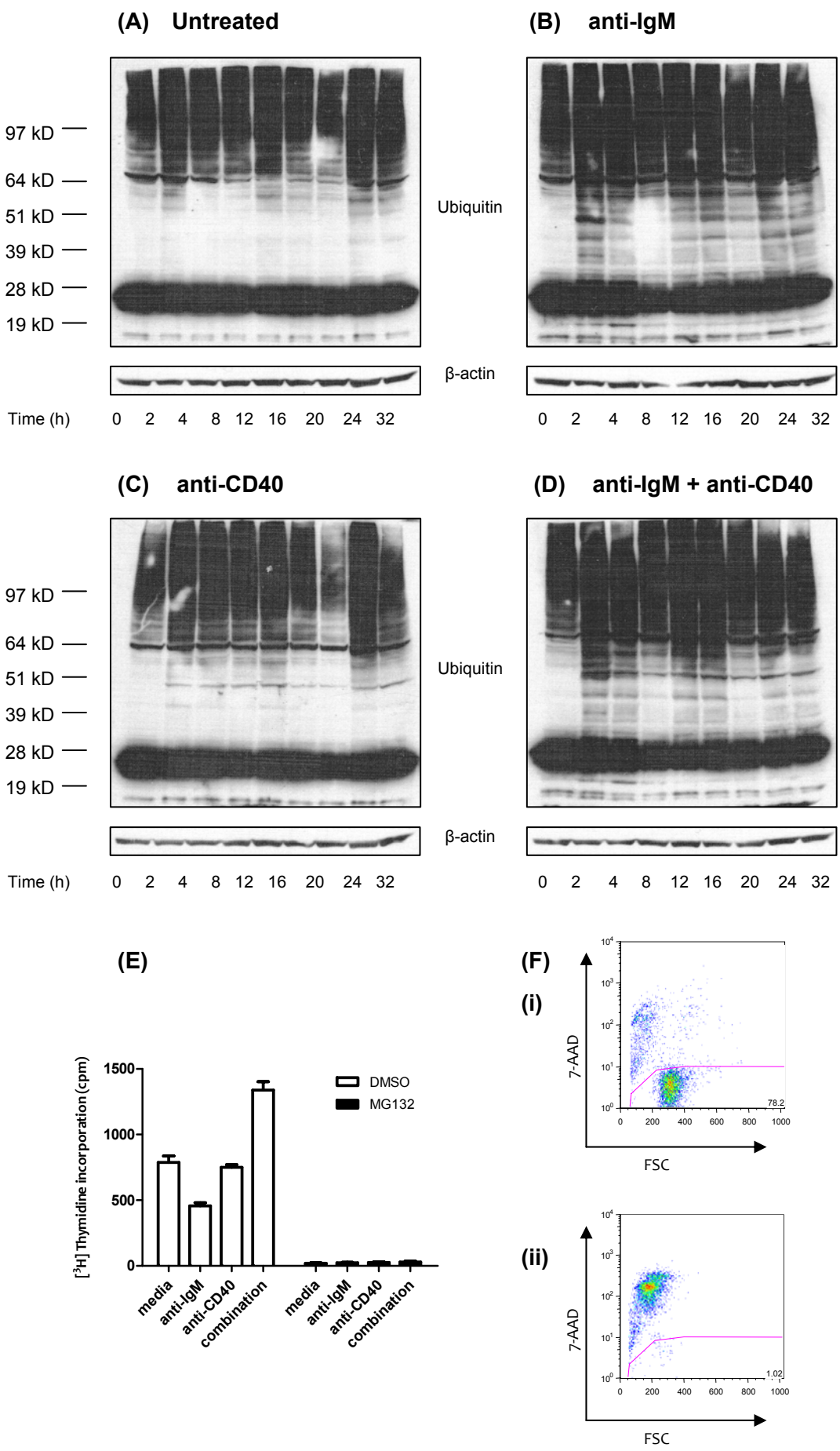
(A) Untreated
(B) anti-IgM
(C) anti-CD40
(D) anti-IgM + anti-CD40
97 kD
64 kD
51 kD
39 kD
28 kD
19 kD
Ubiquitin
β-actin
Time (h) 0 2 4 8 12 16 20 24 32
(E)
[3H] Thymidine incorporation (cpm)
1500
1000
500
0
DMSO
MG132
media
anti-IgM
anti-CD40
combination
(F)
(i)
(ii)
7-AAD
FSC
78.2
1.02

Figure 3.35

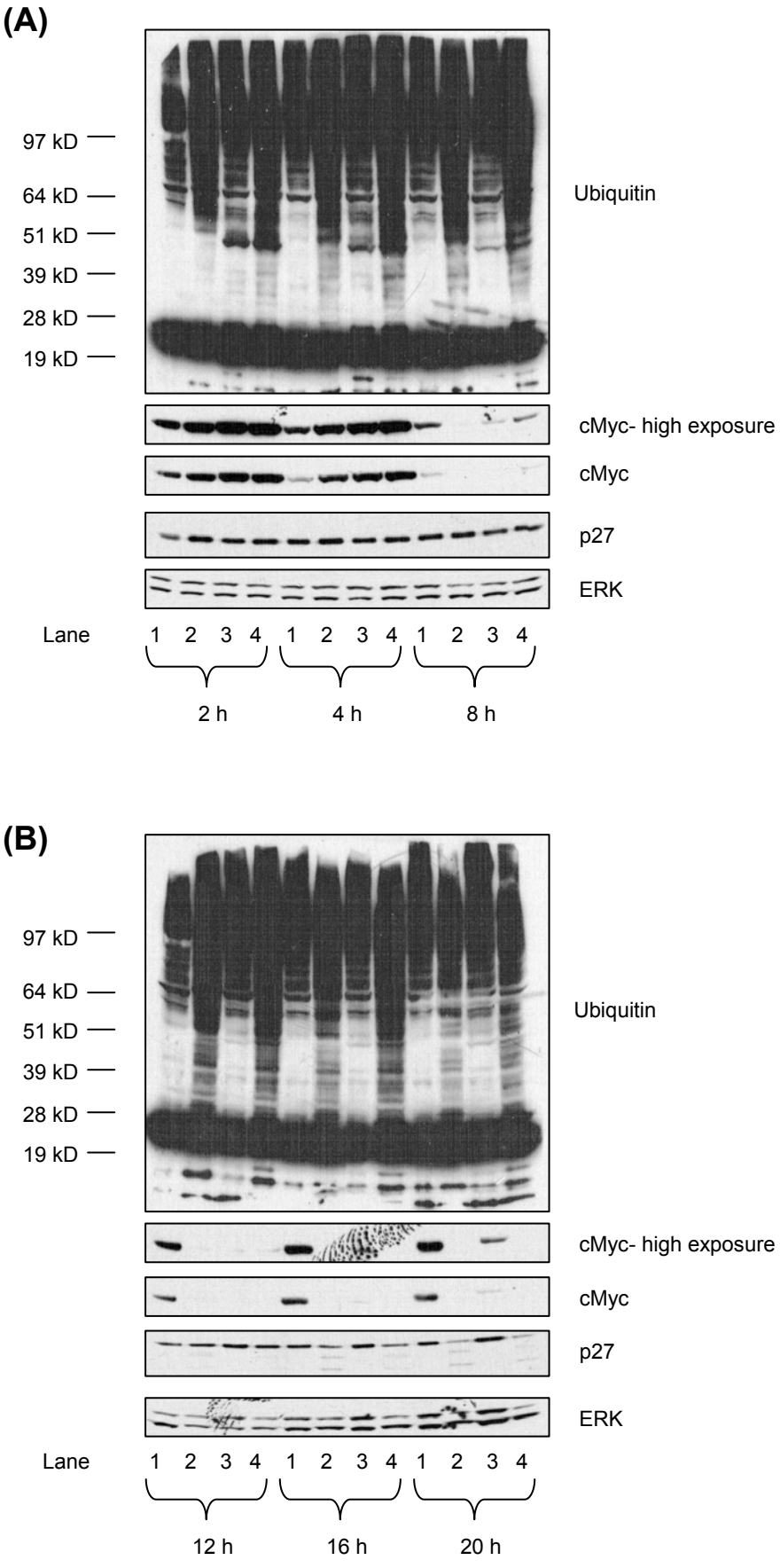
(A)
97 kD
64 kD
51 kD
39 kD
28 kD
19 kD
Ubiquitin
cMyc- high exposure
cMyc
p27
ERK
Lane
1 2 3 4 1 2 3 4 1 2 3 4
2 h
4 h
8 h
(B)
97 kD
64 kD
51 kD
39 kD
28 kD
19 kD
Ubiquitin
cMyc- high exposure
cMyc
p27
ERK
Lane
1 2 3 4 1 2 3 4 1 2 3 4
12 h
16 h
20 h

Figure 3.36

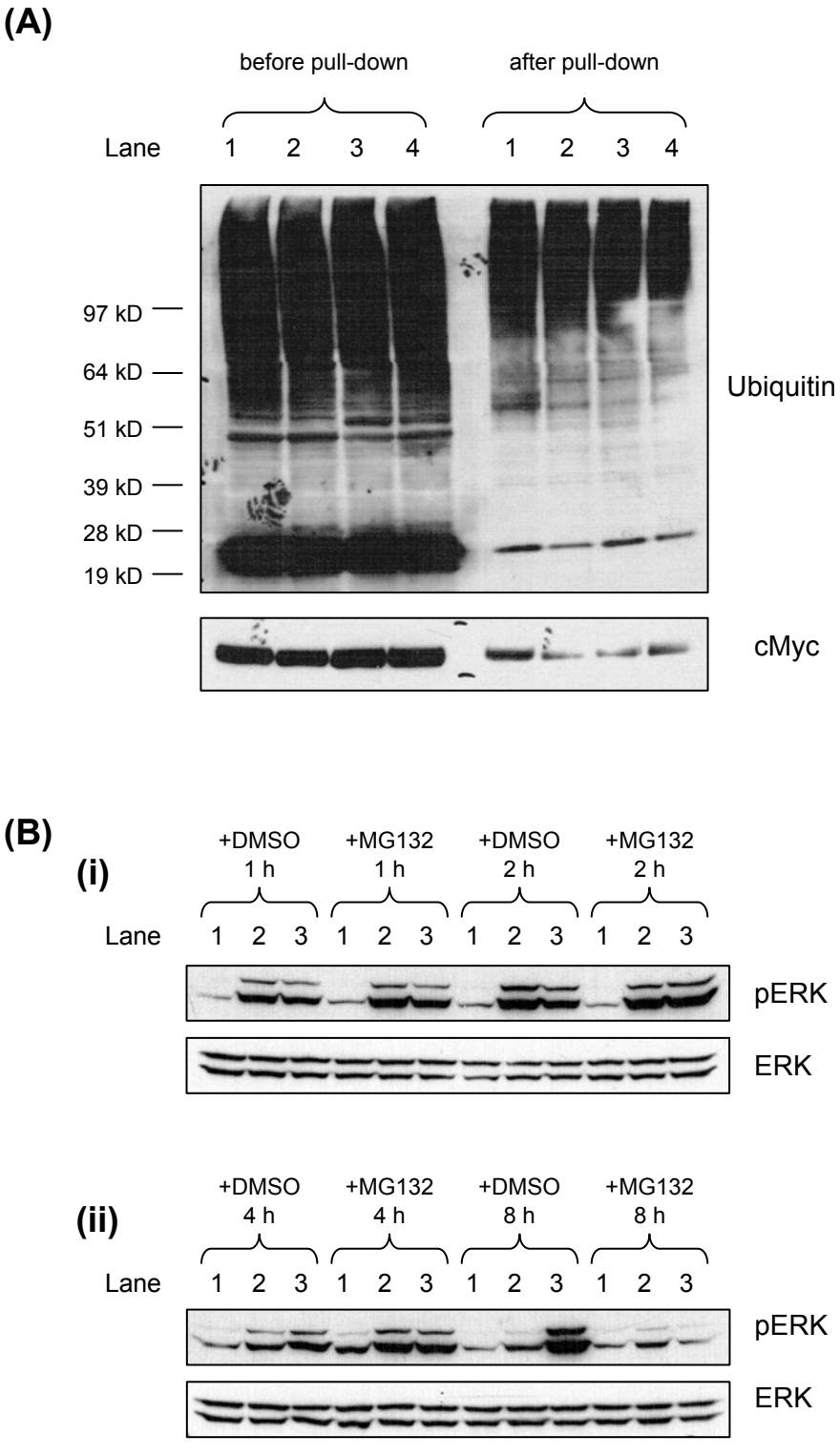
(A)
before pull-down
after pull-down
Lane
1 2 3 4
1 2 3 4
97 kD
64 kD
51 kD
39 kD
28 kD
19 kD
Ubiquitin
cMyc
(B)
(i)
+DMSO 1 h
+MG132 1 h
+DMSO 2 h
+MG132 2 h
Lane
1 2 3 1 2 3 1 2 3 1 2 3
pERK
ERK
(ii)
+DMSO 4 h
+MG132 4 h
+DMSO 8 h
+MG132 8 h
Lane
1 2 3 1 2 3 1 2 3 1 2 3
pERK
ERK

Figure 3.37

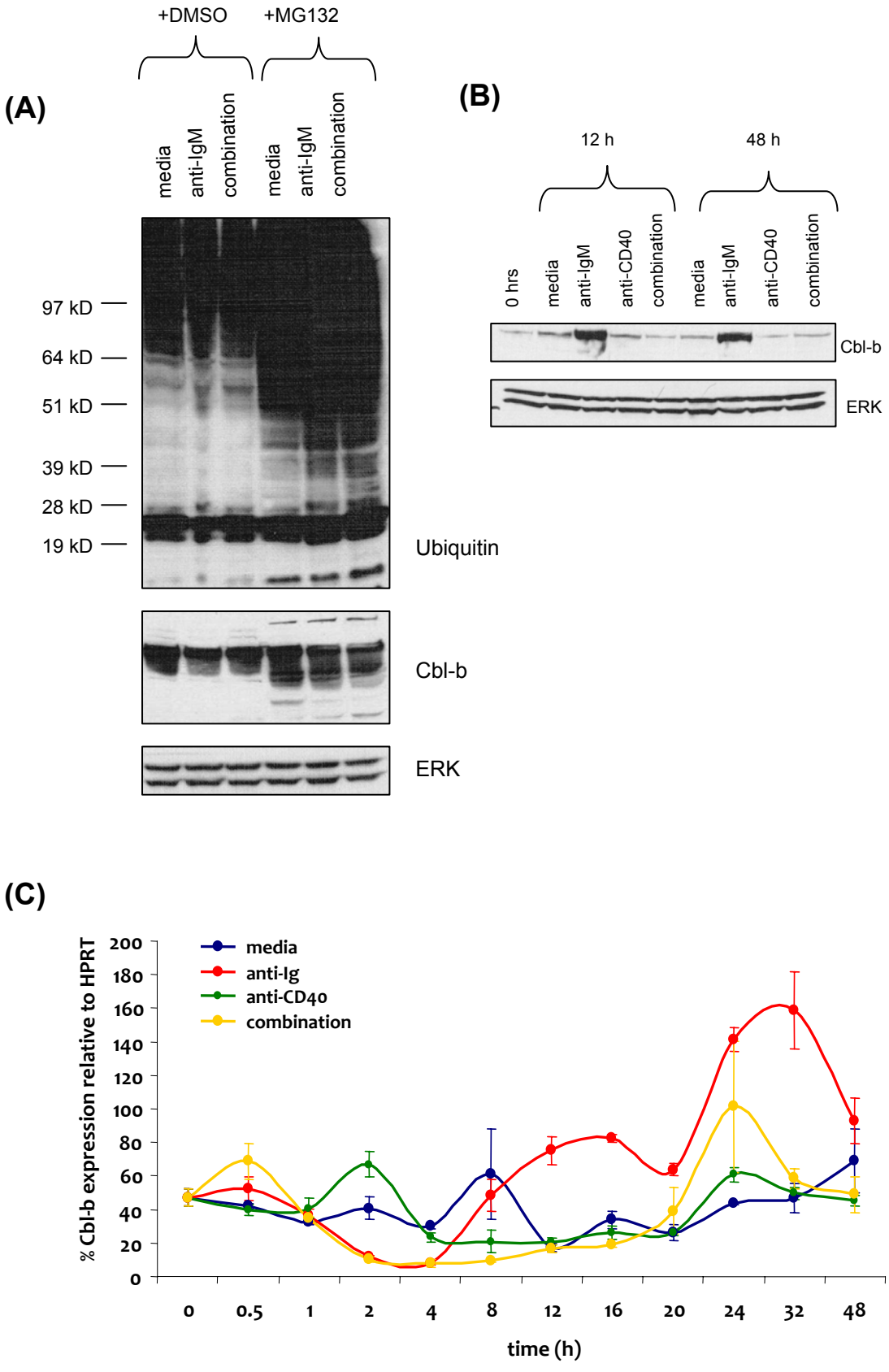
(A)
+DMSO
+MG132
media
anti-IgM
combination
media
anti-IgM
combination
97 kD
64 kD
51 kD
39 kD
28 kD
19 kD
Ubiquitin
Cbl-b
ERK
(B)
12 h
48 h
0 hrs
media
anti-IgM
anti-CD40
combination
media
anti-IgM
anti-CD40
combination
Cbl-b
ERK
(C)
% Cbl-b expression relative to HPRT
200
180
160
140
120
100
80
60
40
20
0
media
anti-Ig
anti-CD40
combination
0
0.5
1
2
4
8
12
16
20
24
32
48
time (h)

Figure 3.38

(A)

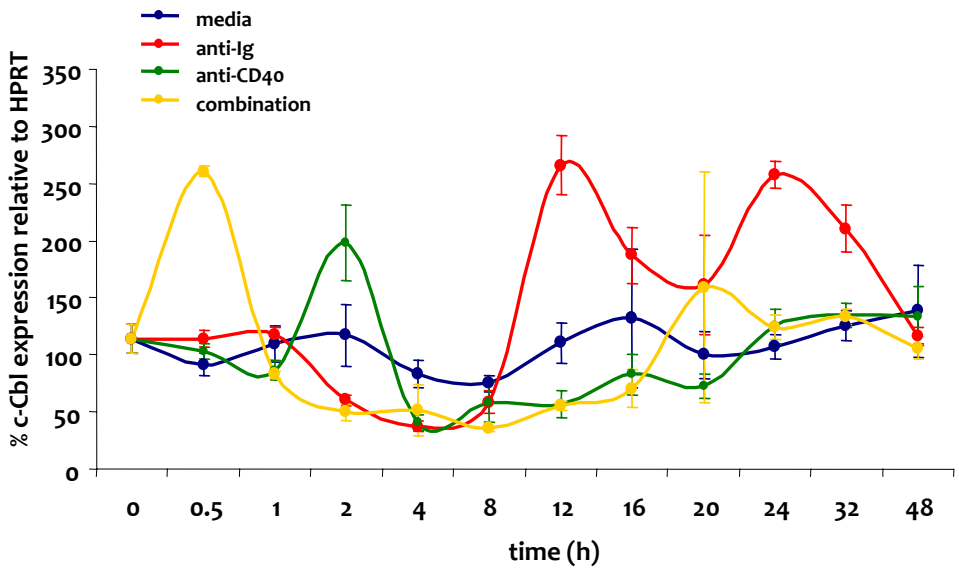

(B)

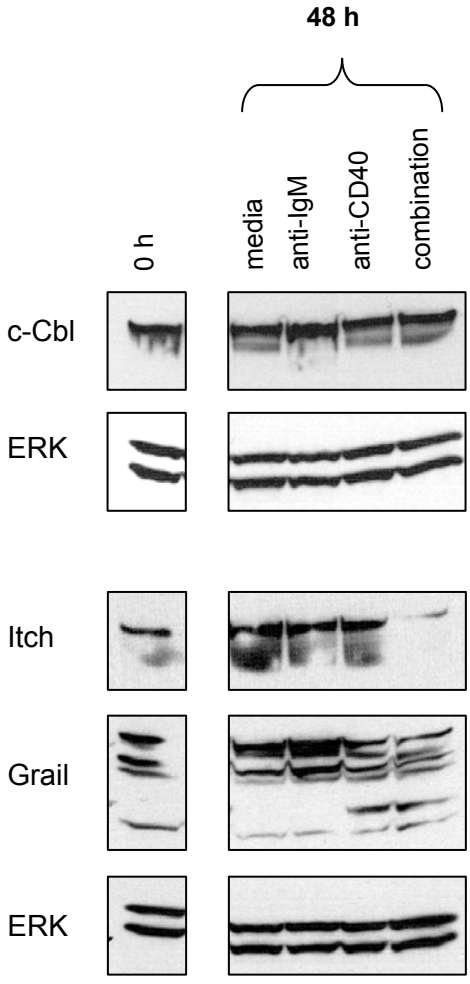

Figure 4.1

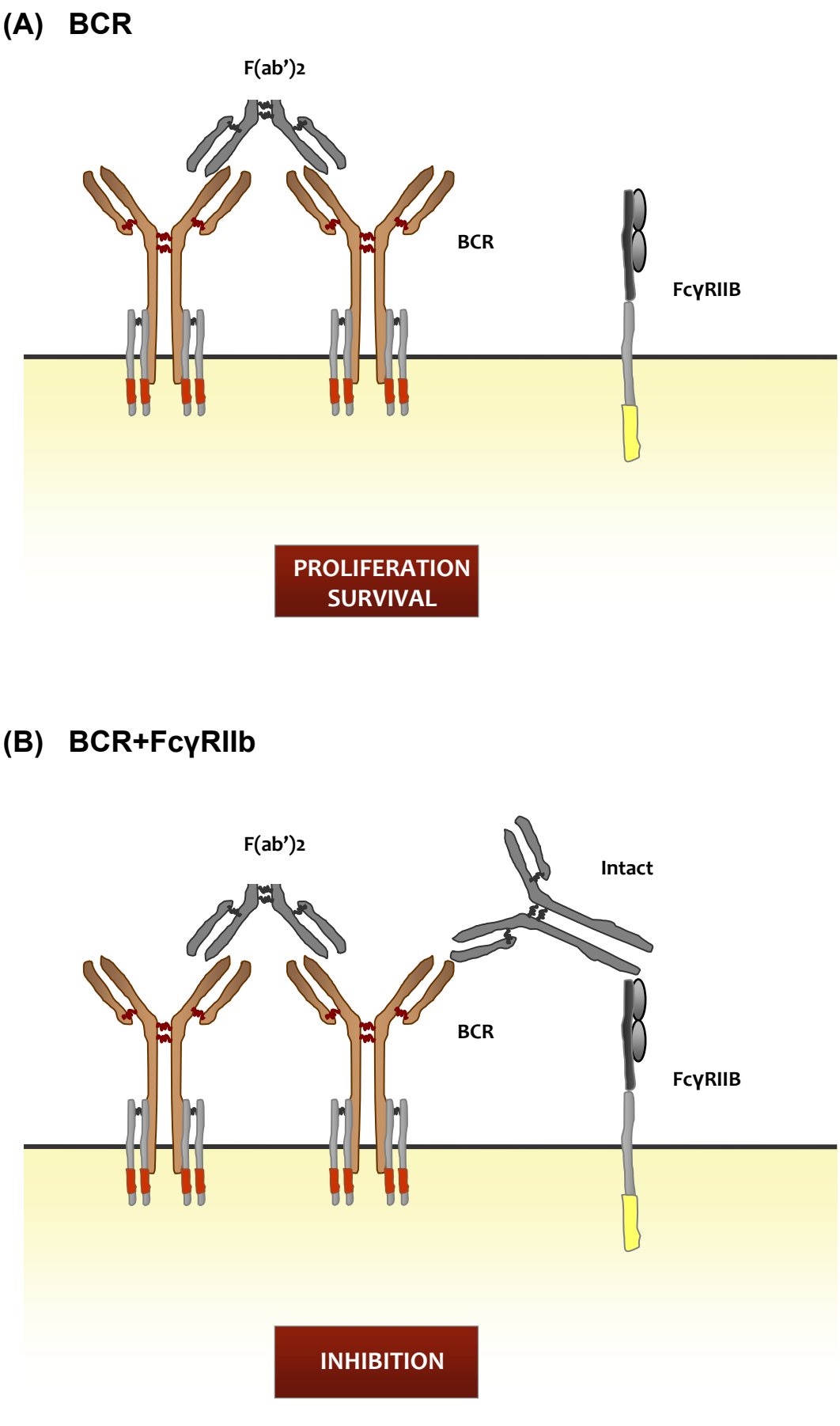
(A) BCR
F(ab')2
BCR
FcγRIIB
PROLIFERATION
SURVIVAL
(B) BCR+FcγRIIb
F(ab')2
Intact
BCR
FcγRIIB
INHIBITION

Figure 4.2

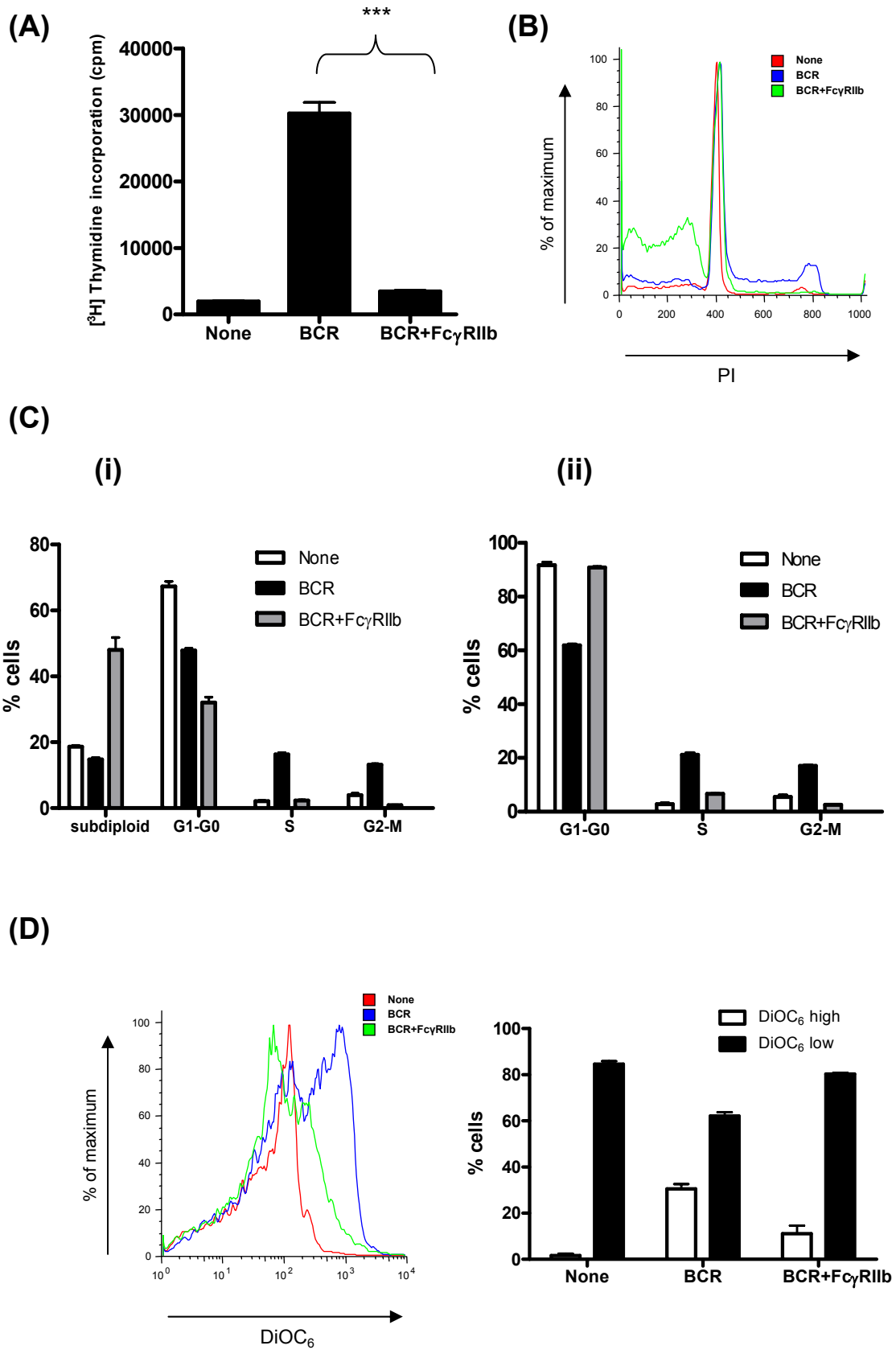
(A)
***
[3H] Thymidine incorporation (cpm)
40000
30000
20000
10000
0
None
BCR
BCR+FcγRIIb
(B)
None
BCR
BCR+FcγRIIb
% of maximum
100
80
60
40
20
0
0
200
400
600
800
1000
PI
(C)
(i)
% cells
80
60
40
20
0
None
BCR
BCR+FcγRIIb
subdiploid
G1-G0
S
G2-M
(ii)
% cells
100
80
60
40
20
0
None
BCR
BCR+FcγRIIb
G1-G0
S
G2-M
(D)
None
BCR
BCR+FcγRIIb
% of maximum
100
80
60
40
20
0
10^0
10^1
10^2
10^3
10^4
DiOC6
DiOC6 high
DiOC6 low
% cells
100
80
60
40
20
0
None
BCR
BCR+FcγRIIb

Figure 4.3

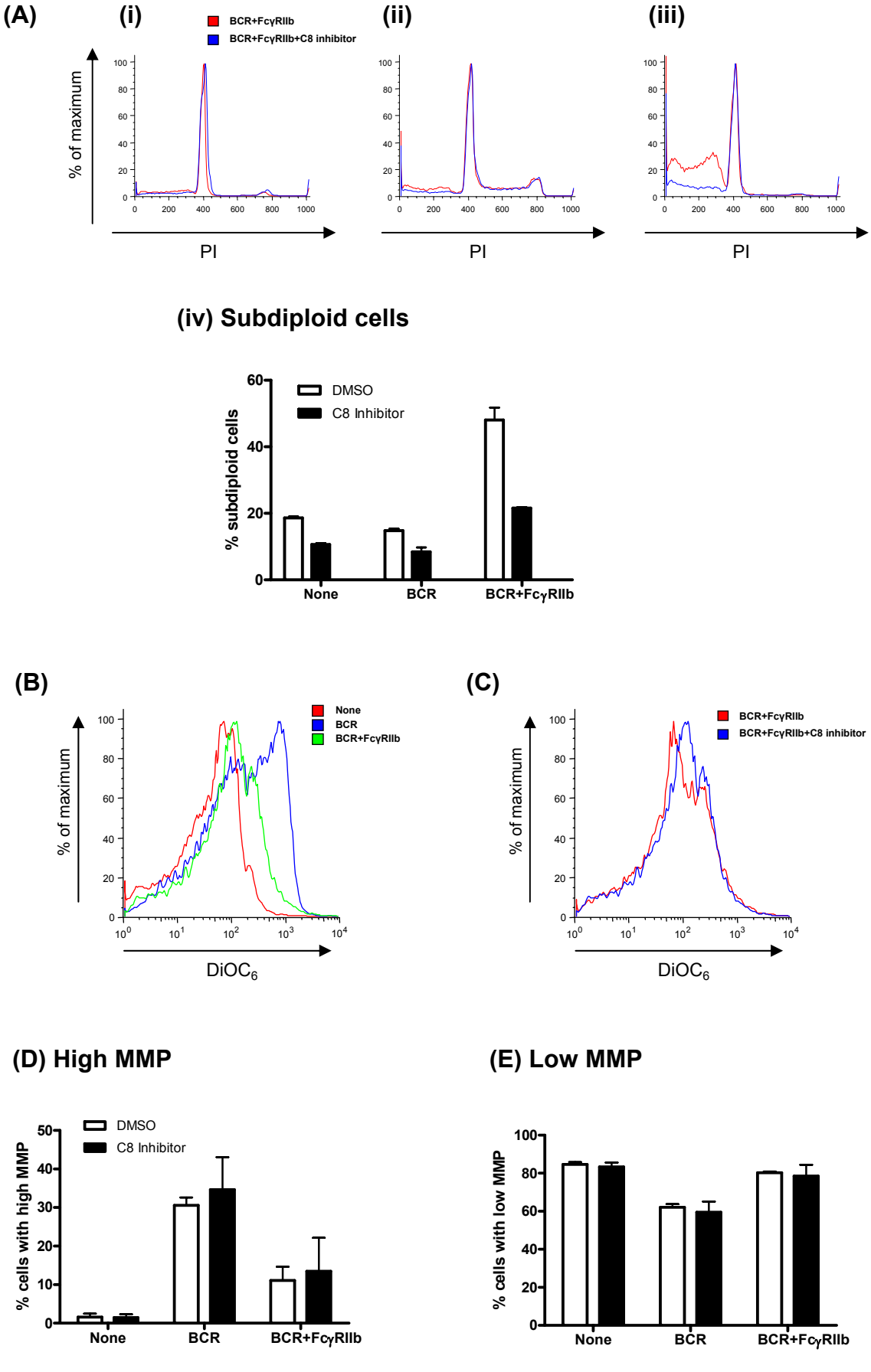
(A)
(i)
BCR+FcγRIIb
BCR+FcγRIIb+C8 inhibitor
(ii)
(iii)
% of maximum
PI
(iv) Subdiploid cells
DMSO
C8 Inhibitor
% subdiploid cells
None
BCR
BCR+FcγRIIb
(B)
None
BCR
BCR+FcγRIIb
% of maximum
DiOC6
(C)
BCR+FcγRIIb
BCR+FcγRIIb+C8 inhibitor
% of maximum
DiOC6
(D) High MMP
DMSO
C8 Inhibitor
% cells with high MMP
None
BCR
BCR+FcγRIIb
(E) Low MMP
% cells with low MMP
None
BCR
BCR+FcγRIIb

Figure 4.4

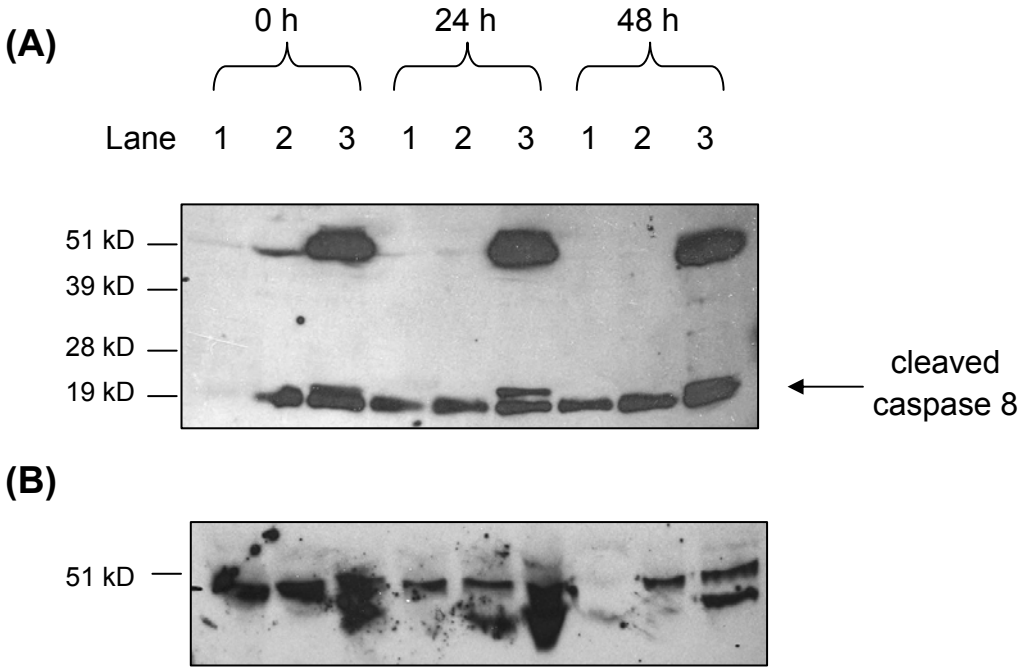
(A)
0 h
24 h
48 h
Lane 1 2 3 1 2 3 1 2 3
51 kD
39 kD
28 kD
19 kD
cleaved caspase 8
(B)
51 kD

Figure 4.5

(A)

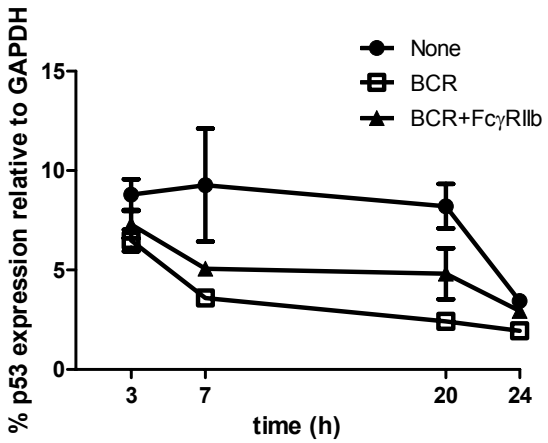

(B) Whole cell lysates

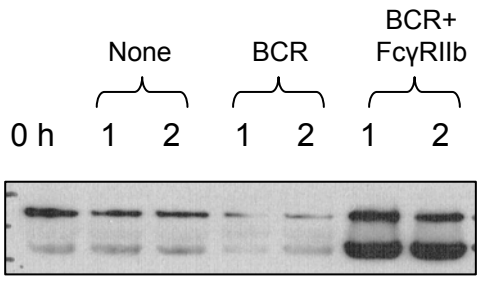

(C) Nuclear fraction

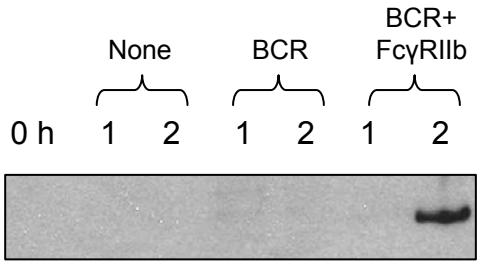

(D) Cytosolic fraction

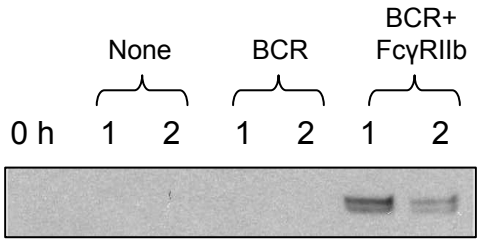

Figure 4.6

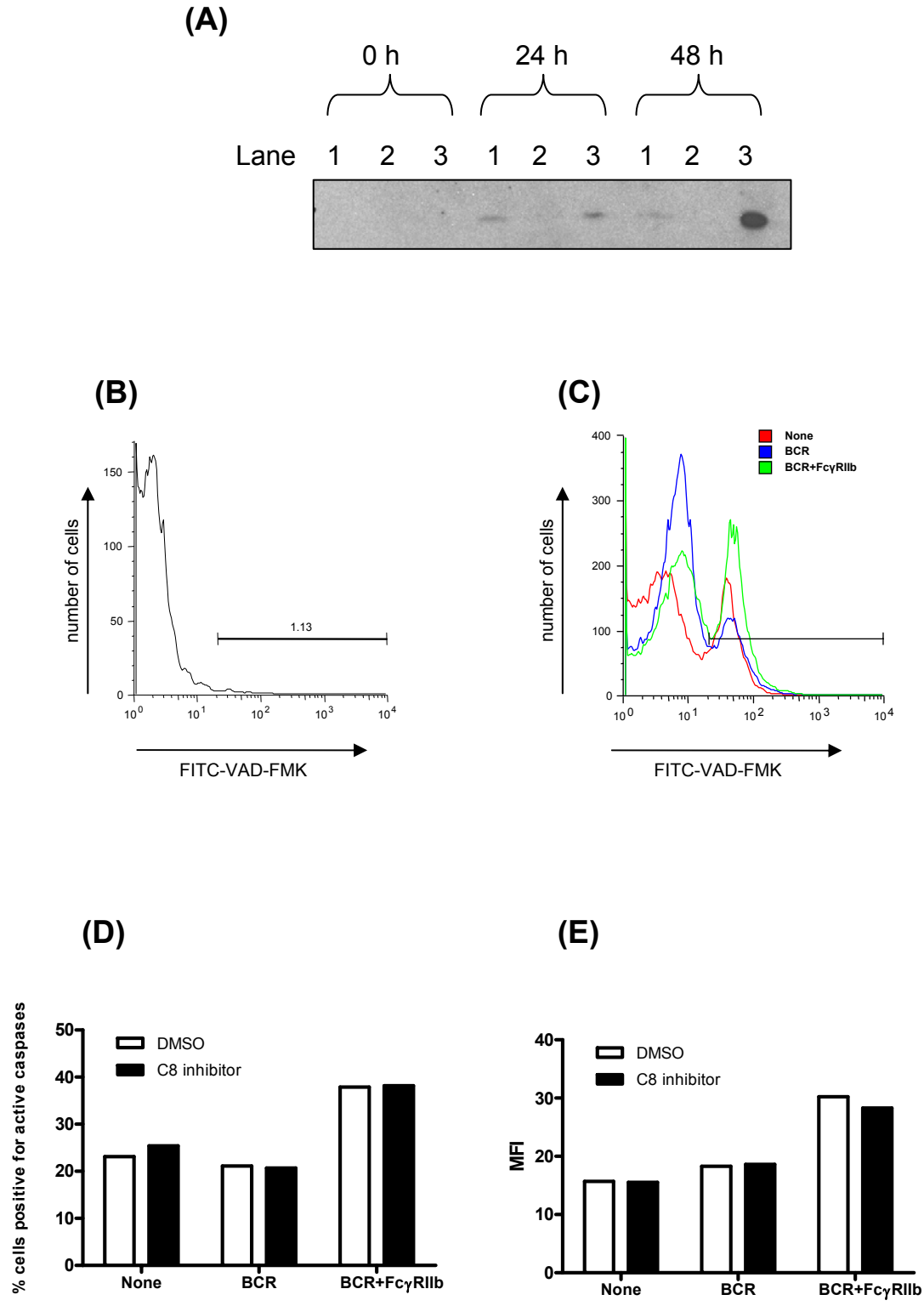
(A)
0 h
24 h
48 h
Lane 1 2 3 1 2 3 1 2 3
(B)
number of cells
1.13
FITC-VAD-FMK
(C)
None
BCR
BCR+FcγRIIb
number of cells
FITC-VAD-FMK
(D)
% cells positive for active caspases
DMSO
C8 inhibitor
None
BCR
BCR+FcγRIIb
(E)
MFI
DMSO
C8 inhibitor
None
BCR
BCR+FcγRIIb

Figure 4.7

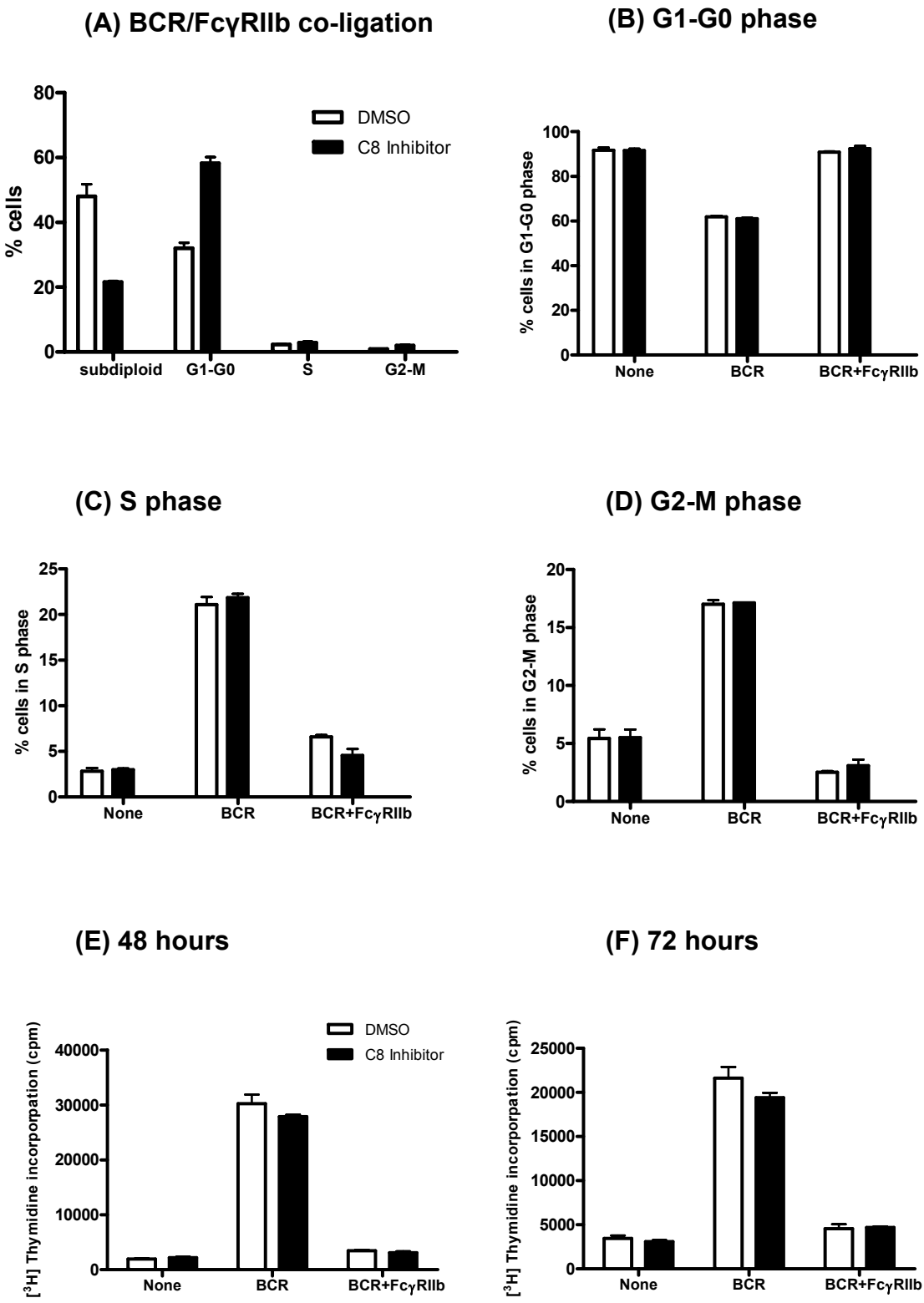
(A) BCR/FcγRIIb co-ligation
% cells
DMSO
C8 Inhibitor
subdiploid
G1-G0
S
G2-M
(B) G1-G0 phase
% cells in G1-G0 phase
None
BCR
BCR+FcγRIIb
(C) S phase
% cells in S phase
(D) G2-M phase
% cells in G2-M phase
(E) 48 hours
[3H] Thymidine incorporation (cpm)
(F) 72 hours

Figure 4.8

(A)

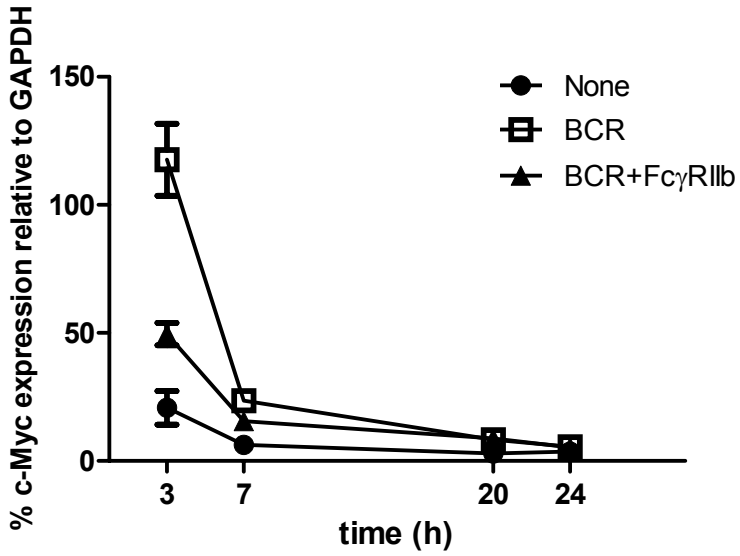
% c-Myc expression relative to GAPDH
150
100
50
0
3
7
20
24
time (h)
None
BCR
BCR+FcγRIIb

(B)

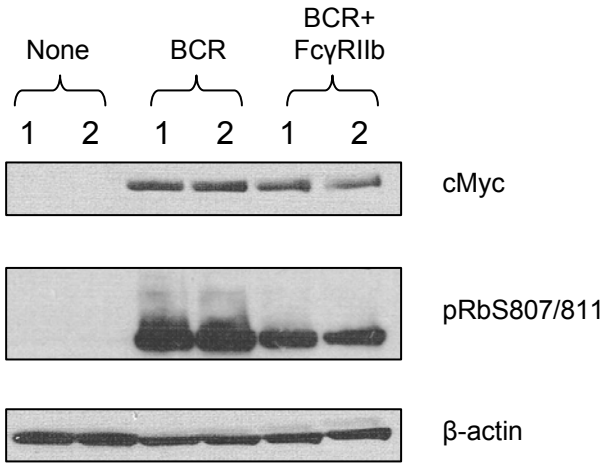
None
BCR
BCR+
FcγRIIb
1 2 1 2 1 2
cMyc
pRbS807/811
β-actin

Figure 4.9

(A) PAC-1

(i)

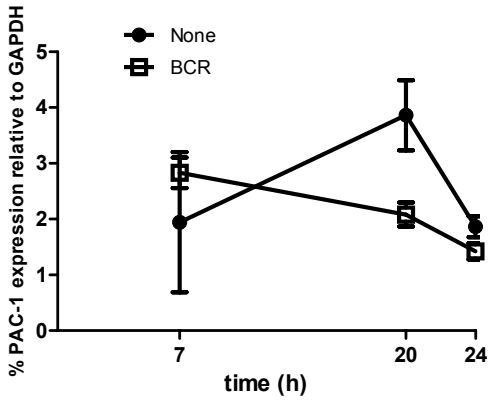

(ii)

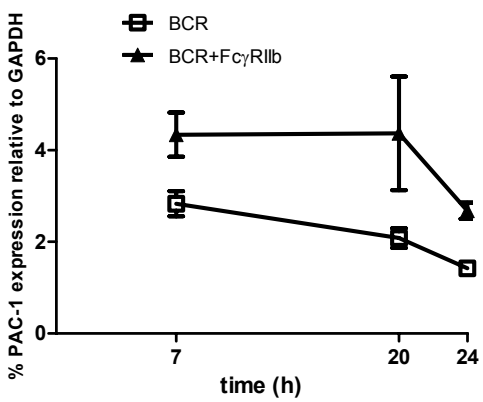

(B) SPA-1

(i)

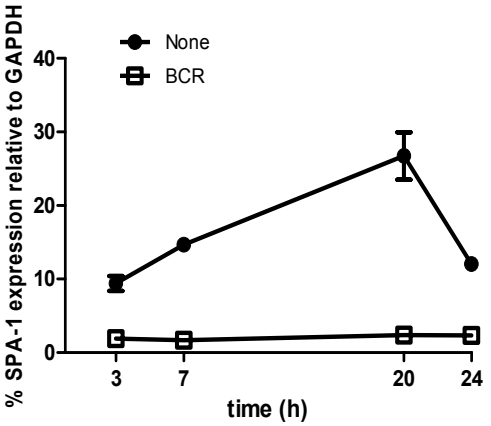

(ii)

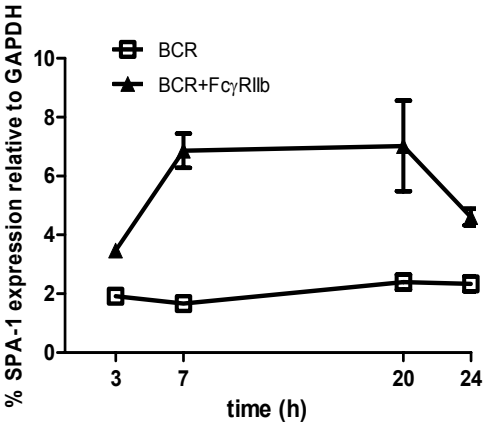

Figure 4.10

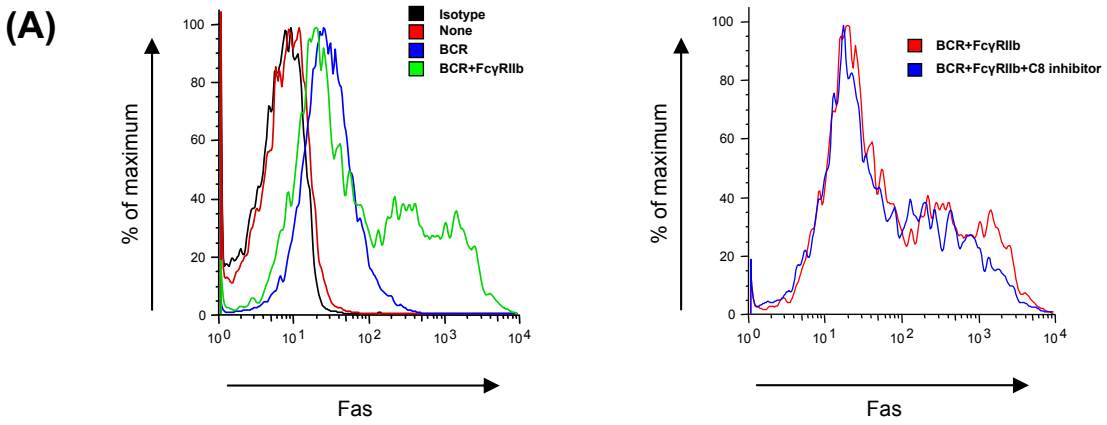
(A)
Isotype
None
BCR
BCR+FcγRIIb
% of maximum
Fas
BCR+FcγRIIb
BCR+FcγRIIb+C8 inhibitor
% of maximum
Fas

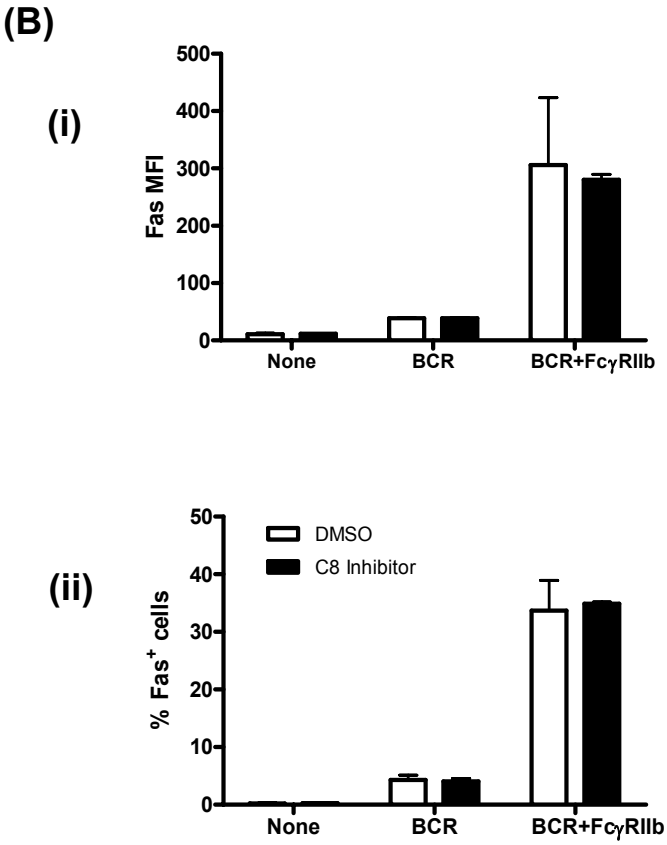
(B)
(i)
Fas MFI
None
BCR
BCR+FcγRIIb
(ii)
DMSO
C8 Inhibitor
% Fas+ cells
None
BCR
BCR+FcγRIIb

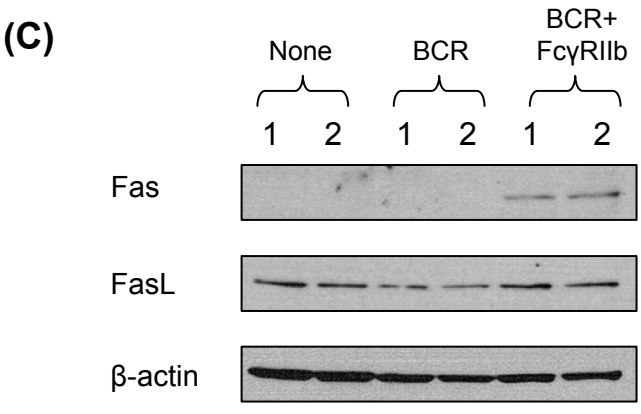
(C)
None
BCR
BCR+ FcγRIIb
1 2 1 2 1 2
Fas
FasL
β-actin

Figure 4.11

(A)

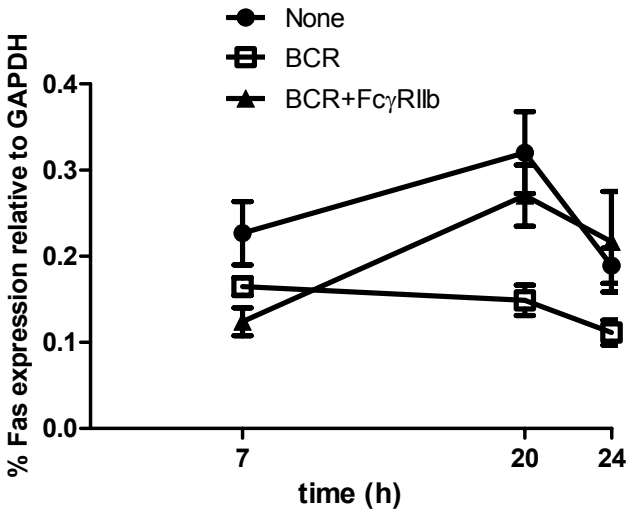

(B) 24 hours

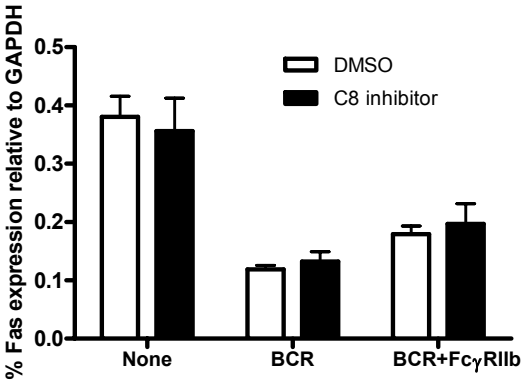

Figure 4.12

(A)

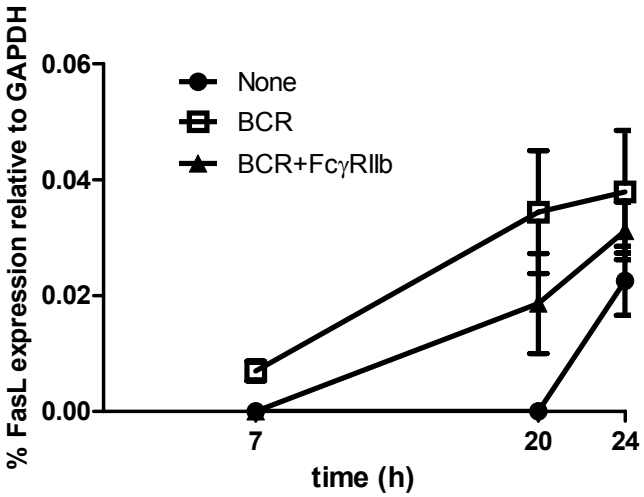

(B) 24 hours

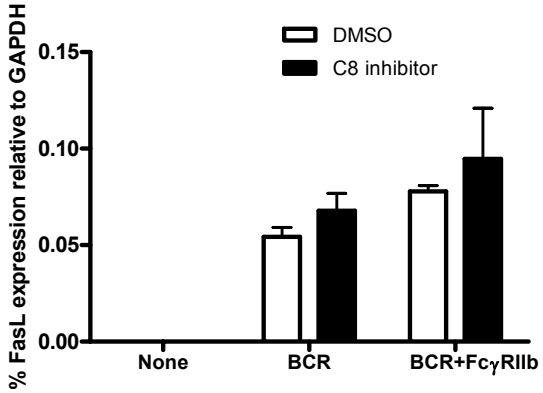

Figure 4.13

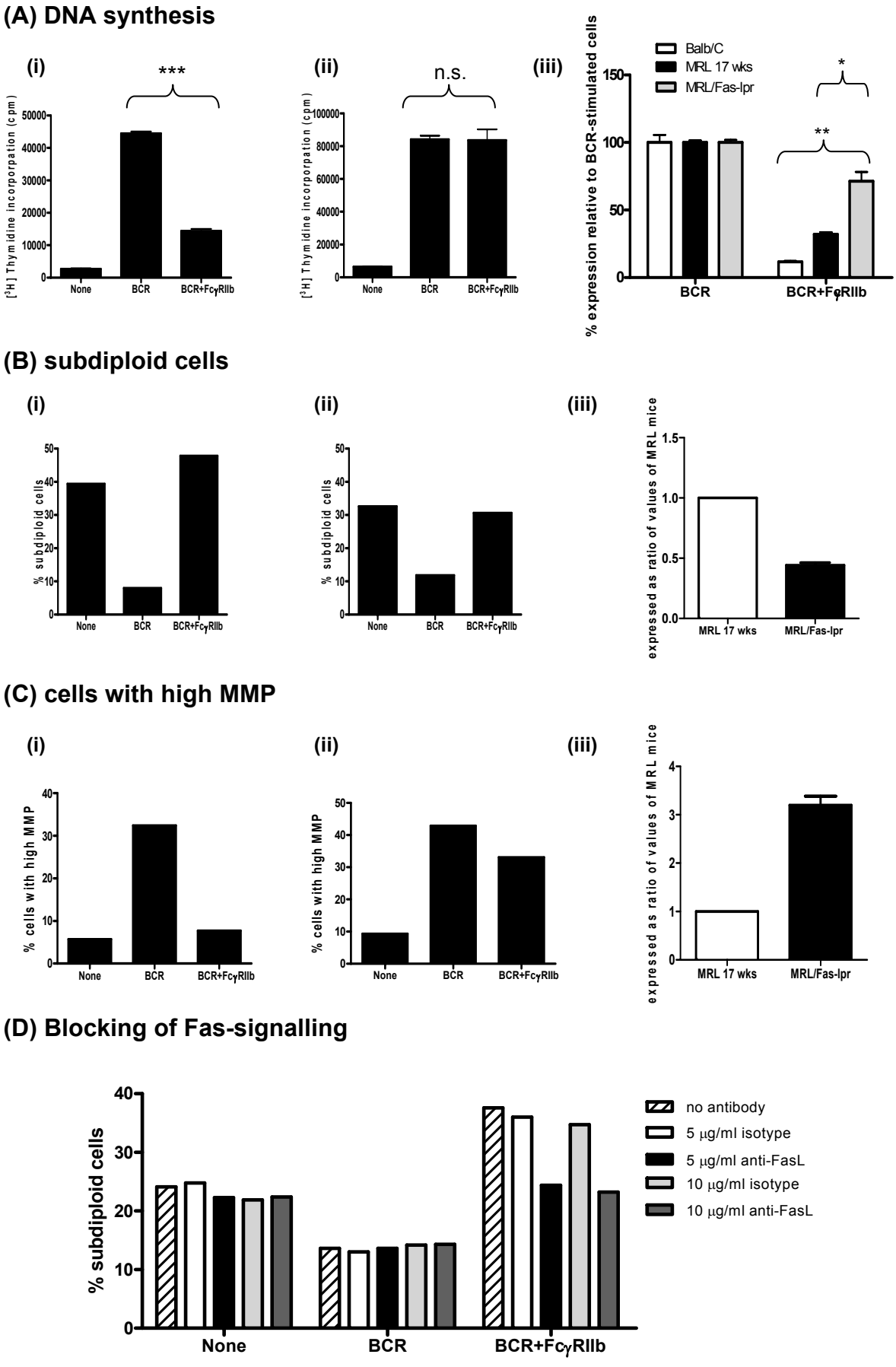
(A) DNA synthesis
(i)
***
[3H] Thymidine incorporation (cpm)
None
BCR
BCR+FcγRIIb
(ii)
n.s.
(iii)
Balb/C
MRL 17 wks
MRL/Fas-lpr
*
**
% expression relative to BCR-stimulated cells
BCR
BCR+FcγRIIb
(B) subdiploid cells
% subdiploid cells
expressed as ratio of values of MRL mice
MRL 17 wks
MRL/Fas-lpr
(C) cells with high MMP
% cells with high MMP
(D) Blocking of Fas-signalling
no antibody
5 μg/ml isotype
5 μg/ml anti-FasL
10 μg/ml isotype
10 μg/ml anti-FasL

Figure 4.14

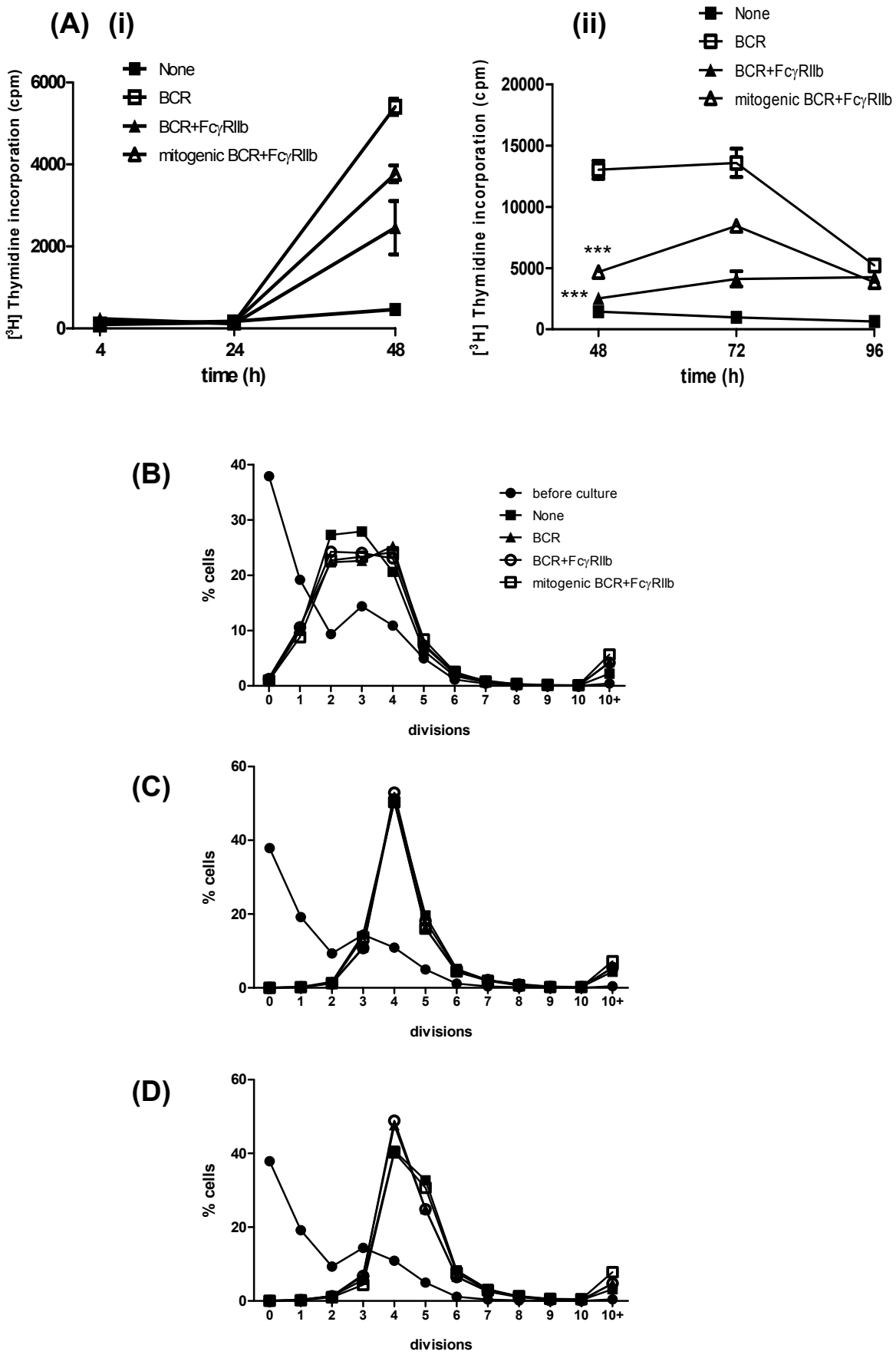
(A) (i)
None
BCR
BCR+FcγRIIb
mitogenic BCR+FcγRIIb
[3H] Thymidine incorporation (cpm)
6000
4000
2000
0
4
24
48
time (h)
(ii)
None
BCR
BCR+FcγRIIb
mitogenic BCR+FcγRIIb
[3H] Thymidine incorporation (cpm)
20000
15000
10000
5000
0
***
***
48
72
96
time (h)
(B)
before culture
None
BCR
BCR+FcγRIIb
mitogenic BCR+FcγRIIb
% cells
40
30
20
10
0
0 1 2 3 4 5 6 7 8 9 10 10+
divisions
(C)
% cells
60
40
20
0
0 1 2 3 4 5 6 7 8 9 10 10+
divisions
(D)
% cells
60
40
20
0
0 1 2 3 4 5 6 7 8 9 10 10+
divisions

Figure 4.15

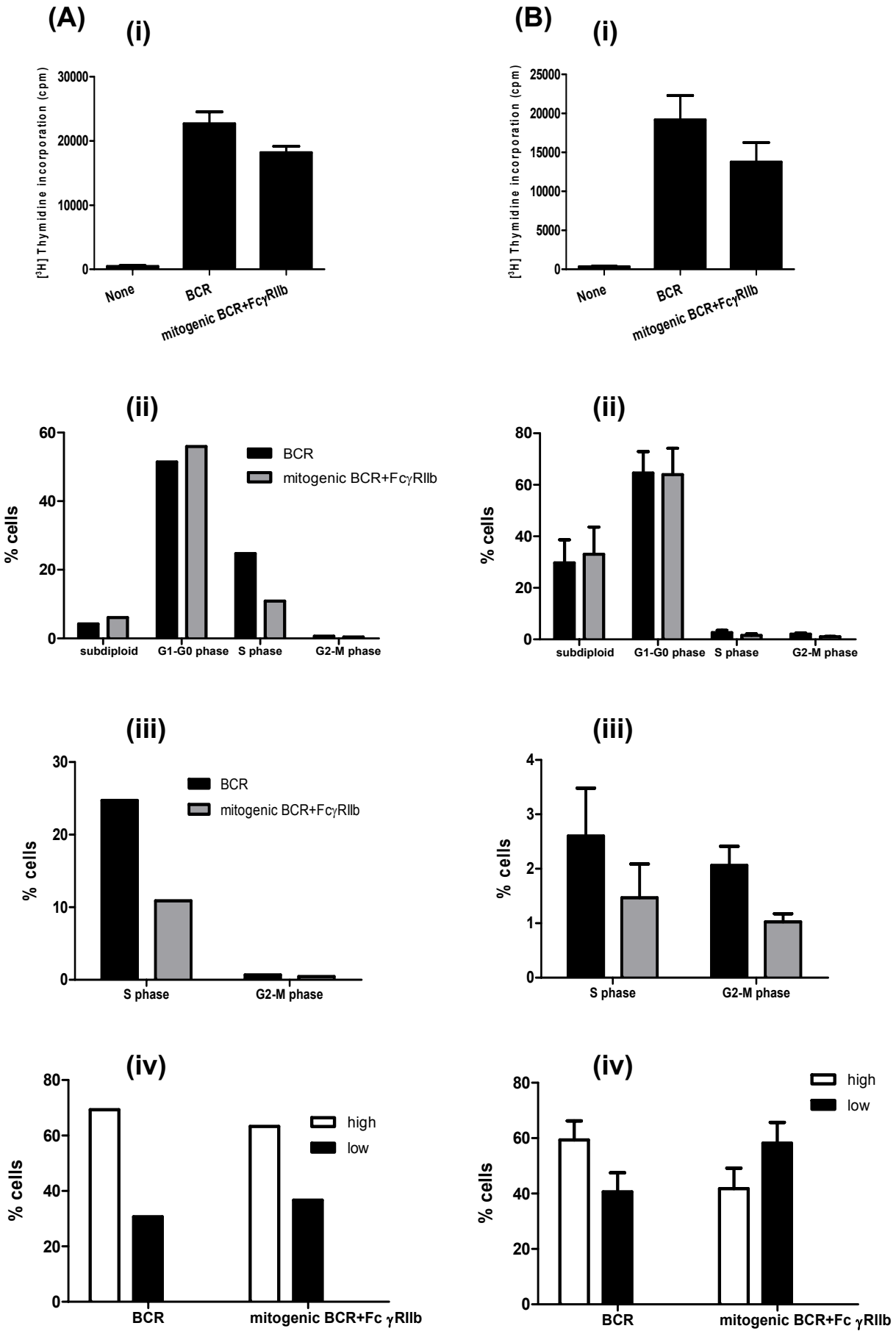
(A)
(i)
[3H] Thymidine incorporation (cpm)
30000
20000
10000
0
None
BCR
mitogenic BCR+FcγRIIb
(ii)
% cells
60
40
20
0
BCR
mitogenic BCR+FcγRIIb
subdiploid
G1-G0 phase
S phase
G2-M phase
(iii)
% cells
30
20
10
0
BCR
mitogenic BCR+FcγRIIb
S phase
G2-M phase
(iv)
% cells
80
60
40
20
0
high
low
BCR
mitogenic BCR+Fc γRIIb
(B)
(i)
[3H] Thymidine incorporation (cpm)
25000
20000
15000
10000
5000
0
None
BCR
mitogenic BCR+FcγRIIb
(ii)
% cells
80
60
40
20
0
subdiploid
G1-G0 phase
S phase
G2-M phase
(iii)
% cells
4
3
2
1
0
S phase
G2-M phase
(iv)
% cells
80
60
40
20
0
high
low
BCR
mitogenic BCR+Fc γRIIb

Figure 4.16

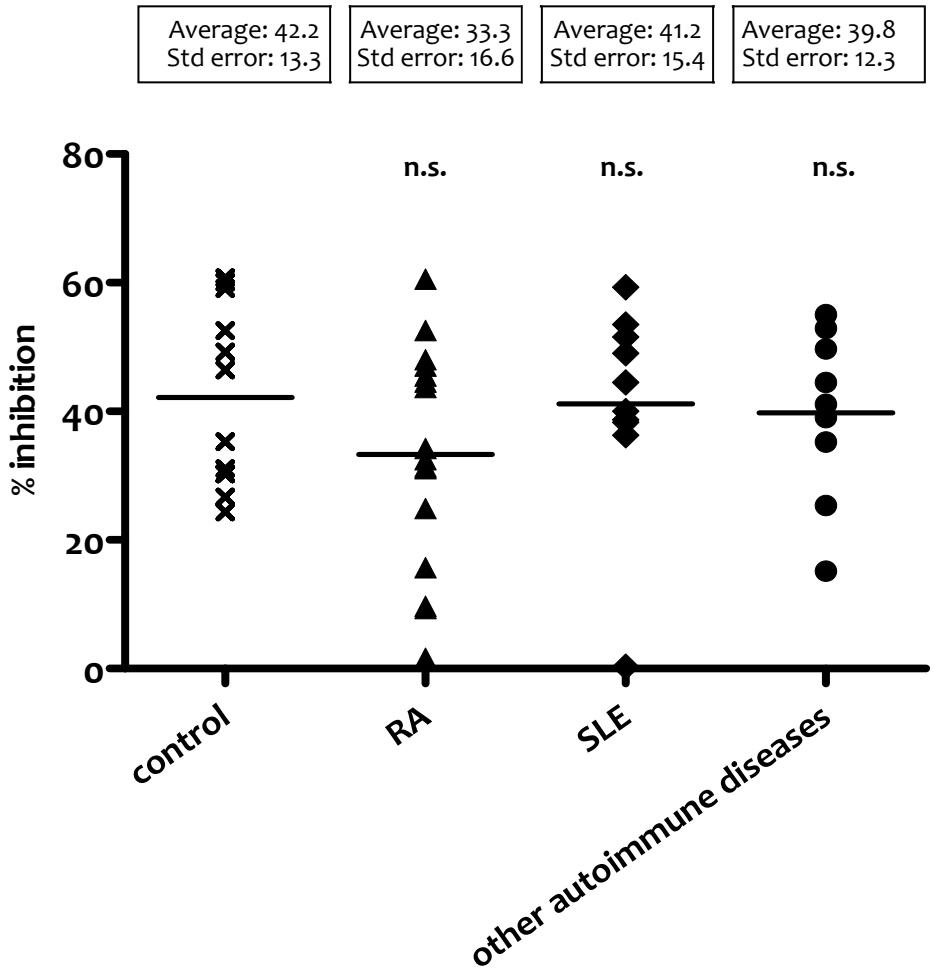
Average: 42.2
Std error: 13.3
Average: 33.3
Std error: 16.6
Average: 41.2
Std error: 15.4
Average: 39.8
Std error: 12.3
n.s.
n.s.
n.s.
80
60
40
20
0
% inhibition
control
RA
SLE
other autoimmune diseases

Figure 4.17

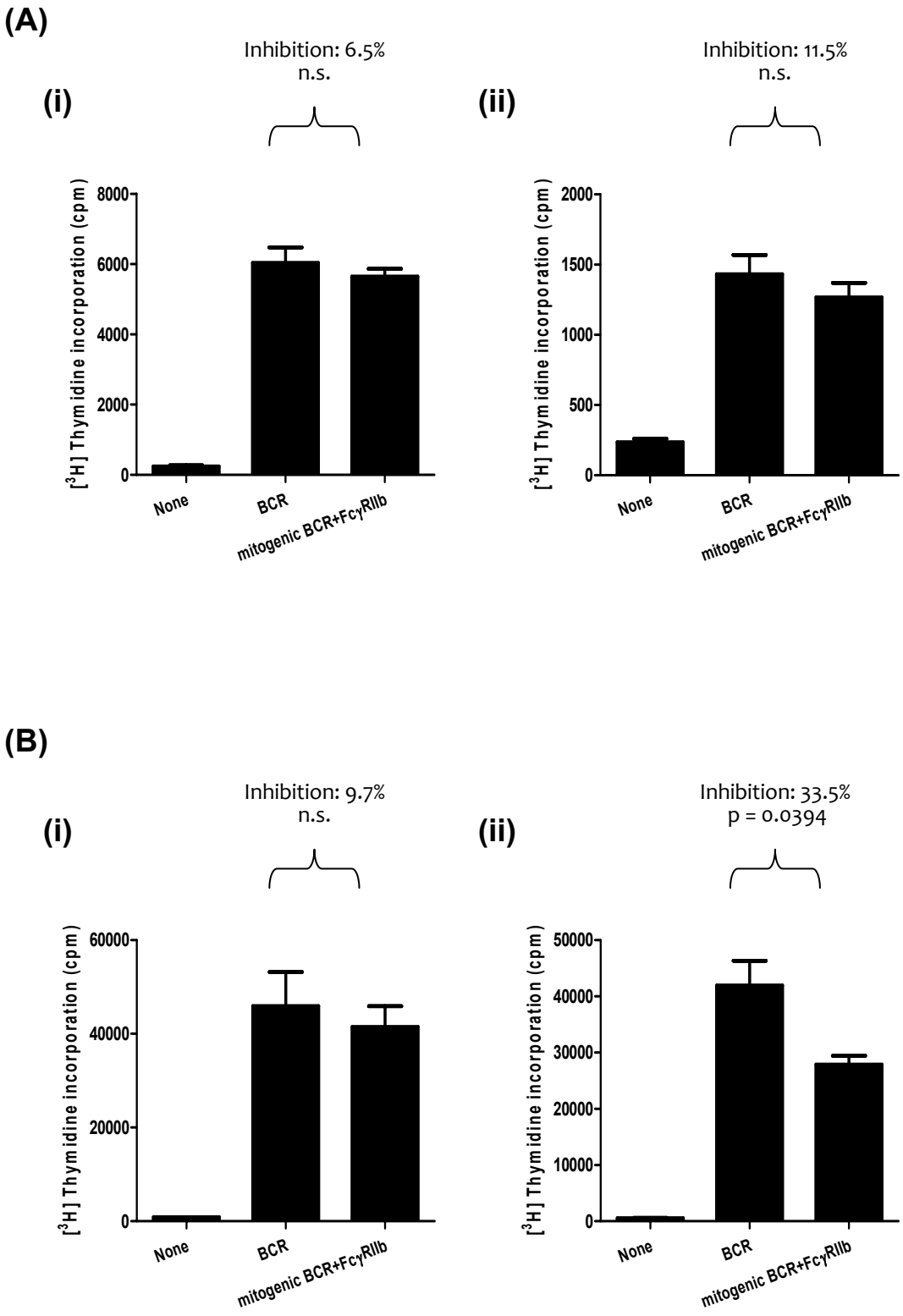
(A)
(i)
Inhibition: 6.5%
n.s.
[3H] Thymidine incorporation (cpm)
8000
6000
4000
2000
0
None
BCR
mitogenic BCR+FcγRIIb
(ii)
Inhibition: 11.5%
n.s.
[3H] Thymidine incorporation (cpm)
2000
1500
1000
500
0
None
BCR
mitogenic BCR+FcγRIIb
(B)
(i)
Inhibition: 9.7%
n.s.
[3H] Thymidine incorporation (cpm)
60000
40000
20000
0
None
BCR
mitogenic BCR+FcγRIIb
(ii)
Inhibition: 33.5%
p = 0.0394
[3H] Thymidine incorporation (cpm)
50000
40000
30000
20000
10000
0
None
BCR
mitogenic BCR+FcγRIIb

Figure 4.18

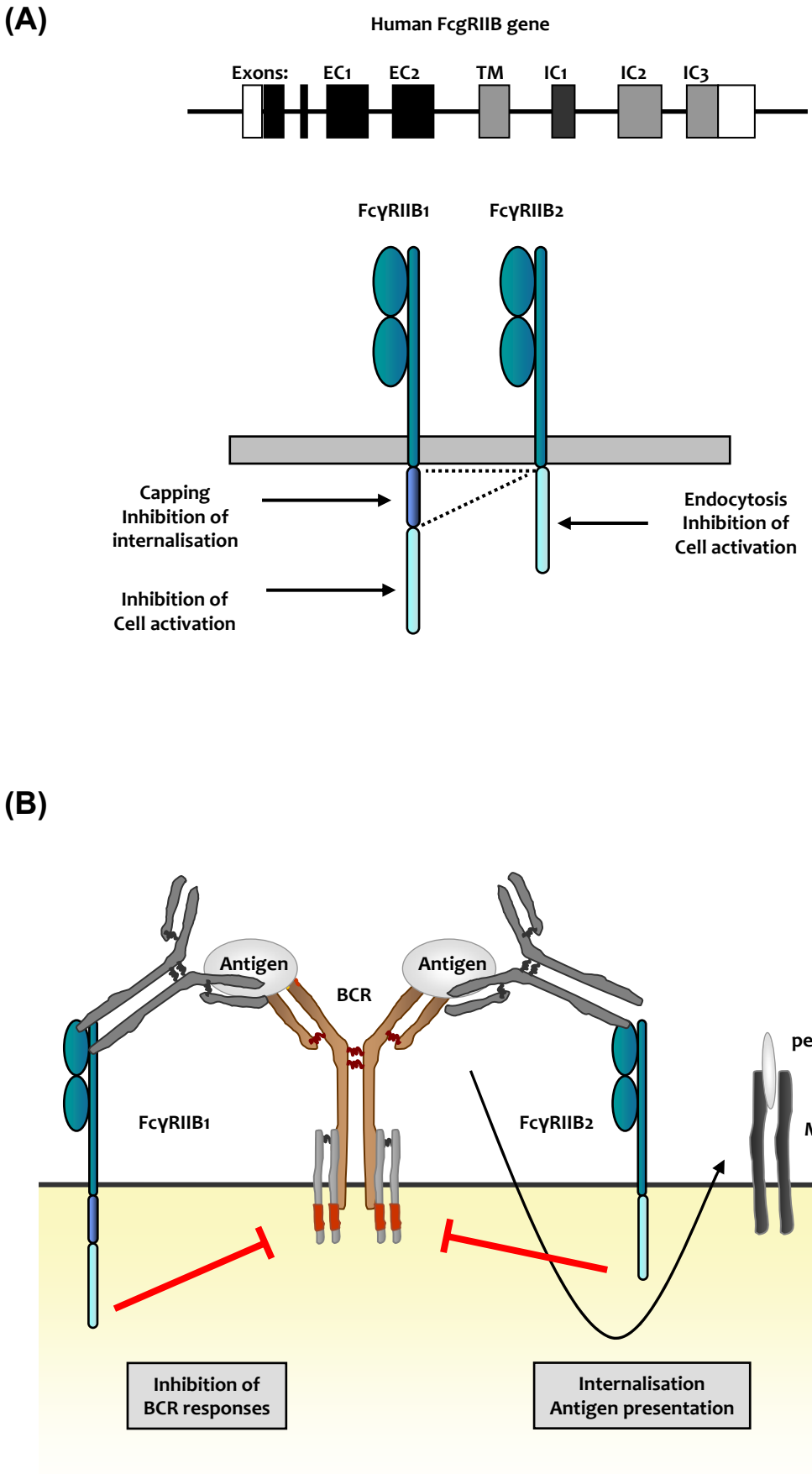
(A)
Human FcgRIIB gene
Exons:
EC1
EC2
TM
IC1
IC2
IC3
FcγRIIB1
FcγRIIB2
Capping
Inhibition of
internalisation
Endocytosis
Inhibition of
Cell activation
Inhibition of
Cell activation
(B)
Antigen
Antigen
BCR
peptide
MHC II
FcγRIIB1
FcγRIIB2
Inhibition of
BCR responses
Internalisation
Antigen presentation

Figure 4.19

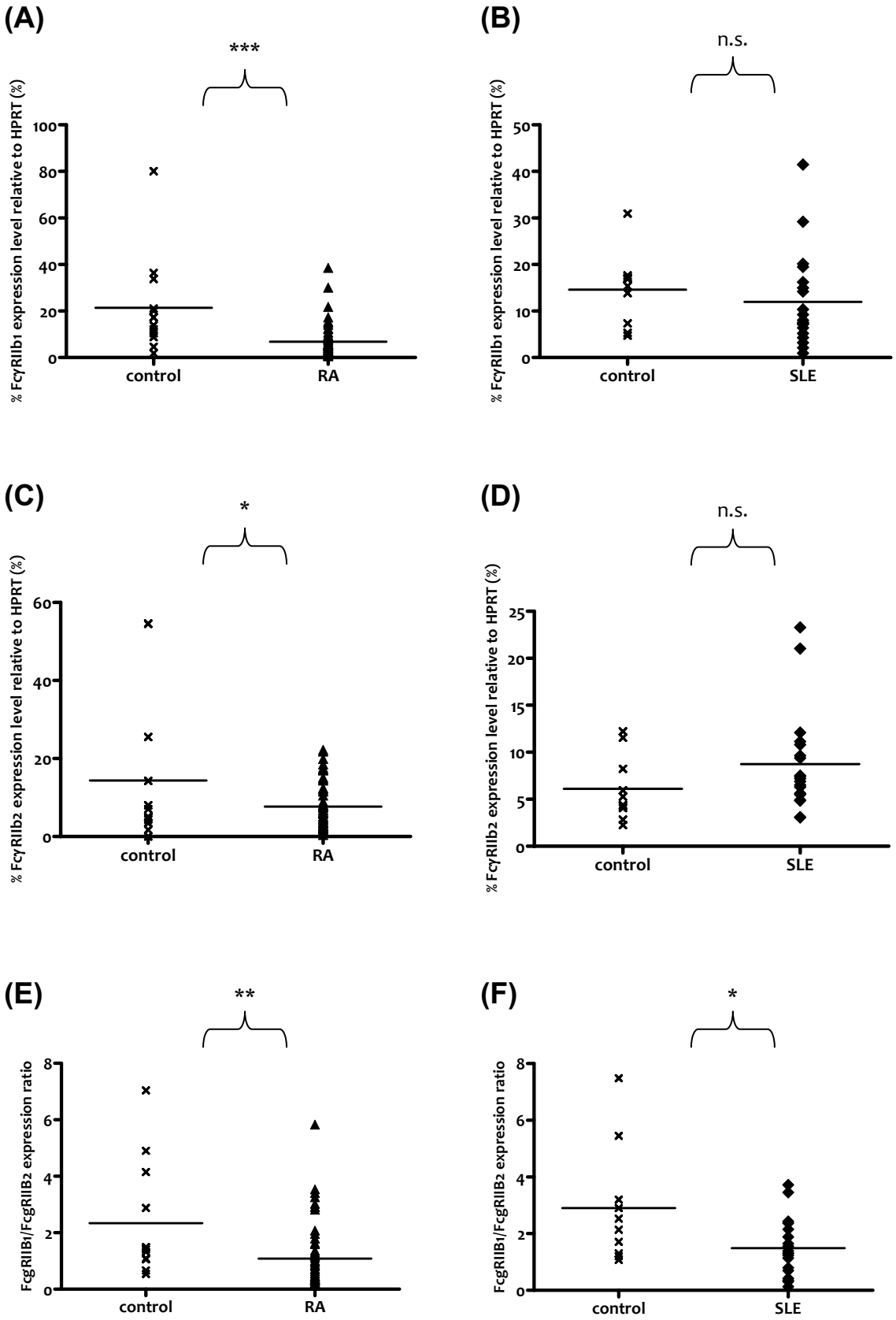
(A)
***
% FcγRIIb1 expression level relative to HPRT (%)
100
80
60
40
20
0
control
RA
(B)
n.s.
% FcγRIIb1 expression level relative to HPRT (%)
50
40
30
20
10
0
control
SLE
(C)
*
% FcγRIIb2 expression level relative to HPRT (%)
60
40
20
0
control
RA
(D)
n.s.
% FcγRIIb2 expression level relative to HPRT (%)
25
20
15
10
5
0
control
SLE
(E)
**
FcgRIIB1/FcgRIIB2 expression ratio
8
6
4
2
0
control
RA
(F)
*
FcgRIIB1/FcgRIIB2 expression ratio
8
6
4
2
0
control
SLE

Figure 4.20

(A)

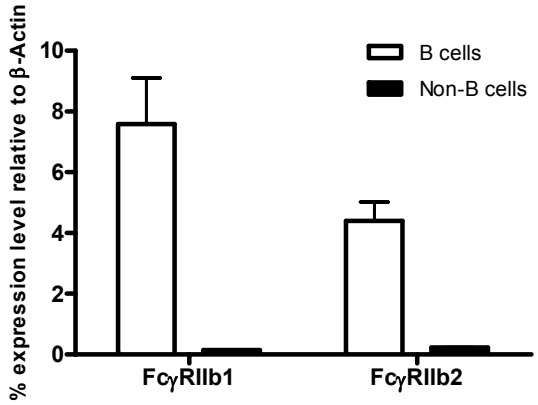

(B)

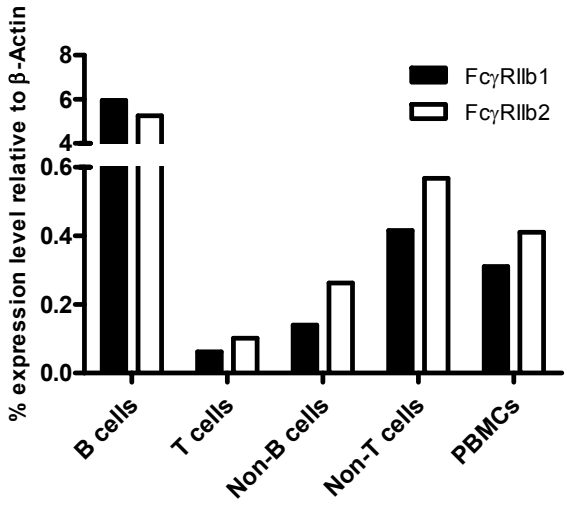

(C)

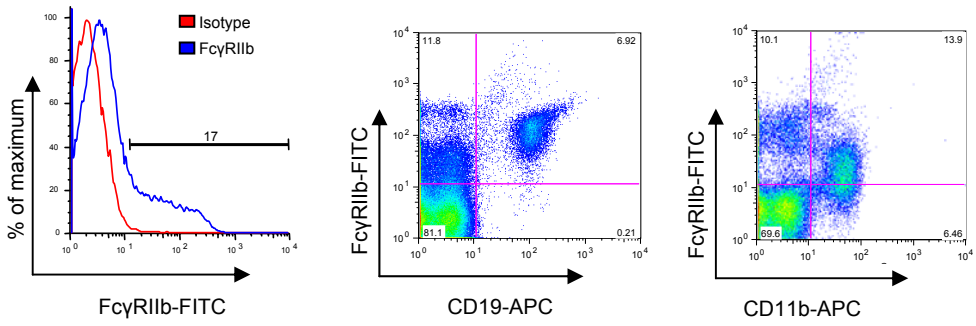

Figure 4.21

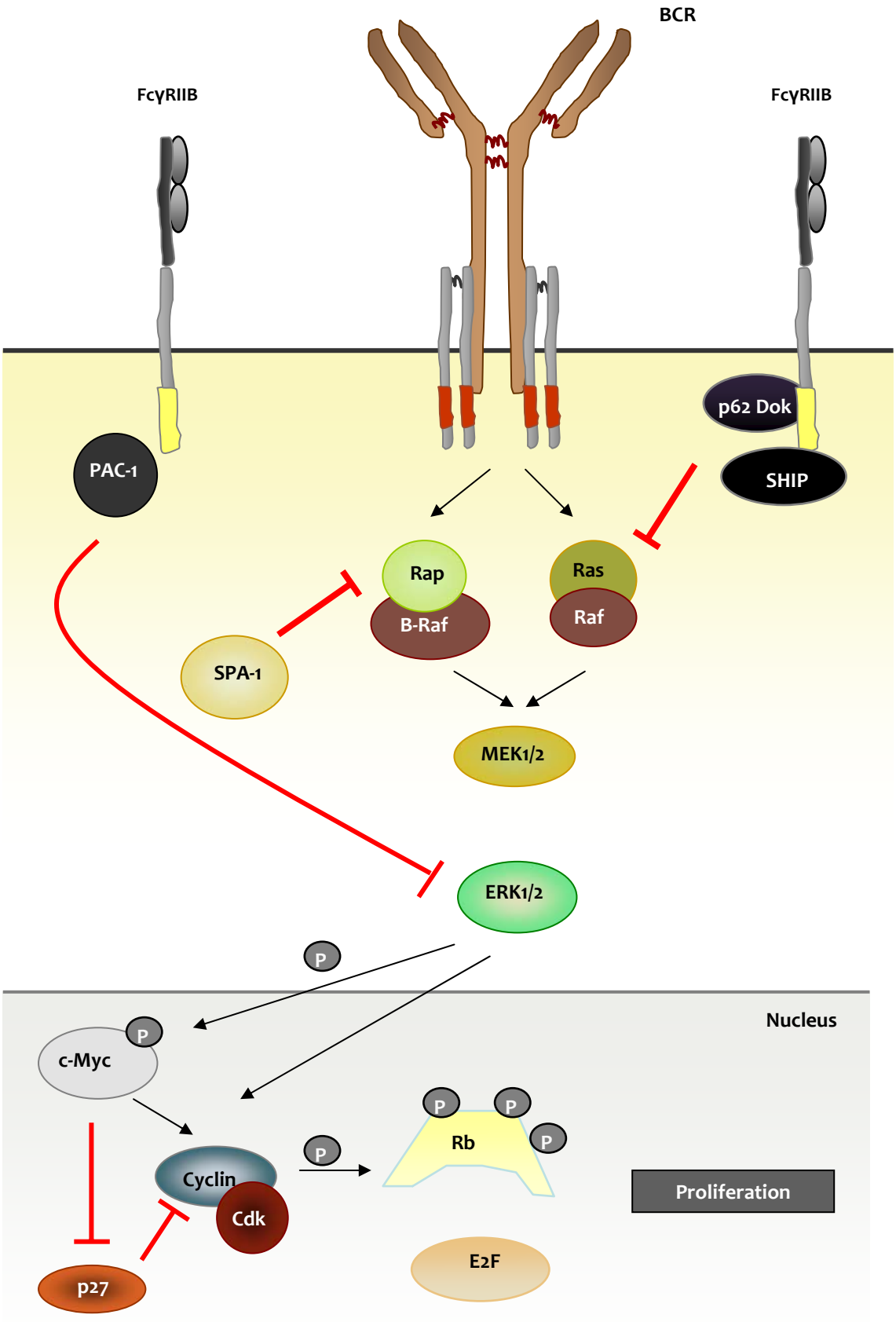
BCR
FcγRIIB
FcγRIIB
p62 Dok
SHIP
PAC-1
Rap
B-Raf
Ras
Raf
SPA-1
MEK1/2
ERK1/2
P
Nucleus
c-Myc
P
P
P
P
Rb
Cyclin
Cdk
P
Proliferation
E2F
p27

Figure 5.1

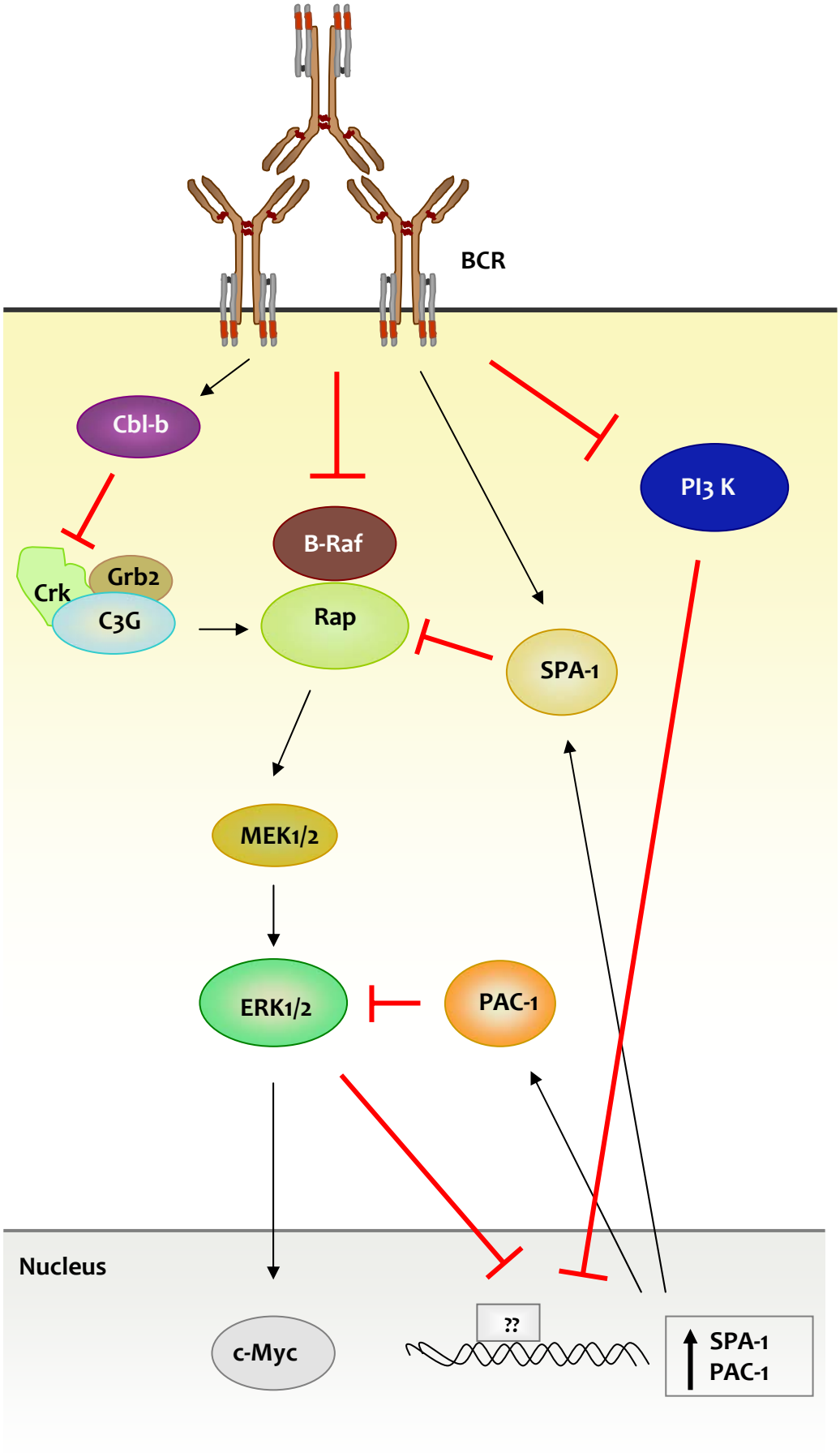
BCR
Cbl-b
PI3 K
B-Raf
Crk
Grb2
C3G
Rap
SPA-1
MEK1/2
ERK1/2
PAC-1
Nucleus
c-Myc
??
SPA-1
PAC-1

Figure 5.2

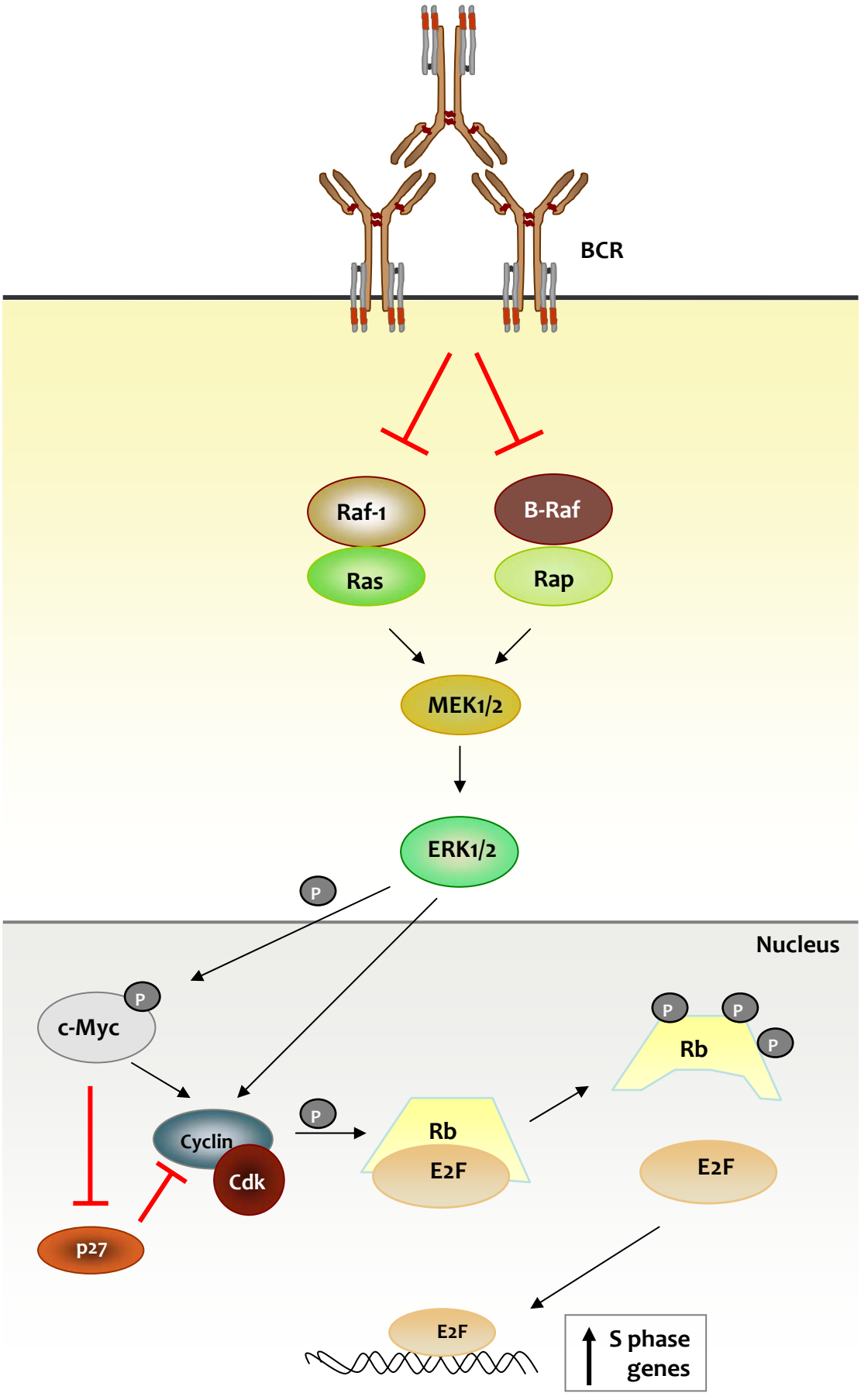
BCR
Raf-1
B-Raf
Ras
Rap
MEK1/2
ERK1/2
P
Nucleus
c-Myc
P
Cyclin
Cdk
p27
P
Rb
E2F
P
P
P
Rb
E2F
E2F
S phase genes

Figure 5.3

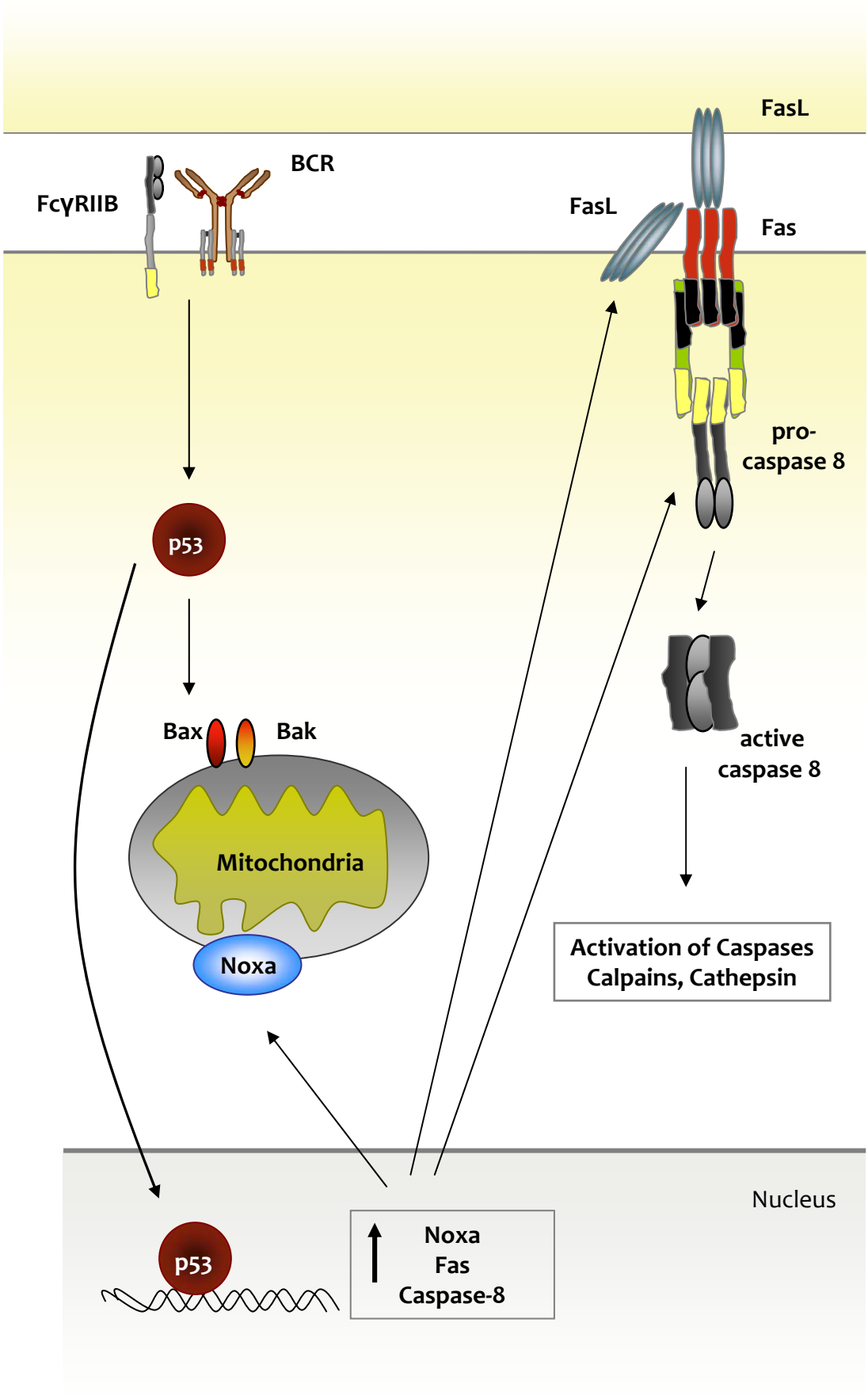
FasL
BCR
FcγRIIB
FasL
Fas
pro-
caspase 8
p53
Bax
Bak
active
caspase 8
Mitochondria
Noxa
Activation of Caspases
Calpains, Cathepsin
Nucleus
p53
Noxa
Fas
Caspase-8